INTEGRATED ANALYTICAL SYSTEMS
Series Editor: Radislav A. Potyrailo, GE Global Research

Functional Nucleic Acids for Analytical Applications

Yingfu Li
Yi Lu
Editors

Springer

Functional Nucleic Acids for Analytical Applications

Yingfu Li • Yi Lu
Editors

Functional Nucleic Acids for Analytical Applications

Springer

Editors
Yingfu Li
Department of Biochemistry and
Biomedical Sciences
McMaster University
Hamilton, Ontario
Canada
liying@mcmaster.ca

Yi Lu
Department of Chemistry
University of Illinois at Urbana-Champaign
Urbana, Illinois
USA
yi-lu@illinois.edu

Cover illustration: Janat Sinn-Hanlon, Imaging Technology Group, Beckman Institute, University of Illinois at Urbana-Champaign.

ISBN: 978-0-387-73710-2 e-ISBN: 978-0-387-73711-9
DOI: 10.1007/978-0-387-73711-9

Library of Congress Control Number: 2008940063

Printed on acid-free paper

springer.com

Preface

Nature long ago solved the problem of finding sequences that code for useful structures, through the endless iteration of the simple algorithm at the heart of Darwinian evolution: variation, selection, reproduction. The deliberate application of this algorithm to the laboratory evolution of useful molecules is a recent development, but the power of this approach is already evident. My introduction to this field came almost 20 years ago when I wanted to explore the rich biochemistry implicit in the strong version of the RNA world hypothesis. Attempting to evolve RNAs that could carry out the key functions of RNA-based life seemed ambitious, so Andrew Ellington and I decided to start with the simple project of selecting for sequences capable of recognizing a given target. In 1990 we showed that it was indeed possible to evolve new RNAs that could bind to and distinguish between closely related small molecules. This was incredibly exciting to us because it was clear that the selected RNAs had to fold into defined three-dimensional structures that contained highly specific ligand-binding sites. Moreover, these ligand-binding RNAs, which we called aptamers, had been selected from a small (only 10^{15}) sample of completely random RNA sequences, implying that functional RNAs were relatively common in sequence space, and that some day really useful aptamers might be evolved! In parallel with our work, Craig Tuerk and Larry Gold found that unexpected sequence variants of a stem-loop RNA had emerged from a randomized population selected for binding to an RNA-binding phage coat protein, and their subsequent work showed that RNAs could be evolved that would bind to almost any protein target. These early findings were soon followed by the evolution of DNA aptamers, novel ribozymes and DNAzymes, and allosterically controlled ribozymes ("aptazymes"). Since then there has been an explosion of work devoted to the evolution of increasingly sophisticated and useful aptamers and nucleic acid catalysts, collectively referred to as functional nucleic acids or FNAs. Perhaps the most scientifically interesting and surprising application of FNAs has been the exciting effort aimed at the development of biosensors and other analytical applications, such as bioseparations, signal amplification, and signal processing, and it is this work that is summarized in a series of thorough and insightful reviews in the present volume.

The book begins with three excellent reviews, the first (by the editors of this volume) introducing the analytical applications of FNAs that are discussed in detail in Parts II and III of the book, the second covering natural riboswitches (Nature's own

RNA-based biosensors) and ribozymes, and the third covering artificially evolved aptamers, ribozymes, and DNAzymes. In Part II we see the remarkable array of amplification and detection technologies that have been coupled to FNAs to allow accurate and sensitive detection of a vast range of target analytes. These methods include a variety of fluorescence and colorimetric and other optical methods, as well as electrochemistry and catalytic signal amplification. Part III on emerging analytical applications is the most forward-looking part of the book, covering diverse topics ranging from aptamer-based separations, to massively parallel microarray detectors, to computational devices and nanomachines built from functional nucleic acids. The myriad of clever ways in which FNAs are now being used is truly remarkable, and this volume provides a wonderful overview for the reader interested in the current state of the art in this rapidly developing field.

Massachusetts General Hospital, USA Jack W. Szostak

Contents

Part I
Overview of Functional Nucleic Acids and Their Analytical Applications

Chapter 1
Introductory Remarks

Yi Lu and Yingfu Li

Abstract The emergence of a large number of natural and artificial functional nucleic acids (FNAs; aptamers and nucleic acid enzymes, collectively termed functional nucleic acids in this book) has generated tremendous enthusiasm and new opportunities for molecular scientists from diverse disciplines to devise new concepts and applications. In this volume, we have assembled some leading experts to provide a timely account of recent progress in sensing and other analytical applications that explore functional nucleic acids.

It is widely known that nucleic acids are the blueprint of life and the foundation of modern biology: they are the hereditary material for the storage and transmission of genetic information in all living organisms on Earth. In some circles, nucleic acids are also known to have the ability to perform other interesting functions, including catalysis and ligand binding. The first discovery in this specific arena was made in early 1980s when some natural RNA molecules were shown to function as enzymes (ribozymes).[1,2] Several years later, several pioneering researchers came up with the idea to perform selection experiments with DNA or RNA in test tubes using a combinatorial technique known as "in vitro selection" or "SELEX" (systematic evolution of ligands by exponential enrichment).[3–5] Subsequent efforts in applying this elegant technique to large random-sequence DNA or RNA pools have led to the creation of a great number of man-made ribozymes, deoxyribozymes (DNAzymes), and aptamers (molecular receptors made of DNA or RNA).[6–12] More recently, many natural RNA molecules, known as "riboswitches," have joined the rank of functional nucleic acids (FNAs). These tiny "molecular wonders" have the ability to regulate gene expression through binding to some important metabolites such as

Y. Lu
Department of Chemistry, University of Illinois at Urbana-Champaign, USA
yi-lu@illinois.edu

Y. Li
Department of Biochemistry and Biomedical Sciences,
McMaster University, Hamilton, Ontario, Canada
liying@mcmaster.ca

Y. Li and Y. Lu (eds.), *Functional Nucleic Acids for Analytical Applications*,

amino acids and nucleotsides.[13–16] We think it is fair to say that the discovery of new functions of nucleic acids has been one of the most fascinating topics in science over the past 25 years.

The existence of many ribozymes and riboswitches in Nature (see Chapter 2, by Lafontaine and coworkers, for a review on natural ribozymes and riboswitches) and our ability to perform test tube evolution experiments to create man-made enzymes and receptors from DNA or RNA (see Chapter 3, by Scott Silverman, for a review on artificial nucleic acid enzymes and aptamers), have generated tremendous enthusiasm in the scientific community. More and more researchers have become interested in studying the fundamental properties of FNAs and examining them for many novel applications in areas including therapeutics,[17–20] molecular imaging,[21] drug screening,[22–24] affinity separation,[25] materials science,[26] nanotechnology,[27–29] and biosensing.[30–36] A timely summary of accomplishments and critical outlook for the future in these areas will be valuable to a wide range of readers who are, or may become, interested in FNAs. However, it is impossible for one book to cover all aspects of FNA-based applications. In this book, we chose to cover FNAs in sensing and other analytical applications because we have witnessed explosive growth of research activities in this area (Fig. 1.1).

To provide a book with the most useful information and authoritative reviews, we have assembled some leading FNA experts whose research activities have contributed significantly to the creation and expansion of each topic covered. The book covers many aspects of functional nucleic acids, from their structures and creation (Chapters 2 and 3) all the way to their applications in analytical chemistry and beyond (Chapters 4–15).

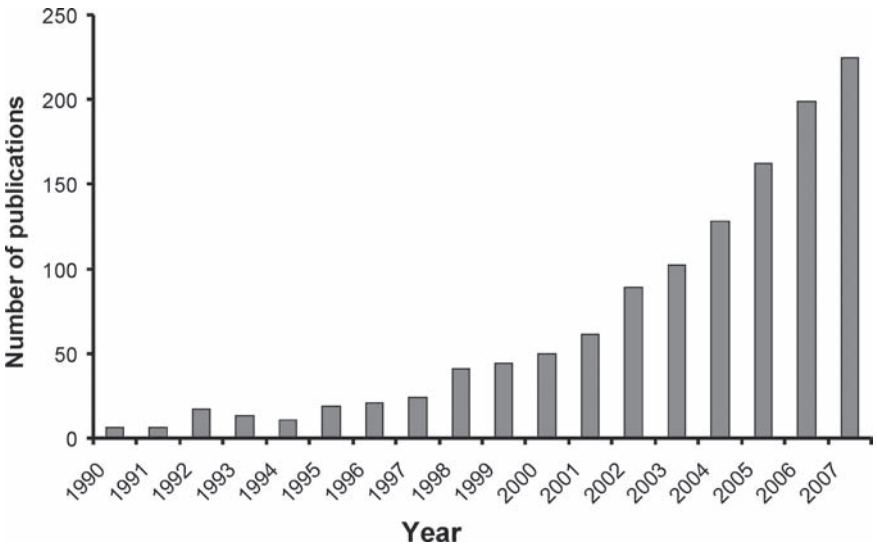

Fig. 1.1 Number of publications related to functional nucleic acids sensors. Results obtained using SciFinder on December 1, 2007. Search terms: sensor and (ribozyme, or deoxyribozyme, or DNAzyme, or aptamer or aptazyme)

Chapter 4, by Tan and coworkers, provides snapshots of recent progress in fluorescent aptamer sensors. Fluorescent sensors have the advantage of being highly sensitive. Many fluorophores can be detected at concentrations less than 1 nM with common benchtop fluorimeters. Many portable fluorimeters are also commercially available, which allows the use of fluorescent sensors in the field. Fluorescence methods give immediate response and can be used in real time Several fluorescence-based signal transduction schemes, such as direct fluorophore labeling, fluorescence resonance energy transfer (FRET), fluorescence quenching, fluorescence anisotropy, and light-switching excimers, are discussed. Examples given have shown that the aptamer sensors can result in simple, rapid, sensitive, and selective biological assays of a wide range of molecules, including organic and protein molecules and tumor cells.

Our ability to create allosteric nucleic acid enzymes (aptazymes) by rational design or in vitro selection has considerably expanded the utility of ribozymes and DNAzymes. Li and Chiuman discuss progress in fluorescent ribozyme and deoxyribozyme sensors in Chapter 5. They begin their chapter by reviewing several strategies that have been used to produce ribozymes or DNAzymes which can generate fluorescent signals upon catalysis. This part is followed by discussion of the efforts in their own laboratory in creating fluorescence-signaling and RNA-cleaving deoxyribozymes by in vitro selection. The third part of their chapter reviews several published approaches that can link the binding action of an aptamer to catalytic activity of a fluorescence-signaling ribozyme or deoxyribozyme.

Recent development in nanotechnology has brought new opportunity in FNA-sensing applications, as nanomaterials possess strong and unique signaling properties for FNA binding of targets and catalysis. FNA-modified nanomaterials are ideally suited for analytical applications. Chapter 6, by Liu and Lu, first discusses simple colorimetric sensors that combine DNAzymes, aptamers, and aptazymes with metallic nanoparticles. Reporting systems obtained from modifying quantum dots with FNAs for fluorescent sensing are also presented. Their chapter closes with an example in which colorimetric sensors are formulated into a “dipstick” test, making it possible for simple on-site real-time detection and quantification without instrumentation.

Electronic devices can be routinely miniaturized in terms of size and power consumption and can usually offer ultrahigh sensitivity, good reproducibility, and fast response; this may explain why electrochemical sensing exploiting FNAs has become a very active research area in recent years. In Chapter 7, Xiao and Plaxco review some exciting sensors that exploit the unusual physical properties of aptamers, properties which render them uniquely well suited for application to impedance- and folding-based electrochemical sensors. These sensors make use of electrode-bound aptamers that undergo reversible, binding-induced folding, which translates into an electronic signal. These sensors can be used to provide reagentless and highly sensitive detection of specific biomolecules in blood serum and other complex, interference-ridden sample matrices.

One of the most important parameters in analytical applications is the detection sensitivity. Although many of the FNAs possess high affinity for their targets, methods

that can further enhance sensitivity of FNA sensors are critical to their wide applicability. In Chapter 8, Willner and coworkers review many interesting methods for the design of FNA sensors with signal amplification capabilities.

In addition to sensing applications, FNAs have been shown to be quite useful in many other analytical applications. This book covers several promising applications such as affinity separation, high-throughput screening, and DNA-based computing. New sensing formats such as aptamer arrays, solid-phase assays, and FNA-based nanostructures provide excellent opportunity for aptamer researchers to take full advantage of FNA-based sensors for a broader range of applications.

In Chapters 9 and 10, the applications of aptamers for affinity separations have been reviewed using capillary electrophoresis (CE) and stationary separations, respectively. In the area of CE-based affinity separation, Guthrie and Le categorize the methods into competitive and noncompetitive assays, fluorescence polarization assays, nonequilibrium capillary electrophoresis of equilibrium mixtures, and affinity-polymerase chain reaction-CE assays. CE not only provides a sensitive detection method but can also be used as a convenient system to determine important parameters of aptamer–target complexation (such dissociation rate and equilibrium binding constants and binding stoichiometries). In Chapter 10, Ravelet and Peyrin provide a discussion on recent activities in using aptamers as target-specific ligands for the separation and capture of various analytes in affinity chromatography and related affinity-based methods such as magnetic bead technology.

The increasingly wider applications of aptamers demand the creation of more aptamers for new targets and the use of many different aptamers for simultaneous detection and quantifications of multiple biological targets. In Chapter 11, Ellington and colleagues discuss recent development both in high-throughput, automated aptamer selection and in construction of aptamer microarrays. For example, the results from their study have shown that arrayed aptamers are almost as sensitive as their solution-phase counterparts and, when assembled together, can provide both specific and general diagnostic signals for proteins and other analytes. Coupling of immobilized aptamers to amplification methods such as those reviewed in Chapter 8 can greatly enhance detection signals.

FNA-based microarrays and other solid-phase applications underscore the importance of developing methods that can immobilize FNAs onto solid supports and maintain the activity of layered FNAs. In Chapter 12, Brennan and coworkers first provide a good overview of methods that can be explored for immobilization of FNAs. This review is followed by discussion of their published efforts in which they studied sol-gel encapsulation of FNAs for the development of solid-phase fluorimetric assays for biosensing and proteomics.

Aptamers and nucleic acid enzymes not only have the potential to be directly exploited as therapeutic agents but can also be explored as tools to derive small-molecule drugs. In Chapter 13, Rentmeister and Famulok have provided a review on research activities where FNA-based sensors have been explored as reporting tools to facilitate high-throughput screens (HTS) to search for small-molecule probes or inhibitors for protein targets that may not have a convenient assay to conduct HTS.

In Chapter 14, Macdonald and Stojanovic discuss an interesting line of research that explores FNAs for DNA-based computation. For example, they have produced various molecular logic gates using RNA-cleaving DNAzymes as switches and single-stranded oligonucleotides as inputs and outputs. These logic gates can be further combined to produce basic computational circuits such as half- and full adders. Their DNAzyme-based logic gates can also be assembled into automata to perform complex computational tasks such as game playing. Their efforts may eventually lead to applications in which FNAs can be utilized as autonomous diagnostic and/or therapeutic molecular devices.

Finally, in Chapter 15, Mao and coworkers provide a review on some of their work on exploring DNA-based enzymes to create interesting DNA assemblies that can function as molecular machines. These DNA machines are regarded as "nanomachines" because their sizes are smaller than 100 nanometer (nm). For example, in Mao's lab, some specific RNA-cleaving DNAzymes are combined with matching substrates and other regulatory DNA strands in unique ways to create autonomous nanomotors, which can extract chemical energy from RNA substrates and convert it into a mechanical motion.

Work reviewed in all the chapters of this book, although quite exciting, represents only a portion of demonstrated examples where FNAs are applied as analytical tools. We hope that by presenting the state-of-the-art methods and technologies concerning FNAs, readers can gain appreciation of what have been accomplished and what remains to achieve. Given the rapid progress made recently in FNAs, we are confident that many of the FNA sensors and emerging analytical applications will be commercially available in the near future. However, many challenges still remain to be tackled before we can realize the full potential of FNAs. Therefore, we hope the information presented in this book can function as an "inducer" to engage more researchers to link their research activities to the expansion of the aptamer arena. We also hope that the demonstrated examples and remaining challenges discussed in this book can motivate future generations of scientists to select this field as their interest of study.

Following the groundbreaking discovery of ribozymes, it took merely 10 years for a group of scientists to come up with the brilliant idea of conducting selection and evolution experiments using DNA or RNA in test tubes. This great invention has now become a powerful vehicle for molecular scientists to travel through the land of nucleic acids for more discoveries and applications. We hope this book can serve as a useful guide for those who would like to take such a journey to search for new frontiers in the amazing "jungle" of functional nucleic acids.

We thank all the authors for their efforts in putting together the excellent chapters and Jack Szostak for writing the preface of the book. We also want to thank the members of our two laboratories for either their assistance or their patience with us while we were working on this project. Special credits go to Juewen Liu and William Chiuman for their assistance in chapter writing and other important issues such as copyright permission acquisition, and Janet Sinn-Hanlon of Imaging Technology Group at the Beckman Institue and Jung Heon Lee and Zidong Wang of Department of Materials Sciences and Engineering at the University of Illinois at Urbana-Champaign, in design of the cover graphics, and

proofreadings. We want to express our gratitude to Kenneth Howell (Springer) and Radislav Potyrailo (GE Global Research Center) for the invitation to assemble this book and for their guidance along the way. Last, but not least, we thank our families for their support and patience.

References

1. Kruger, K., Grabowski, P.J., Zaug, A.J., Sands, J., Gottschling, D.E. and Cech, T.R. (1982) Self-splicing RNA: autoexcision and autocyclization of the ribosomal RNA intervening sequence of *Tetrahymena*. Cell 31:147–157.
2. Guerrier-Takada, C., Gardiner, K., Marsh, T., Pace, N. and Altman, S. (1983) The RNA moiety of ribonuclease P is the catalytic subunit of the enzyme. Cell 35:849–857.
3. Ellington, A.D. and Szostak, J.W. (1990) In vitro selection of RNA molecules that bind specific ligands. Nature (Lond.) 346:818–822.
4. Robertson, D.L. and Joyce, G.F. (1990) Selection in vitro of an RNA enzyme that specifically cleaves single-stranded DNA. Nature (Lond.) 344:467–468.
5. Tuerk, C. and Gold, L. (1990) Systematic evolution of ligands by exponential enrichment: RNA ligands to bacteriophage T4 DNA polymerase. Science 249:505–510.
6. Lee, J.F., Hesselberth, J.R., Meyers, L.A. and Ellington, A.D. (2004) Aptamer database. Nucleic Acids Res. 32:D95–D100.
7. Thodima, V., Piroozina, M. and Deng, Y. (2006) RiboaptDB: a comprehensive database of ribozymes and aptamers. BMC Bioinformatics 7(suppl 2):S6.
8. Breaker, R.R. (2004) Natural and engineered nucleic acids as tools to explore biology. Nature (Lond.) 432:838–845.
9. Fedor, M.J. and Williamson, J.R. (2005) The catalytic diversity of RNAs. Nat. Rev. Mol. Cell. Biol. 6:399–412.
10. Achenbach, J.C., Chiuman, W., Cruz, R.P. and Li, Y. (2004) DNAzymes: from creation in vitro to application in vivo. Curr. Pharm. Biotechnol. 5:321–336.
11. Joyce, G.F. (2004) Directed evolution of nucleic acid enzymes. Annu. Rev. Biochem. 73:791–836.
12. Silverman, S.K. (2005) In vitro selection, characterization, and application of deoxyribozymes that cleave RNA. Nucleic Acids Res. 33:6151–6163.
13. Mandal, M. and Breaker, R.R. (2004) Gene regulation by riboswitches. Nat. Rev. Mol. Cell Biol. 5:451–463.
14. Tucker, B.J. and Breaker, R.R. (2005) Riboswitches as versatile gene control elements. Curr. Opin. Struct. Biol. 15:342–348.
15. Winkler, W.C. (2005) Riboswitches and the role of noncoding RNAs in bacterial metabolic control. Curr. Opin. Chem. Biol. 9:594–602.
16. Winkler, W.C. and Breaker, R.R. (2005) Regulation of bacterial gene expression by riboswitches. Annu. Rev. Microbiol. 59:487–517.
17. Sullenger, B.A. and Gilboa, E. (2002) Emerging clinical applications of RNA. Nature (Lond.) 418:252–258.
18. Nimjee, S.M., Rusconi, C.P. and Sullenger, B.A. (2005) Aptamers: an emerging class of therapeutics. Annu. Rev. Med. 56:555–583, 553 plates.
19. Lee, J.F., Stovall, G.M. and Ellington, A.D. (2006) Aptamer therapeutics advance. Curr. Opin. Chem. Biol. 10:282.
20. Famulok, M., Hartig, J.S. and Mayer, G. (2007) Functional aptamers and aptazymes in biotechnology, diagnostics, and therapy. Chem. Rev. (Washington, DC) 107:3715–3743.
21. Cho, E.J., Rajendran, M. and Ellington, A.D. (2005) Aptamers as emerging probes for macromolecular imaging. Top. Fluoresc. Spectrosc. 10:127–155.

22. Famulok, M. (2005) Allosteric aptamers and aptazymes as probes for screening approaches. Curr. Opin. Mol. Ther. 7:137.
23. Blank, M. and Blind, M. (2005) Aptamers as tools for target validation. Curr. Opin. Chem. Biol. 9:336–342.
24. Famulok, M. and Mayer, G. (2005) Intramers and aptamers: applications in protein-function analyses and potential for drug screening. ChemBioChem 6:19–26.
25. Ravelet, C. and Peyrin, E. (2006) Recent developments in the HPLC enantiomeric separation using chiral selectors identified by a combinatorial strategy. J. Separ. Sci. 29:1322–1331.
26. Lu, Y. and Liu, J. (2007) Smart nanomaterials inspired by biology: dynamic assembly of error-free nanomaterials in response to multiple chemical and biological stimuli. Acc. Chem. Res. 40:315–323.
27. Lu, Y. and Liu, J. (2006) Functional DNA nanotechnology: emerging applications of DNAzymes and aptamers. Curr. Opin. Biotechnol. 17:580–588.
28. Katz, E. and Willner, I. (2004) Nanobiotechnology: integrated nanoparticle–biomolecule hybrid systems: synthesis, properties, and applications. Angew. Chem. Int. Ed. 43:6042–6108.
29. Feldkamp, U. and Niemeyer, C.M. (2006) Rational design of DNA nanoarchitectures. Angew. Chem. Int. Ed. 45:1856–1876.
30. Famulok, M., Mayer, G. and Blind, M. (2000) Nucleic acid aptamers: from selection in vitro to applications in vivo. Acc. Chem. Res. 33:591–599.
31. Rajendran, M. and Ellington, A.D. (2002) Selecting nucleic acids for biosensor applications. Comb. Chem. High Throughput Screen. 5:263–270.
32. Hesselberth, J., Robertson, M.P., Jhaveri, S. and Ellington, A.D. (2000) In vitro selection of nucleic acids for diagnostic applications. Rev. Mol. Biotechnol. 74:15–25.
33. Breaker, R.R. (2002) Engineered allosteric ribozymes as biosensor components. Curr. Opin. Biotechnol. 13:31–39.
34. Lu, Y. (2002) New transition metal-dependent DNAzymes as efficient endonucleases and as selective metal biosensors. Chem. Eur. J. 8:4588–4596.
35. Navani, N.K. and Li, Y. (2006) Nucleic acid aptamers and enzymes as sensors. Curr. Opin. Chem. Biol. 10:272–281.
36. Yang, L. and Ellington, A.D. (2006) Prospects for the de novo design of nucleic acid biosensors. Fluoresc. Sens. Biosens. 5:41, 43.

Chapter 2
Natural Functional Nucleic Acids: Ribozymes and Riboswitches

Renaud Tremblay, Jérôme Mulhbacher, Simon Blouin, J. Carlos Penedo, and Daniel A. Lafontaine

Abstract Natural functional nucleic acids are of primary importance in most cellular processes. Although artificial RNA motifs with functional properties can routinely be generated in research laboratories, the efficiency of their naturally occurring counterparts is hardly matched. Natural ribozymes and riboswitches are examples of Nature's prowess at creating exceedingly good catalysts and ligand-sensing aptamers. This review focuses on natural ribozymes and riboswitches and attempts to highlight how RNA can rival proteins when it comes to show off its capabilities.

2.1 Introduction

RNA molecules are involved in countless essential reactions in living cells – in addition to their roles in information storage and architectural framework, they also perform catalytic reactions, as best exemplified by the peptidyl transfer reaction of ribosomal RNA.[1] However, this nowadays widely accepted notion has not always been the case. Indeed, only 25 years ago, RNA was only considered to be the messenger that would carry genetic information from DNA to the ribosome for the production of proteins. Protein enzymes were considered to be the only true "molecular effectors," which participated in many important biological processes. However, when Thomas Cech[2] and Sidney Altman[3] simultaneously discovered that RNA can exhibit catalytic properties, similar to protein enzymes, it changed the way scientists envisioned how RNA is involved in molecular reactions. These RNA enzymes, the so-called ribozymes, playing both informational and catalytic roles, inspired the "RNA world" hypothesis. This proposal was put forward to address the "chicken-and-egg" problem of how a translation system could evolve without proteins already in place. Thus, if RNA molecules, or some other

R. Tremblay, J. Mulhbacher, S. Blouin, and D.A. Lafontaine
Université de Sherbrooke, Département de Biologie
daniel.lafontaine@usherbrooke.ca

J.C. Penedo
University of St. Andrews, School of Physics and Astronomy
jcp10@st-andrews.ac.uk

Y. Li and Y. Lu (eds.), *Functional Nucleic Acids for Analytical Applications*,

RNA-related biopolymers, could encode information and perform catalysis at the same time, then protein-based processes could well have evolved from those giving rise to the complexity and variety of modern cellular processes. If this is true, it seems plausible to suggest that molecular remnants of that RNA era would still remain today.

A few years ago, RNA came into the spotlight for a second time. Indeed, it was found that RNA was able to use feedback regulatory loops, such as retro-inhibition, to monitor and control its own expression – all of this apparently in the absence of any helper protein. These molecules, the so-called riboswitches, are literally "molecular switches" that can sense the presence of small cellular metabolites and, upon binding to them, switch into a different conformation to either promote or inhibit transcription or translation of the encoded protein. The first examples of this regulatory behavior were found studying the regulation of biosynthetic enzymes producing vitamins B_1, B_2, and B_{12}.[4–8] Because riboswitches can operate in the absence of proteins in vitro, it has been proposed that they could be remnants of the RNA world that was essentially RNA based.[9] Whether riboswitches really work in the absence of protein in the cell still remains elusive, and this point will most probably require additional investigations.

For a primitive world to be viable, it inherently requires that a large array of catalytic reactions and metabolic regulations are performed by RNA molecules. Thus, to probe to what extent RNA is a "good contortionist" at performing various catalytic reactions, a procedure has been put forward that can be described as an accelerated evolution which is done in a test tube. This procedure, called SELEX (systematic evolution of ligands by exponential enrichment),[10–12] relies on the starting hypothesis that, in a given population, at least one RNA sequence exists that is able to perform the desired function. Following this approach, artificially engineered ribozymes have been isolated for a variety of reactions such as hydrolysis, RNA transesterification, peptidyl transfer, ester hydrolysis, isomerization, and Diels–Alder cyclo-addition (recently reviewed[13]). Thus, although RNA has far fewer functional groups compared to proteins, it can still perform a large set of chemical reactions. SELEX has also been used to test RNA molecules for their ligand-binding capacity (recently reviewed[14]). By employing ligands bound to a solid phase, many artificial aptamers have been isolated that respond to various metabolites such as theophylline and adenosine triphosphate (ATP). A natural extension to this was the creation of artificial ribozymes that could be controlled by external signals. Indeed, many allosterically controlled ribozymes were created that could respond to small organic compounds, proteins, pH, light, etc.[14–16] Although a large number of artificial ribozymes and aptamers have been isolated, this review focuses on the natural representatives and attempts to emphasize the variety of tricks that RNA has up its sleeve to rival protein activities. The review of artificially derived functional nucleic acids is provided in Chapter 3 of this volume.

2.2 Ribozymes

RNA catalysis was very likely crucial for the development of early life on Earth. Ribozymes are thought to be "molecular fossils" still in place today. Natural ribozymes perform various enzymatic reactions, and they are usually classified by

their relative size. The large ribozymes [>300 nucleotides (nt)] are constituted of the self-splicing introns (groups I and II) and the protein-assisted RNase P (Fig. 2.1). Although self-splicing introns perform transesterification reactions, the RNase P employs a hydrolysis mechanism to process the 5′-end of transfer RNAs, thus making the reaction practically irreversible. Several crystal structures are available for the group I intron that reveal different steps of the chemical reaction.[17–20] In all cases, the core domain is well conserved and in agreement with previous biochemical data (recently reviewed[21]). Strikingly, a guanine suggested almost 20 years ago[22] to be involved in a triple-base interaction is observed in all crystals. This interaction is also consistent with data from Bass and Cech reporting that the *Tetrahymena* intron is able to use guanosine analogues.[23]

In contrast to other natural ribozymes, RNase P is a multiple turnover enzyme that recognizes and cleaves its substrate in *trans* through recognition of secondary and tertiary structural elements in the substrate.[24] Moreover, RNase P is able to process various structurally different substrates such as pre-tRNAs, 4.5 S RNA, bacteriophage 80-induced RNA, the mRNA from the polycistronic his operon, transient structures adopted by riboswitches, and other cellular substrates.[25] The RNA component of RNase P is strongly conserved, which suggests its importance for cellular metabolism.[26] Evidence of this importance has been recently found on an eukaryotic RNase P, whose RNA moiety is active in absence of proteins, akin to its prokaryotic counterpart.[27] Complete RNase P RNAs from bacterial sources as well as isolated domains have recently been crystallized.[26,28–30] The two complete RNase P crystals were solved for types A and B, which have structurally distinct secondary structures.[25] Unfortunately, neither crystal is able to deliver insights into the conformation of the active structure because both have some associated technical problems.[25] Nevertheless, both structures exhibit a compact fold with a flat surface

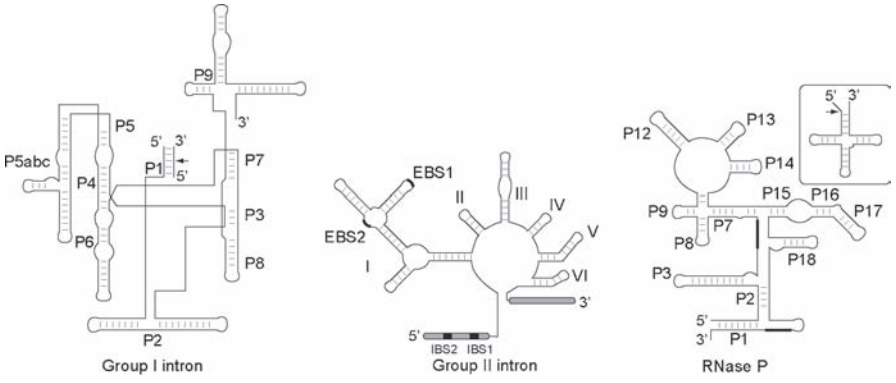

Fig. 2.1 Naturally occurring large ribozymes. Secondary structures are shown for each species. Cleavage sites are shown by *arrows* for the group I intron and the RNase P. The intron and exon binding sequences, *IBS* and *EBS*, respectively, are shown for the group II intron ribozyme. *Gray regions* indicate the exons of the group II intron ribozyme. A tertiary interaction is shown by *bold bars* for the RNase P. The substrate of the RNAse P, a tRNA, is shown in the *inset*

to which a pre-tRNA binds. The nonconserved regions are located away from the binding site and participate in long-range tertiary interactions most probably important for the global folding of the ribozyme. However, even with these crystal structures in hand and together with the huge amount of biochemical data, we are still far from understanding the RNAse P structure and the details of RNA–protein interactions that are part of it. Nevertheless, despite their inherent lack of precision, tertiary models based on isolated crystallized domains of the RNase P and biochemical results provide stimulation for new testable hypotheses.[25]

A mechanistically distinct class of smaller ribozymes also exists that includes the hammerhead, hairpin, hepatitis delta virus (HDV), Varkud satellite (VS), and glmS ribozymes (Fig. 2.2). All these ribozymes perform a self-cleaving transesterification, generating a hydroxyl and a cyclic phosphate terminus that can then be used to catalyze the reverse reaction according to a ligation mechanism. Crystal structures have been obtained for all small ribozymes,[31–37] excluding the VS ribozyme, for which a tertiary model has been built using a combination of comparative gel electrophoresis and fluorescence resonance energy transfer (FRET) distance restraints.[38,39] Because they can function in the absence of divalent ions, in contrast to large ribozymes, it has been suggested that small ribozymes might employ a nucleobase-driven catalysis.[40,41] A new ribozyme seems to have been identified within the human β-globin mRNA that is involved in the cotranscriptional processing.[42] Interestingly, the cleavage site is contained within a region predicted to exhibit a structure similar to the one observed for the hammerhead

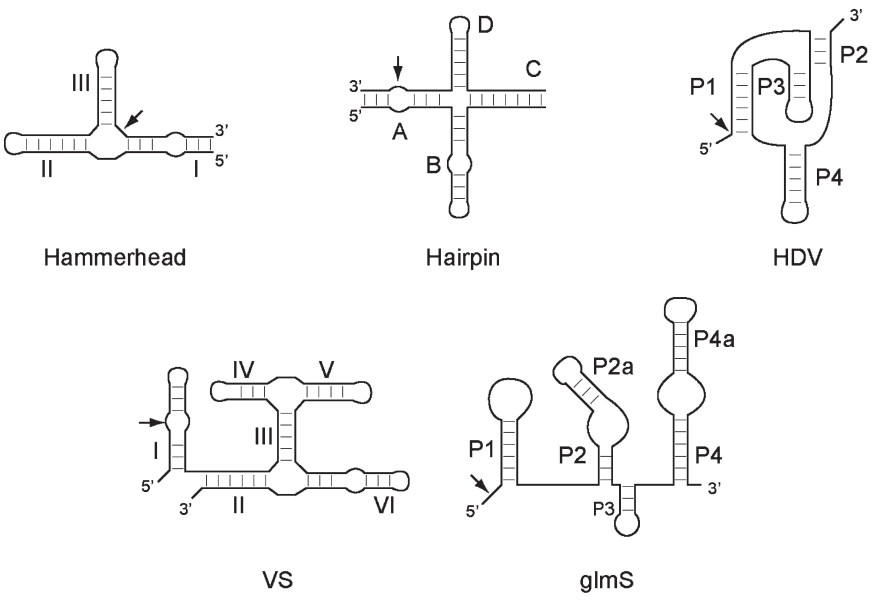

Fig. 2.2 Small nucleolytic ribozymes. Secondary structures and cleavage sites are shown for each ribozyme. The *Schistosoma* variant is represented for the *hammerhead* ribozyme

ribozyme. However, this similarity is only superficial given that the product termini are more related to those generated by the RNase P. Moreover, in addition to providing a model system to study catalysis, small ribozymes are also intensively employed in gene therapy to reduce the expression of specific mRNAs.[43] Although this avenue is promising, various technical problems such as the RNA stability and gene targeting must be addressed to fully exploit this concept.

Natural ribozymes are heavily biased toward transesterification reactions. However, crystallization of the big subunit of the ribosome made clear that the peptidyl transfer reaction that catalyzes the ribosome is very likely performed exclusively by the RNA component, making the ribosome, in fact, a ribozyme.[44] In this case, it has been proposed that a particular adenosine, A2451 in *Escherichia coli*, is involved in a proton transfer reaction during the catalytic step.[1] Interestingly, a peptidyl transferase ribozyme was previously isolated through SELEX,[45] giving support to the notion that the RNA moiety of the ribosome is directly responsible for the catalytic activity, and that ribosomal proteins could function more or less as folding chaperones. Using single-molecule fluorescence spectroscopy, structural information has recently been obtained concerning tRNA dynamics on the ribosome during translation.[46,47] In these studies, it was demonstrated that dynamics of ribosome function are very important for the translation process, and that the ribosomal recognition of correct codon-anticodon pairs drives ribosomal rotational movement during tRNA selection, which is most probably important for the proofreading process.

Various excellent reviews on ribozymes have been published recently.[21,48–54] Here, we focus on the hammerhead ribozyme because it is the one for which a larger body of work on the catalytic mechanism, structure, and folding has been accumulated over the years. Also, a recent crystal structure[36] has shed light on years of discrepancy between structure and function data. Particular attention is also devoted to the VS ribozyme, which is the only natural small ribozyme for which a crystal structure is yet to be solved.

2.2.1 The Hammerhead Ribozyme

The hammerhead is a catalytic motif found in RNA genomes of numerous plant pathogens, and it is involved in the processing of RNA issued from the rolling-circle amplification.[55] For more than 20 years, the hammerhead has been defined as a single three-way junction organized around a conserved core containing the catalytic center (see Fig. 2.2). This autocatalytic species performs the reversible site-specific cleavage of its backbone via a transesterification reaction in which the 2′-oxygen attacks the adjacent 3′-phosphorus, ultimately leading to 5′-hydroxyl and 2′,3′-cyclic phosphate termini. The reaction proceeds with inversion of the configuration at the phosphorus center, indicating that the reaction occurs by transesterification via an S_N2 mechanism. The catalytic reaction is accelerated by at least 10^6-fold compared to the nonenzymatic reaction.[56] The hammerhead

can be engineered as a true enzyme by performing a nick in one of the capping loops, effectively generating a substrate and an enzyme strand. The bimolecular hammerhead catalytic reaction can thus be viewed as follows: association between the substrate and the ribozyme, chemical cleavage step, and dissociation of the ribozyme–products complex. It has been deduced that the substrate association and product dissociation steps have kinetic and thermodynamic properties very similar to an RNA helix-coil transition, and that the chemical step of the cleavage reaction is almost identical throughout all hammerhead ribozymes.[57] In most conditions, the cleavage is at least 100-fold faster than the ligation rate.[58,59]

The hammerhead ribozyme is one of the most studied small catalytic RNAs, and recent advances have shown that, for years, studies were performed on a minimal active form lacking an important loop–loop interaction.[60,61] Indeed, because, of the "RNA reductionism" approach, where an RNA of interest is truncated to its smallest active size, RNA researchers have inadvertently removed a very important loop–loop interaction between stems I and II (Fig. 2.3). It appears that the presence of this tertiary interaction decreases the concentration of divalent ions required for catalytic activity by almost 100-fold compared to the minimal form. This unexpected finding ended a long-standing discrepancy between physiological divalent ions concentrations and that required for significant in vitro activity of the minimal form. Thus, it is important to realize that experiments conducted on the minimal form (i.e., without the loop–loop interaction) might not reflect what

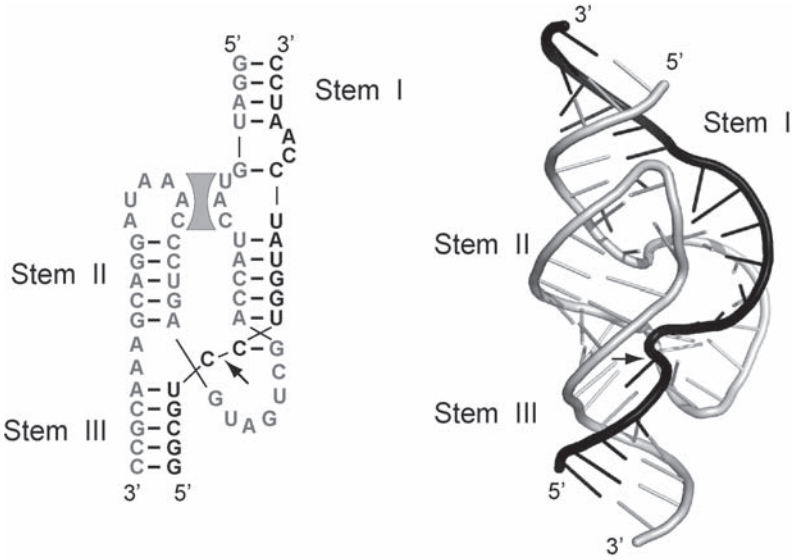

Fig. 2.3 The *Schistosoma* hammerhead ribozyme. The secondary (*left*) and the tertiary (*right*) structures are shown. The substrate and the ribozyme moieties are colored in *gray* and in *black*, respectively. A tertiary interaction and the cleavage site are indicated by the *shaded region* and an *arrow*, respectively[36]

is occurring in the natural sequence. Nevertheless, we believe that a comparison between the biochemical data of the minimal and natural forms of the hammerhead is worthwhile to highlight the importance of what initially were taken as noncrucial structural elements and also to emphasize the need for caution when taking a "reductionist approach."

In its minimal form, the folding and dynamics of the hammerhead have been studied using transient electric birefringence,[62] comparative gel electrophoresis,[63] FRET,[64–66] 2-aminopurine fluorescence,[67,68] binding of bases to abasic sites,[69] cross-linking,[70–73] and solution NMR experiments.[74–76] In agreement with these results, an ion-induced folding scheme of the ribozyme has been elaborated where the folding occurs by a sequential two-stage process, in which both are induced by the noncooperative binding of divalent metal ions.[65,77] During the first step, a series of purine base pairs are formed to produce the domain 2 region, and this occurs in the micromolar (μM) range of magnesium ion concentration, resulting in the coaxial stacking of helices II and III. The second folding transition occurs in the millimolar (mM) range and involves the formation of an uridine turn (domain 1), which brings helix I close to helix II. Because the activity of the ribozyme is observed in the millimolar range of magnesium, this folding step is associated with the active form, as seen in crystal structures of the minimal ribozyme form.[31,32]

The loop–loop interaction was recently discovered, and it was shown that its presence was associated with hammerhead ribozymes active at very low magnesium ion concentrations.[78–80] It is likely that the tertiary interaction restricts internal movements of loops I and II, thus stabilizing states closely resembling the active conformation, consistent with the reduced required magnesium ions. Indeed, the effect of the presence of the loop–loop interaction in the folding pathway of the ribozyme has been studied using FRET analysis. In this study, it was found that the ion-induced folding is greatly enhanced in the presence of the loops promoting the formation of the active conformation in a single step at micromolar magnesium ion concentrations[81]; this is consistent with the loop–loop interaction helping in the close juxtaposition of loops I and II, which lowers the required magnesium ion concentration to achieve the native state. Consistent with this view, recent studies have observed that, under low ionic strength conditions, divalent metal ions appear to stimulate folding of this ribozyme species.[82,83] The loop–loop interaction can thus be seen as a "folding enhancer" element[81] that is essential for the achievement of catalytic activity under a physiologically low magnesium concentration.

The newly solved *Schistosoma mansoni* hammerhead[84] crystal structure[36] clearly illustrates how the loop–loop interaction is involved in the formation of the global structure of the ribozyme (see Fig. 2.3). In their work, Martick and Scott found that the global folding of the molecule primes the ribozyme for catalysis, and that the structure of the core of the *Schistosoma* hammerhead differs from the structures reported for minimal configurations.[36] Because of multiple structural rearrangements, the core of the ribozyme can no longer be considered as having two discrete domains.[85] Instead, a single complex network of interactions span both domains I and II, and in addition, the scissile bond is readily positioned for an in-line attack from the 2′-OH, which is what we expect from a catalytic RNA molecule.

These observations indicate that in addition to altering the global folding of the hammerhead, the presence of the loop–loop interaction modifies the local arrangement of the catalytic core. This concept was emphasized in a recent review where it was attempted to explain the cleavage rates of about 50 minimal hammerhead from available crystallographic data.[56] Half the results could not be readily explained in terms of the structure, highlighting a strong discrepancy between available biochemical and structural data.[85] On the other hand, the *S. mansoni* hammerhead structure is in excellent agreement with available biochemical data and should thus be a reasonable approximation of an active molecule. In the crystal, G12 and the 2′-OH of G8 are positioned very close to the scissile bond, suggesting their roles in an acid–base catalysis. In support of this, a recent study performed on a minimal hammerhead molecule showed the importance of G8 and G12 for the pH profile of the catalytic reaction.[86] In general, the new crystal structure explains most of the previously irreconcilable sets of published results, providing a consistent model.

Interestingly, a similar situation has previously occurred in the context of another small catalytic RNA, the hairpin ribozyme (see Fig. 2.2). The hairpin ribozyme is involved in the cleavage and ligation of the negative strand of sTRSV (tobacco ringspot virus satellite). The minimal sequence of the hairpin ribozyme consists of two stems connected via a hinge region.[87] Both stems include an internal region that contains loops A and B, with the former carrying the substrate cleavage site. However, in the natural sequence, the ribozyme folds as a four-way junction[88] where the presence of the junction is associated with a requirement approximately 1,000-fold lower for magnesium ions to achieve efficient activity.[89] In addition, time-resolved and single-molecule FRET studies have demonstrated that the junction is responsible for the stabilization of the active ribozyme form[90] and the acceleration of the folding via a discrete intermediate.[91] Thus, the loop–loop interaction and the four-way junction in the hammerhead and hairpin ribozymes, respectively, are folding elements that help the RNA molecule to achieve the final folded state under physiological conditions.

2.2.2 The Varkud Satellite Ribozyme

The VS ribozyme is found in the 881 nt VS RNA located in the mitochondria of *Neurospora*, which is transcribed from the Varkud satellite DNA.[92] Although the basic chemistry of the cleavage reaction appears to be close to that of other small ribozymes, the VS ribozyme differs significantly in a number of respects. In addition to being the largest ribozyme and having a secondary structure quite different from other ribozymes, the formation of the ribozyme–substrate complex is not performed via an extensive stretch of Watson–Crick base pairs (see Fig. 2.2). Instead, a loop–loop interaction mediates the formation of the complex, indicating that substrate recognition is mainly achieved via tertiary interactions.[93] This loop–loop interaction has been shown to induce a change in the secondary structure of the substrate by which a number of base pairs are rearranged to yield a “shifted”

substrate conformation,[94] which is most probably important for the creation of an environment favorable to catalysis. Even if the natural configuration of this catalytic RNA is in *cis*, where the substrate is covalently linked to the ribozyme sequence, *trans*-cleavage activity is very efficient and the system can thus be viewed as a bimolecular one, where the substrate is a single stem-loop (stem I), and the ribozyme is composed of five helices (stems II–VI). The ribozyme is organized around two three-way junctions that are arranged as an H shape (see Fig. 2.2). Although a crystal structure of this ribozyme has yet to be obtained, a great amount of biochemical and structural data has been accumulated over the years, from which a detailed catalytic model has been proposed.[95,96]

The substrate contains an asymmetrical internal loop in which the scissile bond is located (see Fig. 2.2). Several NMR studies have found that in the ground state of substrate (i.e., not complexed to the ribozyme), the internal loop is composed of two sheared G•A base pairs and a protonated A^+•C base pair.[97,98] However, by using mutations to obtain a "shifted" substrate, it has been shown that one of the sheared base pairs is disturbed, creating alternative interactions in the internal loops, and additional magnesium ion binding sites.[99] It is clear that additional structural studies on a ribozyme–substrate complex are much needed to fully understand how the ribozyme participates in both the substrate reorganization and the catalytic steps.

Because of the large size of the ribozyme and the lack of available crystal structure, it has been difficult to obtain three-dimensional information describing the global fold of the molecule. Nevertheless, indirect experimental evidence was obtained using biochemical approaches that were used to build a general model. One of the first observations was the discovery of a loop–loop interaction between the substrate and the ribozyme,[93] which effectively places loops I and V in close juxtaposition. A second constraint was revealed by a short-wavelength UV cross-link between two adjacent stems (II and VI) suggesting their close proximity. These results, together with a body of biochemical work, inspired a model for the arrangement of the ribozyme and suggested the importance of the A730 loop.[100–103]

Using a combination of comparative gel electrophoresis and FRET, the global structure of each junction was determined.[38,39] Both junctions were found to undergo coaxial stacking of two helices by the noncooperative binding of magnesium ions. In the 2–3–6 junction, helices III and VI are coaxially stacked, with an acute angle subtended between helices II and VI.[38] Surprisingly, a three-way junction of very similar sequence was found in the *Haloarcula marismortui* 23 S rRNA.[44] When transplanted into the VS ribozyme, an efficient cleavage activity is retained together with complete cleavage of the substrate, indicating that both three-way junctions most probably adopt a very similar global structure. The core of the VS junction was thus modeled using the ribosomal junction. However, no junction similar to the 3–4–5 VS junction was found in the ribosome, leaving uncertainty about the local structure of the VS junction. In addition, because the two VS junctions share a common helix (stem III), a novel comparative gel assay was designed to determine their relative orientation. By extending stems II and V, the amplitude of the end-to-end distance between each stem was magnified and their dihedral angle was thus determined to be about 75°.[39] Although the resulting model does not include base

bulges and internal loops (Fig. 2.4), it still provides an excellent starting point for structure–function analysis of the VS ribozyme.

Using the model described above and a few natural constraints, the location of the substrate can be deduced. First, the substrate is naturally attached to the ribozyme by the 5′-extremity of stem II, and based on previous biochemical analysis, the substrate loop is involved in a tertiary interaction with the loop of stem V.[93,100] Based on these two spatial constraints, it appears logical to position the substrate between stems II and V (see Fig. 2.4). By doing so, the internal loop of the substrate, and hence the scissile bond, is brought in close proximity to the A730 loop located in stem VI. Based on this, it is possible to envision that the A730 loop is directly involved in the catalysis. This hypothesis is in agreement with an extensive mutational analysis which has shown that most of the nucleotide sequence of the VS ribozyme plays an important architectural role, but in contrast, that the A730 loop is most probably an important component of the active site.[104] Moreover, hydroxyl radical probing[105] and nucleotide analogue interference mapping (NAIM)[106] data have revealed that stem II is important for substrate binding, which is in agreement with the proposed model. The substrate is thus thought to

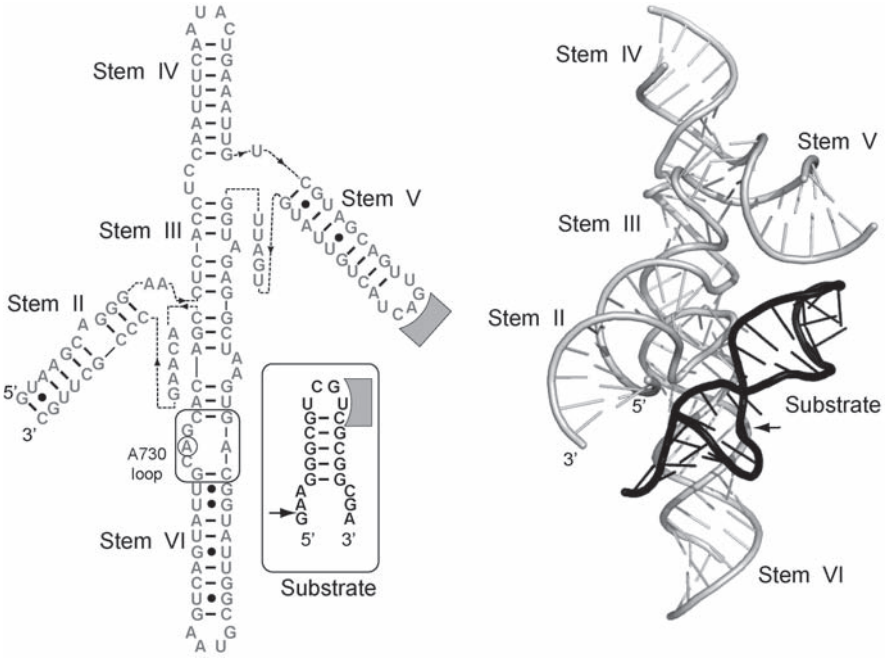

Fig. 2.4 The Varkud satellite (VS) ribozyme. The secondary structure (*left*) is shown to better represent the tertiary arrangement (*right*). The tertiary interaction between the substrate and the stem-loop V is represented by *shaded regions*. *Dotted lines* indicate the polarity of the phosphodiester backbone. The cleavage site is indicated by an *arrow*. The A730 loop is indicated, and the catalytically important nucleotide A756 is *circled*

bind between stems II and VI, and can be tethered to this position via a variety of manners. For instance, it can be attached to the 3′-end of stem II[103] or to the end of stem VI via a linker (D.A. Lafontaine and D.M.J. Lilley, unpublished results), both of which are readily accommodated within the model.

A number of experimental data suggest that the A730 loop is particularly important for the activity of the VS ribozyme. Indeed, using phosphorothioate incorporation, phosphate groups were identified (G757 and G758) in this loop that are important for cleavage activity.[102] Moreover, by using the "manganese rescue" variation, it was also found that the catalytic activity could be restored by using manganese ions, suggesting that metal ion binding sites are present in the loop that are important for the catalytic activity. In addition, the introduction of a variety of nucleotide analogues in this loop resulted in marked reduction in activity.[107]

Of all nucleotides of the A730 loop, the nucleotide A756 is the most sensitive position to point mutations, with most of the atomic positions of the nucleobase being important for activity, therefore suggesting a critical role for A756 in catalysis.[104,108–110] Supporting information has been obtained from cross-linking experiments.[111] Indeed, Collins and coworkers used a covalently attached substrate containing 4-thiouridine at the cleavage site and irradiated the sample with UV light. A cross-link to A756 was obtained, suggesting the close proximity of A756 to the cleavage site. Thus, these results strongly suggest that the A756 nucleobase is a key player during the catalytic reaction of the VS ribozyme. One characteristic aspect of nucleobase-driven catalysis is the dependence of cleavage activity on pH, which has been recently observed using ligation[110] and cleavage assays.[112] Additional evidence about the important role of A756 was obtained using NAIM analysis, which indicated the requirement for a protonated base at position 756.[107] In addition, the importance of A756 in the catalytic reaction has also been emphasized by covalently introducing an imidazole ring in place of the A756 nucleobase and by obtaining significant cleavage activity.[113] A similar procedure was used to show the importance of C75 in the context of the HDV ribozyme.[114] It is likely that a variety of strategies are in place in the VS ribozyme to achieve catalysis, and further experiments will have to be designed to fully grasp the catalytic reaction.

2.3 Riboswitches

Regulation of biological activity is an important cellular process for an organism to be viable. Well-known cellular controls are those involving proteins that regulate at the levels of transcription, translation, and mRNA stability.[115–123] *trans*-Acting RNA factors are also very important in the control of translation and stability of mRNAs,[122,124] as testified by microRNAs (miRNAs) and short-interfering RNAs (siRNAs); these are involved in a series of protein-mediated processing events that ultimately lead to the production of small RNA fragments which form base-paired complexes with target mRNAs, which are then digested by nuclease processing or by other mechanisms.[125,126] In most of these processes, RNA molecules are central

to the biological regulation, which testifies to the growing relevance of RNA in all areas of life.

Recently, a new type of noncoding RNA was uncovered that was found to control numerous fundamental genes using a novel regulation strategy. Indeed, riboswitches are RNA molecules carrying complex folded domains that are located in untranslated regions of mRNAs (recently discussed[127–130]). These molecules are able to sense the concentration of a target cellular metabolite, which is almost always related to the gene product encoded by the downstream sequence of the riboswitch. The sensing domain is called the aptamer and is highly conserved throughout evolution, whereas the expression platform, which is involved in genetic control, shows a much lower degree of conservation. The high degree of conservation of the aptamer most likely results from a selection pressure requiring the sensing of a cellular metabolite, which does not change through evolution. To modulate the expression of a given gene, the expression platform has the ability to fold into various secondary structures that are mutually exclusive. The genetic decision, which relies on the folding of the riboswitch, is dictated by the binding of the target metabolite to the riboswitch. In most cases, when the metabolite is in highly sufficient concentration, its binding to the riboswitch produces the shutdown of the synthesis of encoded biosynthetic proteins. To better illustrate this concept, one of the smallest riboswitches, the guanine-sensing riboswitch, is discussed briefly.

The guanine riboswitch is part of the purine riboswitch family and controls the expression of enzymes that are involved in the metabolism of purines. In *Bacillus subtilis*, it is present in the 5′-untranslated region (5′-UTR) of five transcriptional units, one of them being the *xpt-pbuX* operon that encodes a xanthine phosphoribosyltransferase and a xanthine-specific purine permease, respectively.[131] In the absence of guanine, the structure of the *xpt-pbuX* guanine riboswitch ("ON" state) is characterized by an antiterminator structure whose presence allows the transcription of the entire mRNA molecule and thus the expression of encoded proteins (Fig. 2.5). By contrast, upon binding of guanine to the aptamer domain, the

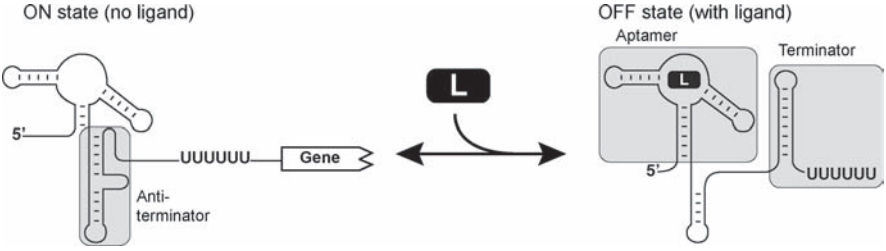

Fig. 2.5 Genetic control of the *xpt-pbuX* guanine riboswitch. In the absence of ligand, the guanine riboswitch adopts a secondary structure characterized by the presence of an anti-antiterminator stem, which allows the transcription of the complete mRNA to take place. However, upon ligand binding (uppercase *L*), the aptamer domain is stabilized, which in turn promotes the formation of a Rho-independent terminator structure, which is associated with the premature transcription termination

antiterminator structure is destabilized, allowing the folding of a Rho-independent terminator to take place, ultimately leading to the premature termination of transcription and to the inhibition of gene expression ("OFF" state). The regulation process is thought to occur without the aid of protein cofactors and thus provides a direct link between the metabolite being monitored and the regulated mRNA.

Various riboswitches have been discovered and shown to specifically recognize a variety of ligands. For instance, aptamer domains have been shown to bind adenine,[132] adenosylcobalamin,[133] flavin mononucleotide,[134,135] guanine,[9] glucosamine-6-phosphate,[123] glycine,[136] lysine,[137,138] S-adenosylmethionine (SAM),[139–142] and thiamine pyrophosphate (TPP).[134,143] The secondary structures of these aptamers are quite diverse (Fig. 2.6) and can be relatively simple (purine) or extremely complex (coenzyme B_{12}). Almost all aptamers shown in Fig. 2.6 control a single expression platform and exhibit a single sensing domain per expression platform. However, the glycine riboswitch (Fig. 2.6) is unique in the sense that it contains a dual aptamer which can sense two glycine molecules. Interestingly, Breaker and coworkers have shown that this riboswitch uses cooperativity to perform a tight regulation control in presence of glycine, and it has been suggested that this tandem configuration provides the riboswitch with a much narrow window toward glycine sensing and thus a higher selectivity in terms of gene activation and shutdown.[136] Moreover, it is important to realize that not all riboswitches negatively regulate expression upon ligand binding. The adenine and the glycine riboswitches are indeed performing a positive regulation in the presence of their respective ligand.[132,136] Riboswitches can also regulate at the level of translation, and in this case, it is not an intrinsic transcription terminator that is modulated but

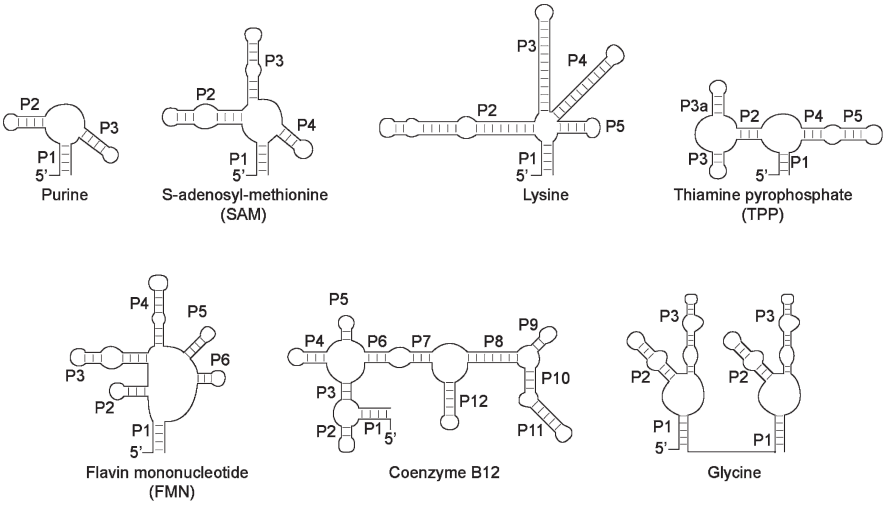

Fig. 2.6 Conventional riboswitches known to regulate on a single expression platform. Only the aptamer region is shown, and the monitored ligand is indicated for each one. The purine riboswitch comprises the adenine and the guanine riboswitches

a helical domain embedding Shine–Dalgarno and translation initiation sequences. Regardless of whether it is transcription or translation that is being regulated, modulation of the RNA structure is always the mechanistic step that controls gene expression, thus making RNA the key player in these regulatory processes.

A few new types of riboswitches have recently been discovered and are referred here as "atypical riboswitches" (Fig. 2.7). A dimeric structure embedding two common single-unit riboswitches, one responding to SAM and the other to coenzyme B_{12}, has recently been characterized in the *Bacillus clausii metE* mRNA.[144] This unique tandem configuration was shown to yield a gene control system functioning as a two-input NOR logic gate. This type of regulatory control expects that either of two chemical inputs yields an output of gene expression, but does not require that the two riboswitches influence each other. However, given that most riboswitches do not require such a tandem arrangement, why does the *B. clausii metE* gene need such a complex riboswitch configuration to be regulated? It turns out that the presence of two distinct riboswitches can be established by examining the metabolic pathway for methionine biosynthesis.[144] Indeed, in *B. clausii*, two proteins (MetE and MetH) are expressed that can independently use homocysteine to produce methionine, which is in turn used to make SAM. As a result, both *metE* and *metH* carry a SAM riboswitch as a control element in response to SAM. While MetE is able to perform the catalytic reaction, MetH uses the more reactive cofactor MeCbl, which is a derivative of AdoCbl. Thus, because cells can much more efficiently produce methionine by expressing MetH rather than MetE, it is energetically unfavorable to sustain MetE synthesis when there is plentiful AdoCbl.[144–146]

An additional atypical riboswitch was recently found in the context of the *B. subtilis glmS* gene.[123] The *glmS* gene encodes the enzyme glutamine-fructose-6-phosphate amidotransferase, which converts fructose-6-phosphate and glutamine into GlcN6P. The secondary structure of this riboswitch is shown in Fig. 2.11 (see later in this chapter). Strikingly, upon ligand binding to the RNA, an autocatalytic cleavage reaction takes place resulting in the scission of the mRNA molecule. The *glmS*

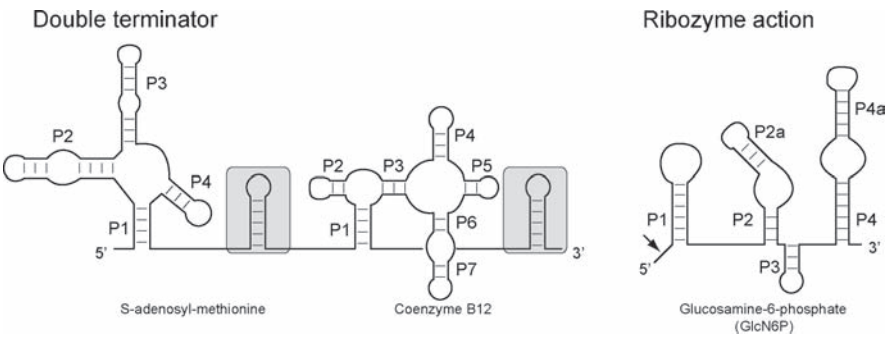

Fig. 2.7 Interestingly, several additional types of tandem configurations were recently reported by Breaker and coworkers,[144] suggesting that relatively simple RNA elements can be assembled to make sophisticated genetic decisions without involving protein factors

riboswitch, or the *glmS* ribozyme, is thus a ligand-dependent processing element that mixes both qualities of riboswitches and ribozymes to achieve genetic regulation of the synthesis of GlcN6P. The structural and mechanistic details of this regulatory RNA are discussed later in this chapter.

Given their natural propensity to bind small cellular metabolites and regulate essential genes, high expectations have been put on riboswitches as antimicrobial agents, partly based on previous successes using small-molecules targeting ribosomes.[147] By using riboswitches as drug targets, it is expected that artificial compounds could be used to bind riboswitches and inhibit the expression of the regulated cellular metabolites, thus heavily destabilizing bacterial pathogens. A proof-of-concept has already been done using the lysine riboswitch.[148] Indeed, several lysine analogues were identified to bind the riboswitch and inhibit cellular growth, most probably by inhibiting the expression of the gene regulated by the riboswitch. Surprisingly, Breaker and coworkers have determined that aminoethyl cysteine (AEC), originally characterized almost 50 years ago,[149] inhibits bacterial growth by targeting the lysine riboswitch.[138,148] Whether riboswitches will really serve as important drug targets needs to be determined, but nevertheless they provide a new avenue that is worthwhile to explore.

Several crystal structures have recently been solved for various riboswitches, which have revealed how ligand binding can be harnessed by RNA molecules to drive gene expression. The following sections are dedicated to discussing each of these in detail.

2.3.1 The Adenine Riboswitch

Purine riboswitches are among the smallest riboswitches that activate or inhibit gene expression in the presence of adenine or guanine, respectively (see Fig. 2.6). Despite the high structural similarity shown between the two aptamers, they display very high specificity, discrimination, and affinity toward their cognate ligand.[9,132] Although regulation by the guanine riboswitch appears to strictly modulate transcription, the adenine riboswitch regulates transcription and also translation. Given that the two riboswitches are very similar in structure, we focus here on the adenine-sensing riboswitch as it has been studied in more detail.

The adenine aptamer folds as a three-way junction where the P1 stem is the only helical region showing some degree of conservation (Fig. 2.8). Helices P2 and P3 are not conserved to a high degree but are involved in a loop–loop interaction.[150,151] The single-stranded core domain of the aptamer is the most conserved region and has been shown to undergo a structural reorganization upon ligand binding using in-line probing assays.[132] This assay exploits the inherent chemical instability of RNA under physiological conditions that is primarily the result of the cleavage of phosphodiester linkages.[152] Spontaneous scissions are more pronounced in unstructured single-stranded regions because internucleotide linkages are free to adopt an in-line conformation that is precluded in the context of an A-type helix.[152]

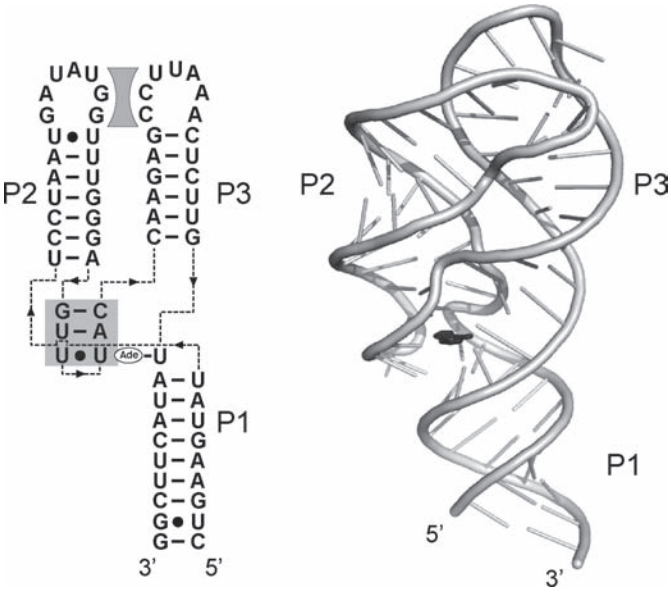

Fig. 2.8 The adenine riboswitch. The secondary (*left*) and the tertiary (*right*) structures are shown. A tertiary interaction (loop–loop) occurring between the stem-loops P2 and P3 is indicated (*shaded region*). *Dotted lines* indicate the polarity of the phosphodiester backbone. The J2/J3 region, observed to stack under P2, is emphasized (*shaded nucleotides*) and shown to make an interaction with the ligand. The bound adenine is shown as "*Ade*" and as a *black residue* in the secondary and tertiary structures, respectively. The Watson–Crick interaction occurring between the ligand and U65 is shown by a *solid line* in the secondary structure

This assay has been used to monitor conformational changes induced by external ligands on numerous mRNA leader regions.[9,132,133,141,143,153–155] Because it is the core region of the adenine aptamer that is reorganized upon ligand binding, it seemed very likely that the ligand-binding site would be formed by this region. Indeed, purine aptamer sequence alignments predicted that the nucleotide at position 65 of the adenine aptamer (position 74 for the guanine aptamer) was the principal specificity determinant of ligand recognition,[132] and based on this evidence it was proposed that ligand recognition was mainly performed by the formation of a Watson–Crick base pair between the ligand and position 65. This prediction was surprising given that the recognition of the ligand by the RNA aptamer is achieved via multiple hydrogen bonds, as observed in most RNA–protein complexes.[156,157]

Five crystal structures of purine riboswitch aptamers have been solved up to the present,[150,151,159] with the overall structure of the aptamer closely matching that deduced using biochemical assays (see Fig. 2.8).[9,132] In each crystallized complex, the fold of the RNA fragment is very compact, with many intricate tertiary interactions.[160] Very importantly, the bound ligand is directly involved in a Watson–Crick base pair with the nucleotide at position 65, which makes this residue particularly important because conversion of an adenine-sensing to a guanine-sensing

riboswitch can be achieved by replacing the uracil at position 65 by a cytosine.[132] In the crystal, the bound adenine is sandwiched between the J2/J3 region and the P1 stem (see Fig. 2.8). A series of Watson–Crick base pairs and stacking interactions are present in the J2/J3 region that are situated at the base of the P2 stem, thus providing the bound ligand with a scaffold from which the P2 loop can be properly oriented for the formation of the loop–loop interaction. Supporting information confirming that the adenine ligand actively helps in the folding process leading to the formation of the loop–loop interaction was obtained by single-molecule FRET.[154] Strikingly, an intermediate state capable of binding the ligand was also detected, suggesting a parallel between the RNA ligand and the role of certain cofactors as protein folding enhancers. Further evidence confirming the active role of the adenine in the folding of the aptamer has emerged from the analysis of the distribution of folding and unfolding rates. The 100-fold variation observed for both rates was significantly reduced in the presence of adenine. Moreover, these studies have also shown that the observed stabilization of the folded state by the ligand results from changes to both folding and unfolding rates. The folding of the core domain has also been studied using an internally incorporated 2AP. In this study, Batey and coworkers have shown that a position in the core domain is exposed to the solvent only upon ligand binding.[159] This finding fits nicely with in-line probing data,[9,132] which suggest that before the binding of the ligand, the core region of the aptamer exists in a flexible state, which is reorganized in the presence of the ligand.

The original working riboswitch model was based on the reorganization of the 5′-UTR RNA sequence following ligand binding.[9,132] However, it was subsequently shown that once the expression platform is fully transcribed, the adenine riboswitch is not able to switch to the alternative conformer.[154,161] In this context, where the ligand affinity is not directly related to the regulation efficiency, the riboswitch is considered to be "kinetically driven." This type of regulation heavily relies on the balance of kinetics of ligand binding and the speed of transcription. Furthermore, transcription pause sites are potentially very important for the adoption of the aptamer–ligand complex, as found for the FMN riboswitch.[162] Clearly, the transcriptional context of riboswitches seems to be an integral part of the regulation control and needs to be further characterized.

RNA has been known before the advent of riboswitches to have the capacity to bind small metabolites. For example, using SELEX, artificial RNA aptamers have been isolated that bind ATP,[163] guanosine,[164] and theophylline.[165] An RNA aptamer has also been obtained that binds xanthine and guanine bases.[166] This aptamer is very small in size (~30 nt) and exhibits a dissociation constant of 1.8 µM for guanine. However, it strongly discriminates adenine (>1,500-fold less affinity), which suggests that it can sense the Watson–Crick face of the ligand, as for purine riboswitches. Whether the aptamer recognizes the ligand in a similar manner as purine riboswitches is hard to predict for now, but this example shows the general tendency of Nature to produce larger aptamers compared to artificially created ones, but with affinities generally higher by a factor of three to four orders of magnitude. Thus, to obtain artificial aptamers with affinities close to the natural ones, a good starting point could be to increase the size of the explored molecules.

2.3.2 The Sam Riboswitch

The S-adenosyl-methionine (SAM) metabolite is an essential coenzyme in all organisms, and it is synthesized directly from methionine by SAM synthetase. It also serves as a source of methyl groups for protein and nucleic acid modification.[129] The regulated genes are related to sulfur metabolism, including genes that are involved in the biosynthesis of cysteine, methionine, and SAM.[140] In *B. subtilis*, 26 genes divided into 11 transcriptional units are controlled by SAM riboswitches.[139,140–142,167–169] SAM riboswitches have been divided into three families based on their secondary structure. Of all three families, the SAM-I family has been the most studied.[139,140–142,167] SAM-II[168,169] and SAM-III[170,171] have been recently uncovered, and although they bind the SAM metabolite, they significantly differ in their predicted secondary structures when compared to SAM-I.

The SAM-I riboswitch aptamer (see Fig. 2.6) has been shown to control both transcription and translation processes depending on the expression platform.[172] The secondary structure of the riboswitch is based on conserved primary sequence elements,[140] which have been confirmed by additional studies.[141,173–175] The aptamer domain (S box) exhibits a high degree of sequence and structural conservation. The core of the S box comprises four helices (P1–P4), forming a distinctive four-way junction. The P1 helix can be viewed as an anti-antiterminator stem given that its formation prevents the adoption of an antiterminator stem. Helices P2–P4 presumably determine the correct folding of the RNA molecule and have been shown to be important for ligand binding and SAM-dependent transcription modulation.[141,167] A secondary structure motif, originally called the GA motif, was described in the P2 helix and found to be important for the transcriptional regulation process.[176] This motif is consistent with the pattern of a K-turn motif that introduces a very tight kink into the helical axis.[177] In addition, conservation of nucleotides in the loop P2 and the unpaired region between helices 3 and 4 (J3/J4) hinted the existence of a tertiary interaction, a pseudoknot structure,[140] that has recently been confirmed to play a key role in the SAM riboswitch regulatory function.[167]

The influence of the pseudoknot interaction (Fig. 2.9) was recently characterized using a combination of in vitro and in vivo techniques.[167] Using site-directed mutagenesis, in vivo expression, transcription termination, SAM binding, and enzymatic probing assays, it was found that the pseudoknot structure plays a key role in the riboswitch function, and that its specific role could depend on the particular aptamer variant. For instance, the formation of the pseudoknot interaction can readily occur in the presence of magnesium ions for the *yitJ* variant. However, SAM is required in the case of the *yrkW* variant, which suggests that although the presence of the pseudoknot is important for binding, its formation before ligand binding is not essential. This suggestion is supported by in-line probing assays, which have shown that some nucleotides involved in the pseudoknot interaction are reorganized upon ligand binding.[141] Thus, these results are in agreement with the general idea that ligand binding to the aptamer domain results in its stabilization, which is crucial for the riboswitch function.

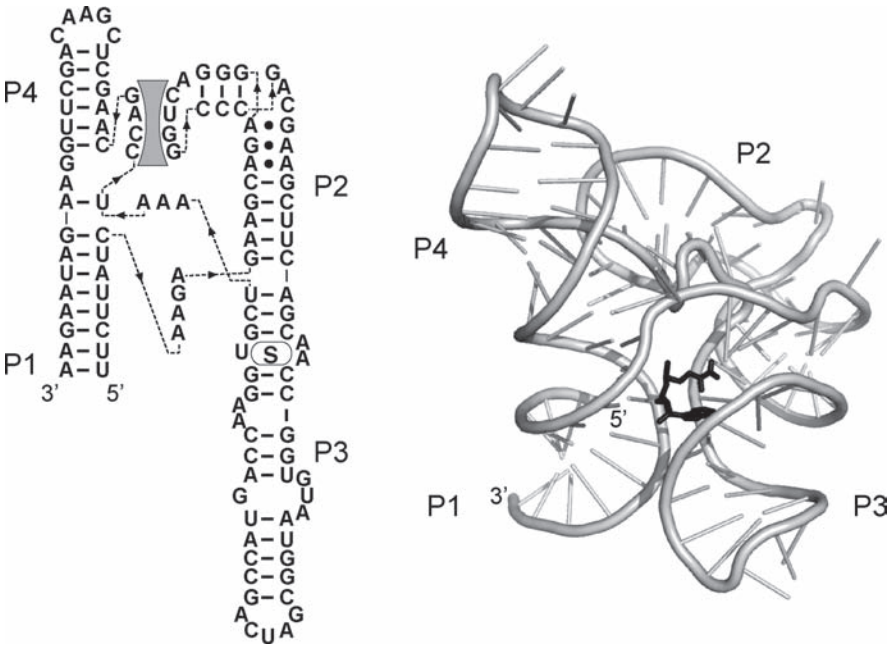

Fig. 2.9 The SAM-I riboswitch. The secondary (*left*) and the tertiary (*right*) structures are shown. A tertiary interaction (pseudoknot) occurring between the stem-loop P2 and the single-strand region J3/J4 is shown (*shaded region*). The bound SAM is shown as "*S*" and as a *black residue* in the secondary and tertiary structures, respectively. *Dotted lines* indicate the polarity of the phosphodiester backbone

Recently, the crystal structure of the complex between the aptamer and the ligand was solved,[178] and it was found that the global architecture of the domain is established through two sets of coaxially stacked helices (see Fig. 2.9). The first pair is formed by the stacking of P1 and P4 stems and the second one by the P2 and P3 stems. The two stacked pairs are oriented relative to each other with an angle of about 70°, with the ligand-binding site located between the minor grooves of P1 and P3 helices,[178] suggesting that the proximity of both helices is important for ligand binding.

The crystal structure shows that the ligand adopts a compact conformation in which the methionine moiety stacks upon the adenine ring (see Fig. 2.9), and interestingly, this conformation is not similar to that which is found in protein enzymes.[178] Instead, the configuration of SAM in the latter is different in that the adenosyl and methionine groups are projecting from each other.[179] The SAM binding site is organized in two different faces: while one is mainly composed by hydrogen bond interactions to the P3 stem, the other uses van der Waals forces to interact with the P1 helix. The adenine base of SAM forms hydrogen bonds with an internal conserved loop of the P3 helical region (see Fig. 2.9), and the main chain of the methionine group is recognized through a series hydrogen bond, also with P3 and

J1/J2 nucleotides. On the other side of the binding site, it is mainly the minor groove of the P1 helix that is interacting with the bound ligand. In general, the crystal structure is largely in agreement with available biochemical and phylogenetic data.

RNA molecules specific to the adenosine moiety of SAM were also isolated using SELEX.[180] The obtained RNA motif was very similar to ATP aptamers known to be specific to adenosine.[163] The binding site corresponds to an asymmetrical bulge in which the 5′- and 3′-single strands comprise 12 and 1 nucleotides, respectively. Both single strands are conserved to a high degree and are purine rich. The structure of the ATP aptamer has been investigated using kethoxal[163] and nuclear magnetic resonance (NMR).[181–183] During these studies, it was established that the binding interaction is characterized by many contacts existing between the ligand and the RNA, and that the latter undergoes a ligand-induced conformational change. The solution structure of the aptamer adopts an L-shaped motif with two nearly orthogonal stems binding the ligand at their junction in a GNRA-like motif.[181–183] Thus, compared to its natural counterpart, the isolated SAM aptamer[180] does not exhibit a relatively complex ligand-binding site, which is most probably why this artificial aptamer exhibits a relatively low specificity toward adenine-containing molecules.

2.3.3 The TPP Riboswitch

Thiamine pyrophosphate (TPP) is a protein cofactor found to be essential in all three kingdoms of life.[184] Most bacteria can synthesize thiamine de novo. In contrast, animals and many fungi rely on external thiamine or immediate precursors.[185] When thiamine is internalized by the cell, it is further processed by phosphorylation, resulting in TPP, which serves as a coenzyme in carbon–carbon bond cleavage reactions involved in metabolic pathways such as glycolysis. Recently, thiamine synthesis was shown to be regulated by a feedback regulation mechanism,[186] and a highly conserved region (*thi*-box) of the leader was identified to be important for this mechanism.[6,186] It became clear that the *thi*-box motif was involved in the regulation of TPP via a riboswitch-related mechanism, and this occurs at both levels of transcription and translation.[134,143]

The TPP riboswitch appears to be a widespread riboswitch given that, as well as being found in prokaryotes, it is also present in several plant and fungal species.[184] However, the putative eukaryotic riboswitches are likely to control different biological functions compared to their prokaryotic counterparts because they are observed in different genomic locations. Indeed, a TPP riboswitch found in the fungus *Fusarium oxysporum* is flanked by 5′- and 3′-splice sites, suggesting its involvement as a splicing regulator control element. Furthermore, another TPP riboswitch was identified in the bluegrass *Poa secunda*, where is it situated in the 3′-UTR region, presumably controlling the processing and the stability of the mRNA. Whether these putative TPP riboswitches really function as sensing and controlling elements needs to be established, but nevertheless it is strongly suggested that additional TPP riboswitches are likely to play essential roles in eukaryotic organisms.

The secondary structure of the TPP aptamer domain is composed of five helical stems that are organized as a standard three-way junction (Fig. 2.10), which is elaborated more in some variants by additional peripheral structural elements.[184] Based on the consensus sequence,[184] it is apparent that most of the helical stems are not conserved so long as their base-pairing potential is maintained. In contrast, single-stranded regions are highly conserved, suggesting their involvement in the formation of the binding site. The formation of the complex between TPP and the aptamer has been studied in detail using in-line probing and in vitro transcription assays.[134,143] In these studies, it was shown that TPP binding to the aptamer domain produces a local rearrangement of the structure that is used to modulate the downstream expression platform and control gene expression. Structural insights to these studies came recently from two independently solved crystal structures of a TPP–aptamer complex.[187,188] The crystal structures revealed that the TPP aptamer exhibits a complex tertiary architecture consisting of two parallel helical domains (P2–P3 and P4–P5) connected to the P1 helix by means of a three-way junction. Given that the two structures are of bacterial and plant origin and that both are highly similar in their tertiary structure, it strongly suggests that prokaryotic and eukaryotic riboswitches may use common mechanisms to perform ligand binding. It was also observed that the riboswitch aptamer specifically recognizes the TPP molecule using conserved nucleotides located within single-strand regions situated in the P2–P3 and P4–P5 helical domains (see Fig. 2.10). Specifically, nucleobases of the P4–P5 helical stack coordinate the pyrophosphate moiety of TPP as well as

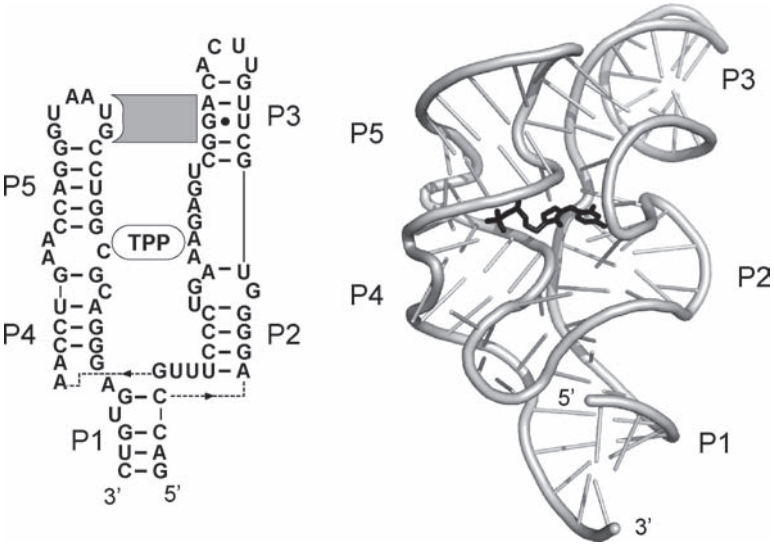

Fig. 2.10 The TPP riboswitch. The secondary (*left*) and the tertiary (*right*) structures are shown. A tertiary interaction (tetraloop–tetraloop receptor-like) occurring between the stem-loop P5 and the stem 3 is shown (*shaded region*). The bound TPP is shown as "*TPP*" and as a *black residue* in the secondary and tertiary structures, respectively. *Dotted lines* indicate the polarity of the phosphodiester backbone

a putative bridging magnesium ion.[189] In addition, on the other side of the ligand, four bases of the P2–P3 helical domain are involved in hydrogen bonds with the pyrimidine ring of TPP. The aptamer also exhibits a type of tetraloop-tetraloop receptor interaction formed by stem 3 and stem-loop 5, which occurs on the TPP upper face, thus covering the ligand-binding site (see Fig. 2.10).

The purine and the TPP riboswitches are similar in their global structure in many respects. First, both are organized around a unique three-way junction that is more elaborated in the case of TPP. Both junctions are constituted at their base by the P1 stem, which is used in the riboswitch regulation mechanism as the "switching helix" involved in the stabilization/destabilization of the terminator stem. In addition, both riboswitches exhibit a tertiary interaction between two of their radiating helices (P2–P3 and P3–P5 for the purine and TPP riboswitches, respectively). In the case of purine riboswitches, it was shown, using FRET analysis for the adenine-sensing aptamer, that formation of the tertiary interaction (loop–loop) can be performed in the absence of ligand.[154] This finding was supported by previous in-line probing assays showing that no additional cleavage protection is observed in presence of purine ligands.[9,132] However, although no biophysical evidence is yet available about the dependence of the tetraloop-tetraloop receptor-like structure on TPP binding, in-line probing assays have shown that the region of the stem-loop 5 exhibits a modulation in the presence of TPP.[143] These findings strongly suggest that the formation of the tetraloop-tetraloop receptor-like structure is adopted only in the presence of ligand, thus differing from the already described behavior of the adenine riboswitch. Last, both the purine and the TPP riboswitch crystal structures revealed that the P1 stem is interacting with a single-strand region (J2/J3 and J3/J4 for the purine and TPP riboswitches, respectively). These interactions should be very important for these riboswitches, given that they most probably stabilize the P1 stem, which is crucial in the gene regulation process carried out by these riboswitches. Because other riboswitches await to be crystallized, it will be interesting to learn whether they are employing completely new folding architectures.

Pyrithiamine is a pyridine analogue of thiamine and is toxic to organisms that rely on externally synthesized thiamine.[190] In cells, pyrithiamine is phosphorylated to yield pyrithiamine pyrophosphate (PTPP), which inhibits enzymes that make use of TPP.[191] The only difference between TPP and PTPP lies in the central part of the ligand: while a thiazole is part of TPP, a pyridine ring is present in PTPP. From the crystal structures of TPP aptamers,[187,188] the antibiotic property of PTPP can be readily explained. Indeed, by holding the ligand on both of its sides using the two distinct helical domains, the riboswitch aptamer does not make productive interactions with the central part of the ligand, which enables PTPP to bind the TPP riboswitch aptamer domain very efficiently. Interestingly, two single-point mutations located in the J1/J2 and J1/J4 have been obtained in the TPP aptamer that rendered host organisms pyrithiamine resistant.[192,193] Biochemical experiments have shown that TPP and PTPP can still bind the mutated aptamers despite the introduced mutations.[193] It is expected that these mutations likely disrupt the native structure of the aptamer and thus prevent the antibiotic from efficiently binding.

2.4 The *glmS* Riboswitch Ribozyme

Typical riboswitches modulate gene expression by using ligand-induced structural changes for controlling transcription and translation. However, a new type of riboswitch has recently been discovered that employs a different regulation strategy. The *glmS* riboswitch is found upstream of genes involved in the metabolism of GlcN6P.[123] In contrast to other riboswitches, the *glmS* riboswitch undergoes a cleavage reaction of the mRNA molecule upon GlcN6P binding. Cleavage products generated by the ribozyme carry 2′,3′-cyclic phosphate and 5′-OH moieties, suggesting a catalytic mechanism similar to that previously described for small nucleolytic ribozymes.[123] The unique character of the *glmS* riboswitch, or the *glmS* ribozyme, has prompted a large number of biochemical and structural studies.[35,37,123,194–204] In the following sections, we discuss in detail the structural characteristics and catalytic mechanisms recently reported and emphasize the role of the ligand in the biological function of this particular riboswitch.

The catalytic mechanism of the *glmS* ribozyme has recently been studied in detail using various ligands.[200] In this work, it was established that several atomic groups of the ligand are important for the cleavage reaction. For instance, it was shown that the amine group of GlcN6P is crucial given that glucose-6-phosphate did not support cleavage reaction (Glc6P). The importance of this position is further emphasized by the ability of serinol, L-serine, and ethanolamine to support catalysis.[200] On the other hand, the phosphate group is not as important as D-glucosamine promotes a very good cleavage activity. In all cases, efficient catalytic activators all share the common feature of an ethanolamine moiety and a vicinal hydroxyl group. Because Glc6P is a potent inhibitor, it suggests that the presence of the amine is not important for binding and that the natural ligand might act as a coenzyme during the self-cleavage reaction. The crucial role of GlcN6P in catalysis was further emphasized in a recent SELEX study.[198] By applying in vitro selection strategy, Breaker and coworkers attempted to identify riboswitch variants that could expand the range of compounds inducing self-cleavage. However, none of the isolated artificial ribozymes exhibited changes in target specificity, this being consistent with the hypothesis that GlcN6P is used by the ribozyme as a coenzyme for RNA cleavage. Supporting results were also obtained from enzymatic studies.[197]

The effect of GlcN6P on the structure of *glmS* was recently characterized using biochemical assays. Indeed, using an engineered *trans*-acting ribozyme construct coupled to a FRET assay, it was observed that the ribozyme–substrate complex does not undergo a global conformational change upon ligand binding.[201] In this study, it was also shown by terbium (III) and RNase protection assays that no significant change is observed in the secondary and tertiary structures upon ligand binding. Supporting data came from hydroxyl radical protection and UV cross-linking assays in which it was established that the riboswitch seems to bind the ligand using a prefolded active site pocket.[195] Combined with previous studies, this suggests a model in which the ligand assists the catalysis via a direct participation in the reaction chemistry. This mode of action is very different from that observed

for other riboswitches, in which structural modulation is a crucial preliminary requirement to achieve gene regulation.

The role of divalent metal ions in the *glmS* catalysis was recently characterized.[202] It was shown that substantial cleavage rate enhancements are supported by an exchange-inert cobalt (III) complex and by molar concentrations of monovalent ions, much like most of the small nucleolytic ribozymes. This finding suggests that metal ions are not directly involved in the chemical step of the catalysis, but rather that the nucleobases per se could be directly involved in the acid–base catalysis. The requirements for metal ions were further studied using nucleotide analogue interference mapping (NAIM).[196] It was found that phosphate oxygen, 2′-OH, and particular nucleobase groups are essential for the catalytic reaction. It was also shown using Co(III) that although certain metal ion contacts are present within the catalytic core, they are not directly chemically involved in the catalytic mechanism. Thus, because the *glmS* ribozyme does not experience structural reorganization in presence of the ligand and because metal ions are not likely to be involved in the chemical step, there is a strong incentive to speculate that GlcN6P is used by the ribozyme as a catalytic cofactor and not as an allosteric one, as for most other riboswitches.

Recently, structural insights came from crystal structures[35,37] solved for the *glmS* ribozyme (Fig. 2.11). The structure is very compact and is formed from two main

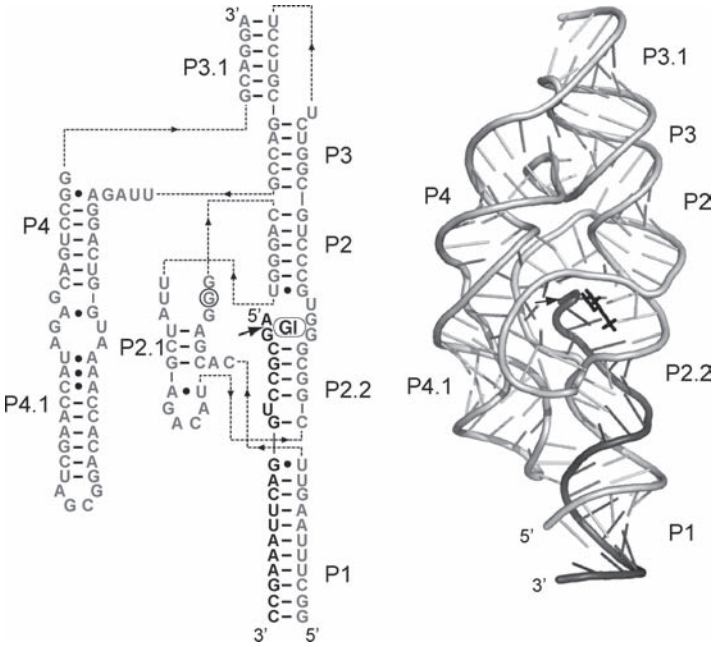

Fig. 2.11 The *glmS* riboswitch. The secondary (*left*) and the tertiary (*right*) structures are shown. The bound GlcN6P is shown as "*Gl*" and as a *black residue* in the secondary and tertiary structures, respectively. *Dotted lines* indicate the polarity of the phosphodiester backbone. The proposed catalytically important G33 is *circled* in the secondary structure

helical stacks (P4–P4.1 and P1–P3) and a GNRA tetraloop (P4.1 loop). A double pseudoknot[203,204] is also present in the structure (P2 loop nucleotides) and forms the ribozyme core, including the GlcN6P binding pocket (see Fig. 2.11). The active site is organized by nonsequential base stacking interactions and pseudoknot structures that are involved in the construction of architectural sides involved in ligand recognition. However, in contrast to other riboswitch crystal structures (see previous sections), the ligand is not completely buried in the RNA structure, suggesting that the ligand can dock on the RNA without any structural changes. This observation is in very good agreement with previously discussed biochemical studies that have established that *glmS* does not undergo structural changes upon ligand binding. In addition, and in agreement with the capacity of the ribozyme to perform cleavage in inert cobalt (III), the active site does not exhibit any metal ion that is positioned for catalysis. Instead, two mechanistically different cleavage reactions have been proposed from the two crystal structures[35,37] directly involving GlcN6P in the cleavage step, and both established that *glmS* is not a metalloenzyme. It has been proposed that, because the pK_a of the GlcN6P amine is closer to neutrality than any RNA functional groups, the ligand could be involved in an acid–base mechanism.[37] Among the two proposed catalytic mechanisms,[35,37] one seems particularly appealing and reconciles previously observed cleavage–pH dependencies.[200] In this model, GlcN6P is thought to induce charge stabilization in the transition state by coordinating the 5′-O leaving group and the pro-Sp nonbridging oxygen of the scissile phosphate.[37] In the crystal structure,[37] while the amine group of the ligand interacts with the 5′-O group, the C1–OH group is involved with the pro-Sp oxygen (Fig. 2.12). The importance of the C1–OH group was shown in cleavage

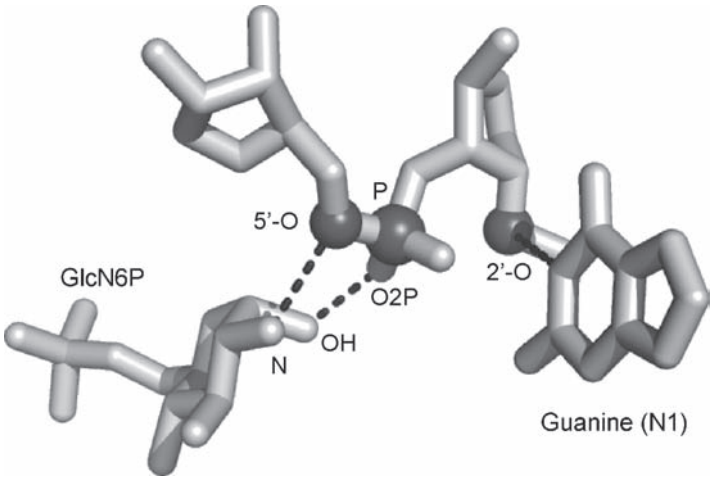

Fig. 2.12 The proposed catalytic mechanism of the *glmS* riboswitch. The 2′-OH (*2′-O*), the phosphate (*P*), and the 5′-OH (*5′-O*) leaving group are poised for an in-line attack. The *N1* group of G33 is postulated to activate the 2′-OH for the catalytic reaction to take place. The bound GlcN6P is shown to make interactions with the 5′-OH and the pro-Sp (O2P) oxygen groups

experiments by using D-serine, which does not support catalysis, and for which the only difference with the catalytically competent L-serine is the stereochemical orientation of functional groups comprising C1–OH.[200]

In the crystal structure, the closest functional group to the 2′-OH of the scissile bond is the N1 of G33 (see Fig. 2.12). This guanine is completely conserved in *glmS* ribozymes.[202] Using mutational analysis, the identity of G33 was found to be very important as even the most active ribozyme mutant was still 1,000-fold less active than the natural sequence.[37] Interestingly, there is a precedent for catalytically important guanines in the case of the hammerhead and hairpin ribozymes.[34–36] Moreover, despite the high pK_a of the N1 of guanine, it could still play a role as a general base by adopting an alternative tautomeric form[37,86,205] Thus, because the *glmS* ribozyme is predicted to use a nucleobase (G33) and GlcN6P to perform catalysis, it strongly suggests that this type of catalytic strategy may have expanded the catalytic repertoire of RNA molecules in a prebiotic RNA world.[37]

So, is the *glmS* RNA a riboswitch, a ribozyme, or both? The fact that *glmS* undergoes autocatalytic cleavage and generates product termini identical to small ribozymes, regardless of the presence of a cofactor, leaves little doubt about its ability to qualify as a ribozyme. However, the readily available answer when trying to define if *glmS* exhibits qualities that are present in riboswitches is less clear cut. This situation is most probably the result of the ambiguity of the scientific community to establish clear criteria defining what is a riboswitch. Historically, the term riboswitch was first coined by Breaker and coworkers, who reported that the 5′-UTR of the *E. coli btuB* mRNA is able to sense the coenzyme B_{12} and to regulate its own expression in absence of proteins.[133] According to this, a riboswitch is mostly referred to a RNA molecule that binds a small metabolic compound and which harnesses the binding event to trigger the reorganization of the secondary structure of the expression platform, which ultimately leads to the control of gene expression. Thus, although the *glmS* ribozyme uses a small metabolite to control gene expression, no change in the structure seems to occur upon binding, and thus it should not qualify as a riboswitch. A similar question could be asked about regulation systems that share all the functional characteristics of conventional riboswitches but do not bind small metabolites. One example of this is the T-box element that modulates gene expression by sensing amino acid-charged tRNAs.[130] At the opposite of the regulation spectrum are RNA switches that regulate in response to infinitely small ligands such as magnesium ions[206] or even temperature.[207] Moreover, additional types of riboswitches may be discovered that challenge even more the actual riboswitch definition. For instance, it is likely that sequences will be found that are very similar to typical riboswitches but which use protein cofactors as chaperones to assist in the folding of the RNA. Such protein candidates are the kink-turn binding proteins that have been shown to be involved in the architectural folding of RNA molecules.[177] Interestingly, SAM and lysine riboswitches possess a kink-turn motif and are thus possibly using kink-turn binding proteins to assist them in vivo. However, it is very clear that there is a very high probability that additional riboswitches will be discovered in the future, as suggested by recent bioinformatic studies.[208]

2.5 Summary and Conclusions

We will never know for certain if ribozymes and riboswitches are really remnants of the RNA world, or even if there was a prebiotic world without proteins to carry out housekeeping and other crucial biochemical tasks. Even without having a formal proof of such a world, the catalytic repertoire of known natural and artificial RNA molecules is staggering, and resoundingly provides tantalizing evidences about a distant past made entirely of RNA or RNA-like molecules. One of the most spectacular successes of Nature undoubtedly consists in the peptidyl transferase activity of the ribosome, which appears to be entirely driven by the RNA moiety.[1,44] Such a level of structural and enzymatic complexity is unmatched by other cellular components, thus making RNA a major component in the cellular machinery.

Natural ribozymes and riboswitches have provided us with a repertoire of tractable systems for structure–function studies that have already expanded our knowledge about RNA molecules. They will undoubtedly be instrumental in the development and applications of modern instrumentation for chemical and biological analysis on a microscale. In the future, a very important challenge will be to efficiently use the gained knowledge in the fight against pathogenic threats and for the use of gene therapy to correct genetic weaknesses or to cure important diseases.

References

1. Nissen, P., Hansen, J., Ban, N., Moore, P.B. and Steitz, T.A. (2000) The structural basis of ribosome activity in peptide bond synthesis. Science 289:920–930.
2. Kruger, K., Grabowski, P.J., Zaug, A.J., Sands, J., Gottschling, D.E. and Cech, T.R. (1982) Self-splicing RNA: autoexcision and autocyclization of the ribosomal RNA intervening sequence of *Tetrahymena*. Cell 31:147–157.
3. Guerrier-Takada, C., Gardiner, K., Marsh, T., Pace, N. and Altman, S. (1983) The RNA moiety of ribonuclease P is the catalytic subunit of the enzyme. Cell 35:849–857.
4. Gelfand, M.S., Mironov, A.A., Jomantas, J., Kozlov, Y.I. and Perumov, D.A. (1999) A conserved RNA structure element involved in the regulation of bacterial riboflavin synthesis genes. Trends Genet. 15:439–442.
5. Nou, X. and Kadner, R.J. (2000) Adenosylcobalamin inhibits ribosome binding to btuB RNA. Proc. Natl. Acad. Sci. USA 97:7190–7195.
6. Miranda-Rios, J., Navarro, M. and Soberon, M. (2001) A conserved RNA structure (thi box) is involved in regulation of thiamin biosynthetic gene expression in bacteria. Proc. Natl. Acad. Sci. USA 98:9736–9741.
7. Stormo, G.D. and Ji, Y. (2001) Do mRNAs act as direct sensors of small molecules to control their expression? Proc. Natl. Acad. Sci. USA 98:9465–9467.
8. Miranda-Rios, J. (2007) The THI-box riboswitch, or how RNA binds thiamin pyrophosphate. Structure 15:259–265.
9. Mandal, M., Boese, B., Barrick, J.E., Winkler, W.C. and Breaker, R.R. (2003) Riboswitches control fundamental biochemical pathways in *Bacillus subtilis* and other bacteria. Cell 113:577–586.
10. Wilson, D.S. and Szostak, J.W. (1999) In vitro selection of functional nucleic acids. Annu. Rev. Biochem. 68:611–647.

11. Tuerk, C. and Gold, L. (1990) Systematic evolution of ligands by exponential enrichment: RNA ligands to bacteriophage T4 DNA polymerase. Science 249:505–510.
12. Ellington, A.D. and Szostak, J.W. (1990) In vitro selection of RNA molecules that bind specific ligands. Nature (Lond.) 346:818–822.
13. Walter, N.G. and Engelke, D.R. (2002) Ribozymes: catalytic RNAs that cut things, make things, and do odd and useful jobs. Biologist (Lond.) 49:199–203.
14. Breaker, R.R. (2004) Natural and engineered nucleic acids as tools to explore biology. Nature (Lond.) 432:838–845.
15. Breaker, R.R. (2002) Engineered allosteric ribozymes as biosensor components. Curr. Opin. Biotechnol. 13:31–39.
16. Silverman, S.K. (2003) Rube Goldberg goes (ribo)nuclear? Molecular switches and sensors made from RNA. RNA 9:377–383.
17. Golden, B.L., Gooding, A.R., Podell, E.R. and Cech, T.R. (1998) A preorganized active site in the crystal structure of the *Tetrahymena* ribozyme. Science 282:259–264.
18. Adams, P.L., Stahley, M.R., Kosek, A.B., Wang, J. and Strobel, S.A. (2004) Crystal structure of a self-splicing group I intron with both exons. Nature (Lond.) 430:45–50.
19. Guo, F., Gooding, A.R. and Cech, T.R. (2004) Structure of the *Tetrahymena* ribozyme: base triple sandwich and metal ion at the active site. Mol. Cell 16:351–362.
20. Golden, B.L., Kim, H. and Chase, E. (2005) Crystal structure of a phage Twort group I ribozyme-product complex. Nat. Struct. Mol. Biol. 12:82–89.
21. Lilley, D.M. (2005) Structure, folding and mechanisms of ribozymes. Curr. Opin. Struct. Biol. 15:313–323.
22. Michel, F., Hanna, M., Green, R., Bartel, D.P. and Szostak, J.W. (1989) The guanosine binding site of the *Tetrahymena* ribozyme. Nature (Lond.) 342:391–395.
23. Bass, B.L. and Cech, T.R. (1984) Specific interaction between the self-splicing RNA of *Tetrahymena* and its guanosine substrate: implications for biological catalysis by RNA. Nature (Lond.) 308:820–826.
24. Torres-Larios, A., Swinger, K.K., Pan, T. and Mondragon, A. (2006) Structure of ribonuclease P: a universal ribozyme. Curr. Opin. Struct. Biol. 16:327–335.
25. Kazantsev, A.V. and Pace, N.R. (2006) Bacterial RNase P: a new view of an ancient enzyme. Nat. Rev. Microbiol. 4:729–740.
26. Kazantsev, A.V., Krivenko, A.A., Harrington, D.J., Holbrook, S.R., Adams, P.D. and Pace, N.R. (2005) Crystal structure of a bacterial ribonuclease P RNA. Proc. Natl. Acad. Sci. USA 102:13392–13397.
27. Kikovska, E., Svard, S.G. and Kirsebom, L.A. (2007) Eukaryotic RNase P RNA mediates cleavage in the absence of protein. Proc. Natl. Acad. Sci. USA 104:2062–2067.
28. Krasilnikov, A.S., Yang, X., Pan, T. and Mondragon, A. (2003) Crystal structure of the specificity domain of ribonuclease P. Nature (Lond.) 421:760–764.
29. Krasilnikov, A.S., Xiao, Y., Pan, T. and Mondragon, A. (2004) Basis for structural diversity in homologous RNAs. Science 306:104–107.
30. Torres-Larios, A., Swinger, K.K., Krasilnikov, A.S., Pan, T. and Mondragon, A. (2005) Crystal structure of the RNA component of bacterial ribonuclease P. Nature (Lond.) 437:584–587.
31. Pley, H.W., Flaherty, K.M. and McKay, D.B. (1994) Three-dimensional structure of a hammerhead ribozyme. Nature (Lond.) 372:68–74.
32. Scott, W.G., Finch, J.T. and Klug, A. (1995) The crystal structure of an all-RNA hammerhead ribozyme: a proposed mechanism for RNA catalytic cleavage. Cell 81:991–1002.
33. Ferre-D'Amare, A.R., Zhou, K. and Doudna, J.A. (1998) Crystal structure of a hepatitis delta virus ribozyme. Nature (Lond.) 395:567–574.
34. Rupert, P.B. and Ferre-D'Amare, A.R. (2001) Crystal structure of a hairpin ribozyme-inhibitor complex with implications for catalysis. Nature (Lond.) 410:780–786.
35. Klein, D.J. and Ferre-D'Amare, A.R. (2006) Structural basis of *glmS* ribozyme activation by glucosamine-6-phosphate. Science 313:1752–1756.
36. Martick, M. and Scott, W.G. (2006) Tertiary contacts distant from the active site prime a ribozyme for catalysis. Cell 126:309–320.

37. Cochrane, J.C., Lipchock, S.V. and Strobel, S.A. (2007) Structural investigation of the GlmS ribozyme bound to its catalytic cofactor. Chem. Biol. 14:97–105.
38. Lafontaine, D.A., Norman, D.G. and Lilley, D.M. (2001) Structure, folding and activity of the VS ribozyme: importance of the 2–3–6 helical junction. EMBO J. 20:1415–1424.
39. Lafontaine, D.A., Norman, D.G. and Lilley, D.M. (2002) The global structure of the VS ribozyme. EMBO J. 21:2461–2471.
40. Murray, J.B., Seyhan, A.A., Walter, N.G., Burke, J.M. and Scott, W.G. (1998) The hammerhead, hairpin and VS ribozymes are catalytically proficient in monovalent cations alone. Chem. Biol. 5:587–595.
41. Bevilacqua, P.C. and Yajima, R. (2006) Nucleobase catalysis in ribozyme mechanism. Curr. Opin. Chem. Biol. 10:455–464.
42. Teixeira, A., Tahiri-Alaoui, A., West, S., Thomas, B., Ramadass, A., Martianov, I., Dye, M., James, W., Proudfoot, N.J. and Akoulitchev, A. (2004) Autocatalytic RNA cleavage in the human beta-globin pre-mRNA promotes transcription termination. Nature (Lond.) 432:526–530.
43. Santiago, F.S. and Khachigian, L.M. (2001) Nucleic acid based strategies as potential therapeutic tools: mechanistic considerations and implications to restenosis. J. Mol. Med. 79:695–706.
44. Ban, N., Nissen, P., Hansen, J., Moore, P.B. and Steitz, T.A. (2000) The complete atomic structure of the large ribosomal subunit at 2.4 Å resolution. Science 289:905–920.
45. Zhang, B. and Cech, T.R. (1997) Peptide bond formation by in vitro selected ribozymes. Nature (Lond.) 390:96–100.
46. Blanchard, S.C., Gonzalez, R.L., Kim, H.D., Chu, S. and Puglisi, J.D. (2004) tRNA selection and kinetic proofreading in translation. Nat. Struct. Mol. Biol. 11:1008–1014.
47. Blanchard, S.C., Kim, H.D., Gonzalez, R.L., Jr., Puglisi, J.D. and Chu, S. (2004) tRNA dynamics on the ribosome during translation. Proc. Natl. Acad. Sci. USA 101:12893–12898.
48. Bevilacqua, P.C., Brown, T.S., Nakano, S. and Yajima, R. (2004) Catalytic roles for proton transfer and protonation in ribozymes. Biopolymers 73:90–109.
49. Doudna, J.A. and Lorsch, J.R. (2005) Ribozyme catalysis: not different, just worse. Nat. Struct. Mol. Biol. 12:395–402.
50. Fedor, M.J. (2002) The role of metal ions in RNA catalysis. Curr. Opin. Struct. Biol. 12:289–295.
51. Fedor, M.J. and Williamson, J.R. (2005) The catalytic diversity of RNAs. Nat. Rev. Mol. Cell. Biol. 6:399–412.
52. Holbrook, S.R. (2005) RNA structure: the long and the short of it. Curr. Opin. Struct. Biol. 15:302–308.
53. Lonnberg, T. and Lonnberg, H. (2005) Chemical models for ribozyme action. Curr. Opin. Chem. Biol. 9:665–673.
54. Woodson, S.A. (2005) Metal ions and RNA folding: a highly charged topic with a dynamic future. Curr. Opin. Chem. Biol. 9:104–109.
55. Symons, R.H. (1992) Small catalytic RNAs. Annu. Rev. Biochem. 61:641–671.
56. Blount, K.F. and Uhlenbeck, O.C. (2005) The structure–function dilemma of the hammerhead ribozyme. Annu. Rev. Biophys. Biomol. Struct. 34:415–440.
57. Stage-Zimmermann, T.K. and Uhlenbeck, O.C. (1998) Hammerhead ribozyme kinetics. RNA 4:875–889.
58. Hertel, K.J., Herschlag, D. and Uhlenbeck, O.C. (1994) A kinetic and thermodynamic framework for the hammerhead ribozyme reaction. Biochemistry 33:3374–3385.
59. Hertel, K.J. and Uhlenbeck, O.C. (1995) The internal equilibrium of the hammerhead ribozyme reaction. Biochemistry 34:1744–1749.
60. Uhlenbeck, O.C. (2003) Less isn't always more. RNA 9:1415–1417.
61. Lilley, D.M. (2003) Ribozymes – a snip too far? Nat. Struct. Biol. 10:672–673.
62. Amiri, K.M. and Hagerman, P.J. (1994) Global conformation of a self-cleaving hammerhead RNA. Biochemistry 33:13172–13177.
63. Bassi, G.S., Mollegaard, N.E., Murchie, A.I., von Kitzing, E. and Lilley, D.M. (1995) Ionic interactions and the global conformations of the hammerhead ribozyme. Nat. Struct. Biol. 2:45–55.

64. Tuschl, T., Gohlke, C., Jovin, T.M., Westhof, E. and Eckstein, F. (1994) A three-dimensional model for the hammerhead ribozyme based on fluorescence measurements. Science 266:785–789.
65. Bassi, G.S., Murchie, A.I., Walter, F., Clegg, R.M. and Lilley, D.M. (1997) Ion-induced folding of the hammerhead ribozyme: a fluorescence resonance energy transfer study. EMBO J. 16:7481–7489.
66. Rueda, D., Wick, K., McDowell, S.E. and Walter, N.G. (2003) Diffusely bound Mg^{2+} ions slightly reorient stems I and II of the hammerhead ribozyme to increase the probability of formation of the catalytic core. Biochemistry 42:9924–9936.
67. Menger, M., Eckstein, F. and Porschke, D. (2000) Multiple conformational states of the hammerhead ribozyme, broad time range of relaxation and topology of dynamics. Nucleic Acids Res. 28:4428–4434.
68. Menger, M., Tuschl, T., Eckstein, F. and Porschke, D. (1996) Mg(2+)-dependent conformational changes in the hammerhead ribozyme. Biochemistry 35:14710–14716.
69. Peracchi, A., Beigelman, L., Usman, N. and Herschlag, D. (1996) Rescue of abasic hammerhead ribozymes by exogenous addition of specific bases. Proc. Natl. Acad. Sci. USA 93:11522–11527.
70. Woisard, A., Fourrey, J.L. and Favre, A. (1994) Multiple folded conformations of a hammerhead ribozyme domain under cleavage conditions. J. Mol. Biol. 239:366–370.
71. Sigurdsson, S.T., Tuschl, T. and Eckstein, F. (1995) Probing RNA tertiary structure: interhelical crosslinking of the hammerhead ribozyme. RNA 1:575–583.
72. Wang, L. and Ruffner, D.E. (1997) An ultraviolet crosslink in the hammerhead ribozyme dependent on 2-thiocytidine or 4-thiouridine substitution. Nucleic Acids Res. 25:4355–4361.
73. Heckman, J.E., Lambert, D. and Burke, J.M. (2005) Photocrosslinking detects a compact, active structure of the hammerhead ribozyme. Biochemistry 44:4148–4156.
74. Simorre, J.P., Legault, P., Hangar, A.B., Michiels, P. and Pardi, A. (1997) A conformational change in the catalytic core of the hammerhead ribozyme upon cleavage of an RNA substrate. Biochemistry 36:518–525.
75. Suzumura, K., Warashina, M., Yoshinari, K., Tanaka, Y., Kuwabara, T., Orita, M. and Taira, K. (2000) Significant change in the structure of a ribozyme upon introduction of a phosphorothioate linkage at P9: NMR reveals a conformational fluctuation in the core region of a hammerhead ribozyme. FEBS Lett. 473:106–112.
76. Bondensgaard, K., Mollova, E.T. and Pardi, A. (2002) The global conformation of the hammerhead ribozyme determined using residual dipolar couplings. Biochemistry 41:11532–11542.
77. Hammann, C. and Lilley, D.M.J. (2002) Folding and activity of the hammerhead ribozyme. ChemBioChem 3:690–700.
78. Khvorova, A., Lescoute, A., Westhof, E. and Jayasena, S.D. (2003) Sequence elements outside the hammerhead ribozyme catalytic core enable intracellular activity. Nat. Struct. Biol. 10:708–712.
79. De la Pena, M., Gago, S. and Flores, R. (2003) Peripheral regions of natural hammerhead ribozymes greatly increase their self-cleavage activity. EMBO J. 22:5561–5570.
80. Canny, M.D., Jucker, F.M., Kellogg, E., Khvorova, A., Jayasena, S.D. and Pardi, A. (2004) Fast cleavage kinetics of a natural hammerhead ribozyme. J. Am. Chem. Soc. 126:10848–10849.
81. Penedo, J.C., Wilson, T.J., Jayasena, S.D., Khvorova, A. and Lilley, D.M. (2004) Folding of the natural hammerhead ribozyme is enhanced by interaction of auxiliary elements. RNA 10:880–888.
82. Kim, N.K., Murali, A. and DeRose, V.J. (2005) Separate metal requirements for loop interactions and catalysis in the extended hammerhead ribozyme. J. Am. Chem. Soc. 127:14134–14135.
83. Osborne, E.M., Schaak, J.E. and Derose, V.J. (2005) Characterization of a native hammerhead ribozyme derived from schistosomes. RNA 11:187–196.
84. Ferbeyre, G., Smith, J.M. and Cedergren, R. (1998) Schistosome satellite DNA encodes active hammerhead ribozymes. Mol. Cell. Biol. 18:3880–3888.
85. Nelson, J.A. and Uhlenbeck, O.C. (2006) When to believe what you see. Mol. Cell. 23:447–450.

86. Han, J. and Burke, J.M. (2005) Model for general acid–base catalysis by the hammerhead ribozyme: pH–activity relationships of G8 and G12 variants at the putative active site. Biochemistry 44:7864–7870.
87. Berzal-Herranz, A., Joseph, S., Chowrira, B.M., Butcher, S.E. and Burke, J.M. (1993) Essential nucleotide sequences and secondary structure elements of the hairpin ribozyme. EMBO J. 12:2567–2573.
88. Murchie, A.I., Thomson, J.B., Walter, F. and Lilley, D.M. (1998) Folding of the hairpin ribozyme in its natural conformation achieves close physical proximity of the loops. Mol. Cell 1:873–881.
89. Zhao, Z.Y., Wilson, T.J., Maxwell, K. and Lilley, D.M. (2000) The folding of the hairpin ribozyme: dependence on the loops and the junction. RNA 6:1833–1846.
90. Walter, N.G., Burke, J.M. and Millar, D.P. (1999) Stability of hairpin ribozyme tertiary structure is governed by the interdomain junction. Nat. Struct. Biol. 6:544–549.
91. Tan, E., Wilson, T.J., Nahas, M.K., Clegg, R.M., Lilley, D.M. and Ha, T. (2003) A four-way junction accelerates hairpin ribozyme folding via a discrete intermediate. Proc. Natl. Acad. Sci. USA 100:9308–9313.
92. Kennell, J.C., Saville, B.J., Mohr, S., Kuiper, M.T., Sabourin, J.R., Collins, R.A. and Lambowitz, A.M. (1995) The VS catalytic RNA replicates by reverse transcription as a satellite of a retroplasmid. Genes Dev. 9:294–303.
93. Guo, H.C. and Collins, R.A. (1995) Efficient trans-cleavage of a stem-loop RNA substrate by a ribozyme derived from neurospora VS RNA. EMBO J. 14:368–376.
94. Andersen, A.A. and Collins, R.A. (2000) Rearrangement of a stable RNA secondary structure during VS ribozyme catalysis. Mol. Cell 5:469–478.
95. Collins, R.A. (2002) The Neurospora Varkud satellite ribozyme. Biochem. Soc. Trans. 30:1122–1126.
96. Lilley, D.M. (2004) The Varkud satellite ribozyme. RNA 10:151–158.
97. Michiels, P.J., Schouten, C.H., Hilbers, C.W. and Heus, H.A. (2000) Structure of the ribozyme substrate hairpin of *Neurospora* VS RNA: a close look at the cleavage site. RNA 6:1821–1832.
98. Flinders, J. and Dieckmann, T. (2001) A pH controlled conformational switch in the cleavage site of the VS ribozyme substrate RNA. J. Mol. Biol. 308:665–679.
99. Hoffmann, B., Mitchell, G.T., Gendron, P., Major, F., Andersen, A.A., Collins, R.A. and Legault, P. (2003) NMR structure of the active conformation of the Varkud satellite ribozyme cleavage site. Proc. Natl. Acad. Sci. USA 100:7003–7008.
100. Beattie, T.L., Olive, J.E. and Collins, R.A. (1995) A secondary-structure model for the self-cleaving region of Neurospora VS RNA. Proc. Natl. Acad. Sci. USA 92:4686–4690.
101. Beattie, T.L. and Collins, R.A. (1997) Identification of functional domains in the self-cleaving Neurospora VS ribozyme using damage selection. J. Mol. Biol. 267:830–840.
102. Sood, V.D., Beattie, T.L. and Collins, R.A. (1998) Identification of phosphate groups involved in metal binding and tertiary interactions in the core of the Neurospora VS ribozyme. J. Mol. Biol. 282:741–750.
103. Rastogi, T. and Collins, R.A. (1998) Smaller, faster ribozymes reveal the catalytic core of Neurospora VS RNA. J. Mol. Biol. 277:215–224.
104. Lafontaine, D.A., Wilson, T.J., Norman, D.G. and Lilley, D.M. (2001) The A730 loop is an important component of the active site of the VS ribozyme. J. Mol. Biol. 312:663–674.
105. Hiley, S.L. and Collins, R.A. (2001) Rapid formation of a solvent-inaccessible core in the Neurospora Varkud satellite ribozyme. EMBO J. 20:5461–5469.
106. Sood, V.D., Yekta, S. and Collins, R.A. (2002) The contribution of 2′-hydroxyls to the cleavage activity of the Neurospora VS ribozyme. Nucleic Acids Res. 30:1132–1138.
107. Jones, F.D. and Strobel, S.A. (2003) Ionization of a critical adenosine residue in the Neurospora Varkud Satellite ribozyme active site. Biochemistry 42:4265–4276.
108. Lafontaine, D.A., Wilson, T.J., Zhao, Z.Y. and Lilley, D.M. (2002) Functional group requirements in the probable active site of the VS ribozyme. J. Mol. Biol. 323:23–34.
109. Sood, V.D. and Collins, R.A. (2002) Identification of the catalytic subdomain of the VS ribozyme and evidence for remarkable sequence tolerance in the active site loop. J. Mol. Biol. 320:443–454.

110. McLeod, A.C. and Lilley, D.M. (2004) Efficient, pH-dependent RNA ligation by the VS ribozyme in trans. Biochemistry 43:1118–1125.
111. Hiley, S.L., Sood, V.D., Fan, J. and Collins, R.A. (2002) 4-thio-U cross-linking identifies the active site of the VS ribozyme. EMBO J. 21:4691–4698.
112. Smith, M.D. and Collins, R.A. (2007) Evidence for proton transfer in the rate-limiting step of a fast-cleaving Varkud satellite ribozyme. Proc. Natl. Acad. Sci. USA 104:5818–5823.
113. Zhao, Z.Y., McLeod, A., Harusawa, S., Araki, L., Yamaguchi, M., Kurihara, T. and Lilley, D.M. (2005) Nucleobase participation in ribozyme catalysis. J. Am. Chem. Soc. 127:5026–5027.
114. Perrotta, A.T., Shih, I. and Been, M.D. (1999) Imidazole rescue of a cytosine mutation in a self-cleaving ribozyme. Science 286:123–126.
115. Mooney, R.A., Artsimovitch, I. and Landick, R. (1998) Information processing by RNA polymerase: recognition of regulatory signals during RNA chain elongation. J. Bacteriol. 180:3265–3275.
116. Stulke, J. (2002) Control of transcription termination in bacteria by RNA-binding proteins that modulate RNA structures. Arch. Microbiol. 177:433–440.
117. Gollnick, P. and Babitzke, P. (2002) Transcription attenuation. Biochim. Biophys. Acta 1577:240–250.
118. Condon, C. (2003) RNA processing and degradation in *Bacillus subtilis*. Microbiol. Mol. Biol. Rev. 67:157–174.
119. Copeland, P.R. (2003) Regulation of gene expression by stop codon recoding: selenocysteine. Gene (Amsterdam) 312:17–25.
120. Browning, D.F. and Busby, S.J. (2004) The regulation of bacterial transcription initiation. Nat. Rev. Microbiol. 2:57–65.
121. Babitzke, P. (2004) Regulation of transcription attenuation and translation initiation by allosteric control of an RNA-binding protein: the *Bacillus subtilis* TRAP protein. Curr. Opin. Microbiol. 7:132–139.
122. Storz, G., Opdyke, J.A. and Zhang, A. (2004) Controlling mRNA stability and translation with small, noncoding RNAs. Curr. Opin. Microbiol. 7:140–144.
123. Winkler, W.C., Nahvi, A., Roth, A., Collins, J.A. and Breaker, R.R. (2004) Control of gene expression by a natural metabolite-responsive ribozyme. Nature (Lond.) 428:281–286.
124. Gottesman, S. (2004) The small RNA regulators of *Escherichia coli*: roles and mechanisms. Annu. Rev. Microbiol. 58:303–328.
125. McManus, M.T. and Sharp, P.A. (2002) Gene silencing in mammals by small interfering RNAs. Nat. Rev. Genet. 3:737–747.
126. Carrington, J.C. and Ambros, V. (2003) Role of microRNAs in plant and animal development. Science 301:336–338.
127. Winkler, W.C. (2005) Metabolic monitoring by bacterial mRNAs. Arch. Microbiol. 183:151–159.
128. Mandal, M. and Breaker, R.R. (2004) Gene regulation by riboswitches. Nat. Rev. Mol. Cell. Biol. 5:451–463.
129. Nudler, E. and Mironov, A.S. (2004) The riboswitch control of bacterial metabolism. Trends Biochem. Sci. 29:11–17.
130. Grundy, F.J. and Henkin, T.M. (2004) Regulation of gene expression by effectors that bind to RNA. Curr. Opin. Microbiol. 7:126–131.
131. Christiansen, L.C., Schou, S., Nygaard, P. and Saxild, H.H. (1997) Xanthine metabolism in *Bacillus subtilis*: characterization of the xpt-pbuX operon and evidence for purine- and nitrogen-controlled expression of genes involved in xanthine salvage and catabolism. J. Bacteriol. 179:2540–2550.
132. Mandal, M. and Breaker, R.R. (2004) Adenine riboswitches and gene activation by disruption of a transcription terminator. Nat. Struct. Mol. Biol. 11:29–35.
133. Nahvi, A., Sudarsan, N., Ebert, M.S., Zou, X., Brown, K.L. and Breaker, R.R. (2002) Genetic control by a metabolite binding mRNA. Chem. Biol. 9:1043.

134. Mironov, A.S., Gusarov, I., Rafikov, R., Lopez, L.E., Shatalin, K., Kreneva, R.A., Perumov, D.A. and Nudler, E. (2002) Sensing small molecules by nascent RNA: a mechanism to control transcription in bacteria. Cell 111:747–756.
135. Winkler, W.C., Cohen-Chalamish, S. and Breaker, R.R. (2002) An mRNA structure that controls gene expression by binding FMN. Proc. Natl. Acad. Sci. USA 99:15908–15913.
136. Mandal, M., Lee, M., Barrick, J.E., Weinberg, Z., Emilsson, G.M., Ruzzo, W.L. and Breaker, R.R. (2004) A glycine-dependent riboswitch that uses cooperative binding to control gene expression. Science 306:275–279.
137. Grundy, F.J., Lehman, S.C. and Henkin, T.M. (2003) The L box regulon: lysine sensing by leader RNAs of bacterial lysine biosynthesis genes. Proc. Natl. Acad. Sci. USA 100:12057–12062.
138. Sudarsan, N., Wickiser, J.K., Nakamura, S., Ebert, M.S. and Breaker, R.R. (2003) An mRNA structure in bacteria that controls gene expression by binding lysine. Genes Dev. 17:2688–2697.
139. Epshtein, V., Mironov, A.S. and Nudler, E. (2003) The riboswitch-mediated control of sulfur metabolism in bacteria. Proc. Natl. Acad. Sci. USA 100:5052–5056.
140. Grundy, F.J. and Henkin, T.M. (1998) The S box regulon: a new global transcription termination control system for methionine and cysteine biosynthesis genes in gram-positive bacteria. Mol. Microbiol. 30:737–749.
141. Winkler, W.C., Nahvi, A., Sudarsan, N., Barrick, J.E. and Breaker, R.R. (2003) An mRNA structure that controls gene expression by binding S-adenosylmethionine. Nat. Struct. Biol. 10:701–707.
142. McDaniel, B.A., Grundy, F.J., Artsimovitch, I. and Henkin, T.M. (2003) Transcription termination control of the S box system: direct measurement of S-adenosylmethionine by the leader RNA. Proc. Natl. Acad. Sci. USA 100:3083–3088.
143. Winkler, W., Nahvi, A. and Breaker, R.R. (2002) Thiamine derivatives bind messenger RNAs directly to regulate bacterial gene expression. Nature (Lond.) 419:952–956.
144. Sudarsan, N., Hammond, M.C., Block, K.F., Welz, R., Barrick, J.E., Roth, A. and Breaker, R.R. (2006) Tandem riboswitch architectures exhibit complex gene control functions. Science 314:300–304.
145. Banerjee, R.V., Frasca, V., Ballou, D.P. and Matthews, R.G. (1990) Participation of cob(I) alamin in the reaction catalyzed by methionine synthase from *Escherichia coli*: a steady-state and rapid reaction kinetic analysis. Biochemistry 29:11101–11109.
146. Gonzalez, J.C., Peariso, K., Penner-Hahn, J.E. and Matthews, R.G. (1996) Cobalamin-independent methionine synthase from *Escherichia coli*: a zinc metalloenzyme. Biochemistry 35:12228–12234.
147. Vicens, Q. and Westhof, E. (2003) RNA as a drug target: the case of aminoglycosides. ChemBioChem 4:1018–1023.
148. Blount, K.F., Wang, J.X., Lim, J., Sudarsan, N. and Breaker, R.R. (2007) Antibacterial lysine analogs that target lysine riboswitches. Nat. Chem. Biol. 3:44–49.
149. Shiota, T., Folk, J.E. and Tietze, F. (1958) Inhibition of lysine utilization in bacteria by S-(beta-aminoethyl) cysteine and its reversal by lysine peptides. Arch. Biochem. Biophys. 77:372–377.
150. Batey, R.T., Gilbert, S.D. and Montange, R.K. (2004) Structure of a natural guanine-responsive riboswitch complexed with the metabolite hypoxanthine. Nature (Lond.) 432:411–415.
151. Serganov, A., Yuan, Y.R., Pikovskaya, O., Polonskaia, A., Malinina, L., Phan, A.T., Hobartner, C., Micura, R., Breaker, R.R. and Patel, D.J. (2004) Structural basis for discriminative regulation of gene expression by adenine- and guanine-sensing mRNAs. Chem. Biol. 11:1729–1741.
152. Soukup, G.A. and Breaker, R.R. (1999) Relationship between internucleotide linkage geometry and the stability of RNA. RNA 5:1308–1325.
153. Winkler, W.C. and Breaker, R.R. (2003) Genetic control by metabolite-binding riboswitches. ChemBioChem 4:1024–1032.
154. Lemay, J.F., Penedo, J.C., Tremblay, R., Lilley, D.M. and Lafontaine, D.A. (2006) Folding of the adenine riboswitch. Chem. Biol. 13:857–868.

155. Lemay, J.F. and Lafontaine, D.A. (2007) Core requirements of the adenine riboswitch aptamer for ligand binding. RNA 13:339–350.
156. Frankel, A.D. (1999) If the loop fits. Nat. Struct. Biol. 6:1081–1083.
157. Williamson, J.R. (2000) Induced fit in RNA–protein recognition. Nat. Struct. Biol. 7:834–837.
158. Gilbert, S.D., Mediatore, S.J. and Batey, R.T. (2006) Modified pyrimidines specifically bind the purine riboswitch. J. Am. Chem. Soc. 128:14214–14215.
159. Gilbert, S.D., Stoddard, C.D., Wise, S.J. and Batey, R.T. (2006) Thermodynamic and kinetic characterization of ligand binding to the purine riboswitch aptamer domain. J. Mol. Biol. 359:754–768.
160. Lescoute, A. and Westhof, E. (2005) Riboswitch structures: purine ligands replace tertiary contacts. Chem. Biol. 12:10–13.
161. Wickiser, J.K., Cheah, M.T., Breaker, R.R. and Crothers, D.M. (2005) The kinetics of ligand binding by an adenine-sensing riboswitch. Biochemistry 44:13404–13414.
162. Wickiser, J.K., Winkler, W.C., Breaker, R.R. and Crothers, D.M. (2005) The speed of RNA transcription and metabolite binding kinetics operate an FMN riboswitch. Mol. Cell 18:49–60.
163. Sassanfar, M. and Szostak, J.W. (1993) An RNA motif that binds ATP. Nature (Lond.) 364:550–553.
164. Connell, G.J. and Yarus, M. (1994) RNAs with dual specificity and dual RNAs with similar specificity. Science 264:1137–1141.
165. Jenison, R.D., Gill, S.C., Pardi, A. and Polisky, B. (1994) High-resolution molecular discrimination by RNA. Science 263:1425–1429.
166. Kiga, D., Futamura, Y., Sakamoto, K. and Yokoyama, S. (1998) An RNA aptamer to the xanthine/guanine base with a distinctive mode of purine recognition. Nucleic Acids Res. 26:1755–1760.
167. McDaniel, B.A., Grundy, F.J. and Henkin, T.M. (2005) A tertiary structural element in S box leader RNAs is required for S-adenosylmethionine-directed transcription termination. Mol. Microbiol. 57:1008–1021.
168. Lim, J., Winkler, W.C., Nakamura, S., Scott, V. and Breaker, R.R. (2006) Molecular-recognition characteristics of SAM-binding riboswitches. Angew. Chem. Int. Ed. Engl. 45:964–968.
169. Corbino, K.A., Barrick, J.E., Lim, J., Welz, R., Tucker, B.J., Puskarz, I., Mandal, M., Rudnick, N.D. and Breaker, R.R. (2005) Evidence for a second class of S-adenosylmethionine riboswitches and other regulatory RNA motifs in alpha-proteobacteria. Genome Biol. 6:R70.
170. Fuchs, R.T., Grundy, F.J. and Henkin, T.M. (2006) The S(MK) box is a new SAM-binding RNA for translational regulation of SAM synthetase. Nat. Struct. Mol. Biol. 13:226–233.
171. Fuchs, R.T., Grundy, F.J. and Henkin, T.M. (2007) S-adenosylmethionine directly inhibits binding of 30S ribosomal subunits to the SMK box translational riboswitch RNA. Proc. Natl. Acad. Sci. USA 104:4876–4880.
172. Winkler, W.C. and Breaker, R.R. (2005) Regulation of bacterial gene expression by riboswitches. Annu. Rev. Microbiol. 59:487–517.
173. Grundy, F.J. and Henkin, T.M. 2002. Synthesis of serine, glycine, cysteine and methionine. American Society for Microbiology Press, Washington, DC.
174. Grundy, F.J. and Henkin, T.M. (2003) The T box and S box transcription termination control systems. Front. Biosci. 8:d20–d31.
175. Rodionov, D.A., Vitreschak, A.G., Mironov, A.A. and Gelfand, M.S. (2004) Comparative genomics of the methionine metabolism in Gram-positive bacteria: a variety of regulatory systems. Nucleic Acids Res. 32:3340–3353.
176. Winkler, W.C., Grundy, F.J., Murphy, B.A. and Henkin, T.M. (2001) The GA motif: an RNA element common to bacterial antitermination systems, rRNA, and eukaryotic RNAs. RNA 7:1165–1172.
177. Klein, D.J., Schmeing, T.M., Moore, P.B. and Steitz, T.A. (2001) The kink-turn: a new RNA secondary structure motif. EMBO J. 20:4214–4221.
178. Montange, R.K. and Batey, R.T. (2006) Structure of the S-adenosylmethionine riboswitch regulatory mRNA element. Nature (Lond.) 441:1172–1175.
179. Schubert, H.L., Blumenthal, R.M. and Cheng, X. (2003) Many paths to methyltransfer: a chronicle of convergence. Trends Biochem. Sci. 28:329–335.

180. Burke, D.H. and Gold, L. (1997) RNA aptamers to the adenosine moiety of S-adenosyl methionine: structural inferences from variations on a theme and the reproducibility of SELEX. Nucleic Acids Res. 25:2020–2024.
181. Dieckmann, T., Suzuki, E., Nakamura, G.K. and Feigon, J. (1996) Solution structure of an ATP-binding RNA aptamer reveals a novel fold. RNA 2:628–640.
182. Jiang, F., Fiala, R., Live, D., Kumar, R.A. and Patel, D.J. (1996a) RNA folding topology and intermolecular contacts in the AMP-RNA aptamer complex. Biochemistry 35:13250–13266.
183. Jiang, F., Kumar, R.A., Jones, R.A. and Patel, D.J. (1996b) Structural basis of RNA folding and recognition in an AMP-RNA aptamer complex. Nature (Lond.) 382:183–186.
184. Sudarsan, N., Barrick, J.E. and Breaker, R.R. (2003a) Metabolite-binding RNA domains are present in the genes of eukaryotes. RNA 9:644–647.
185. Goodwin, T.W. (1963) The biosynthesis of vitamins and related compounds. Academic Press, New York.
186. Begley, T.P., Downs, D.M., Ealick, S.E., McLafferty, F.W., Van Loon, A.P., Taylor, S., Campobasso, N., Chiu, H.J., Kinsland, C., Reddick, J.J. and Xi, J. (1999) Thiamin biosynthesis in prokaryotes. Arch. Microbiol. 171:293–300.
187. Serganov, A., Polonskaia, A., Phan, A.T., Breaker, R.R. and Patel, D.J. (2006) Structural basis for gene regulation by a thiamine pyrophosphate-sensing riboswitch. Nature (Lond.) 441:1167–1171.
188. Thore, S., Leibundgut, M. and Ban, N. (2006) Structure of the eukaryotic thiamine pyrophosphate riboswitch with its regulatory ligand. Science 312:1208–1211.
189. Nudler, E. (2006) Flipping riboswitches. Cell 126:19–22.
190. Robbins, W.J. (1941) The pyridine analog of thiamin and the growth of fungi. Proc. Natl. Acad. Sci. USA 27:419–422.
191. Woolley, D.W. (1951) An enzymatic study of the mode of action of pyrithiamine (neopyrithiamine). J. Biol. Chem. 191:43–54.
192. Kubodera, T., Watanabe, M., Yoshiuchi, K., Yamashita, N., Nishimura, A., Nakai, S., Gomi, K. and Hanamoto, H. (2003) Thiamine-regulated gene expression of *Aspergillus oryzae* thiA requires splicing of the intron containing a riboswitch-like domain in the 5′-UTR. FEBS Lett. 555:516–520.
193. Sudarsan, N., Cohen-Chalamish, S., Nakamura, S., Emilsson, G.M. and Breaker, R.R. (2005) Thiamine pyrophosphate riboswitches are targets for the antimicrobial compound pyrithiamine. Chem. Biol. 12:1325–1335.
194. Blount, K., Puskarz, I., Penchovsky, R. and Breaker, R. (2006) Development and application of a high-throughput assay for glmS riboswitch activators. RNA Biol. 3:77–81.
195. Hampel, K.J. and Tinsley, M.M. (2006) Evidence for preorganization of the glmS ribozyme ligand binding pocket. Biochemistry 45:7861–7871.
196. Jansen, J.A., McCarthy, T.J., Soukup, G.A. and Soukup, J.K. (2006) Backbone and nucleobase contacts to glucosamine-6-phosphate in the glmS ribozyme. Nat. Struct. Mol. Biol. 13:517–523.
197. Lim, J., Grove, B.C., Roth, A. and Breaker, R.R. (2006) Characteristics of ligand recognition by a glmS self-cleaving ribozyme. Angew. Chem. Int. Ed. Engl. 45:6689–6693.
198. Link, K.H., Guo, L. and Breaker, R.R. (2006) Examination of the structural and functional versatility of glmS ribozymes by using in vitro selection. Nucleic Acids Res. 34:4968–4975.
199. Mayer, G. and Famulok, M. (2006) High-throughput-compatible assay for glmS riboswitch metabolite dependence. ChemBioChem 7:602–604.
200. McCarthy, T.J., Plog, M.A., Floy, S.A., Jansen, J.A., Soukup, J.K. and Soukup, G.A. (2005) Ligand requirements for glmS ribozyme self-cleavage. Chem. Biol. 12:1221–1226.
201. Tinsley, R.A., Furchak, J.R. and Walter, N.G. (2007) Trans-acting glmS catalytic riboswitch: locked and loaded. RNA 13:468–477.
202. Roth, A., Nahvi, A., Lee, M., Jona, I. and Breaker, R.R. (2006) Characteristics of the glmS ribozyme suggest only structural roles for divalent metal ions. RNA 12:607–619.
203. Soukup, G.A. (2006) Core requirements for glmS ribozyme self-cleavage reveal a putative pseudoknot structure. Nucleic Acids Res. 34:968–975.

204. Wilkinson, S.R. and Been, M.D. (2005) A pseudoknot in the 3′ non-core region of the glmS ribozyme enhances self-cleavage activity. RNA 11:1788–1794.
205. Wilson, T.J., Ouellet, J., Zhao, Z.Y., Harusawa, S., Araki, L., Kurihara, T. and Lilley, D.M. (2006) Nucleobase catalysis in the hairpin ribozyme. RNA 12:980–987.
206. Cromie, M.J., Shi, Y., Latifi, T. and Groisman, E.A. (2006) An RNA sensor for intracellular Mg(2+). Cell 125:71–84.
207. Chowdhury, S., Ragaz, C., Kreuger, E. and Narberhaus, F. (2003) Temperature-controlled structural alterations of an RNA thermometer. J. Biol. Chem. 278:47915–47921.
208. Barrick, J.E., Corbino, K.A., Winkler, W.C., Nahvi, A., Mandal, M., Collins, J., Lee, M., Roth, A., Sudarsan, N., Jona, I., Wickiser, J.K. and Breaker, R.R. (2004) New RNA motifs suggest an expanded scope for riboswitches in bacterial genetic control. Proc. Natl. Acad. Sci. USA 101:6421–6426.

Chapter 3
Artificial Functional Nucleic Acids: Aptamers, Ribozymes, and Deoxyribozymes Identified by In Vitro Selection

Scott K. Silverman

Abstract The discovery of natural RNA catalysts (ribozymes) inspired the use of in vitro selection methodology to develop artificial functional nucleic acids (FNAs). In vitro selection is the experimental process by which large random-sequence pools of RNA or DNA are used as the starting point to identify particular nucleic acid sequences that have desired functions. When this function is binding of a molecular target, the functional nucleic acid is an RNA or DNA "aptamer." When this function is catalysis of a chemical reaction, the functional nucleic acid is a "ribozyme" or "deoxyribozyme"; these are collectively termed "nucleic acid enzymes." Since the first in vitro selection experiments in 1990, a wide variety of aptamers and nucleic acid enzymes have been identified. This chapter describes how aptamers, ribozymes, and deoxyribozymes are obtained by in vitro selection methodologies. Also addressed are the scope of the molecular targets that are bound and the chemical reactions that are catalyzed. Biochemical and structural characterizations of aptamers and nucleic acid enzymes are discussed. A final section introduces aptazymes, which are allosterically regulated nucleic acid enzymes.

3.1 Introduction to Artificial Functional Nucleic Acids

As described in Chapters 1 and 2, naturally occurring functional nucleic acids (FNAs) are now widely recognized and investigated. In parallel, the development of artificial FNAs is well underway. Broadly speaking, artificial FNAs are either aptamers or enzymes. The term "aptamer" derives from the Latin *aptus*, the past participle of "to fit."[1] Aptamers are RNA or DNA molecules that bind molecular targets. Nature developed RNA aptamers long before researchers reproduced the achievement. The discovery of self-splicing group I introns[2] inherently showed that RNA can bind small molecules, because guanosine or one of its derivatives is an obligatory and specifically bound cofactor for the splicing reaction.[3] Other studies revealed that viruses encode small RNAs which have biological activity. For

S.K. Silverman
Department of Chemistry, University of Illinois at Urbana-Champaign
scott@scs.uiuc.edu

Y. Li and Y. Lu (eds.), *Functional Nucleic Acids for Analytical Applications*,

example, adenovirus encodes the short virus-associated (VA) RNA that inhibits interferon-induced protein kinase R (PKR) activity,[4] and human immunodeficiency virus (HIV) encodes functionally relevant small RNA oligomers such as the *trans*-activation response (TAR) RNA that binds to the viral Tat protein.[5,6] In the same year that the first in vitro aptamer selection experiments were published,[1,7] the naturally occurring TAR aptamer was reported to inhibit HIV replication in vivo.[8] The first artificial nucleic acid enzyme was published in the same year.[9]

All of these FNAs were identified by in vitro selection. The in vitro selection of aptamers was dubbed "systematic evolution of ligands by exponential enrichment," or SELEX, by Tuerk and Gold in 1990.[7] Although this acronym is often applied to all selection experiments, strictly speaking it applies only to aptamer selections but not to nucleic acid enzyme selections. Methodologies for in vitro selection of aptamers and nucleic acid enzymes are growing increasingly sophisticated; e.g., the use of techniques such as microfluidics.[10] Nevertheless, the simple principles and methods that were used in the initial selection experiments are still quite useful and commonly applied. Several general reviews on the in vitro selection of aptamers, ribozymes, and deoxyribozymes have been published.[11–15]

3.2 Methodology for In Vitro Selection of RNA and DNA Aptamers

The most common methodology for in vitro selection of RNA and DNA aptamers depends on exposing a "pool" of random RNA or DNA sequences to a solid support that has been covalently derivatized with the binding target of interest. Sequences that can bind the target remain noncovalently associated with the solid support and can therefore be separated by means of their affinity. This section discusses the affinity chromatography approach and also other methods for identifying nucleic acid sequences that bind to desired targets.

The molecular species bound by an aptamer is often called a "ligand," although the same term is also commonly used for the aptamer itself (note what the L of SELEX stands for). To avoid confusion, in this chapter the molecular species bound by an aptamer is designated as the "target" of that aptamer.

3.2.1 In Vitro Selection of Aptamers by Affinity Chromatography

Although many experimental approaches are used for identification of aptamers by in vitro selection (SELEX), the methodology typically relies upon immobilization of the target on a solid-phase support such as agarose beads.[1] Then, a pool of random RNA or DNA sequences is exposed to the target-derivatized support. Binding of the very small fraction of RNA or DNA sequences that has a high affinity for the

target allows enrichment of those sequences, which are then eluted by addition of underivatized target. Appropriate biochemical manipulations are used to prepare the enriched pool for initiating another round of the selection process. Selection rounds are iterated until an adequately high level of binding is observed. Typically, 5–15 rounds are required until no further enrichment occurs, although occasionally more rounds are needed. Finally, individual aptamer sequences are identified, and their binding and biochemical properties are examined in more detail. The aptamers that emerge from such studies have been used in numerous applications (see Parts II and III of this book).

3.2.1.1 The Basic Procedures of In Vitro Selection (SELEX) of Aptamers

The fundamental choice between RNA and DNA aptamers is largely a matter of personal preference, because both types of nucleic acid are capable of binding a wide range of targets (see Sections 3.3 and 3.4). Once the choice of nucleic acid has been made, a typical aptamer selection experiment (Fig. 3.1) begins with

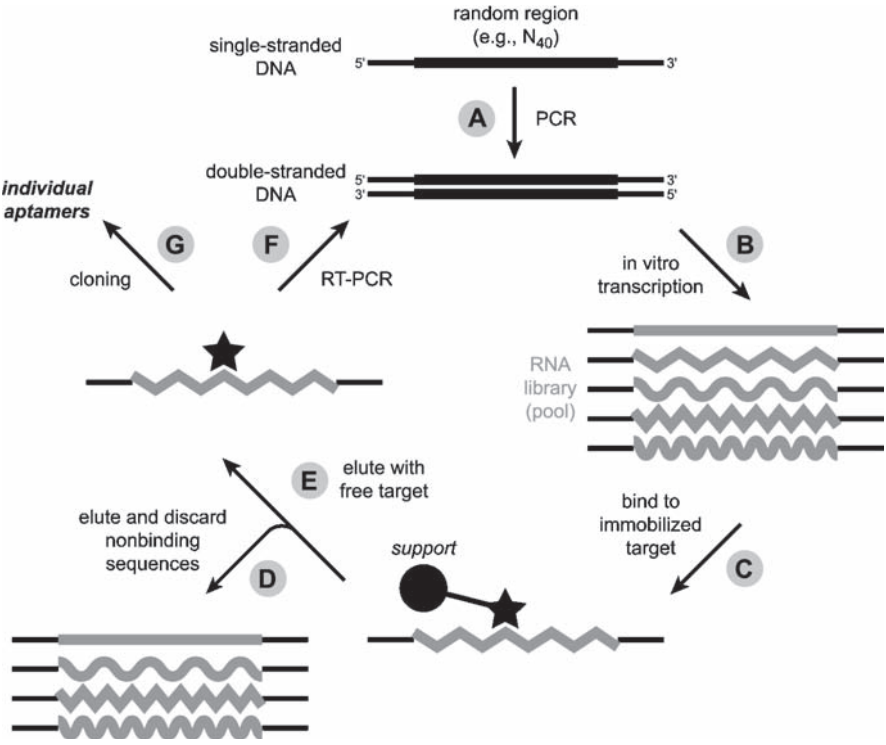

Fig. 3.1 Typical aptamer selection procedure, illustrated for RNA aptamers

solid-phase synthesis of a long DNA oligonucleotide that contains a stretch of random nucleotides. Each random position is introduced by using an appropriate mixture of the four standard DNA phosphoramidites during the solid-phase synthesis coupling step. For RNA aptamers, the long DNA oligonucleotide is amplified by polymerase chain reaction (PCR), and the initially random RNA pool is prepared by transcription using the DNA as a template (see Fig. 3.1, steps A and B). For DNA aptamers, the initially random DNA pool is directly prepared by either primer extension or PCR using the long DNA oligonucleotide as a template. These reactions are facilitated by constant sequence regions that are included adjacent to the random region within the long DNA oligonucleotide.

A key choice at the outset of selection is the length of the random region within the initial pool. The optimal size of the random region is often debated for both binding and catalysis.[16] For a wide range of aptamer targets, random regions as small as 22 nucleotides (i.e., N_{22} regions) have been used successfully.[17,18] Small N_{25} regions have been used to select aptamers for small-molecule targets,[19,20] proteins,[21,22] and a misactivated tRNA.[23] Random regions of N_{40} to N_{80} are more typical, although pools as large as N_{120},[24–30] N_{134},[31] or in an unusual case even N_{228} (!) have been utilized.[32] In one set of experiments, the optimal random-region length was found to reflect a balance between factors,[18] although the generality of the outcome for other targets is uncertain.

For a typical N_{40} pool, the size of "sequence space" is 4^{40} or 10^{24} possible sequences. In practice, technical considerations limit the number of random-pool sequences that can actually be used for initiating the selection to 0.01–10 nmol, which is only 10^{13}–10^{16} sequences. Therefore, sequence space is substantially undersampled, with only one of every 10^{10} possible sequences examined experimentally (i.e., 10^{-10} coverage of sequence space). Larger random regions such as N_{80} have even less coverage of sequence space. Despite these statistical challenges, aptamer selections do succeed, which means that functional sequences (i.e., those that bind the target) must be quite common within sequence space. The weight of experimental evidence indicates that longer random regions are not always superior, for at least two reasons. First, longer stretches of nucleotides offer more possibilities for forming inhibitory interactions with sequences that would otherwise be good target binders. Second, the "tyranny of the short motif"[13,33] must be avoided. Short motifs have a selective advantage because of their very high probability of being present within a random sequence,[34] even if a longer motif would be more highly functional (i.e., have a higher affinity for the target). Initiating the selection process with a longer stretch of random nucleotides increases the probability that a suboptimal short motif may be present and outcompete a more functional but less probable longer motif.

As the next part of the selection procedure, the random pool is exposed to the target-derivatized solid support (step C). The particular incubation conditions must be chosen carefully. Many experimental variables must be considered, including pH, temperature, buffer identity and concentration, organic cosolvent (if included), metal ion identities and concentrations, and incubation time. The choices made

for all of these variables depend on the specific target being used, and there is no general rule for optimal incubation conditions.

The incubation time is usually arranged such that equilibration occurs during the binding time period. Typical incubation times range from 5 min to 1 h. Once equilibration has occurred, nonbinding sequences are eluted and discarded (step D), and the target-binding sequences are eluted with free target (step E). If the selection is for RNA aptamers, then reverse transcription (RT)-PCR (step F) is used to regenerate a DNA template, which is now enriched in those sequences that (when made as RNA) are capable of binding the target. The new RNA pool is then prepared by transcription from the DNA template. If the selection is for DNA aptamers, then PCR is used directly to regenerate the pool DNA (reverse transcription is of course unnecessary). For DNA aptamer selections, the PCR can be performed "asymmetrically" by including a skewed ratio of the two primers,[26,35–37] or "unidirectionally" by including only one primer and obtaining linear amplification.[21] Alternatively, the PCR can be performed normally, but arranged such that the desired single-stranded DNA can be separated physically from its undesired complement. The most common approaches are by binding of the biotinylated form of the undesired DNA strand to immobilized avidin or streptavidin[32,38–42] or by electrophoretic separation of the undesired biotinylated strand.[43–47]

To achieve the desired affinities between the nucleic acid aptamer and the target, the stringency of the selection procedure can be increased as the selection rounds progress. This step is often achieved by decreasing the concentration of the target that is used to displace the binding sequences from the target-derivatized support. A mathematical analysis has been developed for determining the best initial concentration of target to use for elution.[48] For the later rounds of selection, empirical feedback from the results of previous rounds is usually used to guide the choices.

After the selection rounds have been completed, the final PCR product is cloned, leading to individual aptamer sequences (step G). By aligning the sequences of tens or even hundreds of individual clones, consensus aptamer sequences may often be identified. However, highly functional aptamers are sometimes "orphans" with little or no homology to the other sequences, and it is unwise to assume that only repeatedly found sequences are functional. Aptamer candidates from the cloning process are screened to determine their target-binding properties. The "winning" sequences are then studied in greater detail; e.g., to determine their binding constants and secondary structures.

3.2.1.2 Additional Considerations for Aptamer Selection Procedures

Since the first RNA aptamer selection experiments,[1,7] many refinements to the basic procedures have been made. As a key component of the affinity chromatography procedure, different solid supports may be used. The original experiment with the protein T4 DNA polymerase as the target used nitrocellulose filters,[7] as have numerous other experiments with protein targets.[28,29,31,43,44,49–76] For most

small-molecule aptamer selections, agarose (e.g., Sepharose) is used as the support material. Protein targets can sometimes be immobilized directly on agarose rather than nitrocellulose. Alternatively, the protein of interest can be expressed as a GST fusion and bound to glutathione agarose,[67,77] the protein can be bound to beads via biotin-streptavidin or antibody interactions,[78] or the protein can be bound to colloidal gold.[79]

In all these approaches, selectively bound nucleic acid sequences are eluted from the protein-derivatized support during each selection round either by changing the ionic strength,[22] by adding sodium dodecyl sulfate (SDS), Triton X-100, urea, or guanidinium as denaturant,[27,29,31,44,45,51,53–67,70,72–78,80–86] or by cleaving the protein support linker.[68,69,87] Alternatively, the protein target can be immobilized on agarose that has been derivatized with a second protein which interacts tightly with the target; e.g., concanavalin A that binds strongly to thrombin.[38] In such a case, an unrelated ligand that interacts well with the second protein is used to displace and therefore elute selectively bound nucleic acid sequences during each selection round (e.g., α-methylmannoside as a concanavalin A ligand). Other solid supports that have been used to identify aptamers for protein targets include plastic plates or flasks[76,88] or the surfaces of PCR tubes.[21]

In some experiments with small-molecule targets, the functional RNA or DNA sequences are eluted from the affinity column not by adding free target but by changing the ionic strength of the elution buffer or by chelating divalent metal ions, which therefore denatures the nucleic acid. These approaches have been particularly effective in several selections of aptamers that bind to amino acids.[25,39,89]

Measures must be taken to ensure that the RNA or DNA sequences do not merely bind directly to the support itself, regardless of its chemical makeup. Binding directly to the support is usually avoided by exposing the pool to the underivatized support and discarding all sequences that are retained before the pool is exposed to the target-derivatized support. Of course, any sequences that would have been capable of binding to the target but also bind to the support itself are lost. This is an unavoidable drawback of the affinity chromatography procedures. Without discarding the support-binding sequences, in most cases they would overwhelm the selection process and prevent any true target-binding sequences from being discovered.

Some degree of selectivity for the target is usually desired, and several approaches to ensure high selectivity have been developed. Negative selection, also termed counter-selection, is commonly applied.[19,26,31,39,90–98] In negative selection, the pool of nucleic acid sequences is exposed to a secondary target for which binding is *not* desired, and any sequences that bind are discarded. The remaining sequences are then allowed to bind with the desired support-bound target as usual, and the successfully binding sequences are retained to be input into the next round of selection. Exposure of the pool to the underivatized support (as described above) is an essentially universal form of negative selection against nonselective binding to the support material itself.

The first ATP aptamer[24] was rediscovered independently two additional times,[99,100] but a different aptamer was found when discrimination between AMP and ATP was enforced by negative selection.[101] Interestingly, the discriminating aptamer was not

found in the other selection experiments, even though it binds to ATP only slightly less well than the earlier aptamers. Although negative selection is very useful to increase target selectivity, such selectivity does not necessarily *require* the use of negative selection; selectivity may instead emerge fortuitously. For example, the selection of a DNA aptamer for ATP provided a sequence that selectively binds ATP over other nucleoside triphosphates (NTPs), even though negative selection was never applied[102] (DNA aptamers are discussed in more detail in Section 3.3). Similarly, an aptamer that binds both guanine and xanthine did not bind to any of adenine, cytosine, or uracil, even though negative selection against binding of these other nucleobases was never applied.[103,104] Other examples of discrimination against binding of closely related small-molecule targets without negative selection have been described.[105–107] With or without negative selection, selectivity among closely related protein targets has also been achieved in several cases.[27,31,69,72,80,84]

Sometimes, target generality rather than selectivity is sought. For this purpose with protein targets, investigators applied "toggle SELEX," in which the RNA pool is alternately exposed to human and animal versions of the same proteins. This method is advantageous for preclinical studies to ensure cross-reactivity, i.e., to make certain that both forms of the proteins are bound by the aptamer.[68] A similar approach could certainly be applied for other targets such as small molecules to ensure that undesired selectivity is not inadvertently obtained.

Aptamer selections do not necessarily need to begin with an entirely random pool. Instead, in a process termed "reselection," a known aptamer may be partially randomized (mutagenized) to provide the starting point for a new selection effort.[20,63,91,92,94,102,106,108–114] The aptamer starting point for reselection may even be derived from a natural RNA sequence.[54,58] The reselection approach takes advantage both of known target-binding sequences and of the power of selection to improve the original binding activity. Reselection is also used in nucleic acid enzyme selections (see Section 3.6.1.2). As an alternative to reselection via solid-phase synthesis of a mutagenized pool, error-prone PCR[115] or nonstandard nucleotide triphosphates[116] may be used to introduce sequence variation.[87] In one case, appending an additional entirely random region to a known aptamer and repeating the selection process was used to improve the binding affinity of the aptamer.[117]

One important consideration for aptamer selection experiments is whether the constant primer-binding sequences will become involved in the target-binding event. This event is not necessarily detrimental, although a requirement for the primer-binding sequences may make it difficult to minimize (truncate) any aptamers as part of a practical application. Therefore, several approaches have been developed to ensure that the primer-binding sequences do not participate directly or indirectly in target binding. These methods sequester the primer-binding sequences within duplex structures either intramolecularly[118] or intermolecularly,[119] using the logic that duplex nucleic acids are less likely than single strands to interact with a target. Alternatively, ligation is used to append primer-binding sequences during each round of selection, but the primer-binding sequences are absent during the key selection step itself.[120]

3.2.2 Aptamer Selection Methods Other than Affinity Chromatography

In addition to approaches based on binding of nucleic acids to agarose beads or nitrocellulose filters, many other aptamer selection methods have been developed. In one study, the protein target was attached to colloidal gold.[79] This step effectively increased the mass of the protein and allowed a more efficient separation of successfully bound DNA sequences simply by centrifugation to pellet the gold. Another technical advance is the use of magnetic beads, which allow more convenient separations (faster and consuming less material). His_6-tagged proteins may be bound to Ni-NTA magnetic beads to identify aptamers for a protein target.[121] Magnetic beads may also be used with non-His_6-tagged proteins.[116,122,123] Antibody-coated magnetic beads have been used for immunoprecipitation during selection.[80,82,84] Immunoprecipitation using nonmagnetic beads has also been reported.[60,124]

A variant of the magnetic bead approach that additionally uses fluorescence has been termed "FluMag-SELEX."[125,126] In this technique, fluorescent labels replace radioactive (^{32}P) tags to quantify the bound and unbound oligonucleotides during each selection step; this could be particularly advantageous if a laboratory wished completely to avoid the use of radioactivity. In principle, a fluorescence change in the appropriately derivatized target[127] could even be used as the basis for selecting aptamers via a compartmentalization approach.[128,129] However, this approach has not yet been reported.

As an alternative to relying on noncovalent affinity, photoinduced covalent bond formation has been used as the basis for selection.[130] In one set of experiments, selection rounds with or without photo-cross-linking were alternated, leading to aptamers that have both high affinity to the target (HIV-1 REV protein) and high photo-cross-linking efficiency.[131] The photochemistry required incorporation of a nonstandard 5-iodouracil nucleotide into the RNA.

Nondenaturing gel electrophoresis has been used as the basis for separating RNA or DNA that binds to protein targets.[27,43,46,59,74,77,85,132] Often this has been used as an alternative approach to filter binding within a single selection experiment. Alternation of two physical approaches helps to suppress artifacts such as sequences that might opportunistically survive the selection procedure if only one approach were used.

Surface plasmon resonance (SPR; Biacore) has been used directly as part of the selection process in several instances.[133–135] Enrichment of binding sequences is based on the slow dissociation rate of aptamers from the surface-bound target.

Methodology that avoids the need to derivatize the target and then bind it to a bead is desirable for practical reasons. Capillary electrophoresis (CE) methods have been used to identify new DNA aptamers,[136–140] although such methods could presumably be applied to RNA aptamers as well. At present these methods appear promising, and it will be interesting to see the extent to which they supplant the original solid-support methods. CE and other analytical techniques that depend upon aptamers for the binding events are also being developed (see Part III of this book).[141]

Finally, several automated aptamer selection processes have been developed, which has been achieved by the laboratory of Ellington[142–146] and also by others.[10,147,148] The importance of automated selection will certainly increase as aptamer technologies improve and as aptamers are more widely used in practical applications.

3.3 Molecular Targets and Properties of RNA Aptamers

A particularly striking feature of RNA and DNA aptamers is the wide range of targets that may be bound. Not considering divalent metal ion targets,[149–151] the smallest artificial target for which an aptamer has been developed is ethanolamine, which has only four heavy (nonhydrogen) atoms and a molecular weight of merely 61.[126] Despite this small size, the molecule is bound by its (DNA) aptamer with binding constant (K_d) of 6 nM. If nucleic acids can bind tightly to such a small and relatively featureless target, then larger targets should certainly be bindable as well. Indeed, RNA aptamers have been identified that bind well to many targets (Fig. 3.2). This section describes these molecular targets of RNA aptamers and

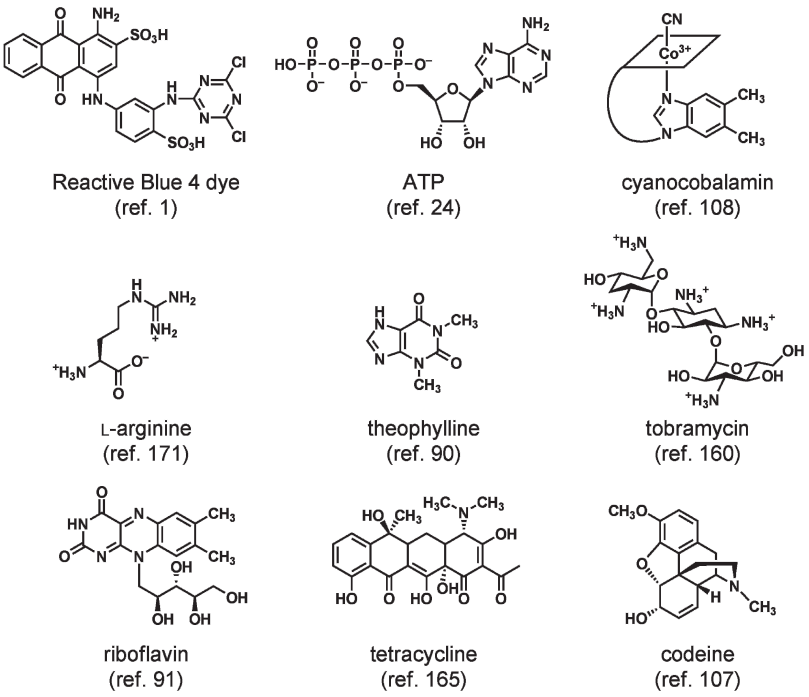

Fig. 3.2 Representative small-molecule targets of RNA aptamers. The corrin ring of *cyanocobalamin* (vitamin B_{12}) is shown schematically

discusses some features of the aptamers themselves. Several examples of aptamers for transition-state analogues are presented in the discussion on ribozymes (see Section 3.6.1.3).

3.3.1 Molecular Targets Bound by RNA Aptamers

3.3.1.1 The First RNA Aptamers

The first RNA aptamers were reported in 1990.[1,7] Ellington and Szostak identified RNAs that bind to small organic dyes, whereas Tuerk and Gold found RNAs that bind to T4 DNA polymerase. These pioneering experiments established that in vitro selection for target binding by nucleic acids is a viable experimental approach. The studies of Ellington and Szostak used organic dyes attached to agarose beads, and the experiments of Tuerk and Gold used T4 DNA polymerase bound to nitrocellulose filters.

One of the first RNA aptamers for a small biomolecule as the target was a sequence that binds ATP and its derivatives.[24] To enable the selection effort, ATP was bound to an agarose support via a tether connected to the C8 position of the adenine nucleobase (Fig. 3.3). Elution of binding sequences with free ATP ensured that the resulting RNA aptamers can bind to untethered ATP as well as to the support-tethered compound. After eight rounds of selection, an aptamer consensus sequence was identified by comparing the sequences of 39 clones. Based on the experimental results, a short 40-nucleotide RNA aptamer (Fig. 3.4) was designed and tested for binding to ATP and numerous derivatives. The data revealed that the adenine nucleobase and ribose sugar moieties are recognized by the RNA aptamer, whereas the 5′-triphosphate is dispensable for binding. At 5 mM Mg^{2+}, which was the concentration of Mg^{2+} present during the selection procedure, the K_d of the aptamer for ATP was of the order of 10 μM, which was improved to 0.7 μM by strategic nucleotide changes. The precise K_d values depended on which measurement method was used (see Section 3.3.2 for more on biochemical characterization of aptamers).

3.3.1.2 Small-Molecule Targets of RNA Aptamers

Small-molecule antibiotic compounds have long been known to interact with ribosomal RNA[152,153] and to disrupt group I intron splicing by either competitive or noncompetitive inhibition.[154–157] The more recent discovery of metabolite-binding "riboswitch" RNAs (see Chapter 2) has strikingly demonstrated that binding of small molecules by RNA can have important natural effects in vivo. Both to advance fundamental understanding and possibly to assist in therapeutic interventions, a large number of in vitro selection experiments have focused on identifying RNA aptamers that bind to small-molecule targets. Here, "small molecules" are defined as compounds of relatively low molecular weight (<1,000), which among

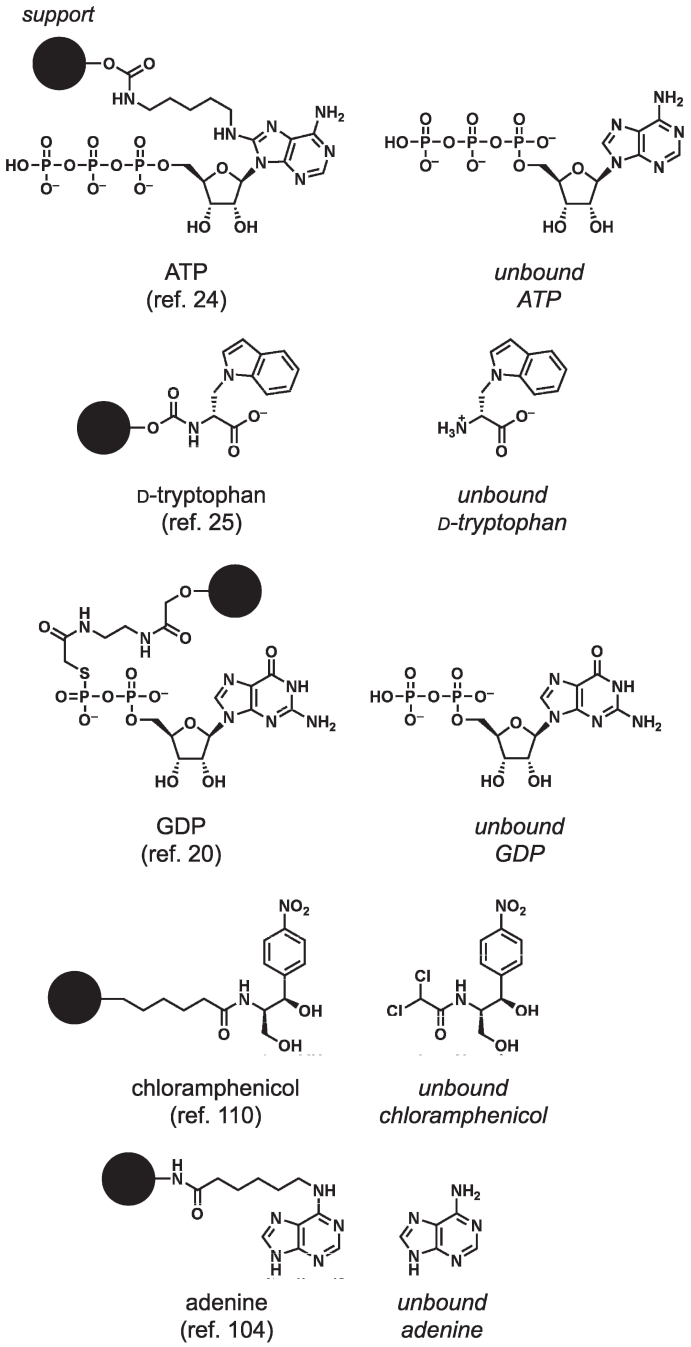

Fig. 3.3 Attachment of small-molecule RNA aptamer targets to solid support. On the *right* are shown unbound versions of each target. *GDP*, guanosine diphosphate

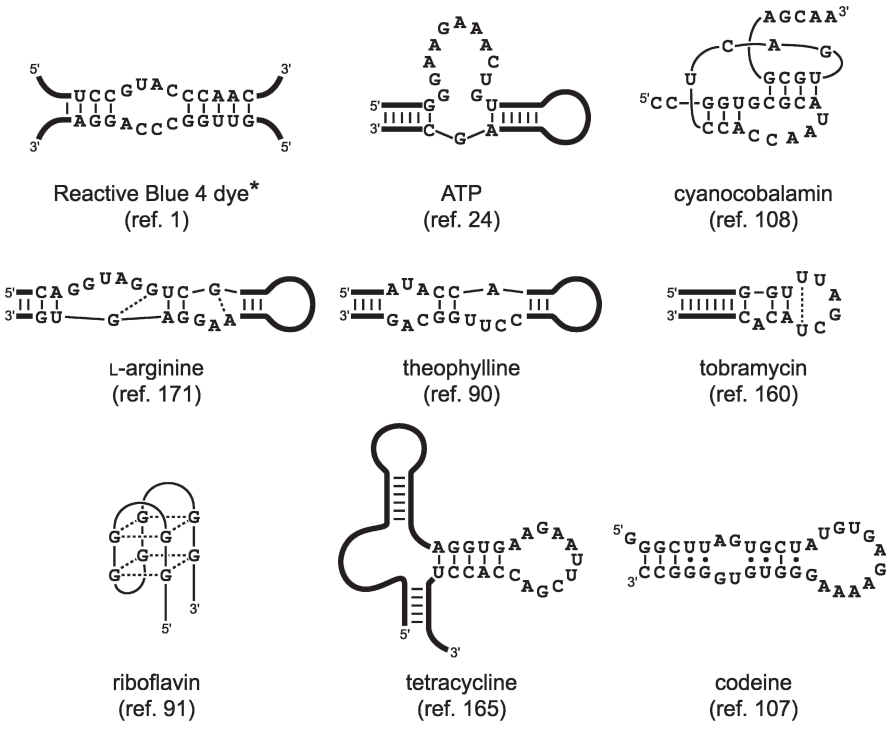

Fig. 3.4 Representative RNA aptamers, shown in proposed secondary structures. The *asterisk* (*) indicates that only the core motif of the dye binding site is illustrated

other targets includes various antibiotics, cofactors, and metabolites. See Table 3.1 for a compilation of RNA aptamer binding constants for small-molecule targets.

Organic dyes were used not only in the initial aptamer selection experiments[1] but in several subsequent studies.[112,158,159] As mentioned earlier, one of the first RNA aptamers was selected for binding to ATP.[24] Soon thereafter, an aptamer for theophylline was reported.[90] This aptamer was identified using negative selection against binding of caffeine, and excellent (10^4-fold) discrimination was observed. Aptamers were subsequently identified that bind to nucleobases,[103] to nucleosides and nucleotides,[20,101,104,106] or to their modified or damaged analogues.[93,95] Aptamers have also been found for the adenosine moiety of *S*-adenosylmethionine (SAM)[100] and for *S*-adenosylhomocysteine (SAH).[97]

Many aptamers have been developed for naturally occurring antibiotics such as tobramycin,[160,161] neomycin,[105] lividomycin,[162,163] kanamycin A,[162] kanamycin B,[164] chloramphenicol,[110] streptomycin,[96] tetracycline,[165] and the peptide antibiotic viomycin.[166] The example of chloramphenicol illustrates that even key functional groups of the target molecule can be missing when tethered to the solid support (see Fig. 3.3), yet the selection process still leads to highly functional aptamers.

Aptamers have been identified for biological cofactors such as cyanocobalamin (vitamin B_{12}),[108] flavin derivatives,[91,99,167] biotin,[113,168] and coenzyme A (CoA).[94,169] Aptamers have also been identified for free amino acids or their derivatives such

Table 3.1 Binding constants (K_d values) of RNA aptamers for small-molecule targets

Small-molecule target	K_d, μM	Reference
Tobramycin	0.002	160, 161
Sialyl Lewis X (sLe^X)	0.003	174
Cyanocobalamin (vitamin B_{12})	0.09	108
Theophylline	0.1	90
S-adenosylhomocysteine	0.1	97
Neomycin	0.1	105
Kanamycin B	0.2	164
L-arginine	0.3	92
Sulforhodamine B dye	0.3	112
8-Oxo-deoxyguanosine	0.3	95
Flavin mononucleotide (FMN)	0.5	99
7-Methyl-guanosine	0.5	93
Coenzyme A (CoA)	0.5	94
4,4′-Methylenedianiline	0.5	98
ATP	0.7	24
Riboflavin	1	91
Guanine	1	103
Streptomycin	1	96
Malachite green dye	1	158
Tetracycline	1	165
Cloramphenicol	2	110
L-dopamine	2	111
Nicotinamide mononucleotide (NMN)	3	91
Codeine	3	107
ATP (recognizing triphosphate)	5	101
Biotin	6	113
Viomycin	10	166
cAMP	10	106
Adenine	10	104
D-tryptophan	20	25
L-tyrosine	40	172
Flavin adenine dinucleotide (FAD)	50	167
L-arginine	60	171
L-citrulline	60	171
Cibacron blue 3G-A dye	100	1
L-arginine	200	170
L-isoleucine	200	173
Reactive blue 4 dye	600	1
L-isoleucine	1,000	17
L-arginine	4,000	20
L-valine	10,000	19

Listed is the best K_d value for each target from the indicated reference

as dopamine.[25,92,111,170–172] One set of experiments found aptamers that bind to either arginine or guanosine, presumably as a result of the related structures of these targets.[20] Another experiment found arginine-binding RNAs that resemble the natural TAR RNA of HIV.[89] A series of experiments from the Yarus laboratory has identified aptamers for aliphatic amino acids and explored their properties.[17,19,173] These efforts have also provided empirical evidence regarding the optimal size of the random region for selection experiments.[18]

Other small-molecule targets that are bound by RNA include codeine[107] and carcinogenic amines.[98] An RNA aptamer has been found that binds with nanomolar affinity to the sialyl Lewis X tetrasaccharide.[174] Finally, aptamers for carbohydrates such as Sephadex may have utility for purification of RNA or RNA–protein complexes.[175]

Because nucleic acids are inherently polyanionic, monovalent or divalent metal ions are always required for structure and therefore function. Mg^{2+} is commonly included in the binding buffer during the selection process. In some cases, the divalent metal ion requirements of the resulting aptamers have been investigated in detail.[94,105] The Mg^{2+} may not actually be required for binding,[108] and indeed no divalent metal ions at all have been included in some selection procedures.[89,162,163] In other experiments, more than one divalent metal ion has been included, and ions other than Mg^{2+} such as Mn^{2+} or Zn^{2+} can be required for target binding.[97,106,173]

3.3.1.3 Peptide and Protein Targets of RNA Aptamers

Many manuscripts have been published on RNA aptamers for peptides and proteins. This profusion reflects the immense practical interest in proteomics methods that use aptamer technologies (see Parts II and III of this book) and also indicates the attention devoted to therapeutic applications of protein–aptamer interactions.[176] Table 3.2 contains a compilation of RNA aptamer-binding constants for protein targets.

Peptide targets for RNA aptamers include techykinin substance P,[87] a peptide derived from the Rev protein,[81] the HTLV-1 Rex ARM peptide,[61] and an Alzheimer's disease amyloid peptide.[183] Protein targets for RNA aptamers include streptavidin,[116] which may find use in affinity purifications,[85] as well as many proteins of more therapeutic interest. These proteins include human immunodeficiency virus (HIV)-1 reverse transcriptase,[49,109] HIV-1 REV protein,[51,185] HIV-1 integrase,[55] bacteriophage R17 coat protein,[50] protein kinase C,[27] vascular endothelial growth factor (VEGF; see next subsection)[52,59,186] and other growth factors,[53,177] *trans*-activating protein Tax from human T-cell leukemia virus,[28] antibodies,[80,82,84,117,124,179] immunoglobulins,[44] selectins,[83,178] interferon-γ,[57] thrombin[68,147] and other serine proteases,[29,65,69,181] prion proteins,[77,86,182] nuclear factor κB,[62] angiopoietin-2,[72] T-cell antigens,[73] integrins,[187,188] and many other proteins.[54,56,58,60,63,64,66,67,70,71,75,76,78,88,122,123,134,146,180,184,189,190]

An RNA aptamer that binds two orders of magnitude more tightly to the Tat protein than the natural TAR RNA aptamer was identified,[30] which indicates that even when Nature has already provided aptamers, improvements to binding can still be made. Several reports show that aptamers selected for a particular "epitope" can bind that target when it is present in a different context; e.g., within a full-length

Table 3.2 Binding constants (K_d values) of RNA aptamers for protein targets

Protein target	K_d, nM	Reference
Keratinocyte growth factor	0.0003	177
Vascular endothelial growth factor (VEGF)	0.05	59
Thrombin	0.05	68
HIV-1 Tat protein	0.1	30
P-selectin	0.2	178
Hemagglutinin	0.2	76
Basic fibroblast growth factor	0.4	53
Human CD4	0.4	78
Rat GPCR for neurotensin	0.4	123
Coagulation factor IXa	0.6	69
Nuclear factor κB (NF-κB)	1	62
Antibody against human insulin receptor	2	80
Interferon-γ	2	57
Human nonpancreatic secretory phospholipase A_2	2	60
Human complement C5 component	2	63
G6-9 anti-DNA autoantibody	2	179
Colicin E3	2	75
Transforming growth factor-β type III receptor	2	180
Elongation factor Tu (EF-Tu)	3	54
L-selectin	3	83
Formamidopyrimidine glycosylase (Fpg)	3	70
Angiopoietin-2	3	72
HIV-1 reverse transcriptase (RT)	5	49
Bbacteriophage R17 coat protein	5	50
Extracellular regulated kinase 2 (ERK2)	5	31
Fibrinogen-like domain of tenascin-C	5	88
HIV-1 surface glycoprotein gp120	5	134
Hepatitis C virus nonstructural protein 3 protease	6	65
Antibody against MIR of AChR	6	117
Streptavidin	7	116
Coagulation factor VIIa	10	181
Cytotoxic T-cell antigen-4 (CTLA-4)	10	73
Elongation factor SelB	20	58
Pepocin	20	67
Prion protein (PrP^{Sc})	20	182
Immunoglobulin IgE	30	44
HTLV-1 Rex ARM peptide	30	61
Alzheimer's βA4(1–40) amyloid peptide	30	183
Heparan sulfate (on cell surface)	40	184
Human epidermal growth factor receptor-3	50	74
Herpes simplex virus-1 US11 protein	70	146
HIV-1 integrase	80	55
Prion protein (PrP)	100	86
Fibronectin (on cell surface)	100	184
Substance P	200	87
Human nerve growth factor	200	56

(continued)

Table 3.2 (continued)

Protein target	K_d, nM	Reference
Streptavidin	200	85
Laminin (on cell surface)	200	184
Ras-binding domain of Raf-1	200	71
HIV-1 Tat protein	300	66
Thrombospondin (on cell surface)	400	184

Listed is the best K_d value for each target from the indicated reference

protein.[81,86,187] An RNA aptamer for a serine protease was developed by conjugating a known small-molecule covalent inhibitor to a random RNA pool and then performing selection.[132]

3.3.1.4 RNA Aptamers for In Vivo and Therapeutic Applications

Substantial efforts have focused upon applying RNA aptamers in vivo and increasingly for therapeutic purposes. For example, aptamers have been identified that act as transcriptional activators[191] and can be controlled in vivo by a small molecule that binds to a fused aptamer domain.[192] Target-regulated aptamers have been developed to control protein activity.[70]

Several aptamers for extracellular targets have been pursued.[193] The first aptamer approved for human medicinal use by the U.S. Food and Drug Administration (FDA) was Macugen,[194–196] which is effective against age-related macular degeneration and has been marketed since January 2005. This aptamer (which is heavily modified chemically; see Section 3.3.3 for a general discussion) binds to the extracellular vascular endothelial growth factor (VEGF) and suppresses angiogenesis. At present, many other RNA aptamers are in various stages of the drug development process. Many of the aptamers mentioned in the previous subsection (e.g., those that bind to growth factors and coagulation factors) interact with extracellular targets.

Aptamers have been selected using live cells as the targets,[180,184,197–201] in some cases with selectivity for certain cell types. These aptamers are thought to interact with particular molecules on the cell surface.[193] By alternation of purified protein with live cells expressing that protein as the target in a "crossover" SELEX technique, aptamers for the tenascin-C protein were identified that bind selectively to tumor cells expressing this protein.[88] Viral particles[76,202,203] or even whole organisms[190,198,204] have also been used successfully as targets.

Aptamers expressed inside of cells ("intramers") can function just as well as they do in vitro.[159,205–210] Indeed, intramers are increasingly being investigated for use in human medicine.[211–213]

3.3.1.5 Other Targets for RNA Aptamers

RNA aptamers have been identified for binding to nucleic acid structures.[214–225] Aptamers have also been selected for binding to host–guest complexes.[226]

A bis-boronic acid host was used to bind guests such as citrate or tartrate, and aptamers were identified that bind to the complex. In this fashion, RNA aptamers for these very small anionic targets were found.

3.3.2 Biochemical Characterization of RNA Aptamers

Because of their fundamental implications for understanding how nucleic acids interact with other molecules, and also for their practical utility, many aptamers have been characterized extensively by biochemical means. These characterizations are presented here. Nuclear magnetic resonance (NMR) and X-ray structural studies of both RNA and DNA aptamers are discussed together in Section 3.5.

3.3.2.1 Secondary Structure Analysis of RNA Aptamers

Before analysis of secondary structure, the minimal range of nucleotides that is required by an aptamer for target binding may be determined by boundary mapping.[43,44,57,60,62,63,65,94,96,100,104–106,110,111,113,167,170,172] In this procedure, the aptamer is radiolabeled at either its 5′-terminus or 3′-terminus. After partial alkaline hydrolysis is used to generate a ladder of cleaved aptamers, the RNA sequences that can bind to (and be eluted from) target-derivatized solid support are revealed by polyacrylamide gel electrophoresis (PAGE). Alternatively, restriction endonucleases can be used to truncate the DNA that encodes an RNA aptamer, and the resulting RNAs can be screened to determine a cutoff point in the sequence beyond which target-binding function is lost.[108]

Aptamers can often tolerate nucleotide changes at particular positions, as long as Watson–Crick base-pairing interactions are maintained.[227] Via analysis of such base-pair covariations, which may be revealed by sequence alignments of many initial clones,[228] individual secondary structures may be proposed (see Fig. 3.4). Such secondary structures may also be proposed even for orphan sequences via secondary structure prediction programs such as mfold.[229] Alternatively, an "artificial phylogeny" may be generated by randomization and reselection.[75,180] By whatever means they are generated, the secondary structure predictions may then be validated by enzymatic and chemical probing experiments[24,31,65–67,71,93,103,113,167,173,230–234] or by mutagenesis in which Watson–Crick covariations are tested empirically. If enzymatic or chemical probing experiments are performed in both the absence and presence of the target, then the data may be used to provide a "footprint" of the target upon the aptamer.[20,30,55,56,58,64,67,70,75,76,89,91,92,96,104,105,107,108,110,111,116,146,164–166,172,179]

Some studies have suggested the value of embedding a nonrandom structured RNA fragment such as a stem-loop within an otherwise random region, which enables more highly functional aptamers to be identified.[227,235] Although it may be useful, this approach has not been widely adopted.

3.3.2.2 Binding Constants of RNA Aptamers: Methodology

Aptamer binding constants are determined by one of several experimental methods, or sometimes by more than one approach. One particularly common method to determine K_d for a small-molecule target is isocratic elution,[236–238] which has been applied many times.[1,17,19,20,24,25,89,98,99,107,108,111,167,170–172,183] Gradient elution may instead be used if a standard curve is first constructed on the basis of isocratic elution data.[89]

A second common method for K_d determination is equilibrium filtration.[24,90,91,94,101,103,104,106,110,111,166,167,171] Binding constants may be determined from the fraction of RNA bound as a function of immobilized target concentration.[113] Competition binding analysis has been performed using a DNA oligonucleotide that contains the target, which was a damaged DNA nucleotide.[95] Other approaches include titration of chemical modification,[105,165] equilibrium dialysis,[92,108] and electrophoretic mobility shift assay.[74,95,116]

If the target is itself a fluorophore, then observables such as fluorescence emission intensity,[91] fluorescence anisotropy,[112] or maximum emission wavelength[158] may be used to determine K_d. Alternatively, if a fluorophore can be conjugated to the target and the properties of this attached fluorophore change upon aptamer–target assocation, then fluorescence-based assay methods can be used.[160,161,164]

Determination of binding constants can be achieved by surface plasmon resonance (SPR) analysis, often called Biacore.[22,97,107,116,134,164,174,180,235] Related to measurements of binding constants are analysis of aptamer–target interactions by atomic force microscopy.[239–241]

For peptide and protein targets, binding constants have been determined by equilibrium dialysis,[87] electrophoretic mobility shift assay,[30,58,61,64,81,82,85,117,146] filter-binding assay,[23,28,29,31,43–45,50,52,53,55–60,62–65,67,68,70,72,73,75,83,86,123,140,177] immunoprecipitation,[80] flow cytometry,[78] binding to protein immobilized on plates,[88] Biacore,[66,88] and saturation analysis of binding to the surface of live cells.[184] In some cases, binding is assessed indirectly, via determining the effect of the aptamer on an appropriate biochemical activity of the protein target.[29,109,122,132]

3.3.2.3 Binding Constants of RNA Aptamers: Quantitative Data

Binding constants (K_d values) for small-molecule targets of RNA aptamers are collected in Table 3.1. The tobramycin aptamer currently has the highest reported affinity for its small-molecule target (~2 nM),[160,161] although much weaker K_d values can be determined experimentally. It is not surprising that an aminoglycoside antibiotic such as tobramycin binds particularly well to RNA, because the protonated amino groups of an aminoglycoside can interact electrostatically with the polyanionic nucleic acid. However, the binding is not solely electrostatic, because substantial selectivity in target binding is observed.

For protein targets, aptamers are frequently compared favorably with antibodies.[242] Aptamers have several advantages compared with antibodies, such as selectability against toxic or nonimmunogenic targets; selectability under nonphysiological

conditions; uniformity of synthetic batches; longer shelf life; relatively small size; and ease of chemical modification. In general, the binding constants of aptamers for their protein targets are competitive with antibody binding constants. Several K_d values for aptamers to protein targets are collected in Table 3.2. Many of these K_d values are low nanomolar or better; currently the best reported is 0.3 pM for keratinocyte growth factor.[177] The origin of this high affinity is not entirely clear, but the 2′-fluoropyrimidine nucleotides used in this selection effort (see Section 3.3.3) are required to achieve the affinity.

To place the nanomolar or stronger K_d values for protein targets in context, it is important to note that even a random RNA pool can bind a protein target with submicromolar affinity. For example, the K_d of the random pool was 200 nM for the VEGF aptamer selection[52] and 30 nM for the keratinocyte growth factor aptamer selection.[177] A typical observation is that two to three orders of magnitude increase in pool affinity (relative to the initial random pool) is obtained during the selection process.

3.3.2.4 Evolutionary Considerations for RNA Aptamers

The relationship between binding ability and "informational complexity" has been explored experimentally with GTP aptamers.[227] One important conclusion was that increasing the binding strength by a factor of 10 requires an RNA structure that is approximately 1,000-fold less frequent within a pool of random sequences. Importantly, the authors concluded on the basis of additional data that selectivity for the target does not automatically increase when the affinity is raised.[243] In addition, the authors noted that improving aptamer binding (i.e., lowering K_d) is easier to achieve via increasing RNA tertiary stability rather than via improving RNA–target interactions, at least in their particular system.

Evolution of one aptamer sequence into another has been explored several times.[114,171,172,244] Stringent minimization of RNA aptamers has been achieved by a combination of computational and empirical approaches.[245,246] Some RNA aptamers for amino acids have a coding triplet in the binding site, which may have implications for the "RNA world" hypothesis and the origin of the genetic code.[247]

3.3.3 RNA Aptamers with Chemical Modifications

For reasons of the interest in using aptamers in vivo (see Section 3.3.1.4), chemical approaches to stabilize RNA in vivo have been investigated. One acute challenge for in vivo application of aptamers is their rapid degradation by cellular nucleases. Chemical modifications to RNA that prevent nuclease degradation allow aptamers to be used in vivo with greater efficacy.

Common chemical modifications are substitutions of the 2′-hydroxyl group of pyrimidine nucleotides with 2′-fluoro or 2′-amino.[44,45,53,57,59,60,63,68,69,72,73,78,82–84,86,88,116, 117,123,132,134,177,182,184,186,198,199,202,203,248–250] Such modifications lead to two to

four orders of magnitude increase in the serum half-life,[53,248,249] although 2′-fluoro RNAs appear superior to 2′-amino RNAs in terms of target affinities, at least in one study.[177] Nucleotides with 2′-*O*-methyl and other modifications are also often used,[251,252] and these alterations can improve the half-life considerably.[253] To reduce renal clearance of aptamers in vivo, addition of polyethylene glycol (PEG) chains,[194,254] covalent appendage of cholesterol[255,256] or biotin-streptavidin,[257] or anchoring to a liposome[258] can be employed. Locked nucleic acids (LNAs) can improve secondary structure stability and in vivo stability of an aptamer.[259] Chemically modified nucleotides may be introduced to enhance target binding rather than for stability reasons,[260–262] or to allow variations of a selection procedure (see Section 3.2.2).

3.3.4 Mirror-Image RNA Aptamers (Spiegelmers)

Natural RNA and DNA nucleotides are built using D-ribose monomers. Symmetry demands that a D-ribose-based aptamer which binds the mirror image of the desired target (such as the opposite enantiomer of a desired peptide target) can be used to subsequently synthesize an L-ribose-based aptamer that binds the correct enantiomer of the target. Cellular nucleases do not degrade RNA made from L-ribose monomers, and therefore L-ribose aptamers should be much more stable than their conventional D-ribose analogues. Based on this logic, a selection strategy has been applied to identify biologically stable L-ribose aptamers for many targets.[263] The mirror-image L-ribose RNA aptamers are termed "Spiegelmers," deriving from the German *Spiegel*, meaning "mirror." It is appropriate that this term also honors the name of Sol Spiegelman, whose work in the 1960s predated almost all the current studies on functional nucleic acids (see introduction to Section 3.6). Spiegelmers were first reported for binding to D-adenosine[264] and L-arginine,[265] and others have been identified.[266] Spiegelmers can have excellent binding activity both in vitro and in vivo.[267,268]

3.4 Molecular Targets and Properties of DNA Aptamers

Many parallels may be drawn between RNA and DNA aptamers. The selection methodologies are very similar. As described in Section 3.2, when selecting DNA aptamers the functional DNA sequences are simply converted directly into DNA for a new selection round by PCR rather than RT-PCR. In general, RNA and DNA aptamers are similar in terms of size and apparent structural complexity, and no obvious distinction has been reported in the range of targets that may be bound. One advantage of DNA over RNA is its relative stability, in terms of both chemistry (a DNA phosphodiester linkage spontaneously hydrolyzes much more slowly than an RNA phosphodiester linkage) and biochemistry (ribonucleases are ubiquitous in biologically derived samples). This section describes the molecular targets and biochemical characterization of DNA aptamers.

3.4.1 Molecular Targets Bound by DNA Aptamers

The first DNA aptamers were obtained by selection for binding of small organic dyes[26] or the protein thrombin.[38] Since then, many DNA aptamers have been developed for a variety of targets, both small molecules (Table 3.3) and proteins (Table 3.4).

One of the first DNA aptamers binds adenosine and related compounds.[102] The DNA aptamer for adenosine and its 5′-phosphate derivatives (e.g., AMP, ATP) binds two molecules of target, whereas the RNA aptamer for ATP[24] binds just one molecule.[269] The RNA aptamer does not bind ATP when made as DNA and vice versa. This lack of RNA–DNA cross-reactivity appears to be a general rule, although a riboflavin RNA aptamer did retain some binding ability when made as the corresponding DNA sequence.[91] One exception to the rule is a porphyrin-binding DNA aptamer that can be converted to an RNA aptamer of identical sequence.[270]

DNA aptamers have been identified for assorted small molecules such as organic dyes,[26,36] cocaine,[271,272] cholic acid and other steroids,[40,273,274] porphyrins,[32,275] amino acids[39] and derivatives,[42] cellobiose and other carbohydrates,[37] thalidomide,[276] and

Table 3.3 Binding constants (K_d values) of DNA aptamers for small-molecule targets

Small-molecule target	K_d, μM	Reference
Ethanolamine	0.006[a]	126
β-estradiol	0.1	274
N-methylmesoporphyrin IX (NMM)	0.4	32
Cocaine	0.4	271
Cellobiose	0.6	37
Sulforhodamine B dye	0.7	36
(*R*)-thalidomide	1	276
Cholic acid	5	40
Adenosine/ATP	6	102
Reactive green 19 dye	30	26
L-tyrosinamide	50	42
L-arginine	3,000	39

Listed is the best K_d value for each target from the indicated reference
[a]The target was immobilized on beads for the K_d measurement

Table 3.4 Binding constants (K_d values) of DNA aptamers for protein targets

Protein target	K_d, nM	Reference
Platelet-derived growth factor B-chain	0.1	43
MUC1 tumor marker	0.1	22
L-selectin	0.3	45
Immunoglobulin IgE	10	44
Thrombin	30	38
Anti-MUC1 IgG3 monoclonal antibody	50	21
Ricin	60	140
Tenascin-C	150	47
Misactivated tRNA synthetase	15,000	23

Listed is the best K_d value for each target from the indicated reference

ethanolamine.[126] As mentioned in Section 3.3, ethanolamine—with its molecular weight of merely 61—represents the smallest organic target for an aptamer known to date. DNA aptamers have also been identified for nucleic acid structures.[277,278]

In the realm of peptides and proteins, DNA aptamers have been identified for tumor marker peptides,[22] growth factors,[43] immunoglobulins,[44] selectins,[45] and other proteins.[21,79,140] This group includes proteins expressed on surface of live cells[41,47] or even anthrax spores,[279] although in the latter case the molecular target of the aptamer was not investigated. As was achieved for an RNA aptamer,[132] a DNA aptamer for a serine protease was developed by conjugating a known small-molecule covalent inhibitor to a random DNA pool and then selecting for binding.[46] Finally, a DNA aptamer has been developed that causes editing of protein synthesis by inducing hydrolysis of a misacylated tRNA synthetase.[23]

3.4.2 Biochemical Characterization of DNA Aptamers

The methods to characterize DNA aptamers are essentially the same as those used to characterize RNA aptamers (see Section 3.3.2). An approach apparently reported only for DNA is UV differential absorption spectroscopy.[36,37] Representative binding constants are listed in Tables 3.3 and 3.4. Structural characterization of DNA aptamers is somewhat more difficult than for RNA aptamers, in part because enzymatic probing with ribonucleases cannot be applied. Procedures functionally analogous to the "boundary mapping" approach applicable to RNA aptamers may be used with DNA.[43]

3.4.3 Other Considerations for DNA Aptamers

DNA aptamers have been identified using chemically modified nucleotides to increase biological stability[280,281] and also to increase binding affinity.[276] DNA Spiegelmers have been developed, in analogy to RNA Spiegelmers (see Section 3.3.4). The first DNA Spiegelmer was developed for the peptide hormone vasopressin.[282] Others have since been identified.[266,283,284]

3.5 Direct Structural Analysis of RNA and DNA Aptamers

3.5.1 NMR and X-Ray Crystallography Analysis of Aptamers

Direct structural studies of aptamer–target complexes by NMR spectroscopy and X-ray crystallography have revealed several basic principles behind the binding events. Aptamers are thought—and in some cases known—to be largely unstructured

in solution in the absence of their target. Upon binding, aptamers adopt highly organized conformations that allow selective target recognition (adaptive folding). The target itself can also undergo conformational changes upon being bound by the aptamer (induced fit).[285] Common features of aptamer–target contacts include stacking interactions between π systems, hydrogen bonding, hydrophobic contacts, and electrostatic interactions.[286] Shape complementarity also plays an important role in many cases. Selectivity for a target generally arises from some combination of steric hindrance, hydrogen bonding, and electrostatic complementarity.

Following are three case studies of aptamers for theophylline, ATP, and thrombin. These experiments used either NMR spectroscopy, X-ray crystallography, or a combination of both methods. In addition, NMR spectroscopy has been used to study aptamers that bind argininamide,[66,287,288] arginine and citrulline,[289] flavin mononucleotide,[290] tobramycin,[291,292] neomycin B,[293] HIV-1 Rev peptide,[294] HIV-1 TAR RNA,[295] and an organic dye.[296] X-ray crystallography has provided structures of aptamers that bind to an organic dye,[297] biotin,[298] vitamin B_{12},[299,300] streptomycin,[301] and various proteins.[302–304] Additional structural information on RNA–target interactions is available from structures of several natural riboswitches (see Chapter 2).

3.5.2 Case Study #1: Theophylline RNA Aptamer

NMR structures of the theophylline RNA aptamer[90] have revealed fundamental principles underlying both aptamer–target interactions and binding selectivity.[305,306] In the free aptamer, the binding site is not stably formed. In contrast, the 15-nucleotide binding pocket within the aptamer–target complex is well ordered, with stacked base triples and numerous hydrogen bonds holding theophylline in place. Selectivity for theophylline versus caffeine (which differs solely by having an additional methyl group) is enforced at least in part by steric clashes involving the methyl group. In addition, two hydrogen bonds would be disrupted by introduction of caffeine's extra methyl group, and stacking interactions would likely be affected as well. Biochemical studies showed that the high affinity of the aptamer for theophylline is primarily the result of a slow dissociation rate.[307] This dissociation rate increases several orders of magnitude in the absence of Mg^{2+}, which explains the requirement for this divalent metal ion.

One particular nucleotide of the theophylline aptamer, C27, can be replaced with an abasic residue while retaining high binding affinity. Nevertheless, this nucleotide may only be A or C; either G or U leads to a much lower affinity. The origin of this requirement was traced using NMR spectroscopy to stable interactions involving the particular nucleobase in the free state of the RNA.[308] No unfavorable contacts are formed in the target-bound state; indeed, C27 is highly dynamic in the aptamer–target complex. These results serve as a reminder that nucleotide requirements do not always originate in interactions involving the bound state of the RNA. In this case, the unbound state of the RNA is clearly the source of the nucleotide requirement.

3.5.3 Case Study #2: ATP RNA and DNA Aptamers

The ATP aptamer identified by Sassanfar and Szostak in 1993[24] also binds ADP, AMP, and adenosine but discriminates against other nucleotide triphosphates. The solution structure of the aptamer–AMP complex was solved by NMR spectroscopy in two research groups.[309,310] The structures agree in both the topology and the key hydrogen bonding and stacking interactions that lead to target recognition.[311] The nucleobase (A) moiety is recognized through a G-A mismatch involving the minor groove edge of G and Watson–Crick edge of A, and not via a Watson–Crick base pair. Follow-up studies further identified the hydrogen-bonding patterns that assist in both target recognition and binding-site organization.[312,313]

An all-DNA version of the RNA aptamer does not bind ATP.[313] Indeed, NMR evidence was obtained for specific 2′-hydroxyls of the RNA aptamer that are important for binding, in addition to the 2′-hydroxyl of the adenosine nucleotide itself. A DNA aptamer for ATP has been identified,[102] and this aptamer was also studied by NMR spectroscopy.[269,314] The RNA–aptamer and DNA–aptamer complexes have different tertiary structures and even different binding stoichiometries; the RNA aptamer binds one molecule of ATP but the DNA aptamer binds two molecules of ATP. In the DNA–aptamer complex, the nucleobase moieties of the two bound target molecules are recognized by noncanonical interactions of the same type as found in the RNA–aptamer complex, despite the differences in overall architecture and stoichiometry.

3.5.4 Case Study #3: Thrombin DNA Aptamer

The thrombin-binding DNA aptamer[38] has been examined by both NMR spectroscopy[315–318] and X-ray crystallography.[319] The structural data agree in revealing two stacked guanine quadruplexes (G-quartets). However, the data disagree with regard to the connectivities among the nucleotides that compose these units. A comparative reevaluation of the two types of data suggested that the original X-ray structure was incorrect with regard to the connectivities.[320] This conclusion was confirmed by the authors of the original X-ray structure.[321] The local but not global symmetry of the aptamer was the source of the structural ambiguity.

3.6 In Vitro Selection of Ribozymes

From one point of view, aptamers are inherently simpler than nucleic acid enzymes. Both types of FNA must bind to something else, but only nucleic acid enzymes then proceed to catalyze a chemical reaction. However, the majority of known nucleic acid enzymes have nucleic acids as their substrates, and these substrates are bound by straightforward Watson–Crick base-pairing interactions. The segregation of many

nucleic acid enzymes into "binding" and "catalysis" regions greatly simplifies the binding process and essentially frees a nucleic acid enzyme to focus its attention on catalysis.

Experiments in the 1960s with Qβ replicase by Sol Spiegelman and coworkers indicated that "test tube evolution" can provide fundamental insight into nucleic acid catalysis.[322,323] Nevertheless, artificial ribozymes did not become a truly realistic objective until researchers were motivated by the discovery of natural ribozymes in the early 1980s.[2,324] Within a decade after those discoveries, selection experiments had demonstrated that RNA aptamers could readily be identified, and soon thereafter reports on artificial ribozymes identified by in vitro selection began to be published. The first in vitro selection procedures to identify artificial ribozymes were initiated with the natural *Tetrahymena* group I intron ribozyme and evolved activities that were related to RNA splicing.[9,325] Since those experiments, many efforts have focused on the selection of new catalytic activities starting from completely random-sequence RNA. One of the earliest selections sought ribozymes that ligate two RNA substrates.[326] This selection experiment is used here to illustrate several facets of ribozyme selection methodology.

3.6.1 Methodology to Identify Ribozymes

Most ribozyme selections have employed a common general approach, although the details necessarily differ for each study depending on the details of the reaction that is catalyzed. As is the case for aptamers, a ribozyme selection typically begins by solid-phase synthesis of a long DNA oligonucleotide that has a random region embedded between two constant regions (see Section 3.2). In vitro transcription is used to provide the initially random RNA pool for the first round of selection. The key design element of any ribozyme selection is to arrange for any catalytically active RNA sequences to become chemically modified during catalysis. In particular, this chemical modification must occur in such a way that the modified RNA sequences may be readily separated from sequences that are catalytically inactive and therefore chemically unmodified.

3.6.1.1 The Basic Procedures of In Vitro Selection of Ribozymes

For the first-reported RNA ligase ribozymes,[326] selection was achieved by using one substrate oligonucleotide with a 5′-terminal "sequence tag" (Fig. 3.5). The other substrate oligonucleotide was covalently joined with the random region, such that ligation of the two substrates inherently connects the sequence tag to the random region. After reverse transcription, the sequence tag then served as one of the two required PCR primer-binding sites for amplification of the catalytically active sequences. Because inactive RNA sequences did not acquire the sequence tag, they were not PCR-amplified and did not survive into the next selection round. Other

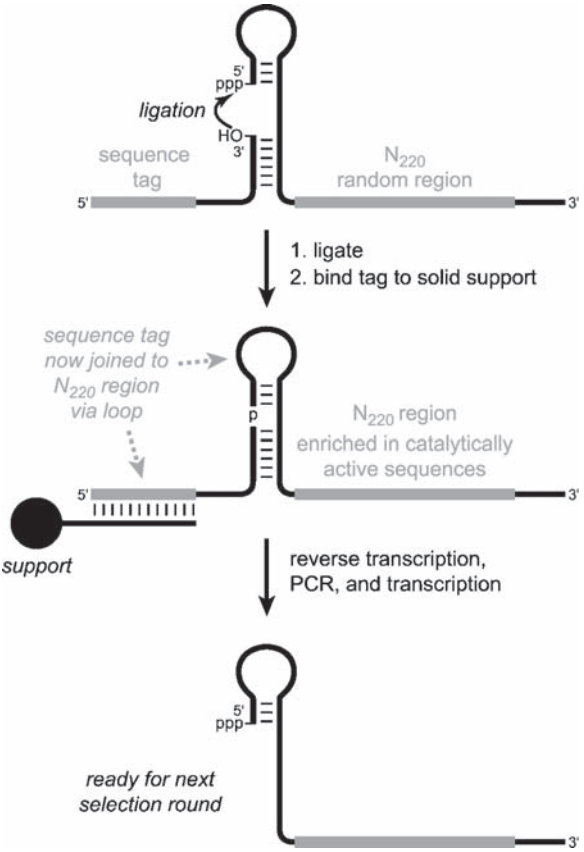

Fig. 3.5 Key selection step of the strategy for identifying the first RNA ligase ribozymes[326]

efforts have instead depended upon addition or removal of a biotin moiety,[168,327–339] addition of a thiol group,[340,341] or shift of a band on polyacrylamide gel electrophoresis (PAGE).[342–345] Occasionally more than one method has been used during the same selection experiment,[346–356] either by using more than one method in the same round or in more serial fashion, with some rounds using one method and other rounds using a different method.

Regardless of which separation method is used, once the "winning" sequences have been separated and subsequently amplified by RT-PCR, the selection rounds are iterated until the catalytic activity of the pool as a whole is satisfactory. Similar to aptamer selections, the number of rounds is typically 5–15, although in some efforts well over 20 rounds have been required. After selection rounds have concluded, individual ribozymes are cloned and tested for catalytic activity. Often this is done before any sequencing is performed; the individual ribozymes may be prepared by transcription even without knowledge of their sequences. Once ribozymes with high catalytic activities have been identified, their sequences may be determined and optimized by more detailed follow-up experiments.

As is the case for aptamer selections, many incubation variables such as pH, temperature, buffer, organic cosolvent, and metal ions must be considered. In addition, the incubation time itself is a particularly important variable, because shorter incubation times impose selection pressure for faster ribozymes. For the original RNA ligase ribozymes,[326] the initial rounds of selection were performed at pH 7.4, 600 mM KCl, and 60 mM $MgCl_2$ at 25°C for 16 h, although changes were made in the later selection rounds. This necessity highlights the large number of variables to consider, each of which may have a wide range of values—and in most cases, the optimal values to favor catalysis are not known at the outset of selection. Therefore, several ribozyme selections are often performed in parallel, with numerous combinations of the variables explored in side-by-side experiments. Particularly when some of these combinations are more successful than others, the results provide information on which specific incubation conditions are essential to optimal catalytic activity.

The length of the random region used in ribozyme selections is an important consideration. Successful ribozyme selections have used random regions up to N_{228}^{350}, for which sequence space encompasses $4^{228} \approx 10^{137}$ possibilities. For N_{228} selections that are initiated with 10^{15} molecules, only the incredibly small fraction 10^{-122} of sequence space is explored, yet these experiments have successfully led to active ribozymes. At least for the investigated catalytic activities, this success implies that the functional RNA sequences are quite common in sequence space.[326,348] More typically, random regions for ribozyme selections are between N_{40} and N_{80}. Complex catalytic motifs benefit from particularly large random regions,[16] but excess sequence elements can inhibit catalysis, so larger is not always better. To account for the various uncertainties in the optimal length of random region, several selection experiments that each have a different length of random region may be performed in parallel.

3.6.1.2 Additional Considerations for Ribozyme Selections

Negative selection (see Section 3.2.1.2) may be applied to eliminate RNA sequences that catalyze undesired reactions and therefore opportunistically survive the selection procedure.[357] Of course, the best approach to success in ribozyme selection is to design the procedure with sufficient care such that the only way that sequences can survive is by catalyzing the reaction of interest. Nevertheless, "parasitic" sequences can survive the selection without actually catalyzing the desired reaction. As just one example, if a selection for RNA ligation depends upon a gel shift to separate active from inactive sequences, those pool sequences that fold in such a way that they migrate at the position of the larger ligated product may opportunistically survive each round. In unfavorable cases, such parasitic sequences may come to dominate the overall effort, in which case it may be imperative to use either negative selection or multiple physical techniques for the key separation steps of successive rounds.

One approach to identify ribozymes is to begin with an RNA aptamer sequence, then add a random region and select for ribozymes that both bind the substrate and

catalyze a reaction of the substrate. This approach has been used successfully,[168,340] although it is not clear that the initially programmed aptamer subunits are functionally retained in the final ribozymes. Furthermore, anecdotal evidence and theoretical considerations suggest that this strategy may not work in all cases. For example, aptamer binding may occlude a site on the target molecule that must be accessible for catalysis to occur. A related approach to achieve a complicated catalytic activity is to start with a known artificial ribozyme and attach a random region to enable an even more challenging catalytic activity. As one example, this approach was used with spectacular success to identify an RNA polymerase ribozyme that is capable of processive nucleotide additions to a growing RNA chain.[347]

Because sequence space is too large to be covered thoroughly when the random region is N_{25} or larger, initially obtained ribozyme sequences are probably not optimal catalysts, and systematic methods to examine variant sequences are useful. Error-prone PCR (mutagenic PCR) is one such method.[115] Appropriate PCR conditions (commonly, inclusion of Mn^{2+}) are known to increase the Taq polymerase error rate, and this can be used to introduce variation into the enzyme pool during any particular selection round. Alternatively, nonstandard nucleotide analogues may be used to promote random mutations during the PCR step.[358] Reselection (see Section 3.2.1.2) is a second approach that may be used to improve ribozyme activity. A new pool is prepared based on a known ribozyme sequence, but with partial randomization. For example, a typical reselection effort might use a pool in which each ribozyme nucleotide position has a 70% probability of being the nucleotide originally present in the ribozyme and a 10% probability (each) of being one of the other three nucleotides. It is straightforward to compute the distribution of expected mutations in the resulting pool,[359–362] although the optimal extent of mutation is difficult to know in advance.

Finally, many ribozymes are converted from a *cis*-acting (intramolecular) to a *trans*-acting (intermolecular) form; i.e., to a form of the ribozyme in which the substrate is not covalently attached to the ribozyme at the outset of the reaction. Of course, only *trans*-acting ribozymes are in principle capable of multiple turnover catalysis, which is often a practical objective. For ribozymes that cleave or ligate nucleic acid substrates, catalysis in *trans* is usually achieved simply by omission of a covalent phosphodiester linkage that is present between the ribozyme and one of its substrates during the selection process. For ribozymes with other catalytic activities, no general prescription exists for conversion into a *trans*-acting form. If during selection a substrate is attached to the ribozyme by a covalent (e.g., PEG) tether, then omitting some or all of the tether may permit multiple-turnover catalysis.[330] However, this is not guaranteed to be successful. In some cases, one may anticipate that achieving multiple-turnover catalysis will require a method that inherently allows selection directly for this feature (see next section).

3.6.1.3 Alternative Methods for Ribozyme Selections

By analogy to efforts with catalytic antibodies, an early approach to ribozymes was to select for binding to transition-state analogues. An aptamer that binds to

a transition-state analogue should be a catalyst for the reaction that proceeds via that transition state. Although this approach was successful in some instances,[363–365] other efforts were unsuccessful.[366] Currently, the conventional wisdom is that selecting directly for catalysis is a superior approach.[326]

Drawbacks of most conventional in vitro selection procedures are their tedious and time-consuming low-throughput nature. As one alternative, continuous evolution has been developed. In this approach, self-replicating molecules are diluted serially (e.g., 1,000-fold dilution) and at constant temperature, in contrast to employing discrete selection rounds and PCR temperature cycling. Many more cycles are possible with continuous evolution; more than 100 serial transfers are common. The early Spiegelman Qβ replicase experiments[322,323] are considered to be the first examples of continuous evolution. More recently, Joyce and coworkers have broadened the field to include evolution of catalytic function.[367] For example, continuous evolution was used to evolve an RNA ligase ribozyme that resists the activity of an RNA-cleaving deoxyribozyme.[368] Despite some advantages of speed and amplification power, continuous evolution suffers from susceptibility to contamination and limitations on the types of reactions that may be catalyzed.[369] Therefore, the true power of continuous evolution approaches to identify new ribozymes is uncertain.

A second alternative approach was spurred by recognizing a key limitation imposed by a covalent linkage between the RNA and its substrate during the selection process. This requirement often means that multiple turnover cannot be engineered into any resulting ribozymes, if the link between the RNA and substrate cannot be broken while retaining catalytic activity (see previous section). The fundamental problem is that the traditional selection procedure inherently cannot, in principle, select for multiple turnover. Therefore, procedures based on in vitro compartmentalization (IVC) have been developed.[128,129] In IVC, the candidate ribozyme sequences are encapsulated within individual droplets in a water-in-oil emulsion. If each droplet contains just one ribozyme candidate, then the encapsulation is functionally equivalent to a covalent bond in terms of linking the RNA sequence information to catalytic ability. Indeed, IVC has been applied to develop several ribozymes that achieve multiple turnover.[370,371] Although such turnover may fortuitously be possible for ribozymes that are identified via the traditional methodologies, the use of IVC allows selection explicitly to achieve this property.

3.6.2 Chemical Reactions Catalyzed by Ribozymes

All natural ribozymes catalyze phosphodiester cleavage or ligation reactions, with the exception of the ribosome that creates peptide bonds (see Chapter 2). A number of artificial ribozymes also catalyze phosphodiester cleavage or ligation, although many ribozymes with other activities have been identified. Figure 3.6 shows some representative examples of particular ribozymes, and Table 3.5 reveals the scope of ribozyme-catalyzed reactions. Although the available data do not suggest any limits on what kinds of reactions can be catalyzed by RNA, more experiments are needed to probe these limits.

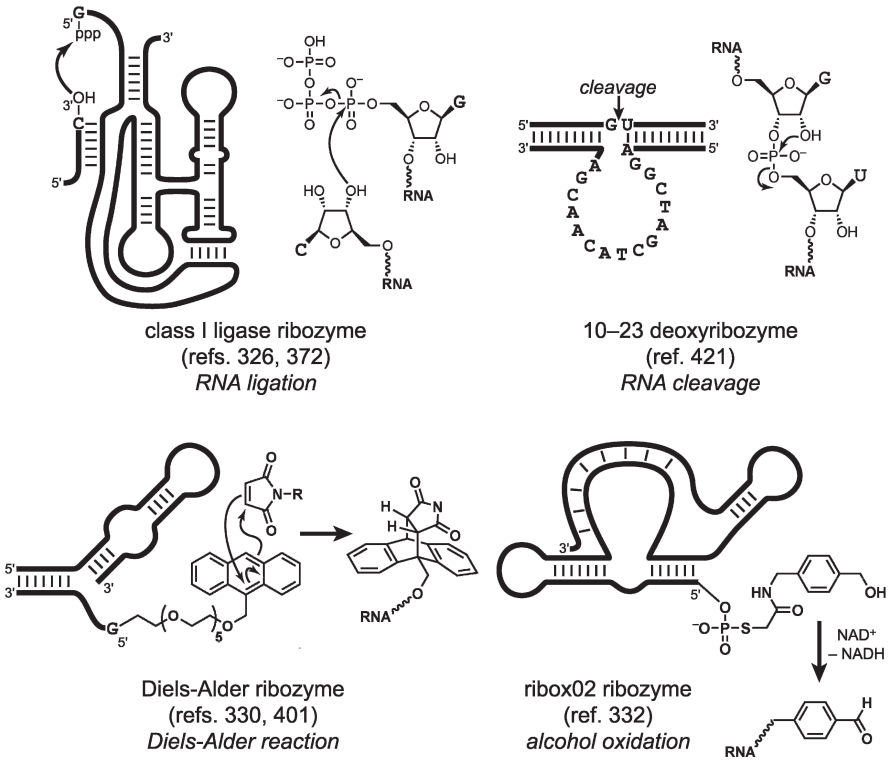

Fig. 3.6 Secondary structures and reactions of representative artificial ribozymes

Table 3.5 Artificial ribozymes

Reaction catalyzed	Bond	Rate enh.	M^{2+} req.	Reference
Cyclic phosphate hydrolysis	O–P	50	Pb^{2+}	342
RNA cleavage	O–P	80	Pb^{2+}	343
RNA cleavage	O–P	200	Mg^{2+}	344
RNA cleavage	O–P	nd	None	345
RNA ligation	O–P	7×10^6	Mg^{2+}	326
RNA ligation	O–P	8×10^8	Mg^{2+}	372
RNA ligation	O–P	5×10^5	Mg^{2+}	373
RNA ligation	O–P	250	Mg^{2+}	327
RNA branching	O–P	nd	Mg^{2+}	328
RNA phosphorylation	O–P	1×10^5	Mg^{2+}	340
RNA phosphorylation	O–P	6×10^6	Mg^{2+}	346
RNA capping	O–P	10^3–10^4	Mg^{2+}	374
RNA capping	O–P	nd	Ca^{2+}	375
RNA capping	O–P	nd	Ca^{2+}	376
Amino acid adenylation	O–P	nd	Ca^{2+}	341
Cofactor synthesis	O–P	nd	Mn^{2+}	377
RNA polymerization	O–P	nd	Mg^{2+}	378
Template-dir. polymerization	O–P	nd	Mg^{2+}	347

(continued)

Table 3.5 (continued)

Reaction catalyzed	Bond	Rate enh.	$M^{2\pm}$ req.	Reference
RNA–protein conjugation	N–P	nd	Mg^{2+}	329
Diels–Alder reaction	C–C	800	Cu^{2+}	348
Diels–Alder reaction	C–C	1×10^4	$Cu^{2+} + Ni^{2+}$	349
Diels–Alder reaction	C–C	1×10^4	Mg^{2+}	331
Aldol reaction	C–C	4×10^3	Zn^{2+}	379
Alcohol oxidation	C–H	1×10^7	$Mg^{2+} + Zn^{2+}$	332
Aldehyde reduction	C–H	3×10^6	$Mg^{2+} + Zn^{2+}$	380
Pyrimidine nt synthesis	C–N	1×10^8	Mg^{2+}	351
Purine nt synthesis	C–N	nd	Mg^{2+}	352
N^7G alkylation	C–N	3×10^6	Mg^{2+}	168
Amide synthesis	C–N	1×10^5	Cu^{2+}	353
Urea synthesis	C–N	1×10^6	nd	354
Peptide bond formation	C–N	1×10^6	Mg^{2+}	333
Peptidyl-RNA synthesis	C–N	100	Ca^{2+}	381
Acyl transfer	C–O	1×10^{10}	Mg^{2+}	335
Acyl transfer	C–O	nd	Mg^{2+}	336
Aminoacylation	C–O	2×10^5	$Mg^{2+} + Ca^{2+}$	355
Ammoacylation	C–O	nd	Mg^{2+}	337
Aminoacylation	C–O	2×10^5	Mg^{2+}	338
Aminoacylation	C–O	6×10^7	Ca^{2+}	382
Carbonate hydrolysis	C–O	100	None	365
Sulfur alkylation	C–S	2×10^3	Mg^{2+}	356
Michael reaction	C–S	3×10^5	Mg^{2+}	339
Porphyrin metalation	Cu–N	500	$Mg^{2+} + Cu^{2+}$	364
Pd nanoparticle formation	Pd–Pd	nd	None	383, 384
Biphenyl isomerization	None	88	Mg^{2+}	363

enh., enhancement; dir., directed; req., required; nd, not determined

3.6.3 Biochemical Characterization of Ribozymes

3.6.3.1 Secondary Structures and Minimization of Ribozymes

As for aptamers (see Section 3.3.2.3), ribozyme secondary structures may be proposed on the basis of computer algorithms and sequence alignments. Then, experimental verification of secondary structures may be performed by enzymatic and chemical probing along with covariation analysis. Sequences and likely secondary structures of some representative ribozymes are illustrated in Fig. 3.6.

A practical goal is often to characterize the minimal version of a particular ribozyme that is still highly functional. Minimal ribozymes are important because smaller ribozymes are more readily synthesized and less susceptible to random degradation; they are also easier to study mechanistically. Minimization efforts are usually guided by the secondary structures already mentioned. One must be careful not to remove nucleotides that may be catalytically important, as shown by a number of studies on the natural hammerhead ribozyme (see Chapter 2 for more discussion of this issue).[385] Nonhomologous random recombination may also

be used in tandem with selection for direct minimization.[386] One advantage of this approach is the lack of bias that would be introduced via any preconceived notions of which secondary structure elements are important for ribozyme activity.

3.6.3.2 Ribozyme Mechanisms and Rate Enhancements

Evidence has increasingly accumulated that natural ribozymes can rely mechanistically upon acid–base catalysis involving the nucleobases.[387,388] It seems likely that artificial ribozymes will be able to take advantage of similar mechanisms. However, little is known about the mechanisms of most artificial ribozymes. Rate parameters and metal ion requirements (see Table 3.5) are usually determined as part of the overall characterization. In contrast, detailed mechanistic analyses are rare, although it is clear that relatively sophisticated physical organic approaches such as kinetic isotope effects may be applied.[389] The catalytic roles of metal ions are often unknown. Because metal ions are required simply for binding of targets by aptamers (see Section 3.3.1), separating the binding and catalysis roles of metal ions for ribozyme activity is a tremendous experimental challenge. The mechanistic roles of metal ions have been explored most extensively for acyl transferase ribozymes.[390–393]

One aspect of ribozyme activity that is often quantified is the rate enhancement (see Table 3.5). For any particular ribozyme, an appropriate background reaction with a relatively low rate can usually be identified. For a ribozyme that ligates two RNA substrates, the relevant background reaction could be taken as the analogous ligation reaction that occurs when the two reacting functional groups are held in together by a complementary splint that lacks an enzyme region, rather than the ribozyme itself (which has both binding and catalytic regions). From the ratio of rates of the background and catalyzed reactions, the rate enhancement may be computed (Fig. 3.7). The observed ribozyme rate enhancements range from modest (10^2) to substantial (10^{10}). Although all these values pale in comparison with rate enhancements for some proteins, the appropriate benchmarks are the natural ribozymes, against which artificial ribozymes compare favorably.

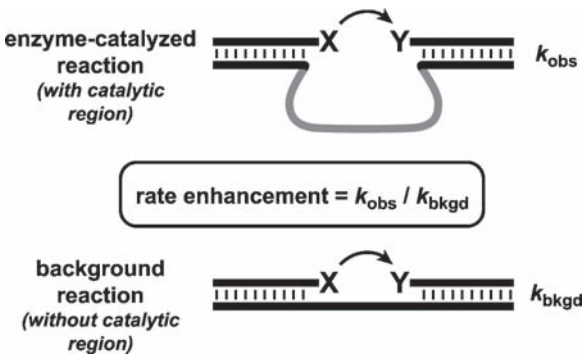

Fig. 3.7 Quantifying the rate enhancement of a ribozyme by comparison of its reaction rate (k_{obs}) to the rate of an analogous "splinted" background (k_{bkgd}) reaction

The large rate enhancements of artificial ribozymes imply that they do more than passively hold their substrates in close proximity via "effective molarity." Consistent with this, almost all ribozymes form just one product, even when multiple products are chemically possible. For example, although the early RNA ligase ribozymes could have made multiple isomeric linkages during synthesis of the ligated RNA, each particular ribozyme was found to make just one type of linkage.[326] This finding is in sharp contrast to effective molarity considerations, which would ordinarily be expected to permit formation of a mixture of isomeric linkages. In most cases, the mechanistic explanation for ribozyme activity is not yet known. As for proteins, the two main possibilities are direct lowering of transition-state energies and precise positioning of the reactive groups (i.e., orientation effects). Given that these mechanistic issues have not been settled for most of the natural ribozymes, including the ribosome,[394–396] it is clear that mechanistic ribozymology is still a nascent field.

3.6.3.3 Ribozyme Structural Biology

X-ray crystal structures or NMR structures are available for many natural ribozymes (see Chapter 2). In contrast, artificial ribozymes have not yet been investigated widely by these structural methods. The Pb^{2+}-dependent RNA-cleaving "leadzyme" has been investigated,[397–400] revealing probable relationships between metal ion binding and structural rearrangements that are required to reach the catalytically active conformation. Separately, a Diels–Alderase ribozyme has been examined,[401] showing that the substrate-binding pocket is hydrophobic and providing a rationale for the observed enantioselectivity. Finally, an RNA ligase ribozyme has been studied; its structure suggests that general base catalysis is involved in the ligation mechanism.[402] Beyond these three examples, much work remains to understand the structural basis of artificial ribozyme catalysis.

3.6.3.4 Evolutionary Considerations for Ribozymes

Certain features of artificial ribozymes have implications for prebiotic chemistry and the "RNA world" hypothesis. For example, ribozymes that incorporate three or fewer different nucleotides (rather than the conventional four) have been investigated. One effort omitted cytidine (C) from the enzyme region and identified ribozymes that ligate RNA.[403] Performing reselection with inclusion of C allowed the catalytic rate to improve 20-fold, which calibrates our understanding of the importance of structural variety in ribozyme function.[404] Remarkably, an RNA ligase ribozyme comprising only two different nucleotides was also identified.[405] This "binary informational system" included only uridine (U) and 2,6-diaminopurine (D), which can form base pairs with each other (Fig. 3.8). Although this ribozyme was fairly inefficient, its identification demonstrates that a highly minimal system can encode relevant catalysis.

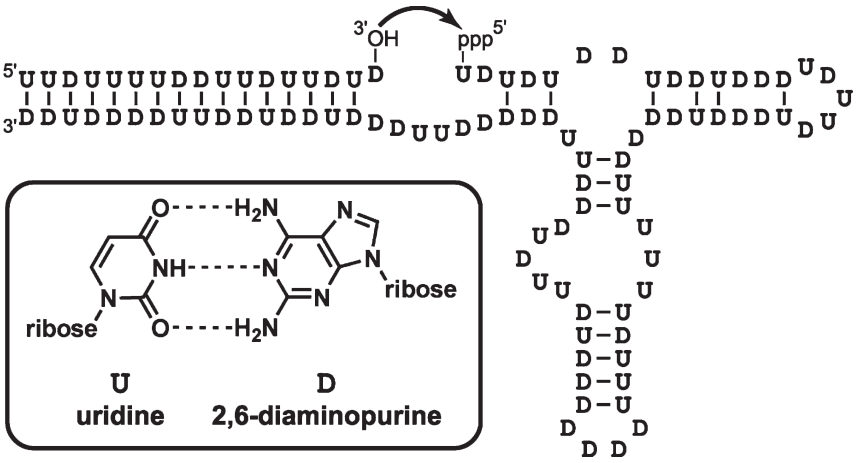

Fig. 3.8 A minimal RNA ligase ribozyme that has only two nucleotides, uridine (*U*) and 2,6-diaminopurine (*D*)[405]

An interesting conceptual challenge is to evolve one ribozyme sequence into another. One study found evidence that a single RNA sequence can adopt either of two entirely distinct secondary structures, each of which has a different catalytic activity.[406] Furthermore, this bifunctional sequence could be accessed by a series of no more than two mutation steps from prototype ribozymes that catalyze only one of the two activities. Therefore, the collection of ribozymes forms a "neutral network" that has implications for understanding early RNA evolution. Another study focused on the evolution of kinase ribozymes starting from an aminoacylase ribozyme.[346] Only a relatively small number of mutations were needed to accomplish the conversion, although the probability of obtaining the new catalytic activity rose sharply when more mutations were introduced.

3.6.4 Ribozymes with Chemical Modifications

Similar to aptamers (see Section 3.3.3), the biochemical stability of ribozymes can be improved by judicious incorporation of nonstandard nucleotides. This approach frequently uses 2′-fluoro or 2′-aminopyrimidine nucleotides, which confer resistance to ribonucleases.[407]

To enhance catalytic activity, several ribozyme selection efforts have used modified nucleotides that introduce functional groups not found naturally in RNA. The first such effort sought ribozymes that catalyze the Diels–Alder reaction, with the assistance of pyridine-modified uridine derivatives.[348,349] Most of the ribozymes required Cu^{2+}, suggesting a role for Lewis acid catalysis, and the pyridine groups were conjectured to participate in some combination of hydrogen bonding,

hydrophobic interactions, dipolar interactions, and metal ion coordination. Because the pyridine was attached via the C5 of uridine, Watson–Crick base-pairing interactions were not disrupted, and the modified nucleotides could be incorporated into RNA via T7 RNA polymerase. Other efforts with modified nucleotides have also been reported, involving 5-imidazolyl-U and amide synthesis,[353] N^6-amine-modified adenosines and RNA ligation,[327] or 5-imidazolyl-U and urea synthesis.[354]

An interesting series of experiments has identified ribozymes that catalyze crystallization of palladium nanoparticles.[383,384] These efforts used pyridine-modified U nucleotides, and these nonstandard nucleotides were required for catalytic activity. Different ribozymes create different crystal shapes, such as hexagonal plates or cubes. The mechanistic basis for the selective crystallization is not known.

3.7 In Vitro Selection of Deoxyribozymes

DNA differs from RNA solely by absence of the 2′-hydroxyl group at every nucleotide position of DNA. Because RNA has relatively few functional groups to begin with, the missing hydroxyl group has long been speculated to render DNA catalytically inferior to RNA.[408] This speculation was reinforced by the natural role of DNA, which is for genetic information storage as a double helix. Nevertheless, just like single-stranded RNA, single-stranded DNA has conformational flexibility that could permit intricate three-dimensional shapes and consequently catalytic activity. In 1994 the first deoxyribozyme was discovered by in vitro selection,[409] and since that time an increasing variety of DNA catalysts has been identified.

3.7.1 Methodology to Identify Deoxyribozymes

Differing from ribozymes, the DNA template does not need to be transcribed into RNA and then (after isolation of the catalytically active sequences) reverse-transcribed back into DNA. Instead, for deoxyribozymes the DNA functions as both information and catalyst throughout the selection process. Other than this procedural difference, the methodology to select deoxyribozymes is essentially the same as for ribozymes (see Section 3.6.1). This method includes several examples of nonstandard nucleotides used to enhance the chemical repertoire of DNA.[410–415] Negative selection may also be used; for example, to improve the metal ion specificity of RNA-cleaving deoxyribozymes.[416]

As is the case for identifying aptamers, single-stranded DNA needs to be separated from its complement after PCR during each round of selection; this can be achieved by incorporating a moiety such as a polyethylene glycol (PEG) spacer in one of the two PCR primers.[417–419] The PCR enzyme—usually Taq polymerase cannot—extend past the spacer within the template strand, and therefore the two unequal-length single strands of the PCR product are separable by PAGE. Other

approaches can be used; for example, based on removal of the biotinylated form of the undesired DNA strand (see Section 3.2.1.1).

3.7.2 Chemical Reactions Catalyzed by Deoxyribozymes

Many fewer types of reactions have been explored using deoxyribozymes rather than ribozymes, reflecting the later discovery of deoxyrbozymes and also the emphasis placed on catalytic RNA by the "RNA world" hypothesis. Nonetheless, deoxyribozymes (which are also termed DNA enzymes, DNAzymes, or catalytic DNA) have proven quite competent catalytically when they have been examined (Table 3.6). Most of the known DNA-catalyzed reactions involve phosphodiester exchange.

3.7.3 Biochemical Characterization of Deoxyribozymes

Experimental data indicate that DNA is quantitatively as competent as RNA in terms of catalytic ability. For example, the RNA-cleaving 10–23 deoxyribozyme can achieve a k_{cat} of $10\,min^{-1}$, which rivals natural ribozymes, and its k_{cat}/K_m is

Table 3.6 Artificial deoxyribozymes

Reaction catalyzed	Bond	Rate enh.	M^{2+} req.	Reference
RNA cleavage	O–P	10^5	Pb^{2+}	409
RNA cleavage	O–P	10^5	Mg^{2+}	420
RNA cleavage	O–P	50	Mg^{2+}	421
RNA cleavage	O–P	1×10^8	None	422
RNA cleavage	O–P	nd	Zn^{2+}	410
RNA cleavage	O–P	nd	None	411
RNA cleavage	O–P	10^5	None	412
RNA ligation	O–P	300	Mg^{2+}	419
RNA ligation	O–P	2×10^4	Zn^{2+}	423
RNA ligation	O–P	10^4	Mg^{2+}	424
RNA ligation	O–P	10^5	Zn^{2+}	424
RNA branching	O–P	5×10^6	Mn^{2+}	425
RNA branching	O–P	10^5	Mg^{2+}	426
RNA lariat formation	O–P	10^5	Mn^{2+}	427
DNA phosphorylation	O–P	10^9	Mn^{2+}	428
DNA adenylation (capping)	O–P	2×10^{10}	$Mg^{2+} + Cu^{2+}$	429
DNA ligation	O–P	3×10^3	Cu^{2+} or Zn^{2+}	430
DNA ligation	O–P	10^5	Mn^{2+}	431
Oxidative DNA cleavage	C–O	10^6	Cu^{2+}	432, 433
DNA deglycosylation	C–N	9×10^5	Ca^{2+}	418
Thymine dimer photoreversal	C–C	3×10^4	None	434
Phosphoramidate cleavage	N–P	10^3	Mg^{2+}	435
Porphyrin metalation	Cu–N	1×10^3	Cu^{2+} or Zn^{2+}	436

enh., enhancement; req., required; nd, not determined

~10^9 M^{-1} min^{-1}, which is higher than that of the protein enzyme ribonuclease A.[421] Furthermore, deoxyribozymes that cleave RNA are at least as proficient as ribozymes that accomplish the same task.[437]

The similarities between RNA and DNA enzymes may relate to common classes of mechanisms, although few deoxyribozymes have been investigated in detail.[438,439] It is intriguing to note that RNA-cleaving deoxyribozymes can use cofactors such as ascorbate or histidine as cofactors,[432,440] thereby demonstrating that DNA can use noncovalently associated small molecules to expand its relatively limited repertoire of functional groups. Structural investigations of deoxyribozymes have also been limited. In the only experiment published to date, the 10–23 deoxyribozyme was crystallized but formed an inactive 2:2 complex with its RNA substrate.[441] Although the resulting structure was an interesting four-way junction that has implications for understanding natural Holliday junction intermediates of recombination, no insights into DNA catalysis could be obtained.

It is interesting to ask if a ribozyme and deoxyribozyme can share the same nucleotide sequence (substituting U for T nucleobases) yet retain catalytic activity. In one study, a deoxyribozyme with hemin-dependent peroxidase activity was shown to retain some activity when all its DNA nucleotides were exchanged for RNA.[270] In the other direction, selection was used to convert a known RNA ligase ribozyme into a deoxyribozyme.[442] The ribozyme was catalytically inactive when made as DNA, and the evolved deoxyribozyme was inactive when made as RNA. If a single nucleotide sequence could be identified that is functional as either RNA or DNA, this would have implications regarding crossover between the two types of informational systems.

3.8 In Vitro Selection of Aptazymes

For practical applications of functional nucleic acids, an important goal is regulation of nucleic acid enzyme catalysis. A key regulatory mechanism for protein enzymes is allostery, in which binding of a target to an enzyme remote from the active site controls the catalytic activity. Similarly, experiments have focused on placing artificial nucleic acid enzymes under the control of targets that bind at sites distant from the active site. These efforts have combined aptamers for target binding with nucleic acid enzymes for catalysis, resulting in allosteric nucleic acid enzymes, or "aptazymes."[443]

3.8.1 Aptazymes Obtained by Rational Fusion of Aptamers with Nucleic Acid Enzymes

In the basic design for an aptazyme, an aptamer that binds a particular target is connected via a "communication module" to a ribozyme. Binding of the target can lead to either an increase or a decrease in ribozyme activity. The first report

of a rationally designed aptazyme was published in 1997, using ATP binding to its aptamer for inhibition of hammerhead ribozyme catalysis (Fig. 3.9).[444] Subsequent efforts with the hammerhead ribozyme were successful with other targets such as flavin mononucleotide,[445,446] theophylline,[445,446] and proteins.[447,448] Additionally, many other ribozymes such as the HDV,[449] hairpin,[450] group I intron,[449,451] and X-motif[449] ribozymes have been converted into aptazymes. In general, a wide range of aptamer targets has been used with many ribozymes.[452]

In many of these cases, no selection at all was involved, in that known aptamer and ribozyme domains were simply joined via strategically placed nucleotides to create the aptazyme. Screening of candidates with different communication modules allowed identification of functional aptazymes. In this fashion, some designed aptazymes can respond to more than one target,[453] presaging analogous discoveries involving natural riboswitches (see Chapter 2). In addition, more than one aptamer domain may be attached to a single enzyme.[454] In a related approach to identifying aptazymes, the power of in vitro selection has been used to find optimal communication modules,[449,455–458] including the use of negative selection to obtain maximal response to the target. In all of these experiments, the aptamer and ribozyme units themselves remain intact. In that context, aptazyme creation by fusion of aptamer

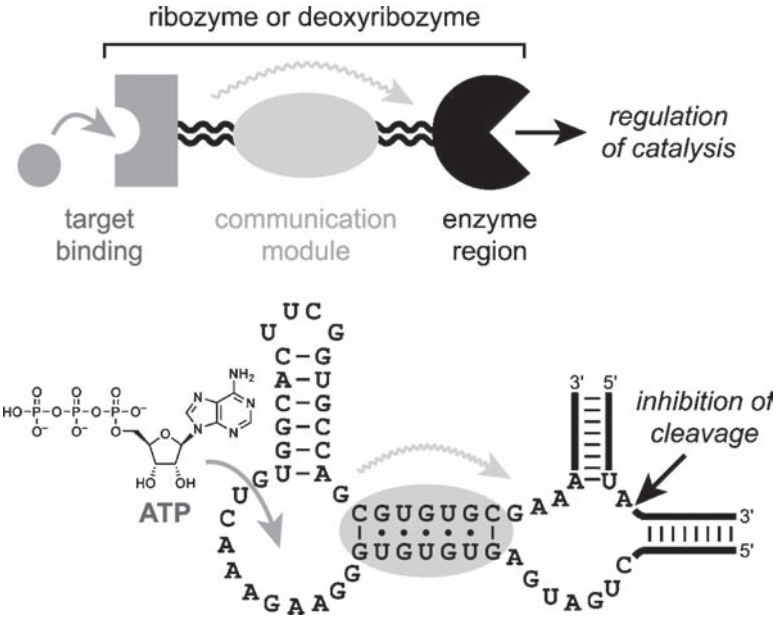

Fig. 3.9 Creating an aptazyme by rational fusion of an aptamer with a ribozyme. Schematic view (*top*); specific example of ATP-inhibited aptazyme (*bottom*)[444]

and enzyme domains (without or with selection to optimize the communication module) may be considered a rational process.

Allosteric deoxyribozymes have been pursued to a limited extent. The sole unambiguous report of an allosteric deoxyribozyme for a small-molecule target (in the general design sense of Fig. 3.9) is an ATP-regulated RNA-cleaving deoxyribozyme, whose allosteric activation was optimized by selecting for functional communication modules.[459] Using related design principles, studies have developed adenosine-activated RNA-cleaving deoxyribozymes[460] for practical applications.[461] Allosteric deoxyribozymes have also been developed by using competition between a regulatory oligonucleotide and the aptamer target to control deoxyribozyme catalysis.[462] Finally, an ATP-responsive RNA-cleaving allosteric deoxyribozyme that functions via an inhibition-reversing strategy was created (as discussed in more detail in Chapter 5).[463] In this approach, the aptamer sequence is embedded within a portion of the deoxyribozyme near the catalytically essential nucleotides, such that these nucleotides are sequestered within a stem-loop. Interaction between the small-molecule target and the aptamer sequence displaces the sequestering nucleotides and allows the catalytic core of the deoxyribozyme to form.

3.8.2 Aptazymes Obtained by In Vitro Selection for Regulated Catalysis

In the foregoing studies, the target-binding domain of the aptazyme was preprogrammed by using a known aptamer. Alternatively, a random region can be fused to a known ribozyme, and in vitro selection can then be used to identify aptazyme sequences that are regulated by the target in the desired fashion. The first report of such direct selection of aptazymes sought regulation of catalysis via binding of cGMP or cAMP.[464] Subsequent experiments identified aptazymes that are controlled by a range of targets including divalent metal ions,[465] caffeine and aspartame,[466] and other small molecules,[467–469] in addition to proteins.[470] Experiments have also used partial randomization and reselection of a known aptamer (as part of an aptazyme) to improve aptazyme function.[457,471]

Aptamer domains within aptazymes can be identified and validated separately for their target-binding ability.[471] Therefore, selection of aptazymes is an indirect way to select for aptamers themselves. One methodological advantage of this approach for identifying aptamers is that the target does not need to be covalently modified for immobilization on a solid support, which is particularly advantageous if the target compound is available in only small quantities or if its chemical modification is difficult. As a separate conceptual advantage of this approach, the aptamer domain can completely engulf the target (analogous to some natural riboswitches[472,473]), which is not possible when a covalent tether must be attached to the target to enable the selection process (see Fig. 3.3, Section 3.3.1.1).

3.8.3 Mechanisms of Aptazyme Signal Transduction

The mechanism by which target binding to the aptamer leads to regulation of nucleic acid enzyme catalysis has been investigated in several studies. The known mechanisms include steric interference between the aptamer and enzyme domains,[474] "slipping" of secondary structure involving the communication module,[455,475,476] and stabilization of catalytically active enzyme structure.[445,446,477] Other mechanisms are presumably possible. Oligonucleotide-dependent nucleic acid enzymes are regulated by different mechanistic principles that involve generally straightforward base-pairing interactions.[443,478–484] Aptazymes that combine regulation by both small molecules and oligonucleotides have also been developed.[485]

3.9 Perspective on Artificial Functional Nucleic Acids

What fundamental questions remain to be addressed for aptamers and nucleic acid enzymes? For aptamers, the wide range of targets that have been recognized—from very small molecules such as ethanolamine all the way to large proteins, some of which have been presented on the exterior of a living organism—lends credence to the notion that an RNA or DNA aptamer can be identified for essentially any desired molecular target. Two research areas are probably the most pressing for future development of aptamers. First, selectivity among closely related targets has been explored in numerous experiments, but the limits of selectivity have probably not been reached. An important goal is a full understanding of how to engineer high target selectivity as a reliable outcome of selection experiments. Second, aptamer selection as typically implemented is labor-intensive and time-consuming. Advances in streamlining selection procedures, including the growing use of automation, will likely prove important in bridging basic research and practical applications.

The in vitro selection of ribozymes and deoxyribozymes is less advanced than analogous studies of aptamers. The scope of chemical reactions that may be catalyzed by RNA and DNA still remains to be determined. The relatively small number of examples other than phosphodiester cleavage or ligation offers substantial hope that a much wider variety of reactions may be catalyzed, but in most cases the difficult work of achieving this new catalysis remains to be done. The payoff for reaching this goal should be the ability to use nucleic acid enzymes (and not just aptamers) in practical applications for which catalyzed chemical reactions are a critical design element.

As demonstrated by the other chapters in this book, the immense body of research on fundamental development of aptamers and nucleic acid enzymes has already enabled several practical applications. These examples of the translation of fundamental research into practical applications should be celebrated, particularly as scientists face ever-increasing pressure to connect their basic research with the challenges of the modern world.

References

1. Ellington, A.D. and Szostak, J.W. (1990) In vitro selection of RNA molecules that bind specific ligands. Nature (Lond.) 346:818–822.
2. Kruger, K., Grabowski, P.J., Zaug, A.J., Sands, J., Gottschling, D.E. and Cech, T.R. (1982) Self-splicing RNA: autoexcision and autocyclization of the ribosomal RNA intervening sequence of *Tetrahymena*. Cell 31:147–157.
3. Bass, B.L. and Cech, T.R. (1984) Specific interaction between the self-splicing RNA of *Tetrahymena* and its guanosine substrate: implications for biological catalysis by RNA. Nature (Lond.) 308:820–826.
4. O'Malley, R.P., Mariano, T.M., Siekierka, J. and Mathews, M.B. (1986) A mechanism for the control of protein synthesis by adenovirus VA RNA_I. Cell 44:391–400.
5. Cullen, B.R. and Greene, W.C. (1989) Regulatory pathways governing HIV-1 replication. Cell 58:423–426.
6. Marciniak, R.A., Garcia-Blanco, M.A. and Sharp, P.A. (1990) Identification and characterization of a HeLa nuclear protein that specifically binds to the trans-activation-response (TAR) element of human immunodeficiency virus. Proc. Natl. Acad. Sci. USA 87:3624–3628.
7. Tuerk, C. and Gold, L. (1990) Systematic evolution of ligands by exponential enrichment: RNA ligands to bacteriophage T4 DNA polymerase. Science 249:505–510.
8. Sullenger, B.A., Gallardo, H.F., Ungers, G.E. and Gilboa, E. (1990) Overexpression of TAR sequences renders cells resistant to human immunodeficiency virus replication. Cell 63:601–608.
9. Robertson, D.L. and Joyce, G.F. (1990) Selection in vitro of an RNA enzyme that specifically cleaves single-stranded DNA. Nature (Lond.) 344:467–468.
10. Hybarger, G., Bynum, J., Williams, R.F., Valdes, J.J. and Chambers, J.P. (2006) A microfluidic SELEX prototype. Anal. Bioanal. Chem. 384:191–198.
11. Gold, L., Polisky, B., Uhlenbeck, O. and Yarus, M. (1995) Diversity of oligonucleotide functions. Annu. Rev. Biochem. 64:763–797.
12. Breaker, R.R. (1997) In vitro selection of catalytic polynucleotides. Chem. Rev. 97: 371–390.
13. Osborne, S.E. and Ellington, A.D. (1997) Nucleic acid selection and the challenge of combinatorial chemistry. Chem. Rev. 97:349–370.
14. Wilson, D.S. and Szostak, J.W. (1999) In vitro selection of functional nucleic acids. Annu. Rev. Biochem. 68:611–647.
15. Joyce, G.F. (2004) Directed evolution of nucleic acid enzymes. Annu. Rev. Biochem. 73:791–836.
16. Sabeti, P.C., Unrau, P.J. and Bartel, D.P. (1997) Accessing rare activities from random RNA sequences: the importance of the length of molecules in the starting pool. Chem. Biol. 4:767–774.
17. Lozupone, C., Changayil, S., Majerfeld, I. and Yarus, M. (2003) Selection of the simplest RNA that binds isoleucine. RNA 9:1315–1322.
18. Legiewicz, M., Lozupone, C., Knight, R. and Yarus, M. (2005) Size, constant sequences, and optimal selection. RNA 11:1701–1709.
19. Majerfeld, I. and Yarus, M. (1994) An RNA pocket for an aliphatic hydrophobe. Nat. Struct. Biol. 1:287–292.
20. Connell, G.J. and Yarus, M. (1994) RNAs with dual specificity and dual RNAs with similar specificity. Science 264:1137–1141.
21. Missailidis, S., Thomaidou, D., Borbas, K.E. and Price, M.R. (2005) Selection of aptamers with high affinity and high specificity against C595, an anti-MUC1 IgG3 monoclonal antibody, for antibody targeting. J. Immunol. Methods 296:45–62.
22. Ferreira, C.S., Matthews, C.S. and Missailidis, S. (2006) DNA aptamers that bind to MUC1 tumour marker: design and characterization of MUC1-binding single-stranded DNA aptamers. Tumor Biol. 27:289–301.

23. Hale, S.P. and Schimmel, P. (1996) Protein synthesis editing by a DNA aptamer. Proc. Natl. Acad. Sci. USA 93:2755–2758.
24. Sassanfar, M. and Szostak, J.W. (1993) An RNA motif that binds ATP. Nature (Lond.) 364:550–553.
25. Famulok, M. and Szostak, J.W. (1992) Stereospecific recognition of tryptophan agarose by in vitro selected RNA. J. Am. Chem. Soc. 114:3990–3991.
26. Ellington, A.D. and Szostak, J.W. (1992) Selection in vitro of single-stranded DNA molecules that fold into specific ligand-binding structures. Nature (Lond.) 355:850–852.
27. Conrad, R., Keranen, L.M., Ellington, A.D. and Newton, A.C. (1994) Isozyme-specific inhibition of protein kinase C by RNA aptamers. J. Biol. Chem. 269:32051–32054.
28. Tian, Y., Adya, N., Wagner, S., Giam, C.Z., Green, M.R. and Ellington, A.D. (1995) Dissecting protein:protein interactions between transcription factors with an RNA aptamer. RNA 1:317–326.
29. Kumar, P.K., Machida, K., Urvil, P.T., Kakiuchi, N., Vishnuvardhan, D., Shimotohno, K., Taira, K. and Nishikawa, S. (1997) Isolation of RNA aptamers specific to the NS3 protein of hepatitis C virus from a pool of completely random RNA. Virology 237:270–282.
30. Yamamoto, R., Katahira, M., Nishikawa, S., Baba, T., Taira, K. and Kumar, P.K. (2000) A novel RNA motif that binds efficiently and specifically to the Tat protein of HIV and inhibits the trans-activation by Tat of transcription in vitro and in vivo. Genes Cells 5:371–388.
31. Seiwert, S.D., Stines Nahreini, T., Aigner, S., Ahn, N.G. and Uhlenbeck, O.C. (2000) RNA aptamers as pathway-specific MAP kinase inhibitors. Chem. Biol. 7:833–843.
32. Li, Y., Geyer, C.R. and Sen, D. (1996) Recognition of anionic porphyrins by DNA aptamers. Biochemistry 35:6911–6922.
33. Conrad, R.C., Giver, L., Tian, Y. and Ellington, A.D. (1996) In vitro selection of nucleic acid aptamers that bind proteins. Methods Enzymol. 267:336–367.
34. Knight, R. and Yarus, M. (2003) Finding specific RNA motifs: function in a zeptomole world? RNA 9:218–230.
35. Gyllensten, U.B. and Erlich, H.A. (1988) Generation of single-stranded DNA by the polymerase chain reaction and its application to direct sequencing of the *HLA-DQA* locus. Proc. Natl. Acad. Sci. USA 85:7652–7656.
36. Wilson, C. and Szostak, J.W. (1998) Isolation of a fluorophore-specific DNA aptamer with weak redox activity. Chem. Biol. 5:609–617.
37. Yang, Q., Goldstein, I.J., Mei, H.Y. and Engelke, D.R. (1998) DNA ligands that bind tightly and selectively to cellobiose. Proc. Natl. Acad. Sci. USA 95:5462–5467.
38. Bock, L.C., Griffin, L.C., Latham, J.A., Vermaas, E.H. and Toole, J.J. (1992) Selection of single-stranded DNA molecules that bind and inhibit human thrombin. Nature (Lond.) 355:564–566.
39. Harada, K. and Frankel, A.D. (1995) Identification of two novel arginine binding DNAs. EMBO J. 14:5798–5811.
40. Kato, T., Takemura, T., Yano, K., Ikebukuro, K. and Karube, I. (2000) In vitro selection of DNA aptamers which bind to cholic acid. Biochem. Biophys. Acta 1493:12–18.
41. Blank, M., Weinschenk, T., Priemer, M. and Schluesener, H. (2001) Systematic evolution of a DNA aptamer binding to rat brain tumor microvessels. Selective targeting of endothelial regulatory protein pigpen. J. Biol. Chem. 276:16464–16468.
42. Vianini, E., Palumbo, M. and Gatto, B. (2001) In vitro selection of DNA aptamers that bind L-tyrosinamide. Bioorg. Med. Chem. 9:2543–2548.
43. Green, L.S., Jellinek, D., Jenison, R., Ostman, A., Heldin, C.H. and Janjic, N. (1996) Inhibitory DNA ligands to platelet-derived growth factor B-chain. Biochemistry 35:14413–14424.
44. Wiegand, T.W., Williams, P.B., Dreskin, S.C., Jouvin, M.H., Kinet, J.P. and Tasset, D. (1996) High-affinity oligonucleotide ligands to human IgE inhibit binding to Fcε receptor I. J. Immunol. 157:221–230.
45. Hicke, B.J., Watson, S.R., Koenig, A., Lynott, C.K., Bargatze, R.F., Chang, Y.F., Ringquist, S., Moon-McDermott, L., Jennings, S., Fitzwater, T., Han, H.L., Varki, N., Albinana, I., Willis, M.C.,

Varki, A. and Parma, D. (1996) DNA aptamers block L-selectin function in vivo. Inhibition of human lymphocyte trafficking in SCID mice. J. Clin. Invest. 98:2688–2692.
46. Charlton, J., Kirschenheuter, G.P. and Smith, D. (1997) Highly potent irreversible inhibitors of neutrophil elastase generated by selection from a randomized DNA-valine phosphonate library. Biochemistry 36:3018–3026.
47. Daniels, D.A., Chen, H., Hicke, B.J., Swiderek, K.M. and Gold, L. (2003) A tenascin-C aptamer identified by tumor cell SELEX: systematic evolution of ligands by exponential enrichment. Proc. Natl. Acad. Sci. USA 100:15416–15421.
48. Ciesiolka, J., Illangasekare, M., Majerfeld, I., Nickles, T., Welch, M., Yarus, M. and Zinnen, S. (1996) Affinity selection-amplification from randomized ribooligonucleotide pools. Methods Enzymol. 267:315–335.
49. Tuerk, C., MacDougal, S. and Gold, L. (1992) RNA pseudoknots that inhibit human immunodeficiency virus type 1 reverse transcriptase. Proc. Natl. Acad. Sci. USA 89:6988–6992.
50. Schneider, D., Tuerk, C. and Gold, L. (1992) Selection of high affinity RNA ligands to the bacteriophage R17 coat protein. J. Mol. Biol. 228:862–869.
51. Giver, L., Bartel, D., Zapp, M., Pawul, A., Green, M. and Ellington, A.D. (1993) Selective optimization of the Rev-binding element of HIV-1. Nucleic Acids Res. 21:5509–5516.
52. Jellinek, D., Green, L.S., Bell, C. and Janjic, N. (1994) Inhibition of receptor binding by high-affinity RNA ligands to vascular endothelial growth factor. Biochemistry 33:10450–10456.
53. Jellinek, D., Green, L.S., Bell, C., Lynott, C.K., Gill, N., Vargeese, C., Kirschenheuter, G., McGee, D.P., Abesinghe, P., Pieken, W.A. et al. (1995) Potent 2′-amino-2′-deoxypyrimidine RNA inhibitors of basic fibroblast growth factor. Biochemistry 34:11363–11372.
54. Nazarenko, I.A. and Uhlenbeck, O.C. (1995) Defining a smaller RNA substrate for elongation factor Tu. Biochemistry 34:2545–2552.
55. Allen, P., Worland, S. and Gold, L. (1995) Isolation of high-affinity RNA ligands to HIV-1 integrase from a random pool. Virology 209:327–336.
56. Binkley, J., Allen, P., Brown, D.M., Green, L., Tuerk, C. and Gold, L. (1995) RNA ligands to human nerve growth factor. Nucleic Acids Res. 23:3198–3205.
57. Kubik, M.F., Bell, C., Fitzwater, T., Watson, S.R. and Tasset, D.M. (1997) Isolation and characterization of 2′-fluoro-, 2′-amino-, and 2′-fluoro-/amino-modified RNA ligands to human IFN-gamma that inhibit receptor binding. J. Immunol. 159:259–267.
58. Klug, S.J., Huttenhofer, A., Kromayer, M. and Famulok, M. (1997) In vitro and in vivo characterization of novel mRNA motifs that bind special elongation factor SelB. Proc. Natl. Acad. Sci. USA 94:6676–6681.
59. Ruckman, J., Green, L.S., Beeson, J., Waugh, S., Gillette, W.L., Henninger, D.D., Claesson-Welsh, L. and Janjic, N. (1998) 2′-Fluoropyrimidine RNA-based aptamers to the 165-amino acid form of vascular endothelial growth factor (VEGF165). Inhibition of receptor binding and VEGF-induced vascular permeability through interactions requiring the exon 7-encoded domain. J. Biol. Chem. 273:20556–20567.
60. Bridonneau, P., Chang, Y.F., O'Connell, D., Gill, S.C., Snyder, D.W., Johnson, L., Goodson, T., Jr., Herron, D.K. and Parma, D.H. (1998) High-affinity aptamers selectively inhibit human nonpancreatic secretory phospholipase A2 (hnps-PLA2). J. Med. Chem. 41:778–786.
61. Baskerville, S., Zapp, M. and Ellington, A.D. (1999) Anti-Rex aptamers as mimics of the Rex-binding element. J. Virol. 73:4962–4971.
62. Lebruska, L.L. and Maher, L.J., III. (1999) Selection and characterization of an RNA decoy for transcription factor NF-κB. Biochemistry 38:3168–3174.
63. Biesecker, G., Dihel, L., Enney, K. and Bendele, R.A. (1999) Derivation of RNA aptamer inhibitors of human complement C5. Immunopharmacology 42:219–230.
64. Klug, S.J., Huttenhofer, A. and Famulok, M. (1999) In vitro selection of RNA aptamers that bind special elongation factor SelB, a protein with multiple RNA-binding sites, reveals one major interaction domain at the carboxyl terminus. RNA 5:1180–1190.
65. Fukuda, K., Vishnuvardhan, D., Sekiya, S., Hwang, J., Kakiuchi, N., Taira, K., Shimotohno, K., Kumar, P.K. and Nishikawa, S. (2000) Isolation and characterization of RNA aptamers specific for the hepatitis C virus nonstructural protein 3 protease. Eur. J. Biochem. 267:3685–3694.

66. Kawakami, J., Imanaka, H., Yokota, Y. and Sugimoto, N. (2000) In vitro selection of aptamers that act with Zn^{2+}. J. Inorg. Biochem. 82:197–206.
67. Hirao, I., Madin, K., Endo, Y., Yokoyama, S. and Ellington, A.D. (2000) RNA aptamers that bind to and inhibit the ribosome-inactivating protein, pepocin. J. Biol. Chem. 275:4943–4948.
68. White, R., Rusconi, C., Scardino, E., Wolberg, A., Lawson, J., Hoffman, M. and Sullenger, B. (2001) Generation of species cross-reactive aptamers using "toggle" SELEX. Mol. Ther. 4:567–573.
69. Rusconi, C.P., Scardino, E., Layzer, J., Pitoc, G.A., Ortel, T.L., Monroe, D. and Sullenger, B.A. (2002) RNA aptamers as reversible antagonists of coagulation factor IXa. Nature (Lond.) 419:90–94.
70. Vuyisich, M. and Beal, P.A. (2002) Controlling protein activity with ligand-regulated RNA aptamers. Chem. Biol. 9:907–913.
71. Kimoto, M., Shirouzu, M., Mizutani, S., Koide, H., Kaziro, Y., Hirao, I. and Yokoyama, S. (2002) Anti-(Raf-1) RNA aptamers that inhibit Ras-induced Raf-1 activation. Eur. J. Biochem. 269:697–704.
72. White, R.R., Shan, S., Rusconi, C.P., Shetty, G., Dewhirst, M.W., Kontos, C.D. and Sullenger, B.A. (2003) Inhibition of rat corneal angiogenesis by a nuclease-resistant RNA aptamer specific for angiopoietin-2. Proc. Natl. Acad. Sci. USA 100:5028–5033.
73. Santulli-Marotto, S., Nair, S.K., Rusconi, C., Sullenger, B. and Gilboa, E. (2003) Multivalent RNA aptamers that inhibit CTLA-4 and enhance tumor immunity. Cancer Res. 63:7483–7489.
74. Chen, C.H., Chernis, G.A., Hoang, V.Q. and Landgraf, R. (2003) Inhibition of heregulin signaling by an aptamer that preferentially binds to the oligomeric form of human epidermal growth factor receptor-3. Proc. Natl. Acad. Sci. USA 100:9226–9231.
75. Hirao, I., Harada, Y., Nojima, T., Osawa, Y., Masaki, H. and Yokoyama, S. (2004) In vitro selection of RNA aptamers that bind to colicin E3 and structurally resemble the decoding site of 16S ribosomal RNA. Biochemistry 43:3214–3221.
76. Gopinath, S.C., Misono, T.S., Kawasaki, K., Mizuno, T., Imai, M., Odagiri, T. and Kumar, P.K. (2006) An RNA aptamer that distinguishes between closely related human influenza viruses and inhibits haemagglutinin-mediated membrane fusion. J. Gen. Virol. 87:479–487.
77. Weiss, S., Proske, D., Neumann, M., Groschup, M.H., Kretzschmar, H.A., Famulok, M. and Winnacker, E.L. (1997) RNA aptamers specifically interact with the prion protein PrP. J. Virol. 71:8790–8797.
78. Davis, K.A., Lin, Y., Abrams, B. and Jayasena, S.D. (1998) Staining of cell surface human CD4 with 2′-F-pyrimidine-containing RNA aptamers for flow cytometry. Nucleic Acids Res. 26:3915–3924.
79. Moreno, M., Rincón, E., Piñeiro, D., Fernández, G., Domingo, A., Jiménez-Ruíz, A., Salinas, M. and González, V.M. (2003) Selection of aptamers against KMP-11 using colloidal gold during the SELEX process. Biochem. Biophys. Res. Commun. 308:214–218.
80. Doudna, J.A., Cech, T.R. and Sullenger, B.A. (1995) Selection of an RNA molecule that mimics a major autoantigenic epitope of human insulin receptor. Proc. Natl. Acad. Sci. USA 92:2355–2359.
81. Xu, W. and Ellington, A.D. (1996) Anti-peptide aptamers recognize amino acid sequence and bind a protein epitope. Proc. Natl. Acad. Sci. USA 93:7475–7480.
82. Lee, S.W. and Sullenger, B.A. (1996) Isolation of a nuclease-resistant decoy RNA that selectively blocks autoantibody binding to insulin receptors on human lymphocytes. J. Exp. Med. 184:315–324.
83. O'Connell, D., Koenig, A., Jennings, S., Hicke, B., Han, H.L., Fitzwater, T., Chang, Y.F., Varki, N., Parma, D. and Varki, A. (1996) Calcium-dependent oligonucleotide antagonists specific for L-selectin. Proc. Natl. Acad. Sci. USA 93:5883–5887.
84. Lee, S.W. and Sullenger, B.A. (1997) Isolation of a nuclease-resistant decoy RNA that can protect human acetylcholine receptors from myasthenic antibodies. Nat. Biotechnol. 15:41–45.
85. Srisawat, C. and Engelke, D.R. (2001) Streptavidin aptamers: affinity tags for the study of RNAs and ribonucleoproteins. RNA 7:632–641.

86. Proske, D., Gilch, S., Wopfner, F., Schatzl, H.M., Winnacker, E.L. and Famulok, M. (2002) Prion-protein-specific aptamer reduces PrPSc formation. ChemBioChem 3:717–725.
87. Nieuwlandt, D., Wecker, M. and Gold, L. (1995) In vitro selection of RNA ligands to substance P. Biochemistry 34:5651–5659.
88. Hicke, B.J., Marion, C., Chang, Y.F., Gould, T., Lynott, C.K., Parma, D., Schmidt, P.G. and Warren, S. (2001) Tenascin-C aptamers are generated using tumor cells and purified protein. J. Biol. Chem. 276:48644–48654.
89. Tao, J. and Frankel, A.D. (1996) Arginine-binding RNAs resembling TAR identified by in vitro selection. Biochemistry 35:2229–2238.
90. Jenison, R.D., Gill, S.C., Pardi, A. and Polisky, B. (1994) High-resolution molecular discrimination by RNA. Science 263:1425–1429.
91. Lauhon, C.T. and Szostak, J.W. (1995) RNA aptamers that bind flavin and nicotinamide redox cofactors. J. Am. Chem. Soc. 117:1246–1257.
92. Geiger, A., Burgstaller, P., von der Eltz, H., Roeder, A. and Famulok, M. (1996) RNA aptamers that bind L-arginine with sub-micromolar dissociation constants and high enantioselectivity. Nucleic Acids Res. 24:1029–1036.
93. Haller, A.A. and Sarnow, P. (1997) In vitro selection of a 7-methyl-guanosine binding RNA that inhibits translation of capped mRNA molecules. Proc. Natl. Acad. Sci. USA 94:8521–8526.
94. Burke, D.H. and Hoffman, D.C. (1998) A novel acidophilic RNA motif that recognizes coenzyme A. Biochemistry 37:4653–4663.
95. Rink, S.M., Shen, J.C. and Loeb, L.A. (1998) Creation of RNA molecules that recognize the oxidative lesion 7,8-dihydro-8-hydroxy-2′-deoxyguanosine (8-oxodG) in DNA. Proc. Natl. Acad. Sci. USA 95:11619–11624.
96. Wallace, S.T. and Schroeder, R. (1998) In vitro selection and characterization of streptomycin-binding RNAs: recognition discrimination between antibiotics. RNA 4:112–123.
97. Gebhardt, K., Shokraei, A., Babaie, E. and Lindqvist, B.H. (2000) RNA aptamers to *S*-adenosylhomocysteine: kinetic properties, divalent cation dependency, and comparison with anti-*S*-adenosylhomocysteine antibody. Biochemistry 39:7255–7265.
98. Brockstedt, U., Uzarowska, A., Montpetit, A., Pfau, W. and Labuda, D. (2004) In vitro evolution of RNA aptamers recognizing carcinogenic aromatic amines. Biochem. Biophys. Res. Commun. 313:1004–1008.
99. Burgstaller, P. and Famulok, M. (1994) Isolation of RNA aptamers for biological cofactors by in vitro selection. Angew. Chem. Int. Ed. Engl. 33:1084–1087.
100. Burke, D.H. and Gold, L. (1997) RNA aptamers to the adenosine moiety of S-adenosyl methionine: structural inferences from variations on a theme and the reproducibility of SELEX. Nucleic Acids Res. 25:2020–2024.
101. Sazani, P.L., Larralde, R. and Szostak, J.W. (2004) A small aptamer with strong and specific recognition of the triphosphate of ATP. J. Am. Chem. Soc. 126:8370–8371.
102. Huizenga, D.E. and Szostak, J.W. (1995) A DNA aptamer that binds adenosine and ATP. Biochemistry 34:656–665.
103. Kiga, D., Futamura, Y., Sakamoto, K. and Yokoyama, S. (1998) An RNA aptamer to the xanthine/guanine base with a distinctive mode of purine recognition. Nucleic Acids Res. 26:1755–1760.
104. Meli, M., Vergne, J., Decout, J.L. and Maurel, M.C. (2002) Adenine-aptamer complexes: a bipartite RNA site that binds the adenine nucleic base. J. Biol. Chem. 277:2104–2111.
105. Wallis, M.G., von Ahsen, U., Schroeder, R. and Famulok, M. (1995) A novel RNA motif for neomycin recognition. Chem. Biol. 2:543–552.
106. Koizumi, M. and Breaker, R.R. (2000) Molecular recognition of cAMP by an RNA aptamer. Biochemistry 39:8983–8992.
107. Win, M.N., Klein, J.S. and Smolke, C.D. (2006) Codeine-binding RNA aptamers and rapid determination of their binding constants using a direct coupling surface plasmon resonance assay. Nucleic Acids Res. 34:5670–5682.
108. Lorsch, J.R. and Szostak, J.W. (1994) In vitro selection of RNA aptamers specific for cyanocobalamin. Biochemistry 33:973–982.

109. Burke, D.H., Scates, L., Andrews, K. and Gold, L. (1996) Bent pseudoknots and novel RNA inhibitors of type 1 human immunodeficiency virus (HIV-1) reverse transcriptase. J. Mol. Biol. 264:650–666.
110. Burke, D.H., Hoffman, D.C., Brown, A., Hansen, M., Pardi, A. and Gold, L. (1997) RNA aptamers to the peptidyl transferase inhibitor chloramphenicol. Chem. Biol. 4:833–843.
111. Mannironi, C., Di Nardo, A., Fruscoloni, P. and Tocchini-Valentini, G.P. (1997) In vitro selection of dopamine RNA ligands. Biochemistry 36:9726–9734.
112. Holeman, L.A., Robinson, S.L., Szostak, J.W. and Wilson, C. (1998) Isolation and characterization of fluorophore-binding RNA aptamers. Fold. Des. 3:423–431.
113. Wilson, C., Nix, J. and Szostak, J. (1998) Functional requirements for specific ligand recognition by a biotin-binding RNA pseudoknot. Biochemistry 37:14410–14419.
114. Held, D.M., Greathouse, S.T., Agrawal, A. and Burke, D.H. (2003) Evolutionary landscapes for the acquisition of new ligand recognition by RNA aptamers. J. Mol. Evol. 57:299–308.
115. Cadwell, R.C. and Joyce, G.F. (1994) Mutagenic PCR. PCR Methods Appl. 3:S136–S140.
116. Tahiri-Alaoui, A., Frigotto, L., Manville, N., Ibrahim, J., Romby, P. and James, W. (2002) High affinity nucleic acid aptamers for streptavidin incorporated into bi-specific capture ligands. Nucleic Acids Res. 30:e45.
117. Hwang, B. and Lee, S.W. (2002) Improvement of RNA aptamer activity against myasthenic autoantibodies by extended sequence selection. Biochem. Biophys. Res. Commun. 290:656–662.
118. Jarosch, F., Buchner, K. and Klussmann, S. (2006) In vitro selection using a dual RNA library that allows primerless selection. Nucleic Acids Res. 34:e86.
119. Nutiu, R. and Li, Y. (2005) In vitro selection of structure-switching signaling aptamers. Angew. Chem. Int. Ed. 44:1061–1065.
120. Vater, A., Jarosch, F., Buchner, K. and Klussmann, S. (2003) Short bioactive Spiegelmers to migraine-associated calcitonin gene-related peptide rapidly identified by a novel approach: tailored-SELEX. Nucleic Acids Res. 31:e130.
121. Murphy, M.B., Fuller, S.T., Richardson, P.M. and Doyle, S.A. (2003) An improved method for the in vitro evolution of aptamers and applications in protein detection and purification. Nucleic Acids Res. 31:e110.
122. Lupold, S.E., Hicke, B.J., Lin, Y. and Coffey, D.S. (2002) Identification and characterization of nuclease-stabilized RNA molecules that bind human prostate cancer cells via the prostate-specific membrane antigen. Cancer Res. 62:4029–4033.
123. Daniels, D.A., Sohal, A.K., Rees, S. and Grisshammer, R. (2002) Generation of RNA aptamers to the G-protein-coupled receptor for neurotensin, NTS-1. Anal. Biochem. 305:214–226.
124. Tsai, D.E., Kenan, D.J. and Keene, J.D. (1992) In vitro selection of an RNA epitope immunologically cross-reactive with a peptide. Proc. Natl. Acad. Sci. USA 89:8864–8868.
125. Stoltenburg, R., Reinemann, C. and Strehlitz, B. (2005) FluMag-SELEX as an advantageous method for DNA aptamer selection. Anal. Bioanal. Chem. 383:83–91.
126. Mann, D., Reinemann, C., Stoltenburg, R. and Strehlitz, B. (2005) In vitro selection of DNA aptamers binding ethanolamine. Biochem. Biophys. Res. Commun. 338:1928–1934.
127. Babendure, J.R., Adams, S.R. and Tsien, R.Y. (2003) Aptamers switch on fluorescence of triphenylmethane dyes. J. Am. Chem. Soc. 125:14716–14717.
128. Tawfik, D.S. and Griffiths, A.D. (1998) Man-made cell-like compartments for molecular evolution. Nat. Biotechnol. 16:652–656.
129. Miller, O.J., Bernath, K., Agresti, J.J., Amitai, G., Kelly, B.T., Mastrobattista, E., Taly, V., Magdassi, S., Tawfik, D.S. and Griffiths, A.D. (2006) Directed evolution by in vitro compartmentalization. Nat. Methods 3:561–570.
130. Golden, M.C., Collins, B.D., Willis, M.C. and Koch, T.H. (2000) Diagnostic potential of PhotoSELEX-evolved ssDNA aptamers. J. Biotechnol. 81:167–178.
131. Jensen, K.B., Atkinson, B.L., Willis, M.C., Koch, T.H. and Gold, L. (1995) Using in vitro selection to direct the covalent attachment of human immunodeficiency virus type 1 Rev protein to high-affinity RNA ligands. Proc. Natl. Acad. Sci. USA 92:12220–12224.

132. Smith, D., Kirschenheuter, G.P., Charlton, J., Guidot, D.M. and Repine, J.E. (1995) In vitro selection of RNA-based irreversible inhibitors of human neutrophil elastase. Chem. Biol. 2:741–750.
133. Pileur, F., Andreola, M.L., Dausse, E., Michel, J., Moreau, S., Yamada, H., Gaidamakov, S.A., Crouch, R.J., Toulme, J.J. and Cazenave, C. (2003) Selective inhibitory DNA aptamers of the human RNase H1. Nucleic Acids Res. 31:5776–5788.
134. Khati, M., Schuman, M., Ibrahim, J., Sattentau, Q., Gordon, S. and James, W. (2003) Neutralization of infectivity of diverse R5 clinical isolates of human immunodeficiency virus type 1 by gp120-binding 2′F-RNA aptamers. J. Virol. 77:12692–12698.
135. Misono, T.S. and Kumar, P.K. (2005) Selection of RNA aptamers against human influenza virus hemagglutinin using surface plasmon resonance. Anal. Biochem. 342:312–317.
136. Mendonsa, S.D. and Bowser, M.T. (2004) In vitro evolution of functional DNA using capillary electrophoresis. J. Am. Chem. Soc. 126:20–21.
137. Berezovski, M., Drabovich, A., Krylova, S.M., Musheev, M., Okhonin, V., Petrov, A. and Krylov, S.N. (2005) Nonequilibrium capillary electrophoresis of equilibrium mixtures: a universal tool for development of aptamers. J. Am. Chem. Soc. 127:3165–3171.
138. Berezovski, M., Musheev, M., Drabovich, A. and Krylov, S.N. (2006) Non-SELEX selection of aptamers. J. Am. Chem. Soc. 128:1410–1411.
139. Drabovich, A.P., Berezovski, M., Okhonin, V. and Krylov, S.N. (2006) Selection of smart aptamers by methods of kinetic capillary electrophoresis. Anal. Chem. 78:3171–3178.
140. Tang, J., Xie, J., Shao, N. and Yan, Y. (2006) The DNA aptamers that specifically recognize ricin toxin are selected by two in vitro selection methods. Electrophoresis 27:1303–1311.
141. Ravelet, C., Grosset, C. and Peyrin, E. (2006) Liquid chromatography, electrochromatography and capillary electrophoresis applications of DNA and RNA aptamers. J. Chromatogr. A 1117:1–10.
142. Cox, J.C. and Ellington, A.D. (2001) Automated selection of anti-protein aptamers. Bioorg. Med. Chem. 9:2525–2531.
143. Sooter, L.J., Riedel, T., Davidson, E.A., Levy, M., Cox, J.C. and Ellington, A.D. (2001) Toward automated nucleic acid enzyme selection. Biol. Chem. 382:1327–1334.
144. Cox, J.C., Rajendran, M., Riedel, T., Davidson, E.A., Sooter, L.J., Bayer, T.S., Schmitz-Brown, M. and Ellington, A.D. (2002) Automated acquisition of aptamer sequences. Comb. Chem. High Throughput Screen. 5:289–299.
145. Cox, J.C., Hayhurst, A., Hesselberth, J., Bayer, T.S., Georgiou, G. and Ellington, A.D. (2002) Automated selection of aptamers against protein targets translated in vitro: from gene to aptamer. Nucleic Acids Res. 30:e108.
146. Bryant, K.F., Cox, J.C., Wang, H., Hogle, J.M., Ellington, A.D. and Coen, D.M. (2005) Binding of herpes simplex virus-1 US11 to specific RNA sequences. Nucleic Acids Res. 33:6090–6100.
147. Drolet, D.W., Jenison, R.D., Smith, D.E., Pratt, D. and Hicke, B.J. (1999) A high throughput platform for systematic evolution of ligands by exponential enrichment (SELEX). Comb. Chem. High Throughput Screen. 2:271–278.
148. Eulberg, D., Buchner, K., Maasch, C. and Klussmann, S. (2005) Development of an automated in vitro selection protocol to obtain RNA-based aptamers: identification of a biostable substance P antagonist. Nucleic Acids Res. 33:e45.
149. Ciesiolka, J., Gorski, J. and Yarus, M. (1995) Selection of an RNA domain that binds Zn^{2+}. RNA 1:538–550.
150. Ciesiolka, J. and Yarus, M. (1996) Small RNA-divalent domains. RNA 2:785–793.
151. Hofmann, H.P., Limmer, S., Hornung, V. and Sprinzl, M. (1997) Ni^{2+}-binding RNA motifs with an asymmetric purine-rich internal loop and a G-A base pair. RNA 3:1289–1300.
152. Moazed, D. and Noller, H.F. (1987) Interaction of antibiotics with functional sites in 16*S* ribosomal RNA. Nature (Lond.) 327:389–394.
153. Hermann, T. (2003) Chemical and functional diversity of small molecule ligands for RNA. Biopolymers 70:4–18.
154. von Ahsen, U. and Schroeder, R. (1990) Streptomycin and self-splicing. Nature (Lond.) 346:801.

155. von Ahsen, U. and Schroeder, R. (1991) Streptomycin inhibits splicing of group I introns by competition with the guanosine substrate. Nucleic Acids Res. 19:2261–2265.
156. von Ahsen, U., Davies, J. and Schroeder, R. (1991) Antibiotic inhibition of group I ribozyme function. Nature (Lond.) 353:368–370.
157. von Ahsen, U., Davies, J. and Schroeder, R. (1992) Non-competitive inhibition of group I intron RNA self-splicing by aminoglycoside antibiotics. J. Mol. Biol. 226:935–941.
158. Grate, D. and Wilson, C. (1999) Laser-mediated, site-specific inactivation of RNA transcripts. Proc. Natl. Acad. Sci. USA 96:6131–6136.
159. Werstuck, G. and Green, M.R. (1998) Controlling gene expression in living cells through small molecule–RNA interactions. Science 282:296–298.
160. Wang, Y. and Rando, R.R. (1995) Specific binding of aminoglycoside antibiotics to RNA. Chem. Biol. 2:281–290.
161. Wang, Y., Killian, J., Hamasaki, K. and Rando, R.R. (1996) RNA molecules that specifically and stoichiometrically bind aminoglycoside antibiotics with high affinities. Biochemistry 35:12338–12346.
162. Lato, S.M., Boles, A.R. and Ellington, A.D. (1995) In vitro selection of RNA lectins: using combinatorial chemistry to interpret ribozyme evolution. Chem. Biol. 2:291–303.
163. Lato, S.M. and Ellington, A.D. (1996) Screening chemical libraries for nucleic-acid-binding drugs by in vitro selection: a test case with lividomycin. Mol. Divers. 2:103–110.
164. Kwon, M., Chun, S.M., Jeong, S. and Yu, J. (2001) In vitro selection of RNA against kanamycin B. Mol. Cells 11:303–311.
165. Berens, C., Thain, A. and Schroeder, R. (2001) A tetracycline-binding RNA aptamer. Bioorg. Med. Chem. 9:2549–2556.
166. Wallis, M.G., Streicher, B., Wank, H., von Ahsen, U., Clodi, E., Wallace, S.T., Famulok, M. and Schroeder, R. (1997) In vitro selection of a viomycin-binding RNA pseudoknot. Chem. Biol. 4:357–366.
167. Roychowdhury-Saha, M., Lato, S.M., Shank, E.D. and Burke, D.H. (2002) Flavin recognition by an RNA aptamer targeted toward FAD. Biochemistry 41:2492–2499.
168. Wilson, C. and Szostak, J.W. (1995) In vitro evolution of a self-alkylating ribozyme. Nature (Lond.) 374:777–782.
169. Saran, D., Frank, J. and Burke, D.H. (2003) The tyranny of adenosine recognition among RNA aptamers to coenzyme A. BMC Evol. Biol. 3:26.
170. Connell, G.J., Illangesekare, M. and Yarus, M. (1993) Three small ribooligonucleotides with specific arginine sites. Biochemistry 32:5497–5502.
171. Famulok, M. (1994) Molecular recognition of amino acids by RNA-aptamers: an L-citrulline binding motif and its evolution into an L-arginine binder. J. Am. Chem. Soc. 116:1698–1706.
172. Mannironi, C., Scerch, C., Fruscoloni, P. and Tocchini-Valentini, G.P. (2000) Molecular recognition of amino acids by RNA aptamers: the evolution into an L-tyrosine binder of a dopamine-binding RNA motif. RNA 6:520–527.
173. Majerfeld, I. and Yarus, M. (1998) Isoleucine: RNA sites with associated coding sequences. RNA 4:471–478.
174. Jeong, S., Eom, T., Kim, S., Lee, S. and Yu, J. (2001) In vitro selection of the RNA aptamer against the Sialyl Lewis X and its inhibition of the cell adhesion. Biochem. Biophys. Res. Commun. 281:237–243.
175. Srisawat, C., Goldstein, I.J. and Engelke, D.R. (2001) Sephadex-binding RNA ligands: rapid affinity purification of RNA from complex RNA mixtures. Nucleic Acids Res. 29:e4.
176. Lee, J.F., Stovall, G.M. and Ellington, A.D. (2006) Aptamer therapeutics advance. Curr. Opin. Chem. Biol. 10:282–289.
177. Pagratis, N.C., Bell, C., Chang, Y.F., Jennings, S., Fitzwater, T., Jellinek, D. and Dang, C. (1997) Potent 2′-amino-, and 2′-fluoro-2′-deoxyribonucleotide RNA inhibitors of keratinocyte growth factor. Nat. Biotechnol. 15:68–73.
178. Jenison, R.D., Jennings, S.D., Walker, D.W., Bargatze, R.F. and Parma, D. (1998) Oligonucleotide inhibitors of P-selectin-dependent neutrophil-platelet adhesion. Antisense Nucleic Acid Drug Dev. 8:265–279.

179. Kim, Y.M., Choi, K.H., Jang, Y.J., Yu, J. and Jeong, S. (2003) Specific modulation of the anti-DNA autoantibody–nucleic acids interaction by the high affinity RNA aptamer. Biochem. Biophys. Res. Commun. 300:516–523.
180. Ohuchi, S.P., Ohtsu, T. and Nakamura, Y. (2006) Selection of RNA aptamers against recombinant transforming growth factor-β type III receptor displayed on cell surface. Biochimie 88:897–904.
181. Rusconi, C.P., Yeh, A., Lyerly, H.K., Lawson, J.H. and Sullenger, B.A. (2000) Blocking the initiation of coagulation by RNA aptamers to factor VIIa. Thromb. Haemost. 84: 841–848.
182. Rhie, A., Kirby, L., Sayer, N., Wellesley, R., Disterer, P., Sylvester, I., Gill, A., Hope, J., James, W. and Tahiri-Alaoui, A. (2003) Characterization of 2′-fluoro-RNA aptamers that bind preferentially to disease-associated conformations of prion protein and inhibit conversion. J. Biol. Chem. 278:39697–39705.
183. Ylera, F., Lurz, R., Erdmann, V.A. and Furste, J.P. (2002) Selection of RNA aptamers to the Alzheimer's disease amyloid peptide. Biochem. Biophys. Res. Commun. 290: 1583–1588.
184. Ulrich, H., Magdesian, M.H., Alves, M.J. and Colli, W. (2002) In vitro selection of RNA aptamers that bind to cell adhesion receptors of *Trypanosoma cruzi* and inhibit cell invasion. J. Biol. Chem. 277:20756–20762.
185. Giver, L., Bartel, D.P., Zapp, M.L., Green, M.R. and Ellington, A.D. (1993) Selection and design of high-affinity RNA ligands for HIV-1 Rev. Gene 137:19–24.
186. Green, L.S., Jellinek, D., Bell, C., Beebe, L.A., Feistner, B.D., Gill, S.C., Jucker, F.M. and Janjic, N. (1995) Nuclease-resistant nucleic acid ligands to vascular permeability factor/vascular endothelial growth factor. Chem. Biol. 2:683–695.
187. Blind, M., Kolanus, W. and Famulok, M. (1999) Cytoplasmic RNA modulators of an inside-out signal-transduction cascade. Proc. Natl. Acad. Sci. USA 96:3606–3610.
188. Mi, J., Zhang, X., Giangrande, P.H., McNamara, J.O., II, Nimjee, S.M., Sarraf-Yazdi, S., Sullenger, B.A. and Clary, B.M. (2005) Targeted inhibition of αvβ3 integrin with an RNA aptamer impairs endothelial cell growth and survival. Biochem. Biophys. Res. Commun. 338:956–963.
189. Romero-López, C., Barroso-del Jesus, A., Puerta-Fernández, E. and Berzal-Herranz, A. (2005) Interfering with hepatitis C virus IRES activity using RNA molecules identified by a novel in vitro selection method. Biol. Chem. 386:183–190.
190. Homann, M., Lorger, M., Engstler, M., Zacharias, M. and Göringer, H.U. (2006) Serum-stable RNA aptamers to an invariant surface domain of live African trypanosomes. Comb. Chem. High Throughput Screen. 9:491–499.
191. Buskirk, A.R., Kehayova, P.D., Landrigan, A. and Liu, D.R. (2003) In vivo evolution of an RNA-based transcriptional activator. Chem. Biol. 10:533–540.
192. Buskirk, A.R., Landrigan, A. and Liu, D.R. (2004) Engineering a ligand-dependent RNA transcriptional activator. Chem. Biol. 11:1157–1163.
193. Pestourie, C., Tavitian, B. and Duconge, F. (2005) Aptamers against extracellular targets for in vivo applications. Biochimie 87:921–930.
194. Tucker, C.E., Chen, L.S., Judkins, M.B., Farmer, J.A., Gill, S.C. and Drolet, D.W. (1999) Detection and plasma pharmacokinetics of an anti-vascular endothelial growth factor oligonucleotide-aptamer (NX1838) in rhesus monkeys. J. Chromatogr. B 732:203–212.
195. Kim, E.S., Serur, A., Huang, J., Manley, C.A., McCrudden, K.W., Frischer, J.S., Soffer, S.Z., Ring, L., New, T., Zabski, S., Rudge, J.S., Holash, J., Yancopoulos, G.D., Kandel, J.J. and Yamashiro, D.J. (2002) Potent VEGF blockade causes regression of coopted vessels in a model of neuroblastoma. Proc. Natl. Acad. Sci. USA 99:11399–11404.
196. Eyetech Study Group. (2003) Anti-vascular endothelial growth factor therapy for subfoveal choroidal neovascularization secondary to age-related macular degeneration: phase II study results. Ophthalmology 110:979–986.
197. Morris, K.N., Jensen, K.B., Julin, C.M., Weil, M. and Gold, L. (1998) High affinity ligands from in vitro selection: complex targets. Proc. Natl. Acad. Sci. USA 95:2902–2907.

198. Lorger, M., Engstler, M., Homann, M. and Göringer, H.U. (2003) Targeting the variable surface of African trypanosomes with variant surface glycoprotein-specific, serum-stable RNA aptamers. Eukaryot. Cell 2:84–94.
199. Cerchia, L., Duconge, F., Pestourie, C., Boulay, J., Aissouni, Y., Gombert, K., Tavitian, B., de Franciscis, V. and Libri, D. (2005) Neutralizing aptamers from whole-cell SELEX inhibit the RET receptor tyrosine kinase. PLoS Biol. 3:e123.
200. Shangguan, D., Li, Y., Tang, Z., Cao, Z.C., Chen, H.W., Mallikaratchy, P., Sefah, K., Yang, C.J. and Tan, W. (2006) Aptamers evolved from live cells as effective molecular probes for cancer study. Proc. Natl. Acad. Sci. USA 103:11838–11843.
201. Chu, T.C., Twu, K.Y., Ellington, A.D. and Levy, M. (2006) Aptamer mediated siRNA delivery. Nucleic Acids Res. 34:e73.
202. Pan, W., Craven, R.C., Qiu, Q., Wilson, C.B., Wills, J.W., Golovine, S. and Wang, J.F. (1995) Isolation of virus-neutralizing RNAs from a large pool of random sequences. Proc. Natl. Acad. Sci. USA 92:11509–11513.
203. Wang, J., Jiang, H. and Liu, F. (2000) In vitro selection of novel RNA ligands that bind human cytomegalovirus and block viral infection. RNA 6:571–583.
204. Homann, M. and Göringer, H.U. (1999) Combinatorial selection of high affinity RNA ligands to live African trypanosomes. Nucleic Acids Res. 27:2006–2014.
205. Famulok, M., Blind, M. and Mayer, G. (2001) Intramers as promising new tools in functional proteomics. Chem. Biol. 8:931–939.
206. Famulok, M. and Verma, S. (2002) In vivo-applied functional RNAs as tools in proteomics and genomics research. Trends Biotechnol. 20:462–466.
207. Toulmé, J.J., Di Primo, C. and Boucard, D. (2004) Regulating eukaryotic gene expression with aptamers. FEBS Lett. 567:55–62.
208. Kim, M.Y. and Jeong, S. (2004) Inhibition of the functions of the nucleocapsid protein of human immunodeficiency virus-1 by an RNA aptamer. Biochem. Biophys. Res. Commun. 320:1181–1186.
209. Theis, M.G., Knorre, A., Kellersch, B., Moelleken, J., Wieland, F., Kolanus, W. and Famulok, M. (2004) Discriminatory aptamer reveals serum response element transcription regulated by cytohesin-2. Proc. Natl. Acad. Sci. USA 101:11221–11226.
210. Choi, K.H., Park, M.W., Lee, S.Y., Jeon, M.Y., Kim, M.Y., Lee, H.K., Yu, J., Kim, H.J., Han, K., Lee, H., Park, K., Park, W.J. and Jeong, S. (2006) Intracellular expression of the T-cell factor-1 RNA aptamer as an intramer. Mol. Cancer Ther. 5:2428–2434.
211. Cerchia, L., Hamm, J., Libri, D., Tavitian, B. and de Franciscis, V. (2002) Nucleic acid aptamers in cancer medicine. FEBS Lett. 528:12–16.
212. Nimjee, S.M., Rusconi, C.P. and Sullenger, B.A. (2005) Aptamers: an emerging class of therapeutics. Annu. Rev. Med. 56:555–583.
213. Ireson, C.R. and Kelland, L.R. (2006) Discovery and development of anticancer aptamers. Mol. Cancer Ther. 5:2957–2962.
214. Pei, D.H., Ulrich, H.D. and Schultz, P.G. (1991) A combinatorial approach toward DNA recognition. Science 253:1408–1411.
215. Soukup, G.A., Ellington, A.D. and Maher, L.J., III. (1996) Selection of RNAs that bind to duplex DNA at neutral pH. J. Mol. Biol. 259:216–228.
216. Mishra, R.K., Le Tinévez, R. and Toulmé, J.J. (1996) Targeting nucleic acid secondary structures by antisense oligonucleotides designed through in vitro selection. Proc. Natl. Acad. Sci. USA 93:10679–10684.
217. Boiziau, C., Dausse, E., Mishra, R., Ducongé, F. and Toulmé, J.J. (1997) Identification of aptamers against the DNA template for in vitro transcription of the HIV-1 TAR element. Antisense Nucleic Acid Drug Dev. 7:369–380.
218. Ducongé, F. and Toulmé, J.J. (1999) In vitro selection identifies key determinants for loop–loop interactions: RNA aptamers selective for the TAR RNA element of HIV-1. RNA 5:1605–1614.
219. Scarabino, D., Crisari, A., Lorenzini, S., Williams, K. and Tocchini-Valentini, G.P. (1999) tRNA prefers to kiss. EMBO J. 18:4571–4578.

220. Tok, J.B., Cho, J. and Rando, R.R. (2000) RNA aptamers that specifically bind to a 16S ribosomal RNA decoding region construct. Nucleic Acids Res. 28:2902–2910.
221. Aldaz-Carroll, L., Tallet, B., Dausse, E., Yurchenko, L. and Toulmé, J.J. (2002) Apical loop–internal loop interactions: a new RNA–RNA recognition motif identified through in vitro selection against RNA hairpins of the hepatitis C virus mRNA. Biochemistry 41:5883–5893.
222. Kikuchi, K., Umehara, T., Fukuda, K., Hwang, J., Kuno, A., Hasegawa, T. and Nishikawa, S. (2003) RNA aptamers targeted to domain II of hepatitis C virus IRES that bind to its apical loop region. J. Biochem. 133:263–270.
223. Da Rocha Gomes, S., Dausse, E. and Toulme, J.J. (2004) Determinants of apical loop–internal loop RNA–RNA interactions involving the HCV IRES. Biochem. Biophys. Res. Commun. 322:820–826.
224. Kikuchi, K., Umehara, T., Fukuda, K., Kuno, A., Hasegawa, T. and Nishikawa, S. (2005) A hepatitis C virus (HCV) internal ribosome entry site (IRES) domain III-IV-targeted aptamer inhibits translation by binding to an apical loop of domain IIId. Nucleic Acids Res. 33:683–692.
225. Fauzi, H., Jack, K.D. and Hines, J.V. (2005) In vitro selection to identify determinants in tRNA for *Bacillus subtilis tyr*S T box antiterminator mRNA binding. Nucleic Acids Res. 33:2595–2602.
226. Manimala, J.C., Wiskur, S.L., Ellington, A.D. and Anslyn, E.V. (2004) Tuning the specificity of a synthetic receptor using a selected nucleic acid receptor. J. Am. Chem. Soc. 126:16515–16519.
227. Carothers, J.M., Oestreich, S.C., Davis, J.H. and Szostak, J.W. (2004) Informational complexity and functional activity of RNA structures. J. Am. Chem. Soc. 126:5130–5137.
228. Davis, J.P., Janjic, N., Javornik, B.E. and Zichi, D.A. (1996) Identifying consensus patterns and secondary structure in SELEX sequence sets. Methods Enzymol. 267:302–314.
229. Zuker, M. (2003) Mfold web server for nucleic acid folding and hybridization prediction. Nucleic Acids Res. 31:3406–3415.
230. Burgstaller, P., Kochoyan, M. and Famulok, M. (1995) Structural probing and damage selection of citrulline- and arginine-specific RNA aptamers identify base positions required for binding. Nucleic Acids Res. 23:4769–4776.
231. Burgstaller, P. and Famulok, M. (1996) Structural characterization of a flavin-specific RNA aptamer by chemical probing. Bioorg. Med. Chem. Lett. 6:1157–1162.
232. McGregor, A., Murray, J.B., Adams, C.J., Stockley, P.G. and Connolly, B.A. (1999) Secondary structure mapping of an RNA ligand that has high affinity for the MetJ repressor protein and interference modification analysis of the protein–RNA complex. J. Biol. Chem. 274:2255–2262.
233. Sayer, N.M., Cubin, M., Rhie, A., Bullock, M., Tahiri-Alaoui, A. and James, W. (2004) Structural determinants of conformationally selective, prion-binding aptamers. J. Biol. Chem. 279:13102–13109.
234. Dey, A.K., Griffiths, C., Lea, S.M. and James, W. (2005) Structural characterization of an anti-gp120 RNA aptamer that neutralizes R5 strains of HIV-1. RNA 11:873–884.
235. Davis, J.H. and Szostak, J.W. (2002) Isolation of high-affinity GTP aptamers from partially structured RNA libraries. Proc. Natl. Acad. Sci. USA 99:11616–11621.
236. Dunn, B.M. and Chaiken, I.M. (1974) Quantitative affinity chromatography. Determination of binding constants by elution with competitive inhibitors. Proc. Natl. Acad. Sci. USA 71:2382–2385.
237. Arnold, F.H., Schofield, S.A. and Blanch, H.W. (1986) Analytical affinity chromatography. I. Local equilibrium theory and the measurement of assocation and inhibition constants. J. Chromatogr. 355:1–12.
238. Arnold, F.H. and Blanch, H.W. (1986) Analytical affinity chromatography. II. Rate theory and the measurement of biological binding kinetics. J. Chromatogr. 355:13–27.
239. Jiang, Y., Zhu, C., Ling, L., Wan, L., Fang, X. and Bai, C. (2003) Specific aptamer–protein interaction studied by atomic force microscopy. Anal. Chem. 75:2112–2116.

240. Jiang, Y., Wang, J., Fang, X. and Bai, C. (2004) Study of the effect of metal ion on the specific interaction between protein and aptamer by atomic force microscopy. J. Nanosci. Nanotechnol. 4:611–615.
241. Basnar, B., Elnathan, R. and Willner, I. (2006) Following aptamer-thrombin binding by force measurements. Anal. Chem. 78:3638–3642.
242. Jayasena, S.D. (1999) Aptamers: an emerging class of molecules that rival antibodies in diagnostics. Clin. Chem. 45:1628–1650.
243. Carothers, J.M., Oestreich, S.C. and Szostak, J.W. (2006) Aptamers selected for higher-affinity binding are not more specific for the target ligand. J. Am. Chem. Soc. 128:7929–7937.
244. Huang, Z. and Szostak, J.W. (2003) Evolution of aptamers with a new specificity and new secondary structures from an ATP aptamer. RNA 9:1456–1463.
245. Anderson, P.C. and Mecozzi, S. (2005) Unusually short RNA sequences: design of a 13-mer RNA that selectively binds and recognizes theophylline. J. Am. Chem. Soc. 127:5290–5291.
246. Anderson, P.C. and Mecozzi, S. (2005) Identification of a 14mer RNA that recognizes and binds flavin mononucleotide with high affinity. Nucleic Acids Res. 33:6992–6999.
247. Yarus, M. (2000) RNA-ligand chemistry: a testable source for the genetic code. RNA 6:475–484.
248. Lin, Y., Qiu, Q., Gill, S.C. and Jayasena, S.D. (1994) Modified RNA sequence pools for in vitro selection. Nucleic Acids Res. 22:5229–5234.
249. Lin, Y., Nieuwlandt, D., Magallanez, A., Feistner, B. and Jayasena, S.D. (1996) High-affinity and specific recognition of human thyroid stimulating hormone (hTSH) by in vitro-selected 2′-amino-modified RNA. Nucleic Acids Res. 24:3407–3414.
250. Beaudry, A., DeFoe, J., Zinnen, S., Burgin, A. and Beigelman, L. (2000) In vitro selection of a novel nuclease-resistant RNA phosphodiesterase. Chem. Biol. 7:323–334.
251. Beigelman, L., McSwiggen, J.A., Draper, K.G., Gonzalez, C., Jensen, K., Karpeisky, A.M., Modak, A.S., Matulic-Adamic, J., DiRenzo, A.B., Haeberli, P., Sweedler, D., Trace D., Grimm, S., Wincott, F.E., Thackray, V.G., and Usman, N. (1995) Chemical modification of hammerhead ribozymes. Catalytic activity and nuclease resistance. J. Biol. Chem. 270: 25702–25708.
252. Kato, Y., Minakawa, N., Komatsu, Y., Kamiya, H., Ogawa, N., Harashima, H. and Matsuda, A. (2005) New NTP analogs: the synthesis of 4′-thioUTP and 4′-thioCTP and their utility for SELEX. Nucleic Acids Res. 33:2942–2951.
253. Green, L., Waugh, S., Binkley, J.P., Hostomska, Z., Hostomsky, Z. and Tuerk, C. (1995) Comprehensive chemical modification interference and nucleotide substitution analysis of an RNA pseudoknot inhibitor to HIV-1 reverse transcriptase. J. Mol. Biol. 247:60–68.
254. Bell, C., Lynam, E., Landfair, D.J., Janjic, N. and Wiles, M.E. (1999) Oligonucleotide NX1838 inhibits VEGF165-mediated cellular responses in vitro. In Vitro Cell Dev. Biol. Anim. 35:533–542.
255. de Smidt, P.C., Le Doan, T., de Falco, S. and van Berkel, T.J. (1991) Association of antisense oligonucleotides with lipoproteins prolongs the plasma half-life and modifies the tissue distribution. Nucleic Acids Res. 19:4695–4700.
256. Rusconi, C.P., Roberts, J.D., Pitoc, G.A., Nimjee, S.M., White, R.R., Quick, G., Jr., Scardino, E., Fay, W.P. and Sullenger, B.A. (2004) Antidote-mediated control of an anticoagulant aptamer in vivo. Nat. Biotechnol. 22:1423–1428.
257. Dougan, H., Lyster, D.M., Vo, C.V., Stafford, A., Weitz, J.I. and Hobbs, J.B. (2000) Extending the lifetime of anticoagulant oligodeoxynucleotide aptamers in blood. Nucl. Med. Biol. 27:289–297.
258. Willis, M.C., Collins, B.D., Zhang, T., Green, L.S., Sebesta, D.P., Bell, C., Kellogg, E., Gill, S.C., Magallanez, A., Knauer, S., Bendele, R.A., Gill, P.S. and Janjic, N. (1998) Liposome-anchored vascular endothelial growth factor aptamers. Bioconjug. Chem. 9:573–582.
259. Schmidt, K.S., Borkowski, S., Kurreck, J., Stephens, A.W., Bald, R., Hecht, M., Friebe, M., Dinkelborg, L. and Erdmann, V.A. (2004) Application of locked nucleic acids to improve aptamer in vivo stability and targeting function. Nucleic Acids Res. 32:5757–5765.
260. Battersby, T.R., Ang, D.N., Burgstaller, P., Jurczyk, S.C., Bowser, M.T., Buchanan, D.D., Kennedy, R.T. and Benner, S.A. (1999) Quantitative analysis of receptors for adenosine

nucleotides obtained via in vitro selection from a library incorporating a cationic nucleotide analog. J. Am. Chem. Soc. 121:9781–9789.
261. Teramoto, N., Ichinari, H., Kawazoe, N., Imanishi, Y. and Ito, Y. (2001) Peroxidase activity of in vitro-selected 2′-amino RNAs. Biotechnol. Bioeng. 75:463–468.
262. Vaish, N.K., Larralde, R., Fraley, A.W., Szostak, J.W. and McLaughlin, L.W. (2003) A novel, modification-dependent ATP-binding aptamer selected from an RNA library incorporating a cationic functionality. Biochemistry 42:8842–8851.
263. Vater, A. and Klussmann, S. (2003) Toward third-generation aptamers: Spiegelmers and their therapeutic prospects. Curr. Opin. Drug Disc. Dev. 6:253–261.
264. Klussmann, S., Nolte, A., Bald, R., Erdmann, V.A. and Furste, J.P. (1996) Mirror-image RNA that binds D-adenosine. Nat. Biotechnol. 14:1112–1115.
265. Nolte, A., Klussmann, S., Bald, R., Erdmann, V.A. and Furste, J.P. (1996) Mirror-design of L-oligonucleotide ligands binding to L-arginine. Nat. Biotechnol. 14:1116–1119.
266. Leva, S., Lichte, A., Burmeister, J., Muhn, P., Jahnke, B., Fesser, D., Erfurth, J., Burgstaller, P. and Klussmann, S. (2002) GnRH binding RNA and DNA Spiegelmers: a novel approach toward GnRH antagonism. Chem. Biol. 9:351–359.
267. Helmling, S., Maasch, C., Eulberg, D., Buchner, K., Schroder, W., Lange, C., Vonhoff, S., Wlotzka, B., Tschop, M.H., Rosewicz, S. and Klussmann, S. (2004) Inhibition of ghrelin action in vitro and in vivo by an RNA-Spiegelmer. Proc. Natl. Acad. Sci. USA 101:13174–13179.
268. Faulhammer, D., Eschgfäller, B., Stark, S., Burgstaller, P., Englberger, W., Erfurth, J., Kleinjung, F., Rupp, J., Dan Vulcu, S., Schröder, W., Vonhoff, S., Nawrath, H., Gillen, C. and Klussmann, S. (2004) Biostable aptamers with antagonistic properties to the neuropeptide nociceptin/orphanin FQ. RNA 10:516–527.
269. Lin, C.H. and Patel, D.J. (1997) Structural basis of DNA folding and recognition in an AMP–DNA aptamer complex: distinct architectures but common recognition motifs for DNA and RNA aptamers complexed to AMP. Chem. Biol. 4:817–832.
270. Travascio, P., Bennet, A.J., Wang, D.Y. and Sen, D. (1999) A ribozyme and a catalytic DNA with peroxidase activity: active sites versus cofactor-binding sites. Chem. Biol. 6:779–787.
271. Stojanovic, M.N., de Prada, P. and Landry, D.W. (2001) Aptamer-based folding fluorescent sensor for cocaine. J. Am. Chem. Soc. 123:4928–4931.
272. Stojanovic, M.N. and Landry, D.W. (2002) Aptamer-based colorimetric probe for cocaine. J. Am. Chem. Soc. 124:9678–9679.
273. Kato, T., Yano, K., Ikebukuro, K. and Karube, I. (2000) Interaction of three-way DNA junctions with steroids. Nucleic Acids Res. 28:1963–1968.
274. Kim, Y.S., Jung, H.S., Matsuura, T., Lee, H.Y., Kawai, T. and Gu, M.B. (2007) Electrochemical detection of 17β-estradiol using DNA aptamer immobilized gold electrode chip. Biosens. Bioelectron. 22:2525–2531.
275. Chinnapen, D.J. and Sen, D. (2002) Hemin-stimulated docking of cytochrome c to a hemin-DNA aptamer complex. Biochemistry 41:5202–5212.
276. Shoji, A., Kuwahara, M., Ozaki, H. and Sawai, H. (2007) Modified DNA aptamer that binds the (*R*)-isomer of a thalidomide derivative with high enantioselectivity. J. Am. Chem. Soc. 129:1456–1464.
277. Boiziau, C., Dausse, E., Yurchenko, L. and Toulmé, J.J. (1999) DNA aptamers selected against the HIV-1 trans-activation-responsive RNA element form RNA–DNA kissing complexes. J. Biol. Chem. 274:12730–12737.
278. Sekkai, D., Dausse, E., Di Primo, C., Darfeuille, F., Boiziau, C. and Toulmé, J.J. (2002) In vitro selection of DNA aptamers against the HIV-1 TAR RNA hairpin. Antisense Nucleic Acid Drug Dev. 12:265–274.
279. Bruno, J.G. and Kiel, J.L. (1999) In vitro selection of DNA aptamers to anthrax spores with electrochemiluminescence detection. Biosens. Bioelectron. 14:457–464.
280. Latham, J.A., Johnson, R. and Toole, J.J. (1994) The application of a modified nucleotide in aptamer selection: novel thrombin aptamers containing 5-(1-pentynyl)-2′-deoxyuridine. Nucleic Acids Res. 22:2817–2822.

281. Masud, M.M., Kuwahara, M., Ozaki, H. and Sawai, H. (2004) Sialyllactose-binding modified DNA aptamer bearing additional functionality by SELEX. Bioorg. Med. Chem. 12:1111–1120.
282. Williams, K.P., Liu, X.H., Schumacher, T.N., Lin, H.Y., Ausiello, D.A., Kim, P.S. and Bartel, D.P. (1997) Bioactive and nuclease-resistant L-DNA ligand of vasopressin. Proc. Natl. Acad. Sci. USA 94:11285–11290.
283. Wlotzka, B., Leva, S., Eschgfaller, B., Burmeister, J., Kleinjung, F., Kaduk, C., Muhn, P., Hess-Stumpp, H. and Klussmann, S. (2002) In vivo properties of an anti-GnRH Spiegelmer: an example of an oligonucleotide-based therapeutic substance class. Proc. Natl. Acad. Sci. USA 99:8898–8902.
284. Purschke, W.G., Radtke, F., Kleinjung, F. and Klussmann, S. (2003) A DNA Spiegelmer to staphylococcal enterotoxin B. Nucleic Acids Res. 31:3027–3032.
285. Nguyen, D.H., DeFina, S.C., Fink, W.H. and Dieckmann, T. (2002) Binding to an RNA aptamer changes the charge distribution and conformation of malachite green. J. Am. Chem. Soc. 124:15081–15084.
286. Hermann, T. and Patel, D.J. (2000) Adaptive recognition by nucleic acid aptamers. Science 287:820–825.
287. Lin, C.H. and Patel, D.J. (1996) Encapsulating an amino acid in a DNA fold. Nat. Struct. Biol. 3:1046–1050.
288. Lin, C.H., Wang, W., Jones, R.A. and Patel, D.J. (1998) Formation of an amino-acid-binding pocket through adaptive zippering-up of a large DNA hairpin loop. Chem. Biol. 5:555–572.
289. Yang, Y., Kochoyan, M., Burgstaller, P., Westhof, E. and Famulok, M. (1996) Structural basis of ligand discrimination by two related RNA aptamers resolved by NMR spectroscopy. Science 272:1343–1347.
290. Fan, P., Suri, A.K., Fiala, R., Live, D. and Patel, D.J. (1996) Molecular recognition in the FMN–RNA aptamer complex. J. Mol. Biol. 258:480–500.
291. Jiang, L., Suri, A.K., Fiala, R. and Patel, D.J. (1997) Saccharide–RNA recognition in an aminoglycoside antibiotic–RNA aptamer complex. Chem. Biol. 4:35–50.
292. Jiang, L. and Patel, D.J. (1998) Solution structure of the tobramycin–RNA aptamer complex. Nat. Struct. Biol. 5:769–774.
293. Jiang, L., Majumdar, A., Hu, W., Jaishree, T.J., Xu, W. and Patel, D.J. (1999) Saccharide–RNA recognition in a complex formed between neomycin B and an RNA aptamer. Structure 7:817–827.
294. Ye, X., Gorin, A., Ellington, A.D. and Patel, D.J. (1996) Deep penetration of an α-helix into a widened RNA major groove in the HIV-1 rev peptide–RNA aptamer complex. Nat. Struct. Biol. 3:1026–1033.
295. Collin, D., van Heijenoort, C., Boiziau, C., Toulmé, J.J. and Guittet, E. (2000) NMR characterization of a kissing complex formed between the TAR RNA element of HIV-1 and a DNA aptamer. Nucleic Acids Res. 28:3386–3391.
296. Flinders, J., DeFina, S.C., Brackett, D.M., Baugh, C., Wilson, C. and Dieckmann, T. (2004) Recognition of planar and nonplanar ligands in the malachite green–RNA aptamer complex. ChemBioChem 5:62–72.
297. Baugh, C., Grate, D. and Wilson, C. (2000) 2.8 Å crystal structure of the malachite green aptamer. J. Mol. Biol. 301:117–128.
298. Nix, J., Sussman, D. and Wilson, C. (2000) The 1.3 Å crystal structure of a biotin-binding pseudoknot and the basis for RNA molecular recognition. J. Mol. Biol. 296:1235–1244.
299. Sussman, D., Nix, J.C. and Wilson, C. (2000) The structural basis for molecular recognition by the vitamin B_{12} RNA aptamer. Nat. Struct. Biol. 7:53–57.
300. Sussman, D. and Wilson, C. (2000) A water channel in the core of the vitamin B_{12} RNA aptamer. Structure 8:719–727.
301. Tereshko, V., Skripkin, E. and Patel, D.J. (2003) Encapsulating streptomycin within a small 40-mer RNA. Chem. Biol. 10:175–187.
302. Rowsell, S., Stonehouse, N.J., Convery, M.A., Adams, C.J., Ellington, A.D., Hirao, I., Peabody, D.S., Stockley, P.G. and Phillips, S.E. (1998) Crystal structures of a series of RNA aptamers complexed to the same protein target. Nat. Struct. Biol. 5:970–975.

303. Convery, M.A., Rowsell, S., Stonehouse, N.J., Ellington, A.D., Hirao, I., Murray, J.B., Peabody, D.S., Phillips, S.E. and Stockley, P.G. (1998) Crystal structure of an RNA aptamer–protein complex at 2.8 Å resolution. Nat. Struct. Biol. 5:133–139.
304. Horn, W.T., Convery, M.A., Stonehouse, N.J., Adams, C.J., Liljas, L., Phillips, S.E. and Stockley, P.G. (2004) The crystal structure of a high affinity RNA stem-loop complexed with the bacteriophage MS2 capsid: further challenges in the modeling of ligand–RNA interactions. RNA 10:1776–1782.
305. Zimmermann, G.R., Jenison, R.D., Wick, C.L., Simorre, J.P. and Pardi, A. (1997) Interlocking structural motifs mediate molecular discrimination by a theophylline-binding RNA. Nat. Struct. Biol. 4:644–649.
306. Zimmermann, G.R., Wick, C.L., Shields, T.P., Jenison, R.D. and Pardi, A. (2000) Molecular interactions and metal binding in the theophylline-binding core of an RNA aptamer. RNA 6:659–667.
307. Jucker, F.M., Phillips, R.M., McCallum, S.A. and Pardi, A. (2003) Role of a heterogeneous free state in the formation of a specific RNA–theophylline complex. Biochemistry 42:2560–2567.
308. Zimmermann, G.R., Shields, T.P., Jenison, R.D., Wick, C.L. and Pardi, A. (1998) A semiconserved residue inhibits complex formation by stabilizing interactions in the free state of a theophylline-binding RNA. Biochemistry 37:9186–9192.
309. Jiang, F., Kumar, R.A., Jones, R.A. and Patel, D.J. (1996) Structural basis of RNA folding and recognition in an AMP–RNA aptamer complex. Nature (Lond.) 382:183–186.
310. Dieckmann, T., Suzuki, E., Nakamura, G.K. and Feigon, J. (1996) Solution structure of an ATP-binding RNA aptamer reveals a novel fold. RNA 2:628–640.
311. Patel, D.J., Suri, A.K., Jiang, F., Jiang, L., Fan, P., Kumar, R.A. and Nonin, S. (1997) Structure, recognition and adaptive binding in RNA aptamer complexes. J. Mol. Biol. 272:645–664.
312. Nonin, S., Jiang, F. and Patel, D.J. (1997) Imino proton exchange and base-pair kinetics in the AMP–RNA aptamer complex. J. Mol. Biol. 268:359–374.
313. Dieckmann, T., Butcher, S.E., Sassanfar, M., Szostak, J.W. and Feigon, J. (1997) Mutant ATP-binding RNA aptamers reveal the structural basis for ligand binding. J. Mol. Biol. 273:467–478.
314. Nonin-Lecomte, S., Lin, C.H. and Patel, D.J. (2001) Additional hydrogen bonds and base-pair kinetics in the symmetrical AMP–DNA aptamer complex. Biophys. J. 81:3422–3431.
315. Macaya, R.F., Schultze, P., Smith, F.W., Roe, J.A. and Feigon, J. (1993) Thrombin-binding DNA aptamer forms a unimolecular quadruplex structure in solution. Proc. Natl. Acad. Sci. USA 90:3745–3749.
316. Wang, K.Y., McCurdy, S., Shea, R.G., Swaminathan, S. and Bolton, P.H. (1993) A DNA aptamer which binds to and inhibits thrombin exhibits a new structural motif for DNA. Biochemistry 32:1899–1904.
317. Schultze, P., Macaya, R.F. and Feigon, J. (1994) Three-dimensional solution structure of the thrombin-binding DNA aptamer d(GGTTGGTGTGGTTGG). J. Mol. Biol. 235:1532–1547.
318. Wang, K.Y., Krawczyk, S.H., Bischofberger, N., Swaminathan, S. and Bolton, P.H. (1993) The tertiary structure of a DNA aptamer which binds to and inhibits thrombin determines activity. Biochemistry 32:11285–11292.
319. Padmanabhan, K., Padmanabhan, K.P., Ferrara, J.D., Sadler, J.E. and Tulinsky, A. (1993) The structure of α-thrombin inhibited by a 15-mer single-stranded DNA aptamer. J. Biol. Chem. 268:17651–17654.
320. Kelly, J.A., Feigon, J. and Yeates, T.O. (1996) Reconciliation of the X-ray and NMR structures of the thrombin-binding aptamer d(GGTTGGTGTGGTTGG). J. Mol. Biol. 256:417–422.
321. Padmanabhan, K. and Tulinsky, A. (1996) An ambiguous structure of a DNA 15-mer thrombin complex. Acta Crystallogr. D 52:272–282.
322. Mills, D.R., Peterson, R.L. and Spiegelman, S. (1967) An extracellular Darwinian experiment with a self-duplicating nucleic acid molecule. Proc. Natl. Acad. Sci. USA 58:217–224.

323. Spiegelman, S. (1971) An approach to the experimental analysis of precellular evolution. Q. Rev. Biophys. 4:213–253.
324. Guerrier-Takada, C., Gardiner, K., Marsh, T., Pace, N. and Altman, S. (1983) The RNA moiety of ribonuclease P is the catalytic subunit of the enzyme. Cell 35:849–857.
325. Green, R., Ellington, A.D. and Szostak, J.W. (1990) In vitro genetic analysis of the *Tetrahymena* self-splicing intron. Nature (Lond.) 347:406–408.
326. Bartel, D.P. and Szostak, J.W. (1993) Isolation of new ribozymes from a large pool of random sequences. Science 261:1411–1418.
327. Teramoto, N., Imanishi, Y. and Ito, Y. (2000) In vitro selection of a ligase ribozyme carrying alkylamino groups in the side chains. Bioconjug. Chem. 11:744–748.
328. Tuschl, T., Sharp, P.A. and Bartel, D.P. (1998) Selection in vitro of novel ribozymes from a partially randomized U2 and U6 snRNA library. EMBO J. 17:2637–2650.
329. Baskerville, S. and Bartel, D.P. (2002) A ribozyme that ligates RNA to protein. Proc. Natl. Acad. Sci. USA 99:9154–9159.
330. Seelig, B. and Jäschke, A. (1999) A small catalytic RNA motif with Diels–Alderase activity. Chem. Biol. 6:167–176.
331. Seelig, B., Keiper, S., Stuhlmann, F. and Jäschke, A. (2000) Enantioselective ribozyme catalysis of a bimolecular cycloaddition reaction. Angew. Chem. Int. Ed. 39:4576–4579.
332. Tsukiji, S., Pattnaik, S.B. and Suga, H. (2003) An alcohol dehydrogenase ribozyme. Nat. Struct. Biol. 10:713–717.
333. Zhang, B. and Cech, T.R. (1997) Peptide bond formation by in vitro selected ribozymes. Nature (Lond.) 390:96–100.
334. Lohse, P.A. and Szostak, J.W. (1996) Ribozyme-catalysed amino-acid transfer reactions. Nature (Lond.) 381:442–444.
335. Suga, H., Lohse, P.A. and Szostak, J.W. (1998) Structural and kinetic characterization of an acyl transferase ribozyme. J. Am. Chem. Soc. 120:1151–1156.
336. Jenne, A. and Famulok, M. (1998) A novel ribozyme with ester transferase activity. Chem. Biol. 5:23–34.
337. Lee, N., Bessho, Y., Wei, K., Szostak, J.W. and Suga, H. (2000) Ribozyme-catalyzed tRNA aminoacylation. Nat. Struct. Biol. 7:28–33.
338. Saito, H., Kourouklis, D. and Suga, H. (2001) An in vitro evolved precursor tRNA with aminoacylation activity. EMBO J. 20:1797–1806.
339. Sengle, G., Eisenführ, A., Arora, P.S., Nowick, J.S. and Famulok, M. (2001) Novel RNA catalysts for the Michael reaction. Chem. Biol. 8:459–473.
340. Lorsch, J.R. and Szostak, J.W. (1994) In vitro evolution of new ribozymes with polynucleotide kinase activity. Nature (Lond.) 371:31–36.
341. Kumar, R.K. and Yarus, M. (2001) RNA-catalyzed amino acid activation. Biochemistry 40:6998–7004.
342. Pan, T. and Uhlenbeck, O.C. (1992) A small metalloribozyme with a two-step mechanism. Nature (Lond.) 358:560–563.
343. Pan, T. and Uhlenbeck, O.C. (1992) In vitro selection of RNAs that undergo autolytic cleavage with Pb^{2+}. Biochemistry 31:3887–3895.
344. Williams, K.P., Ciafre, S. and Tocchini-Valentini, G.P. (1995) Selection of novel Mg^{2+}-dependent self-cleaving ribozymes. EMBO J. 14:4551–4557.
345. Jayasena, V.K. and Gold, L. (1997) In vitro selection of self-cleaving RNAs with a low pH optimum. Proc. Natl. Acad. Sci. USA 94:10612–10617.
346. Curtis, E.A. and Bartel, D.P. (2005) New catalytic structures from an existing ribozyme. Nat. Struct. Mol. Biol. 12:994–1000.
347. Johnston, W.K., Unrau, P.J., Lawrence, M.S., Glasner, M.E. and Bartel, D.P. (2001) RNA-catalyzed RNA polymerization: accurate and general RNA-templated primer extension. Science 292:1319–1325.
348. Tarasow, T.M., Tarasow, S.L. and Eaton, B.E. (1997) RNA-catalysed carbon–carbon bond formation. Nature (Lond.) 389:54–57.

349. Tarasow, T.M., Kellogg, E., Holley, B.L., Nieuwlandt, D., Tarasow, S.L. and Eaton, B.E. (2004) The effect of mutation on RNA Diels–Alderases. J. Am. Chem. Soc. 126:11843–11851.
350. Unrau, P.J. and Bartel, D.P. (1998) RNA-catalysed nucleotide synthesis. Nature (Lond.) 395:260–263.
351. Chapple, K.E., Bartel, D.P. and Unrau, P.J. (2003) Combinatorial minimization and secondary structure determination of a nucleotide synthase ribozyme. RNA 9:1208–1220.
352. Lau, M.W., Cadieux, K.E. and Unrau, P.J. (2004) Isolation of fast purine nucleotide synthase ribozymes. J. Am. Chem. Soc. 126:15686–15693.
353. Wiegand, T.W., Janssen, R.C. and Eaton, B.E. (1997) Selection of RNA amide synthases. Chem. Biol. 4:675–683.
354. Nieuwlandt, D., West, M., Cheng, X., Kirshenheuter, G. and Eaton, B.E. (2003) The first example of an RNA urea synthase: selection through the enzyme active site of human neutrophile elastase. ChemBioChem 4:651–654.
355. Illangasekare, M., Sanchez, G., Nickles, T. and Yarus, M. (1995) Aminoacyl–RNA synthesis catalyzed by an RNA. Science 267:643–647.
356. Wecker, M., Smith, D. and Gold, L. (1996) In vitro selection of a novel catalytic RNA: characterization of a sulfur alkylation reaction and interaction with a small peptide. RNA 2:982–994.
357. Tsang, J. and Joyce, G.F. (1996) Specialization of the DNA-cleaving activity of a group I ribozyme through in vitro evolution. J. Mol. Biol. 262:31–42.
358. Kore, A.R., Vaish, N.K., Morris, J.A. and Eckstein, F. (2000) In vitro evolution of the hammerhead ribozyme to a purine-specific ribozyme using mutagenic PCR with two nucleotide analogues. J. Mol. Biol. 301:1113–1121.
359. Breaker, R.R. and Joyce, G.F. (1994) Inventing and improving ribozyme function: rational design versus iterative selection methods. Trends Biotechnol. 12:268–275.
360. Tsang, J. and Joyce, G.F. (1996) In vitro evolution of randomized ribozymes. Methods Enzymol. 267:410–426.
361. Flynn-Charlebois, A., Prior, T.K., Hoadley, K.A. and Silverman, S.K. (2003) In vitro evolution of an RNA-cleaving DNA enzyme into an RNA ligase switches the selectivity from 3′-5′ to 2′-5′. J. Am. Chem. Soc. 125:5346–5350.
362. Knight, R. and Yarus, M. (2003) Analyzing partially randomized nucleic acid pools: straight dope on doping. Nucleic Acids Res. 31:e30.
363. Prudent, J.R., Uno, T. and Schultz, P.G. (1994) Expanding the scope of RNA catalysis. Science 264:1924–1927.
364. Conn, M.M., Prudent, J.R. and Schultz, P.G. (1996) Porphyrin metalation catalyzed by a small RNA molecule. J. Am. Chem. Soc. 118:7012–7013.
365. Chun, S.-M., Jeong, S., Kim, J.-M., Chong, B.-O., Park, Y.-K., Park, K. and Yu, J. (1999) Cholesterol esterase activity by in vitro selection of RNA against a phosphate transition-state analogue. J. Am. Chem. Soc. 121:10844–10845.
366. Morris, K.N., Tarasow, T.M., Julin, C.M., Simons, S.L., Hilvert, D. and Gold, L. (1994) Enrichment for RNA molecules that bind a Diels–Alder transition state analog. Proc. Natl. Acad. Sci. USA 91:13028–13032.
367. Wright, M.C. and Joyce, G.F. (1997) Continuous in vitro evolution of catalytic function. Science 276:614–617.
368. Ordoukhanian, P. and Joyce, G.F. (1999) A molecular description of the evolution of resistance. Chem. Biol. 6:881–889.
369. Johns, G.C. and Joyce, G.F. (2005) The promise and peril of continuous in vitro evolution. J. Mol. Evol. 61:253–263.
370. Agresti, J.J., Kelly, B.T., Jäschke, A. and Griffiths, A.D. (2005) Selection of ribozymes that catalyse multiple-turnover Diels–Alder cycloadditions by using in vitro compartmentalization. Proc. Natl. Acad. Sci. USA 102:16170–16175.
371. Levy, M., Griswold, K.E. and Ellington, A.D. (2005) Direct selection of trans-acting ligase ribozymes by in vitro compartmentalization. RNA 11:1555–1562.

372. Ekland, E.H., Szostak, J.W. and Bartel, D.P. (1995) Structurally complex and highly active RNA ligases derived from random RNA sequences. Science 269:364–370.
373. Hager, A.J. and Szostak, J.W. (1997) Isolation of novel ribozymes that ligate AMP-activated RNA substrates. Chem. Biol. 4:607–617.
374. Chapman, K.B. and Szostak, J.W. (1995) Isolation of a ribozyme with 5′-5′ ligase activity. Chem. Biol. 2:325–333.
375. Huang, F. and Yarus, M. (1997) 5′-RNA self-capping from guanosine diphosphate. Biochemistry 36:6557–6563.
376. Huang, F., Yang, Z. and Yarus, M. (1998) RNA enzymes with two small-molecule substrates. Chem. Biol. 5:669–678.
377. Huang, F., Bugg, C.W. and Yarus, M. (2000) RNA-catalyzed CoA, NAD, and FAD synthesis from phosphopantetheine, NMN, and FMN. Biochemistry 39:15548–15555.
378. Ekland, E.H. and Bartel, D.P. (1996) RNA-catalysed RNA polymerization using nucleoside triphosphates. Nature (Lond.) 382:373–376.
379. Fusz, S., Eisenfuhr, A., Srivatsan, S.G., Heckel, A. and Famulok, M. (2005) A ribozyme for the aldol reaction. Chem. Biol. 12:941–950.
380. Tsukiji, S., Pattnaik, S.B. and Suga, H. (2004) Reduction of an aldehyde by a NADH/Zn^{2+}-dependent redox active ribozyme. J. Am. Chem. Soc. 126:5044–5045.
381. Illangasekare, M. and Yarus, M. (1999) A tiny RNA that catalyzes both aminoacyl–RNA and peptidyl–RNA synthesis. RNA 5:1482–1489.
382. Illangasekare, M. and Yarus, M. (1999) Specific, rapid synthesis of Phe-RNA by RNA. Proc. Natl. Acad. Sci. USA 96:5470–5475.
383. Gugliotti, L.A., Feldheim, D.L. and Eaton, B.E. (2004) RNA-mediated metal–metal bond formation in the synthesis of hexagonal palladium nanoparticles. Science 304:850–852.
384. Gugliotti, L.A., Feldheim, D.L. and Eaton, B.E. (2005) RNA-mediated control of metal nanoparticle shape. J. Am. Chem. Soc. 127:17814–17818.
385. Uhlenbeck, O.C. (2003) Less isn't always more. RNA 9:1415–1417.
386. Wang, Q.S. and Unrau, P.J. (2005) Ribozyme motif structure mapped using random recombination and selection. RNA 11:404–411.
387. Das, S.R. and Piccirilli, J.A. (2005) General acid catalysis by the hepatitis delta virus ribozyme. Nat. Chem. Biol. 1:45–52.
388. Bevilacqua, P.C. and Yajima, R. (2006) Nucleobase catalysis in ribozyme mechanism. Curr. Opin. Chem. Biol. 10:455–464.
389. Unrau, P.J. and Bartel, D.P. (2003) An oxocarbenium-ion intermediate of a ribozyme reaction indicated by kinetic isotope effects. Proc. Natl. Acad. Sci. USA 100:15393–15397.
390. Suga, H., Cowan, J.A. and Szostak, J.W. (1998) Unusual metal ion catalysis in an acyltransferase ribozyme. Biochemistry 37:10118–10125.
391. Vaidya, A. and Suga, H. (2001) Diverse roles of metal ions in acyl-transferase ribozymes. Biochemistry 40:7200–7210.
392. Saito, H. and Suga, H. (2002) Outersphere and innersphere coordinated metal ions in an aminoacyl-tRNA synthetase ribozyme. Nucleic Acids Res. 30:5151–5159.
393. Flynn-Charlebois, A., Lee, N. and Suga, H. (2001) A single metal ion plays structural and chemical roles in an aminoacyl-transferase ribozyme. Biochemistry 40:13623–13632.
394. Sievers, A., Beringer, M., Rodnina, M.V. and Wolfenden, R. (2004) The ribosome as an entropy trap. Proc. Natl. Acad. Sci. USA 101:7897–7901.
395. Weinger, J.S., Parnell, K.M., Dorner, S., Green, R. and Strobel, S.A. (2004) Substrate-assisted catalysis of peptide bond formation by the ribosome. Nat. Struct. Mol. Biol. 11:1101–1106.
396. Bieling, P., Beringer, M., Adio, S. and Rodnina, M.V. (2006) Peptide bond formation does not involve acid–base catalysis by ribosomal residues. Nat. Struct. Mol. Biol. 13:423–428.
397. Wedekind, J.E. and McKay, D.B. (1999) Crystal structure of a lead-dependent ribozyme revealing metal binding sites relevant to catalysis. Nat. Struct. Biol. 6:261–268.
398. Wedekind, J.E. and McKay, D.B. (2003) Crystal structure of the leadzyme at 1.8 Å resolution: metal ion binding and the implications for catalytic mechanism and allo site ion regulation. Biochemistry 42:9554–9563.

399. Legault, P., Hoogstraten, C.G., Metlitzky, E. and Pardi, A. (1998) Order, dynamics and metal-binding in the lead-dependent ribozyme. J. Mol. Biol. 284:325–335.
400. Hoogstraten, C.G., Legault, P. and Pardi, A. (1998) NMR solution structure of the lead-dependent ribozyme: evidence for dynamics in RNA catalysis. J. Mol. Biol. 284:337–350.
401. Serganov, A., Keiper, S., Malinina, L., Tereshko, V., Skripkin, E., Höbartner, C., Polonskaia, A., Phan, A.T., Wombacher, R., Micura, R., Dauter, Z., Jäschke, A. and Patel, D.J. (2005) Structural basis for Diels–Alder ribozyme-catalyzed carbon–carbon bond formation. Nat. Struct. Mol. Biol. 12:218–224.
402. Robertson, M.P. and Scott, W.G. (2007) The structural basis of ribozyme-catalyzed RNA assembly. Science 315:1549–1553.
403. Rogers, J. and Joyce, G.F. (1999) A ribozyme that lacks cytidine. Nature (Lond.) 402:323–325.
404. Rogers, J. and Joyce, G.F. (2001) The effect of cytidine on the structure and function of an RNA ligase ribozyme. RNA 7:395–404.
405. Reader, J.S. and Joyce, G.F. (2002) A ribozyme composed of only two different nucleotides. Nature (Lond.) 420:841–844.
406. Schultes, E.A. and Bartel, D.P. (2000) One sequence, two ribozymes: implications for the emergence of new ribozyme folds. Science 289:448–452.
407. Pieken, W.A., Olsen, D.B., Benseler, F., Aurup, H. and Eckstein, F. (1991) Kinetic characterization of ribonuclease-resistant 2′-modified hammerhead ribozymes. Science 253:314–317.
408. Cech, T.R. (1987) The chemistry of self-splicing RNA and RNA enzymes. Science 236: 1532–1539.
409. Breaker, R.R. and Joyce, G.F. (1994) A DNA enzyme that cleaves RNA. Chem. Biol. 1:223–229.
410. Santoro, S.W., Joyce, G.F., Sakthivel, K., Gramatikova, S. and Barbas, C.F., III. (2000) RNA cleavage by a DNA enzyme with extended chemical functionality. J. Am. Chem. Soc. 122:2433–2439.
411. Perrin, D.M., Garestier, T. and Hélène, C. (2001) Bridging the gap between proteins and nucleic acids: a metal-independent RNAseA mimic with two protein-like functionalities. J. Am. Chem. Soc. 123:1556–1563.
412. Sidorov, A.V., Grasby, J.A. and Williams, D.M. (2004) Sequence-specific cleavage of RNA in the absence of divalent metal ions by a DNAzyme incorporating imidazolyl and amino functionalities. Nucleic Acids Res. 32:1591–1601.
413. Thum, O., Jager, S. and Famulok, M. (2001) Functionalized DNA: a new replicable biopolymer. Angew. Chem. Int. Ed. 40:3990–3993.
414. Liu, Y. and Sen, D. (2004) Light-regulated catalysis by an RNA-cleaving deoxyribozyme. J. Mol. Biol. 341:887–892.
415. Keiper, S. and Vyle, J.S. (2006) Reversible photocontrol of deoxyribozyme-catalyzed RNA cleavage under multiple-turnover conditions. Angew. Chem. Int. Ed. 45:3306–3309.
416. Bruesehoff, P.J., Li, J., Augustine, A.J., III and Lu, Y. (2002) Improving metal ion specificity during in vitro selection of catalytic DNA. Comb. Chem. High Throughput Screen. 5:327–335.
417. Williams, K.P. and Bartel, D.P. (1995) PCR product with strands of unequal length. Nucleic Acids Res. 23:4220–4221.
418. Sheppard, T.L., Ordoukhanian, P. and Joyce, G.F. (2000) A DNA enzyme with *N*-glycosylase activity. Proc. Natl. Acad. Sci. USA 97:7802–7807.
419. Flynn-Charlebois, A., Wang, Y., Prior, T.K., Rashid, I., Hoadley, K.A., Coppins, R.L., Wolf, A.C. and Silverman, S.K. (2003) Deoxyribozymes with 2′-5′ RNA ligase activity. J. Am. Chem. Soc. 125:2444–2454.
420. Breaker, R.R. and Joyce, G.F. (1995) A DNA enzyme with Mg^{2+}-dependent RNA phosphoesterase activity. Chem. Biol. 2:655–660.
421. Santoro, S.W. and Joyce, G.F. (1997) A general purpose RNA-cleaving DNA enzyme. Proc. Natl. Acad. Sci. USA 94:4262–4266.
422. Geyer, C.R. and Sen, D. (1997) Evidence for the metal-cofactor independence of an RNA phosphodiester-cleaving DNA enzyme. Chem. Biol. 4:579–593.

423. Hoadley, K.A., Purtha, W.E., Wolf, A.C., Flynn-Charlebois, A. and Silverman, S.K. (2005) Zn^{2+}-dependent deoxyribozymes that form natural and unnatural RNA linkages. Biochemistry 44:9217–9231.
424. Purtha, W.E., Coppins, R.L., Smalley, M.K. and Silverman, S.K. (2005) General deoxyribozyme-catalyzed synthesis of native 3′–5′ RNA linkages. J. Am. Chem. Soc. 127:13124–13125.
425. Wang, Y. and Silverman, S.K. (2003) Deoxyribozymes that synthesize branched and lariat RNA. J. Am. Chem. Soc. 125:6880–6881.
426. Coppins, R.L. and Silverman, S.K. (2005) A deoxyribozyme that forms a three-helix-junction complex with its RNA substrates and has general RNA branch-forming activity. J. Am. Chem. Soc. 127:2900–2907.
427. Wang, Y. and Silverman, S.K. (2005) Efficient one-step synthesis of biologically related lariat RNAs by a deoxyribozyme. Angew. Chem. Int. Ed. 44:5863–5866.
428. Wang, W., Billen, L.P. and Li, Y. (2002) Sequence diversity, metal specificity, and catalytic proficiency of metal-dependent phosphorylating DNA enzymes. Chem. Biol. 9:507–517.
429. Li, Y., Liu, Y. and Breaker, R.R. (2000) Capping DNA with DNA. Biochemistry 39:3106–3114.
430. Cuenoud, B. and Szostak, J.W. (1995) A DNA metalloenzyme with DNA ligase activity. Nature (Lond.) 375:611–614.
431. Sreedhara, A., Li, Y. and Breaker, R.R. (2004) Ligating DNA with DNA. J. Am. Chem. Soc. 126:3454–3460.
432. Carmi, N., Shultz, L.A. and Breaker, R.R. (1996) In vitro selection of self-cleaving DNAs. Chem. Biol. 3:1039–1046.
433. Carmi, N., Balkhi, S.R. and Breaker, R.R. (1998) Cleaving DNA with DNA. Proc. Natl. Acad. Sci. USA 95:2233–2237.
434. Chinnapen, D.J. and Sen, D. (2004) A deoxyribozyme that harnesses light to repair thymine dimers in DNA. Proc. Natl. Acad. Sci. USA 101:65–69.
435. Burmeister, J., von Kiedrowski, G. and Ellington, A.D. (1997) Cofactor-assisted self-cleavage in DNA libraries with a 3′-5′ phosphoramidate bond. Angew. Chem. Int. Ed. Engl. 36:1321–1324.
436. Li, Y. and Sen, D. (1996) A catalytic DNA for porphyrin metallation. Nat. Struct. Biol. 3:743–747.
437. Silverman, S.K. (2005) In vitro selection, characterization, and application of deoxyribozymes that cleave RNA. Nucleic Acids Res. 33:6151–6163.
438. Santoro, S.W. and Joyce, G.F. (1998) Mechanism and utility of an RNA-cleaving DNA enzyme. Biochemistry 37:13330–13342.
439. Brown, A.K., Li, J., Pavot, C.M. and Lu, Y. (2003) A lead-dependent DNAzyme with a two-step mechanism. Biochemistry 42:7152–7161.
440. Roth, A. and Breaker, R.R. (1998) An amino acid as a cofactor for a catalytic polynucleotide. Proc. Natl. Acad. Sci. USA 95:6027–6031.
441. Nowakowski, J., Shim, P.J., Prasad, G.S., Stout, C.D. and Joyce, G.F. (1999) Crystal structure of an 82-nucleotide RNA–DNA complex formed by the 10–23 DNA enzyme. Nat. Struct. Biol. 6:151–156.
442. Paul, N., Springsteen, G. and Joyce, G.F. (2006) Conversion of a ribozyme to a deoxyribozyme through in vitro evolution. Chem. Biol. 13:329–338.
443. Robertson, M.P. and Ellington, A.D. (1999) In vitro selection of an allosteric ribozyme that transduces analytes to amplicons. Nat. Biotechnol. 17:62–66.
444. Tang, J. and Breaker, R.R. (1997) Rational design of allosteric ribozymes. Chem. Biol. 4:453–459.
445. Araki, M., Okuno, Y., Hara, Y. and Sugiura, Y. (1998) Allosteric regulation of a ribozyme activity through ligand-induced conformational change. Nucleic Acids Res. 26:3379–3384.
446. Soukup, G.A. and Breaker, R.R. (1999) Design of allosteric hammerhead ribozymes activated by ligand-induced structure stabilization. Structure 7:783–791.
447. Vaish, N.K., Dong, F., Andrews, L., Schweppe, R.E., Ahn, N.G., Blatt, L. and Seiwert, S.D. (2002) Monitoring post-translational modification of proteins with allosteric ribozymes. Nat. Biotechnol. 20:810–815.

448. Wang, D.Y. and Sen, D. (2002) Rationally designed allosteric variants of hammerhead ribozymes responsive to the HIV-1 Tat protein. Comb. Chem. High Throughput Screen. 5:301–312.
449. Kertsburg, A. and Soukup, G.A. (2002) A versatile communication module for controlling RNA folding and catalysis. Nucleic Acids Res. 30:4599–4606.
450. Hartig, J.S., Najafi-Shoushtari, S.H., Grune, I., Yan, A., Ellington, A.D. and Famulok, M. (2002) Protein-dependent ribozymes report molecular interactions in real time. Nat. Biotechnol. 20:717–722.
451. Thompson, K.M., Syrett, H.A., Knudsen, S.M. and Ellington, A.D. (2002) Group I aptazymes as genetic regulatory switches. BMC Biotechnol. 2:21.
452. Silverman, S.K. (2003) Rube Goldberg goes (ribo)nuclear? Molecular switches and sensors made from RNA. RNA 9:377–383.
453. Jose, A.M., Soukup, G.A. and Breaker, R.R. (2001) Cooperative binding of effectors by an allosteric ribozyme. Nucleic Acids Res. 29:1631–1637.
454. Cho, S., Kim, J.E., Lee, B.R., Kim, J.H. and Kim, B.G. (2005) Bis-aptazyme sensors for hepatitis C virus replicase and helicase without blank signal. Nucleic Acids Res. 33:e177.
455. Soukup, G.A. and Breaker, R.R. (1999) Engineering precision RNA molecular switches. Proc. Natl. Acad. Sci. USA 96:3584–3589.
456. Robertson, M.P. and Ellington, A.D. (2000) Design and optimization of effector-activated ribozyme ligases. Nucleic Acids Res. 28:1751–1759.
457. Soukup, G.A., Emilsson, G.A. and Breaker, R.R. (2000) Altering molecular recognition of RNA aptamers by allosteric selection. J. Mol. Biol. 298:623–632.
458. Srinivasan, J., Cload, S.T., Hamaguchi, N., Kurz, J., Keene, S., Kurz, M., Boomer, R.M., Blanchard, J., Epstein, D., Wilson, C. and Diener, J.L. (2004) ADP-specific sensors enable universal assay of protein kinase activity. Chem. Biol. 11:499–508.
459. Levy, M. and Ellington, A.D. (2002) ATP-dependent allosteric DNA enzymes. Chem. Biol. 9:417–426.
460. Wang, D.Y., Lai, B.H. and Sen, D. (2002) A general strategy for effector-mediated control of RNA-cleaving ribozymes and DNA enzymes. J. Mol. Biol. 318:33–43.
461. Liu, J. and Lu, Y. (2004) Adenosine-dependent assembly of aptazyme-functionalized gold nanoparticles and its application as a colorimetric biosensor. Anal. Chem. 76:1627–1632.
462. Achenbach, J.C., Nutiu, R. and Li, Y. (2005) Structure-switching allosteric deoxyribozymes. Anal. Chim. Acta 534:41–51.
463. Shen, Y., Chiuman, W., Brennan, J.D. and Li, Y. (2006) Catalysis and rational engineering of trans-acting pH6DZ1, an RNA-cleaving and fluorescence-signaling deoxyribozyme with a four-way junction structure. ChemBioChem 7:1343–1348.
464. Koizumi, M., Soukup, G.A., Kerr, J.N. and Breaker, R.R. (1999) Allosteric selection of ribozymes that respond to the second messengers cGMP and cAMP. Nat. Struct. Biol. 6:1062–1071.
465. Zivarts, M., Liu, Y. and Breaker, R.R. (2005) Engineered allosteric ribozymes that respond to specific divalent metal ions. Nucleic Acids Res. 33:622–631.
466. Ferguson, A., Boomer, R.M., Kurz, M., Keene, S.C., Diener, J.L., Keefe, A.D., Wilson, C. and Cload, S.T. (2004) A novel strategy for selection of allosteric ribozymes yields RiboReporter sensors for caffeine and aspartame. Nucleic Acids Res. 32:1756–1766.
467. Piganeau, N., Jenne, A., Thuillier, V. and Famulok, M. (2000) An allosteric ribozyme regulated by doxycycline. Angew. Chem. Int. Ed. 39:4369–4373.
468. Piganeau, N., Thuillier, V. and Famulok, M. (2001) In vitro selection of allosteric ribozymes: theory and experimental validation. J. Mol. Biol. 312:1177–1190.
469. Seetharaman, S., Zivarts, M., Sudarsan, N. and Breaker, R.R. (2001) Immobilized RNA switches for the analysis of complex chemical and biological mixtures. Nat. Biotechnol. 19:336–341.
470. Robertson, M.P. and Ellington, A.D. (2001) In vitro selection of nucleoprotein enzymes. Nat. Biotechnol. 19:650–655.
471. Soukup, G.A., DeRose, E.C., Koizumi, M. and Breaker, R.R. (2001) Generating new ligand-binding RNAs by affinity maturation and disintegration of allosteric ribozymes. RNA 7:524–536.

472. Batey, R.T., Gilbert, S.D. and Montange, R.K. (2004) Structure of a natural guanine-responsive riboswitch complexed with the metabolite hypoxanthine. Nature (Lond.) 432: 411–415.
473. Serganov, A., Yuan, Y.R., Pikovskaya, O., Polonskaia, A., Malinina, L., Phan, A.T., Hobartner, C., Micura, R., Breaker, R.R. and Patel, D.J. (2004) Structural basis for discriminative regulation of gene expression by adenine- and guanine-sensing mRNAs. Chem. Biol. 11:1729–1741.
474. Tang, J. and Breaker, R.R. (1998) Mechanism for allosteric inhibition of an ATP-sensitive ribozyme. Nucleic Acids Res. 26:4214–4221.
475. Suess, B., Fink, B., Berens, C., Stentz, R. and Hillen, W. (2004) A theophylline responsive riboswitch based on helix slipping controls gene expression in vivo. Nucleic Acids Res. 32:1610, 1614.
476. Hall, B., Hesselberth, J.R. and Ellington, A.D. (2007) Computational selection of nucleic acid biosensors via a slip structure model. Biosens. Bioelectron. 22:1939–1747.
477. Atsumi, S., Ikawa, Y., Shiraishi, H. and Inoue, T. (2001) Design and development of a catalytic ribonucleoprotein. EMBO J. 20:5453–5460.
478. Kuwabara, T., Warashina, M., Tanabe, T., Tani, K., Asano, S. and Taira, K. (1998) A novel allosterically trans-activated ribozyme, the maxizyme, with exceptional specificity in vitro and in vivo. Mol. Cell 2:617–627.
479. Komatsu, Y., Yamashita, S., Kazama, N., Nobuoka, K. and Ohtsuka, E. (2000) Construction of new ribozymes requiring short regulator oligonucleotides as a cofactor. J. Mol. Biol. 299:1231–1243.
480. Wang, D.Y. and Sen, D. (2001) A novel mode of regulation of an RNA-cleaving DNAzyme by effectors that bind to both enzyme and substrate. J. Mol. Biol. 310:723–734.
481. Wang, D.Y., Lai, B.H., Feldman, A.R. and Sen, D. (2002) A general approach for the use of oligonucleotide effectors to regulate the catalysis of RNA-cleaving ribozymes and DNAzymes. Nucleic Acids Res. 30:1735–1742.
482. Burke, D.H., Ozerova, N.D. and Nilsen-Hamilton, M. (2002) Allosteric hammerhead ribozyme TRAPs. Biochemistry 41:6588–6594.
483. Najafi-Shoushtari, S.H., Mayer, G. and Famulok, M. (2004) Sensing complex regulatory networks by conformationally controlled hairpin ribozymes. Nucleic Acids Res. 32:3212–3219.
484. Penchovsky, R. and Breaker, R.R. (2005) Computational design and experimental validation of oligonucleotide-sensing allosteric ribozymes. Nat. Biotechnol. 23:1424–1433.
485. Najafi-Shoushtari, S.H. and Famulok, M. (2005) Competitive regulation of modular allosteric aptazymes by a small molecule and oligonucleotide effector. RNA 11:1514–1520.

Part II
Functional Nucleic Acid Sensors Based on Different Transduction Principles

Chapter 4
Fluorescent Aptamer Sensors

Hui William Chen, Youngmi Kim, Ling Meng, Prabodhika Mallikaratchy, Jennifer Martin, Zhiwen Tang, Dihua Shangguan, Meghan O'Donoghue, and Weihong Tan

Abstract Aptamers are single-stranded nucleic acid probes that can be evolved to have high specificity and affinity for different targets. These targets include biomarker proteins, small molecules, and even whole live cells that express a variety of surface proteins of interest. Aptamers offer several advantages over protein-based molecular probes such as low immunogenic activity, flexible modification, and in vitro synthesis. In addition, aptamers used as molecular probes can be made with easy signaling for binding with their corresponding targets. There are a few different fluorescence-based signal transduction mechanisms, such as direct fluorophore labeling, fluorescence resonance energy transfer (FRET), fluorescence quenching, fluorescence anisotropy, and light-switching excimers. These signaling processes in combination with various labeling strategies of nucleic acid aptamers contribute to simple, rapid, sensitive, and selective biological assays. In this chapter, we discuss the optical signaling of aptamers for single proteins such as α-thrombin and platelet-derived growth factor (PDGF). We also present detailed discussion about fluorescent aptamers developed from cell-based systematic evolution of ligands by exponential enrichment (SELEX) for the recognition of different target tumor cells.

4.1 Overview

During the past few decades, the rapid development of molecular sensing systems has resulted in diversified platforms for both basic biomedical studies and advanced bioanalytical applications. The benefited areas include medicine and health care (gene chips, clinical diagnosis, biomedicine, pharmaceutical and drug analysis), microbiology (bacterial and viral analysis), environment (pollution and contamination detection), and homeland security (chemical and biological weapons

H.W. Chen, Y. Kim, L. Meng, P. Mallikaratchy, J. Martin, Z. Tang, D. Shangguan, M. O'Donoghue, and W. Tan
Center for Research at the Bio/Nano Interface, Department of Chemistry, Shands Cancer Center, University of Florida Genetics Institute and McKnight Brain Institute, University of Florida,
tan@chem.ufl.edu

Y. Li and Y. Lu (eds.), *Functional Nucleic Acids for Analytical Applications*,

detection). Generally, molecular sensing systems are composed of molecular recognition elements and signal transduction mechanisms.

To achieve specific detection, different biological molecular recognition elements such as enzymes, receptor proteins, antibodies, nucleic acids, aptamers, cells, and tissues have been exploited, along with several synthetic molecular recognition elements. Among all of the natural biological molecular recognition elements, antibodies and aptamers can be developed for almost any target molecules. Aptamers came of age decades after the beginning of antibodies and their adoption as an everyday tool by researchers in the 1950s. While both have comparable specificity and affinity, aptamers are more applicable to a variety of targets including proteins, organic molecules, ions, virus, organelles, and even cells. In addition, low molecular weight aptamers are easily synthesized and suitable for modification so that they have more chances to maintain necessary functions when exposed to undesirable conditions. These merits of aptamers give rise to the flexibility for the design of novel bioanalytical sensors.

Aptamers are synthetic DNA or RNA molecules evolved from a random library of 10^{15}–10^{18} candidates. The binding ability of aptamers comes from their tertiary structures in the presence of target molecules, which derive from the combinatorial secondary structures of nucleic acid molecules during the systematic evolution of ligands by exponential enrichment (SELEX).[1,2] Besides their early applications in bioanalytical chemistry as a basic molecular recognition element, aptamers have recently begun to be utilized in personalized disease diagnosis and therapy. Single-stranded nucleic acid aptamers can be evolved to have high specificity and affinity against different disease-related metabolites, biomarker proteins, and even whole live cells expressing a variety of surface proteins of interest. When coupled with suitable signal transduction mechanisms, aptamers show great potential as a new tool for biomedical studies.

Several different fluorescence-based signal transduction mechanisms such as direct fluorophore labeling,[3] fluorescence resonance energy transfer (FRET),[4,5] fluorescence quenching,[4,6,7] fluorescence anisotropy,[5,8,9] and light-switching excimers[10] have been developed for different aptamer sensing systems. Because of its inherent stability and sensitivity, the direct fluorophore labeling strategy was extensively used for rapid and simple detection of biological entities including proteins, nucleic acids, and cells by aptamer sensors.[3,11] Although some assays, such as cancer cell detection by aptamers, have benefited greatly from direct labeling with dye molecules, aptamer-based FRET and fluorescence anisotropy worked together to provide detailed information of protein binding and interaction.[5] It is worthy to mention that light-switching excimer-based aptamer probes also found important applications in cancer biology by achieving sensitive and selective real-time detection of disease biomarker proteins in the presence of intense biological background interference with the help of both wavelength switching and the long fluorescence lifetime of the excimers.[10] Besides, there are also numerous other fluorescent aptamer sensor design strategies, as reviewed in detail elsewhere.[12] Combining the molecular recognition ability of aptamers with specific fluorescence signal transduction mechanisms provides simple, rapid, sensitive, and selective assays of biological molecules.

4.2 Fluorescent Aptamers Developed from Cell-Based SELEX for Recognition of Cancer Cells and Biomarker Discovery

Effective diagnosis, therapy, and prevention of diseases require the understanding of diseases at the molecular level, which relies not only on the genetic character but also on the proteomic character of diseases, especially for cancer, the number one killing disease of humans. For the diagnosis of cancer, accurate and flexible criteria are indispensable for the classification of types as well as subtypes of certain cancers to support the appropriate treatment and the detection of minimal residual disease. Current criteria for cancer diagnosis based on genetic and morphological features instead of proteomic features are complicated and insufficient for clinical practice, which is partially caused by the lack of well-defined cancer biomarker proteins and specific molecular probes to recognize and identify them. Although cancer diagnosis by recognition of molecular signatures is relatively simple and direct, it is very challenging to discover enough cancer biomarker proteins for conclusive diagnosis because of the limits of current biomarker discovery techniques. Therefore, it is highly desirable to have an efficient and reliable method to develop specific molecular probes suitable for appropriate signal transduction mechanisms to distinguish the differences among cancer cells at the molecular level without prior knowledge of target biomarker proteins. In addition, with these molecular probes, biologically meaningful biomarker proteins can be revealed to provide great insight of cancer.

Shangguan et al. recently developed some new fluorescent molecular sensors using aptamers evolved from cell-based SELEX as recognition elements to probe the molecular signatures of different leukemia cells in a direct and simple manner.[3] These molecular signatures expressed on live cell membranes may imply important disease mechanisms if validated as biomarkers. Not only are these fluorescent aptamer sensors as accurate as, if not better than, antibody-based sensors for the differentiation of subtypes of leukemia, they also reveal more subtle molecular-level differences. Theoretically, any molecular-level variance among different types or subtypes of cancer cells could be revealed by a similar methodology, something that was previously impractical. To develop such aptamer probes for molecular differences between two types of leukemia, a methodology called cell-based SELEX dealing with whole live cancer cells was used (Fig. 4.1). This methodology is unlike previous attempts of SELEX against other complex targets such as isolated cell membranes, organelles, and purified proteins.[13–16] Another distinct aspect of this methodology is the use of a counter-selection strategy to screen out those aptamers bound to common target proteins expressed on the cell membranes of different cancer cells. In this specific case, two different leukemia cell lines were chosen to study the molecular-level differences. A cultured precursor T-cell acute lymphoblastic leukemia (ALL) cell line, CCRF-CEM, was used as a positive target and a cultured B-cell human Burkitt's lymphoma cell line, Ramos, was used as the negative control. After iterative binding with both positive and negative cell lines, a panel of aptamer probes became enriched, among

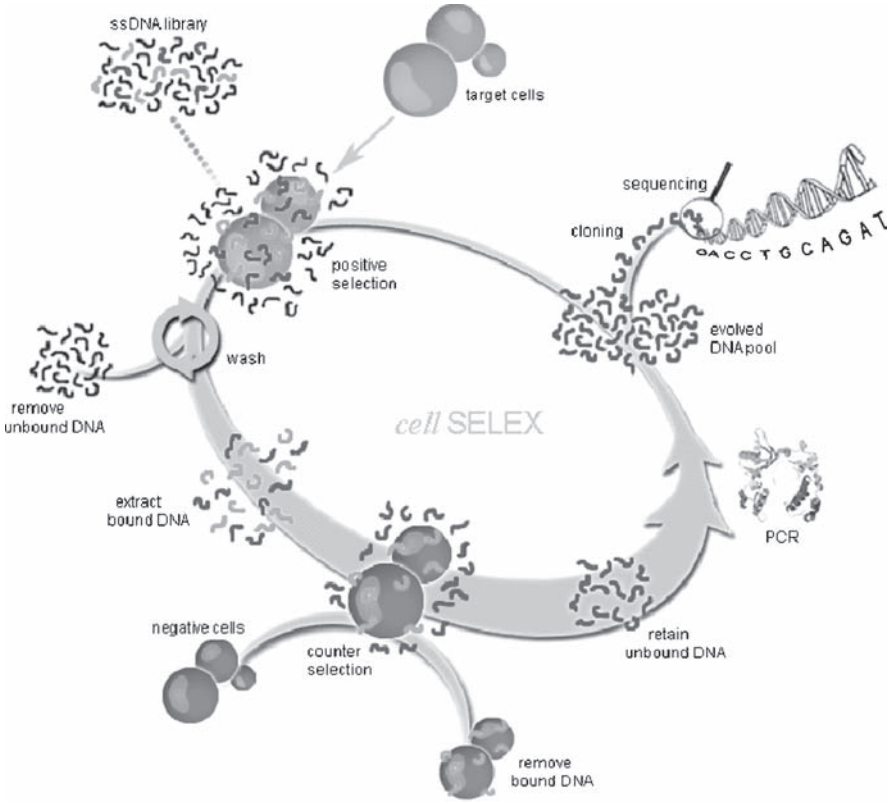

Fig. 4.1 Scheme of cell-based systematic evolution of ligands by exponential enrichment (SELEX).[3] First, the single-stranded DNA (ssDNA) pool was incubated with CCRF-CEM target cells. After washing, the bound DNAs were eluted by heating to 95°C. The eluted DNAs were then incubated with Ramos negative cells for counter-selection. After centrifugation, the collected DNAs were amplified by PCR. The double-stranded PCR products were then separated into ssDNA for next round of selection or subjected to cloning and sequencing for aptamer identification (Copyright [2007] National Academy of Sciences, USA)

which probes can be used either individually for bioanalytical applications or together in multiprobe-based assays to provide more information for diagnostics.

Flow cytometry assays can be easily carried out with direct fluorophore-labeled aptamers. After incubation with dye-labeled aptamers, the fluorescence intensity of DNA-bound cells measured by flow cytometry represents the binding capacity of the aptamers to the cells (Fig. 4.2). As predicted, most of the aptamers selected by this methodology only recognized target cells and were not interfered by an excess of DNA library. These aptamers exhibited not only great specificity but also high affinity for the target cells, which ranges from submicromolar to subnanomolar. At the same time, none of these aptamers competed with known antibodies for the binding of receptor proteins expressed on the target cell surfaces, which indicated

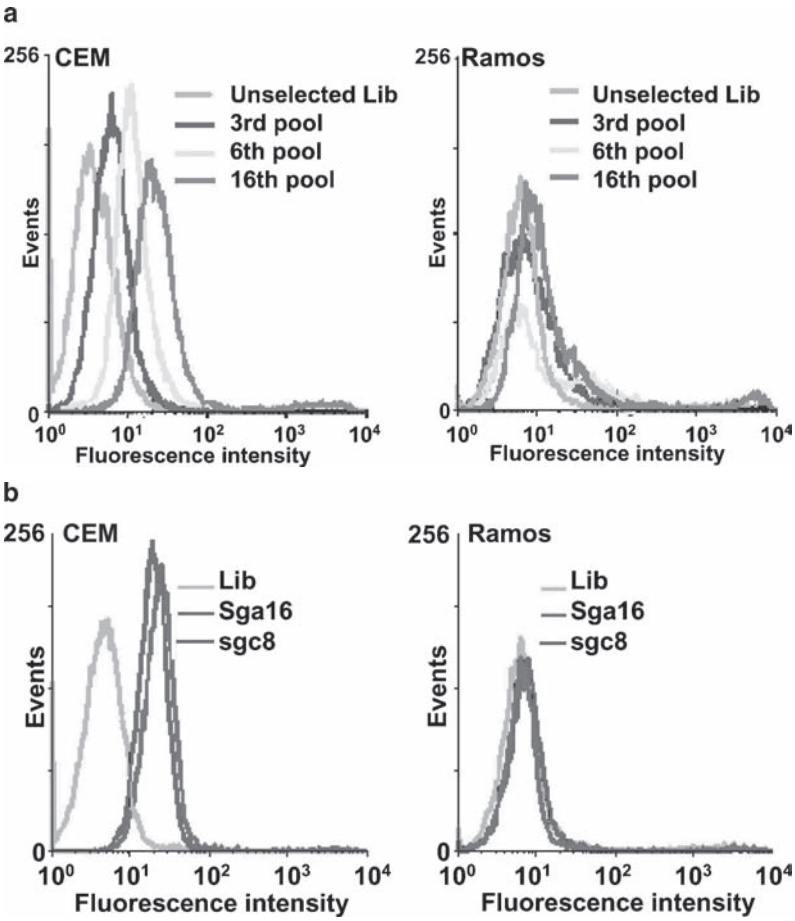

Fig. 4.2 (**a**) Flow cytometry assay of FITC-labeled selected pools with CCRF-CEM target cells and Ramos control cells.[3] The *green curve* represents the nonspecific binding of unselected DNA library. For CEM cells, there were gradual increases in binding capacity of the DNA pools as the selection progressed, whereas there was little change for the Ramos cells. (**b**) Flow cytometry assay of FITC-labeled aptamers sga16 and sgc8 with CCRF-CEM target cells and Ramos control cells. The *green curve* represents the nonspecific binding of unselected DNA library. The final concentration of the aptamers was 250 nM (Copyright [2007] National Academy of Sciences, USA)

that the discovered molecular signatures are new and may have great importance for leukemia studies. It was also noticed that some of the selected aptamers can only recognize certain sub-populations of target cells, which may be explained as aptamers can be evolved to recognize any small molecular difference among cells by cell-based SELEX and counter-selection. As the aptamers were generated against whole live cells in their native state, the clinical assays can be directly performed. When mixed with normal human bone marrow aspirates, target cells were still recognized by fluorescent aptamer probes (Fig. 4.3).

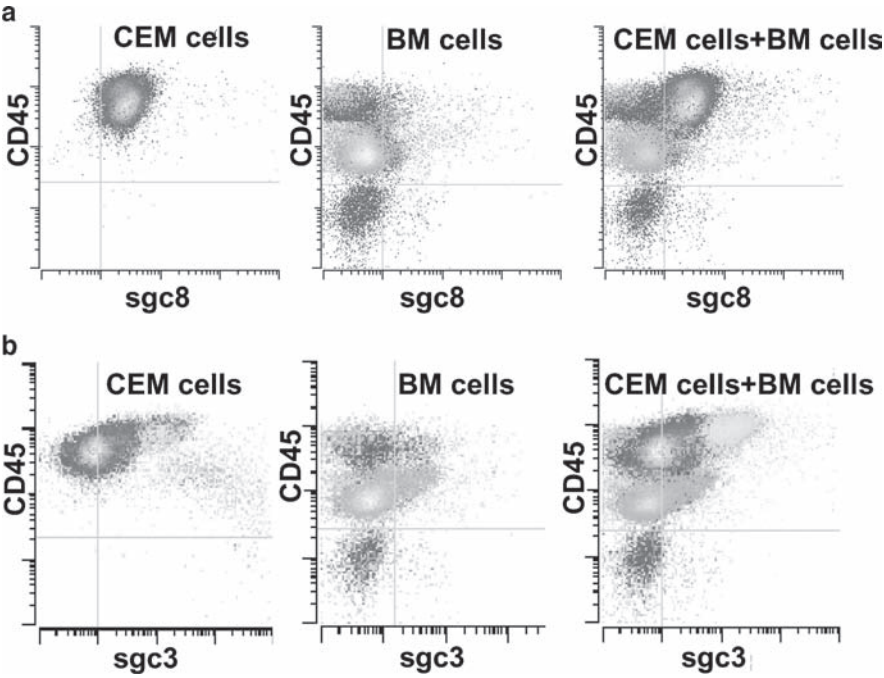

Fig. 4.3 Molecular recognition of CCRF-CEM cells mixed with human bone marrow cells by FITC-labeled sgc8, sgc3, and PerCP labeled anti-CD45 antibody.[3] The sgc8 (**a**) and sgc3 (**b**) were able to distinguish the target leukemia cells from human bone marrow aspirates in the mixture. (Copyright [2007] National Academy of Sciences, USA)

To demonstrate the widespread usefulness of these selected aptamer probes, they were tested against other T-cell ALL cell lines, which are similar to the target cells used in aptamer selection, B-cell lymphoma cell lines, which are close to control cells, and acute myloid leukemia cell lines, which represent another type of leukemia. The results showed that these aptamers recognize most "target cell-like cell lines" and do not recognize either most "control cell-like cell lines" or other types of leukemia. It was encouraging to see that real clinical T-cell ALL patient bone marrow aspirates also responded to the aptamer probes. Thus, the capability of aptamers generated by cell-based SELEX for the recognition of molecular differences among cancer cells was clearly demonstrated. Similar results were obtained using B-cell lymphoma as target cells and T-cell ALL as control cells.

Recently, cell-based SELEX was also used to successfully develop molecular probes for solid tumors such as lung and liver cancer.[17,18] Later on, these aptamer probes were used for biomarker discovery and validation, which confirmed that the molecular differences discovered are biologically meaningful.

Not only can a group of aptamers selected based on cell differences be used as molecular probes for the recognition and detection of specific disease cells, but also they can be used to purify and identify biomarkers that had not been studied before

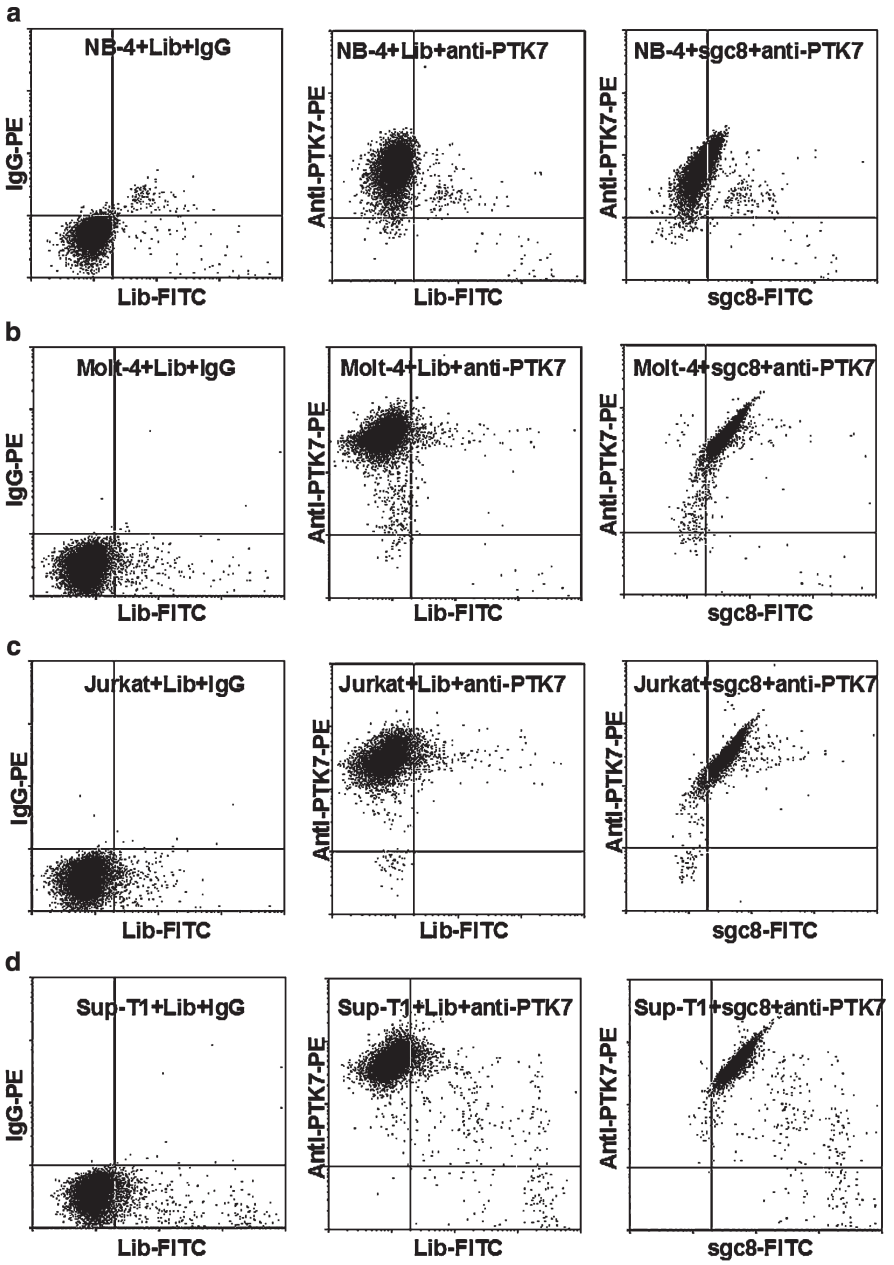

Fig. 4.4 Flow cytometry assay of leukemia cells stained with anti-PTK7-PE and sgc8-FITC.[19] (**a**) Acute promyelocytic leukemia, NB-4; (**b**) human acute lymphoblastic leukemia (T-cell line), Molt-4; (**c**) human acute lymphoblastic leukemia (T-cell line), Jurkat; (**d**) human acute lymphoblastic leukemia (T-cell line), Sup-T1. FITC-labeled Library (Lib) and IgG-PE were used as negative controls

the probes were generated. Therefore, the strategy of cell-specific aptamer-directed disease biomarker discovery greatly facilitates biomarker discovery by identifying more biologically important biomarkers for specific types of diseases and reducing the effort required for biomarker screening and biomarker validation. As distinct biomarkers can be discovered for specific diseases, they will eventually help achieve more accurate diagnoses and more effective treatments, which are essential for the goal of personalized medicine.

One aptamer, sgc8, demonstrating high specificity and affinity to T-cell acute lymphoblastic leukemia cells,[3] was used to purify and identify the target protein on the cell surface through affinity chromatography coupled with LC-MS/MS.[19]

Table 4.1 Aptamer sgc8 tests with hematopoietic cancer cells and normal bone marrow[19]

Cultured cell lines		sgc8	Patient's samples		sgc8	Patient's samples		sgc8
T-ALL	CCRF-CEM	+++	T-ALL	T ALL 1	++	B-ALL	B ALL 1	0
	Molt-4	++++		T ALL 2	++		B ALL 2	0
	Sup-T1	++++		T ALL 3	+		B ALL 3	++
	Jurkat	++++		T ALL 4	+	Other clinical samples	1, T-cell lymphoma	0
B-ALL	SUP-B15	+		T ALL 5	+		2, follicular lymphoma	0
AML	NB-4 (APL)	+		T ALL 6	0		3, B-cell lymphoma	0
	Kasumi-1	+++		T ALL 7	0		4, T-cell lymphoma,	0
							5, B-cell lymphoma	0
Myeloma	U266	0	AML	AML 1	+		6, plasma cell neoplasm	0
B-cell lymphoma	Ramos	0		AML 2	+	Normal bone marrow	CD3 (+) T cells	0
	Toledo	0		AML 3	+		Mature B cells[b]	0
	UF1[a]	0		AML 4	0		Immature B cells[c]	0
	Mo2058	0		AML 5	0		Granulocytes	0
				AML 6	+		Monocytes	0
							Erythrocytes	0

0, <10%; +, 10–35%; ++, 35–60%; +++, 60–85%; ++++, >85%

In the flow cytometry analysis, a threshold based on fluorescence intensity of FITC was chosen so that 99% of cells incubated with the FITC-labeled unselected DNA library would have fluorescence intensity below it. When FITC-labeled aptamer was allowed to interact with the cells, the percentage of the cells with fluorescence intensity above the set threshold was used to evaluate the binding capacity of the aptamer to the cells

AML, acute myeloid leukemia; T-ALL, T-cell acute lymphoblastic leukemia; B-ALL: B-cell acute lymphoblastic leukemia

[a]UF1, follicular large B-cell lymphoma

[b]Mature B cells, CD19(+), CD10(−)

[c]Immature B cells, CD19(+), CD10(+)

The target protein was determined to be transmembrane protein tyrosine kinase-7 (PTK7), a known colon cancer biomarker whose functions in tumor development are unknown.[20] This protein has never previously been reported as a significant biomarker for T-cell leukemia (Fig. 4.4). By testing the aptamer together with anti-PTK7 antibody, it was also found that no competition exists between the binding of the aptamer and the antibody with PTK7; instead, they may colocalize with each other when bound to PTK7. Control cells were then transfected with cDNA of PTK7 and found to bind with both anti-PTK7 antibody and sgc8 after treatment, confirming PTK7 as the target protein of aptamer sgc8. To validate PTK7 as an effective biomarker, a series of cultured cell lines and clinical patient cells of T-cell ALL and AML were tested with anti-PTK7 aptamer. These samples showed significant binding, whereas most of the lymphoma cells and normal bone marrow cells had negligible binding with the aptamer probes (Table 4.1).

From the results discussed above, it can be concluded that PTK7 is, indeed, an important biomarker for the development of specific types of leukemia. In addition, both the biomarker and selected aptamer probe have great potential to be used for diagnosis, targeted therapy, and minimal residual disease detection. Similar to the biomarker discovery by T-cell ALL-specific aptamer, an aptamer selected for B-cell lymphoma cells also allowed the identification of its target protein with a photo-cross-linking strategy. It was found that membrane-bound IgM is a significant biomarker for B cell lymphoma.[21] As demonstrated here, it is clear that the integration of probe development and biomarker discovery gives rise to extra advantages, resulting in a shortened time gap between laboratory research and clinical application.

4.3 FRET and Fluorescence Anisotropy-Based Aptamer Sensors for Protein Studies

Protein detection and protein–protein interaction studies are two other important aspects for understanding cellular functions and disease mechanisms. However, most current techniques involve labeling and/or genetic manipulation of proteins, which may affect the protein folding and functions. Recently, protein studies using molecular aptamer probes coupled with fluorescence-based signal transduction mechanisms such as fluorescence resonance energy transfer (FRET) and fluorescence anisotropy are becoming a trend. These simple methods provide sensitive protein detection and detailed protein–protein interaction information without labeling the proteins.

FRET is an energy transfer mechanism between a fluorescent donor and a nearby acceptor whose excitation spectrum partially overlaps with the donor emission spectrum. A classic example of the FRET mechanism is seen in the molecular beacon (MB), nucleic acid probes dually labeled with a fluorophore and a quencher, used for nucleic acid detection.[22] As a separation-free assay, MBs have been used in a variety of applications, such as detection of single nucleotide polymorphisms

(SNPs),[23,24] real-time polymerase chain reaction (PCR),[25] and detection of mRNA in living cells.[26,27] Along with nucleic acid detection, FRET has also been used to detect proteins with molecular beacon aptamers (MBAs). In this case, when a dual-labeled aptamer binds with its target protein, a conformational change occurs, resulting in FRET, and signaling a protein-binding event. MBAs have been proven to be very sensitive for the detection of some important proteins such as thrombin and platelet-derived growth factor (PDGF).

Fluorescence anisotropy is another useful signal transduction mechanism, which involves labeling aptamers with a single fluorophore. The binding of aptamers to relatively large proteins can cause slow rotational diffusion, resulting in increased fluorescence anisotropy.

One of the most studied families of aptamers that binds to and inhibits α-thrombin, a crucial regulator enzyme of blood clotting, was discovered in 1992 through the first in vitro selection against a protein not previously known to bind with nucleic acids.[28] The ssDNA aptamer has a 15-nucleotide consensus sequence, six thymidine and nine guanine nucleotides, which switches between two tertiary structures: a random coil and a G-quartet structure.[29–32] When in a solution free of target protein and with low levels of monovalent cations such as potassium ions, the aptamer exists as a relaxed random coil. Upon binding to its target protein or interacting with a cation, the aptamer adopts a compact quadruplex structure formed by a two-layer G-quartet, which is usually referred to as a "chair structure" (Fig. 4.5a).[33] In this chair structure, the four guanines of each quartet organize into

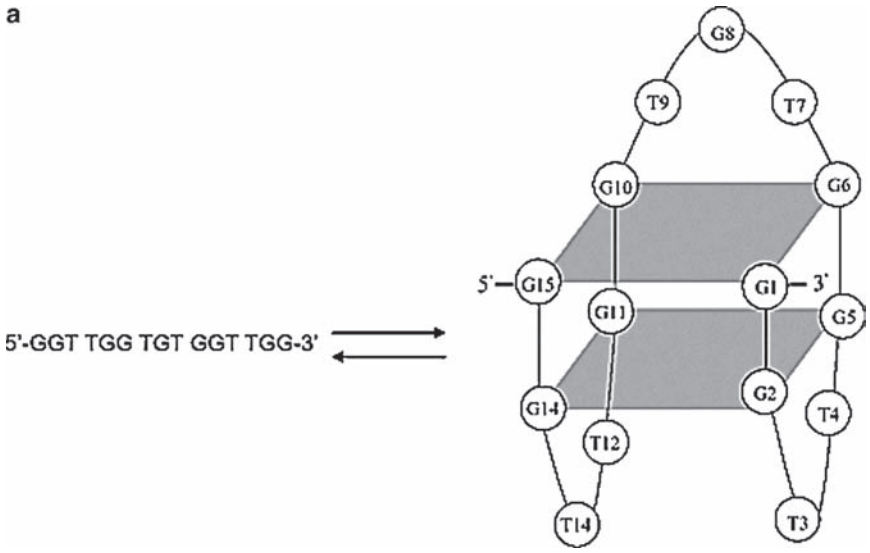

Fig. 4.5 (**a**) Linear and G-quartet (chair) structures of thrombin-binding DNA aptamer. *Shaded squares* represent guanine quartet.[30] (**b**) *Top*: Binding of thrombin aptamer to thrombin. *F*, fluorophore; *Q*, quencher. *Bottom*: Time-course of molecular beacon aptamers (MBA) showing how addition of thrombin decreases fluorescence intensity[33]

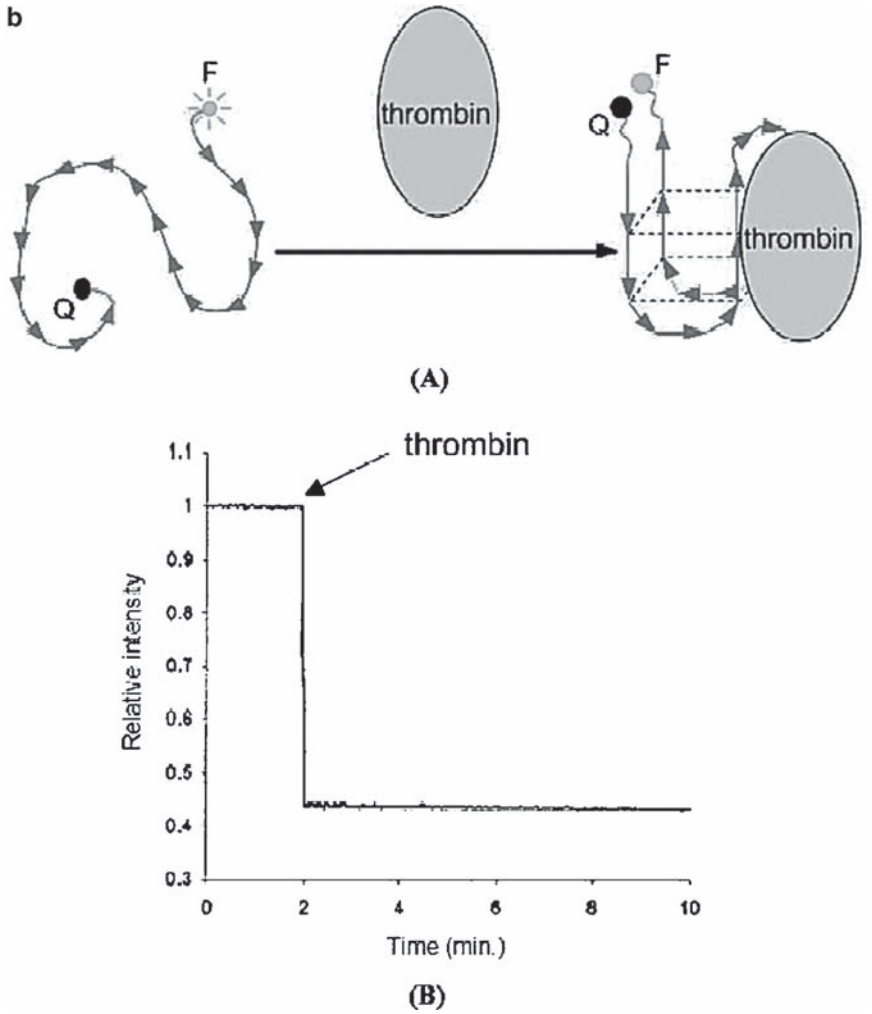

Fig. 4.5 (continued)

a square planar configuration, with each guanine interacting with its adjacent two guanines through hydrogen bonds known as a Hoogsteen base pair.

This structural switching of the thrombin aptamer between a relaxed coil and a G-quartet chair structure was then used by researchers to construct the first molecular beacon aptamer (MBA).[4,34,35] To do this, the Tan group added one thymidine at each end of the thrombin aptamer, and labeled them with a fluorophore and a quencher, respectively. When thrombin binds to the aptamer, it takes the G-quartet chair structure, and the distance between the fluorophore and quencher decreases, resulting in a decline in fluorescence intensity (Fig. 4.5b).[36] This MBA signal transduction mechanism based on fluorescence quenching has several advantages;

namely, it is fast (less then 30 s), sensitive (sub-nM thrombin in physiological buffer), and does not affect aptamer binding affinity.[4]

Similarly, the Tan group created another MBA that increases in fluorescence upon binding to a protein target. This aptamer was accomplished by replacing the dye-quencher pair with coumarin as the donor, and 6-FAM as the acceptor, to form a FRET pair.[35] When in the relaxed coil form, the two fluorophores have negligible FRET; however, upon binding to the thrombin target, the fluorophores are brought in close proximity, resulting in FRET. Using a ratiometric assay that compares fluorescence before and after thrombin addition, thrombin detection at ~112 pM was achieved.

At about the same time, Hamaguchi et al. also developed a thrombin MBA.[34] This MBA was formed by adding several bases to one end of the aptamer and complementary bases to the other end. Both ends were then capped with a fluorophore–quencher pair. In the absence of thrombin, the fluorophore and quencher are held tightly together by the complementary stem, resulting in quenched fluorescence. Upon thrombin binding, the aptamer switches to the G-quartet chair structure, separating the stem ends to produce unquenched fluorescence. Aside from the development of thrombin-based MBAs for protein detection, advances have been made on other fluorescence-based signal transduction mechanisms for different applications including label-free monitoring of protein–protein interactions, potassium detection, and electronic protein sensors.

Although protein–protein interactions play pivotal roles in cellular functions, most current techniques for these studies require direct manipulation of the proteins to determine how they interact with each other and their environment. As proteins rely on their tertiary structures for function, direct manipulation of proteins, such as dye labeling and fusing with fluorescent proteins, may interfere with their properties. Innovative approaches obviating the need of direct protein manipulation include the use of aptamer-based FRET and fluorescence anisotropy as signal transduction mechanisms. With these two signal transduction mechanisms, competition assays using MBAs that bind to two different sites on the thrombin protein have succeeded in real-time monitoring of protein–protein interactions. The thrombin enzyme binds to several different proteins at different sites; for instance, one site binds to fibrinogen and hirudin while another binds to heparin. Using two different MBAs with G-quartet structures – the 15mer discussed above, which binds to the fibrinogen/hirudin site, and a 27mer that binds to the heparin site – the competition between the aptamers initially bound to the specific thrombin sites and other thrombin-binding proteins can be observed in real time.[5] The scheme for this system and a similar one that records the change in fluorescence anisotropy between bound aptamer and free aptamer dislodged by other thrombin-binding proteins is shown in Fig. 4.6.

Platelet-derived growth factor (PDGF) aptamers are another major family extensively used for FRET-based protein detections. As an important serum mitogenic factor, the biological function of PDGF is to stimulate the division and proliferation of cells through binding to its receptors on cell surfaces.[37,38] PDGF is composed of two distinct, but structurally related, peptide chains designated as A and B. Dimeric isoforms PDGF-AA, -AB, and -BB are differentially expressed in various cell types, and their effects are mediated through two distinct receptors, named α and β.

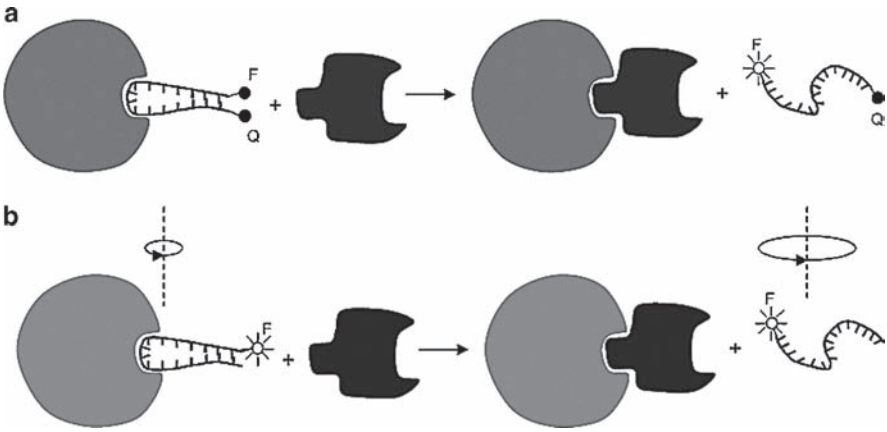

Fig. 4.6 Dye-labeled protein–binding DNA aptamers reporting protein–protein interactions.[5] (**a**) Dual-labeled aptamer with a fluorophore and a quencher. The folded form of the aptamer results in a quenched fluorescence when it binds to the bait protein. The bait–prey protein interaction causes the release of the aptamer from the bait protein, leading to a restored fluorescence. (**b**) Single-labeled aptamer. When bound to the much larger bait protein, the aptamer displays slow rotational diffusion. The interaction between bait and prey proteins displaces the aptamer. The unbound aptamer has much faster rotational diffusion. The change in the rotation rate is reported by fluorescence anisotropy of the dye molecule. *F*, fluorophore; *Q*, quencher

PDGF is considered a cancer biomarker that is overexpressed in many types of cancer, while the autocrine and paracrine effects of PDGF-BB increase with the degree of malignancy.[39,40] The calculated biological folding of PDGF-BB is shown in Fig. 4.7.

For this important protein, two DNA aptamers (41t and 36t) sharing a similar secondary structure, a three-way helix junction with a three-nucleotide loop at the branch point, have been developed by Louis Green and colleagues using the SELEX methodology.[41] Both PDGF aptamers have high affinity and selectivity against the B-chain of PDGF-BB. The 36t aptamer is a 39mer with a kd of 0.093 nM, and the 41t aptamer is a 44mer with a kd of 0.129 nM. Both sequences are predicted to undergo conformational changes upon binding with the target protein, and these changes provide many opportunities for different signal transduction mechanisms to be used in biological studies. As with thrombin aptamers, the FRET mechanism was applied to PDGF aptamers for PDGF detection.

In 2003, a FRET-based PDGF aptamer probe, also called PDGF MBA (Fig. 4.8), was reported to demonstrate the versatility of FRET-based aptamers. In this case, the PDGF-bound aptamer produced low fluorescence signal, and the unbound aptamer generated high fluorescence signal. According to in vitro assay results, the PDGF MBA showed enough specificity to distinguish PDGF from many other proteins existing in biological systems. Meanwhile, different PDGF isomeric dimers such as PDGF-AA, -BB, and -AB could also be differentiated (Fig. 4.9). In addition to the great selectivity, the PDGF MBA also showed very high sensitivity, with a picomolar detection limit.

Fig. 4.7 Calculated biological folding of platelet-derived growth factor (PDGF)

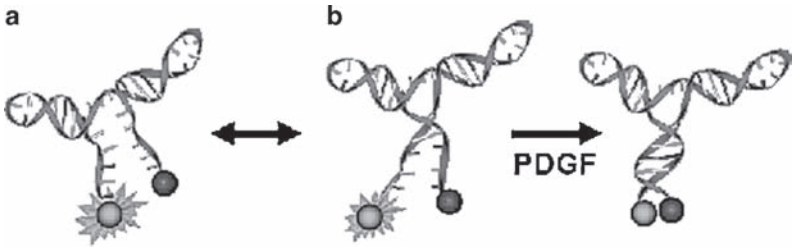

Fig. 4.8 Proposed mechanism of PDGF-BB-induced FRET responses for the 36t probe. When the MBA is free in homogeneous solution, multiple conformations are possible. Upon binding to PDGF-BB, the probe conformation shifts from the opened (**a**) or partially opened (**b**) to the closed conformation. The fluorescence signal, therefore, is high before binding; the signal is quenched on stem formation

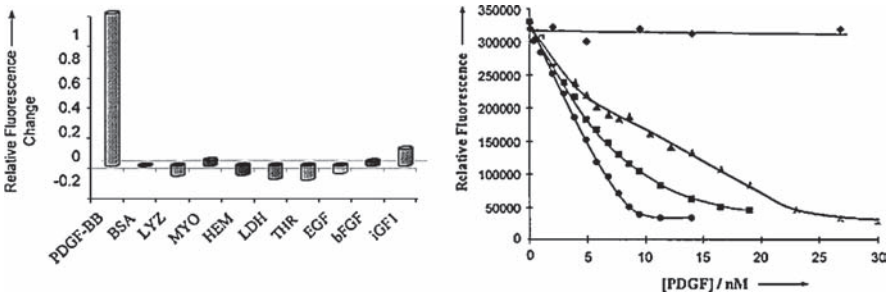

Fig. 4.9 Binding specificity of PDGF-BB MBA.[6] *Left*: Fluorescence signals of incubation mixtures containing *PDGF-BB* MBA (20nM) and one of the following proteins (100nM): bovine serum albumin (*BSA*), hemoglobin (*HEM*), lactate dehydrogenase (*LDH*), lysozyme (*LYZ*), myoglobin (*MYO*), thrombin (*THR*), or one of the following growth factors (20nM): epidermal growth factor (*EGF*), basic fibroblast growth factor (*bFGF*), or insulin-like growth factor-1 (*iGF1*). *Right*: Dose–response curves of PDGF variants: fluorescence signals of MBA for PDGF-AA (*triangles*), PDGF-AB (*squares*), PDGF-BB (*circles*), and denatured PDGF-BB (*diamonds*). The concentration of MBA was 10nM

In addition to the tests in buffer, the PDGF MBA was also applied to real samples, including the culture media of HTB-26 (human breast cancer cell line) known to secrete high levels of PDGF-BB, the culture media of normal cells (BALB/3t3 fibroblast cell line), and pure PDGF-BB solution used as a control. It was found that the pure solution of PDGF-BB responded to PDGF MBA more similarly to cancer cell culture media than to normal cell culture media. This observation clearly demonstrated that MBA was able to detect low levels of proteins selectively in their native environment without any purification or sample treatment.

4.4 Light-Switching Excimer-Based Aptamer Probes for Cancer Biomarker Detection in Complex Biological Fluids

Even with the great specificity and sensitivity of FRET-based aptamer probes, detection of proteins in their native environment is still a challenge, mainly due to interfering background signals. While the probes always experience some incomplete quenching, another source of background signal comes from the biological sample itself, and its surrounding environment. These problems can decrease sensitivity, compromise selectivity, and hinder the detection of proteins. To solve these problems, another signal transduction mechanism using light-switching excimer was developed, and demonstrated great potential.[10]

Pyrene, classified as a fluorescent molecule, is one of the light-switching excimer-forming species. The pyrene monomer behaves like a normal fluorescent molecule with a maximum emission at 400 nm. However, when two pyrene molecules are superimposed in an appropriate position, an excimer (excited-state dimer) will be formed, and the maximum emission wavelength is shifted from 400 to 485 nm (Fig. 4.10, left). With this light-switching feature of the pyrene excimer, the presence of PDGF can be detected by the naked eye (Fig. 4.10, right). The binding of

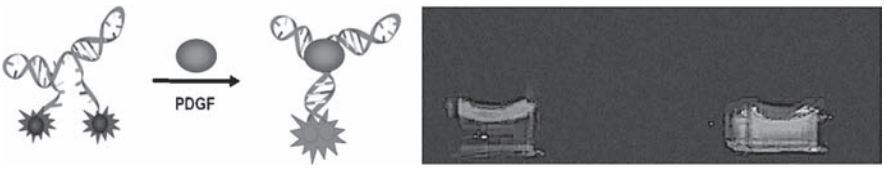

Fig. 4.10 Light-switching excimer-based aptamer probes for PDGF detection (*left*). PDGF aptamer (*red*) is end-labeled with pyrene molecules (*blue*) that are separated from each other without target binding. The pyrene molecule has monomer emission peaks at 378 and 398 nm. After binding to PDGF (*purple*), the aptamer forms a closed conformation, bringing two pyrene molecules close to each other. Consequently, pyrene excimer (*green*) forms and green light (485 nm) is emitted after photoexcitation. Visual detection of PDGF-BB after illumination with an UV lamp (*right*). Solutions of 100 nM excimer probe were excited without (*left*) and with (*right*) 40 nM PDGF-BB. The total volume of the solutions was 100 µl[10]

light-switching aptamers to their target molecules is as rapid as with the unmodified aptamer, taking place in only seconds. This new type of aptamer probe also preserves the great sensitivity needed to quantify the target protein (Fig. 4.11).

Although the most desirable properties of the PDGF aptamer are maintained in the light-switching excimer probe, the signals generated can still be buried by strong autofluorescence from complex biological samples. Light-switching excimer probes are able to provide a solution to this using a time-resolved fluorescence measurement technique. It is the unusually long fluorescence lifetime of the pyrene excimer that makes the difference. The lifetime of this excimer can be up to 20 times longer than that of complex biological samples, which is less than 5 ns.[42] Thus, target binding-induced excimer signals can be easily separated from biological background interference by delaying the signal measurement at 485 nm. This unique characteristic of the excimer enables PDGF detection in raw samples to be highly reliable. Combining light-switching properties with time-resolved measurements allows the detection of picomolar PDGF-BB in a few

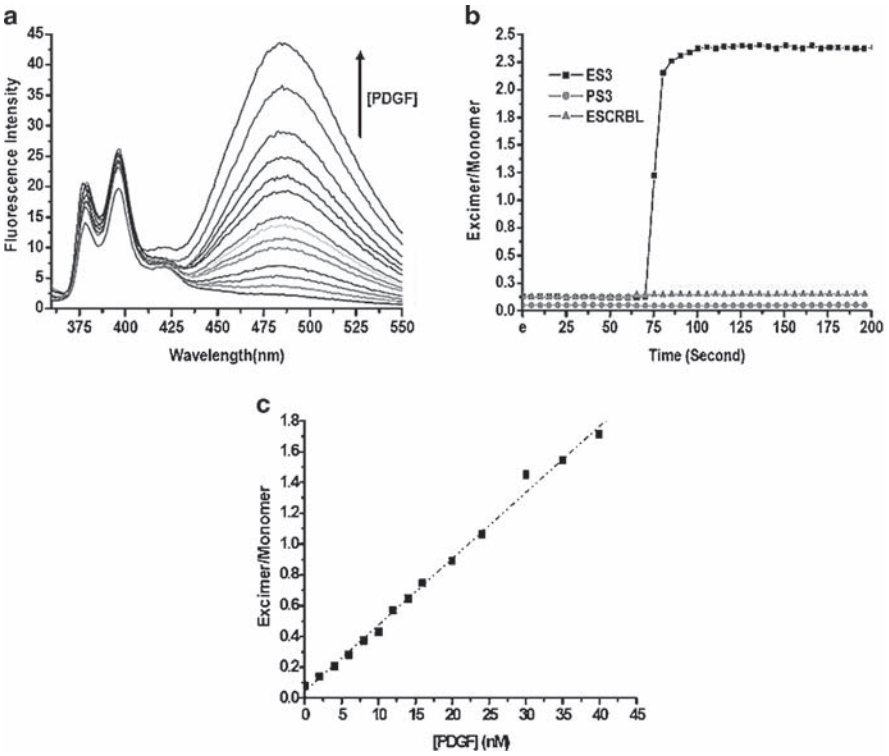

Fig. 4.11 (**a**) Response of the excimer probe (ES3) to different concentrations of PDGF-BB (0–40 nM). (probe [ES3]) = 100 nM. (**b**) Real-time response of the probe (ES3) and two pyrene-labeled control sequences to 50 nM PDGF-BB. PS3 is an aptamer sequence with one pyrene labeled at 5′. The ESCRBLE is a random DNA sequence with pyrene labeled at both ends. [ES3] = [PS3] = [ESCRBLE] = 100 nM. **c** Fluorescence ratio of excimer over monomer as a function of target protein concentration. [ES3] = 100 nM[10]

seconds. Direct detection and quantification of target molecules in complex biological samples then can be carried out without any pretreatment.

As shown in Fig. 4.12, fluorescence spectra measured in 20 ns do not show a distinguishable increase at 485 nm, presumably because of severe background interference from the cell media. However, the background interference was effectively removed by delaying the fluorescence measurement to 40–60 ns. This result was also confirmed with lifetime measurements. The fluorescence decay measured at 398 nm, the maximum emission wavelength of monomeric pyrene, was very rapid and did not change with different conditions. In contrast, the decay measured at 480 nm, known as the maximum emission wavelength of the pyrene excimer, was much slower, and the differences in the conditions (such as with or without target) was noticeable. Making use of this difference, rapid detection of PDGF in complex biological fluids without any sample pretreatment was attained (Fig. 4.13).

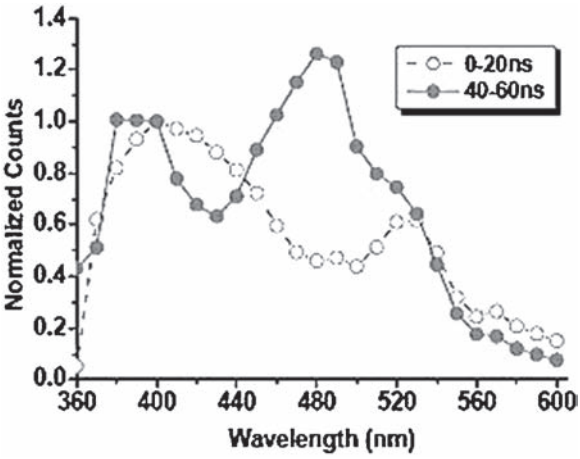

Fig. 4.12 Time-resolved fluorescence spectrum of 200 nM ES3 and 50 nM PDGF-BB in cell media at different time windows after the excitation pulse: 0–20 ns (*blue*) and 40–60 ns (*red*)[10]

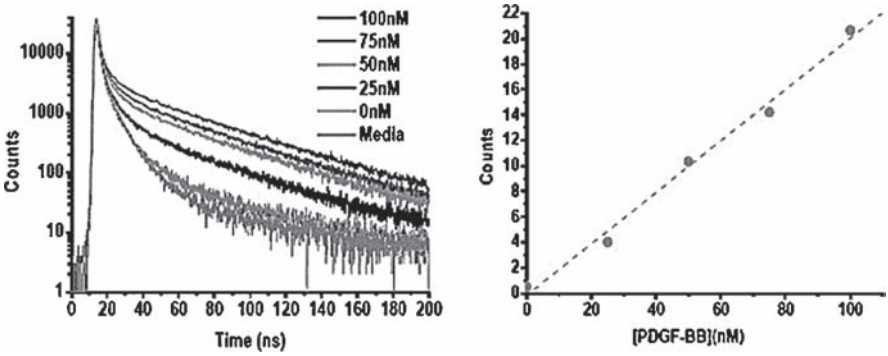

Fig. 4.13 Fluorescence decays of 200 nM light-switching PDGF aptamer in cell media with various concentrations of PDGF-BB (*left*) and the response of fluorescence intensity to the change of protein concentration (*right*)[10]

4.5 Future Perspectives

Fluorescent aptamer sensors combine the strength of both aptamers and fluorescence-based signal transduction mechanisms to perform a variety of biological studies. Their merits such as specificity, robustness, and flexibility for modification lead to the recruitment of aptamers as one of the most desirable molecular recognition elements. The sensitivity, stability, and simplicity of fluorescence-based signal transduction mechanisms, including direct fluorophore labeling, fluorescence resonance energy transfer (FRET), fluorescence quenching, fluorescence anisotropy, and light-switching excimer strategy, also contribute to the many successful applications of aptamers. In the future, the development of specific aptamer probes for molecular signatures of disease cells will allow us to find more important biomarkers, define diseases, and create tailored treatment regime for more "personalized" medicine.

Acknowledgments The authors thank our group members, whose work is reported here. We also thank the NIH and NSF for grants for financial support.

References

1. Ellington, A.D. and Szostak, J.W. (1990) In vitro selection of RNA molecules that bind specific ligands. Nature (Lond.) 346:818–822.
2. Tuerk, C. and Gold, L. (1990) Systematic evolution of ligands by exponential enrichment – RNA ligands to bacteriophage-T4 DNA-polymerase. Science 249:505–510.
3. Shangguan, D., Li, Y., Tang, Z., Cao, Z.C., Chen, H.W., Mallikaratchy, P., Sefah, K., Yang, C.J. and Tan, W. (2006) Aptamers evolved from live cells as effective molecular probes for cancer study. Proc. Natl. Acad. Sci. USA 103:11838–11843.
4. Li, J., Fang, X. and Tan, W. (2002) Molecular aptamer beacons for real-time protein recognition. Biochem. Biophys. Res. Commun. 292:31–40.
5. Cao, Z. and Tan, W. (2005) Molecular aptamers for real-time protein–protein interaction study. Chem. Eur. J. 11:4502–4508.
6. Fang, X., Sen, A., Vicens, M. and Tan, W. (2003) Synthetic DNA aptamers to detect protein molecular variants in a high-throughput fluorescence quenching assay. ChemBioChem 4:829–834.
7. Nutiu, R. and Li, Y. (2004) Structure-switching signaling aptamers: transducing molecular recognition into fluorescence signaling. Chem. Eur. J. 10:1868–1876.
8. Fang, X., Cao, Z.C., Beck, T. and Tan, W. (2001) Molecular aptamer for real-time oncoprotein platelet-derived growth factor monitoring by fluorescence anisotropy. Anal. Chem. 73:5752–5757.
9. Potyrailo, R.A., Conrad, R.C., Ellington, A.D. and Hieftje, G.M. (1998) Adapting selected nucleic acid ligands (aptamers) to biosensors. Anal. Chem. 70:3419–3425.
10. Yang, C.J., Jockusch, S., Vicens, M., Turro, N.J. and Tan, W. (2005) Light-switching excimer probes for rapid protein monitoring in complex biological fluids. Proc. Natl. Acad. Sci. USA 102:17278–17283.
11. Mallikaratchy, P., Stahelin, R.V., Cao, Z.C., Cho, W. and Tan, W. (2006) Selection of DNA ligands for protein kinase C-delta. Chem. Commun. 30:3229–3231.
12. Nutiu, R. and Li, Y. (2005) Aptamers with fluorescence-signaling properties. Methods 37:16–25.

13. Morris, K.N., Jensen, K.B., Julin, C.M., Weil, M. and Gold, L. (1998) High affinity ligands from in vitro selection: complex targets. Proc. Natl. Acad. Sci. USA 95:2902–2907.
14. Blank, M., Weinschenk, T., Priemer, M. and Schluesener, H. (2001) Systematic evolution of a DNA aptamer binding to rat brain tumor microvessels: selective targeting of endothelial regulatory protein pigpen. J. Biol. Chem. 276:16464–16468.
15. Daniels, D.A., Chen, H., Hicke, B.J., Swiderek, K.M. and Gold, L. (2003) A tenascin-C aptamer identified by tumor cell SELEX: systematic evolution of ligands by exponential enrichment. Proc. Natl. Acad. Sci. USA 100:15416–15421.
16. Wang, C., Zhang, M., Yang, G., Zhang, D., Ding, H., Wang, H., Fan, M., Shen, B. and Shao, N. (2003) Single-stranded DNA aptamers that bind differentiated but not parental cells: subtractive systematic evolution of ligands by exponential enrichment. J. Biotechnol. 102:15–22.
17. Chen, H., Medley, C., Sefah, K., Shangguan, D., Tang, Z., Meng, L., Smith, J., and Tan, W. (2008) Molecular recognition of small-cell lung cancer cells using aptamers. CHEMMEDCHEM 3:991–1001.
18. Shangguan, D., Meng, L., Cao, Z., Xiao, Z., Fang, X., Li, Y., Cardona, D., Witek, R., Liu, C., and Tan, W. (2008) Identification of liver cancer-specific aptamers using whole live cells. Analytical Chemistry 80: 721–728.
19. Shangguan D., Cao, Z., Meng, L., Mallikaratchy, P., Sefah, K., Wang, H., Li, Y., and Tan, W. (2008) Cell-specific aptamer probes for membrane protein elucidation in cancer cells. Journal of Proteome Research 7: 2133–2139.
20. Mossie, K., Jallal, B., Alves, F., Sures, I., Plowman, G. and Ullrich, A. (1995) Colon-carcinoma kinase-4 defines a new subclass of the receptor tyrosine kinase family. Oncogene 11:2179–2184.
21. Mallikaratchy, P., Tang, Z., Kwame, S., Meng, L., Shangguan, D., and Tan, W. (2007) Aptamer directly evolved from live cells recognizes membrane bound immunoglobin heavy mu chain in Burkitt's lymphoma cells. Molecular & Cellular Proteomics 6: 2230–2238.
22. Tyagi, S. and Kramer, F.R. (1996) Molecular beacons: probes that fluoresce upon hybridization. Nat. Biotechnol. 14:303–308.
23. Kostrikis, L.G., Tyagi, S., Mhlanga, M.M., Ho, D.D. and Kramer, F.R. (1998) Molecular beacons: spectral genotyping of human alleles. Science 279:1228–1229.
24. Giesendorf, B.A.J., Vet, J.A.M., Tyagi, S., Mensink, E.J.M.G., Trijbels, F.J.M. and Blom, H.J. (1998) Molecular beacons: a new approach for semiautomated mutation analysis. Clin. Chem. 44:482–486.
25. Manganelli, R., Dubnau, E., Tyagi, S., Kramer, F.R. and Smith, I. (1999) Differential expression of 10 sigma factor genes in mycobacterium tuberculosis. Mol. Microbiol. 31:715–724.
26. Matsuo, T. (1998) In situ visualization of messenger RNA for basic fibroblast growth factor in living cells. Biochem. Biophys. Acta Gen. Subj. 1379:178–184.
27. Sokol, D.L., Zhang, X.L., Lu, P.Z. and Gewitz, A.M. (1998) Real time detection of DNA RNA hybridization in living cells. Proc. Natl. Acad. Sci. USA 95:11538–11543.
28. Bock, L.C., Griffin, L.C., Latham, J.A., Vermaas, E.H. and Toole, J.J. (1992) Selection of single-stranded DNA molecules that bind and inhibit human thrombin. Nature (Lond.) 355:564–566.
29. Baldrich, E. and O'Sullivan, C.K. (2005) Ability of thrombin to act as molecular chaperone, inducing formation of quadruplex structure of thrombin-binding aptamer. Anal. Biochem. 341:194–197.
30. Fialova, M., Kypr, J. and Vorlickova, M. (2006) The thrombin binding aptamer GGTTGGTGTGGTTGG forms a bimolecular guanine tetraplex. Biochem. Biophys. Res. Commun. 344:50–54.
31. Mayer, G., Krock, L., Mikat, V., Engeser, M. and Heckel, A. (2005) Light-induced formation of G-quadruplex DNA secondary structures. ChemBioChem 6:1966–1970.
32. Nagatoishi, S., Nojima, T., Galezowska, E., Juskowiak, B. and Takenaka, S. (2006) G quadruplex-based FRET probes with the thrombin-binding aptamer (TBA) sequence designed for the efficient fluorometric detection of the potassium ion. ChemBioChem 7:1730–1737.

33. Huang, C., Cao, Z., Chang, H. and Tan, W. (2004) Protein–protein interaction studies based on molecular aptamers by affinity capillary electrophoresis. Anal. Chem. 76:6973–6981.
34. Hamaguchi, N., Ellington, A. and Stanton, M. (2001) Aptamer beacons for the direct detection of proteins. Anal. Biochem. 294:126–131.
35. Zhang, P., Beck, T. and Tan, W. (2001) Design of a molecular beacon DNA probe with two fluorophores. Angew. Chem. Int. Ed. 40:402–405.
36. Wang, J., Cao, Z., Jiang, Y., Zhou, C., Fang, X. and Tan, W. (2005) Molecular signaling aptamers for real-time fluorescence analysis of protein. IUBMB LIFE 57:123–128.
37. Oefner, C., Darcy, A., Winkler, F.K., Eggimann, B. and Hosang, M. (1992) Crystal-structure of human platelet-derived growth factor-BB. EMBO J. 11:3921–3926.
38. Bergsten, E., Uutela, M., Li, X.R., Pietras, K., Ostman, A., Heldin, C.H., Alitalo, K. and Eriksson, U. (2001) PDGF-D is a specific, protease-activated ligand for the PDGF beta-receptor. Nat. Cell Biol. 3:512–516.
39. Heldin, C.H., Johnsson, A., Betsholtz, C. and Westermark, B. (1986) Platelet-derived growth-factor-structure, function and possible role in cell-transformation. Biol. Chem. Hoppe-Seyler 367:265–265.
40. Peres, R., Betsholtz, C., Westermark, B. and Heldin, C.H. (1987) Frequent expression of growth-factors for mesenchymal cells in human mammary-carcinoma cell-lines. Cancer Res. 47:3425–3429.
41. Green, L.S., Jellinek, D., Bell, C., Beebe, L.A., Feistner, B.D., Gill, S.C., Jucker, F.M. and Janjic, N. (1996) Nuclease-resistant nucleic acid ligands to vascular permeability factor vascular endothelial growth factor (vol. 2, pp 683, 1995). Chem. Biol. 3:960.
42. Birks, J.B. and Leite, M.S.S.C.P. (1970) Energy transfer in organic systems. 8. Quenching of naphthalene fluorescence by biacetyl. J. Phys. Part B Atom. Mol. Phys. 3:417.

Chapter 5
Fluorescent Ribozyme and Deoxyribozyme Sensors

William Chiuman and Yingfu Li

Abstract The development of allosteric nucleic acid enzymes (NAEs) has made NAEs very attractive for a wide variety of biotechnological applications, including biosensing, diagnostics, drug screening, and molecular computation. Although NAEs alone might have limited values for analytical application due to the rather small scope of their substrates and cofactors, modular characteristics of aptamers and NAEs permit the easy design of combined sensors where the aptamer acts as the molecular recognition element (MRE) and the NAE functions as a reporter. To facilitate the exploitation of NAEs for biosensing applications, fluorescence methods have been increasingly explored as better alternatives to radioisotope-based detection techniques. In this chapter, we first survey the strategies that have been employed to graft fluorescence-signaling moieties onto NAEs. We then review our experimental efforts in creating a group of fluorescence-signaling and RNA-cleaving deoxyribozymes (DNAzymes) intended for the design of fluorescent sensors. Last, we discuss the diverse engineering approaches that can transmit the binding status of an aptamer to the activation or repression of catalytic activity in fluorescent NAE sensors.

5.1 Introduction

Fluorescent nucleic acid enzyme (NAE) sensors have three essential components: a molecular recognition element (MRE), a catalytic platform, and a fluorescence-signaling unit. Similar to protein enzymes that are allosterically regulated by the presence of intracellular or extracellular signals, a functional NAE sensor operates by inducing or suppressing its catalytic activity when the MRE identifies its target. For NAEs that require a cofactor (e.g., a specific metal ion) or an environmental cue (e.g., pH) to carry out their catalytic functions, they can be directly utilized

W. Chiuman and Y. Li
Department of Biochemistry and Biomedical Sciences, McMaster University, Hamilton, Ontario, Canada
liying@mcmaster.ca

Y. Li and Y. Lu (eds.), *Functional Nucleic Acids for Analytical Applications*,

for sensing applications as they already contain an inherent recognition element. However, to build an NAE sensor that reports the presence of a substance other than its catalytic constraint, an external MRE must be introduced.

Aptamers are single-stranded RNA or DNA molecules that can selectively bind to a specific target with high affinity. Although natural RNA aptamers have been discovered for several metabolites,[1–4] most of the existing aptamers were isolated from vast random-sequence libraries through in vitro selection or SELEX (systematic evolution of ligands by exponential enrichment).[5–7] The SELEX techniques have been applied to many targets ranging from small organic compounds to proteins and even whole cells.[8,9] The modular nature of aptamers and NAEs allows them to be conjoined to each other while still retaining their functional properties (see Section 5.4). With this principle in mind, one can derive NAE sensors for essentially any target of interest, provided the concerned aptamers are available. Alternatively, one can conduct in vitro selection experiments to directly derive NAE sensors from properly designed random-sequence libraries.

The catalytic platforms of NAE sensors reported to date are mostly RNA-cleaving ribozymes found in nature (e.g., hammerhead and hairpin ribozymes)[10,11] or RNA-cleaving deoxyribozymes artificially created by in vitro selection (e.g., E6 and 8-17).[12–14] To better illustrate the advance in NAE sensor development, we focus solely on the RNA-cleaving ribozyme and deoxyribozyme sensors in this chapter. For brevity, nucleic acid enzymes with RNA-cleaving activity will be referred to as NAERs. There are three main reasons why RNA-cleaving systems are usually favored over NAEs that catalyze other chemical reactions: (1) NAERs have been exhaustively studied because of their relatively high occurrence in nature and their potential for gene therapeutics. Hence, the catalytic and structural properties of most NAERs are well understood. The availability of such information can significantly facilitate the engineering of biosensors, especially if full structural characterization has been achieved. (2) The progress of RNA cleavage can be easily monitored, as a typical RNA-cleavage reaction produces two shorter oligonucleotide fragments with respect to the substrate input. (3) The catalyzed rates of RNA cleavage are among the fastest of all reactions catalyzed by NAEs and are on the time scale for analytical applications.

The most common RNA-cleavage assay, which is still widely used today, involves labeling the substrate with ^{32}P at one terminus (thus one of the cleavage products would also carry the radioisotope), gel separation of the substrate from the cleavage fragments based on their sizes by denaturing polyacrylamide gel electrophoresis (PAGE), and, ultimately, quantification of the cleavage fraction from the autoradiography (phosphor image) of the gel. Fluorescence methods, on the other hand, have several merits over radioisotope-based detection: (1) fluorophore-attached oligonucleotides do not carry the risk encountered in the handling and disposal of radioisotope-labeled nucleic acids; (2) fluorescence signal outputs can be used to monitor the reaction progress in real time and, thus, are faster and more convenient than the discontinuous analyses in radioisotope-based assay; and (3) the fluorophore shelf life is, in essence, unlimited.

The fluorescence-signaling module of NAER sensors is most often (but not limited to) a pair of donor (D) and acceptor (A) dye molecules that interact by fluorescence resonance energy transfer (FRET).[15] D and A can either be chemically conjugated to modified nucleotides of an NAER, or directly added to the nucleic acid sequence during solid-phase oligonucleotide synthesis, provided the concerned dye phosphoramidites or dye-labeled nucleoside phosphoramidites are available. The efficiency of FRET is inversely proportional to the sixth power of intermolecular separation; more specifically, FRET efficiency = $R_o^6/(R_o^6 + r^6)$, where R_o is the distance at which energy transfer is 50% efficient and r is the distance between D and A.[16] Therefore, to render a change in fluorescence signal upon each RNA-cleavage event, the dye molecules have to be attached to the substrate–NAER complex in such a way that D and A are in close proximity for FRET or contact-mediated quenching[17,18] before RNA cleavage. When the substrate is cleaved, the products dissociate from NAER, and the physical separation of D from A generates a high fluorescence signal. For example, if a fluorescein and a nonfluorescent quencher, DABCYL [4-(4-dimethylaminophenylazo) benzoic acid], are situated immediately on either side of the scissile phosphodiester linkage of the substrate (Fig. 5.1a), fluorescein will be severely quenched by DABCYL. However, when the substrate is cleaved, a high fluorescence signal would result.

In the following sections, we first discuss the effects of various dye arrangements in the substrate–NAER complex on the catalytic and signaling performance of NAER in general. We then focus on a series of RNA-cleaving deoxyribozymes that were intentionally created for fluorescence-signaling purposes. Last, several fluorescent NAER sensors are used as representative examples to demonstrate the different mechanisms that govern the functions of allosteric NAERs and to provide insights into the combinatorial and rational approaches to build NAER sensors.

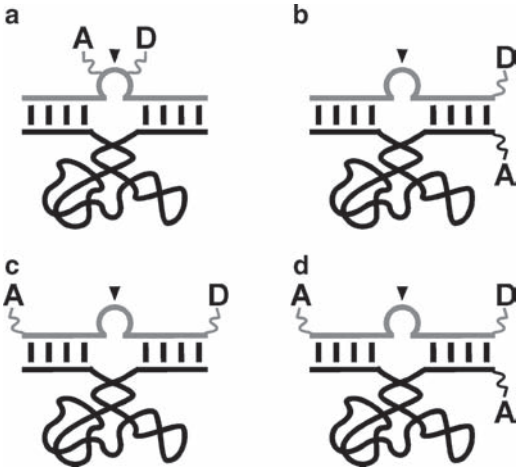

Fig. 5.1 Dye arrangements in fluorescent NAERs. NAERs and their substrates are shown as *black and gray lines*, respectively. The cleavage site is highlighted with "▼." *D*, donor fluorophore; *A*, acceptor fluorophore (or quencher)

5.2 Synchronization of Catalytic Activity with Fluorescence Signals for Existing RNA-Cleaving Nucleic Acid Enzymes

There are primarily two types of dye arrangements in fluorescent NAERs: (1) D and A are located at the opposing termini of an NAER and its substrate (Fig. 5.1b) such that when NAER binds the substrate, D is placed adjacent to A[19–22]; or (2) D and A are at either end of the substrate (Fig. 5.1c).[23–25] In the first case, FRET is only diminished when NAER cleaves the substrate, and the products dissociate from the NAER. However, not all the substrates can effectively associate with NAER in the beginning, and therefore the system yields high background fluorescence. The second dye arrangement, in contrast, does not have the substrate–NAER association problem as both D and A are situated on the same oligonucleotide strand. Nevertheless, a separating distance of more than ten nucleotides between D and A usually renders FRET inefficient, resulting in small signal deviation upon RNA cleavage. Liu and Lu have attempted to improve the signaling performance of a Pb^{2+}-deoxyribozyme sensor, which initially adopted the arrangement of D and A as depicted in Fig. 5.1b, by adding another acceptor molecule to the other end of the substrate (see Fig. 5.1d). The new design was found to be able to significantly suppress the elevated background fluorescence inherent in the previous design, thereby improving the signaling magnitude by approximately fivefold.[26] A similar dye arrangement has also been applied to the newly isolated uranyl-specific deoxyribozyme, and it registered ≤17-fold fluorescence enhancement upon addition of uranyl.[27]

The maximum signal enhancement/deviation that could be attained from the dye arrangements just mentioned is typically less than or equal to tenfold, which may not be ideal for sensitive and highly quantitative detection. Despite that there is an exceptional case of uranyl-specific deoxyribozyme generating greater than tenfold fluorescence emission over the background, it is conceivable that the signaling magnitude of an NAER can be greatly improved by simply moving D and A closer to the cleavage site of a double dye-labeled substrate. Nonetheless, such operation might make NAERs incompetent at cleaving the substrates for the following reasons: (1) Most NAERs were not intentionally selected to process RNA substrates with a crowded cleavage site. (2) Dye molecules are often bulky. Thus, having them nearby the scissile phosphodiester linkage might sterically hinder an NAER to access its cleavage site. (3) Some dyes contain chemical groups that might interact with nucleic acids. Hence, putting them closer to the cleavage site might alter the catalytic mechanism or disrupt the folding of an NAER.

We have recently conducted a detailed study on the effects of the nature of dyes and their attaching positions on the catalytic and signaling performance of 8-17 deoxyribozyme (Fig. 5.2) by screening a series of substrates that are attached with three different fluorophore–quencher pairs (AF488-QSY9, AF546-QSY9, and AF647-QSY21; AF represents Alexa Fluor) at various locations.[28] To our surprise, 8-17 is able to accommodate every dye molecule on most of the nucleotide positions

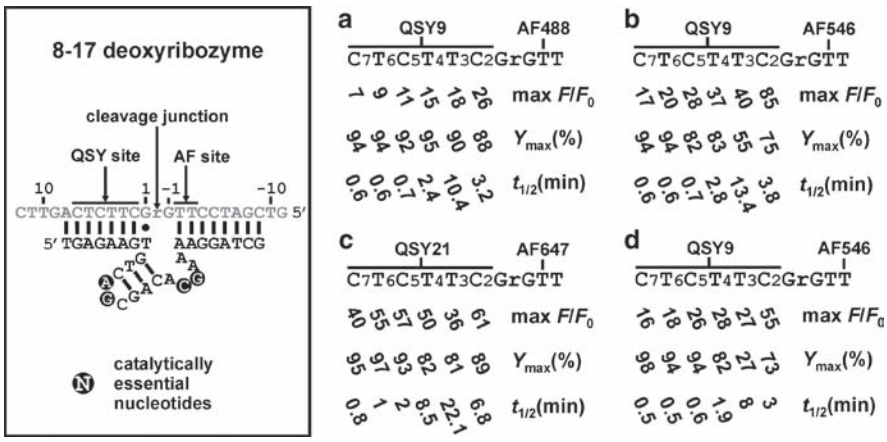

Fig. 5.2 Signaling performance of 8-17 containing Alexa Fluor fluorophore and QSY quencher at various locations. The 8-17 system tested is *boxed*. The chimeric DNA/RNA substrate (top strand) has "rG" as the lone RNA unit. Substrate nucleotides are numbered with respect to "r" as indicated. (**a–d**) For each AF-QSY pair examined (AF488-QSY9, AF546-QSY9, and AF647-QSY21), 12 different substrates were made with the QSY location varying among six nucleotide positions downstream of the cleavage site and the AF location varying between two positions upstream. The substrates were tested on three parameters: max *F/Fo* (maximum fluorescence enhancement), *Y*max (maximum cleavage yield), and $t_{1/2}$ (the time required to reach half of the signaling plateau). The collected data are organized into six groups, of which every substrate shares a common AF attached to a chosen nucleotide upstream of the cleavage site and a QSY quencher on a downstream nucleotide. The data for substrate groups that have AF488 or AF647 at position −3 are omitted here (Panels **a–d** are adopted with copyright permission from ref. 28)

along the substrate strand, including the ones that are only one nucleotide away from the cleavage site (see Y_{max} in panels a–d of Fig. 5.2). The only exceptions are the substrates that contain QSY9 at position +3 and AF546 at position −2 or −3 as they could only be cleaved to 55% and 27%, respectively (see panels b and d, Fig. 5.2), whereas the other substrates were cleaved to the range of 73–98%. As almost all the modified substrates are able to generate 15- to 85-fold signal enhancement (F/F_o) within 10 min, the 8-17 system is no doubt a very attractive catalytic platform for the design of effective fluorescent NAER sensors.

5.3 Creating and Characterizing a Group of New Fluorescence-Signaling and RNA-Cleaving Deoxyribozymes

As discussed earlier, most naturally occurring RNA-cleaving ribozymes and artificially created RNA-cleaving deoxyribozymes are not specifically geared toward fluorescence signaling. Hence, it poses a significant challenge to use those catalytic

platforms to design NAER sensors that have strong catalytic activity and at the same time yield high signaling performance. One way to deal with this issue is to create new NAERs that are capable of efficiently cleaving a substrate that contains the scissile phosphodiester linkage flanked immediately on either side by D and A. In this section, we describe the efforts from our laboratory in creating and characterizing a group of deoxyribozymes that can cleave a DNA substrate which contains an adenine ribonucleotide (denoted as rA) sitting immediately adjacent to a fluorescein-labeled deoxyribothymidine on the 5′-side and a DABCYL-labeled deoxyribothymidine on the 3′-side.

5.3.1 The In Vitro Selection Scheme

The overall process of in vitro selection mainly constitutes iterative cycles of a selection step followed by an amplification procedure. The key to the success of in vitro selection is to devise an effective selection technique to partition the nucleic acid species with the function of interest apart from the inert species, so that only the interesting molecules are progressively enriched in the pool. To date, we have performed two in vitro selection experiments to obtain fluorescence-signaling and RNA-cleaving deoxyribozymes (abbreviated as "FRD"), using the in vitro selection scheme outlined in Fig. 5.3.[29,30]

Briefly, a random-sequence library containing ~10^{14} single-stranded DNA species is first phosphorylated at the 5′-end by polynucleotide kinase (I), followed by ligation to the specially designed substrates described above (II). The ligated molecules are purified by denaturing PAGE (III) and then allowed to self-cleave in the presence of divalent metal ion cofactors (IV). The shortened DNA molecules

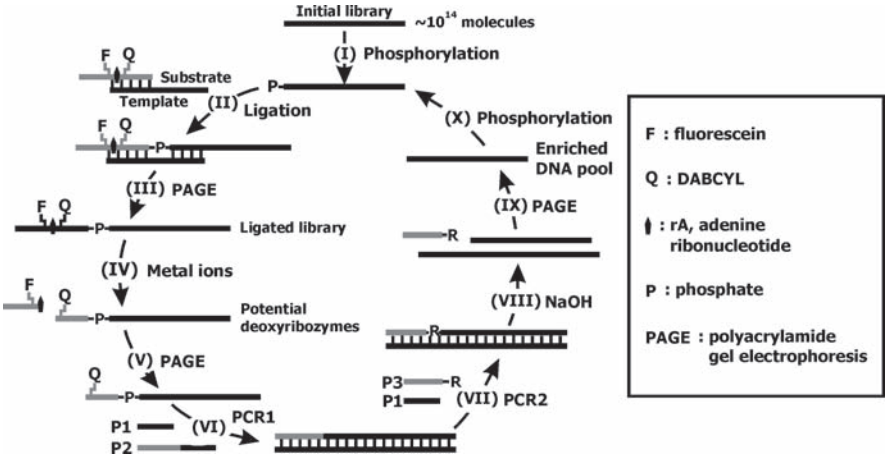

Fig. 5.3 Schematic of in vitro selection for FRD. The details of each step are described in the main text

(deoxyribozyme candidates) are isolated by PAGE (V) and amplified by polymerase chain reaction (PCR) with the use of two DNA primers, P1 and P2 (VI). Another PCR step is then conducted (VII) in which a ribo-terminated primer (P3, replacing P2 in VI) is used to introduce a ribonucleotide into the double-stranded PCR product. To recover the deoxyribozyme strands, the PCR products are treated with NaOH, thereby cleaving the ribonucleotide linkages, resulting in DNA fragments of unequal lengths (VIII). The middle-sized DNA fragment, which represents the deoxyribozyme strand, is purified by PAGE (IX), phosphorylated at the 5′-end by PNK (X), and subjected to the next selection cycle. When the cleavage activity of the population reaches a desirable level, standard cloning and sequencing protocols are applied to obtain the sequences of the final DNA pool. Eventually, several cloned species are arbitrarily chosen to assess their catalytic activities and fluorescence-signaling capabilities.

5.3.2 *Fluorescence-Signaling and RNA-Cleaving Deoxyribozymes from the First In Vitro Selection Attempt*

Our first selection effort on creating FRD utilized a library of 86-nucleotide (nt) DNA molecules containing 43 random nucleotides (Fig. 5.4a).[29] A total of 22 rounds of selective amplification were performed, and the progress is summarized in Fig. 5.4b. Briefly, the DNA population, which had the substrate attached at the 5′-end, was allowed to self-cleave in 5 h in the initial rounds of selection. When a strong cleavage activity was observed in G_{11} (G, generation), the reaction time was progressively reduced from 5 h to 1 s in subsequent selection cycles. A single class of deoxyribozymes was found in the G_{22} pool, and one cloned species named DEC22-18 (which stands for DNA enzyme that acts in *cis* and was found in G_{22} as clone 18) was thoroughly examined.

Based on a secondary structure model of DEC22-18, the *cis*-acting catalyst was successfully converted into a *trans*-acting deoxyribozyme denoted as DET22-18 (Fig. 5.5a; T, *trans*). DET22-18 was reported to exhibit a k_{cat} of ~7 min^{-1} under

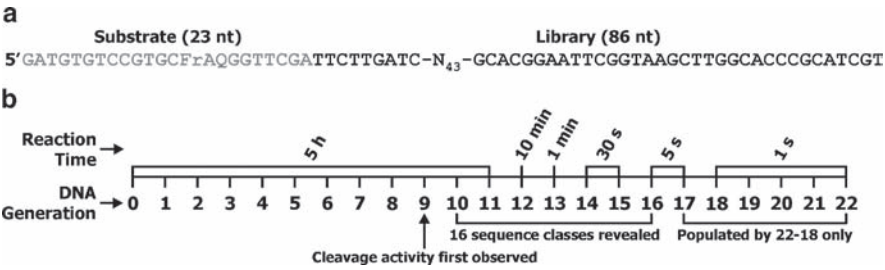

Fig. 5.4 The first in vitro selection attempt. (**a**) DNA library for the selection experiment. (**b**) The entire selection trajectory

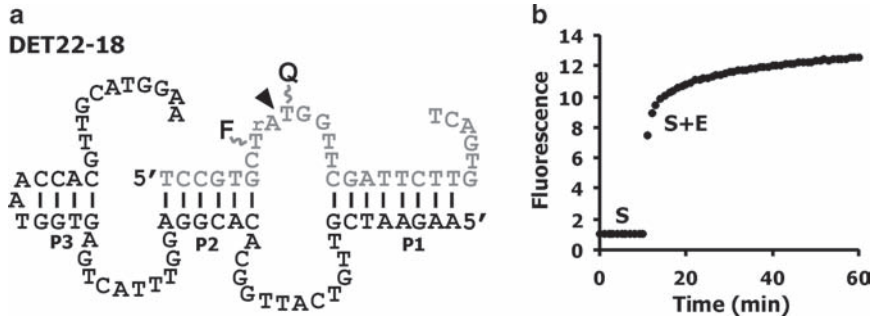

Fig. 5.5 DET22-18. (**a**) Proposed secondary structure of DET22-18. (**b**) Fluorescence-signaling profile of DET22-18. The deoxyribozyme strand was added at the tenth minute

the optimal reaction condition, specifically 50 mM HEPES, pH 6.8 at 23°C, 5 mM $MgCl_2$, and 10 mM $CoCl_2$. However, because a high concentration of Co^{2+} in the reaction mixture was found to cause severe fluorescence quenching,[29,31] $CoCl_2$ was reduced to 1 mM to obtain a maximum of ~13-fold fluorescence enhancement upon DET22-18-mediated substrate cleavage.

Cloning and sequencing of several earlier generations revealed that the only surviving deoxyribozyme species in G_{17}–G_{22} were all similar to DEC22-18 in terms of the sequence context (see Fig. 5.4b; Kenny Schlosser and Yingfu Li, 2006). However, in G_{10}–G_{16}, 15 additional deoxyribozyme sequence classes were also discovered. We named them the "OA" classes (OA stands for "once abandoned"), largely for the reason that they were lost toward the end of the selection trajectory.

While DEC22-18 appeared to have a complicated secondary structure that has yet to be fully elucidated, we wondered whether these OA species have a simpler secondary structure and are perhaps more suitable for sensor engineering. In view of that, we arbitrarily chose six different OA species (namely, OA-I to OA-VI) and created an artificial phylogeny for each deoxyribozyme by performing six parallel reselection experiments, each with a library of synthetic variants of the given deoxyribozyme.[32] The six libraries were subjected to six rounds of selective amplification with the reaction time progressively decreased from 1 h in G_0 to 1 min in G_2–G_5. Through comparative sequence analyses of the cloned species from G_5 of each OA class, followed by cleavage activity assessment of various synthetic mutants, we were able to show that all six OA species use a common three-way junction framework to support their catalytic functions. The secondary structures of the minimized *trans*-acting OA-I to OA-VI are shown in Fig. 5.6.

For each OA species, in general, the absolutely conserved residues (highlighted in black circles; presumably most crucial to the catalytic function of each deoxyribozyme) are mostly located in J2/J3 and J3/J1 (the single-stranded region that join P2 and P3, and P3 and P1, respectively; P represents base-pair stem). Although P3 is required for catalysis in every deoxyribozyme, the base-pairing partners can be covaried (e.g., A=T to T=A or A=T to G≡C) without a drastic effect on the cleavage activity, except the first C≡G pair of P3 facing toward the cleavage site

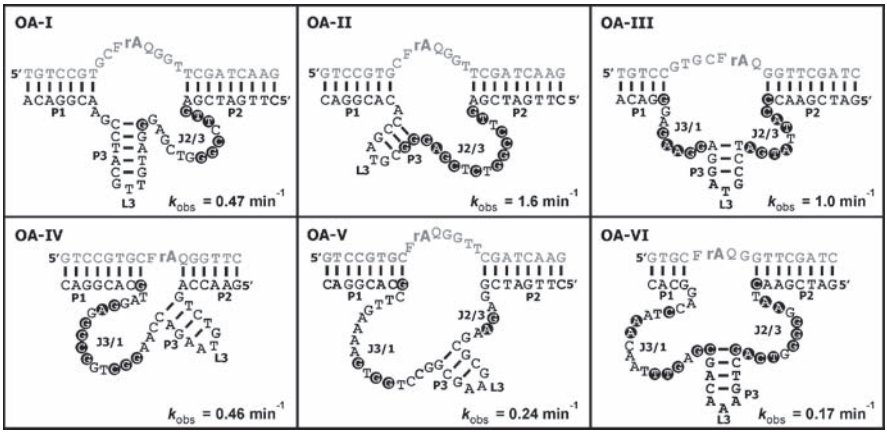

Fig. 5.6 Secondary structures of the six OA deoxyribozymes

in OA-II. The sequence context of L3 (L = loop) is not important for catalysis and, thus, the combined P3–L3 motif might pose a good site for aptamer incorporation (see Section 5.4).

In contrast, the covariability and the catalytic relevance of the substrate-binding stems, P1 and P2, vary among the OA deoxyribozymes: P1 and P2 of OA-I and OA-V can be altered so long as the Watson–Crick interactions are maintained. The base-pairing partners in P1 and P2 of OA-III and OA-IV can also be covaried, but these changes would lead to catalytic constructs with slower kinetics. Both P1 and P2 are essential for the catalytic function of these four OA species, as the incorporation of mismatched pairs or further stem-trimming could deactivate the deoxyribozymes. For OA-II and OA-VI, however, P2 plays a more prominent role in substrate recognition than P1, based on the observation that P1 of both deoxyribozymes can tolerate mismatched pairs or can be significantly truncated.

Considering that the rate constants of the minimized OA deoxyribozymes fall in the range of ~0.2–1.6 min^{-1},[32] which are comparable to those of similar ribozymes, the simple secondary structures of OA deoxyribozymes should open up many opportunities for effective biosensor engineering.

5.3.3 Evolution of a Fluorescence-Signaling and RNA-Cleaving Deoxyribozyme with a Five-Way Junction Structure

In an attempt to further optimize the catalytic performance of the six OA deoxyribozymes, the G4 population of each OA reselection was subjected to six additional selection cycles with online mutagenesis introduced by error-prone PCR and under more stringent time pressure. To our surprise, a few new deoxyribozyme sequences

have emerged along with the parent sequence in four of the six OA pools. In particular, two new sequence classes from the OA-IV population – 5JA and 5JB – share a common five-stem structure arranged in a star-like configuration.[33]

A consensus 5J structure model is shown in Fig. 5.7, where the nucleotides that are conserved in all the sequenced clones of 5J-A and 5J-B are indicated with filled circles. All helical stems (P1–P5) were found to be required for deoxyribozyme activity. Deletion of either DNA strand of any helix or incorporation of mismatches within the stem motifs was detrimental to catalytic function. The sequence context of P1 can be changed so long as the equivalent Watson–Crick base pairs are retained. P2a, the GGH bulge between P2a and P2b, and the two base pairs of P2b lying closest to P2a all play significant roles in catalytic function. The rest of P2 can be covaried with no significant effect on catalysis. None of the conserved nucleotides in P4 and P5 can be mutated. The sequence content and the size of all loops are unimportant for catalysis, thus posing several good sites for biosensor engineering. With all the helical stems being partially covariable, the 5J deoxyribozymes can potentially be equipped with up to five MREs. Our optimized 5J deoxyribozyme exhibited a biphasic kinetics with $k_1 = 2.96\,\text{min}^{-1}$ and $Y_1 = 65\%$ in the fast phase, and $k_2 = 3.27 \times 10^{-2}\,\text{min}^{-1}$ and $Y_2 = 21\%$ in the slow phase.[33]

5.3.4 *Fluorescence-Signaling and RNA-Cleaving Deoxyribozymes from the Second In Vitro Selection Attempt*

A second in vitro selection experiment was conducted to derive FRDs that could be utilized for biosensing applications under various pH conditions.[30] For this experiment, the substrate and the selection scheme used were similar to those adopted in the first selection experiment described above. The selection was initially performed at pH 4.0 with an allowed reaction time of 5 h, using a DNA library that contains a 70-nt random region (Fig. 5.8a). When a strong cleavage activity was observed after eight rounds of selective amplification, the population was subjected

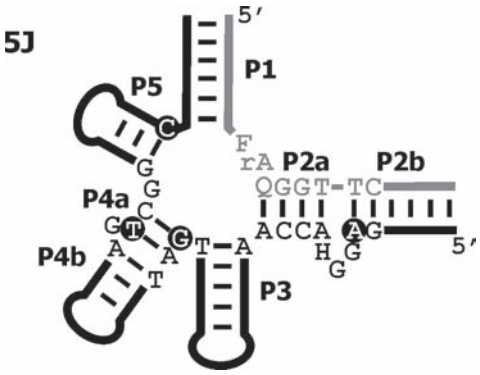

Fig. 5.7 Secondary structure of 5J. H = A, C, or T

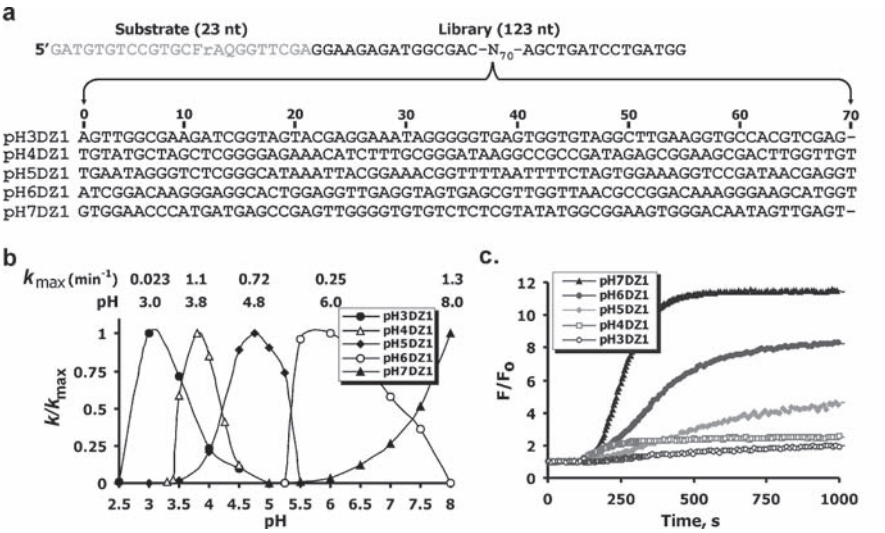

Fig. 5.8 Fluorescence-signaling and RNA-cleaving deoxyribozymes (FRDs) from the second in vitro selection attempt. (**a**) DNA library for the selection experiment and the dominant deoxyribozyme species from five pH-selection trajectories. *Top sequence* is the full-length library construct; *bottom sequences* are the five dominant deoxyribozymes as indicated (note: only the random region is shown). (**b**) Cleavage activity versus pH profiles. Optimal pH for each deoxyribozyme is shown above the figure. (**c**) Fluorescence signaling profiles

to five parallel selection trajectories with the permissive reaction pH set individually at 3.0, 4.0, 5.0, 6.0, and 7.0. Over the course of each selection, the reaction time was progressively reduced from 5 h to as low as 1 s.

Each selected pool was found to contain various deoxyribozyme sequences. The dominant catalyst from each pool was named pH3DZ1, pH4DZ1, pH5DZ1, pH6DZ1, and pH7DZ1 to reflect appropriately their pH heritage and dominance (Fig. 5.8a). Four of these five deoxyribozymes, pH3DZ1, pH4DZ1, pH5DZ1, and pH6DZ1, displayed a maximal cleavage activity at (or near) the pH that was specifically set for the relevant selection trajectory and had a rather narrow functional pH range of less than 3 pH units (Fig. 5.8b). The only exception was pH7DZ1, whose cleavage activity was found to increase in an exponential fashion from pH 5.5 to 8.0. Most of these deoxyribozymes exhibited relatively large k_{obs} values, ranging from 0.2 to 1.3 min^{-1}; only pH3DZ1 was less efficient, with a k_{obs} of 0.023 min^{-1}.[30]

The cleavage-promoted fluorescence enhancement of the five pH-dependent deoxyribozymes was found to vary between twofold and 14-fold (see Fig. 5.8c).[30] Larger enhancement was observed for the deoxyribozymes selected at higher pH, a trend that appears to reflect the inherent pH dependence of fluorescence emission associated with the fluorescein dye. The most likely reasons for the decrease in fluorescence enhancement generated by the lower pH-dependent deoxyribozymes could be that the fluorescein compound is not only less bright but is also less efficiently quenched by the resonance energy transfer mechanism at a lower pH.

The potentials of the pH-dependent signaling deoxyribozymes could be fully realized only if their secondary structures and the catalytically important nucleotides could be identified. To date, three of the five deoxyribozymes – pH6DZ1, pH4DZ1, and pH3DZ1 – have been comprehensively examined for these features. The studies of pH7DZ1 and pH5DZ1 are currently underway. Below, we first discuss the biochemical properties of pH6DZ1; then, we move on to pH4DZ1 and pH3DZ1.

The minimized *trans*-acting pH6DZ1 comprises 48 nucleotides that form a four-way junction structure with the substrate (Fig. 5.9).[34,35] The base-pairing partners in all four helical stems were found to play only structural roles that support catalysis, based on the observation that each of these nucleotides can tolerate mutation to some degree. Most of the base pairs can be covaried without a significant loss of catalytic activity. The only exceptions are the two T=A pairs in P4 and the G≡C pair at the bottom edge of P2, where substitution with alternative base pairs would greatly suppress the cleavage activity. A total of seven catalytically essential nucleotides have been identified, located in J2/J3 and L4. It is reasonable to assume that these seven residues play a major role in forming the active site of the deoxyribozyme. In contrast, L3 does not contain any functionally important nucleotides. Given that the size and content of L3 can be altered without any restriction, the P3–L3 motif is a good site for biosensor engineering (see Section 5.4.1 for an allosteric system built from pH6DZ1 and an ATP aptamer).

The minimized *trans*-acting constructs of pH4DZ1 and pH3DZ1 are shown in Fig. 5.10. The pH4DZ1 system consists of a 59-nt catalyst and 17-nt substrate,[36] and

Fig. 5.9 Secondary structure of pH6DZ1

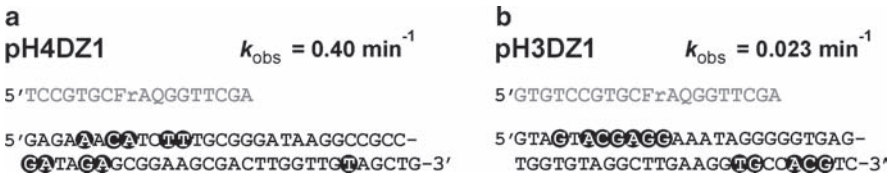

Fig. 5.10 Minimized sequences of pH4DZ1 (**a**) and pH3DZ1 (**b**)

the pH3DZ1 system consists of a 51-nt catalyst and 20-nt substrate.[37] Reselection experiments followed by comparative sequence analyses have identified 10 and 11 absolutely conserved nucleotides for pH4DZ1 and pH3DZ1, correspondingly. In addition, >50% of the remaining nucleotides were also found to be highly conserved, but they are scattered throughout the entire deoxyribozyme strand. Due to the extensive protonation at the N1 atom of adenosine and the N3 atom of cytosine (both of which involve in hydrogen bond formation in the Watson–Crick geometry) at pH ≤ 4, the Watson–Crick pairing rules might not apply to these deoxyribozymes. Indeed, not even a single Watson–Crick base pair was experimentally identified for either pH4DZ1 or pH3DZ1. It was speculated that the tertiary structures of these two deoxyribozymes are built from many molecular interactions between distal nucleotides and probably a few structural domains.

5.3.5 Catalytic Relevance of F, Q, and rA Moieties Within the Substrate

All the aforementioned FRDs were created using the common substrate that contains three special nucleotides – rA (the scissile ribonucleotide), fluorescein-modified dT, and DABCYL-modified dT. Requirement of these moieties for catalysis have been examined for DEC22-18,[29] pH4DZ1,[36] and pH6DZ1.[34] Surprisingly, these FRDs were found to incorporate all three special moieties on the substrate strand as some of the essential structural and/or catalytic components, based on the results that neither the fluorophore nor the quencher can be removed and that the adenine located on the ribose cannot be mutated into other nucleobases. Therefore, the current exploration of these FRDs for biosensor engineering is limited to the use of the fluorescein–DABCYL pair only. To extend to other fluorophore–quencher pairs, new in vitro selection experiments are required to derive new FRDs either from a completely random pool or a partially random pool synthesized according to the sequence of any existing FRDs. To avoid the dependence of a particular fluorophore–quencher pair for catalysis, it should be better to alternate the use of a few substrates, each carrying a different fluorophore–quencher pair, over the course of selection.

5.4 Engineering Allostery into Fluorogenic RNA-Cleaving Nucleic Acid Enzymes

The principle of allostery in NAER sensors mainly relies on the “adaptive binding” characteristic of aptamers.[38,39] That is, the loop(s), bulge(s), and short duplex(es) of an aptamer would only fold into defined conformations when the target is bound. Otherwise, these structural constituents are mostly disordered in the bare aptamer state. The energy that is generated from the formation of the aptamer–target

complex then forces the adjoining NAER to shift from inactive to active conformation (or vice versa, depending on the sensor design). Eventually, a differential signal corresponds to the target absence or presence could be detected. In this section, we describe three general ways by which allosteric NAERs can transduce a ligand-recognition event to a conformational switch in its catalytic domain.

5.4.1 Communication Module Approach

Communication module is a structural bridge that connects aptamer and NAER.[40,41] This module is a part of the aptamer structure, and is most often a weak duplex scaffold that replaces a secondary structure element essential for the catalytic function of NAER. For example, a structural bridge (Fig. 5.11), which comprises two Watson–Crick base pairs sandwiching a single non-Watson–Crick G•A base pair, was exploited to conjugate an ATP-binding DNA aptamer to DEC22-18 at stem P1 to form an ATP-responsive deoxyribozyme (see Fig. 5.5a for the unmodified P1).[29] In the absence of ATP, the bridge stays denatured, rendering the catalytic domain inactive. When ATP is added, the aptamer adaptively folds around ATP, which in turn stabilizes the bridge and triggers the deoxyribozyme activity. Self-cleavage then leads to dissociation of the 5′-cleavage fragment from DEC22-18 and at the same time, causes fluorescein to separate from DABCYL, resulting in a high fluorescence signal. The ATP-responsive DEC22-18 was reported to register ~20-fold increase in fluorescence-signaling rate in the presence of ATP.

The assembly of aptamer, communication module, and NAER into a tripartite system through modular rational design, such as the ATP-responsive DEC22-18, has been quite effective for designing allosteric NAERs. Nevertheless, the sequence context of the communication module is, in most cases, not optimal for either the aptamer or NAER or both. That is, the binding affinity of the aptamer and the catalytic activity of NAER are always hindered in the setting of a rationally designed tripartite assembly. To overcome this deficiency, a library with only the bridge region randomized can be used to search for bridge permutations that are able to couple the aptamer with NAER, but without affecting their wild-type properties, via in vitro selection.

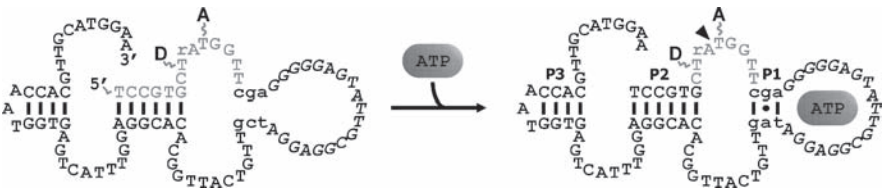

Fig. 5.11 A tripartite ATP sensor comprising DEC22-18 (*black*), a communication module (*P1*), and an ATP aptamer (*Italic letters*). "▼" indicates that substrate cleavage takes place at the scissile phosphodiester

Shown in Fig. 5.12a is a library that consists of a flavin mononucleotide (FMN)-binding RNA aptamer, hammerhead ribozyme (see Fig. 5.12b for the original sequence), and an 8-nt random region at P2 to be selected for the communication module that can activate the hammerhead ribozyme in the presence of FMN.[42] To isolate bridges that confer allosteric activation, the population was first subjected to a "negative selection" for self-cleavage in the absence of FMN. RNA species that remained uncleaved in this screening process were recovered and subsequently subjected to a "positive selection" for self-cleavage in the presence of FMN. After iterative cycles of selection and amplification, the resulting population would contain enriched allosteric ribozymes that are only turned on if FMN is bound.

One selected allosteric ribozyme (Fig. 5.12c) was shown to register ~270-fold enhancement in cleavage activity in the presence of FMN.[42] The authors proposed that the base pairings within the bridge might slip one base pair relative to the G•A interaction in the absence of FMN, which, as a consequence, displaces the G≡C base pair needed for the ribozyme activity. In the presence of FMN, however, the binding energy derived from the new interactions in the FMN–aptamer complex stabilizes the G•A interaction, entails the specific base pairings within the bridge, and, as a result, restores the G≡C base pair required for catalysis. The same authors also demonstrated that their tripartite assembly can be rapidly engineered to detect other molecular compounds by simply swapping the FMN aptamer with another aptamer of interest, such as the aptamer for ATP or theophylline; the ATP-inducible ribozyme registered ~40-fold rate enhancement while the theophylline-responsive ribozyme sensor registered ~110-fold rate enhancement.[42]

A fluorogenic version of the theophylline-inducible hammerhead ribozyme created by a different group[43] is shown in Fig. 5.13. Similar to the aforementioned FMN-dependent ribozyme, the fluorescent sensor for theophylline triggers its cleavage activity through the local alteration of base-pairing patterns within the communication module upon binding of theophylline to the aptamer domain.

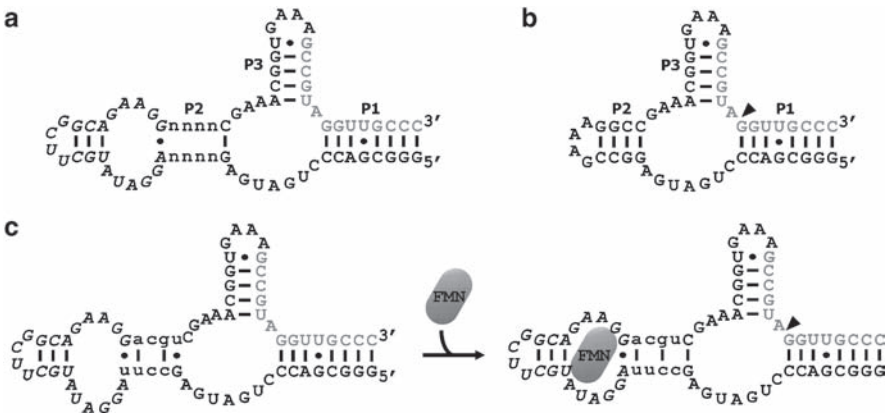

Fig. 5.12 Allosteric ribozyme for FMN detection. (**a**) RNA library used for allosteric selection. (**b**) Hammerhead ribozyme. (**c**) FMN-triggered hammerhead ribozyme

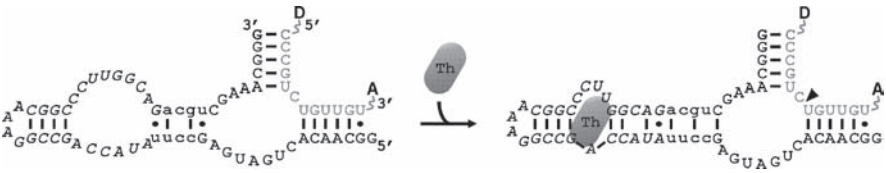

Fig. 5.13 Allosteric ribozyme for theophylline (*Th*) detection

When the substrate labeled with Cy3 and Cy5 at the opposite ends is cleaved, a drop in FRET signal could be detected as the cleavage products dissociate from the ribozyme. The acceleration in FRET decrease was reported to be enhanced by ~12-fold in the presence of theophylline.

It is important to note that the communication module indicated in Fig. 5.12c or Fig. 5.13 is not universally applicable to every aptamer. For instance, when an arginine aptamer was swapped in, the bridge element failed to confer allosteric activation.[42] Therefore, successful design of allosteric NAERs using the modular approach might still require the search for a matching bridge that is compatible with the aptamer of interest either by testing other communication modules that have been used in other sensor systems[44–47] or via a new selection experiment.

Alternatively, one could also derive allosteric NAERs by direct isolation of new aptamers, which are able to confer allosteric transition in a tripartite setting, from a library that contains a NAER with one of its essential stem structures (such as P2) replaced by a long random nucleic acid sequence (Fig. 5.14).[48–51] The selection scheme for allosteric NAERs that are activated by the ligand presence is similar to the one described earlier for the FMN-dependent hammerhead ribozyme. For ligand suppression, on the contrary, the "negative selection" in each selection cycle is carried out in the presence of the target. The remaining uncleaved RNAs are then screened for self-cleavage activity in the target absence.

5.4.2 Antisense Sequestration Approach

Most NAERs reported in the literature recognize their substrates with one or two binding arm(s) through Watson–Crick interactions.[10–14] If an aptamer could be modified in such a way that a part of its sequence is complementary to any binding arm of a NAER, a simple end-to-end joining between the two could then render the catalytic segment incapable of binding the substrate. When the target is present, the binding arm would be released from the aptamer due to the more thermodynamically favorable binding of the aptamer to the target. For example, the Rev-binding aptamer (Rev is a protein that allows fragments of HIV mRNA that contain the Rev response element to be exported from the nucleus to the cytoplasm) attached to the 5′-end of hammerhead ribozyme (via a penta-A linker) inhibits the substrate binding and cleavage of the ribozyme in the absence of Rev by hybridizing to the

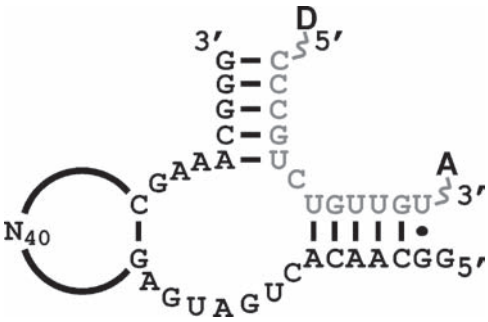

Fig. 5.14 A hammerhead ribozyme-based library construct that allows selection for an aptamer which confers allosteric transition

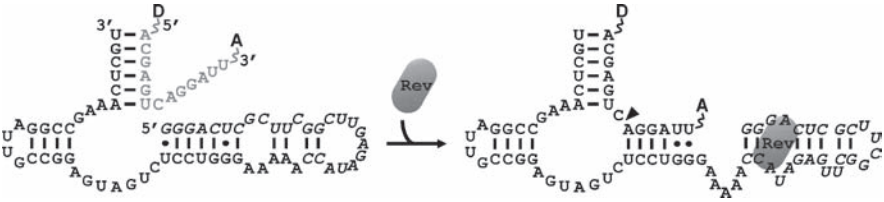

Fig. 5.15 Rev-responsive hammerhead ribozyme

5′-substrate-binding arm of the ribozyme (Fig. 5.15). When Rev is introduced, the aptamer domain rearranges to form the aptamer–Rev complex, allowing the annealing and subsequent cleavage of the substrate. By using a substrate that carries a fluorescein label and a TAMRA quencher at the opposite ends, the presence of Rev brought about ~34-fold enhancement in fluorescence-signaling rate in the aptamer-inhibited ribozyme system.[52]

Besides sequestering the substrate-binding arm, another way to build an allosteric NAER using the antisense approach is to block the catalytic core from folding into its native structure. For example, the ATP-dependent pH6DZ1 deoxyribozyme (Fig. 5.16) was constructed by replacing a part of the nonconserved stem loop P3–L3 with the ATP aptamer, which was modified at its alterable loop region with a sequence complementary to several catalytically essential nucleotides (highlighted in black circles) in the junction between P2 and P3 (J2/J3).[35] In the absence of ATP, a fraction of J2/J3 and the 5′-hybridization arm of P3 are sequestered by the ATP-binding DNA aptamer in a rigid helical structure, rendering the deoxyribozyme inactive. When ATP is added, the aptamer domain pulls the inhibitory strand away from J2/J3 and allows the formation of P3 and subsequent tertiary folding of the catalytic core. With the use of a substrate that contains the lone RNA phosphodiester linkage sandwiched in between fluorescein- and DABCYL-labeled nucleotides, the ATP-inducible pH6DZ1 system was reported to yield ~15-fold increase in fluorescence-signaling rate in the presence of ATP.

In comparison with the communication module method, the antisense approach offers a simpler way of allosteric design for the following reasons. First, inhibitory

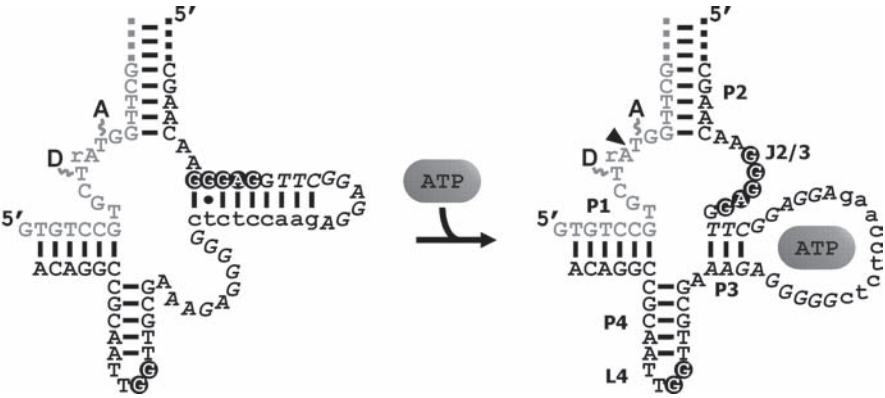

Fig. 5.16 ATP-dependent pH6DZ1

antisense sequences can be easily designed as the Watson–Crick interactions are highly predictable. Second, no modification on NAER is involved, which enables the preservation of wild-type activity. Third, a preliminary screening of aptamer constructs that have different inhibitory strands with blocking activity can be quickly performed in *trans* (or in the intermolecular fashion). Nevertheless, similar to the communication module, there is no guarantee that any molecular engineering approach can definitely yield a nucleic acid construct that confers effective allosteric transition. In the case where the rational design falls short or no significant allosteric transition is inherited from any of the rationally designed aptamer constructs, a combinatorial library might be worth exploring for potential inhibitors.

5.4.3 Catalytic Molecular Beacon Approach

Molecular beacons (MBs) are DNA oligonucleotides that bind to specific nucleic acid targets and have the capability to achieve one mismatch discrimination.[53] An MB has a stem-loop structure where the loop portion is designed to have a sequence complementary to the target and the stem portion is formed by hybridization of the complementary arm sequences at the ends of the probe. The stem only opens when the target hybridizes to the loop and forms a rigid helical structure. Due to the 1:1 stoichiometry of the MB–target complex, a fusion of MB and NAER was modularly designed to amplify the target presence with multiple substrate turnovers. The resulting fusion is called "catalytic MB."[54]

Shown in Fig. 5.17 is a catalytic MB consisting of E6 deoxyribozyme and two MB modules that are able to exert positive and negative regulation, respectively, on its catalytic domain.[55] To confer allosteric activation of E6 by the presence of oligonucleotide input A, an MB module (MB-1) was attached to the 5′-substrate-binding arm of E6 and was designed to have the following three traits: (1) the

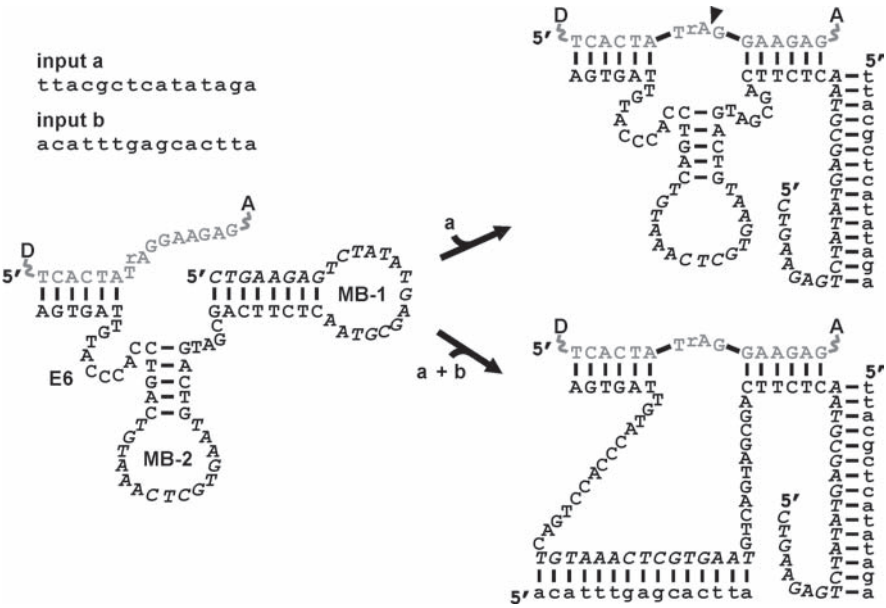

Fig. 5.17 Catalytic MB

5′-hybridization arm is complementary to the 5′-substrate-binding arm of E6; (2) the loop sequence is complementary to input A; and (3) the 3′-hybridization arm is also the 5′-substrate-binding arm of E6.

In the absence of input A, MB-1 stays in its closed form, preventing the substrate from completely annealing to E6. When input A is introduced, MB-1 opens and allows the substrate to fully access E6 for enzymatic cleavage. Dissociation of the cleavage fragments from E6 [and thus separation of fluorescein (D) from TAMRA (A)] decreases the FRET signal. Consequently, a high fluorescence intrinsic to fluorescein could be detected. To exert negative regulation on E6 by oligonucleotide input B, the nonconserved L3 of E6 was designed to have a sequence that is complementary to input B such that a new MB module (MB-2) could form a duplex structure with input B. In the absence of input B, P3 stays intact and substrate cleavage occurs. When input B is present, the hybridization of input B to L3 breaks P2, rendering the system catalytically inactive.

Catalytic MBs have been extensively explored to mimic the computational logic gates,[55–57] such as input A and not input B depicted in Fig. 5.17, where the inputs are the target oligonucleotides and the outputs are distinct fluorescence signals corresponding to the gate functions (see Chapter 14 for more discussions on this topic). By integrating various catalytic MBs, molecular automata were assembled to perform increasingly complex tasks, such as playing a complete tic-tac-toe game.[58,59] With more and more highly branched and fluorescence-signaling deoxyribozymes uncovered (see Section 5.3), the complexity of catalytic MBs can be further expanded and integrated to perform even more challenging tasks.

To summarize, the design of allosteric NAERs requires the knowledge of at least the secondary structures as well as the conserved nucleotide patterns of both aptamers and NAERs. Although rational modular design by itself has proved to be fruitful in developing NAER-based sensors, the combined rational and combinatorial approach remains to be the most effective and convenient method to build NAER sensors, regardless of the allosteric mechanism chosen to be in play.

5.5 Concluding Remarks

The many examples of NAE-based sensors reported to date have illustrated that the versatility of NAEs can be easily extended beyond catalysis of chemical reactions to biosensing, diagnostics, drug screening, molecular computation, and even more applications that are awaited. It is the advent of in vitro selection that has brought us to appreciate what nucleic acids are capable of and, consequently, to utilize them as building blocks to make a variety of useful molecular tools. For detection purposes in particular, molecular engineers have been quite successful in manipulating functional nucleic acids into more complex and sophisticated molecular entities that can report the presence of a ligand target with high specificity and a dynamic range of sensitivity.

To lend NAE-based sensors to automation, different dye moieties have been used to tailor allosteric NAEs with a fluorescence-signaling unit such that the catalytic activity can be synchronized with fluorescence signals, which in turn, indicate the absence/presence of the targets depending on the sensor design. We have discussed the advantages as well as the drawbacks in positioning dye moieties onto preexisting NAER systems. However, to maximize the signaling potential of an NAER, it is necessary to conduct a comprehensive study on the effects of the dye positions on its catalytic and signaling performance, such as the 8-17 study we have described in Section 5.2. Alternatively, one could directly derive new catalytic platforms with robust signaling feature via in vitro selection. The existence of a considerably large collection of FRDs will provide a good opportunity for the design of highly effective reporters for drug screening, metabolite profiling, and any other sensing-based application in demand.

Despite the success in making fluorescent NAE sensors, the challenges to bring them into practices, such as low copy detection and in vivo probing, are yet to be overcome with further research and development. It is conceivable that the sensitivity of an allosteric NAE can be improved with the combination of an aptamer domain having higher affinity for its target, a more efficient catalytic platform with high substrate turnovers, and a more robust signaling component. Nevertheless, to transduce one single recognition event (or a few such events) to a detectable signal, even an improved sensor might not have the amplification power to do so. One way to circumvent this problem is to couple the sensor with an external nucleic acid- or protein-based signal amplification system, which is discussed in Chapter 8 by Willner and coworkers.

The completion of sequencing the human genome and the genomes of many other organisms at an accelerating pace has undoubtedly marked the need to understand in details the functions and interplay of numerous metabolites and macromolecules (including RNAs and proteins) in individual cells, different tissues, or the whole organism. To use NAE sensors for real-time analyses of the healthy/diseased states of an organism or isolated cells, there are still many issues to be addressed: (1) steady expression of allosteric NAEs within the cell; (2) precise delivery of allosteric NAEs to specific intracellular organelles; (3) chemical stability of nucleic acids (i.e., nuclease resistance); (4) biological compatibility and effective delivery of fluorescence-signaling moieties; and (5) correct folding of allosteric NAEs in cellular environments.

With the increasing demand of molecular reporters that can make quick response to the presence of the target of interest with high specificity, a dynamic range of sensitivity, and a fluorescence output, we hope this chapter will guide researchers to consider fluorescent NAER sensors as alternatives to other detection tools and to design them appropriately for their applications of interest.

Acknowledgments We thank the Canadian Institutes of Health Research, the Natural Sciences and Engineering Research Council of Canada, Canada Foundation for Innovation, Canada Research Chairs Program, Ontario Innovation Trust, and Ontario Premier Research Excellence Award Program for research support.

References

1. Mandal, M. and Breaker, R.R. (2004) Gene regulation by riboswitches. Nat. Rev. Mol. Cell Biol. 5:451–463.
2. Tucker, B.J. and Breaker, R.R. (2005) Riboswitches as versatile gene control elements. Curr. Opin. Struct. Biol. 15:342–348.
3. Winkler, W.C. (2005) Riboswitches and the role of noncoding RNAs in bacterial metabolic control. Curr. Opin. Chem. Biol. 9:594–602.
4. Winkler, W.C. and Breaker, R.R. (2005) Regulation of bacterial gene expression by riboswitches. Annu. Rev. Microbiol. 59:487–517.
5. Ellington, A.D. and Szostak, J.W. (1990) In vitro selection of RNA molecules that bind specific ligands. Nature (Lond.) 346:818–822.
6. Robertson, D.L. and Joyce, G.F. (1990) Selection in vitro of an RNA enzyme that specifically cleaves single-stranded DNA. Nature (Lond.) 344:467–468.
7. Tuerk, C. and Gold, L. (1990) Systematic evolution of ligands by exponential enrichment: RNA ligands to bacteriophage T4 DNA polymerase. Science 249:505–510.
8. Lee, J.F., Hesselberth, J.R., Meyers, L.A. and Ellington, A.D. (2004) Aptamer database. Nucleic Acids Res. 32:D95–D100.
9. Thodima, V., Piroozina, M. and Deng, Y. (2006) RiboaptDB: a comprehensive database of ribozymes and aptamers. BMC Bioinf. 7(suppl. 2):S6.
10. Breaker, R.R. (2004) Natural and engineered nucleic acids as tools to explore biology. Nature (Lond.) 432:838–845.
11. Fedor, M.J. and Williamson, J.R. (2005) The catalytic diversity of RNAs. Nat. Rev. Mol. Cell. Biol. 6:399–412.
12. Achenbach, J.C., Chiuman, W., Cruz, R.P. and Li, Y. (2004) DNAzymes: from creation in vitro to application in vivo. Curr. Pharm. Biotechnol. 5:321–336.

13. Joyce, G.F. (2004) Directed evolution of nucleic acid enzymes. Annu. Rev. Biochem. 73: 791–836.
14. Silverman, S.K. (2005) In vitro selection, characterization, and application of deoxyribozymes that cleave RNA. Nucleic Acids Res. 33:6151–6163.
15. Förster, T. (1948) Intermolecular energy migration and fluorescence. Ann. Phys. 2:55–75.
16. Lakowicz, J.R. (1999) Principles of fluorescence spectroscopy, 2nd edn. Kluwer/Plenum, New York.
17. Bernacchi, S. and Mély, Y. (2001) Exciton interaction in molecular beacons: a sensitive sensor for short range modifications of the nucleic acid structure. Nucleic Acids Res. 29:e62.
18. Marras, S.A.E., Kramer, F.R. and Tyagi, S. (2002) Efficiencies of fluorescence resonance energy transfer and contact-mediated quenching in oligonucleotide probes. Nucleic Acids Res. 30:e122.
19. Perkins, T.A., Wolf, D.E. and Goodchild, J. (1996) Fluorescence resonance energy transfer analysis of ribozyme kinetics reveals the mode of action of a facilitator oligonucleotide. Biochemistry 35:16370–16377.
20. Walter, N.G. and Burke, J.M. (1997) Real-time monitoring of hairpin ribozyme kinetics through base-specific quenching of fluorescein-labeled substrates. RNA 3:392–404.
21. Li, J. and Lu, Y. (2000) A highly sensitive and selective catalytic DNA biosensor for lead ions. J. Am. Chem. Soc. 122:10466–10467.
22. Lu, Y., Liu, J., Li, J., Bruesehoff, P.J., Pavot, C.M.B. and Brown, A.K. (2003) New highly sensitive and selective catalytic DNA biosensors for metal ions. Biosens. Bioelectron. 18:529–540.
23. Jenne, A., Gmlein, W., Raffler, N. and Famulok, M. (1999) Real-time characterization of ribozymes by fluorescence resonance energy transfer. Angew. Chem. Int. Ed. 38:1300–1303.
24. Vitiello, D., Pecchia, B. and Burke, J.M. (2000) Intracellular ribozyme-catalyzed trans-cleavage of RNA monitored by fluorescence resonance energy transfer. RNA 6:628–637.
25. Stojanovic, M.N., de Prada, P. and Landry, D.W. (2000) Homogeneous assays based on deoxyribozyme catalysis. Nucleic Acids Res. 28:2915–2918.
26. Liu, J. and Lu, Y. (2003) Improving fluorescent DNAzyme biosensors by combining inter- and intramolecular quenchers. Anal. Chem. 75:6666–6672.
27. Liu, J., Brown, A.K., Meng, X., Cropek, D.M., Istok, J.D., Watson, D.B. and Lu, Y. (2007) A catalytic beacon sensor for uranium with parts-per-trillion sensitivity and millionfold selectivity. Proc. Natl. Acad. Sci. USA 104:2056–2061.
28. Chiuman, W. and Li, Y. (2007) Efficient signaling platforms built from a small catalytic DNA and doubly labeled fluorogenic substrates. Nucleic Acids Res. 35:401–405.
29. Mei, S.H., Liu, Z., Brennan, J.D. and Li, Y. (2003) An efficient RNA-cleaving DNA enzyme that synchronizes catalysis with fluorescence signaling. J. Am. Chem. Soc. 125:412–420.
30. Liu, Z., Mei, S.H., Brennan, J.D. and Li, Y. (2003) Assemblage of signaling DNA enzymes with intriguing metal-ion specificities and pH dependences. J. Am. Chem. Soc. 125:7539–7545.
31. Rupcich, N., Chiuman, W., Nutiu, R., Mei, S., Flora, K.K., Li, Y. and Brennan, J.D. (2006) Quenching of fluorophore-labeled DNA oligonucleotides by divalent metal ions: implications for selection, design, and applications of signaling aptamers and signaling deoxyribozymes. J. Am. Chem. Soc. 128:780–790.
32. Chiuman, W. and Li, Y. (2006) Revitalization of six abandoned catalytic DNA species reveals a common three-way junction framework and diverse catalytic cores. J. Mol. Biol. 357:748–754.
33. Chiuman, W. and Li, Y. (2006) Evolution of high-branching deoxyribozymes from a catalytic DNA with a three-way junction. Chem. Biol. 13:1061–1069.
34. Shen, Y., Brennan, J.D. and Li, Y. (2005) Characterizing the secondary structure and identifying functionally essential nucleotides of pH6DZ1, a fluorescence-signaling and RNA-cleaving deoxyribozyme. Biochemistry 44:12066–12076.
35. Shen, Y., Chiuman, W., Brennan, J.D. and Li, Y. (2006) Catalysis and rational engineering of trans-acting pH6DZ1, an RNA-cleaving and fluorescence-signaling deoxyribozyme with a four-way junction structure. ChemBioChem 7:1343–1348.
36. Kandadai, S.A. and Li, Y. (2006) Characterization of a catalytically efficient acidic RNA-cleaving deoxyribozyme. Nucleic Acids Res. 33:7164–7175.

37. Ali, M.M., Kandadai, S.A. and Li, Y. (2007) Characterization of pH3DZ1: an RNA-cleaving deoxyribozyme with optimal activity at pH 3. Can. J. Chem. 85:261–273.
38. Patel, D.J., Suri, A.K., Jiang, F., Jiang, L., Fan, P., Kumar, R.A. and Nonin, S. (1997) Structure, recognition and adaptive binding in RNA aptamer complexes. J. Mol. Biol. 272:645–664.
39. Hermann, T. and Patel, D.J. (2000) Adaptive recognition by nucleic acid aptamers. Science 287:820–825.
40. Tang, J. and Breaker, R.R. (1997) Rational design of allosteric ribozymes. Chem. Biol. 4: 453–459.
41. Tang, J. and Breaker, R.R. (1997) Examination of the catalytic fitness of the hammerhead ribozyme by in vitro selection. RNA 3:914–925.
42. Soukup, G.A. and Breaker, R.R. (1999) Engineering precision RNA molecular switches. Proc. Natl. Acad. Sci. USA 96:3584–3589.
43. Sekella, P.T., Rueda, D. and Walter, N.G. (2002) A biosensor for theophylline based on fluorescence detection of ligand-induced hammerhead ribozyme cleavage. RNA 8:1242–1252.
44. Araki, M., Okuno, Y., Hara, Y. and Sugiura, Y. (1998) Allosteric regulation of a ribozyme activity through ligand-induced conformational change. Nucleic Acids Res. 26:3379–3384.
45. Robertson, M.P. and Ellington, A.D. (2000) Design and optimization of effector-activated ribozyme ligases. Nucleic Acids Res. 28:1751–1759.
46. Soukup, G.A., Emilsson, G.A.M. and Breaker, R.R. (2000) Altering molecular recognition of RNA aptamers by allosteric selection. J. Mol. Biol. 298:623–632.
47. Kertsburg, A. and Soukup, G.A. (2002) A versatile communication module for controlling RNA folding and catalysis. Nucleic Acids Res. 30:4599–4606.
48. Koizumi, M., Soukup, G.A., Kerr, J.N.Q. and Breaker, R.R. (1999) Allosteric selection of ribozymes that respond to the second messengers cGMP and cAMP. Nat. Struct. Biol. 6: 1062–1071.
49. Piganeau, N., Thuillier, V. and Famulok, M. (2001) In vitro selection of allosteric ribozymes: theory and experimental validation. J. Mol. Biol. 312:1177–1190.
50. Srinivasan, J., Cload, S.T., Hamaguchi, N., Kurz, J., Keene, S., Kurz, M., Boomer, R.M., Blanchard, J., Epstein, D., Wilson, C. and Diener, J.L. (2004) ADP-specific sensors enable universal assay of protein kinase activity. Chem. Biol. 11:499–508.
51. Ferguson, A., Boomer, R.M., Kurz, M., Keene, S.C., Diener, J.L., Keefe, A.D., Wilson, C. and Cload, S.T. (2004) A novel strategy for selection of allosteric ribozymes yields RiboReporter sensors for caffeine and aspartame. Nucleic Acids Res. 32:1756–1766.
52. Hartig, J.S., Najafi-Shoushtari, S.H., Grüne, I., Yan, A., Ellington, A.D. and Famulok, M. (2002) Protein-dependent ribozymes report molecular interactions in real time. Nat. Biotechnol. 20:717–722.
53. Tyagi, S. and Kramer, F.R. (1996) Molecular beacons: probes that fluoresce upon hybridization. Nat. Biotechnol. 14:303–308.
54. Stojanovic, M.N., de Prada, P. and Landry, D.W. (2001) Catalytic molecular beacons. ChemBioChem 2:411–415.
55. Stojanovic, M.N. and Stefanovic, D. (2003) Deoxyribozyme-based half adder. J. Am. Chem. Soc. 125:6673–6676.
56. Stojanovic, M.N., Mitchell, T.E. and Stefanovic, D. (2002) Deoxyribozyme-based logic gates. J. Am. Chem. Soc. 124:3555–3561.
57. Lederman, H., Macdonald, J., Stefanovic, D. and Stojanovic, M.N. (2006) Deoxyribozyme-based three-input logic gates and construction of a molecular full adder. Biochemistry 45: 1194–1199.
58. Stojanovic, M.N. and Stefanovic, D. (2003) A deoxyribozyme-based molecular automaton. Nat. Biotechnol. 21:1069–1074.
59. Macdonald, J., Li, Y., Sutovic, M., Lederman, H., Pendri, K., Lu, W., Andrews, B.L., Stefanovic, D. and Stojanovic, M.N. (2006) Medium scale integration of molecular logic gates in an automaton. Nano Lett. 6:2598–2603.

Chapter 6
Colorimetric and Fluorescent Biosensors Based on Directed Assembly of Nanomaterials with Functional DNA

Juewen Liu and Yi Lu

Abstract This chapter reviews recent progress in the interface between functional nucleic acids and nanoscale science and technology, and its analytical applications. In particular, the use of metallic nanoparticles as the color reporting groups for the action (binding, catalysis, or both) of aptamers, DNAzymes, and aptazymes is described in detail. Because metallic nanoparticles possess high extinction coefficients and distance-dependent optical properties, they allow highly sensitive detections with minimal consumption of materials. The combination of quantum dots (QDs) with functional nucleic acids as fluorescent sensors is also described. The chapter starts with the design of colorimetric and fluorescent sensors responsive to single analytes, followed by sensors responsive to multiple analytes with controllable cooperativity and multiplex detection using both colorimetric and fluorescent signals in one pot, and ends by transferring solution-based detections into litmus paper type of tests, making them generally applicable and usable for a wide range of on-site and real-time analytical applications such as household tests, environmental monitoring, and clinical diagnostics.

6.1 Introduction

6.1.1 Functional DNA as Sensing Molecules

In the past 2 decades, our understanding of nucleic acid chemistry and biology has expanded remarkably with the new discoveries of their functions such as catalysis and molecular recognition. These chemical functions have long been thought to be possessed only by proteins, and their realization in nucleic acids is largely attributed to the development of molecular biology technologies. Naturally occurring catalytic RNAs (ribozymes) were first reported in the early 1980s.[1,2] In addition

Juewen Liu and Yi Lu
Department of Chemistry, University of Illinois at Urbana-Champaign
yi-lu@illinois.edu

Y. Li and Y. Lu (eds.), *Functional Nucleic Acids for Analytical Applications*,

to catalytic functions, natural RNA elements have recently been found to bind small-molecule metabolites and regulate gene expression in bacterial cells. These RNA-based gene regulators are termed riboswitches.[3,4] Chapter 1 of this book extensively reviews all natural functional nucleic acids. Although none has been found in Nature thus far, many catalytic DNAs (deoxyribozymes or DNAzymes) have been isolated in test tubes (in vitro) with combinational selection methods since 1994.[5] Similar selection methods have also been developed to isolate artificial ribozymes and nucleic acid-based binding molecules (aptamers) from large nucleic acid pools containing as many as 10^{15} random sequences.[6,7] Aptamers can be selected to bind essentially any molecule of choice. During the past 17 years, hundreds of aptamers targeting different analytes have been obtained. The affinity and specificity of aptamers are proven to rival those of antibodies.[8,9] Appending aptamers to nucleic acid enzymes results in allosteric enzymes or aptazymes.[10] Aptazymes have the properties of both aptamers and nucleic acid enzymes. Chapter 2 of this book describes the in vitro selected functional nucleic acids. Nucleic acid enzymes, aptamers, and aptazymes are collectively termed functional nucleic acids to set them apart from DNA and RNA with traditional biological functions.

The advent of functional nucleic acids provides vast opportunities for analytical chemistry, particularly for sensing applications. Compared to sensors based on other types of molecules, such as small organic molecules, polymers, proteins, and cells, functional nucleic acids have several advantages.[11] Probably the greatest advantage is that they can be subject to in vitro selection, and such a combinatorial selection is one of the few general methods to obtain sensing molecules for virtually any class of molecule. In vitro selection from a library of 10^{14} to 10^{15} random nucleic acid sequences offers considerable possibilities.[12–18] Target selectivity can be rationally increased by using negative selections,[19] which can overcome our limited knowledge about the ligand-binding affinity and selectivity. Selection of nucleic acids is also time- and cost-effective. Compared to the antibody approach, nucleic acid selections are carried out in test tubes, in a shorter time span, and with limited cost, thus resulting in significant savings of time and funds. DNA molecules have high stability. In contrast to proteins or antibodies, most catalytic DNA and DNA aptamers can be denatured and renatured many times without losing their functions. They can be stored under rather harsh conditions and can be used when correct conditions are restored. Therefore, DNA has a much longer shelf life and is more suitable for field applications, which is the focus of this chapter. Furthermore, nucleic acids have predictable secondary structures. To signal nucleic acid binding or catalytic events, chemical labels (fluorophores, nanoparticles, and electrochemical labels) can be placed remotely from the binding or cleavage sites so that binding and sensing do not interfere with each other and can be optimized independently. Finally, the effective placement of such labels can be accomplished with little knowledge of the three-dimensional structure of the system. These valuable properties make functional nucleic acids (especially DNA) a primary candidate for sensor design.

6.1.2 Optical Properties of Inorganic Nanomaterials

In addition to sensing molecules that can bind target analytes tightly and selectivity, sensors require reporting groups to generate signals for detection and quantification. Optical signals such as color and fluorescence are commonly employed. Because optical sensors require only simple analytical instruments or, in the case of colorimetric sensors, even no instrumentation at all, on-site real-time detection is possible. One good example is pH paper. For colorimetric sensors, organic chromophores are the most frequently used because of their widespread availability and the ease with which they can be attached to nucleic acids.[20] The main drawback, however, comes from the relatively low extinction coefficient. Most organic dyes have extinction coefficients of the order of 10^5 M^{-1} cm^{-1}. Therefore, micromolar concentrations of dye or DNA are needed to allow visible color detection using the naked eye. In contrast, metallic nanoparticles have much higher extinction coefficients due to the surface plasmon effect.[21,22] For example, the extinction coefficients for 13- and 50-nm gold nanoparticles (Au NPs) were reported to be 2.7×10^8 and 1.5×10^{10} M^{-1} cm^{-1}, respectively.[23] These values are three to five orders of magnitude higher than those for the brightest organic dyes. Therefore, only nanomolar concentrations of materials are needed for visual detection. In addition to being highly sensitive, metallic nanoparticles display distance-dependent optical properties.[24] For example, Au NPs are red in the dispersed state, and blue or purple upon aggregation, making it possible for ratiometric detection to minimize background signals that often interfere with color intensity-based detection. Finally, DNA molecules can be conveniently attached to Au NPs via the thiol-gold chemistry, and these DNA-functionalized Au NPs have been used for nucleic acid detection.[24–26] Therefore, metallic nanoparticles are an excellent choice for colorimetric sensing.

Similarly, organic fluorophores are the common choice for designing fluorescent sensors. However, organic fluorophores often display broad absorption and emission spectra, making it difficult to use multiple fluorophores in the same system for multiplex sensing with a single excitation source. They also suffer from photobleaching, preventing long-time monitoring for processes such as cellular activities. Quantum dots (QDs) are nanocrystalline semiconductors.[27–29] Thanks to recent developments in synthesis and functionalization, QDs are increasingly becoming a superior alternative to organic fluorophores. Because of their large Stokes shifts and narrow emission bands, essentially any emission wavelength covering the whole visible region, and even beyond, can be obtained under the same excitation light; the exact emission wavelength can be controlled by employing QDs of different compositions and sizes.[27] Conversely, for organic fluorophores, it is difficult to simultaneously excite even two molecules with distinct emission wavelengths.[29] QDs are highly photostable and resistant to photobleaching. In addition, QDs also possess high extinction coefficients and quantum yields. Therefore, QDs are also ideal labeling groups for sensing and imaging applications.

6.2 Colorimetric Sensors

6.2.1 Colorimetric Sensors for Metal Ions Based on Directed Assembly of Au NPs Using DNAzymes

Most DNAzymes require metal ions for their structure and function, and such a requirement is often quite specific for a certain metal ion, especially for DNAzymes obtained through in vitro selections.[11] For example, DNAzymes that are specific for Pb^{2+},[5,30] Zn^{2+},[31] Cu^{2+},[32,33] Co^{2+},[34] and UO_2^{2+},[35] have been obtained. Therefore, it would be interesting and useful to convert these DNAzymes into selective metal sensors. The 8–17 DNAzyme is one of the examples of metal-specific DNAzymes (Fig. 6.1a), which contains a DNA enzyme strand (the lower strand) and a substrate strand (the upper strand) with a single RNA linkage (rA). This DNAzyme showed very high activity in the presence of low concentrations of Pb^{2+}.[36] At low metal

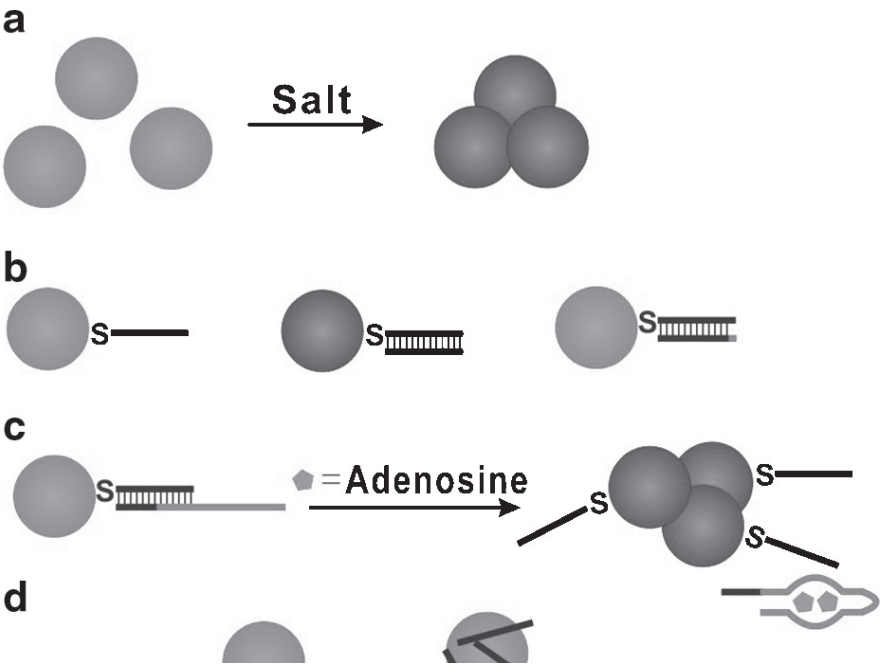

Fig. 6.1 (**a**) The secondary structure of the Pb^{2+}-specific DNAzyme. Mutating the G•T wobble pair to a G•C pair abolishes enzyme activity. (**b**) In the presence of Pb^{2+}, the substrate is cleaved into two pieces. (**c**) Pb^{2+} sensing based on Pb^{2+}-directed assembly of DNAzyme-linked nanoparticles aligned in a head-to-tail manner. (**d**) UV–vis spectra of disassembled (*solid line*) and assembled (*dashed line*) nanoparticles. (**e**) The assembly state or color of nanoparticles in response to Pb^{2+} concentration (*triangles*). (**f**) Color of the gold nanoparticles in the presence of different divalent metal ions (spotted on a TLC plate). All color figures in this chapter are available online (Reproduced with permission from ref. 37. Copyright © [2003] American Chemical Society)

concentrations (nanomolar to low micromolar range), Pb^{2+} is the only metal that can activate the enzyme.

The Pb^{2+}-specific 8-17 DNAzyme was chosen as a model DNAzyme for metal sensor design. In the presence of Pb^{2+}, the enzyme cleaves the substrate into two pieces (Fig. 6.1b). To allow the DNAzyme to bind DNA-functionalized Au NPs, the substrate strand was extended on both ends and the extended substrate was named Sub_{Au} (Fig. 6.1c).[37] The Au NPs were aligned in a head-to-tail manner so that only one set of nanoparticles (5′-DNA_{Au}) was used. The Au NPs were preassembled by the DNAzyme to assure an optimal ratio between the DNAzyme and nanoparticles, and the assembled Au NPs can be used as colorimetric sensors for Pb^{2+} detection. To detect Pb^{2+}, the sensor was heated to 50°C to fully disassemble the aggregates. In the subsequent slow cooling process to room temperature (annealing), Pb^{2+} can direct the color of the system. If Pb^{2+} was present, the substrate was cleaved by the enzyme and assembly was inhibited, resulting in a red color. Otherwise, Au NPs were reassembled by the DNAzyme to form aggregated structures, accompanied by a red-to-blue color change caused by surface plasmon coupling. Upon aggregation, the 522-nm plasmon peak decreased while the extinction in the 700-nm region increased (Fig. 6.1d). Therefore, the extinction ratio at 522 nm over 700 nm was used to quantify the Au NP assembly state. A higher ratio is associated with dispersed particles of red color, and a lower ratio is associated with aggregated particles of blue color. With increasing concentrations of Pb^{2+}, the extinction ratio increased, suggesting the Au NPs were in the disassembled state (Fig. 6.1e). The detection limit was determined to be 100 nM. The color change was also conveniently observed by spotting the Au NPs on a thin-layer chromatography (TLC) plate (Fig. 6.1f). A color progression from blue/purple to red was observed with increasing Pb^{2+} concentrations, whereas competing metal ions resulted in only a background blue/purple color.

The colorimetric sensor based on head-to-tail aligned aggregates was sensitive and selective. In addition, the color of the sensor changed from blue to red in the presence of Pb^{2+}, and such a color change was desirable because from a sensor point of view it was a “turn-on” sensor. However, an annealing step (heating to 50°C and subsequent cooling slowly to room temperature over 2 h) was needed to form the head-to-tail aligned aggregates shown in Fig. 6.1c, and no assembly occurred by simple mixing of the DNAzyme and Au NPs at room temperature (Fig. 6.2b, solid dots), which impeded practical applications of the sensor.

The need for the annealing process was attributed to the relatively large steric effects related to the head-to-tail nanoparticle alignment.[38,39] Indeed, by changing the alignment to tail-to-tail (Fig. 6.2a), assembly at constant temperature was observed (Fig. 6.2b, empty squares). However, the rate of assembly was relatively slow. It is known that the optical properties of a Au NP aggregate are governed by the size of the aggregate, instead of the number of nanoparticles in it.[40] Therefore, by using larger Au NPs, the time needed to form an aggregate with a defined size should decrease, although the rate of assembly may not change. By changing both nanoparticles (3′-DNA_{Au} and 5′-DNA_{Au}) from 13 to 42 nm, a clear color change was observed in 5 min (Fig. 6.2b, solid triangles). Similarly, Pb^{2+} can control the

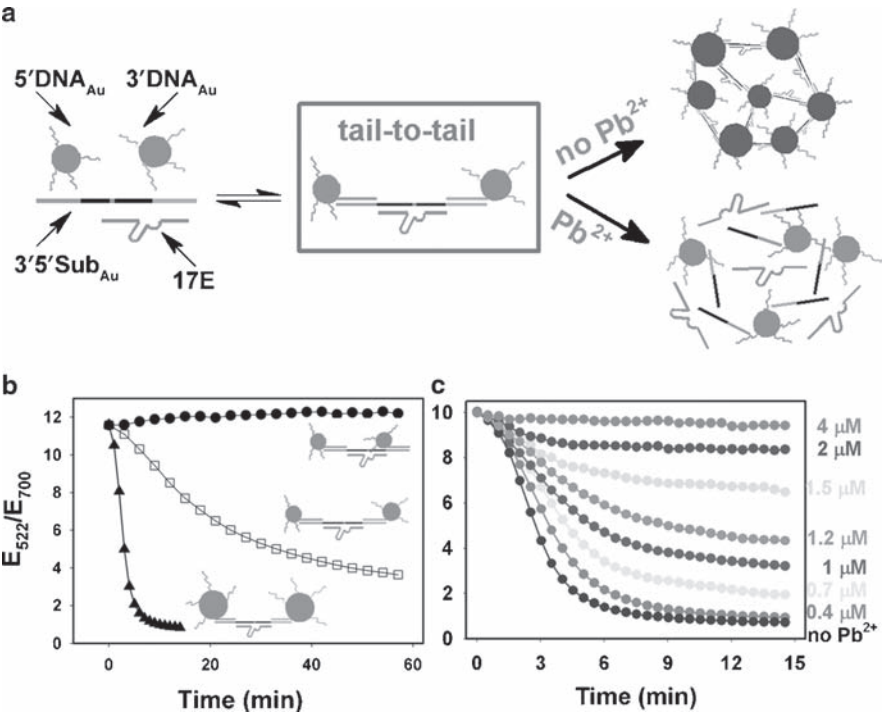

Fig. 6.2 (**a**) Pb^{2+} sensing based on Pb^{2+}-directed assembly of DNAzyme-linked nanoparticles aligned in a tail-to-tail manner. (**b**) The effect of nanoparticle alignment and size on the rate of color change. (**c**) The kinetics of nanoparticle assembly in the presence of different Pb^{2+} concentrations (Reproduced with permission from ref. 39. Copyright © [2004] American Chemical Society)

assembly state of the system (see Fig. 6.2a). The nanoparticles aggregated to different degrees at different Pb^{2+} concentrations (see Fig. 6.2c). Therefore, this system is also useful for colorimetric sensing of Pb^{2+}.[39] Compared to the previous system, this sensor has similar sensitivity, but with a much faster response time, and can be operated at ambient temperatures. One disadvantage, however, was the lack of a positive color change in the presence of Pb^{2+}. As shown in Fig. 6.2a, there was no color change in the presence of Pb^{2+}, and the red-to-blue color change was only observed in the absence of Pb^{2+}. Therefore, this is not a "turn-on" sensor and is susceptible to environmental factors that may induce false-positive results.

To further improve the sensor performance and design "turn-on" colorimetric sensors with fast responses, Pb^{2+}-induced disassembly of DNAzyme-linked Au NPs was studied.[41,42] As characterized by transmission electron microscopy (TEM), most DNAzyme-linked Au NPs contained hundreds to thousands of nanoparticles. Surprisingly, when Pb^{2+} was added to Au NP aggregates aligned in either configuration, no disassembly or color change was observed. To investigate the reason behind this, the 5′-ends of the substrates were labeled with ^{32}P, and the kinetics of Pb^{2+}-induced substrate cleavage in nanoparticle aggregates was monitored. In the

head-to-tail aligned system, 22% of substrate was cleaved in 1 h; in the tail-to-tail aligned aggregates, 60% cleavage was observed (Fig. 6.3c). From this study, it appeared that the DNAzyme was active in both aggregates, and we hypothesized that there could be inhibition of nanoparticle release after cleavage. To facilitate Au NP release, the NaCl concentration was decreased from 300 to 30 mM for the tail-to-tail aligned aggregates, and a slow color change was observed upon addition of Pb^{2+} (Fig. 6.3b). This color change was inhibited in 300 mM NaCl. However, even in low-NaCl buffers, Pb^{2+} did not accelerate the disassembly of head-to-tail aligned aggregates, which suggested that the observed 22% cleavage was from dangling DNAzymes with only one of its ends attached to Au NPs, while the linking DNAzymes were not active (Fig. 6.3a).

To further accelerate the rate of disassembly and color change in tail-to-tail aligned aggregates, two methods were developed. First, a short DNA complementary to the cleaved substrate pieces was added to invade the cleaved substrate,

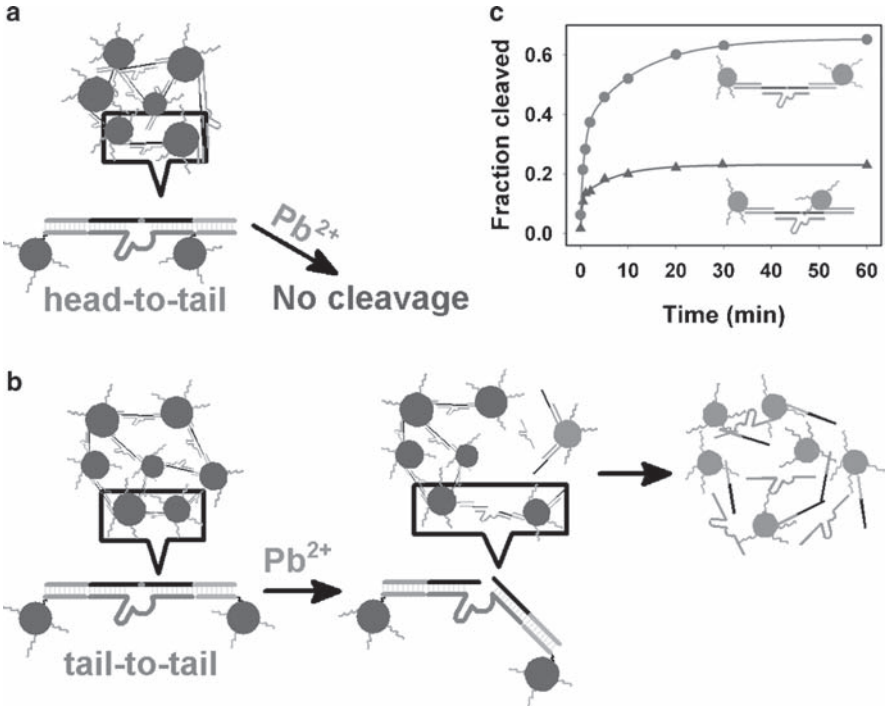

Fig. 6.3 Colorimetric sensing by Pb^{2+}-induced disassembly of DNAzyme-linked Au NPs. (**a**) In head-to-tail aligned aggregates, the linking DNAzyme was inactive. (**b**) In tail-to-tail aligned aggregates, the linking DNAzyme was active, and a blue-to-red color transition was observed in the presence of Pb^{2+}. (**c**) Activity assay of DNAzyme embedded in Au NP aggregates. The 22% cleavage from head-to-tail aligned aggregates was attributed to nonbridging DNAzymes with only one end linked to the Au NPs[41] (Reproduced with permission from ref. 41. Copyright © [2005] American Chemical Society)

which significantly accelerated the rate of disassembly, and as such, the added DNA was called invasive DNA.[41] Under optimized conditions, color change from blue to red was observed in 5 min at room temperature. Alternatively, asymmetrical DNAzymes were designed with one of the substrate-binding arms elongated and the other one shortened to facilitate release of Au NPs after cleavage.[42]

6.2.2 *Beyond Colorimetric Metal Sensors*

The DNAzymes described above provide a valuable means for analyte recognition that is coupled with catalytic reactions, and the catalytic turnover property could allow sensing with ultrahigh sensitivity. Because of the chemical nature of DNAzyme-catalyzed reactions, most known DNAzymes employ only metal ions as cofactors, and few other species can replace metal ions to catalyze the same kind of reactions.[43,44] Aptamers are known to bind a broad range of molecules beyond metal ions, but cannot catalyze chemical reactions as do DNAzymes. To expand the DNAzyme-based methodology to design sensors responsive to other molecules such as small organic molecules, proteins, or even cells, one can take advantage of aptamer-binding events to regulate DNAzyme activities, and such DNAzymes are known as allosteric DNAzymes or aptazymes.[45] An aptazyme designed by Sen and coworkers was chosen to assemble Au NPs responsive to adenosine.[46] The aptazyme was built on the Pb^{2+}-specific DNAzyme catalytic core. An adenosine aptamer was inserted into one of the substrate-binding arms of the enzyme strand (Fig. 6.4).[47] In the absence of adenosine, binding to the substrate was disrupted by the bulging aptamer motif. As a result, the aptazyme activity was inhibited. In the presence of adenosine, the interaction between the aptamer and adenosine strengthened the binding of the substrate and the enzyme, and cleavage of the substrate was allowed. Therefore, a Pb^{2+}-dependent DNAzyme was converted into an adenosine-dependent aptazyme. Similar to the Pb^{2+}-DNAzyme, an adenosine sensor based on the assembly of Au NPs was demonstrated. In the TLC plate in Fig. 6.4, only the sample with adenosine showed a red color, while other nucleosides induced blue colors.[48]

DNAzymes and aptazymes are catalysts and chemical transformations are involved in the sensing process. Therefore, such sensors are generally not reversible,

Fig. 6.4 An adenosine-activated aptazyme based on the Pb^{2+}-specific RNA-cleaving DNAzyme

making continuous monitoring of a sample for a long period of time difficult. Most traditional sensors solely rely on binding for molecular recognition, such as those based on antibodies and organic chelators. Compared to binding-based sensors, DNAzyme sensors could take longer time for sensing because binding events are usually faster than DNAzyme catalysis. Aptamers are nucleic acid-based binding molecules that represent another class of important nucleic acid-sensing molecules. To convert aptamers into colorimetric sensors, many research efforts have been undertaken.

Stojanovic and coworkers screened 35 different dyes by incubating the dyes with a cocaine aptamer and then adding cocaine to the mixture.[20] Only a cyanine dye showed some differences in the absorption spectrum upon addition of cocaine. The authors suggested that cocaine may displace the cyanine dye in the aptamer-binding pocket and push the cyanine dye into solution. The cyanine dye formed dimers in solution whose absorption spectrum was different from that of the monomer, which resulted in a color change. However, to visualize the color change by the naked eye, 20-μM aptamer was used and a waiting time of 12 h was needed. It is also difficult for this method to be generalized to design other colorimetric aptamer sensors, because it is not certain whether there will be an appropriate dye for any chosen aptamer. Leclerc and coworkers employed cationic conjugated polymers for colorimetric sensing of aptamer binding events.[49–51] When the polymer was in a random coil conformation in solution, the effective conjugation length decreased and an absorption maximum of 390 nm was observed. In comparison, the absorption maximum shifted to 540 nm in the solid state, which was attributed to the formation of a conjugated form. The cationic polymer interacted strongly with negatively charged DNA. Using the thrombin aptamer as an example, the polymer formed a stiff duplex with the free aptamer, shifting the absorption to a longer wavelength. When the aptamer bound thrombin and folded into a compact structure, the polymer wrapped around the aptamer and displayed an absorption maximum at a shorter wavelength. The colorimetric sensor had a detection limit of 100 nM for thrombin. The method has also been successfully applied to detect nucleic acids and potassium ions. However, similar to organic chromophores, micromolar concentration of aptamers had to be used for visualization by the naked eye.

Willner and coworkers functionalized Au NPs with the 15-mer antithrombin aptamer via a poly-T spacer. After mixing these Au NPs with a high concentration of thrombin, some turbidity was observed.[52] The authors suggested that each thrombin can interact with two aptamers.[53] As a result, Au NPs were linked by thrombin to result in aggregates. The aggregates were also separated and used as seeds to grow larger Au NPs to facilitate detection. A detection limit of 20 nM was reported with this method. Similarly, Chang and coworkers have functionalized PDGF aptamers on Au NPs.[54] It is known that each PDGF can bind two aptamers, and a red-to-purple color change was observed with addition of platelet-derived growth factor (PDGF), which was again attributed to the cross-linking of nanoparticles by PDGF. Interestingly, the authors were able to show that too much PDGF can also inhibit assembly, because at high PDGF concentrations, Au NPs were

completely covered by PDGF and no aptamers were available for cross-linking. A competitive binding assay for PDGF receptor-β was also developed. Being highly sensitive, the aggregation-based method requires that a target molecule has two or more aptamer-binding sites. Therefore, it is difficult to be generalized, especially for small-molecule detection.

As an extension of the work performed on Pb^{2+}-induced disassembly of DNAzyme-linked Au NPs, small-molecule detection using aptamer and Au NPs was also pursued.[55] Instead of using aptamers to directly functionalize Au NPs, aptamers were used as linker DNA to assemble nanoparticles. The sensor design for adenosine detection is shown in Fig. 6.5a. Two kinds of DNA-functionalized Au NPs (1 and 2) were assembled by a linker DNA containing an adenosine aptamer fragment. The aptamer was extended by 17 nucleotides on the 5′-end. The first 12 nucleotides were complementary to the DNA on particle 1, while the next 5 on the extension with an additional 7 from the aptamer can hybridize to the DNA on particle 2. In the presence of adenosine, the aptamer switched its structure and bound to the target. As a result, the number of base pairs left to bind particle 2 decreased from 12 to 5, which was not strong enough to hold particle 2 and led to its dissociation. Such an aptamer structure switch method was first applied by Li and coworkers to design fluorescent sensors,[56–60] and more detailed discussion on this topic is provided in Chapter 12 of this book. A color change from blue/purple to red was observed in the disassembly process. In contrast to the relatively slow assembly-based process, disassembly can finish in seconds. As shown in Fig. 6.5d, increasing concentrations of adenosine led to faster rates of color change, while other ribonucleosides did not induce any color change (Fig. 6.5c). The sensor design is very general. Au NPs linked by a cocaine aptamer were also prepared (Fig. 6.5b). In the presence of cocaine, a red color was produced, while in the presence of adenosine, no color change was observed (Fig. 6.5e). The degree of disassembly also varied with cocaine concentration (Fig. 6.5f). Similarly, sensors responsive to K^+ have also been obtained.[61]

6.2.3 Colorimetric Sensors with Tunable Dynamic Ranges

The colorimetric sensors described above have a relatively sharp color transition, resulting in high sensitivity, i.e., sharp colorimetric signal rises with small changes in analyte concentration. This advantage of nanoparticle-based sensors, however, can become a disadvantage as its narrow dynamic range means signals can saturate easily, making it difficult to quantify in a wide concentration range. For some applications such as the detection of lead in dust or paint, such a narrow dynamic range is desirable because the only information needed is whether the lead level is above or below the regulation threshold. For many other applications, more quantitative results covering a wide dynamic range are desirable. To have sharp signal increases while still possessing wide dynamic ranges, we designed DNAzyme-based Pb^{2+}

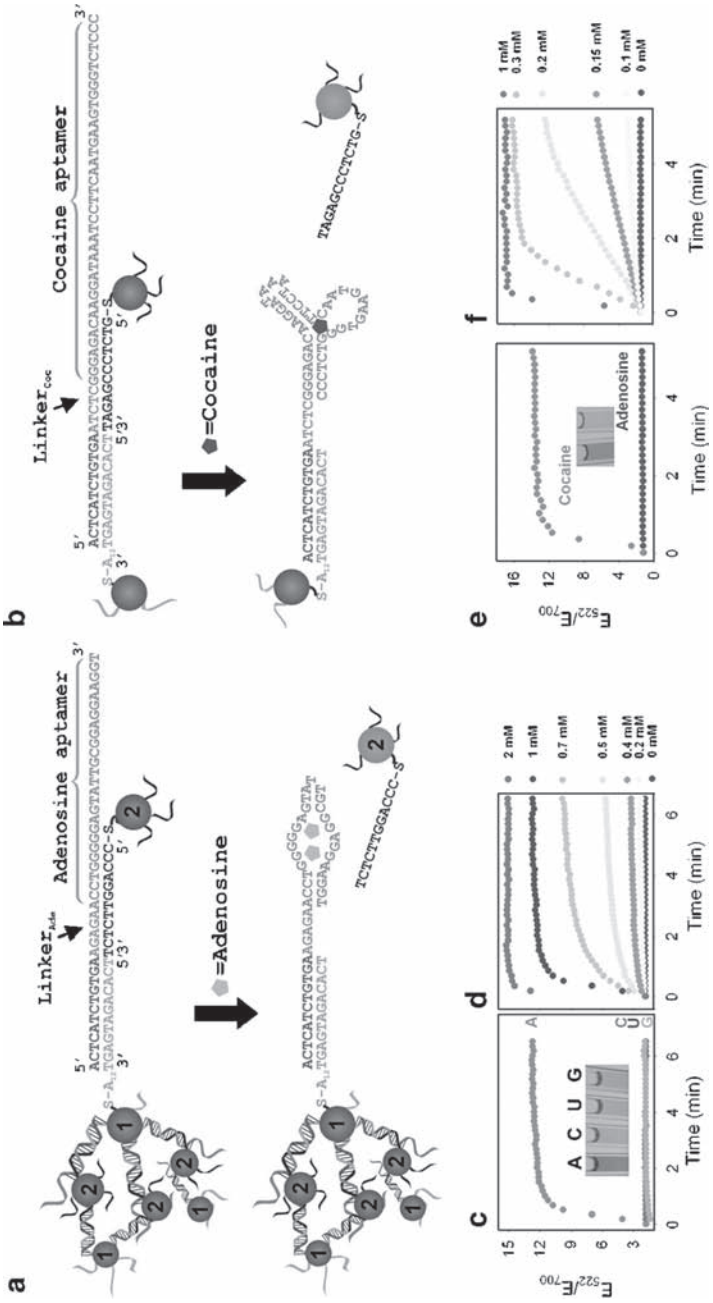

Fig. 6.5 Colorimetric sensors based on the disassembly of Au NPs linked by an adenosine aptamer (**a**) or a cocaine aptamer (**b**). Analyte specificity of the adenosine (**c**) and cocaine (**e**) sensors. *Insets*: Images of the sensor solutions after treatment with analytes. Kinetics of sensor color change in the presence of different concentrations of adenosine for the adenosine sensor (**d**), or cocaine for the cocaine sensor (**f**) (Reproduced with permission from ref. 55. Copyright © [2006] Wiley.)

sensors with tunable detection ranges. As a catalyst, the DNAzyme possesses multiple turnover properties, which allows tuning of the Pb^{2+} dynamic range over several orders of magnitude. By changing the G•T wobble pair to a G•C Watson–Crick pair (see Fig. 6.1a; highlighted by a circle), the DNAzyme activity was abolished. However, the mutated DNAzyme can still assemble nanoparticles. If only a small fraction of the active enzyme (17E) was used (i.e., 5%) with the rest being the inactive enzyme (17Ec), the Pb^{2+} dynamic range shifted about one order of magnitude to higher Pb^{2+} concentrations (Fig. 6.1e, squares). This tuning property is unique and useful for sensing applications because it allows detection of Pb^{2+} in a wide concentration range without signal saturation problems.[37]

6.2.4 From Single Analyte Detection to Multiple Analyte Detection

Most sensors, including those described above, can detect only one specific analyte. For certain applications, it is desirable to design sensors that can detect multiple analytes in the same system. The aptamer-linked Au NPs allowed us to design more complex sensors that are sensitive to multiple analytes. Importantly, we show that the cooperativity between the analytes can be tuned by using different sensor designs. Such sensors are useful because they can be used to sense complex chemical environments. First, a system with high analyte cooperativity was designed.[61] This system contained two kinds of Au NPs: 1 and 2 (Fig. 6.6a). Particle 1 was functionalized with one kind of DNA and particle 2 was functionalized with two kinds of DNA. Both the adenosine aptamer and the cocaine aptamer were used to assemble the particles. To disassemble the Au NPs, both adenosine and cocaine were needed. Neither molecule alone can induce significant color change. Therefore, the two molecules were highly cooperative in performing the disassembly task. Indeed, as shown in Fig. 6.6c, only when both molecules were present (black curve) was a fast color change observed. Either adenosine or cocaine alone cannot produce much color change. The inset of Fig. 6.6c shows the color of the sensors when exposed to different analytes, and an intense red color was observed only in the presence of both molecules. Concentration-dependent studies (Fig. 6.6d) were also performed, and high extinction ratios were observed only in the presence of both adenosine and cocaine.

After demonstrating sensors with high cooperative responses to adenosine and cocaine, an independent system without cooperativity was also designed (Fig. 6.6b). This system contained two kinds of Au NPs, 3 and 4, and a linker DNA, which is flanked by an adenosine aptamer (green) and a cocaine aptamer (red). In the presence of either adenosine or cocaine, Au NPs 3 and 4 should be separated. Indeed, as shown in Fig. 6.6e, time-dependent color change was observed in the presence of either adenosine, or cocaine, or both. The inset of Fig. 6.6e shows the color of the sensors exposed to different analytes, and an intense red color was seen in the presence of either molecule. A concentration-dependent study was also performed

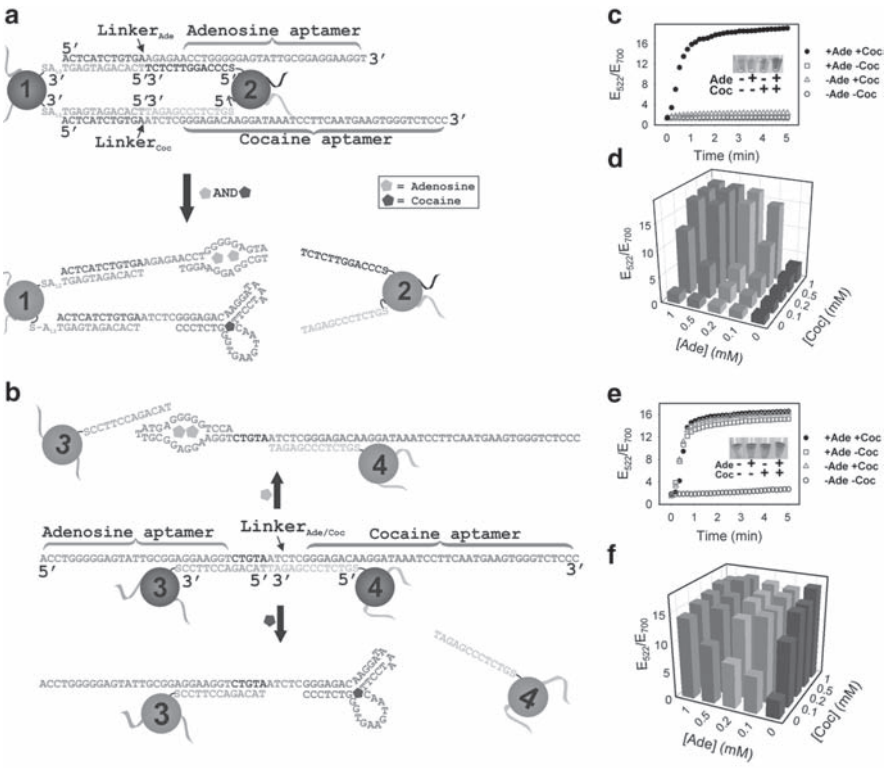

Fig. 6.6 Sensors that requires both adenosine and cocaine (**a**) or either adenosine or cocaine (**b**) to change color. Kinetics of color change in the presence of 1 mM adenosine (*open squares*), 1 mM cocaine (*open triangles*), or 0.5 mM adenosine and 0.5 mM cocaine (*solid dots*), or none (*open dots*) for aggregates shown in Fig. 6.1a (**c**) and Fig. 6.1b (**e**). *Insets* are the color of the systems with or without adenosine and/or cocaine after 5 min reaction time. Adenosine- and cocaine-dependent color change for aggregates shown in Fig. 6.1a (**d**) and Fig. 6.1b (**f**) (Reproduced with permission from ref. 61. Copyright © [2006] Wiley)

(Fig. 6.6f). Either adenosine or cocaine induced a significant degree of color change at high concentrations.

6.3 Fluorescent Sensors

In addition to metallic nanoparticles, semiconductor nanocrystals (QDs) have also recently been employed to design aptamer-based sensors. Compared to organic fluorophores, QDs give stable emissions and allow multiplex detection of several targets in a single solution. Ellington and coworkers functionalized QDs with a thrombin-binding aptamer.[62] A short piece of quencher-labeled DNA was hybridized

to the thrombin aptamer on QDs. Therefore, the QD emission was initially quenched. Addition of thrombin resulted in dissociation of the quencher labeled DNA and unmasked the QD emission. In the presence of 1-μM thrombin, a remarkable 19-fold emission increase was observed. In a separate example, Strano and coworkers prepared thrombin aptamer passivated PbS QDs and found that addition of thrombin decreased PbS emission, which was attributed to charge transfer from functional groups on thrombin to the QD.[63] Although other proteins could also be adsorbed onto the surface of the QD, quenching was observed only for thrombin. A detection limit of ~1 nM was obtained with this method. In other examples, QD and aptamer conjugates have also been applied to stain cancer cells and bacteria cells.[64–66] Because of their superior optical properties, functional nucleic acid-tagged QDs will see more applications in analytical chemistry.

6.4 "One-Pot" Multiplex Colorimetric and Fluorescent Detection of Multiple Analytes Using Au NPs and QDs

In the foregoing multiplex detection systems (see Section 6.2.4) with Au NPs, even though multiple chemical analytes can be detected with a single sensor, only one kind of signal was produced (purple to red color change). As a result, the identity of each analyte in the mixture cannot be distinguished. To improve upon this, an encoding mechanism needs to be introduced. Because of the highly tunable emission properties of QDs, QD-encoded adenosine and cocaine sensors were constructed. The sensors were designed as shown in Fig. 6.7a. Using adenosine as an example, in addition to Au NPs 1 and 2, QD Q1 (emission at 525 nm) was also used. Q1 and Au NP 2 were functionalized with DNA of the same sequence, and therefore both can be linked to Au NP 1 by the adenosine aptamer linker. In the assembled state, the QD emission was quenched because of energy transfer to nearby Au NPs.[67–71] Addition of adenosine disassembles the aggregates, resulting in increased emission intensity at 525 nm. Similarly, cocaine sensors were also prepared by incorporation of Q2, which emitted at 585 nm. As the detection of adenosine and cocaine can be carried out under the same external conditions (i.e., temperature, buffer pH, and ionic strength), it is possible to mix the two sensors and achieve detection of both molecules in one pot. As shown in Fig. 6.7b, two emission peaks at 525 and 585 nm were observed (solid line), corresponding to the adenosine and cocaine sensors, respectively. Addition of cytidine and uridine (Fig. 6.7b, dashed line) did not change the emission intensity of either peak. Addition of 1 mM adenosine alone increased the 525-nm peak but not the 585-nm peak (Fig. 6.7c), while addition of 1 mM cocaine alone increased the 585-nm peak but not the 525-nm peak (Fig. 6.7d). Addition of both analytes resulted in enhancements in both peaks (Fig. 6.7e). This result proved the high selectivity of both systems and the feasibility of using aptamer-linked nanoparticles for simultaneous detection of multiple analytes in one pot.

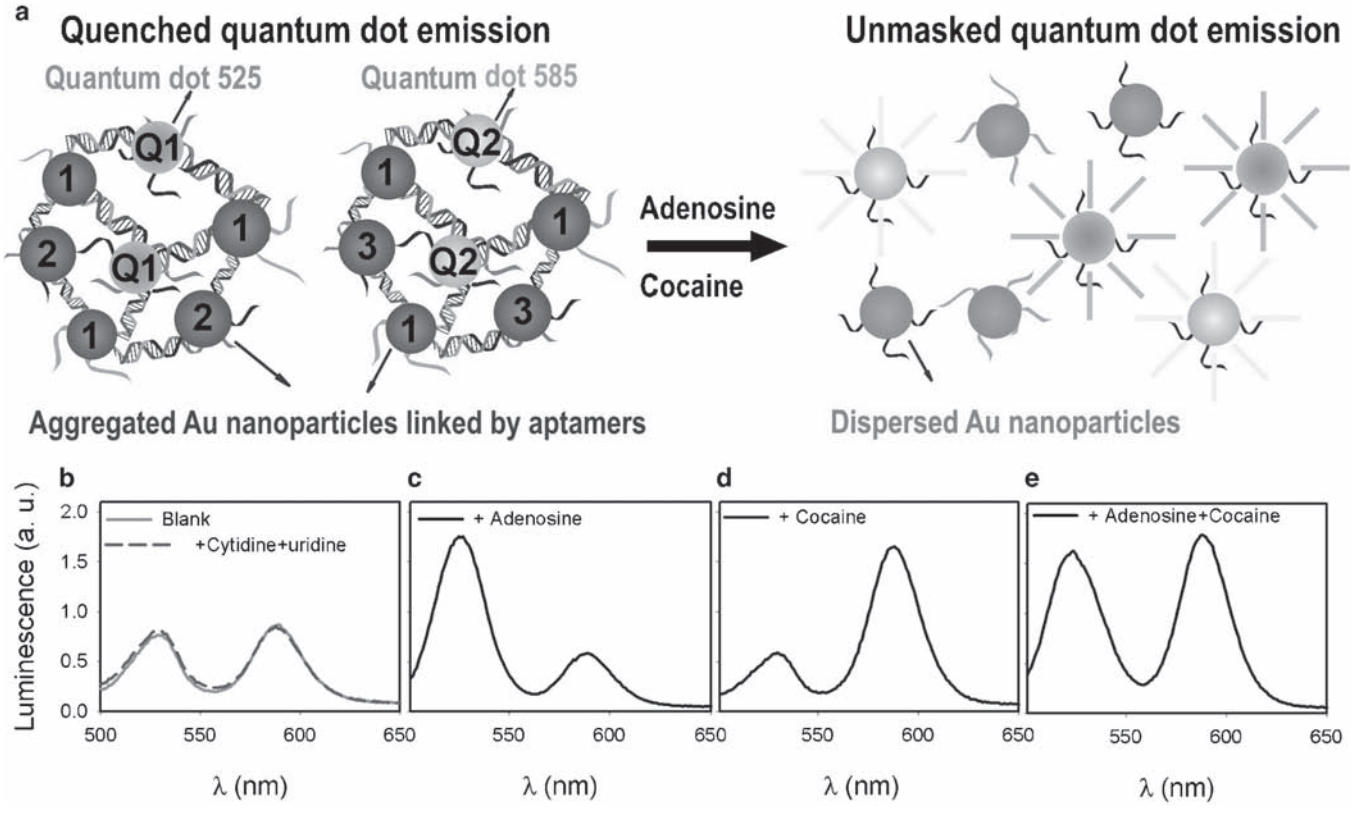

Fig. 6.7 (**a**) Quantum dot (QD)-encoded aptamer-linked nanostructures for multiplex detection. Au NPs 1, 2, and QD Q1 were assembled by the adenosine aptamer DNA; 1, 2, and Q2 were assembled by the cocaine aptamer. In both aggregates, QD emissions were quenched. Addition of adenosine and cocaine disassembled the aggregates with increased QD emission observed. (**b–e**) Emission spectra of mixed sensors. (**b**) Mixed sensors alone, or with 1 mM cytidine and 1 mM uridine. Mixed sensors with 1 mM adenosine added (**c**), with 1 mM cocaine added (**d**), or with 1 mM adenosine and 1 mM cocaine added (**e**)

6.5 Detection Based on Non-cross-Linking DNA

In the above Au NP-based colorimetric aptamer sensors, the color change was due to the cross-linking of DNA on Au NPs or aptamers with their targets. Interestingly, it has been shown that non-DNA cross-linking-based Au NP aggregation is also useful for developing colorimetric aptamer sensors. The stability of Au NPs is dependent on the concentration of salt in solution, and high concentrations of salt can induce aggregation of colloids, giving a similar red-to-blue color change. A schematic of such a process is shown in Fig. 6.8a. Au NPs are usually made from reduction of $HAuCl_4$ by sodium citrate, and Au NPs protected by the citrate ligand are relatively unstable. They tend to aggregate irreversibly in low-salt buffers (i.e., tens of millimolar NaCl). Thiol DNA-functionalized Au NPs, on the other hand, are much more stable and can withstand even molar concentrations of NaCl.[24] The Au NP stability against salt is also dependent on the condition of DNA. For example,

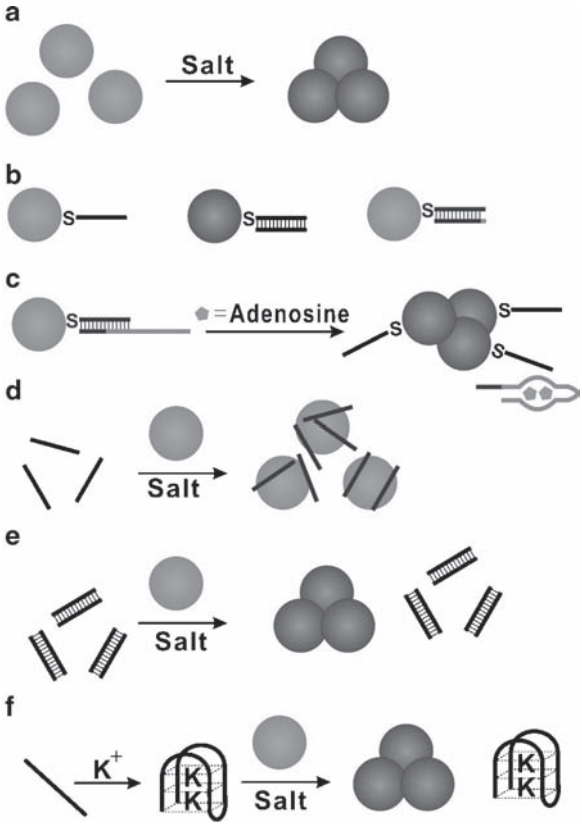

Fig. 6.8 Colorimetric sensors based on non-cross-linking DNA and Au NPs. (**a**) Schematics of Au NP aggregation induced by electrolytes. (**b**) Stability of Au NPs with different DNA in high-salt buffers.[72] (**c**) Colorimetric detection of adenosine.[73] There are ~100 DNA on each Au NP; only 1 is shown for clarity of the figure. Non-thiol-modified single-stranded DNA can also protect Au NPs from aggregation (**d**), but double-stranded DNA cannot (**e**).[75] (**f**) Colorimetric detection of K^+.[77]

single- or double-stranded, folded or unfolded, short or long, thiolated or non-thiolated DNA all give different Au NP stabilities, which provides another means for colorimetric sensor design. Because such aggregation processes are not induced by DNA hybridization, they are usually called non-cross-linking Au NP aggregation. Sato et al. attached thiol-modified 15-mer single-stranded DNA to Au NPs.[72] These particles were highly stable, and they remained dispersed and red in color even in 2.5 M NaCl (Fig. 6.8b, left panel). There were more than 100 DNA on each Au NP, and only 1 is drawn in the figure. In the presence of complementary DNA, the salt stability of the Au NPs decreased, and a purple-colored precipitant was observed with 0.5 M NaCl (Fig. 6.8b, middle panel). If the DNA contained a single mismatch in the end, the Au NPs could also survive 2.5 M NaCl and remained red in color (Fig. 6.8b, middle panel. This system, however, required a target DNA:Au NP ratio of 200:1 to induce aggregation, which had limited sensitivity of 500 nM. The difference in Au NP stability was attributed to the rigidity of double-stranded DNA.

Li and coworkers also functionalized Au NPs with short thiol DNA, upon which an adenosine DNA aptamer was hybridized. The stability of Au NPs was so high that they were stable even in 500 mM $MgCl_2$. Such high ionic strengths were undesirable to carry out aptamer-binding and structure-switching reactions. Au NP stability was then tuned down by treating Au NPs with 6-mercaptohexanol (MCH). It was determined that the number of thiol DNA dropped from ~150 to ~100 after MCH treatment, and 90% of them were hybridized to the adenosine DNA aptamer. These Au NPs were stable in 35 mM $MgCl_2$ for more than 1 min. Addition of adenosine led to the structure switching of the aptamer and its dissociation from Au NPs (Fig. 6.8c). The salt stability of the Au NPs then decreased, giving a red to purple color change. Such color changes can be observed in 1 min, and a detection limit of 10 μM was reported.[73]

Instead of using thiol-modified DNA to functionalize Au NPs, Rothberg and coworkers found that nonthiolated short single-stranded DNA can also be absorbed onto the Au NP surface and have protection effects (Fig. 6.8d).[74–76] The kinetics of DNA adsorption was dependent upon the length of DNA and temperature. Shorter DNA (10–20 nucleotides) and higher temperature gave faster adsorption.[75] Long or double-stranded DNA cannot be associated with Au NPs effectively, and Au NPs remained susceptible to salt-induced precipitation (Fig. 6.8e). Because no labeling of the AuNPs with DNA is required for sensing, this method is also called label-free colorimetric sensing. Along this line, Fan and coworkers designed a colorimetric K^+ sensor.[77] A piece of guanine-rich DNA folded into a G-quadruplex structure in the presence of K^+. Similar to a double-stranded DNA, this folded DNA cannot be effectively absorbed on the Au NP surface and therefore Au NPs were aggregated in the presence of NaCl. In the absence of K^+, the Au NPs were stabilized and remained red (Fig. 6.8f). The detection limit was ~1 mM K^+. This sensor did not use thiol DNA, which can reduce the cost associated with sensor production and simplify the experiment protocol. This very reason, however, also attributed to the relatively low stability of Au NPs even with protection from short single-stranded DNA. For example, thiol DNA-protected Au NPs are stable in several molar NaCl, but the stability goes down tenfold for nonthiolated DNA-protected Au NPs. Therefore, high ionic strength samples may give false-positive results whereas the presence of other single-stranded DNA or ligands may give false-negative results.

For all non-cross-linking-based detection systems, an advantage is the fast color change kinetics. To assemble Au NPs by DNA base-pairing interactions, it usually takes several minutes to hours, because the Au NPs contain negative charges from DNA and are repulsive to each other. DNA hybridization needs to overcome such repulsive forces. For non-cross-linking systems, on the other hand, the charges are screened by high concentrations of salt and aggregation is driven by van der Waals forces.[72,73] Usually color changes in such systems can be observed in 1 min.

6.6 Toward More Practical Applications: Simple "Dipstick" Tests

Even though nanoparticle-based colorimetric sensors can eliminate the use of analytical instruments for detection, one limitation that prevents their practical application is the handling of solutions, such as transfer of microliter volumes of sensors and their subsequent mixing with target solutions. This limitation may make the sensors difficult to use for ordinary users. One of the most useful methods to convert antibody-based assays to user-friendly test kits is the lateral flow technology, and a well-known example is the commercially available pregnancy test kit. Despite wide applications in antibody assays, nucleic acid-based lateral flow devices were demonstrated only for DNA detection.[78] We pursued the feasibility of using lateral flow devices to design aptamer-based sensors that can be used as simple dipsticks.[79,80]

First, the adenosine aptamer was used to build a model system to study aptamer-based lateral flow devices. The adenosine-responsive nanoparticle aggregates are similar to that shown in Fig. 6.5a. To be captured by streptavidin, some nanoparticles were labeled with biotinylated DNA (black stars in Fig. 6.9a). The lateral flow device contained four overlapping pads placed on a backing (Fig. 6.9a). The four pads were (from top to bottom): absorption pad, membrane, glass fiber conjugation pad, and wicking pad. The aptamer-linked nanoparticle aggregates were spotted on the conjugation pad while streptavidin was applied on the membrane as a thin line (Fig. 6.9a, left strip). The whole device was then dried overnight at room temperature before use. We hypothesize that nanoparticle aggregates are too large to migrate along the membrane, while dispersed nanoparticles can. If the wicking pad of the device is dipped into a solution, the solution will move up along the device and rehydrate the aggregates. In the absence of adenosine, the rehydrated aggregates will migrate to the bottom of the membrane where they stop because of their large size (Fig. 6.9a, middle strip). In the presence of adenosine, the nanoparticles would be disassembled by binding of adenosine by the aptamer.[55,56] The dispersed nanoparticles can then migrate along the membrane and be captured by streptavidin to form a red line (Fig. 6.9a, right strip).

To carry out detection, the adenosine-sensitive devices were dipped into buffers containing various nucleoside species at different concentrations (see Fig. 6.9b). No red band was observed in the absence of adenosine. With increasing adeno-

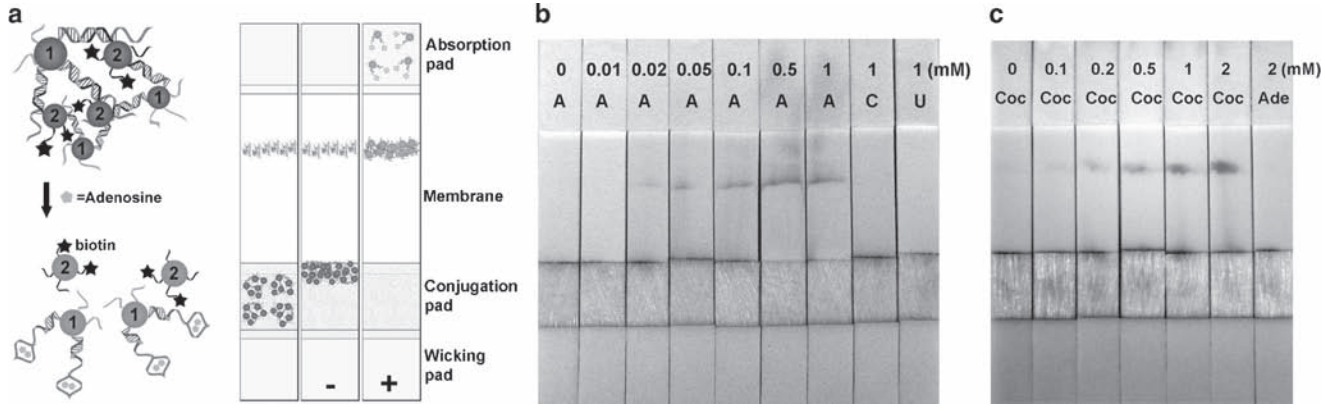

Fig. 6.9 Aptamer- and Au NP-based lateral flow device. (**a**) *Left*: adenosine-induced disassembly of nanoparticle aggregates into red-colored dispersed nanoparticles. Biotin is denoted as a *black star. Right*: lateral flow devices loaded with the Au NP aggregates (on the conjugation pad) and streptavidin (on the membrane in cyan) before use (*left strip*), in a negative (*middle strip*), or a positive (*right strip*) test. (**b**) Adenosine-sensing lateral flow device with varying concentrations of nucleosides. *A*, adenosine; *C*, cytidine; *U*, uridine. (**c**) Cocaine lateral flow device with varying concentrations of cocaine in undiluted human blood serum. *Coc*, cocaine; *Ade*, adenosine (Reproduced with permission from ref. 79. Copyright © [2006] Wiley)

sine concentrations, more intense red bands were observed, and the detection limit was ~20 μM. For the other ribonucleosides, no red bands were observed with 1 mM cytidine or uridine, suggesting that the high selectivity of the aptamer was maintained. Similarly, cocaine-sensitive strips were also prepared and the possibility of using such devices to detect analytes in human blood serum was tested. Cocaine was spiked into untreated serum, and 10 μL of serum samples was added to the conjugation pads directly to rehydrate and react with the nanoparticle aggregates. After 20 s, the wicking pad part of the device was dipped into a running buffer. As can be observed from Fig. 6.9c, a distinct red line can be observed when the serum contained 0.2 mM cocaine, and the color intensity increased with increasing cocaine concentration, while adenosine failed to produce a red line. These results demonstrate that the device is compatible with biological samples, making applications in medical diagnostics possible.

6.7 Conclusions and Outlook

In conclusion, incorporation of inorganic nanoparticles into functional nucleic acid (DNAzyme, aptamer, and aptazyme) has proven to be a useful method to design highly sensitive and selective colorimetric and fluorescent sensors. Because nucleic acids can be selected for essentially any target molecule of choice, the methods of sensor design described in this chapter should be applicable to the detection of many other analytes of interest. Future work in this area can be focused on increasing sensor sensitivity, selectivity, stability, and user-friendliness. These improvements can be achieved by performing detailed characterizations to understand nucleic acid and nanoparticle interactions, introducing signal amplification mechanisms, and introducing novel sensing platforms such as lateral flow devices.

Acknowledgments We thank other Lu group members for helpful discussions and Ms. Natasha Yeung for proofreading the chapter. The Lu group research described in this chapter has been generously supported by the U.S. Department of Energy, National Science Foundation, Department of Defense, Department of Housing and Urban Development, and National Institute of Health.

References

1. Kruger, K., Grabowski, P.J., Zaug, A.J., Sands, J., Gottschling, D.E. and Cech, T.R. (1982) Self-splicing RNA: autoexcision and autocyclization of the ribosomal RNA intervening sequence of tetrahymena. Cell 31:147–157.
2. Guerrier-Takada, C., Gardiner, K., Marsh, T., Pace, N. and Altman, S. (1983) The RNA moiety of ribonuclease p is the catalytic subunit of the enzyme. Cell 35:849–857.
3. Winkler, W., Nahvi, A. and Breaker, R.R. (2002) Thiamine derivatives bind messenger RNAs directly to regulate bacterial gene expression. Nature (Lond.) 419:952–956.

4. Breaker, R.R. (2004) Natural and engineered nucleic acids as tools to explore biology. Nature (Lond.) 432:838.
5. Breaker, R.R. and Joyce, G.F. (1994) A DNA enzyme that cleaves RNA. Chem. Biol. 1: 223–229.
6. Tuerk, C. and Gold, L. (1990) Systematic evolution of ligands by exponential enrichment: RNA ligands to bacteriophage t4 DNA polymerase. Science 249:505–510.
7. Ellington, A.D. and Szostak, J.W. (1990) In vitro selection of RNA molecules that bind specific ligands. Nature (Lond.) 346:818–822.
8. Wilson, D.S. and Szostak, J.W. (1999) In vitro selection of functional nucleic acids. Annu. Rev. Biochem. 68:611–647.
9. Jayasena, S.D. (1999) Aptamers: an emerging class of molecules that rival antibodies in diagnostics. Clin. Chem. 45:1628–1650.
10. Tang, J. and Breaker, R.R. (1997) Rational design of allosteric ribozymes. Chem. Biol. 4: 453–459.
11. Lu, Y. (2002) New transition metal-dependent DNAzymes as efficient endonucleases and as selective metal biosensors. Chem. Eur. J. 8:4588–4596.
12. Osborne, S.E. and Ellington, A.D. (1997) Nucleic acid selection and the challenge of combinatorial chemistry. Chem. Rev. 97:349–370.
13. Breaker, R.R. (1997) In vitro selection of catalytic polynucleotides. Chem. Rev. 97:371–390.
14. Sen, D. and Geyer, C.R. (1998) DNA enzymes. Curr. Opin. Chem. Biol. 2:680–687.
15. Famulok, M. and Jenne, A. (1999) Catalysis based on nucleic acid structures. Top. Curr. Chem. 202:101–131.
16. Joyce, G.F. (2004) Directed evolution of nucleic acid enzymes. Annu. Rev. Biochem. 73: 791–836.
17. Achenbach, J.C., Chiuman, W., Cruz, R.P.G. and Li, Y. (2004) DNAzymes: from creation in vitro to application in vivo. Curr. Pharm. Biotechnol. 5:312–336.
18. Silverman, S.K. (2005) In vitro selection, characterization, and application of deoxyribozymes that cleave RNA. Nucleic Acids Res. 33:6151–6163.
19. Bruesehoff, P.J., Li, J., Augustine, A.J. and Lu, Y. (2002) Improving metal ion specificity during in vitro selection of catalytic DNA. Comb. Chem. High Throughput Screen. 5:327–335.
20. Stojanovic, M.N. and Landry, D.W. (2002) Aptamer-based colorimetric probe for cocaine. J. Am. Chem. Soc. 124:9678–9679.
21. Yguerabide, J. and Yguerabide, E.E. (1998) Light-scattering submicroscopic particles as highly fluorescent analogs and their use as tracer labels in clinical and biological applications. I. Theory. Anal. Biochem. 262:137–156.
22. Bohren, C.F. and Huffman, D.R. (1993) Absorption and scattering of light by small particles. Wiley, New York.
23. Jin, R., Wu, G., Li, Z., Mirkin, C.A. and Schatz, G.C. (2003) What controls the melting properties of DNA-linked gold nanoparticle assemblies? J. Am. Chem. Soc. 125:1643–1654.
24. Mirkin, C.A., Letsinger, R.L., Mucic, R.C. and Storhoff, J.J. (1996) A DNA-based method for rationally assembling nanoparticles into macroscopic materials. Nature (Lond.) 382:607–609.
25. Elghanian, R., Storhoff, J.J., Mucic, R.C., Letsinger, R.L. and Mirkin, C.A. (1997) Selective colorimetric detection of polynucleotides based on the distance-dependent optical properties of gold nanoparticles. Science 277:1078–1080.
26. Rosi, N.L. and Mirkin, C.A. (2005) Nanostructures in biodiagnostics. Chem. Rev. 105: 1547–1562.
27. Han, M., Gao, X., Su, J.Z. and Nie, S. (2001) Quantum-dot-tagged microbeads for multiplexed optical coding of biomolecules. Nat. Biotechnol. 19:631–635.
28. Alivisatos, A.P., Gu, W. and Larabell, C. (2005) Quantum dots as cellular probes. Annu. Rev. Biomed. Eng. 7:55–76.
29. Medintz, I.L., Uyeda, H.T., Goldman, E.R. and Mattoussi, H. (2005) Quantum dot bioconjugates for imaging, labelling and sensing. Nat. Mater. 4:435–446.

30. Li, J., Zheng, W., Kwon, A.H. and Lu, Y. (2000) In vitro selection and characterization of a highly efficient Zn(ii)-dependent RNA-cleaving deoxyribozyme. Nucleic Acids Res. 28: 481–488.
31. Santoro, S.W., Joyce, G.F., Sakthivel, K., Gramatikova, S. and Barbas, C.F., III. (2000) RNA cleavage by a DNA enzyme with extended chemical functionality. J. Am. Chem. Soc. 122: 2433–2439.
32. Carmi, N., Shultz, L.A. and Breaker, R.R. (1996) In vitro selection of self-cleaving DNAs. Chem. Biol. 3:1039–1046.
33. Carmi, N., Balkhi, H.R. and Breaker, R.R. (1998) Cleaving DNA with DNA. Proc. Natl. Acad. Sci. USA 95:2233–2237.
34. Mei, S.H.J., Liu, Z., Brennan, J.D. and Li, Y. (2003) An efficient RNA-cleaving DNA enzyme that synchronizes catalysis with fluorescence signaling. J. Am. Chem. Soc. 125:412–420.
35. Liu, J., Brown, A.K., Meng, X., Cropek, D.M., Istok, J.D., Watson, D.B. and Lu, Y. (2007) A catalytic beacon sensor for uranium with parts-per-trillion sensitivity and million-fold selectivity. Proc. Natl. Acad. Sci. USA 104:2056.
36. Brown, A.K., Li, J., Pavot, C.M.B. and Lu, Y. (2003) A lead-dependent DNAzyme with a two-step mechanism. Biochemistry 42:7152–7161.
37. Liu, J. and Lu, Y. (2003) A colorimetric lead biosensor using DNAzyme-directed assembly of gold nanoparticles. J. Am. Chem. Soc. 125:6642–6643.
38. Liu, J. and Lu, Y. (2004) Optimization of a Pb^{2+}-directed gold nanoparticle/DNAzyme assembly and its application as a colorimetric biosensor for Pb^{2+}. Chem. Mater. 16:3231–3238.
39. Liu, J. and Lu, Y. (2004) Accelerated color change of gold nanoparticles assembled by DNAzymes for simple and fast colorimetric Pb^{2+} detection. J. Am. Chem. Soc. 126: 12298–12305.
40. Storhoff, J.J., Lazarides, A.A., Mucic, R.C., Mirkin, C.A., Letsinger, R.L. and Schatz, G.C. (2000) What controls the optical properties of DNA-linked gold nanoparticle assemblies? J. Am. Chem. Soc. 122:4640–4650.
41. Liu, J. and Lu, Y. (2005) Stimuli-responsive disassembly of nanoparticle aggregates for light-up colorimetric sensing. J. Am. Chem. Soc. 127:12677–12683.
42. Liu, J. and Lu, Y. (2006) Design of asymmetric DNAzymes for dynamic control of nanoparticle aggregation states in response to chemical stimuli. Org. Biomol. Chem. 4:3435–3441.
43. Geyer, C.R. and Sen, D. (1997) Evidence for the metal-cofactor independence of an RNA phosphodiester-cleaving DNA enzyme. Chem. Biol. 4:579–593.
44. Roth, A. and Breaker, R.R. (1998) An amino acid as a cofactor for a catalytic polynucleotide. Proc. Natl. Acad. Sci. USA 95:6027–6031.
45. Breaker, R.R. (2002) Engineered allosteric ribozymes as biosensor components. Curr. Opin. Biotechnol. 13:31–39.
46. Wang, D.Y., Lai, B.H.Y. and Sen, D. (2002) A general strategy for effector-mediated control of RNA-cleaving ribozymes and DNA enzymes. J. Mol. Biol. 318:33–43.
47. Huizenga, D.E. and Szostak, J.W. (1995) A DNA aptamer that binds adenosine and ATP. Biochemistry 34:656–665.
48. Liu, J. and Lu, Y. (2004) Adenosine-dependent assembly of aptazyme-functionalized gold nanoparticles and its application as a colorimetric biosensor. Anal. Chem. 76:1627–1632.
49. Ho, H.-A. and Leclerc, M. (2004) Optical sensors based on hybrid aptamer/conjugated polymer complexes. J. Am. Chem. Soc. 126:1384–1387.
50. Ho, H.-A., Bera-Aberem, M. and Leclerc, M. (2005) Optical sensors based on hybrid DNA/conjugated polymer complexes. Chem. Eur. J 11:1718–1724.
51. Dore, K., Dubus, S., Ho, H.-A., Levesque, I., Brunette, M., Corbeil, G., Boissinot, M., Boivin, G., Bergeron, M.G., Boudreau, D. and Leclerc, M. (2004) Fluorescent polymeric transducer for the rapid, simple, and specific detection of nucleic acids at the zeptomole level. J. Am. Chem. Soc. 126:4240–4244.
52. Pavlov, V., Xiao, Y., Shlyahovsky, B. and Willner, I. (2004) Aptamer-functionalized Au nanoparticles for the amplified optical detection of thrombin. J. Am. Chem. Soc. 126:11768–11769.

53. Padmanabhan, K., Padmanabhan, K.P., Ferrara, J.D., Sadler, J.E. and Tulinsky, A. (1993) The structure of a-thrombin inhibited by a 15-mer single-stranded DNA aptamer. J. Biol. Chem. 268:17651–17654.
54. Huang, C.-C., Huang, Y.-F., Cao, Z., Tan, W. and Chang, H.-T. (2005) Aptamer-modified gold nanoparticles for colorimetric determination of platelet-derived growth factors and their receptors. Anal. Chem. 77:5735–5741.
55. Liu, J. and Lu, Y. (2006) Fast colorimetric sensing of adenosine and cocaine based on a general sensor design involving aptamers and nanoparticles. Angew. Chem. Int. Ed. 45:90–94.
56. Nutiu, R. and Li, Y. (2003) Structure-switching signaling aptamers. J. Am. Chem. Soc. 125: 4771–4778.
57. Nutiu, R., Mei, S., Liu, Z. and Li, Y. (2004) Engineering DNA aptamers and DNA enzymes with fluorescence-signaling properties. Pure Appl. Chem. 76:1547–1561.
58. Nutiu, R. and Li, Y. (2004) Structure-switching signaling aptamers: transducing molecular recognition into fluorescence signaling. Chem. Eur. J. 10:1868–1876.
59. Nutiu, R. and Li, Y. (2005) In vitro selection of structure-switching signaling aptamers. Angew. Chem. Int. Ed. 44:1061–1065; S1061/1–S1061/3.
60. Nutiu, R. and Li, Y. (2005) Aptamers with fluorescence-signaling properties. Methods 37:16–25.
61. Liu, J. and Lu, Y. (2006) Smart nanomaterials responsive to multiple chemical stimuli with controllable cooperativity. Adv. Mater. 18:1667–1671.
62. Levy, M., Cater, S.F. and Ellington, A.D. (2005) Quantum-dot aptamer beacons for the detection of proteins. ChemBioChem 6:2163–2166.
63. Choi, J.H., Chen, K.H. and Strano, M.S. (2006) Aptamer-capped nanocrystal quantum dots: a new method for label-free protein detection. J. Am. Chem. Soc. 128:15584–15585.
64. Dwarakanath, S., Bruno, J.G., Shastry, A., Phillips, T., John, A.A., Kumar, A. and Stephenson, L.D. (2004) Quantum dot-antibody and aptamer conjugates shift fluorescence upon binding bacteria. Biochem. Biophys. Res. Commun. 325:739–743.
65. Shieh, F., Lavery, L., Chu, C.T., Richards-Kortum, R., Ellington, A.D. and Korgel, B.A. (2005) Semiconductor nanocrystal-aptamer bioconjugate probes for specific prostate carcinoma cell targeting. Proc. SPIE (Int. Soc. Opt. Eng.) 5705:159–165.
66. Chu, T.C., Shieh, F., Lavery, L.A., Levy, M., Richards-Kortum, R., Korgel, B.A. and Ellington, A.D. (2006) Labeling tumor cells with fluorescent nanocrystal-aptamer bioconjugates. Biosens. Bioelectron. 21:1859–1866.
67. Mitchell, G.P., Mirkin, C.A. and Letsinger, R.L. (1999) Programmed assembly of DNA functionalized quantum dots. J. Am. Chem. Soc. 121:8122–8123.
68. Gueroui, Z. and Libchaber, A. (2004) Single-molecule measurements of gold-quenched quantum dots. Phys. Rev. Lett. 93:166108/1–166108/4.
69. Wargnier, R., Baranov, A.V., Maslov, V.G., Stsiapura, V., Artemyev, M., Pluot, M., Sukhanova, A. and Nabiev, I. (2004) Energy transfer in aqueous solutions of oppositely charged CdSe/ZnS core/shell quantum dots and in quantum dot-nanogold assemblies. Nano Lett. 4:451–457.
70. Oh, E., Hong, M.-Y., Lee, D., Nam, S.-H., Yoon, H.C. and Kim, H.-S. (2005) Inhibition assay of biomolecules based on fluorescence resonance energy transfer (FRET) between quantum dots and gold nanoparticles. J. Am. Chem. Soc. 127:3270–3271.
71. Dyadyusha, L., Yin, H., Jaiswal, S., Brown, T., Baumberg, J.J., Booy, F.P. and Melvin, T. (2005) Quenching of CdSe quantum dot emission, a new approach for biosensing. Chem. Commun. 25:3201–3203.
72. Sato, K., Hosokawa, K. and Maeda, M. (2003) Rapid aggregation of gold nanoparticles induced by non-cross-linking DNA hybridization. J. Am. Chem. Soc. 125:8102–8103.
73. Zhao, W., Chiuman, W., Brook, M.A. and Li, Y. (2007) Simple and rapid colorimetric biosensors based on DNA aptamer and noncrosslinking gold nanoparticle aggregation. ChemBioChem 8:727–731.
74. Li, H. and Rothberg, L. (2004) Colorimetric detection of DNA sequences based on electrostatic interactions with unmodified gold nanoparticles. Proc. Natl. Acad. Sci. USA 101: 14036–14039.

75. Li, H. and Rothberg, L.J. (2004) Label-free colorimetric detection of specific sequences in genomic DNA amplified by the polymerase chain reaction. J. Am. Chem. Soc. 126: 10958–10961.
76. Li, H. and Rothberg, L.J. (2004) DNA sequence detection using selective fluorescence quenching of tagged oligonucleotide probes by gold nanoparticles. Anal. Chem. 76:5414–5417.
77. Wang, L., Liu, X., Hu, X., Song, S. and Fan, C. (2006) Unmodified gold nanoparticles as a colorimetric probe for potassium DNA aptamers. Chem. Commun. 28:3780–3782.
78. Glynou, K., Ioannou, P.C., Christopoulos, T.K. and Syriopoulou, V. (2003) Oligonucleotide-functionalized gold nanoparticles as probes in a dry-reagent strip biosensor for DNA analysis by hybridization. Anal. Chem. 75:4155–4160.
79. Liu, J., Mazumdar, D. and Lu, Y. (2006) A simple and sensitive "dipstick" test in serum based on lateral flow separation of aptamer-linked nanostructures. Angew. Chem. Int. Ed. 45: 7955–7959.
80. Famulok, M. and Mayer, G. (2006) Chemical biology: aptamers in nanoland. Nature (Lond.) 439:666–669.

Chapter 7
Electrochemical Approaches to Aptamer-Based Sensing

Yi Xiao and Kevin W. Plaxco

Abstract Motivated by the potential convenience of electronic detection, a wide range of electrochemical, aptamer-based sensors have been reported since the first was described only in 2005. Although many of these are simply electrochemical, aptamer-based equivalents of traditional immunochemical approaches (e.g., sandwich and competition assays employing electroactive signaling moieties), others exploit the unusual physical properties of aptamers, properties that render them uniquely well suited for application to impedance and folding-based electrochemical sensors. In particular, the ability of electrode-bound aptamers to undergo reversible, binding-induced folding provides a robust, reagentless means of transducing target binding into an electronic signal that is largely impervious to nonspecific signals arising from contaminants. This capability enables the direct detection of specific proteins at physiologically relevant, picomolar concentrations in blood serum and other complex, contaminant-ridden sample matrices.

7.1 Introduction

The potential applications of aptamers to molecular sensing are readily apparent.[1–6] It was thus not a surprise when, within a decade after the first description of aptamers, a wide range of optical, aptamer-based sensors had been reported (reviewed in Chapters 4–6). Unfortunately, however, while convenient to implement (and thus first-out-of-the-box), optical methods suffer from a number of potential drawbacks, including false-positive signals arising from contaminating fluorophores

Yi Xiao
Department of Physics, Materials Department, Department of Chemistry and Biochemistry, University of California, Santa Barbara
yixiao@physics.ucsb.edu

K.W. Plaxco
Department of Chemistry and Biochemistry,
Interdepartmental program in Biomolecular Science and Engineering,
University of California, Santa Barbara
kwp@chem.ucsb.edu

Y. Li and Y. Lu (eds.), *Functional Nucleic Acids for Analytical Applications*,

or quenchers and a requirement for sophisticated, often bulky optical instrumentation. Electrochemical methods, in contrast, potentially benefit from the relative paucity of electroactive contaminants, the relative stability and environmental insensitivity of electroactive labels, and the impressive miniaturization of modern microelectronics.[7–12] They thus offer solutions to some of the problems that have hindered optical approaches, particularly in applications involving complex, contaminant-ridden samples. Here we discuss recent advances in electrochemical aptasensors (aptamer-based sensors) in light of these potential advantages.

Because electrochemistry implies interrogation via an electrode, electrochemical devices are fundamentally heterogeneous; the sensing "action" takes place at an interface. The type of action occurring at this surface allows us to separate electrochemical biosensors into three broad classes. The first class of electrochemical aptasensors that we discuss are sandwich- and competition-type assays in which an electrode-bound aptamer is used to bring a complex composed of the target and some redox-active species to the electrode, or remove a preformed target–redox complex from the electrode. These sensors are, in effect, electrochemistry-and-aptamer analogues of well-established immunochemical approaches. The second class of electrochemical aptamer sensors are those based on *generically* detecting targets adsorbed to an aptamer-modified electrode surface using electrochemical impedance spectroscopy, an approach that was also pioneered with immunochemical sensors, albeit with perhaps limited success. The final broad class of electrochemical aptasensor involves the use of electrochemistry to monitor binding-specific conformational changes in an electrode-bound aptamer. This class of electrochemical aptasensors, for which no antibody-based analogue has been reported, appears to offer particular promise with regard to rapid, reagent-less detection under realistically complex, "real-world" conditions.

The metrics with which one judges the success of a sensor, which include sensitivity, selectivity, generality, response time, and operational convenience, are easy to define and relatively objective.[13,14] Using these criteria, we attempt to provide a *critical* review of the electrochemical aptasensor literature. We note, however, that "relatively objective" is a key phrase; although ostensibly objective, the metrics used to describe detection limits, for example, vary dramatically from author to author, rendering discussion of reported detection limits an apples-and-oranges comparison at best, and substantially misleading at worst. We thus adopt here the convention of reporting the lowest target concentration *actually detected* (with apparent or confirmed statistical significance) in the literature under discussion; while this approach, too, suffers from potentially damning laboratory-to-laboratory variations, it appears a more defensible standard than the simple reiteration of reported detection limits based on often wildly differing standards. And while we limit ourselves to discussion of *electrochemical* (as opposed to electronic, electromechanical, or electroacoustic; see ref. 15 for a review and refs. 16–19 for specific examples) aptamer-based approaches, we also attempt an exhaustive review of this specific subfield. To this end we also note that, while the electrochemical aptasensor literature is expanding rapidly, the field is very young: fewer than two dozen electrochemical aptasensor papers have appeared in the literature since O'Sullivan and coworkers[20] published the first in 2005, and those have been directed against only a handful of distinct targets.

7.2 Sandwich or Competition-Based Electrochemical Techniques

A range of antibody-based electrochemical sensors have been described to date that have been, more or less, recapitulated using aptamers; these include electrochemical sandwich assays reminiscent of the exceedingly well-established ELISA (enzyme-linked immunosorbent assay) approach. A second, related aptasensor architecture is the competition assay in which unlabeled target molecules compete with exogenously added, redox-labeled target molecules for a limited number of binding sites on the sensing electrode.

Immunochemical sandwich assays are among the most frequently employed clinical testing approaches in use today. In one implementation of this approach, a surface-immobilized antibody binds to the target molecule, which is subsequently "labeled" using a second antibody (often this labeling occurs before binding to the immobilized antibody, but the order of the events is of little relevance to our discussion) that has, in turn, been (directly or indirectly) modified with an enzyme producing a colorimetric or fluorescent signal.[21–24] More recently, this approach has been adapted to electrochemical detection by immobilizing the first antibody on an electrode and modifying the second with an inorganic or biochemical "electrocatalyst" that produces a small-molecule redox mediator (such as H_2O_2) which transfers electrons to or from this surface.[25–27] This action produces an increase in current (called the Faradic current to distinguish it from currents arising due to capacitance) when the potential on the electrode reaches a voltage sufficient to support the transfer of electrons from or to the redox mediator.

Perhaps not surprisingly, several groups have adapted aptamers to such sandwich approaches (Fig. 7.1). In the first of these, Sode and coworkers exploited the

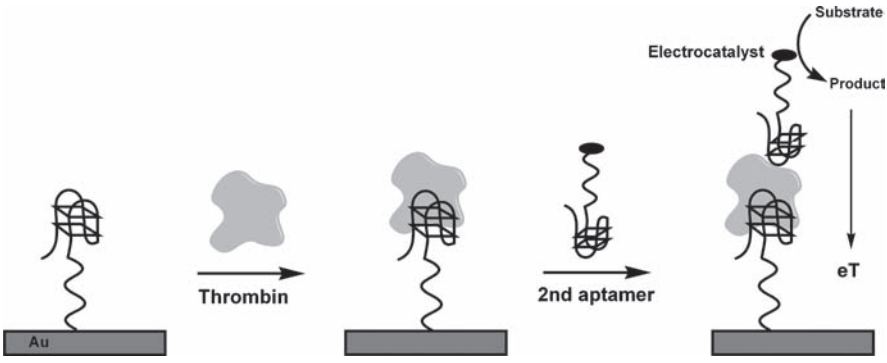

Fig. 7.1 Some protein targets exhibit more than one high-affinity aptamer-binding site. Such proteins are readily detected using sandwich assays in which one binding site (and its cognate aptamers) is used to direct the target to the electrode surface and a second is used to affix an electroactive label.[28,30] Such labels are usually electrocatalysts, such as horseradish peroxidase (HRP), that produce multiple molecules of a redox-active product per binding event, thus amplifying the electrochemical signal

fact that two distinct aptamers are available the protein thrombin, binding to two nonoverlapping sites on the protein. Using the one aptamer to immobilize the target to the electrode and a second to label the target with the electrocatalyst glucose dehydrogenase, they report a thrombin detection limit of just 10 nM, approximately threefold below the dissociation constant of the lower affinity of the two aptamers employed in the sandwich.[28] More recently, two groups have reported sandwich sensors based on the surprising fact that the 15-base antithrombin aptamer of Bock et al.[29] binds to two, nonidentical, nonoverlapping sites on the protein. Thus, this single aptamer sequence can be employed both to adsorb the target to the electrode (using a surface-immobilized variant of the aptamer) and as a secondary reagent with which to label the bound target with an electrocatalyst. Using horseradish peroxidase (HRP) as the electrocatalyst and an osmium-based mediator, Katakis and coworkers[30] report a thrombin detection limit of 80 nM, approximately three times higher than the 26-nM dissociation constant of the Bock aptamer. In a parallel study, Willner and coworkers used platinum nanocrystals on the secondary aptamer as electrocatalysts to reduce hydrogen peroxide and transfer electrons directly from the electrode.[31] Using this approach they report thrombin detection at an impressive 1 nM, which is more than 25-fold below the aptamer solution-phase dissociation constant.[29]

While their operational convenience may suffer (they are inherently slow, multi-step batch processes), the sensitivity and selectivity of electrocatalytic sandwich assays should, in theory, be excellent. For example, the catalytic production of redox mediators by the electrocatalysts means that multiple electrons are produced for each binding event, which can give rise to significant signal amplification. Unfortunately, however, the high sensitivity potentially on offer appears difficult to achieve in practice: only the Willner group has reported a sandwich assay detection limit more than a factor of three below the dissociation constant of the aptamer employed.[30] Sandwich assays should also achieve excellent specificity, provided that the electroactive label (or its associated aptamer) does not adhere to either the electrode or to any contaminants nonspecifically bound to the electrode. Whether this can be achieved in practice, however, is difficult to judge as only very limited studies of this issue have been reported in the afore-described literature: Katakis and coworkers report only that "the assay as designed suffered from significant nonspecific adsorption of HRP labeled aptamer,"[30] Willner and coworkers report, as data not shown, only that "no electrocatalytic current was observed with control samples without thrombin or a control sample that included 1 μM BSA (bovine serum albumin),"[30] and Sode and coworkers report that no increase in current was observed "for the electrode onto which (1 μM) BSA was released."[28] Given that physiological serum albumin levels are approximately 600 times higher than the concentration employed by the latter two groups,[32,33] it is difficult to judge whether aptamer sandwich assays will live up to their potential promise and allow for the direct detection of specific proteins in, for example, blood serum.

The generality of aptamer-based sandwich approaches also remains an open question: it is not clear how many proteins share thrombin's property of exhibiting multiple, high-affinity aptamer-binding sites. Two potential solutions to this problem,

however, have been reported. In the first, Katakis and coworkers[30] have dispensed with the immobilized aptamer by instead chemi-adsorbing the target protein directly onto the electrode. They then produce an electrochemical signal by incubating the adsorbed target with the Bock antithrombin aptamer modified with the electrocatalyst HRP, achieving a reported detection limit of 3.5 nM. The approach, however, is significantly hindered by nonspecific adsorption of the modified aptamer: despite efforts to passivate the sensing electrode, the background current observed in the absence of target is nearly half that observed in the presence of target. Evtugyn and coworkers[34] have, in contrast, maintained the primary aptamer (responsible for surface adsorption) and instead replaced the secondary aptamer with the simple, redox-active dye methylene blue. Because methylene blue itself binds thrombin (and, reportedly, to proteins in general), they are able to detect the protein at concentrations as low as 28.5 nM. Unfortunately, however, methylene blue also binds to the aptamer-modified electrode in the absence of thrombin and, presumably, to any target protein molecules that absorb nonspecifically to the sensor surface. This binding leads to high background currents and significantly degraded selectivity; the sensor responses to mixed IgGs and human serum albumin, for example, are fully one-half and one-quarter, respectively of those observed at the same concentration of thrombin.[34]

A second, commonly employed immunochemical approach is the competition or displacement assay in which authentic target molecules compete with exogenously added, artificially labeled target molecules for specific binding sites on the sensor surface (Fig. 7.2). To date, two groups have developed electrochemical aptasensors based on this approach. In the first, O'Sullivan and coworkers measured thrombin at concentrations down to 5 nM via competition between horseradish peroxidase (HRP) modified thrombin and unlabeled target molecules in the sample.[20] More recently Collins and coworkers have developed a "two-color" aptamer-based competition assay

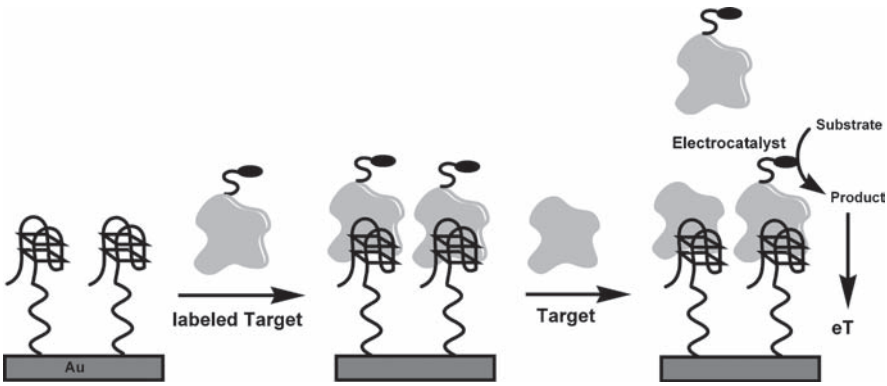

Fig. 7.2 Competition (or displacement) assays monitor the presence of their target by measuring the extent to which target molecules in a sample displace labeled-target molecules previously bound to the sensor surface. To date, two groups have adapted aptamer recognition elements and electrochemical detection to this well-established approach

employing antithrombin and antilysozyme aptamers as recognition elements and cadmium sulfide- and lead sulfide-modified thrombin and lysozyme as the labeled reagents.[35] In this approach, the amount of each sulfide retained, which provides a measure of the concentration of the unmodified target present, is determined by first removing and solubilizing the sulfides (via acid wash and extensive sonication) before quantification via electrochemical stripping detection. The detection limits of this approach appear to be an impressive 0.5 pM, and no significant signal is observed when the sensor is treated with either BSA or IgG at concentrations a million times the detection limit. Likewise, the operational convenience of being able to simultaneously monitor two targets is to be applauded. This said, the approach, like all competition approaches, is a cumbersome batch process that is, in this case, rather slow (>1 h).

Sandwich and competition aptasensor approaches closely parallel the equivalent, well-established antibody-based technologies. This has advantages: although reagent intensive and somewhat cumbersome, these approaches have been optimized to the extreme for antibody-based sensing and are sensitive, robust, and, in their automated forms, exceedingly cost-effective. This said, it is not clear to the authors of this review that aptamers provide significant advantages over antibodies for such applications; this is all the more true when one considers the potential limitations of aptamers (e.g., the paucity of targets exhibiting two distinct aptamer-binding sites). In contrast, aptamers appear significantly better suited than antibodies for use in the next class of sensors that we discuss, a class of sensors that is also more rapid and more operationally convenient than the above-described, direct analogues of existing immunochemical techniques.

7.3 Impedance-Based Electrochemical Aptasensors

A second, generic approach to electrochemical aptasensors is based on a presumably rather general means of monitoring the adsorption of macromolecules onto an electrode surface. Electrochemistry can be performed using alternating current (AC), but under these conditions the approach is rendered dependent on the rate with which the redox species can diffuse to the electrode surface. A significant reduction in redox current will be observed as the AC frequency is increased beyond the rate with which the redox moiety reaches the electrode surface. Any process that inhibits the accessibility of the electrode surface will, under these circumstances, produce a frequency-dependent phase lag between the AC voltage and the observed current. Such a phase lag is analogous to that produced by an electronic circuit exhibiting significant "impedance," and thus AC voltammetric measurements of this effect are often called electrochemical (or faradic) impedance spectroscopy. If diffusion of the redox mediator is modulated when a target molecule binds to the electrode, the resulting impedance changes (as measured by the interfacial resistance) provide a ready means of monitoring the binding event (Fig. 7.3).

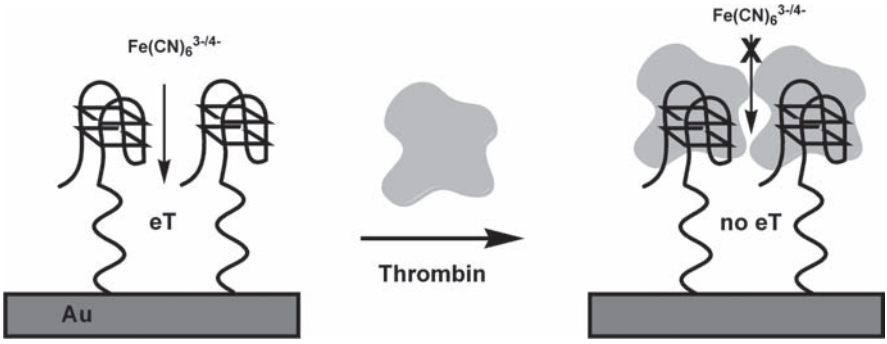

Fig. 7.3 The binding of a macromolecule to the surface of an aptamer-covered electrode will affect the rate at which a small redox mediator diffuses to the electrode surface. This changes the interfacial resistance, which, in turn, provides a ready means of measuring the concentration of bound target via impedance spectroscopy (see text). In general the binding of a macromolecule to such a sensor reduces electron transfer (*eT*), as shown here.[43–45,47] In some cases, however, target binding leads to an increase in electron transfer,[46] presumably because the target partially counteracts the dense negative charge of the aptamer layer and thus enhances the rate with which a negatively charged mediator diffuses to the electrode

Impedance spectroscopy has been employed in a number of antibody-based sensors[36–41] and, more recently, in aptamer-based sensing applications. In contrast to the limited advantages that aptamers appear to provide in competition and sandwich assays, they appear to provide two significant advantages for the fabrication of impedance-based sensors: First, the relatively small size of a typical aptamer can, at least in theory, lead to much larger changes in relative impedance than occurs when a relatively large antibody binds to the equivalent target[42] (but see ref. 43 for a counterexample). Second, it appears that the homogeneous negative charge of the aptamer repels negatively charged mediators, such as commonly employed ferrocyanide [$Fe(CN)_6^{-3/-4}$], providing an alternative mechanism by which binding can modulate the interfacial resistance via changes in the net charge on the electrode surface. Motivated by these potential advantages, several groups have reported impedance- or impedance-like aptasensors, including sensors directed against the proteins thrombin,[44–46] IgE,[42] and lysozyme.[47] The reported detection limits of these sensors generally range from 1 μM to 0.1 nM, and the sensors are reasonably rapid (the equilibration times required to achieve these detection limits are typically 10–90 min). Of note, the lower end of the detection limit range represents concentration more than two orders of magnitude lower than the dissociation constant of the employed aptamers (e.g., 0.1 nM detection limit[45] obtained using the Bock antithrombin aptamer, for which the dissociation constant is 26 nM[29]). The detection of sub-K_D target concentrations corresponds to the detection of submonolayer adsorption on the sensor surface, which is certainly possible given that an increasing interfacial resistance requires only that transport of the mediator is impeded, not abolished. Nevertheless, the robust detection of such significantly submonolayer adsorption is surprising to the authors of this review. An even more

extreme example of this is provided by the work of Xu and coworkers, who claim a sub-100 *femto*molar (fM) detection limit for native thrombin and an even more impressive 10 fM detection limit when the protein is denatured (and thus expanded) using guanidine hydrochloride after it is bound to the recognition aptamer.[48] No explanation is provided (or apparent to the authors of this review), however, as to how the limited occupancy expected to arise due to specific binding at a target concentration *millions* of times lower than the aptamer dissociation constant could produce the large changes in impedance reported in this work. Given our inability to imagine a plausible mechanism by which specific binding could lead to such an effect we are, unfortunately, disinclined to believe these extraordinary claims.

The requirement of impedance sensors that target binding significantly increases molecular crowding on the electrode surface has historically precluded the development of both antibody- and aptamer-based impedance sensors directed against small-molecule targets. Recently, however, two methods have been described by which this difficulty can be overcome using aptamers. In the first, Radi and O'Sullivan folded aptamers into a compact, G-quadruplex structure in the presence of potassium ions.[49] This folding is associated with a large, rapid increase in interfacial resistance, allowing for the detection of as little as 0.1 mM of the target. As a demonstration of the second approach, Willner and coworkers developed an impedance aptasensor against the small-molecule AMP.[50] To do so they fabricated a sensor comprised of an AMP-binding aptamer and a short, complementary DNA sequence (Fig. 7.4). During sensor fabrication, both DNA molecules are present and the aptamer adopts a nonbinding, double-stranded conformation. Because the target nucleotide only binds to the folded, native state of the aptamer, the target drives the aptamer into its folded state, releasing the complementary DNA. The loss of bulky, negatively charged complementary DNA, in turn, produces a readily measurable decrease in impedance. Using this approach, the authors achieve an AMP detection limit of 2 μM (after a 4-min incubation) and did not observe any detectable signal from CMP at concentrations as high as 10 mM.

The detection limits and convenience of impedance-based sensors are impressive. We fear, however, they may nevertheless be poorly suited for real-world applications because the same attribute that ensures their generality (signaling requires only adsorption to the sensor surface) may also degrade their selectivity. That is, the adsorption of contaminants to the sensor surface would also impede the transport of the redox mediator, producing a signal that would be difficult to distinguish from that produced by the authentic target.[36,46] Consistent with this argument, the nonspecific adsorption of target molecules to the electrode could account for the significantly subdissociation-constant detection limits reported for some of the impedance aptasensors described above[48] (although the results of control studies with binding-incompetent aptamers indicates this is not a universal problem[45]). We must admit, however, that this concern remains speculative, as the extent to which any impedance-based aptasensor meets the challenge of complex, contaminant-ridden samples has not been reported; even the most detailed studies published to date only report testing the specificity of their sensors using a handful of specific, highly purified proteins as contaminants, and these at concentrations

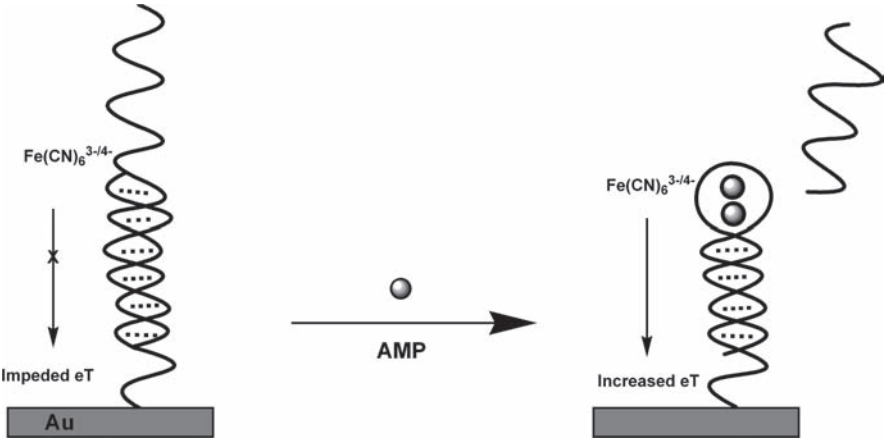

Fig. 7.4 Impedance sensors require that target binding significantly increases molecular crowding on the electrode surface, an issue that has historically precluded the development of impedance sensors directed against small-molecule targets. Recently, however, two methods have been described by which this difficulty can be overcome using aptamers.[48,49] Shown here is the method of Willner and coworkers,[50] who fabricated a sensor composed of an AMP-binding aptamer hybridized to a short, complementary DNA sequence. During sensor fabrication, both DNA molecules are present and the aptamer adopts a non-AMP-binding, double-stranded conformation. Because the target nucleotide only binds to the folded, native state of the aptamer, the target drives the aptamer into its folded state, releasing the complementary DNA. The loss of bulky, negatively charged complementary DNA, in turn, produces a readily measurable decrease in impedance

only four times higher than those of the target molecule.[44,47] Similarly, while sensor reusability would provide further evidence for a specific signaling mechanism (if the observed signals arise due to specific target–aptamer interactions they should be readily reversible, whereas nonspecific interactions between the target and the electrode may well be less so), the regeneration of impedance-based sensors has seen relatively little exploration in the literature.[44] More generally, the demonstration of sensor regeneration is crucial in order to ensure that the observed signal change is not originating from processes unrelated to the target, such as sensor degradation.

7.4 Electrochemical Sensors Based on Target Binding-Induced Aptamer Folding

False signals arising from the nonspecific adsorption of contaminants remain a significant hurdle for adsorption-based biosensors, limiting them to applications involving relatively clean samples and preventing their application in clinical settings (where blood, urine, and other complex, contaminant-ridden samples are the norm). This hurdle is not limited to impedance-based sensors[36] (such as those described here) but also affects sensors based on monitoring changes in index of

refraction[51–53] or on measures of absorbed mass[54–56] or charge.[57–61] A solution to this problem would be to design sensors that, rather than detecting adsorption, detect a binding-specific change in the conformation of the aptamer, an approach that has seen application to the problem of optical aptasensors with the invention of aptamer beacons (reviewed in Chapter 4 and named after an analogous optical DNA sensing strategy).[62–65] Moreover, given the apparent ease with which the property of binding-induced folding can be selected for[66–69] or rationally engineered[70–75] into otherwise well-folded aptamers, aptamers appear even better suited for application in folding-based sensors than do proteins.[76,77]

Binding-induced folding couples target recognition with the least subtle of all possible changes in the physics of the polymer: folding. How, then, to convert this wholesale conformational change into an easily detectable electrochemical signal? To date, three approaches have been described. One of these, based on an increase in impedance that occurs when an electrode-bound aptamer folds, is described above.[44] The other two we describe below.

In contrast to single-stranded oligonucleotides, double-stranded DNA binds to a wide range of intercalators. Exploiting this effect, Bang et al.[78] have produced a folding-based, aptasensor based on a modified version of the thrombin aptamer beacon.[79] The addition of seven bases to the 5′-end of the Bock antithrombin aptamer induces the sequence to adopt an alternative, stem-loop conformation. Target binding converts the stem-loop back into the aptamer functional, G-quadruplex structure, rupturing the double-stranded stem and reducing the oligonucleotide affinity for the redox-active intercalator methylene blue. Target binding is thus signaled by a decrease in Faradaic current arising from bound methylene blue. Rather limited data suggest that the limit of detection for this sensor approaches 11 nM, approximately a factor of 2 below the dissociation constant of the aptamer employed. Almost equally limited data hint that the approach is specific: neither ovalbumin nor β-casein produce significant signals at concentrations ~35 times higher than the thrombin detection limit. This said, Evtugyn and coworkers have argued that many proteins bind methylene blue,[34] which suggests that this approach may be thwarted by the nonspecific adsorption of contaminants. The limited data available regarding the intercalation of redox-active species into folded aptamers (to generate a signal, the intercalator must not bind the folded aptamer) lead to further questions regarding the generality of this approach.

More recently our research group, and the groups of O'Sullivan and Fan, have explored an alternative approach to monitoring the binding-induced folding of aptamers that appears to be both general and largely impervious to the nonspecific adsorption of contaminants. This approach, which we have termed E-AB sensors, is based on the observation that electron-transfer rates are exponentially sensitive to the transfer distance. Because of this the efficiency of transfer from a redox moiety affixed to a surface-immobilized DNA will depend critically on the rate with which the moiety collides with the electrode surface.[80] If the DNA molecule in question is an aptamer that undergoes binding-induced folding, we can expect to see large changes in faradic current at the collision rate is either increased or decreased by the formation of the native structure (Fig. 7.5). To date such folding-based E-AB

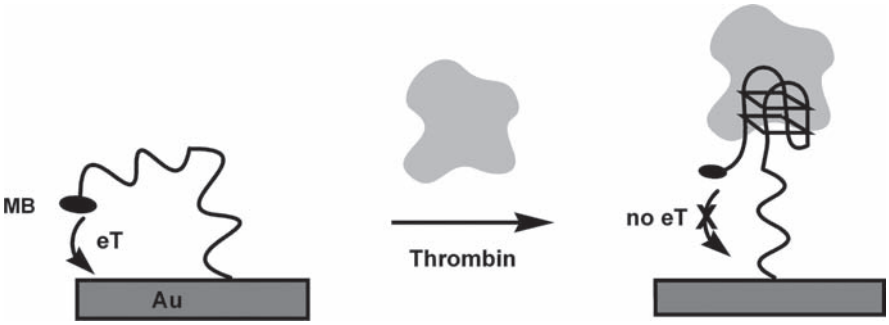

Fig. 7.5 A half-dozen electrochemical sensors have been reported to date based on the binding-induced folding of aptamers.[48,81–88] Shown is a schematic of one of these E-AB (electronic, aptamer-based) sensors, here directed against the protein thrombin. (Reproduced with permission from ref. 81. Copyright Wiley-VCH Verlag GmbH & Co. Kga.) In the absence of thrombin the aptamer is largely unfolded, allowing for frequent collisions between the terminal redox moiety and the electrode. Upon target binding the aptamer folds, reducing the collision rate and, with that, the efficiency of electron transfer. Whether binding-induced folding increases electron transfer (i.e., produces a signal-on sensor[83,85,86]) or, as shown, decreases electron transfer depends on the precise dynamics and structure of the unfolded and bound, folded states[80]

sensors have been reported against a half-dozen targets, including the proteins thrombin and platelet-derived growth factor (PDGF),[81–85] the small-molecules cocaine and AMP,[86,87] and the inorganic ions potassium and lead.[49,88]

The first reported E-AB sensor,[81] which (once again!) was directed against the target thrombin, was composed of a version of the thrombin Bock aptamer that had been modified to undergo binding-induced folding. One end of the modified aptamer was bound to a gold electrode via a six-carbon alkane-thīol, and the opposite terminus was covalently modified with the redox moiety methylene blue. In the absence of target, a large faradic current is observed from the methylene blue. Upon target binding this current is reduced, presumably because the binding-induced folding of the aptamer reduces the rate of collision between the redox moiety and the electrode. The sensor is reagentless (all the signaling components are covalently attached to the electrode), readily reusable (93% signal recovery upon a room temperature wash with 6 M guanidine hydrochloride), and achieves a ~20 nM detection limit, albeit after a 3-h incubation. The sensor is also highly selective; because the sensing mechanism is predicated on a binding-specific conformational change in the aptamer, rather than simple adsorption to the sensor surface; it is almost entirely impervious to the nonspecific binding of contaminants. For this reason, the E-AB sensor is capable of detecting its target even when faced with complex, contaminant-ridden sample matrices such as blood serum.[81]

Closely following the first reported E-AB sensor, O'Sullivan and coworkers described a near-identical discovery.[83,84] Of note, however, despite employing the same core aptamer sequence, the O'Sullivan sensor is signal-on (current increasing upon target binding) rather than the signal-off architecture originally reported by us. This difference represents a potentially significant advance: signal-off sensors

suffer from a number of drawbacks, not the least of which is limited signal gain (at best the target can suppress only 100% of the signal). Consistent with this, the detection limit of the O'Sullivan thrombin sensor is below 5 nM, a significant improvement over the 20 nM achieved by our original, signal-off architecture. The discrepancy between the O'Sullivan signal-on sensor and our signal-off sensor presumably arises from differences in the structure of the aptamer (O'Sullivan's group employed shorter linker sequences), the redox moiety (methylene blue versus ferrocene), or differences in the electrochemical methods employed; the sign of the E-AB signal depends on the relative efficiency of electron transfer in the target-bound or target-free states, which are sensitive functions of all these factors.[80] These issues not withstanding, we have recently demonstrated a means of converting signal-off E-AB sensors into a signal-on architectures via a strand-displacement mechanism (Fig. 7.6) that is, presumably, general. The gain of this signal-on sensor is improved by an order of magnitude over that of our original E-AB thrombin sensor (from a 30% signal suppression at saturation to a 300% signal increase) and concomitantly improves our detection limit by a factor of 7 to just 3 nM.[82]

The E-AB approach appears to be general with, for example, several additional E-AB sensors having been reported in the last year alone.[49,85–87] The first, inspired by an optical aptamer beacon engineered by Stojanovic et al.,[72] achieves a 10 μM detection limit for the small-molecule cocaine and performs well even when challenged with complex, contaminant-ridden media such as pure blood serum and the commonly employed drug-cutting and -masking agents flour, coffee, and mustard.[86] In the second, Radi and O'Sullivan employed the potassium-induced folding of a G-quadruplex aptamer to monitor the presence of this ion at concentrations as low as 0.1 mM.[49] The third new E-AB sensor[85] was directed against the blood protein platelet-derived growth factor (PDGF) and achieves a 50-pM detection limit even when deployed directly in 50% blood serum, and exhibits a sub-10-min equilibration time constant. Finally, Fan and coworkers[87] have described an E-AB sensor

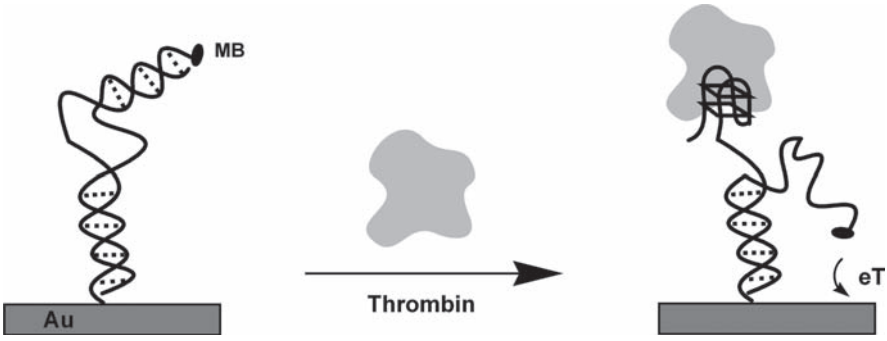

Fig. 7.6 We have recently demonstrated a presumably systematic means of converting signal-off E-AB sensors into signal-on sensors via strand displacement.[82] The relatively low background currents afforded by the unbound, duplex DNA (*left*) lead to high signal gain and, consequently, significant improvements in sensitivity

similar to the strand-displacement impedance sensor of Willner and coworkers[50] that achieves a 10-nM detection limit and works even when challenged with crude cellular extracts. Of note, all these detection limits are several fold below the reported, solution-phase dissociation constants of the aptamers from which these sensors were fabricated.

More recently, the E-AB approach has been expanded to the detection of lead using a DNAzyme rather than a simple aptamer. DNAzymes are catalytic DNA sequences isolated via in vitro selection.[89,90] Cofactor-dependent DNAzymes can often be generated from this approach by adding varying cofactors and cofactor concentrations during the selection process.[91–93] Using this approach, Lu and coworkers have developed a lead-dependent DNAzyme with sequence-specific nuclease activity and converted it into a family of optical lead sensors.[94–97] We have recently demonstrated a sensitive electrochemical lead sensor composed of a methylene blue-modified version of this catalytic DNA hybridized to its complementary, 20-base substrate.[88] The DNAzyme–substrate complex, which is linked to a gold electrode via a thiol on the catalytic strand, is relatively rigid, presumably preventing the redox moiety from approaching the electrode and transferring electrons. In the presence of Pb^{2+}, the *trans*-acting catalytic strand cleaves the sessile phosphodiester of the substrate into two fragments. Subsequent dissociation of these fragments allows the redox moiety to approach the electrode and transfer electrons. The resulting increase in faradic current allows the sensor to detect its target with excellent sensitivity and selectivity: the sensor's detection limit for lead is 0.3 μM (after 1 h incubation), and it does not respond measurably to Mn^{2+}, Ni^{2+}, Zn^{2+}, Co^{2+}, Mg^{2+}, Ca^{2+}, Cu^{2+}, or Hg^{2+} at concentrations as high as 10 μM. Finally, the sensor is selective enough to deploy under realistic field conditions; using it, we have conveniently and accurately determined parts-per-million or lower lead concentrations in acid extracts of lead-contaminated soils.[88]

7.5 A Comparison: Optical Versus Electrochemical Aptasensors

The sensitivity and generalizability of E-AB sensors are competitive with those of other electrochemical aptasensors, and the platform has been tested rather more thoroughly than any other electrochemical approach with regard to its ability to perform in complex, contaminate-ridden samples. It should thus prove informative to compare E-AB sensors with the best equivalent optical aptasensors. The recent description of an E-AB sensor directed against the blood protein PDGF[85] and the availability of several previously reported optical approaches employing the same aptamer provides an opportunity for just such a head-to-head comparison.

The sensitivity of the best optical PDGF aptasensors approaches the 50-pM detection limit reported for the equivalent E-AB sensor. For example, although the detection limit of a recently reported colorimetric sensor based on the PDGF-induced aggregation of aptamer-coated gold nanoparticles is ~50 times poorer than

that of the relevant E-AB sensor,[98] an alternative approach based on fluorescence anisotropy has a reported limit of detection of 220 pM.[99] Two fluorescence-based aptamer-beacon approaches have also been described, which are exact optical analogues of the E-AB platform. The first, which works via the binding-induced segregation of a quencher-fluorophore pair, has achieved a detection limit of 110 pM when deployed in pure buffer.[100] The second employs a binding-induced increase in the excimer fluorescence of pyrene to monitor the binding-induced folding of the aptamer and exhibits a demonstrated detection limit of 2,500 pM when tested in pure buffer.[101]

In terms of operational convenience, neither optical nor electrochemical aptasensor approaches appear to have the upper hand. For example, the E-AB sensor is effectively reagentless and is based on simple, handheld electronics and millimeter-scale electrodes. Conversely, however, E-AB sensors are based on a surface-immobilized, redox-modified aptamer, the fabrication of which is rather more cumbersome than the fabrication of optical aptamer beacons, which are generally deployed homogeneously in solution rather than as surface-attached probes. The heterogeneous nature of E-AB sensors also renders them somewhat slower to equilibrate than their homogeneous optical brethren; while the equilibrium time constant of the cocaine and potassium E-AB sensors are less than 1 min,[49,86] the time constants of the PDGF and thrombin sensors are ~8 and ~40 min, respectively.[81,85] Finally, however, because both the sensing aptamer and its attached redox moiety are immobilized on the electrode, the E-AB platform is readily reusable: the PDGF E-AB sensor can be regenerated in minutes using simple, denaturing buffers,[85] the cocaine E-AB sensor achieves >99% signal recovery in seconds via room temperature buffer washes,[86] and the thrombin sensor of Radi and O'Sullivan achieves a standard deviation of only 5% across 25 cycles of use and regeneration.[83]

In contrast to the issues of sensitivity and operational convenience, attributes for which optical and E-AB approaches appear reasonably closely matched, the *selectivity* of the E-AB platform appears to very significantly outpace that of optical approaches. As already noted, two aspects of the E-AB sensing mechanism lend themselves to improved selectivity. First, rather than being based on the detection of absorption (which is easily spoofed by the adsorption of contaminants), E-AB sensors are based on the detection of a specific, binding-induced conformational change in the sensing aptamer. Second, electroactive contaminants are relatively sparse and, in typical clinical or environmental samples, are far rarer than the equivalent fluorescent or colorimetric contaminants. Taken together, these attributes assure that the nonspecific background associated with E-AB sensors is exceptionally low, thus allowing for their direct deployment in complex, contaminant-rich samples such as blood serum and foodstuffs. For example, the PDGF sensor achieves a detection limit of 50 *pico*molar when deployed directly in 50% blood serum[85]; this corresponds to detection against an approximately 25,000,000-fold excess of contaminating blood proteins. This parameter contrasts sharply with the selectivity of the optical approaches described above, the best of which achieves a detection limit of 25 *nano*molar in culture media containing only 10% serum.[101] It thus appears that the selectivity of at least the PDGF E-AB sensor is several thousand times higher than that of the most selective of the comparable optical aptasensor approaches.

7.6 Conclusions

Nearly two dozen papers have appeared on the subject of electrochemical aptasensors since the first in 2005. These articles describe a wide range of sensors, some mirroring well-established immunochemical approaches and others depending critically on the unique physical properties of aptamers (and thus largely or entirely new to the sensing arena). This latter class of sensors includes a number of sensing architectures based on the binding-induced folding of aptamers and exhibiting not only sub-dissociation constant detection limits but also sufficient selectivity to work directly in blood serum and other complex, contaminant-ridden samples. The fact that this rich literature, and the impressive sensitivity, selectivity, and operational convenience it often describes, has accumulated in less than 3 years leaves us optimistic that the future is bright for electrochemical aptamer sensors.

Acknowledgments This work was supported in part by NIH EB002046, by NSF DMR 0099843, by Lawrence Livermore National Laboratory (URP-06–019), and by the Institute for Collaborative Biotechnologies through grant DAAD19-03-D-0004 from the US Army Research Office.

References

1. Potyrailo, R.A., Conrad, R.C., Ellington, A.D. and Hieftje, G.M. (1998) Adapting selected nucleic acid ligands (aptamers) to biosensors. Anal. Chem. 70:3419–3425.
2. Tombelli, S., Minunni, M., Luzi, E. and Mascini, M. (2004) New trends in nucleic acids based biosensors. Anal. Lett. 37:1037–1052.
3. Dittmer, W.U., Reuter, A. and Simmel, F.C. (2004) A DNA-based machine that can cyclically bind and release thrombin. Angew. Chem. Int. Ed. 43:3550–3553.
4. Zhang, Z.R., Blank, M. and Schluesener, H.J. (2004) Nucleic acid aptamers in human viral disease. Arch. Immunol. Ther. Exp. 52:307–315.
5. Proske, D., Blank, M., Buhmann, R. and Resch, A. (2005) Aptamers: basic research, drug development, and clinical applications. Appl. Microbiol. Biotechnol. 69:367–374.
6. Liao, W., Guo, S. and Zhao, X.S. (2006) Novel probes for protein chip applications. Front. Biosci. 11:186–197.
7. Bakker, E. and Qin, Y. (2006) Electrochemical sensors. Anal. Chem. 78:3965–3983.
8. Kuhr, W.G. (2000) Electrochemical DNA analysis comes of age. Nat. Biotechnol. 18:1042–1043.
9. Willner, I. (2002) Biomaterials for sensors, fuel cells, and circuitry. Science 298:2407–2408.
10. Fritz, J., Cooper, E.B., Gaudet, S., Sorger, P.K. and Manalis, S.R. (2002) Electronic detection of DNA by its intrinsic molecular charge. Proc. Natl. Acad. Sci. USA 99:14142–14146.
11. Bard, A.J. and Faulkner, L.R. (2001) Electrochemical methods. Wiley, New York.
12. Gooding, J.J. (2005) Nanostructuring electrodes with carbon nanotubes: a review on electrochemistry and applications for sensing. Electrochim. Acta 50:3049–3060.
13. Kissinger, P.T. (2005) Biosensors: a perspective. Biosens. Bioelectron. 20:2512–2516.
14. Crouch, S.R. (2005) Kinetic aspects of analytical chemistry: progress and emerging trends. Anal. Bioanal. Chem. 381:1323–1327.
15. Willner, I. and Zayats, M. (2007) Electronic aptamer-based sensors. Angew. Chem. Int. Ed. 46:6408–6418.
16. Shipway, A.N., Katz, E. and Willner, I. (2000) Nanoparticle arrays on surfaces for electronic, optical, and sensor applications. Chem. Phys. Chem. 1:18–52.

17. Savran, C.A., Knudsen, S.M., Ellington, A.D. and Manalis, S.R. (2004) Micromechanical detection of proteins using aptamer-based receptor molecules. Anal. Chem. 76:3194–3198.
18. Staples, M., Daniel, K., Cima, M.J. and Langer, R. (2006) Application of micro- and nano-electromechanical devices to drug delivery. Pharm. Res. 23:847–863.
19. Dukhin, A.S. and Goetz, P.J. (2001) Acoustic and electroacoustic spectroscopy characterizing concentrated dispersions emulsions. Adv. Colloid Interface Sci. 92:73–132.
20. Baldrich, E., Acero, J.L., Reekmans, G., Laureyn, W. and O'Sullivan, C.K. (2005) Displacement enzyme linked aptamer assay. Anal. Chem. 77:4774–4784.
21. Martin, R., Wardale, R.J., Jones, S.J., Hernandez, P.E. and Patterson, R.L.S. (1991) Monoclonal-antibody sandwich ELISA for the potential detection of chicken meat in mixtures of raw beef and pork. Meat Sci. 30:23–31.
22. Garcia, T., Martin, R., Rodrigueze, E., Azcona, J.I., Sanz, B. and Hernandez, P.E. (1991) Detection of bovine-milk in ovine milk by a sandwich enzyme-linked immunosorbent-assay (ELISA). J. Food Prot. 54:366–369.
23. Honda, M., Yamamoto, S., Cheng, M., Yasukawa, K., Suzuki, H., Saito, T., Osugi, Y., Tokunaga, T. and Kishimoto, T. (1992) Human soluble IL-6 receptor: its detection and enhanced release by HIV-infection. J. Immunol. 148:2175–2180.
24. Kitamura, K., Matsuda, K., Ide, M., Tokunaga, T. and Honda, M. (1989) A fluorescence sandwich ELISA for detecting soluble and cell-associated human interleukin-2. J. Immunol. Methods 121:281–288.
25. Krishnan, R., Ghindilis, A.L., Atanasov, P. and Wilkins, E. (1995) Fast amperometric immunoassay utilizing highly dispersed electrode material. Anal. Lett. 28:2459–2474.
26. Campbell, C.N., de Lumley-Woodyear, T. and Heller, A. (1999) Towards immunoassay in whole blood: separationless sandwich-type electrochemical immunoassay based on in-situ generation of the substrate of the labeling enzyme. Fresenius J. Anal. Chem. 364:165–169.
27. Eteshola, E. and Leckband, D. (2001) Development and characterization of an ELISA assay in PDMS microfluidic channels. Sens. Actuators B 72:129–133.
28. Ikebukuro, K., Kiyohara, C. and Sode, K. (2005) Novel electrochemical sensor system for protein using the aptamers in sandwich manner. Biosens. Bioelectron. 20:2168–2172.
29. Bock, L.C., Griffin, L.C., Latham, J.A., Vermaas, E.H. and Toole, J.J. (1992) Selection of single-stranded-DNA molecules that bind and inhibit human thrombin. Nature (Lond.) 355:564–566.
30. Mir, M., Vreeke, M. and Katakis, I. (2006) Different strategies to develop an electrochemical thrombin aptasensor. Electrochem. Commun. 8:505–511.
31. Polsky, R., Gill, R., Kaganovsky, L. and Willner, I. (2006) Nucleic acid-functionalized Pt nanoparticles: catalytic labels for the amplified electrochemical detection of biomolecules. Anal. Chem. 78:2268–2271.
32. Greer, R.W., Hatipoglu, M. and Glancy, D.L. (1975) Normal ranges and diagnostic value of serum albumin and leucine aminopeptidase activity in Egyptian children. Environ. Child Health December:301–306.
33. Carvounis, C.P. and Feinfeld, D.A. (2000) A simple estimate of the effect of the serum albumin level on the anion gap. Am. J. Nephrol. 20:369–372.
34. Hianik, T., Ostatna, V., Zajacova, Z., Stoikova, E. and Evtugyn, G. (2005) Detection of aptamer–protein interactions using QCM and electrochemical indicator methods. Bioinorg. Med. Chem. Lett. 15:291–295.
35. Hansen, J.A., Wang, J., Kawde, A.N., Xiang, Y., Gothelf, K.V. and Collins, G. (2006) Quantum-dot/aptamer-based ultrasensitive multi-analyte electrochemical biosensor. J. Am. Chem. Soc. 128:2228–2229.
36. Katz, E. and Willner, I. (2003) Probing biomolecular interactions at conductive and semiconductive surfaces by impedance spectroscopy: routes to impedimetric immunosensors, DNA-sensors, and enzyme biosensors. Electroanalysis 15:913–947.
37. Pejcic, B. and De Marco, R. (2006) Impedance spectroscopy: over 35 years of electrochemical sensor optimization. Electrochim. Acta 51:6217–6229.

38. Diaz-Gonzalez, M., Gonzalez-Garcia, M.B. and Costa-Garcia, A. (2005) Recent advances in electrochemical enzyme immunoassays. Electroanalysis 17:1901–1918.
39. Guan, J.G., Miao, Y.Q. and Zhang, Q.J. (2004) Impedimetric biosensors. J. Biosci. Bioeng. 97:219–226.
40. Lillie, G., Payne, P. and Vadgama, P. (2001) Electrochemical impedance spectroscopy as a platform for reagentless bioaffinity sensing. Sens. Actuators B 78:249–256.
41. Taira, H., Nakano, K., Maeda, M. and Takagi, M. (1993) Electrode modification by long-chain, dialkyl disulfide reagent having terminal dinitrophenyl group and its application to impedimetric immunosensors. Anal. Sci. 9:199–206.
42. Xu, D.K., Xu, D.W., Yu, X.B., Liu, Z.H., He, W. and Ma, Z.Q. (2005) Label-free electrochemical detection for aptamer-based array electrodes. Anal. Chem. 77:5107–5113.
43. Schlecht, U., Malave, A., Gronewold, T., Tewes, M. and Lohndorf, M. (2006) Comparison of antibody and aptamer receptors for the specific detection of thrombin with a nanometer gap-sized impedance biosensor. Anal. Chim. Acta 573:65–68.
44. Radi, A.E., Sanchez, J.L.A., Baldrich, E. and O'Sullivan, C.K. (2005) Reusable impedimetric aptasensor. Anal. Chem. 77:6320–6323.
45. Cai, H., Lee, T.M.-H. and Hzing, I.-M. (2006) Label-free protein recognition using an aptamer-based impedance measurement assay. Sens. Actuators B 114:433–437.
46. Le Floch, F., Ho, H.A. and Leclerc, M. (2006) Label-free electrochemical detection of protein based on a ferrocene-bearing cationic polythiophene and aptamers. Anal. Chem. 78:4727–4731.
47. Rodriquez, M.C., Kawde, A.-N. and Wang, J. (2005) Aptamer biosensor for label-free impedance spectroscopy detection of proteins based on recognition-induced switching of the surface charge. Chem. Commun. 34:4267–4269.
48. Xu, Y., Yang, L., Ye, X., He, P. and Fang, Y. (2006) An aptamer-based protein biosensor by detecting the amplified impedance signal. Electroanalysis 18:1449–1456.
49. Radi, A.E. and O'Sullivan, C.K. (2006) Aptamer conformational switch as sensitive electrochemical biosensor for potassium ion recognition. Chem. Commun. 32:3432–3434.
50. Zayats, M., Huang, Y., Gill, R., Ma, C. and Willner, I. (2006) Label-free and reagentless aptamer-based sensors for small molecules. J. Am. Chem. Soc. 128:13666–13667.
51. Homola, J., Yeea, S.S. and Gauglitzb, G. (1999) Surface plasmon resonance sensors: review. Sens. Actuators B 54:3–15.
52. Rahman, M.A., Won, M.S. and Shim, Y.B. (2005) The potential use of hydrazine as an alternative to peroxidase in a biosensor: comparison between hydrazine and HRP-based glucose sensors. Biosens. Bioelectron. 21:257–265.
53. Homola, J. (2003) Present and future of surface plasmon resonance biosensors. Anal. Bioanal. Chem. 377:528–539.
54. Andersson, J., Larsson, R., Richter, R., Ekdahl, K.N. and Nilsson, B. (2001) Binding of a model regulator of complement activation (RCA) to a biomaterial surface: surface-bound factor H inhibits complement activation. Biomaterials 22:2435–2443.
55. Janshoff, A., Galla, H.J. and Steinem, C. (2000) Piezoelectric mass-sensing devices as biosensors: an alternative to optical biosensors? Angew. Chem. Int. Ed. 39:4004–4032.
56. Raiteri, R., Grattarola, M., Butt, H.J. and Skladal, P. (2001) Micromechanical cantilever-based biosensors. Sens. Actuators B 79:115–126.
57. Zurn, A., Rabolt, B., Grafe, M. and Muller, H. (1994) Advances in photolithographically fabricated ENFET membranes. Fresenius J. Anal. Chem. 349:666–669.
58. Barbaro, M., Bonfiglio, A., Raffo, L., Alessandrini, A., Facci, P. and Barak, I. (2006) Fully electronic DNA hybridization detection by a standard CMOS biochip. Sens. Actuators B 118:41–46.
59. Shin, J.K., Kim, D.S., Park, H.J. and Lim, G. (2004) Detection of DNA and protein molecules using an FET-type biosensor with gold as a gate metal. Electroanalysis 16:1912–1918.
60. Xu, J.J., Luo, X.L. and Chen, H.Y. (2005) Analytical aspects of FET-based biosensors. Front. Biosci. 10:420–430.

61. Barbaro, M., Bonfiglio, A., Raffo, L., Alessandrini, A., Facci, P. and Barak, I. (2006) A CMOS, fully integrated sensor for electronic detection of DNA hybridization. IEEE Electron. Device Lett. 27:595–597.
62. Yamamoto, R. and Kumar, P.K.R. (2000) Molecular beacon aptamer fluoresces in the presence of Tat protein of HIV-1. Genes Cells 5:389–396.
63. Li, J.W.J., Fang, X.H. and Tan, W.H. (2002) Molecular aptamer beacons for real-time protein recognition. Biochem. Biophys. Res. Commun. 292:31–40.
64. Rajendran, M. and Ellington, A.D. (2003) In vitro selection of molecular beacons. Nucleic Acids Res. 31:5700–5713.
65. Tan, W.H., Wang, K.M. and Drake, T.J. (2004) Molecular beacons. Curr. Opin. Chem. Biol. 8:547–553.
66. Lin, C.H. and Patel, D.J. (1997) Structural basis of DNA folding and recognition in an AMP–DNA aptamer complex: distinct architectures but common recognition motifs for DNA and RNA aptamers complexed to AMP. Chem. Biol. 4:817–832.
67. Baldrich, E., Restrepo, A. and O'Sullivan, C.K. (2004) Aptasensor development: elucidation of critical parameters for optimal aptamer performance. Anal. Chem. 76:7053–7063.
68. Famulok, M. (1999) Oligonucleotide aptamers that recognize small molecules. Curr. Opin. Struct. Biol. 9:324–329.
69. Perrin, D.M. (2000) Nucleic acids for recognition and catalysis: landmarks, limitations, and looking to the future. Comb. Chem. High Throughput Screen. 3:243–269.
70. Jhaveri, S.D., Kirby, R., Conrad, R., Maglott, E.J., Bowser, M., Kennedy, R.T., Glick, G. and Ellington, A.D. (2000) Designed signaling aptamers that transduce molecular recognition to changes in fluorescence intensity. J. Am. Chem. Soc. 122:2469–2473.
71. Tang, J. and Breaker, R.R. (1997) Examination of the catalytic fitness of the hammerhead ribozyme by in vitro selection. RNA 3:914–925.
72. Stojanovic, M.N., de Prada, P. and Landry, D.W. (2001) Aptamer-based folding fluorescent sensor for cocaine. J. Am. Chem. Soc. 123:4928–4931.
73. Hamaguchi, N., Ellington, A. and Stanton, M. (2001) Aptamer beacons for the direct detection of proteins. Anal. Biochem. 294:126–131.
74. Hesselberth, J.R., Robertson, M.P., Knudsen, S.M. and Ellington, A.D. (2003) Simultaneous detection of diverse analytes with an aptazyme ligase array. Anal. Biochem. 312:106–112.
75. Rupcich, N., Chiuman, W., Nutiu, R., Mei, S., Flora, K.K., Li, Y.F. and Brennan, J.D. (2006) Quenching of fluorophore-labeled DNA oligonucleotides by divalent metal ions: implications for selection, design, and applications of signaling aptamers and signaling deoxyribozymes. J. Am. Chem. Soc. 128:780–790.
76. Oh, K.J., Cash, K.J. and Plaxco, K.W. (2006) Excimer-based peptide beacons: a convenient experimental approach for monitoring polypeptide–protein and polypeptide–oligonucleotide interactions. J. Am. Chem. Soc. 128:14018–14019.
77. Kohn, J.E. and Plaxco, K.W. (2005) Engineering a signal transduction mechanism for protein-based biosensors. Proc. Natl. Acad. Sci. USA 102:10841–10845.
78. Bang, G.S., Cho, S. and Kim, B.G. (2005) A novel electrochemical detection method for aptamer biosensors. Biosens. Bioelectron. 21:863–870.
79. Hamaguchi, N., Ellington, A. and Stanton, M. (2001) Aptamer beacons for the direct detection of proteins. Anal. Biochem. 294:126–131.
80. Ricci, F., Lai, R.Y., Heeger, A.J. and Plaxco, K.W. (2007) Effect of molecular crowding on the response of an electrochemical DNA sensor. Langmuir 23:6827.
81. Xiao, Y., Lubin, A.A., Heeger, A.J. and Plaxco, K.W. (2005) Label-free electronic detection of thrombin in blood serum using an aptamer based sensor. Angew. Chem. Int. Ed. 44:5456–5459.
82. Xiao, Y., Piorek, B.D., Plaxco, K.W. and Heeger, A.J. (2005) A reagentless, signal-on design for electronic aptamer-based sensors via target-induced strand displacement. J. Am. Chem. Soc. 127:17990–17991.
83. Radi, A.E., Sanchez, J.L.A., Baldrich, E. and O'Sullivan, C.K. (2006) Reagentless, reusable, ultrasensitive electrochemical molecular beacon aptasensor. J. Am. Chem. Soc. 128:117–124.

84. Sanchez, J.L.A., Baldrich, E., Radi, A.E.G., Dondapati, S., Sanchez, P.L., Katakis, I. and O'Sullivan, C.K. (2006) Electronic "off-on" molecular switch for rapid detection of thrombin. Electroanalysis 18:1957–1962.
85. Lai, R.Y., Plaxco, K.W. and Heeger, A.J. (2006) Rapid, aptamer-based electrochemical detection of platelet-derived growth factor at picomolar concentrations directly in blood serum. Anal. Chem. 79:229–233.
86. Baker, B.R., Lai, R.Y., Wood, M.S., Doctor, E.H., Heeger, A.J. and Plaxco, K.W. (2006) An electronic, aptamer-based small molecule sensor for the rapid, reagentless detection of cocaine in adulterated samples and biological fluids. J. Am. Chem. Soc. 128:3138–3139.
87. Zuo, X., Song, S., Zhang, J., Pan, D., Wang, L. and Fan, C. (2007) A target-responsive electrochemical aptamer switch (TREAS) for reagentless detection of nanomolar ATP. J. Am. Chem. Soc. 129:1042–1043.
88. Xiao, Y., Rowe, A.A. and Plaxco, K.W. (2006) Electrochemical detection of parts per billion lead via an electrode-bound DNAzyme assembly. J. Am. Chem. Soc. 129:262–263.
89. Breaker, R.R. and Joyce, G.F. (1994) A DNA enzyme that cleaves RNA. Chem. Biol. 1:223–229.
90. Breaker, R.R. (2000) Molecular biology: making catalytic DNAs. Science 290:2095–2096.
91. Faulhammer, D. and Famulok, M. (1996) The Ca^{2+} ion as a cofactor for a novel RNA-cleaving deoxyribozyme. Angew. Chem. Int. Ed. 35:2837–2841.
92. Lu, Y. (2002) New transition-metal-dependent DNAzymes as efficient endonucleases and as selective metal biosensors. Chem. Eur. J. 8:4588–4596.
93. Lu, Y., Liu, J.W., Li, J., Bruesehoff, P.J., Pavot, C.M.B. and Brown, A.K. (2003) New highly sensitive and selective catalytic DNA biosensors for metal ions. Biosens. Bioelectron. 18:529–540.
94. Li, J. and Lu, Y. (2000) A highly sensitive and selective catalytic DNA biosensor for lead ions. J. Am. Chem. Soc. 122:10466–10467.
95. Liu, J. and Lu, Y. (2003) Improving fluorescent DNAzyme biosensors by combining inter- and intramolecular quenchers. Anal. Chem. 75:6666–6672.
96. Swearingen, C.B., Wernette, D.P., Cropek, D.M., Lu, Y. Sweedler, J.V. and Bohn, P.W. (2005) Immobilization of a catalytic DNA molecular beacon on Au for Pb(II) detection. Anal. Chem. 77:442–448.
97. He, Q., Miller, E.W., Wong, A.P. and Chang, C.J. (2006) A selective fluorescent sensor for detecting lead in living cells. J. Am. Chem. Soc. 128:9316–9317.
98. Huang, C.C., Huang, Y.F., Cao, Z., Tan, W. and Chang, H.T. (2005) Aptamer-modified gold nanoparticles for colorimetric determination of platelet-derived growth factors and their receptors. Anal. Chem. 77:5735–5741.
99. Fang, X., Cao, Z., Beck, T. and Tan, W. (2001) Molecular aptamer for real-time oncoprotein platelet-derived growth factor monitoring by fluorescence anisotropy. Anal. Chem. 73:5752–5757.
100. Fang, X., Sen, A., Vicens, M. and Tan, W. (2003) Synthetic DNA aptamers to detect protein molecular variants in a high-throughput fluorescence quenching assay. ChemBioChem 4:829–834.
101. Yang, C.J., Jockusch, S., Vicens, M., Turro, N.J. and Tan, W. (2005) Light-switching excimer probes for rapid protein monitoring in complex biological fluids. Proc. Natl. Acad. Sci. USA 102:17278–17283.

Chapter 8
Amplified DNA Biosensors

Itamar Willner, Bella Shlyahovsky, Bilha Willner, and Maya Zayats

Abstract Amplified detection of DNA is a central research topic in modern bioanalytical science. Electronic or optical transduction of DNA recognition events provides readout signals for DNA biosensors. Amplification of the DNA analysis is accomplished by the coupling of nucleic acid-functionalized enzymes or nucleic acid-functionalized nanoparticles (NP) as labels for the DNA duplex formation. This chapter discusses the amplified amperometric analysis of DNA by redox enzymes, the amplified optical sensing of DNA by enzymes or DNAzymes, and the amplified voltammetric, optical, or microgravimetric analysis of DNA using metallic or semiconductor nanoparticles. Further approaches to amplify DNA detection involve the use of micro-carriers of redox compounds as labels for DNA complex formation on electrodes, or the use of micro-objects such as liposomes, that label the resulting DNA complexes on electrodes and alter the interfacial properties of the electrodes. Finally, DNA machines are used for the optical detection of DNA, and the systems are suggested as future analytical procedures that could substitute the polymerase chain reaction (PCR) process.

8.1 Introduction

The development of biosensors attracts substantial fundamental and applied research efforts, and numerous uses of biosensors can be envisaged, such as clinical diagnostics, analysis of environmental pollutants, homeland security, food analysis, and forensic applications.[1–4] The biosensor devices include the biomolecule recognition element coupled to a transducer unit. The recognition events with the biomolecular matrix are then transduced in the form of optical, electronic, magnetic or other signals. Among the different biomolecular recognition events, such as enzyme–substrate, protein–ligand, and antibody–antigen binding processes, the interactions of complementary nucleic acids hybridization are of special interest.

I. Willner, B. Shlyahovsky, B. Willner, and M. Zayats
Institute of Chemistry, The Hebrew University of Jerusalem, Jerusalem 91904, Israel, willnea@vms.huji.ac.il

Y. Li and Y. Lu (eds.), *Functional Nucleic Acids for Analytical Applications*,

The sensitive high-throughput analysis of DNA or DNA mutants has significant diagnostic importance for the early detection of genetic disorders, the analysis of mutations that lead to cancer, or the rapid detection of infectious pathogens. Other important uses of DNA analysis include homeland security and the detection of biological warfare, forensic applications, tissue matching, and analysis of bacterial contamination of water resources or food.

Indeed, the development of DNA detection methods has attracted substantial research activity in the past decades. Optical, chemiluminescent, electronic, and microgravimetric DNA sensors were designed, and several comprehensive reviews describing the advances in the field were reported.[5–10]

Optical biosensors for DNA detection attracted intense research efforts. The discovery of the unique size-controlled optical properties of metallic nanoparticles (NPs), reflected by intense localized plasmon excitons,[11–13] turned the NPs into powerful optical tags for the optical detection of DNA. A colorimetric detection method of nucleic acids is based on the distance-dependent optical properties of DNA-functionalized Au NPs. The aggregation of Au NPs leads to a red shift in the plasmon resonance absorbance of the Au NPs as a result of an interparticle coupled plasmon exciton. Thus, the hybridization-induced aggregation of DNA-functionalized Au NPs changed the solution color from red to blue.[14] Changes in the optical properties of the Au NPs upon their aggregation provide an effective method for the sensitive detection of DNA hybridization, and this allowed the design of optical DNA biosensors (Fig. 8.1).[15–18] Au NPs were separately functionalized with two thiolated nucleic acids, complementary to the two ends of the analyte DNA (Fig. 8.1a). Each of the nucleic acid-functionalized Au NPs includes many modifying oligonucleotides, complementary to the 3′- and 5′-ends of the target DNA. Addition of the target DNA to a solution of the two DNA-functionalized Au NPs resulted in the cross-linking and aggregation of the nanoparticles through hybridization, and this changed the color of the solution from red to purple as a result of interparticle-coupled plasmon absorbance (Fig. 8.1b). The aggregation process was found to be temperature-dependent, and the aggregated Au NPs could be reversibly dissociated upon elevation of the temperature through the melting of the double strands and reassociate upon decreasing the temperature, effecting the rehybridization process, which resulted in the reversible changes of the spectrum.[19] These melting transitions, aggregation and deaggregation, occurred in a narrow temperature range (Fig. 8.1c), and this allowed the design of selective assays for DNA targets and high discrimination of the mismatched targets.

Chemiluminescence provides an alternative approach for the optical detection of DNA. For example, the detection of DNA hybridization based on electrogenerated chemiluminescence (ECL) using tris(2,2′-bipyridyl)ruthenium(II) ($Ru(bpy)_3^{2+}$) as the ECL label was reported.[20] An anthrax-related specific single-stranded DNA probe was attached to the gold surface and then hybridized with a single-stranded target DNA tagged with $Ru(bpy)_3^{2+}$. The ECL response was generated by the modified electrode upon interaction with a tri-*n*-propylamine (TPrA) solution that acted as an ECL coreactant upon applying different potentials. The

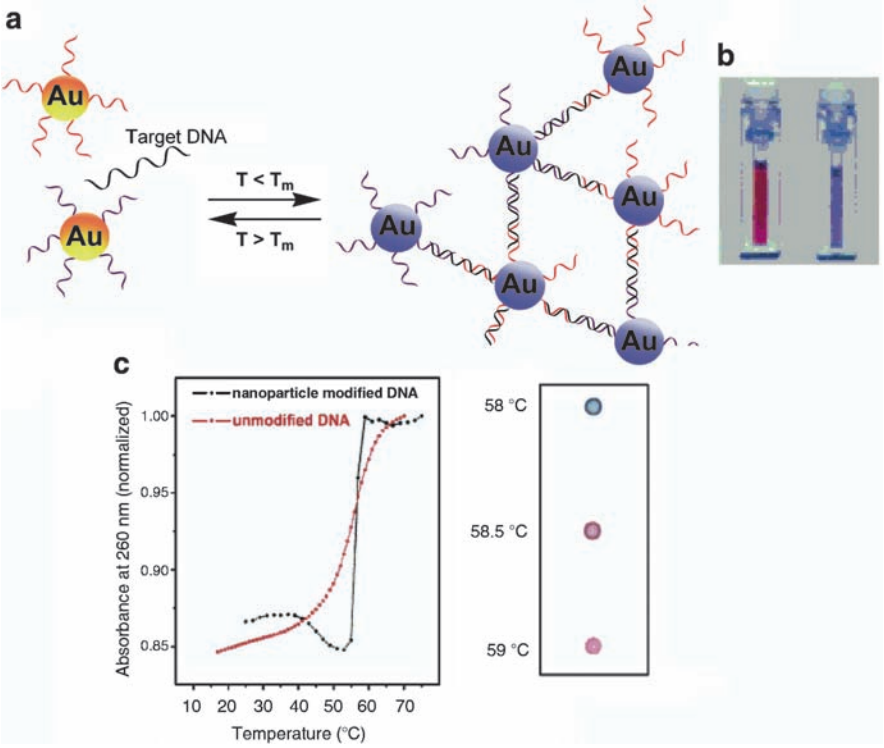

Fig. 8.1 The optical detection of a target DNA through the hybridization of two kinds of nucleic acid-functionalized Au nanoparticles (NPs) complementary to the ends of the target DNA. The hybridization leads to the aggregation of the NPs (**a**), and to a red-to-purple color transition (**b**). The deaggregation of the nanoparticles is stimulated by the melting of the cross-linked DNA duplexes (**c**) (Reprinted with permission from ref. 19. Copyright American Chemical Society)

method allowed discriminating the hybridization event of target DNA with complementary DNA probe from noncomplementary probe that included four base-pair mismatches.

Electronic, and particularly, electrochemical DNA sensors were developed. While early efforts have examined the direct electrochemical responses of the DNA bases,[21] later studies have employed redox-active intercalators to probe the formation of double-stranded DNA.[22,23] For example, the composite bisferrocene-tethered naphthalene diimide, (**1**), was used as an intercalator for probing the formation of double-stranded DNA on surfaces with a detection limit of $\sim 1 \times 10^{-20}$ mol[24] (Fig. 8.2). A different approach for the electrochemical analysis of DNA is depicted in Fig. 8.3, where a redox-active hairpin structure of a nucleic acid, (**2**), was functionalized with a ferrocene label, and immobilized on an electrode surface. The hybridization of the analyte DNA with the single-stranded region of (**2**) opened the hairpin structure and prohibited the electrical communication between the redox

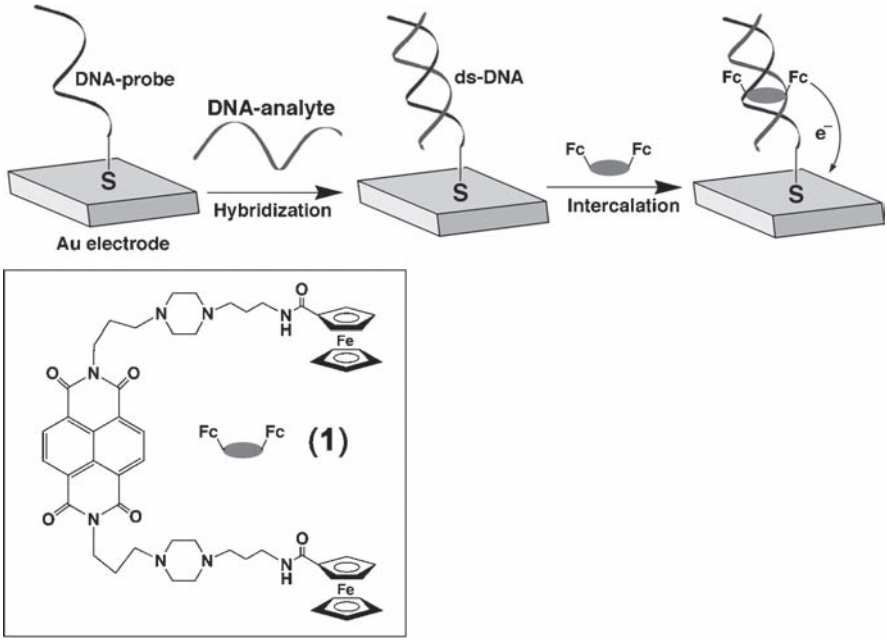

Fig. 8.2 Electrochemical analysis of DNA using the bis-ferrocene-tethered naphthalene diimide (**1**) as a redox-active intercalator associated with the surface-confined dsDNA

label and the electrode.[25] Figure 8.3b exemplifies the decrease of the voltammetric responses of the (**2**)-functionalized electrode upon analyzing different concentrations of the analyte DNA. Other electronic transduction methods of DNA hybridization events included the use of field-effect transistors (ISFET) that monitored potential changes on the ISFET gate as a result of hybridization,[26] or changes in the frequency of piezoelectric crystals[27] as a result of the mass changes occurring upon the formation of the duplex DNAs on the sensing surfaces (microgravimetric, quartz crystal microbalance analysis [QCM]).

The development of DNA biosensors of practical utility requires, however, the design of sensitive analytical systems. Most of the electronic or optical DNA biosensors use pre-polymerase chain reaction (PCR) amplification of the target nucleic acids. The intrinsic limitation of PCR that is error-prone, and requires the amplification of the analytes by replication/thermal dissociation time intervals, suggests that the development of analytical procedures that include internal amplification paths analyzing the target might be an attractive means for DNA sensing. The most obvious approach to amplify the analysis of a target DNA is schematically described in Fig. 8.4a. The nucleic acid, (**3**), acts as the recognition element, and it is immobilized on a surface. The analyte DNA, (**4**), is captured by the sensing interface through hybridization, and a catalytic label bound to a nucleic acid, (**5**), associates to the surface by a secondary hybridization process. The catalytic

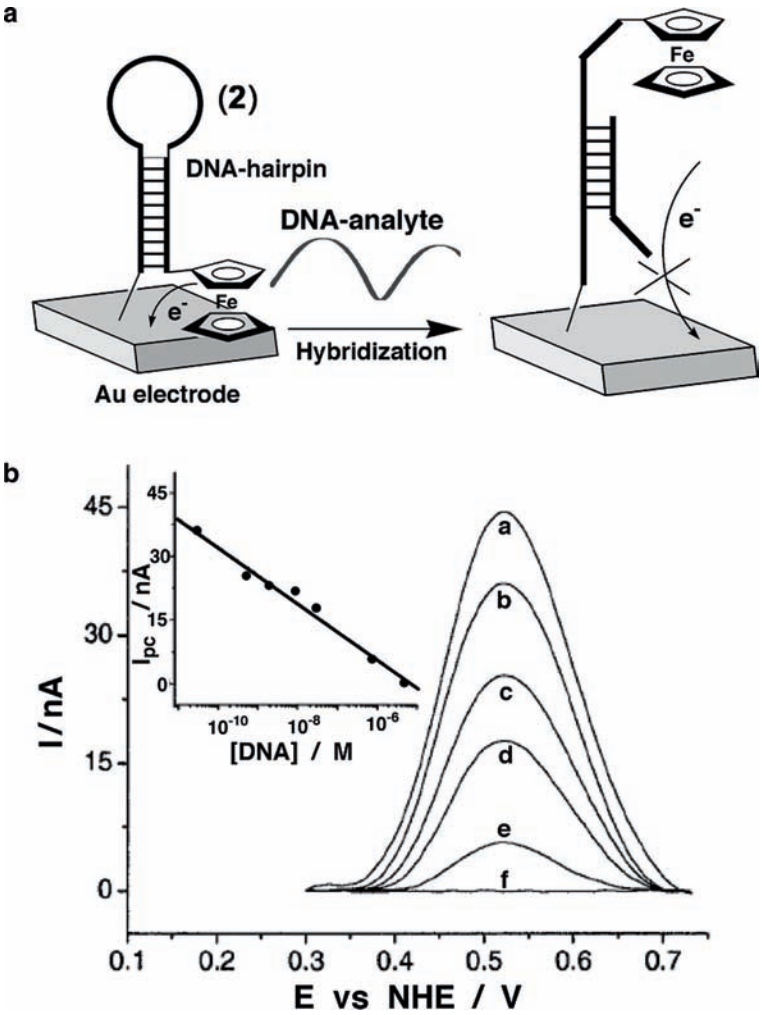

Fig. 8.3 (**a**) Electrochemical DNA sensor based on a redox-active label-functionalized DNA hairpin self-assembled monolayer on a Au electrode. (**b**) Anodic linear sweep voltammograms of the DNA sensor in the presence of different concentrations of the complementary DNA: *a*, 0 M; *b*, 30 pM; *c*, 500 pM; *d*, 30 nM; *e*, 800 nM; *f*, 5 μM. The hybridization time interval was 30 min. *Inset*: The calibration curve of the anodic peak currents recorded at different concentrations of the DNA analyte (Reproduced with permission from ref. 25. Copyright 2003, National Academy of Science, USA)

conjugate might be a molecular, macromolecular, biomolecular, or nanoparticle catalyst. The catalytic conversion of the substrate to the product translates a single DNA hybridization event to numerous product molecules that could be analyzed by optical, electrical, or microgravimetric means. A different amplification route is depicted in Fig. 8.4b, where the label hybridized with the nucleic acid/analyte

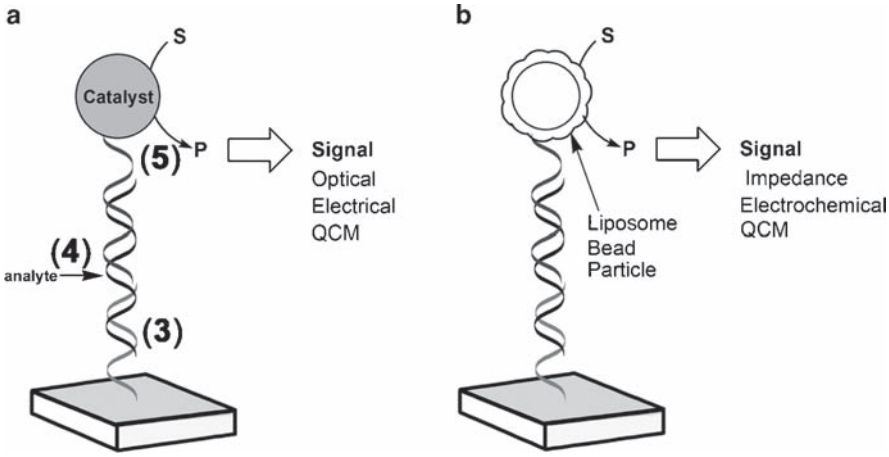

Fig. 8.4 Amplified analysis of DNA: by the application of a catalytic label tethered to a nucleic acid probe (**a**), and by anchoring a nano/micro-object, to the nucleic acid probe that controls the surface properties (**b**)

duplex consists of a micro- or nano-object such as a nanoparticle, a liposome, or even a bead. The control of the interface properties by the label, the dissolution of the label into numerous product molecules, or mass changes introduced by the label may then act as amplification paths. The electrochemical analysis of the interface properties, e.g., by impedance spectroscopy, the electrochemical detection of the dissolved ions/molecules, or the microgravimetric analysis of the bound particles, exemplify different readout methods (transduction) for the primary hybridization of the DNA analyte.

The present chapter summarizes the advances that have been accomplished in the development of amplified electronic and optical DNA biosensor systems.

8.2 Enzyme-Amplified Electrochemical DNA Biosensors

The high turnover of enzymes, the ability to modify them with nucleic acids to yield biocatalytic nucleic acid conjugates, and the diversity of enzymes, e.g., redox enzymes and hydrolytic enzymes, provides different configurations to construct amplified electrochemical biosensors.

The biocatalytic process may lead to a redox-active product, or to the control of the electrical properties of the electrode surface, thus enabling the amplified electrochemical sensing of the target DNA. Alternatively, the biocatalytic transformation might lead to color or fluorescent products, or to the generation of a chemiluminescence signal, thus resulting in optical readout methods for the detection of the target DNA.

8.2.1 *Enzyme-Amplified Electrochemical Detection of DNA*

The amplified amperometric detection of DNA was achieved by the use of the nucleic acid-functionalized horseradish peroxidase (HRP), a biocatalytic conjugate in an electrically contacting medium. An electrode was modified with a polyacrylamide-hydrazide hydrogel functionalized with $[Os(dmebpy)_2Cl]^{+/2+}$ (dmebpy = 4,4′-dimethyl-2,2′-bipyridine) redox-active units, (**6**) (Fig. 8.5). The nucleic acid, (**7**), was covalently linked to the hydrogel, and the hybridization of the nucleic acid, (**8**), functionalized with HRP, was followed by the biocatalyzed reduction of H_2O_3 using the redox polymer as an electron-transfer mediator between HRP and the electrode.[28] In a related system, the detection of single-base mismatches in DNA was demonstrated[29] (Fig. 8.6). The nucleic acid (**9**) was linked to the redox polymer, and the fully complementary nucleic acid (**10**) bound to

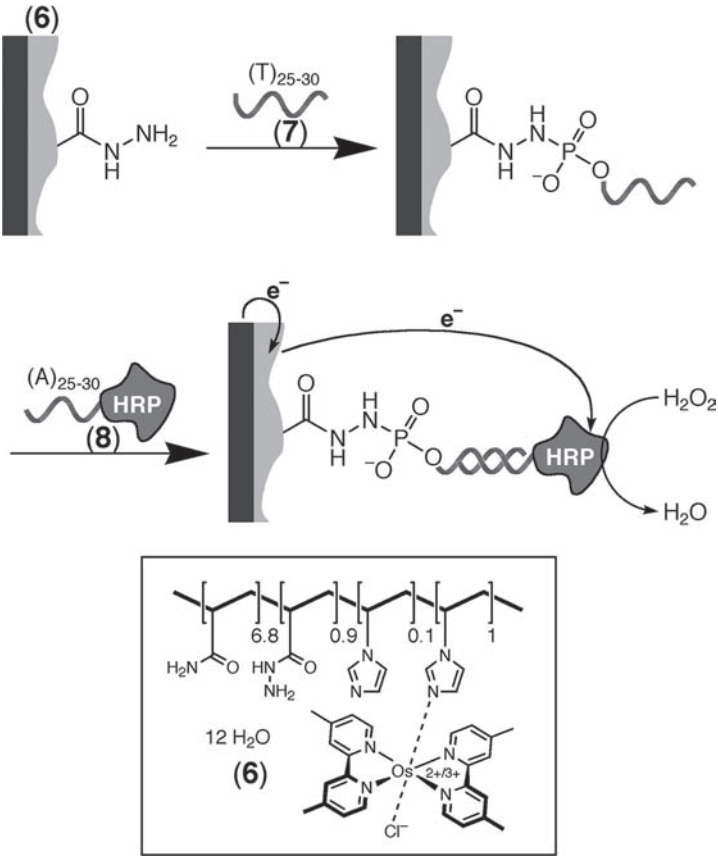

Fig. 8.5 Enzyme-amplified analysis of DNA in a redox-active hydrogel

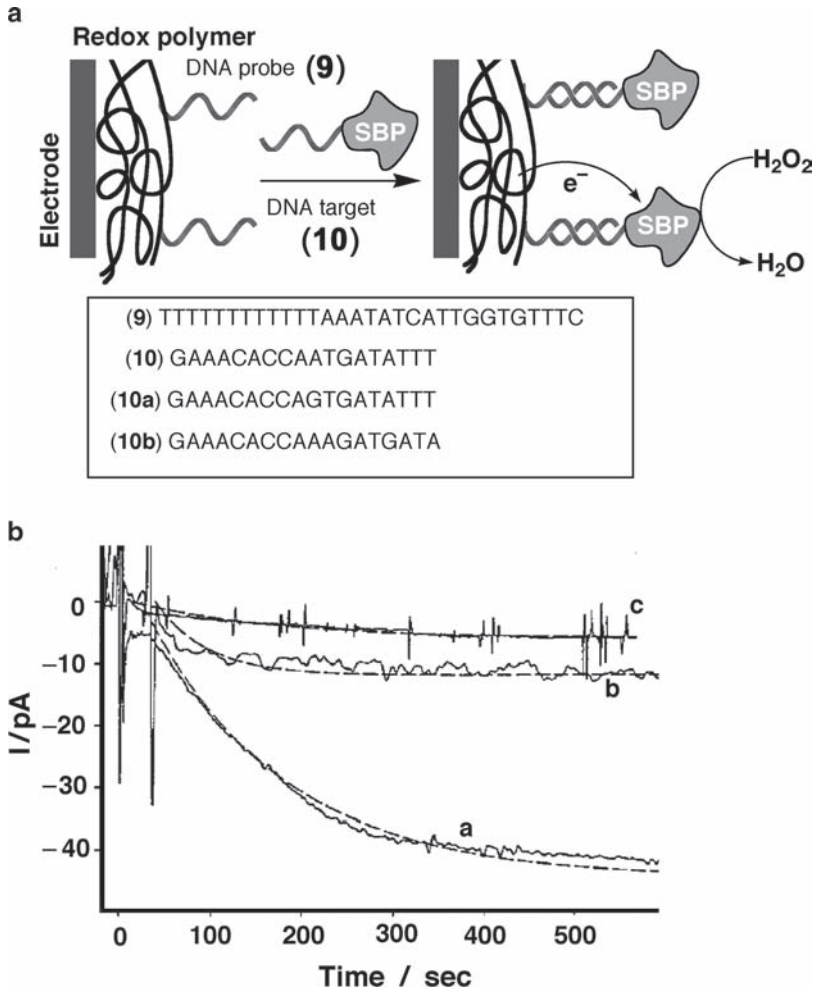

Fig. 8.6 (**a**) Amperometric transduction of the formation of a double-stranded complementary DNA complex using a soybean peroxidase (SBP)–DNA conjugate as a bioelectrocatalytic amplifier. (**b**) Increase of the electrocatalytic currents recorded at 57°C after adding the SBP-labeled target DNA: *a*, perfectly matched target; *b*, target with a single mismatched base; *c*, target with four mismatched bases. The *dashed lines* represent the best fit of the data to the theory (Reprinted with permission from ref. 29. Copyright American Chemical Society)

soybean peroxidase (SBP) was hybridized with the DNA probe (Fig. 8.6a). The nucleic acids (**10a**) or (**10b**), that include a single-base mismatch or a four-base mismatch to the probe, were similarly linked to the SBP biocatalyst. By controlling the hybridization temperature (57°C), the conjugates that included the mismatches could be discriminated by the (**9**)-modified redox polymer. Figure 8.6b shows the chronoamperometric transients observed upon the bioelectrocatalyzed reduction

of H_2O_2 by the fully complementary duplex (**9**)/(**10**)–SBP (curve a), and the very low responses of the duplexes that include the single-base mismatched nucleic acid-SBP (curve b), or the almost zero response of **10b–**SBP that includes four-base mismatches (curve c). Similarly, the avidin-glucose dehydrogenase (GDH) conjugate was employed to amplify the DNA hybridization on electrode surfaces by the bioelectrocatalyzed oxidation of glucose.[30] The formation of the duplex between a probe DNA linked to the electrode and the biotinylated target DNA, followed by the binding of the avidin–GDH conjugate, led to an electrocatalytic anodic current in the presence of glucose and 1-methoxyphenazine methosulfate as electron mediator.

A related approach for the amplified amperometric detection of DNA made use of the polymerase-induced incorporation of redox mediators into the replicated duplex structure formed between the probe nucleic acid and the target DNA on the electrode surface[31] (Fig. 8.7). The thiolated nucleic acid, (**11**), was immobilized on

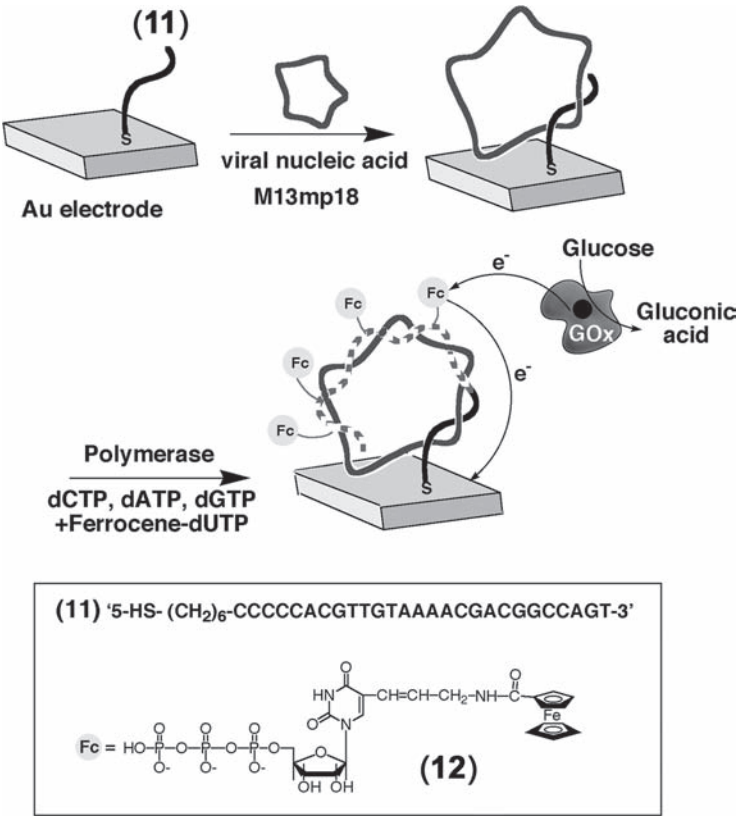

Fig. 8.7 Amplified electrochemical detection of the viral M13mp18 DNA by the generation of a redox-active replica and the bioelectrocatalyzed oxidation of glucose (Reproduced with permission from ref. 31. Copyright American Chemical Society)

an electrode surface, and it captured the target M13 phage DNA. The replication of the resulting duplex in the presence of polymerase (Klenow fragment) and the nucleotide mixture dNTPs that included the ferrocene-labeled deoxyuridine triphosphate (dUTP), (**12**), led to the incorporation of the ferrocene labels into the replicated DNA. The redox labels acted then as mediators that activated the bioelectrocatalyzed oxidation of glucose by glucose oxidase (GOx). The resulting currents enabled the amplified detection of M13 phage DNA with a detection limit that corresponded to 1×10^{-13} M.

A different method to amplify the electrochemical detection of DNA used a hydrolytic enzyme as conjugate for the generation of an electroactive product.[32] The duplex structure between the probe DNA and the biotinylated target DNA was generated on the electrode. The avidin–alkaline phosphatase was then bound to the DNA duplex as biocatalytic conjugate that hydrolyzed α-naphthol phosphate to the electrochemically active α-naphthol. The system enabled the analysis of DNA with a detection limit that corresponded to 2.5×10^{-10} M, and it was successfully applied for analyzing the 355 promoter of the GMO genome that regulates transgene expression.

The biocatalytic precipitation of an insoluble product on electrode surfaces is a further means to amplify DNA recognition events.[33,34] In contrast to the previous electrochemical sensors that probe the hybridization of the analyte DNA by the redox response of the reaction product generated by the biocatalytic process, the latter method probes the changes in the electrical properties of the electrode surface as a result of the precipitation of an insulating non-redox-active product on the electrode by the biocatalytic process. Figure 8.8a exemplifies this approach by analyzing the nucleic acid (**13**) on an electrode modified with the probe nucleic acid, (**14**). The secondary hybridization of the nucleic acid (**15**)-functionalized alkaline phosphatase (AlkPh) with the duplex DNA associated with the electrode, followed by the biocatalytic oxidative hydrolysis of 5-bromo-4-chloro-indolyl phosphate, (**16**), to the insoluble indigo derivative, (**17**), yields the precipitate on the electrode surface.[33] The formation of the precipitate on the electrode surface generated an electrically insulating film that increased the electron-transfer resistance at the electrode–solution interface. Faradaic impedance spectroscopy provides an effective method to probe the changes of electron-transfer resistances at electrode surfaces.[7,35] Figure 8.8b shows the Faradaic impedance spectra observed by the AlkPh-labeled electrode upon analyzing variable concentrations of the target DNA, (**13**) (in the form of Nyquist plots). As the concentration of (**13**) increased, the interfacial electron-transfer resistance was higher, and the resulting calibration curve (Fig. 8.8c), revealed that (**13**) was analyzed with a detection limit that corresponded to 1×10^{-13} M. A different method to link the biocatalytic label to the DNA recognition complex was developed by applying the avidin–AlkPh as the biocatalytic label, and the incorporation of biotin labels into the DNA recognition complex through replication.[34] This was demonstrated with the analysis of DNA or RNA viral genes. For example, the primer (**18**) that is complementary to a segment of the 11,161-base RNA of the vesicular stomatitis virus (VSV) (**19**) was immobilized on an Au electrode

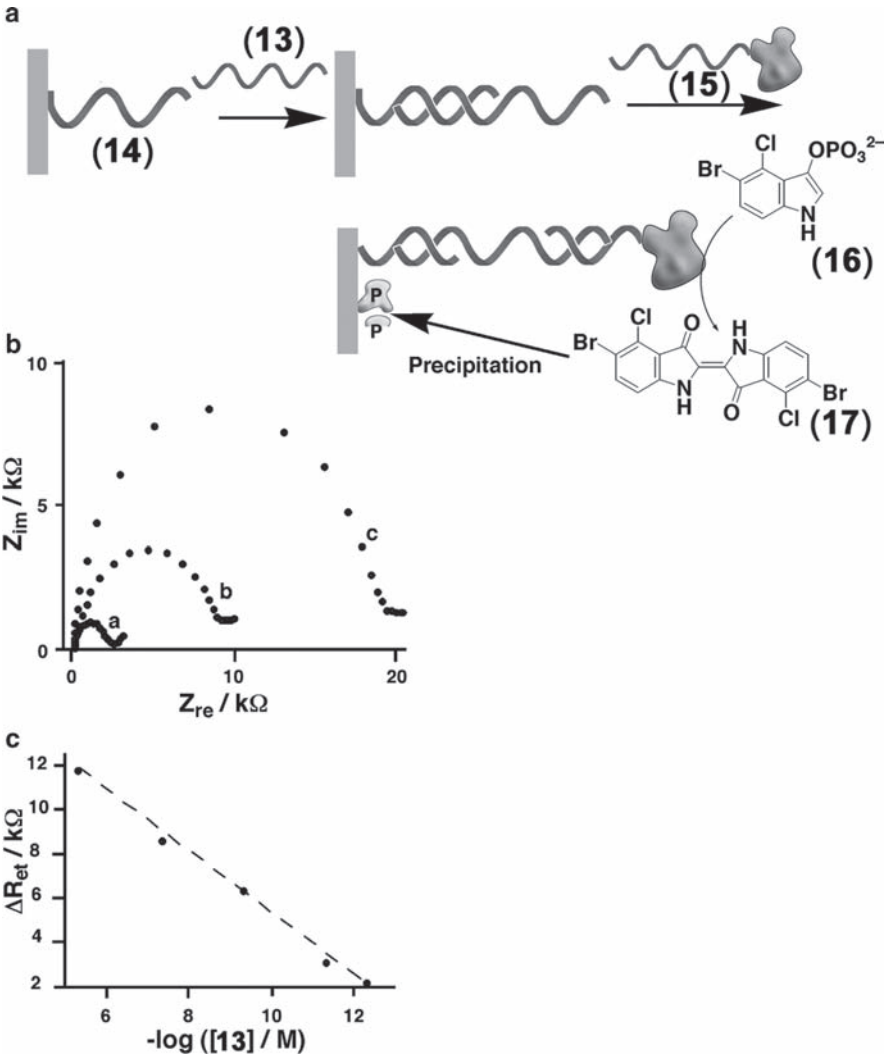

Fig. 8.8 (**a**) Amplified detection of target DNA by the biocatalyzed precipitation of an insoluble product (**17**) on the electrode support using a nucleic acid-functionalized alkaline phosphatase conjugate. (**b**) Faradaic impedance spectra (Nyquist plots) of: (*a*) the **14**-functionalized Au electrode, (*b*) after the interaction of the sensing electrode with the target DNA (**13**) (5×10^{-6} M) pretreated with the **15**/alkaline phosphatase conjugate (7×10^{-5} M) for a period of 60 min, (*c*) after the biocatalyzed precipitation of **17** for 30 min in the presence of **16** (2×10^{-3} M) in 0.1 M Tris-HCl buffer at pH = 7.4. (**c**) The changes in the electron-transfer resistance, R_{et}, upon the sensing of different concentrations of the target DNA (**13**) by the amplified biocatalyzed precipitation of **17** onto the transducer for a period of 30 min (Reproduced with permission from ref. 33. Copyright Wiley-VCH Verlag GmbH & Co.KGaA)

(Fig. 8.9a). The hybridization of **19** with the probe, followed by the replication of the double-stranded DNA in the presence of reverse transcriptase and the nucleotide mixture dNTPs that included biotinylated dUTP, resulted in the incorporation of the biotin labels into the replicated strands. The subsequent binding of the

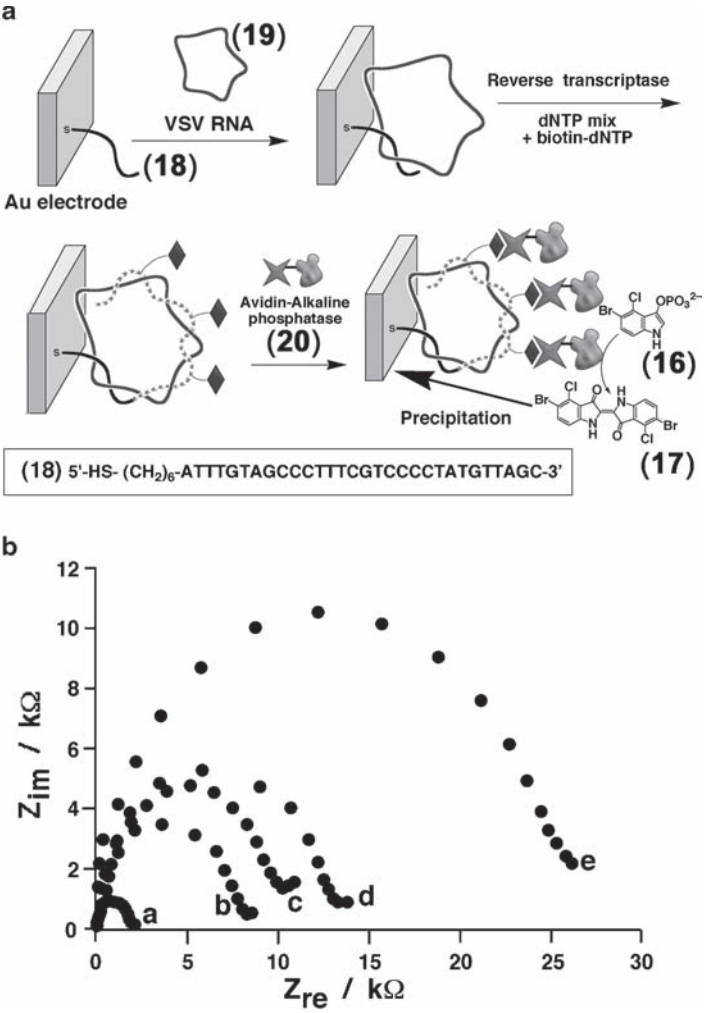

Fig. 8.9 (**a**) Amplified electronic transduction of the analysis of a viral RNA by the reverse transcriptase-induced replication of **19** while incorporating biotin labels into the replica, and the biocatalyzed precipitation of an insoluble product on the transducer. (**b**) Faradaic impedance spectra (Nyquist plots) upon the amplified sensing of vesicular stomatitis virus (VSV) RNA: *a*, the **18**-functionalized Au electrode; *b*, after hybridization with the VSV RNA (**19**), 1×10^{-12} M; *c*, after the reverse transcription for 45 min in the presence of dGTP, dATP, dTTP, dCTP, and biotinylated dUTP (1:1:2/3:1:1/3, each base 1 mM); *d*, after the association of the avidin–alkaline phosphatase conjugate (**20**); *e*, after the biocatalyzed precipitation of **17** for 20 min in the presence of **16** (2×10^{-3} M) (Reproduced with permission from ref. 34. Copyright Wiley-VCH Verlag GmbH & Co. KGaA)

avidin–AlkPh conjugate (**20**) and the biocatalyzed precipitation of the insoluble product (**17**) on the electrode enabled, then, the impedimetric readout of the analysis of (**19**). Figure 8.9b displays the impedance spectra observed upon the analysis of 1×10^{-12} M of the VSV RNA. The increase in the interfacial electron-transfer resistance as a result of the reverse transcriptase-stimulated replication of the primary duplex, $\Delta R_{et} = 4.5\,k\Omega$, was attributed to the negative charge that was generated on the electrode that results in the electrostatic repulsion of the negatively charged redox label $(Fe(CN)_6^{3-/4-})$ in solution. The precipitation of the insoluble product (**17**) on the electrode increased the interfacial electron-transfer resistance to $\Delta R_{et} = 14.0\,k\Omega$ due to the insulating effect of the precipitate on the electrode. The extent of the insulation of the electrode by (**17**) was controlled by the concentration of the VSV RNA in the analyte sample, and by the coverage of (**18**)/(**19**) on the electrode, and the method enabled the analysis of the viral RNA with a detection limit of 1×10^{-17} M. A similar method was applied to analyze the M13 phage DNA, using polymerase as replication biocatalyst.[34] The use of this method to amplify the detection of a single-base mismatch in DNA[36] is outlined in Fig. 8.10. The analyte DNA (**21**), consisting of 41 bases, included a single G-mutation as compared to the normal gene (**22**), that included the A base at the mutation site. Accordingly, electrodes were modified with the primer DNA (**23**) that is complementary to the mutant or the normal gene up to one base before the mutation site. Knowing the nature of the sought mutant, the electrodes treated and hybridized with either the mutant or the normal gene were treated with biotinylated dCTP and polymerase. The incorporation of the biotin-labeled

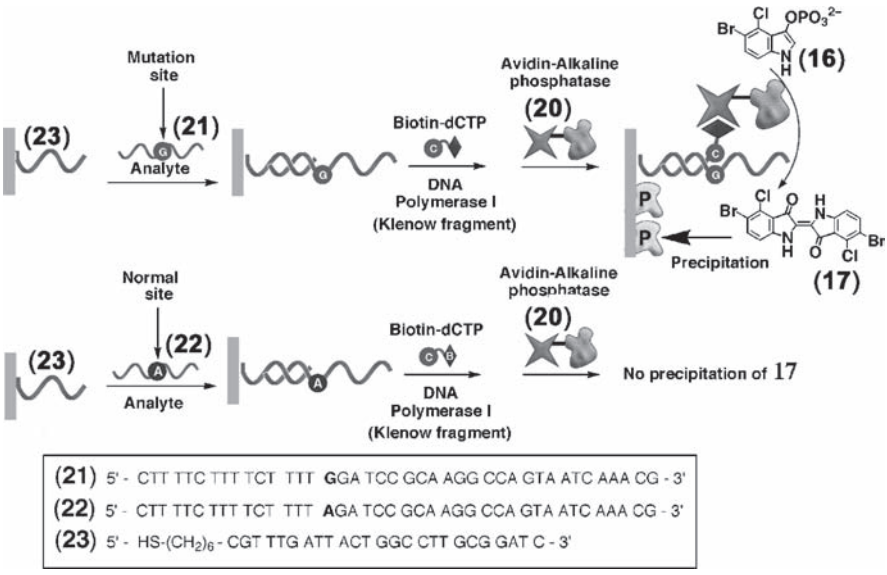

Fig. 8.10 Electronic transduction of the analysis of a single-base mutation in an analyte DNA using the biocatalytic precipitation of an insoluble product on the transducer as an amplification route (Adapted with permission from ref. 36. Copyright Nature Publishing Group, 2001)

C-base occurred only on the surface that included the hybridized mutant. The subsequent binding of the avidin–alkaline phosphatase conjugate, followed by the biocatalyzed precipitation of (**17**), enabled then the impedimetric detection of the electrode at which the mutant was hybridized. This method was successfully applied to analyze real blood samples that included the Tay–Sachs genetic disorder mutated gene with no need for PCR preamplification.

8.2.2 Enzyme- and DNAzyme-Amplified Optical Detection of DNA

The enzyme-catalyzed generation of color or fluoregenic products is one of the fundamental procedures to amplify biorecognition events, e.g., the enzyme-linked immunosorbent assay (ELISA) protocol. Because these ELISA configurations have been extensively discussed in the past,[37,38] they are not addressed here. We mention, however, several recent approaches to apply enzymes for the amplified optical detection of DNA with systems of enhanced complexity.

The biocatalytic evolution of a biocatalyst was suggested as a versatile method to amplify DNA detection[39] (Fig. 8.11a). According to this method, the complex between the probe nucleic acid, (**24**), and the analyte DNA, (**25**), was generated on a surface, and a biotin-labeled nucleic acid, (**26**), was linked to the resulting duplex structure as an anchoring site for the biocatalytic cascade. The attachment of ecarin to the biotin label through the avidin bridge yielded the biocatalytic unit on the recognition complex and activated the biocatalyzed transformation of prothrombin to thrombin. The latter product acted as biocatalyst for the hydrolysis of bis-(*p*-tosyl-Gly-Pro-Arg)-Rhodamine110, (**27**), to the fluorescent product, (**28**). Thus, the biocatalytic evolution of a biocatalyst presents a two-step nonlinear amplification cascade for the detection of the DNA. This method enabled the analysis of DNA with a detection limit that corresponded to 1×10^{-12} M.

An enzyme-amplified optical detection scheme of DNA was developed by the use of aptamer–thrombin conjugates[40] (Fig. 8.11b). The thrombin was functionalized with nucleic acid tethers (**29**) consisting of a region complementary to the analyte DNA and a domain that functions as an anti-thrombin aptamer. Binding of the aptamer to the thrombin inhibited its biocatalytic functions, and the hydrolysis of (**27**) was blocked. The hybridization of the analyte, (**30**), with the nucleic acid, (**29**), rigidified the nucleic acid, and this resulted in the release of the aptamer structure and the activation of thrombin toward the hydrolysis of (**27**) to the fluorescent product, (**28**). Thus, a single hybridization event activated the thrombin, resulting in the amplified detection of (**30**) through the generation of numerous fluorescent product molecules.

The enzyme-catalyzed generation of chemiluminescence was employed to analyze DNA.[41] The double-stranded DNA formed on an electrode surface upon analyzing the target DNA was interacted with the doxorubicin intercalator. The electrochemically reduced duplex-incorporated doxorubicin catalyzed the reduction of O_2 to H_2O_2, and the latter product stimulated, in the presence of HRP and

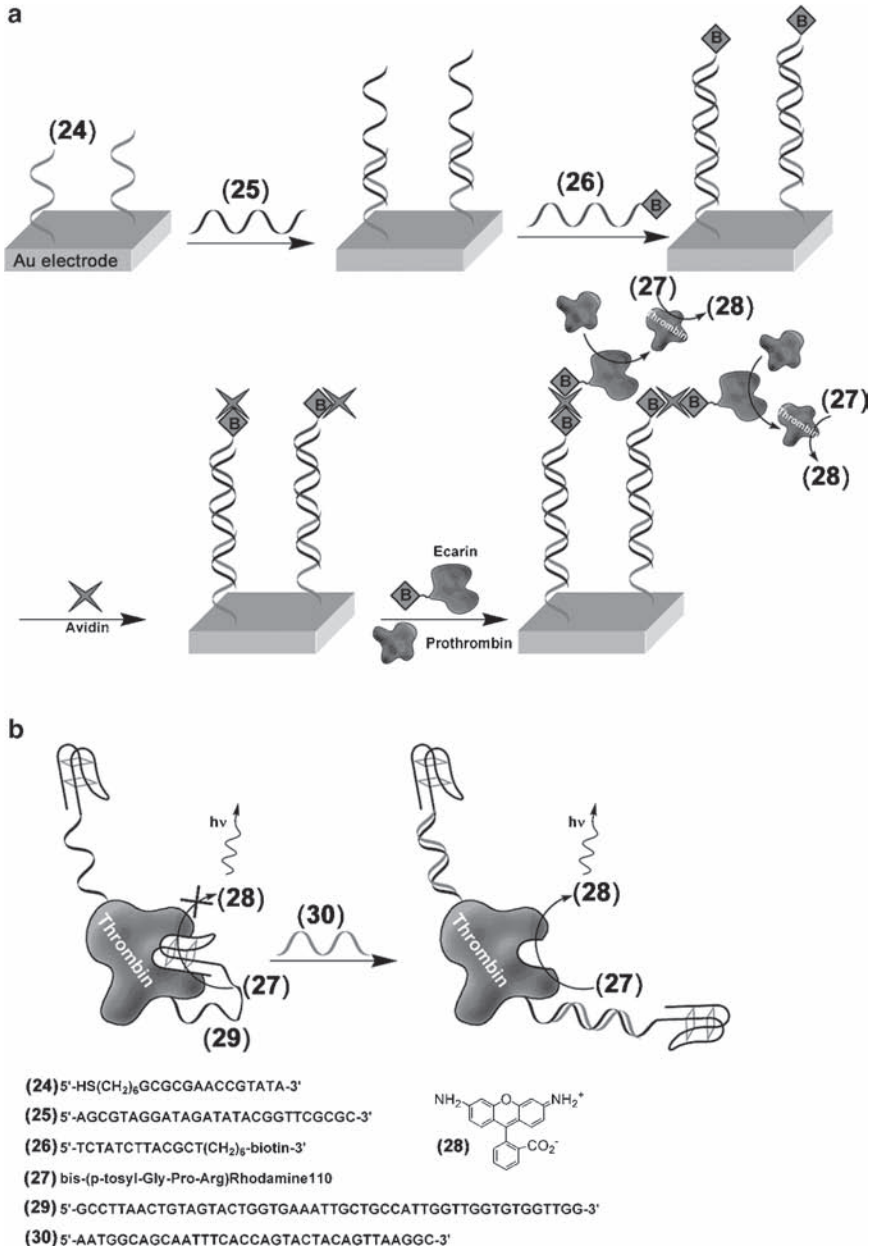

Fig. 8.11 (**a**) Amplified analysis of DNA by the ecarin-catalyzed evolution of the thrombin biocatalyst and the generation of the fluorescent product (**28**). (**b**) Optical analysis of DNA by the catalytic activation of thrombin through the dissociation of a anti-thrombin–aptamer complex (Part **a** reproduced with permission from ref. 39. Copyright Wiley-VCH Verlag GmbH& Co. KGaA)

luminol, the generation of chemiluminescence. The intensities of the emitted light were controlled by the content of the surface-bound intercalator, and this related to the surface coverage of the duplex DNA on the surface, or the bulk concentration of the analyzed DNA. The method enabled the detection of the target nucleic acid with a detection limit that corresponded to 1×10^{-12} M.

The discovery of the biocatalytic functions of nucleic acids[42] and the versatile method to design DNA- (or RNA)-based biocatalysts by the systematic evolution of ligands by exponential enrichment (SELEX) procedure[43,44] led to the preparation of nucleic acid-based biocatalysts (DNAzymes). Different DNA architectures incorporated recognition sites for the target DNA and catalytic sequences (DNAzyme units) that enabled the amplified optical readout of the hybridization process at the recognition site. The DNAzyme that was used is a G-rich sequence, which forms a G-quadruplex structure that intercalates hemin. The hemin-interlayered G-quadruplex structure was found to mimic the horseradish peroxidase (HRP) functions.[45,46] This HRP-mimicking DNAzyme was used as a catalytic label for the amplified optical detection of DNA.[47] The hairpin nucleic acid structure (**31**) included in its "stem" component the sequence "A," tethered to sequence "B," that included the encoded sequence to form the G-quadruplex-hemin DNAzyme. The single-stranded loop of the hairpin structure included the recognition sequence for the hybridization with the target DNA, (**32**) (Fig. 8.12). Hybridization of the

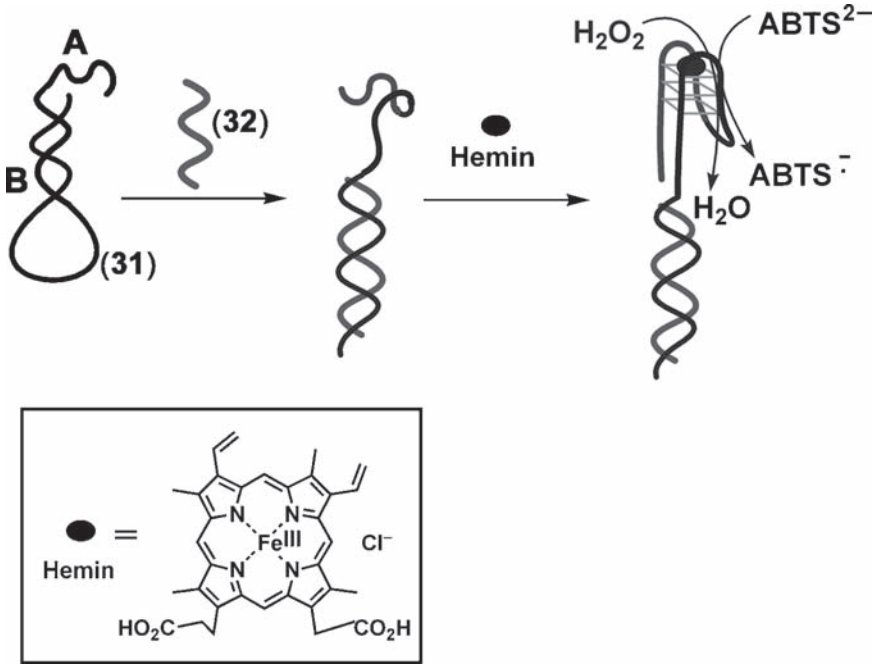

Fig. 8.12 Analysis of DNA by opening of a hairpin nucleic acid (**31**) and the generation of a DNAzyme

target DNA with the loop opened the "stem" and parts "A" and "B" self-assembled in the presence of hemin to the HRP-mimicking DNAzyme. The latter mediated the H_2O_2-catalyzed oxidation of 2,2′-azino-bis(3-ethylbenzothiazoline)-6-sulfonic acid, $ABTS^{2-}$, to the oxidized colored product ABTS. The tailored DNAzyme enabled the sensing of DNA with a detection limit that corresponded to 2×10^{-7} M. The hybridization of the target DNA with the loop region was sensitive to a single-base mismatch in the target DNA, and the method enabled the analysis of single-base mismatches in the analyzed DNA.

The hemin/G-quadruplex DNAzyme revealed also horseradish peroxidase-type reactivity that was reflected by the generation of chemiluminescence in the presence of H_2O_2 and luminol.[48] This property was used to develop an amplified DNAzyme-based chemiluminescence DNA biosensor (Fig. 8.13a). A thiolated nucleic acid, (**33**), was assembled on an Au surface, and it captured the analyte nucleic acid, (**34**). The subsequent hybridization of the DNAzyme tethered to the reporter nucleic acid sequence, (**35**), that hybridizes to the single-stranded domain of the analyte resulted in the labeling of the recognition complex. The rinsed, surface-confined, biocatalytic complex stimulated the generation of chemiluminescence (Fig. 8.13b). The method enabled the analysis of the target DNA with a detection limit that corresponded to 1×10^{-9} M. A further extension of this method included the application of Au NPs as carriers of the reporting DNAzyme labels[49] (Fig. 8.13c). By this approach the duplex generated on the surface between the capturing nucleic acid, (**33**), and the analyte, (**34**), was interacted with Au NPs (13 nm) that carried the nucleic acid units composed of the horseradish peroxidase-mimicking DNAzyme tethered to a nucleic acid chain, (**36**), complementary to the analyte, (**34**). This reaction resulted in the association of a nanoparticles carrying multicomponent DNAzyme units that reported the analyte hybridization with the capturing surface by the generation of chemiluminescence. By applying the multi-DNAzyme-functionalized Au NPs as reporters for the DNA hybridization event, the detection limit could be improved by one order of magnitude as compared to the use of a single DNAzyme-nucleic acid nanostructure as reporter unit.

Semiconductor quantum dots (QDs) exhibit unique size-controlled photophysical properties.[50] The intense fluorescence of the QDs and their stability against photobleaching was extensively used to develop fluorescence-based biosensors.[51] Specifically, the size-controlled fluorescence properties of semiconductor QDs were used for multiplexed parallel analysis of different analytes using the different-sized QDs as fluorescence codes for the different analytes.[52] The combination of biocatalytic replication of DNA on semiconductor QDs enabled the amplified optical analysis of the M13 phage DNA.[53] CdSe/ZnS core-shell QDs were functionalized with the thiolated nucleic acid, (**37**), that is complementary to M13 phage DNA, (**38**). Hybridization of the M13 phage DNA with the capturing nucleic acid on the CdSe/ZnS QDs, was followed by the replication of the single-stranded M13 phage in the presence of polymerase and the dNTPs mixture that included the Texas phage DNA Red-modified dUTP, (**39**). The replication resulted in the incorporation of the dye units into the replicated DNA, and this stimulated the fluorescence resonance energy transfer (FRET) from the QDs to the dye units (Fig. 8.14a). As the number

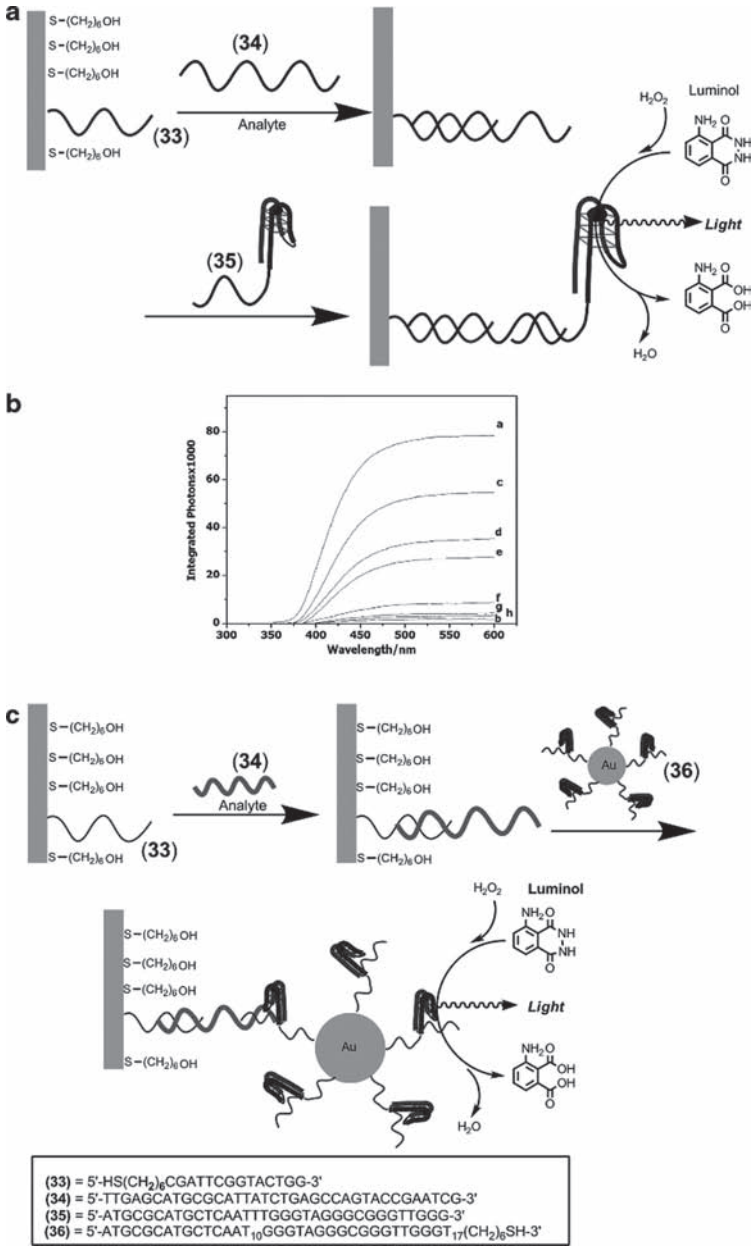

Fig. 8.13 (**a**) Analysis of a DNA using a DNAzyme label and chemiluminescence as a detection signal. (**b**) Integrated light intensities corresponding to: (*a*) the analysis of (**34**), 0.5 μM, using the DNAzyme label (**35**), 2.5 μM; (*b*) the analysis of (**34**) without added DNAzyme label but upon treatment with hemin 2.5 μM; (*c*) to (*h*), analyzing (**34**), at 0.1, 0.07, 0.04, 0.01, 0.005, and 0.001 μM, respectively. (**c**) The amplified chemiluminescence detection of DNA using DNAzyme-functionalized Au NPs (Part **a** reproduced with permission from ref. 48. Copyright American Chemical Society. Part **b** reproduced with permission from ref. 49. Copyright American Chemical Society)

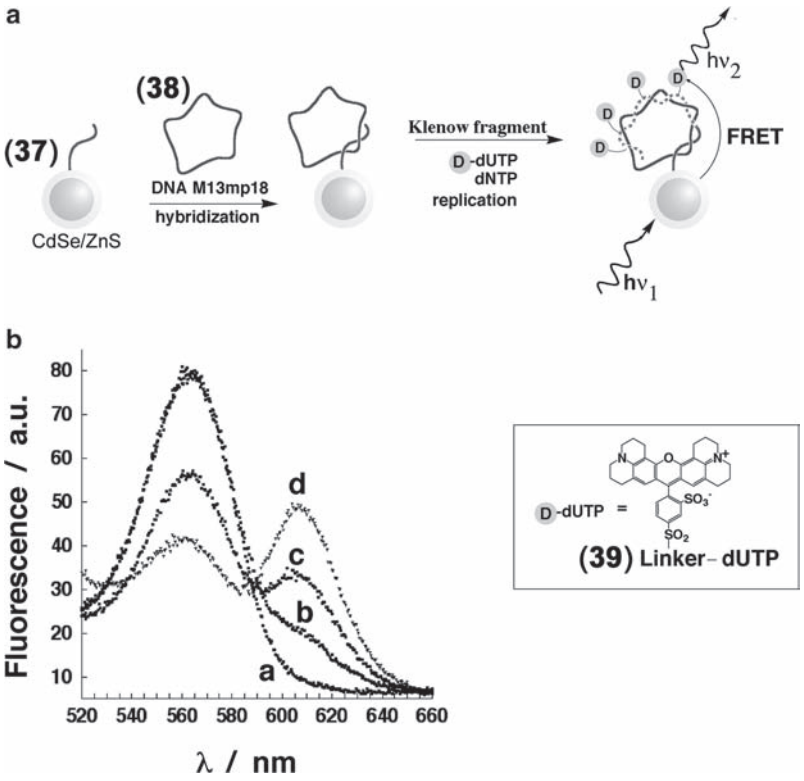

Fig. 8.14 (**a**) The optical detection of M13 phage DNA (**38**) by nucleic acid-functionalized CdSe/ZnS quantum dots (QDs). The replication of the analyte in the presence of the dNTP mixture that includes the Texas-Red labeled dUTP (**39**) results in the incorporation of the dye into the replica and stimulates a fluorescence resonance energy transfer (FRET) process. (**b**) Time-dependent fluorescence changes upon incorporation of the dye (**39**), into the DNA replica and the analysis of the M13 phage DNA according to **a**: (*a*) 0, (*b*) 10, (*c*) 30, and (*d*) 60 min (Reproduced with permission from ref. 53. Copyright American Chemical Society)

of the dye units increased with the time interval of replication, the fluorescence of the dye was intensified (Fig. 8.14b).

8.3 Amplified Electrochemical or Optical Detection of DNA Using Metal Nanoparticles (NPs)

Metal NPs may substitute the enzyme labels as catalysts for amplifying DNA analysis. Pt NPs were found to catalyze the electrochemical reduction of H_2O_2 and thus could substitute HRP as a biocatalytic label[54] (Fig. 8.15). The duplex between the probe DNA, (**40**), and the analyte DNA, (**41**), was generated on an electrode, and Pt NPs (~4 nm) modified with the nucleic acid, (**42**), that is complementary to

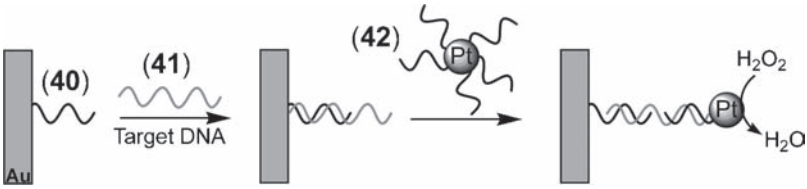

Fig. 8.15 The amplified electrochemical analysis of a DNA by nucleic acid-functionalized Pt NPs acting as electrocatalysts for the reduction of H_2O_2 (Reproduced with permission from ref. 54. Copyright American Chemical Society)

the single strand of (**41**) were conjugated as labels to the sensing electrode. The amperometric response of the system that resulted upon the Pt NP-mediated electrocatalyzed reduction of H_2O_2 was used as readout signal. The method enabled the analysis of DNA with a detection limit of 1×10^{-11} M.

The Pt NPs were found to catalyze, similarly to HRP, the generation of chemiluminescence in the presence of luminol–H_2O_2. Using the conjugate shown in Fig. 8.15, the DNA could be analyzed with a detection limit that corresponded to 1×10^{-11} M.[55]

The functions of NPs as catalysts to reduce metal salts and to grow NPs of identical composition or of core-shell structures are extensively used to develop biosensors, and specifically, DNA sensor systems.[56] The amplified electrical detection of DNA by the catalytic enlargement of Au NPs and using conductivity as readout signal was accomplished by the generation of conductivity paths between microelectrodes through the catalytic process[57,58] (Fig. 8.16). The probe nucleic acid, (**43**), was immobilized in between two microelectrodes, and the target DNA, (**44**), was hybridized with the surface and further functionalized with the (**45**)-functionalized Au NPs (Fig. 8.16a). The catalytic enlargement of the Au NP by Ag^+ with hydroquinone yielded conductivity routes between the microelectrodes. Figure 8.16b (curve a) shows the resistivity of the microelectrode gap upon analyzing the DNA, (**44**), as a function of the time employed to enlarge the NPs by the Ag^+/hydroquinone system. The gap revealed high resistance, $R > 2 \times 10^8$ Ω, before the enlargement process, and it dropped to R ~ 100 Ω after 25 min of silver deposition. The method proved to be successful to detect single-base mismatches in DNA. For example, exchange of the A-base in the capture nucleic acid, (**43**), with a G-base enabled the temperature-controlled elimination of the hybridization of (**44**), due to a lower melting temperature. Figure 8.16b (curve b) reveals that the single-base mismatch between the capture DNA and the analyte, (**44**), eliminated the hybridization of the nucleic acid and, thus, prevented the secondary binding of the (**45**)-modified NPs. As a result, the insulating features of the gap were preserved. The conductivity of the gap was controlled by the concentration of the analyte DNA, because the content of the catalytic NPs that provide the origin of the conductivity paths is dominated by the surface coverage of (**44**) (Fig. 8.16c). This technology to detect DNA was already practically implemented in DNA chips that included electrode arrays for multiplexed analyses of DNAs, and conductivity analyzers that probe the NP-enlarged microelectode gaps were fabricated.[59] The method was further developed[60] by employing Al microelectrodes on Al_2O_3 supports

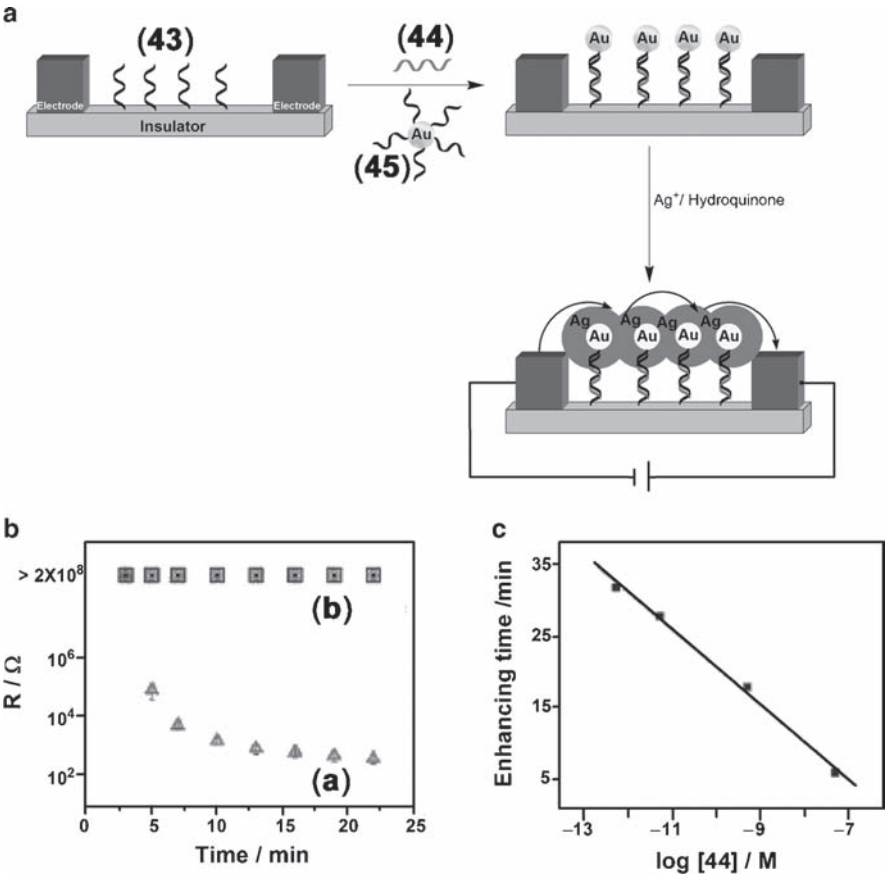

Fig. 8.16 (**a**) Analysis of DNA by the enhancement of the conductivity between electrodes by the catalytic enlargement of Au nanoparticles associated with the DNA assembly. (**b**) Resistance of the electrode array measured as a function of the time interval of silver enhancing in the presence of (*a*) the complementary and (*b*) noncomplementary DNA. **(c)** A graph of the silver enhancing time required to reach a resistance value of 100 kΩ as a function of target DNA concentration (Reproduced with permission from ref. 57. Copyright 2002, AAAS)

as the transducing element. The functionalization of the oxide surface with an amine-functionalized nucleic acid, followed by the hybridization of a biotin-modified nucleic acid to the surface-linked capture nucleic acid–analyte duplex, resulted in the labeled conjugate. The subsequent binding of the conjugate consisting of Au NPs linked to antibiotin Ab to the DNA complex and the catalytic deposition of Ag^0 on the Au NPs yielded the conductive routes that traced the primary capturing of the analyte (for other amplified electrochemical DNA sensors that employ the catalytic growth of metal NPs, see Section 8.4). Metal NPs, aggregated in the presence of the target DNA, were used as a conductive three-dimensional structure for the amplified electrochemical analysis of DNA by the intercalation of a redox-active intercalator into the double-stranded matrix of the aggregated NPs[61] (Fig. 8.17a). Two kinds of Au NPs functionalized with the nucleic acids, (**46**) and

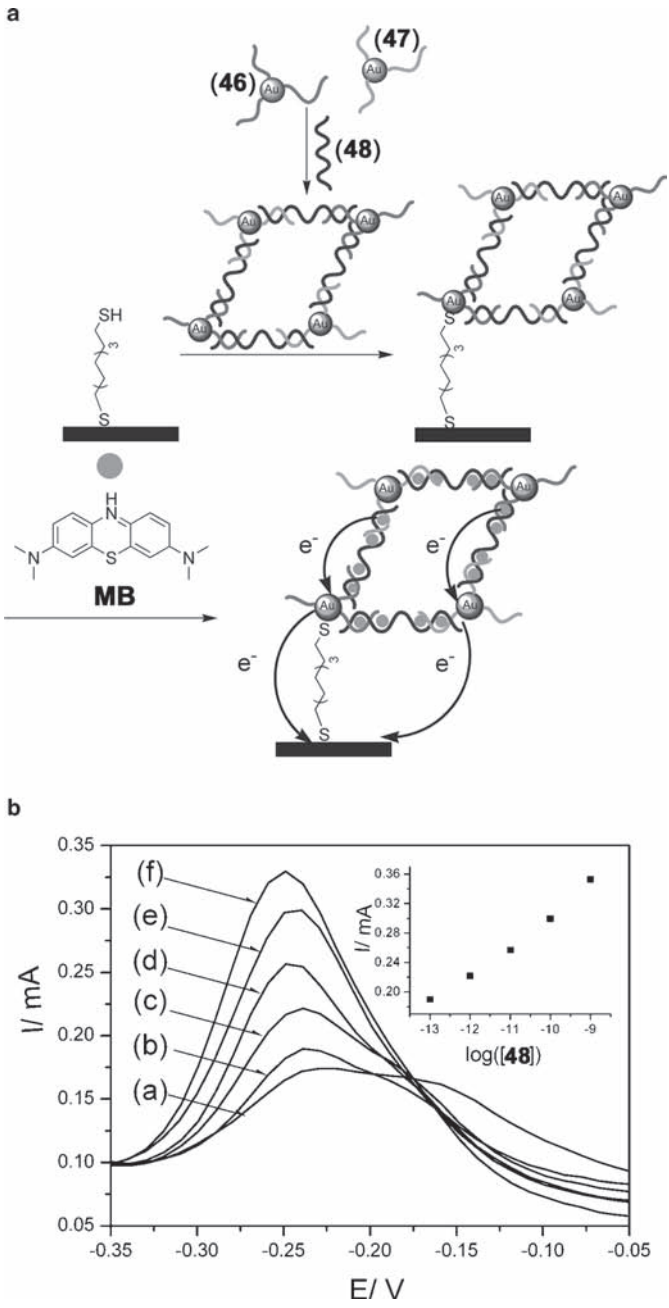

Fig. 8.17 (**a**) Electrochemical detection of DNA through the aggregation of Au NPs and the voltammetric response of the redox-active MB intercalator in the duplex-aggregated NPs. (**b**) Differential pulse voltammograms corresponding to the analysis of different concentrations of (**48**): (*a*) 0 M, (*b*) 1×10^{-13} M, (*c*) 1×10^{-12} M, (*d*) 1×10^{-11} M, (*e*) 1×10^{-10} M, (*f*) 1×10^{-9} M. *Inset*: Resulting calibration curve. In all experiments, the concentration of the probe (**46**)- and (**47**)-functionalized Au NPs was 6×10^{-9} M, and the aggregation time interval before the deposition of the aggregates on the electrode surfaces was 20 min (Reproduced from ref. 61 by permission of The Royal Society of Chemistry)

(**47**), that are complementary to the 3′- and 5′-ends of the target DNA, were reacted with the analyte, (**48**). The hybridization resulted in the aggregation of the NPs. The collection of the Au NPs aggregated on a dithiol-functionalized monolayer, followed by the intercalation of methylene blue, provided the electrochemical path for the voltammetric detection of (**48**) (Fig. 8.17b). The Au NP aggregates provided a three-dimensional structure for the electrical contacting of the numerous redox-active intercalator units with the electrode. The method enabled the detection of DNA with a sensitivity that corresponded to 1×10^{-13} M.

A scanometric detection method was developed, as an alternative approach for DNA analysis, and it is based on a sandwich array format involving a DNA-functionalized glass slide, the target DNA, and Au NP probes.[62] In a typical setup for scanometric detection, the modified glass slide was illuminated in the plane of the slide with white light. The slide served in such configuration as a planar waveguide that prevented any light from reaching the microscope objective by total internal reflectance. Wherever NP probes were attached to the surface, evanescently coupled light was scattered from the slide, and the NP labels were imaged as bright, colored spots. This approach was used for the detection of target DNA molecules (**49**) that were specifically bound to a DNA (**50**)-functionalized surface. The resulting DNA hybrid was labeled with nucleic acid-functionalized gold nanoparticles (**51**) that enabled the scanometric detection of the DNA (Fig. 8.18). At high target concentrations (≥1 nM), the Au NPs on the surface could be visualized by naked eyes. At low target concentrations (≤100 pM), the coverage of surface-bound Au NPs was too low, and an enhancement process was needed. Enlargement of the Au NPs by the catalytic reduction of silver ions and the deposition of silver metal on the Au NPs resulted in a 100-fold increase of the light-scattered signal, and thus increased the sensitivity detection of target DNA (50 fM).[62] This method was used to detect single-base mismatches in oligonucleotides, which were hybridized to DNA probes and were immobilized at different domains of a glass support. High sensitivities were provided by the deposition of silver, whereas the selectivity was achieved by examining of the melting properties of the spots: the mismatched DNA spot reveals a lower

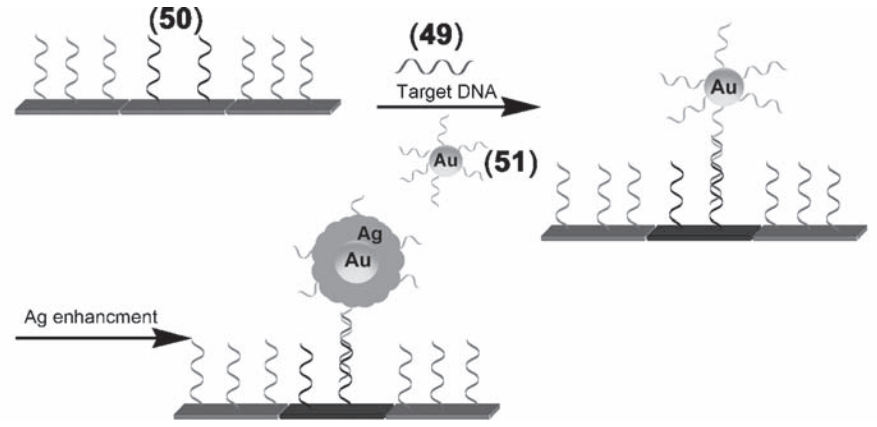

Fig. 8.18 Scanometric detection of DNA on a surface using gold-silver core-shell NPs

melting temperature owing to its lower association constant. The scattering of light is size-dependent, and hence, by using different-sized nanoparticles, the simultaneous detection of different DNA sequences was feasible. Accordingly, the light scattered by DNA-functionalized 50- and 100-nm Au NP probes was used to identify two different target DNAs in solution.[63] The scanometric method was successfully

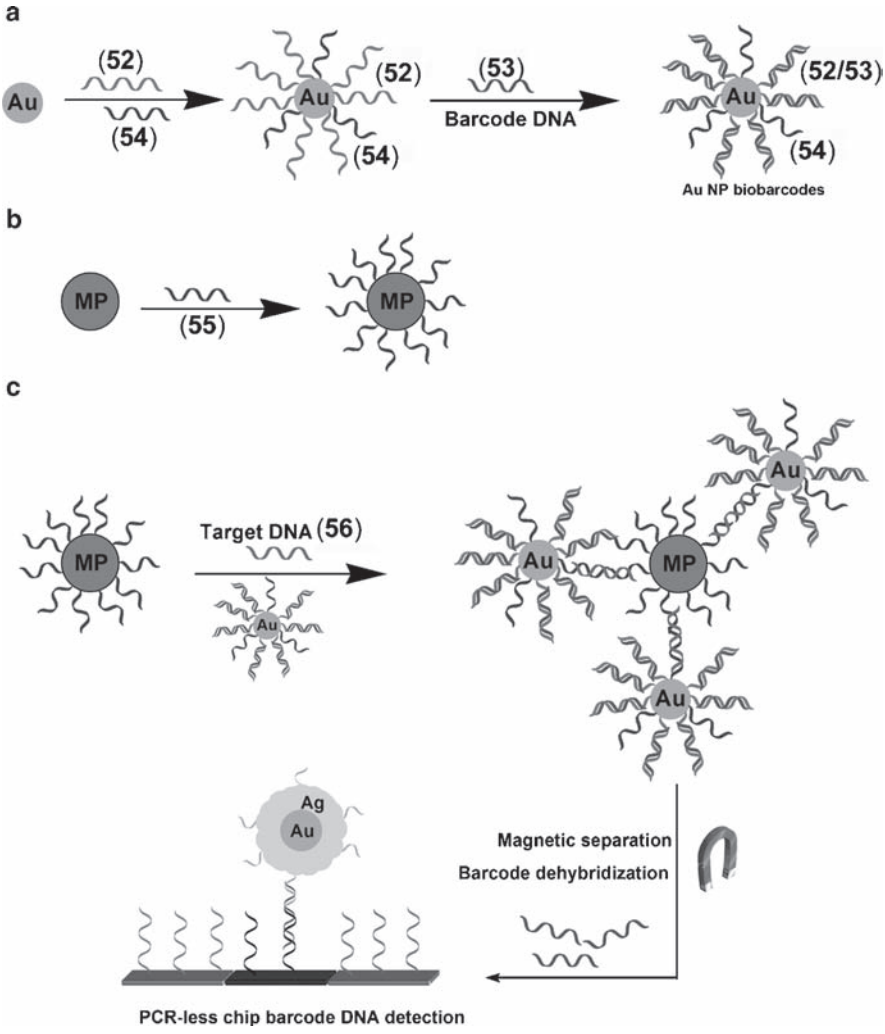

Fig. 8.19 Scanometric detection of a DNA by a nucleic acid barcode-functionalized Au NP. (**a**) Synthesis of Au NP labeled with the nucleic acid (**52**), complementary to the DNA barcode (**53**) and the nucleic acid (**54**) complementary to the target. (**b**) Preparation of the magnetic particles modified with the nucleic acid (**55**) complementary to the other end of the target. (**c**) Aggregation of the functionalized Au NPs and the magnetic particles through hybridization to the target, magnetic separation of the aggregates, thermal separation of the DNA barcode, and its scanometric detection

applied to detect the MTHFR gene from genomic DNA at a concentration as low as 200 fM without PCR amplification of the target, by the application-improved optical imaging instruments.[64] A similar approach was used to identify single nucleotide polymorphisms (SNPs) in unamplified human genomic DNA samples representing all possible genotypes for three genes involved in thrombotic disorders.[65]

The scanometric method was also applied as an optical detection means in a series of systems that employ nucleic acid-functionalized Au NPs as barcodes for biorecognition events such as DNA hybridization. For example, the scanometric method was used to analyze DNA by nucleic acid-functionalized Au NPs that acted as signaling barcodes (Fig. 8.19).[66] By this method, the functionalized Au NPs included the duplex DNA barcode, (**52/53**), and the nucleic acid units, (**54**), that recognize the target DNA (**56**). In the presence of the target DNA, (**56**), the magnetic particles modified with the nucleic acids, (**55**), and the (**52/54**)-functionalized Au NPs, the magnetic particle-Au NP aggregate was formed through cross-linking the particles by (**56**). The subsequent magnetic separation of the aggregate and the thermal separation of the DNA barcode (**53**) were followed by the scanometric detection of the released DNA code on surfaces. A PCR-like sensitivity that corresponded to 500 zM was claimed for the analysis of DNA. The DNA barcode-based sensing protocols were used to analyze the genes of various pathogens such as hepatitis B, Ebola virus, variola virus (smallpox, VV), and human immunodeficiency virus (HIV).[67]

8.4 Amplified Electrochemical, Microgravimetric, and Optical Analysis of DNA Using Nanoparticles (NPs) as Labels

An alternative approach to amplify DNA binding events includes the use of nanoparticles as tracer units that report the hybridization between the analyte and the probe nucleic acid. Different properties of the nanoparticles (NPs) are utilized in these amplification paths: (i) The labeling of the analyzed duplex with the NPs, followed by the chemical dissolution of the particles, yields numerous product ions as a result of a single recognition event. The electrochemical analysis of the released ions provides then a reporting signal to the primary hybridization event. (ii) The NPs that bind as labels to the DNA complexes introduce a weight label that may report, through microgravimetric analyses on a piezoelectric crystal, the DNA hybridization events. (iii) The NPs may catalyze secondary chemical transformations such as the deposition of metals on seed metal NPs. The subsequent dissolution of the deposited metal and the electrochemical analysis of the released ions may then be used as a route to amplify the DNA hybridization process. Alternatively, the catalytic deposition of metals on the NP seeds may substantially alter the weight or the optical features (e.g., reflectivity) of the NPs, and thus provide amplification paths for the analysis of DNA. Furthermore, the use of NPs as labels allows not only amplifying the DNA recognition but also performing the parallel multiplexed analysis of several DNAs by using different NPs as reporter units.

8.4.1 Amplified Electrochemical Analysis of DNA Using Nanoparticles

Two general electrochemical procedures for the amplified analysis of DNA using NPs were developed (Fig. 8.20). By one approach, the formation of the nucleic acid probe–DNA analyte complex on a surface was followed by the binding of the corresponding nucleic acid-functionalized NPs onto the complex. The subsequent chemical or electrochemical dissolution of the particles was followed by the electrochemical reduction of the released ions and their deposition on the electrodes. The electrochemical stripping off of the deposited product provided the quantitative voltammetric readout of the DNA analysis (Fig. 8.20, route A). The primary surface on which the recognition of DNA occurs might be a magnetic particle that enables the separation of the recognition complex with the bound NP labels, or an electrode that allows the specific electrochemical dissolution of the tracer NPs associated with the DNA complex on the electrode. The second method that enabled the enhanced amplified analysis of DNA by means of NP labels is depicted in Fig. 8.20 (route B). By this method, the primary formation of the conjugate between the DNA duplex and the NP label is followed by the catalytic enlargement of the NPs (e.g., with the same metal or a different metal). The chemical or electrochemical dissolution of the enlarged particles, followed by the electrochemical reductive collection of the metal on the electrode, and its electrochemical stripping off, yield an amplified voltammetric signal that originates from the catalytic enlargement of the NP labels.

Different configurations that follow the approach outlined in Fig. 8.20 (route A) were developed.[68] Magnetic particles functionalized with avidin were used as active surfaces for the immobilization of the biotinylated nucleic acid (**57**) that acted as a capturing probe. The hybridization of the biotinylated nucleic acid (**58**), followed by the association of avidin modified with Au NPs, enabled the magnetic collection of the Au NPs-labeled duplex DNA. The chemical dissolution of the particles, followed by the electrochemical reduction and deposition of the released ions onto the electrode, and the subsequent stripping off of the collected metal (Fig. 8.21a), provided a current readout signal for the formation of the duplex DNA.[69] A related approach[70] used metal (indium) micro-rods as the tracing labels that substitute the metal NPs (Fig. 8.21b). The use of micro-rods has the advantage that the content of the released metal ions is substantially higher than from the NPs. The indium nano-rods were prepared in porous membranes and isolated by the dissolution of the membrane template.[71] The analysis of the target DNA, (**59**), was achieved by the association of the capture biotinylated nucleic acid, (**60**), onto avidin-functionalized magnetic particles, and the formation of the (**59/60**) duplex on the magnetic particles. The subsequent hybridization of the (**61**)-functionalized In micro-rods onto the (**59/60**) duplex was followed by the magnetic attraction of the magnetic particles/In nano-rods to the electrode and the analysis of the DNA through the chronopotentiometric stripping off of the metal. Using this method, the analysis of DNA with a detection limit of 250 zmol was reported.

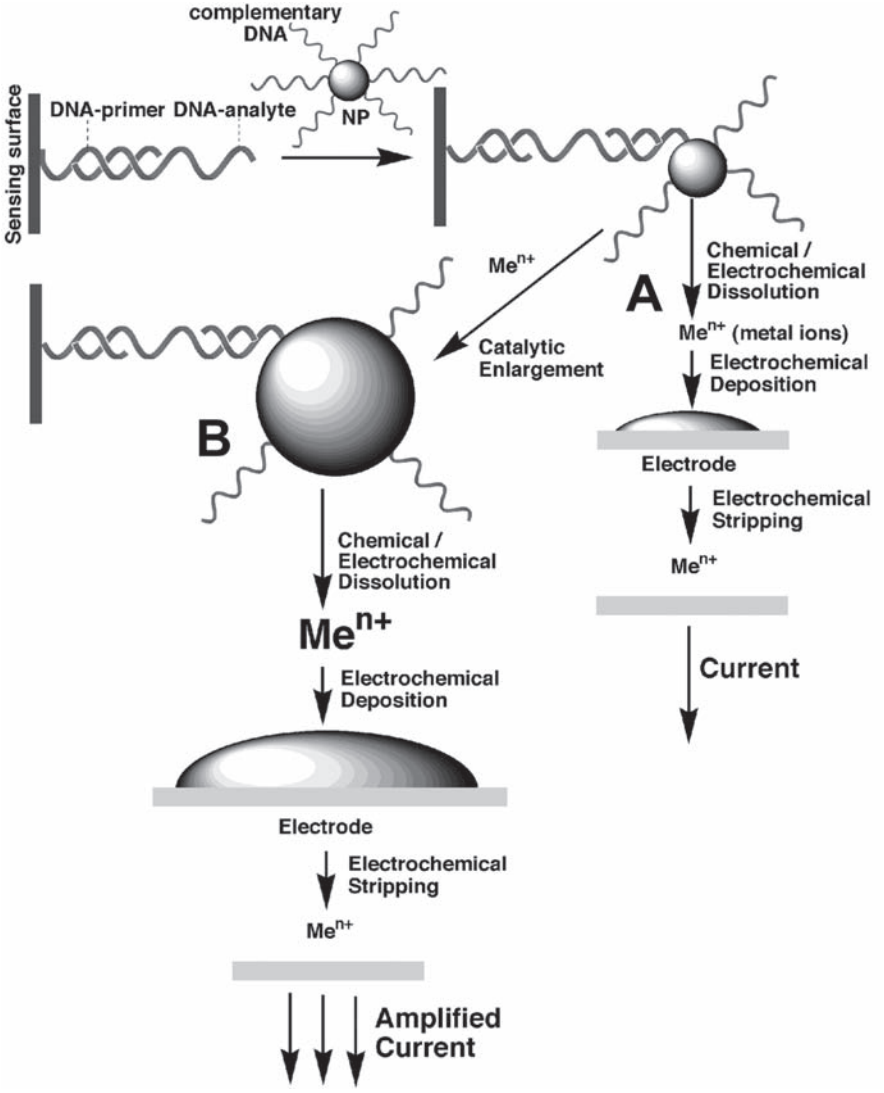

Fig. 8.20 (**A**) DNA analysis based on stripping voltammetry of metal NPs associated with the sensing interface. (**B**) Sequential amplification of DNA analysis by stripping analysis using the catalytic enlargement of the metal NPs associated with the sensing interface, and the dissolution of the enlarged NPs

The nanoparticles that act as amplifying tracers for DNA analysis can be from other inorganic compositions. For example, metal sulfides, such as PbS, enable the surface association of thiolated nucleic acids and the formation of a labeling conjugate.[72] Accordingly, a probe nucleic acid was immobilized onto a polypyrrole-functionalized glassy carbon electrode. The hybridization of the complementary

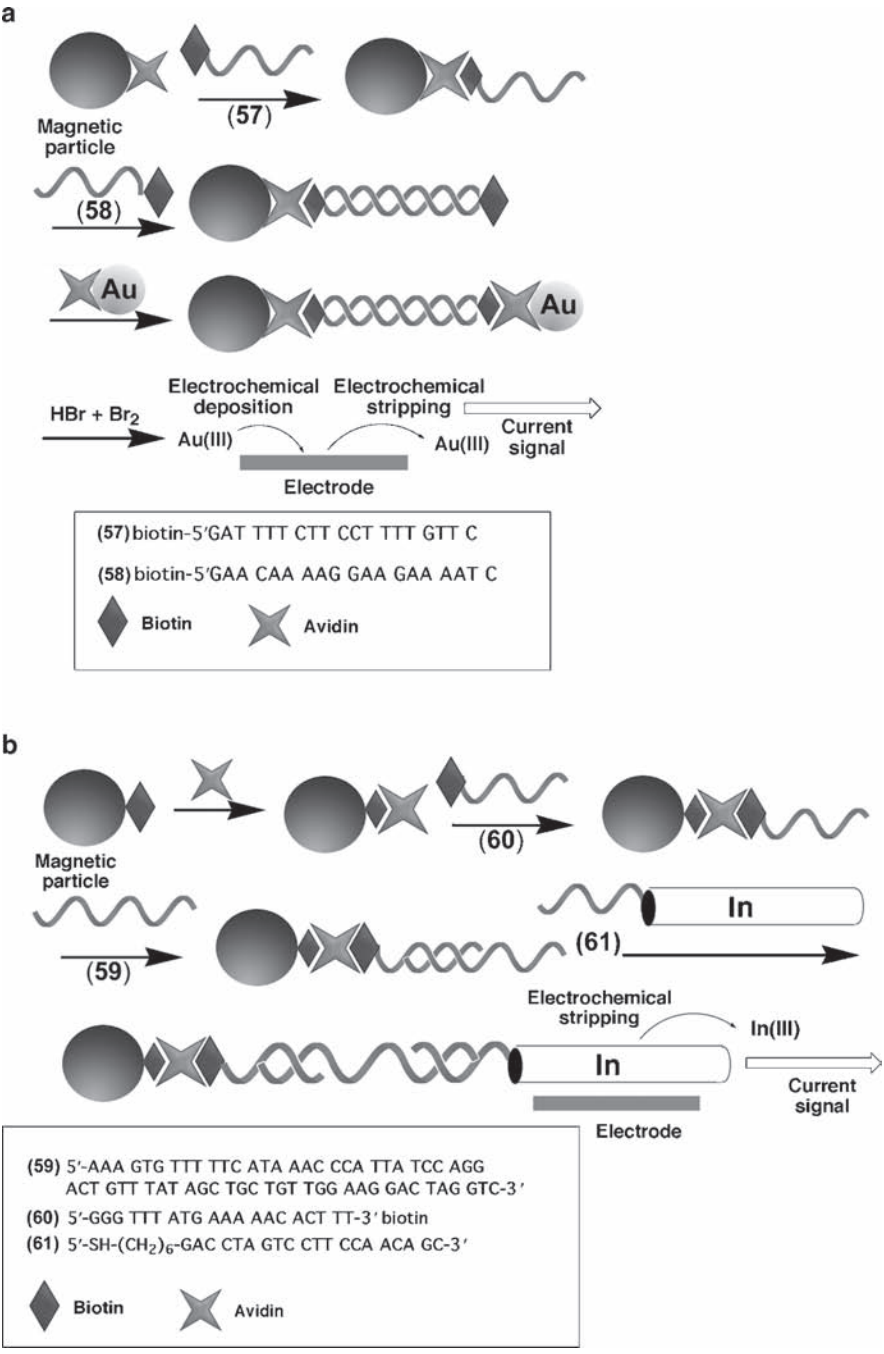

Fig. 8.21 (**a**) Analysis of DNA by stripping voltammetry of metal NPs associated with the sensing interface linked to magnetic particles. (**b**) Analysis of DNA using anodic stripping voltammetry of In nano-rods associated with an oligonucleotide duplex assembly

nucleic acid-functionalized PbS NPs was followed by the acidic dissolution of the particles. The electrochemical reduction of the released ions and the deposition of Pb^0 onto the electrode, followed by the anodic potentiometric stripping off of the deposited metal, were used for the electrochemical transduction of the DNA hybridization event. Other metal sulfides, such as CdS, were similarly employed for the amplified analysis of DNA.[73] The variety of metal sulfides, and the different stripping potentials of the metals, enable the use of mixtures of metal sulfides as a composite for the parallel amplified analysis of different DNAs; this has been demonstrated[74] with the parallel analysis of three different mutants related to the BRCA1 breast cancer gene (Fig. 8.22a). Magnetic particles were functionalized with three different probe nucleic acids, (**62**), (**63**), and (**64**), each complementary to a different BRCA1 mutant, (**65**), (**66**), and (**67**), respectively. Treatment of the magnetic particles with a mixture of all mutants (or a part of them) resulted in the hybridization of the mutants with the respective probe units. Three different

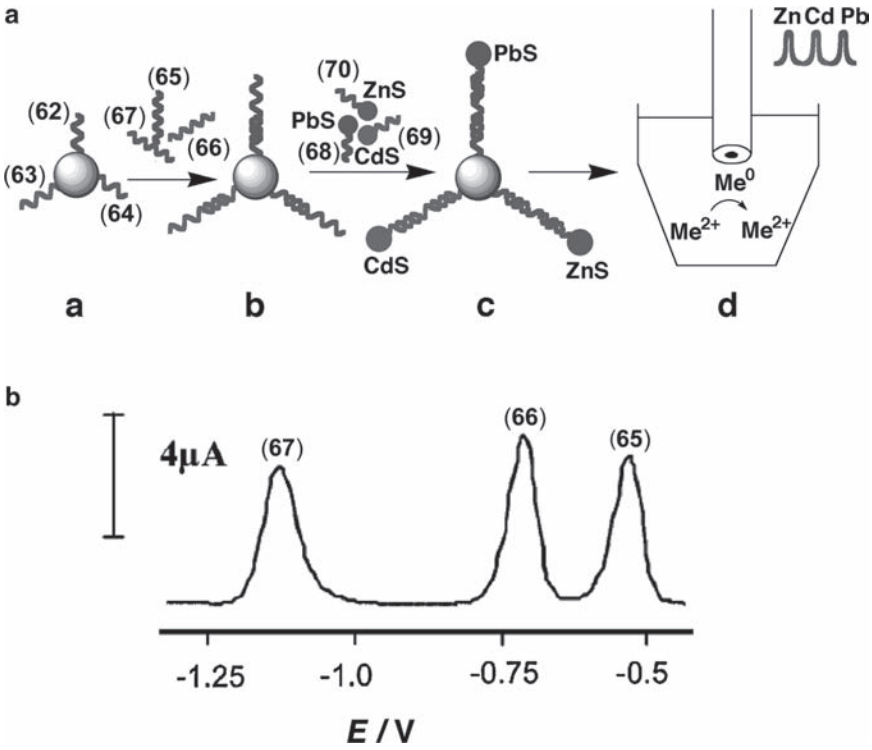

Fig. 8.22 (**a**) Multitarget electrochemical detection of DNA by different nanocrystal labels: (*a*) introduction of probe-modified magnetic beads; (*b*) hybridization with the DNA targets; (*c*) second hybridization with the NP-labeled oligonucleotides; (*d*) Dissolution of the NPs and the electrochemical detection of the released ions. (**b**) Stripping voltammogram corresponding to the simultaneous analysis of three different 60-mer DNA targets (**65**–**67**; 54 nM each), which are related to the BRCA1 breast cancer gene. The DNA molecules are labeled with ZnS NPs, CdS NPs, and PbS NPs (Reprinted with permission from ref. 74. Copyright American Chemical Society)

metal sulfide NPs, ZnS, CdS and PbS, were each functionalized with the nucleic acids, (**68**), (**69**), and (**70**) that are complementary to the single-stranded end of the mutants, (**65**), (**66**), and (**67**), respectively. Provided that all the mutants were in the analyzed sample, all three tracer nucleic acid-functionalized metal sulfides hybridize with the nucleic acid complexes bound to the magnetic particles. The subsequent separation of the magnetic particles and the dissolution of the different metal sulfide NPs associated with the magnetic particles were followed by the electrochemical reduction of the released ions on the electrodes. The electrochemical stripping of the different metals (Fig. 8.22b) enabled then the quantitative analysis of each of the mutants by the encoded metal sulfide. This method allowed the simultaneous analysis of the different mutants with a detection limit of 2.7×10^{-10} M.

Nucleotide-functionalized Au NPs were used as labels for the detection of single-base polymorphism.[75] Au NPs functionalized with the C or T nucleotides (C-Au NP and T-Au NP) were reacted with a double-stranded duplex DNA that included a G-A base mismatch. The lack of interduplex H bonds between the two bases enabled the H-bonded association of the two labeled Au NPs to the mutation sites and the subsequent electrochemical detection of the base polymorphism. A related method[76] employed four different metal sulfide NPs (ZnS, CdS, PbS, or CuS), functionalized with the different nucleotides A, C, G, or T, as specific encoded labels for the bioelectronic detection of all possible eight one-base mismatches. Figure 8.23a depicts the eight possible polymorphic structures of a duplex DNA that includes a single-base mismatch, and the resulting H-bonded complex with the set of four nucleotide-functionalized metal sulfides. Each of the mutations is encoded with a different composition of tracing NPs. Figure 8.23b shows the stripping voltammograms upon analyzing eight different single-base mismatches by the mixture of the nucleotide-functionalized metal sulfide. Although the fully matched duplex DNA did not allow the association of any of the particles to the double-stranded nucleic acid, and hence led to no voltammetric response, each of the single-base mismatches led to the association of the complementary NPs. By decoding of the voltammetric responses, the base composition of the mismatched site could be elucidated. This method was extended to analyze several base mismatches in a single DNA duplex.

The properties of metallic NPs that act as catalysts for the growth of particles provide a secondary means to amplify DNA analysis (see Fig. 8.20b). For example, the nanoparticle-promoted precipitation of gold[77] or silver[78] on Au NP labels associated with DNA duplexes, and the subsequent electrochemical stripping of the enlarged particles, enable the sub-picomolar detection of DNA. A related approach to amplify DNA detection via the catalytic enlargement of metallic nanoclusters made use of the fact that ions bind to the phosphate residues of DNA. The reduction of these ions yields metallic nanoclusters on the DNA backbone that act as catalytic seeds for their enlargement. Electrochemical stripping of the deposited metal provides then the readout signal for the formation of the duplex DNA.[78] Silver ions were linked to duplex DNA formed on an electrode. The chemical reduction of the ions by hydroquinone led to the formation of Ag^0 nanoclusters that were further enlarged by chemical means. The electrochemical stripping of the deposited metal was then used to transduce the formation of the double-stranded DNA.

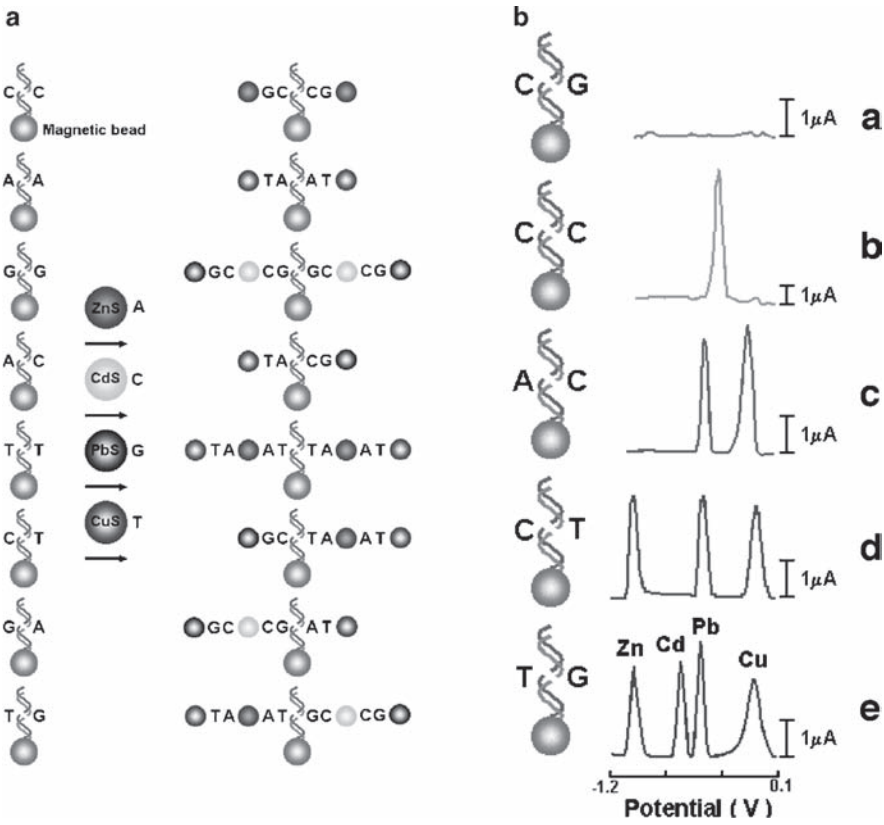

Fig. 8.23 (**a**) Electrochemical coding of all eight possible one-base mismatches in duplex DNAs using inorganic nanocrystal tracers. Use of mismatch-containing hybrids (captured on magnetic beads) followed by sequential additions of ZnS-linked adenosine-5′-monophosphate, CdS-linked cytidine-5′-monophosphate, PbS-linked guanosine-5′-monophosphate, and CuS-linked thymidine-5′-monophosphate. Also shown (*right*) are the corresponding assemblies of nanocrystal-linked DNA/magnetic beads. (**b**) Stripping voltammograms for the analysis of fully complementary DNA (*a*), and hybrids containing C-C (*b*), A-C (c), C-T (*d*), and T-G (*e*) mismatches using adenosine-5′ monophosphate/ZnS, cytidine-5′ monophosphate/CdS, guanosine-5′ monophosphate/PbS, and thymidine-5′monophosphate/CuS conjugates. The data were recorded in a 0.1 M acetate buffer (pH 4.9) containing 10 μg ml^{-1} Hg(II) (Reprinted with permission from ref. 76. Copyright American Chemical Society)

8.4.2 Amplified Microgravimetric Analysis of DNA with NPs

Nanoparticles provide a "weight label" that may be utilized for the development of amplified microgravimetric sensing methods (quartz crystal microbalance, QCM). Also, the catalytic properties of metallic NPs may be further employed to deposit metals on the NP-functionalized biorecognition complexes, thus enabling enhanced mass changes on the transducers (piezoelectric crystals) and thus amplified biosensing. For a quartz piezoelectric crystal (AT-cut), the resonance frequency of the

crystal changes by Δf when a mass change Δ*m* occurs on the crystal, according to the Sauerbrey equation (Eq. 8.1),[79] where f_0 is the fundamental frequency of the quartz crystal, Δ*m* is the mass change, A is the piezoelectrically active area, ρ_q is the density of quartz (2.648 g·m^{-3}), and μ_q is the shear modulus (2.947×10^{11} dyn·cm^{-2} for AT-cut quartz). Thus, any mass changes on the piezoelectric crystals are accompanied by a frequency change in the resonance frequency of the crystal.

$$\Delta f = -2f_0^2 [\Delta m / A (\mu_q \rho_q)^{1/2}] \tag{8.1}$$

The microgravimetric quartz crystal microbalance (QCM) method was applied for the amplified detection of DNA using nucleic acid-functionalized Au NPs as "weight labels."[80–82] A target DNA molecule (**72**) was hybridized to a Au–quartz crystal that was modified with a probe oligonucleotide (**71**), and the (**73**)-functionalized Au NPs were hybridized to the 3′-end of the duplex DNA associated with the crystal (Fig. 8.24). The subsequent secondary dendritic amplification was achieved by the interaction of the resulting interface with the target DNA (**72**) that was pretreated with the (**71**)-functionalized Au NP.[81,83] Concentrations of DNA (**72**) as low as 1×10^{-10} M could be detected by the amplification of the target DNA by the nucleic acid-functionalized Au NP labels. Also, the detection of DNA using nucleic acid-functionalized Au NPs and catalytic metal deposition on the NP labels was reported.[84,85] The Au NPs act as catalytic "seeds" and catalyze the reduction of $AuCl_4^-$ and the deposition of gold on the Au NPs. Thus, the catalytic enlargement of the nanoparticles increased the mass associated with the piezoelectric crystal and provided an active amplification route for the amplified microgravimetric detection of the DNA. For example, Fig. 8.25a depicts the amplified detection of the 7249-base M13mp18 DNA by using the catalytic deposition of gold on an Au NP conjugate.[85] The DNA primer (**74**) was assembled on an Au–quartz crystal. After hybridization with M13mp18 DNA (**75**), the double-stranded assembly was replicated in the presence of a mixture of nucleotides (deoxynucleotide triphosphates, dNTP mixture) that included dATP, dGTP, dUTP, and biotinylated dCTP (B-dCTP), and polymerase (Klenow fragment). The resulting biotin-labeled replica was then treated with the streptavidin–Au NP conjugate (Sav-Au NP) (**76**), and the resulting Au-labeled replica was subjected to the Au NP-catalyzed deposition of gold by the NH_2OH-stimulated reduction of $AuCl_4^-$. The replication process represents the primary amplification step, as it increases the mass associated with the crystal and simultaneously generates a high number of biotin labels for the association of the streptavidin–Au NP conjugate (Sav-Au NP). The binding of the conjugate represents the secondary amplification step for the analysis of M13mp18 DNA. The third step, which involves the catalyzed precipitation of the metal, led to the greatest amplification in the sensing process as a result of the increase in the mass of the Au NPs. This method enabled to sense the M13mp18 DNA with a detection limit corresponding to $\approx 1 \times 10^{-15}$ M.

This amplification method was also applied for analyzing a single-base mismatch in DNA (Fig. 8.25b),[84,85] exemplified with the analysis of the DNA mutant, (**78**), which differs from the normal gene, (**78a**), by the substitution of an A base

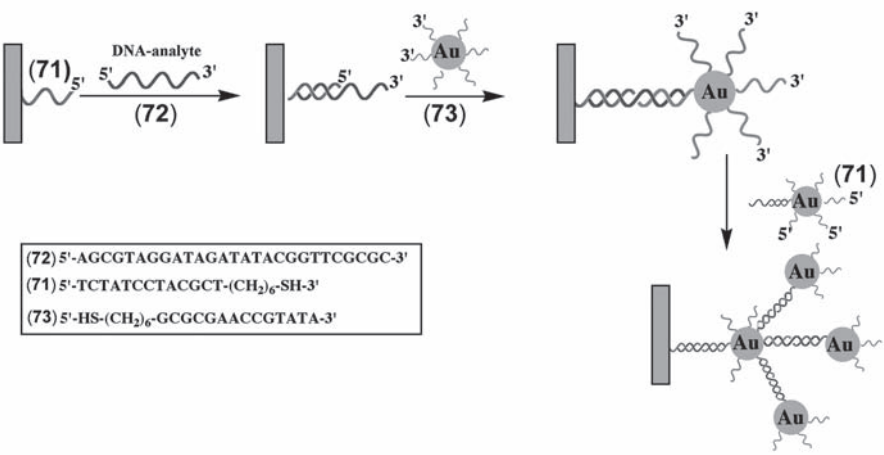

Fig. 8.24 Dendritic amplified DNA sensing by the use of oligonucleotide-functionalized Au NPs, which are assembled on a quartz crystal microbalance (QCM) electrode (Reproduced from ref. 81 by permission of The Royal Society of Chemistry)

with a G base. The analysis of the mutant was performed by the immobilization of the probe DNA, (**77**), which is complementary to the normal gene, (**78a**), as well as to the mutant, (**78**) (up to one base before the mutation site), on the Au–quartz crystal. Hybridization of the normal gene, or the mutant, with the probe interface, followed by the reaction of the hybridized surfaces with biotinylated dCTP (B-dCTP) in the presence of polymerase (Klenow fragment), led to the incorporation of the biotin-labeled base only into the assembly that included the mutant, (**78**). The subsequent association of the Sav-Au NP conjugate, (**76**), followed by the catalyzed deposition of gold on the Au NPs, led to the amplified analysis of the single-base mismatch in (**78**). Figure 8.25c (curve a) shows the microgravimetric detection of the mutant, (**78a**), revealing a frequency change of $\Delta f = -700$ Hz upon analyzing (**78a**), 3×10^{-9} M. The normal gene, (**78a**), does not alter the frequency of the crystal (Fig. 8.25c, curve b). The mutant could be detected with a detection limit of 3×10^{-16} M.

8.5 Amplified Electrochemical Analysis of DNA Using Micro-/Nano-carriers of Labels or Micro-/Nano-objects That Control the Interface Properties of Electrodes

Different micro-carriers of electrochemically detectable labels were employed to amplify the detection of DNA. For example, polystyrene beads or carbon nanotubes (CNT) were employed as carriers of electrochemically detectable substrates.

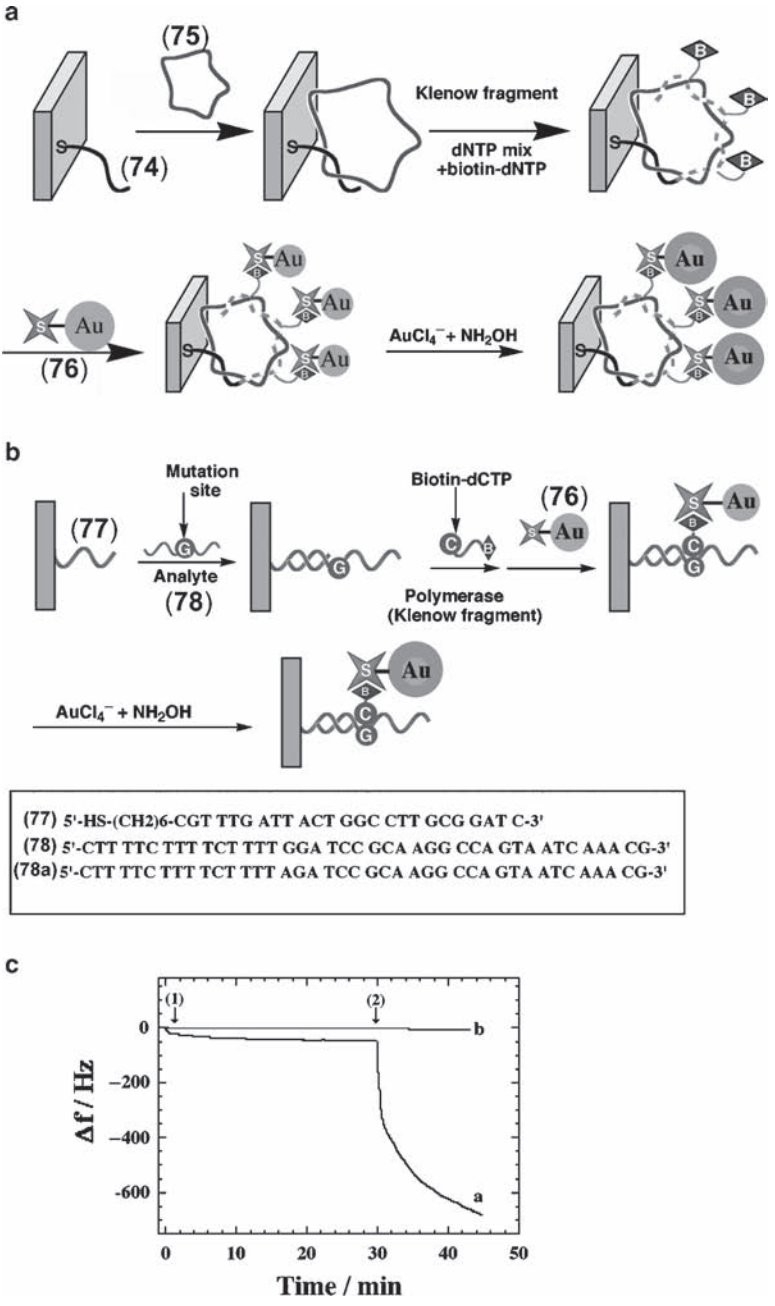

Fig. 8.25 (**a**) Amplified detection of the 7249-base M13mp18 DNA (**75**) using the catalytic deposition of gold on an Au NP conjugate. (**b**) Analysis of a single-base mismatch in DNA (**78**) using the catalytic deposition of gold on an Au NP conjugate. (**c**) Microgravimetric detection of a single-base mutant (**78**) enhanced by the catalytic deposition of gold on an Au NP conjugate. The frequency responses were observed with a mutant DNA (**78**) (*a*), and with a normal DNA (**78a**) (*b*). *Arrow 1* shows the attachment of the Sav-Au NP conjugate (**76**) and *arrow 2* shows catalytic deposition of gold on the Au NPs (Reproduced from ref. 85 by permission of The Royal Society of Chemistry)

Magnetic particles were functionalized with the probe nucleic acid, (**79**), and ferrocene carboxaldehyde, (**80**), was embedded in polystyrene beads that were modified with the nucleic acid, (**81**), that is complementary to the probe nucleic acid (Fig. 8.26a).[86] The hybridization of the polystyrene beads, that acted as carriers of the redox labels, with the (**79**)-modified magnetic particles was followed by the magnetic separation of the magnetic particles/polystyrene beads aggregates. The dissolution of the phystyrene beads resulted in the release of numerous redox relay units as a result of a low number of recognition events. The voltammetric response of the ferrocene units then provided a quantitative assay for the DNA detection. A related system has employed the polystyrene beads as a micro-carrier of Au NPs that were detected electrochemically (Fig. 8.26b).[87] Magnetic particles were modified with the probe nucleic acid (**82**), and the complementary biotinylated nucleic acid (**83**) was linked to the Au NP-modified avidin-functionalized polystyrene beads. The formation of the duplex DNA between the probe nucleic acid and the polystyrene beads was followed by the magnetic separation of the aggregates. The subsequent binding of biotin-labeled NPs to the avidin capping layer, the catalytic enlargement of the NPs, and the final dissolution of the enlarged NPs released numerous Au^{3+} ions that were voltammetrically analyzed. Similarly, carbon nanotubes (CNTs) were used as carriers for the electrochemically detectable labels.[88] Surfaces were functionalized with the probe nucleic acid, and CNTs modified with Au or CdS NPs were linked to the probe–analyte nucleic acid tracing duplex structure through biotin–avidin bridges. The acidic dissolution of the NPs and the voltammetric stripping of the released ions was then used to amplify the detection of DNA.

Liposomes were used as nanostructures for the amplified electrochemical detection of DNA through the control of the surface properties of the electrode. The labeling of DNA duplex structures assembled on electrodes with liposomes could control the surface properties of electrodes by the formation of a double-layer hydrophobic interface or by the use of charged liposomes that yield a double charged layer with electrostatic repulsive properties. Accordingly, electrodes functionalized with the probe nucleic acid, (**84**), were used as the sensing surfaces of the analyte nucleic acid, (**85**) (see Fig. 8.27a). The hybridization of the nucleic acid (**86**)-functionalized liposomes with the DNA duplex associated with the electrode generated a negatively charged interface on the electrode surface.[89] Faradaic impedance spectroscopy provides an effective means to probe the capacitance and electron-transfer resistances at electrode surfaces.[7,35] As the (**86**)-functionalized liposomes (~10 nm diameter) generate a negatively charged interface on the electrode, the electron transfer from the electrode to a negatively charged redox label in the solution is perturbed by the electrostatic repulsion of the redox label from the electrode. Figure 8.27b shows the Faradaic impedance spectra in the form of the Nyquist plot upon the stepwise analysis of (**85**) according to Fig. 8.27a, while using $Fe(CN)_6^{3-/4-}$ as redox label. The immobilization of the probe nucleic acid, (**84**), and its hybridization with (**85**) were accompanied by slight increases in the interfacial electron-transfer resistances (the diameter of the semicircle domain on the Z_{re} axis), due to the electrostatic repulsion of the redox

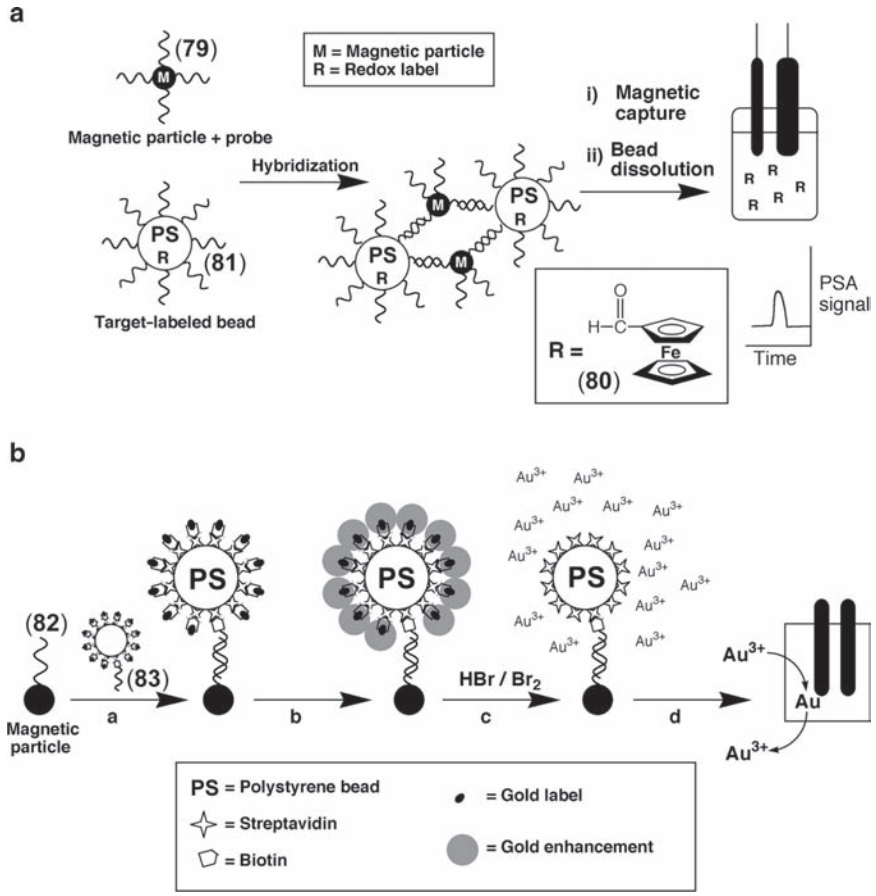

Fig. 8.26 (**a**) The amplified detection of DNA with polystyrene beads loaded with the ferrocene redox marker, (**80**). (**b**) Amplified detection of DNA by using nucleic acid–Au NP-functionalized beads as labels and electroless catalytic deposition of gold on the NPs as a means of amplification: *a*, hybridization of the nucleic acid–Au NP-functionalized beads with the target DNA that is associated with a magnetic particle; *b*, enhanced catalytic deposition of gold on the NPs; *c*, dissolution of the gold clusters; *d*, detection of the released Au^{3+} ions by stripping voltammetry (Part **a** reprinted with permission from ref. 86. Copyright American Chemical Society)

label by the single-stranded nucleic acid and the duplex structure, respectively. The association of the (**86**)-tagged liposome to the duplex DNA associated with the electrode resulted in a pronounced increase in the interfacial electron-transfer resistance, $\Delta R_{et} = 11.0\,k\Omega$, consistent with the electrostatic barrier generated by the negatively charged liposomes. As the number of recognition events controls the coverage of the electrode by the labeled liposomes, the changes in the interfacial electron-transfer resistances at the electrode relate to the bulk concentration of the analyzed DNA (**85**). The inset in Fig. 8.27b depicts the resulting calibration curve.

The sensitivity limit for analyzing (**85**) by the (**86**)-labeled liposomes as amplifying units was 1×10^{-12} M.

A different configuration for the amplified analysis of DNA by biotin-tagged liposomes and using Faradaic impedance spectroscopy as transduction means is displayed in Fig. 8.28a.[89] The duplex DNA generated on the electrode support by the hybridization of (**85**) with the probe nucleic acid (**84**) was further hybridized with the biotin-labeled nucleic acid (**87**). The association of avidin to the electrode surface followed by the binding of biotin-tagged liposomes (**88**) onto the interface led to the coverage of the electrode with the blocking interface of the liposomes. The resulting liposome-modified electrode enabled the subsequent dendritic

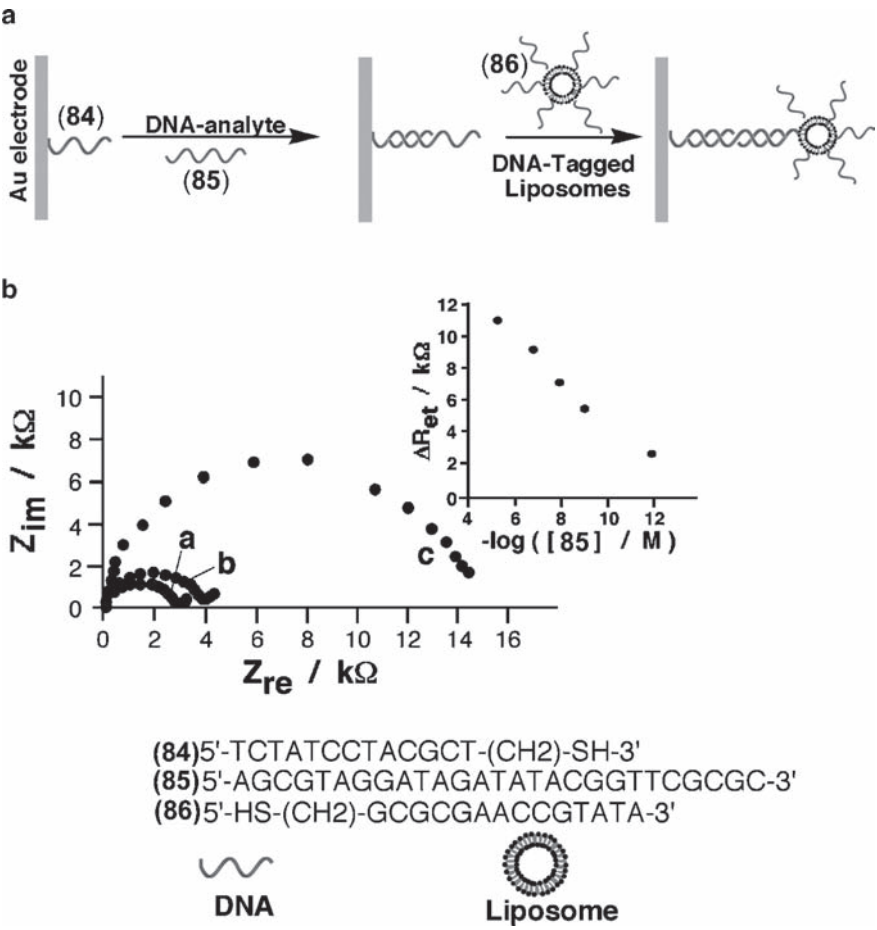

Fig. 8.27 (**a**) Amplified analysis of a target DNA by oligonucleotide-functionalized liposomes. (**b**) Faradaic impedance spectra of the **84**-functionalized Au electrode (a) The 84-functionalized Au electrode; (b) After hybridization of the electrode surface with (**85**), 5×10^{-6}M. (c) After association of the **86**-functionalized liposomes. (Reproduced with permission from ref. 89. Copyright American Chemical Society)

amplification of the primary hybridization event of (**85**) by the generation of a second and third shell of the biotin-tagged liposomes onto the surface using avidin-bridging units. Figure 8.28b shows the Faradaic impedance spectra observed upon the analysis of (**85**) according to Fig. 8.28a. The association of the first shell of the avidin–biotin-tagged liposomes increased the interfacial electron-transfer resistance to a value of 15.5 kΩ (Fig. 8.28b, curve d), while the association of the second shell of avidin/biotin-tagged liposome further enhanced the interfacial electron-transfer resistance to the value of 21 kΩ (Fig. 8.28b, curve f). The resulting calibration curve for analyzing (**85**) (Fig. 8.28b, inset) indicates that the detection limit for analyzing (**85**) by the two-step amplification was 1×10^{-15} M. This result indicates that the dendritic amplification by the two-shell liposomes assembly enhanced by a factor of 10^3 the detection limit for analyzing (**85**) as compared to a single shell of tagged liposomes, albeit the analytical procedure is of higher complexity.

The biotin-functionalized liposomes were also employed for the amplified detection of single-base mutations (Fig. 8.29a),[89] as is exemplified with the analysis of genes, where the A-base in the normal gene, (**89**), is exchanged with a G-base to yield the mutant, (**90**). The probe nucleic acid, (**91**), that is complementary to the normal gene, as well as to the mutant up to the base before the mutation site, was immobilized through thiolated functionality to Au electrodes. The resulting modified electrodes were reacted with the mutant, (**90**), or the normal gene, (**89**), and these yield the respective duplexes on the electrodes. The subsequent reaction of the electrodes with biotinylated-dCTP in the presence of polymerase resulted in the incorporation of the biotin label into the duplex structure that included the G-mutation site, while the duplex containing the normal gene stayed unreacted. The subsequent binding of the biotin-labeled liposomes onto the biotin-tagged duplex through an avidin bridge enabled, then, the amplified detection of the mutant using Faradaic impedance spectroscopy as electronic transduction means. The normal gene-containing duplex did not allow, however, the association of the biotinylated label, and thus a tagged liposome was not linked to this interface. Figure 8.29b shows the Faradaic impedance spectra observed upon the analysis of the mutant, (**90**), where a change in the interfacial electron-transfer resistance of $\Delta R_{et} = 12.5\,\text{k}\Omega$ was observed upon analyzing 1×10^{-9} M of the mutant. As the surface coverage of the electrode is controlled by the surface coverage of the electrode with the mutant, the interfacial electron-transfer resistance upon the association of the liposomes is related to the bulk concentration of (**90**) (Fig. 8.29b, inset). Accordingly, the mutant was analyzed with a sensitivity limit that corresponded to 1×10^{-13} M.

Other nano-objects carrying tags that control the interfacial electron-transfer resistance at electrodes were similarly employed to amplify the detection of DNA using Faradaic impedance spectroscopy as transduction means. CdS nanoparticles functionalized with nucleic acids were used as tagged nano-objects that bind to duplex DNA assemblies associated with electrodes and, accordingly, increase the interfacial electron-transfer resistances to negatively charged redox labels in the electrolyte solution ($Fe(CN)_6^{3-/4-}$).[90]

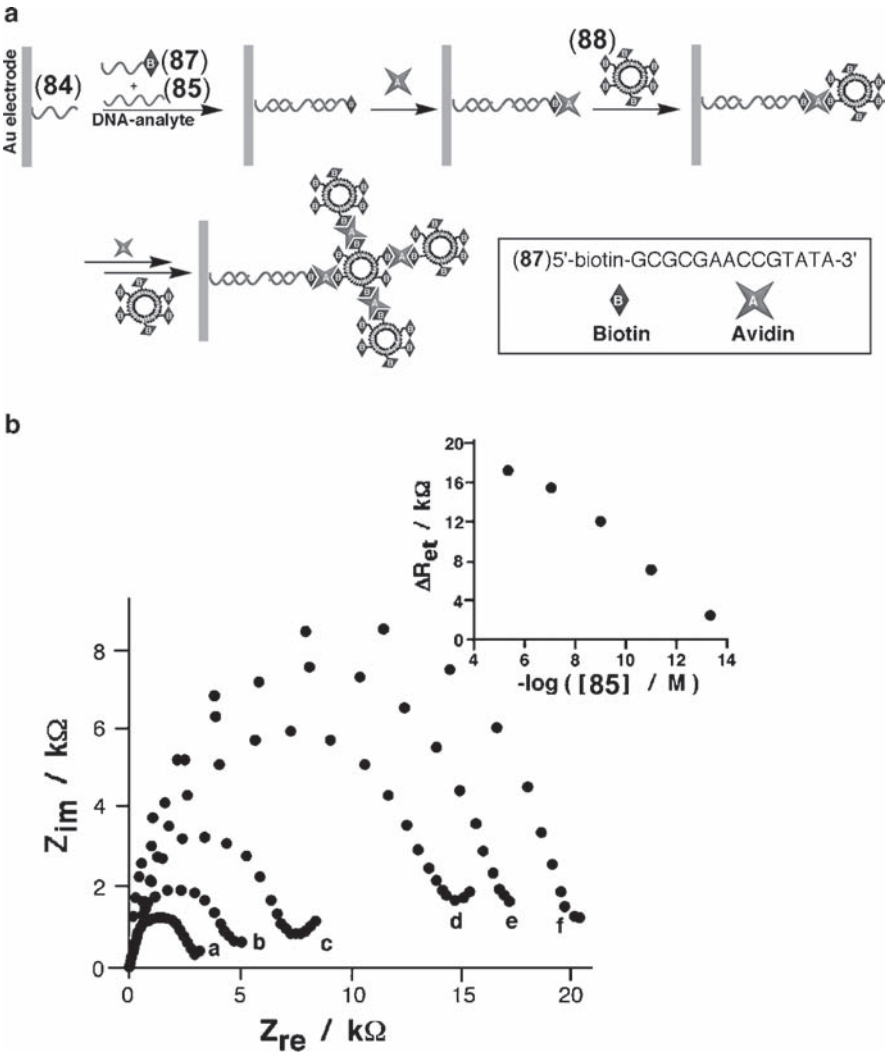

Fig. 8.28 (**a**) Amplified analysis of a target DNA by biotin-functionalized liposomes using avidin as a linker. (**b**) Faradaic impedance spectra of *a*, the **84**-functionalized Au electrode; *b*, after interaction of the sensing electrode with **85**, 5×10^{-6} M, that was pretreated with DNA–biotin conjugate (**87**) (**c**) After treatment with avidin; (**d**), after interaction with the biotinylated liposomes (**88**); *d*, after treatment of the interface for a second time with avidin; and (**f**) after interaction of the interface for a second time with the biotinylated liposomes. *Inset*: Calibration plot corresponding to the changes in the electron-transfer resistance of the sensing interface upon analyzing different concentrations of DNA (**85**), and enhancement of the sensing process by a double-step avidin/biotinylated liposome amplification path (Reproduced with permission from ref. 89. Copyright American Chemical Society)

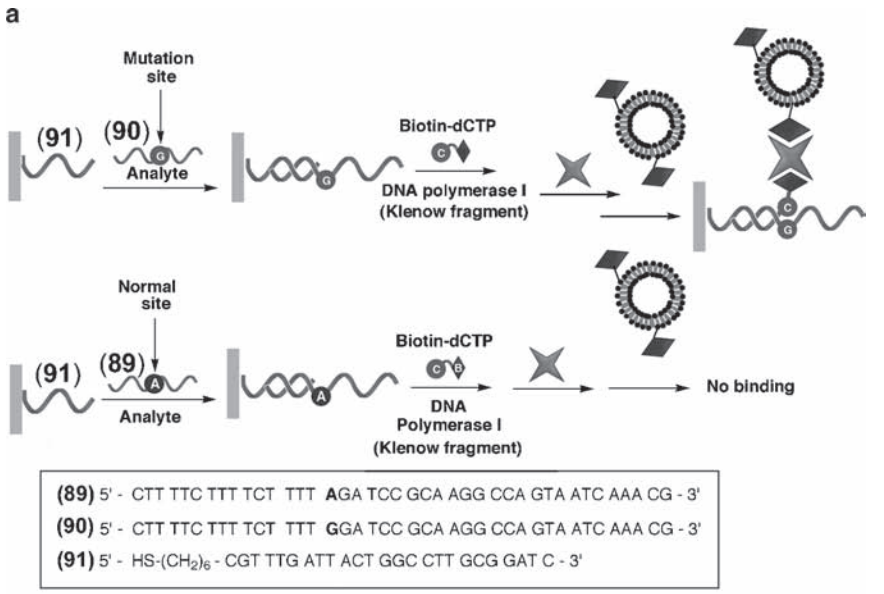

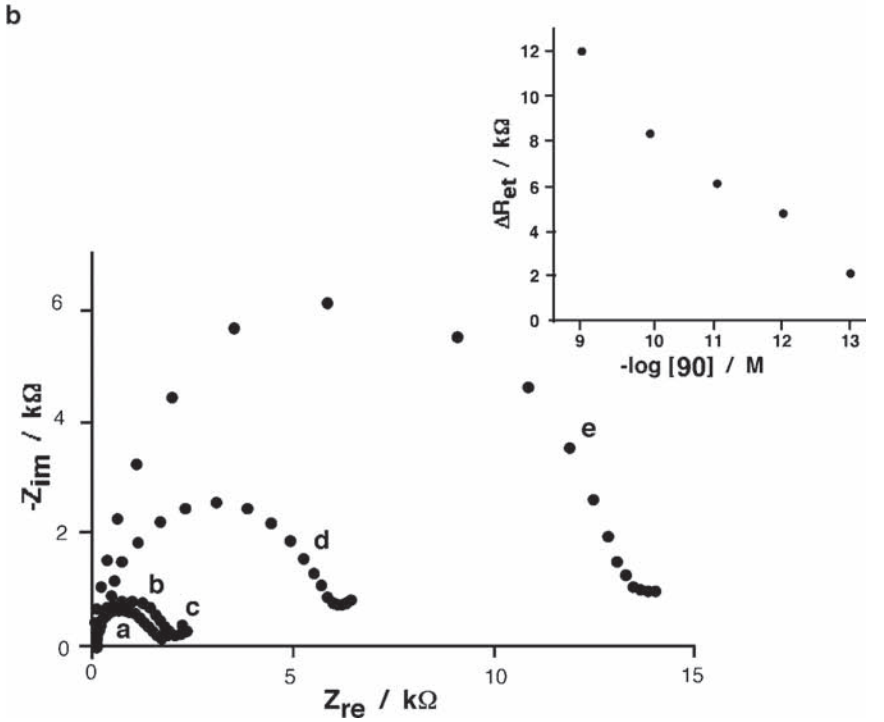

Fig. 8.29 (**a**) Electronic transduction of a single-base mutation in the target DNA, (**90**), using the polymerase-induced coupling of a biotinylated-base to the probe, (**91**), and the use of biotin-labeled liposomes as an amplification route. (**b**) Faradaic impedance spectra (Z_{im} vs. Z_{re}) upon the analysis of the single-base mismatch in **90**: a, the **91**-functionalized electrodes; b, the **91**-functionalized electrode after hybridization with **90**, 1×10^{-9} M; c, after reaction of the double-stranded

8.6 Amplified Optical Detection of DNA by DNA-Based Machines

The inherent dynamic properties of double-stranded DNA reflected by the thermally controlled sequence-dependent hybridization and separation of duplex DNA or by biocatalytic replication, scission, and strand displacement enable the use of DNA nanostructures as machinery elements. Substantial progress was recently accomplished with the design of DNA structures that duplicate machine functions such as tweezers,[91] walkers,[92] gears,[93] and more.[94,95] The advances in the area of DNA machines were recently reviewed.[96–98] The concept of DNA machines was extended to design amplified DNA sensors. The "DNA machine sensor" consists of a nucleic acid sequence that provides a template on which the machine operates. The template includes a recognition unit that, upon hybridizing with the target (analyte) DNA, triggers on the operation of the machine that reveals some fundamental features: (i) the machine requires for its operation a fuel; (ii) the machine performs a mechanical function (scission, rolling, etc.); and (iii) the operation of the machine yields a "waste product." This waste product might yield either an optical signal or act as a DNAzyme, and hence, the "waste product" may transduce the operation of the machine and amplify the primary recognition of the analyte DNA by the machine. The continuous generation of the waste product by the machine, and particularly, the generation of DNAzymes as a waste product, amplified the DNA sensing. Not surprising, such DNA-based machines were suggested as isothermal DNA sensor systems that could substitute PCR.

An autonomous DNA machine for the amplified detection of M13 phage DNA was developed by the use of polymerase and a nicking enzyme as biocatalysts that drive the operation of the DNA machine[99] (Fig. 8.30a). The nucleic acid, (**92**), acted as a "track" for operating the machine. It consisted of three domains, where domain I acts as the recognition unit for activating the machine, domain II is the domain where the machine is operating by repeated replication and scission, and domain III included the sequence complementary to the horseradish peroxidase-mimicking DNAzyme (see Section 8.2.2). A hairpin nucleic acid, (**93**), was used as the capture nucleic acid for analyzing the M13 phage DNA (**94**). In the presence of the M13 phage DNA analyte, the hairpin structure was opened, and the single-stranded released nucleic acid was hybridized with the recognition sequence of the DNA track, and this triggered the autonomous operation of the machine. In the presence of the dNTPs, the nucleotide mixture, acting as fuel, and polymerase the replication of the track was activated. The replication of domain I

Fig. 8.29 (continued) interface with biotinylated-dCTP, 20 μM, and polymerase Klenow fragment, 20 U ml^{-1}; d, after the interaction of the electrode with avidin, 2.5 μg ml^{-1}; and e, after the interaction of the interface with the biotinylated liposomes (lipid concentration, 0.25 mM). Inset: Calibration curve corresponding to the R_{et} values observed upon the sensing of different concentrations of the mutant, (**90**), according to the process outlined in **a** (Reproduced with permission from ref. 89. Copyright American Chemical Society)

generated the nicking site of the N.BbvC IA biocatalyst. Scission of the replicated DNA reactivated the polymerization at the nicking site and the displacement of the formerly synthesized DNA. The displaced nucleic acid, (**95**), self-assembled,

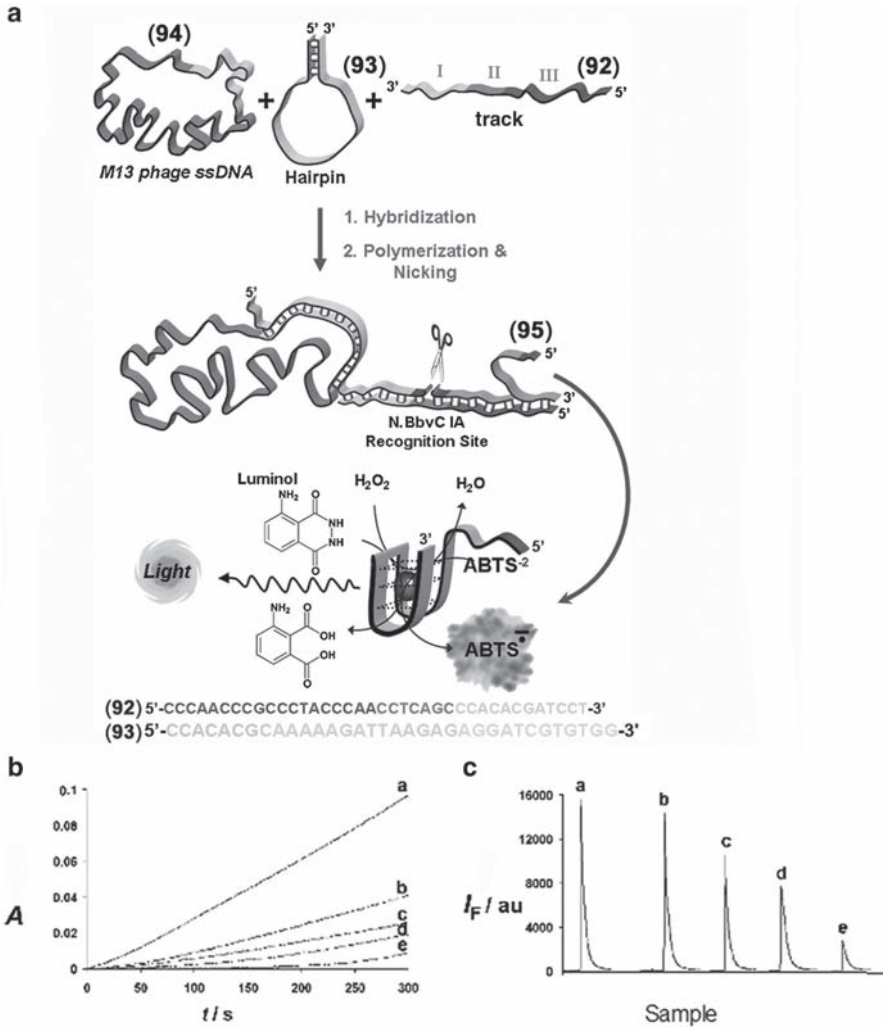

Fig. 8.30 (**a**) Primer-induced autonomous synthesis of DNAzyme units on a template DNA using polymerase/dNTPs and a nicking enzyme as biocatalysts. (**b**) Absorbance changes and (**c**) chemiluminescence intensities upon the oxidation of $ABTS^{2-}$ by H_2O_2 or the light emission by luminol/H_2O_2 by the DNA-based machine, upon analyzing different concentrations of M13 phage ssDNA (**94**): (*a*) 1×10^{-9} M, (*b*) 1×10^{-11} M, (*c*) 1×10^{-12} M, (*d*) 1×10^{-14} M, (*e*) analysis of the foreign calf-thymus ssDNA, 1×10^{-8} M. In all systems fixed concentrations of the hairpin, (**93**), 1×10^{-6} M, and the template, (**92**), 1×10^{-6} M, were used (Reproduced with permission from ref. 99. Copyright Wiley-VCH Verlag GmbH & Co. KGaA)

in the presence of hemin, to the horseradish peroxidase-mimicking DNAzyme that led to the colorimetric detection of the analyte M13 phage DNA through the DNAzyme-catalyzed oxidation of $ABTS^{2-}$ to its colored oxidized product ABTS., or by the biocatalyzed generation of chemiluminescence. The color signal or the chemiluminescence signal generated by the DNA machine was controlled by the concentration of the M13 phage DNA (Fig. 8.30b and c, respectively). The analyte could be detected with a sensitivity that corresponded to 1×10^{-15} M. A related approach has employed the displaced "waste product" as a nucleic acid that bridged Au NPs that included nucleic acid residues complementary to the released product.[100] The aggregation of the Au NPs and the color change of the system from red to blue, upon the aggregation of the Au NPs, resulting from the coupled interparticle exciton within the aggregate, was used as optical readout signal of the biosensing process.

A different method to amplify the detection of DNA has used[101,102] the rolling-circle amplification process (RCA) as machinery reaction (Fig. 8.31a). The circular DNA, (**97**), included the DNA recognition domain and three separated domains, each complementary to the horseradish peroxidase-mimicking DNAzyme. Upon the recognition of the target DNA, (**96**), and its hybridization with the circular DNA, (**97**), the RCA process was initiated by polymerase and the oligonucleotide dNTPs mixture, acting as fuel. The RCA process led to the formation of long DNA bands consisting of the self-assembled hemin/G-quadruplex DNAzyme units. Each evolution around the circular DNA led to the formation of three DNAzyme units. The resulting DNAzyme strips enabled the amplified colorimetric or chemiluminescent readout of the primary hybridization event of (**96**) to the circular DNA (Fig. 8.31b and c, respectively). The method was applied to analyze the M13 phage DNA with a sensitivity that corresponded to 1×10^{-14} M.

A different DNA machine for the amplified optical detection of DNA used the enzyme Fok I as catalyst for the replication of nucleic acid templates that utilize as fuel a nucleic acid that synthesizes the template and generates a fluorescent nucleotide as readout signal[103,104] (Fig. 8.32). This amplified detection method was demonstrated with the analysis of the Tay–Sachs genetic disorder mutant, (**98**). A double hairpin oligonucleotide, (**99**), was designed to include the specific duplex region for the specific binding of the Fok I biocatalyst, and the loop region for capturing the target mutant, (**98**). In the presence of the analyte mutant, (**98**), the duplex structure, (**100**), was generated, and these yield the duplex region that remotely cleaved by the enzyme to yield the products, (**101**) and (**102**), and the nucleic acid–Fok I complex, (**103**). The latter complex acted as an active cutter that produced the fluorescent product and replicated the molecular cutter templates. The fuel, (**104**), included the base sequence that binds to the cutter, (**103**), and it was modified by the fluorophore (FAM) and quencher (TAMRA) units. The hybridized configuration of the fuel resulted in a quenched, nonfluorescent, structure. The hybridization of the fuel with the cutter resulted in the Fok I-catalyzed scission of the fuel to generate the fluorophore-labeled nucleic acid, (**105**), the quencher-functionalized oligonucleotide, (**106**), and a new cutter unit. That is, the sensing of the mutant, (**98**), is accompanied

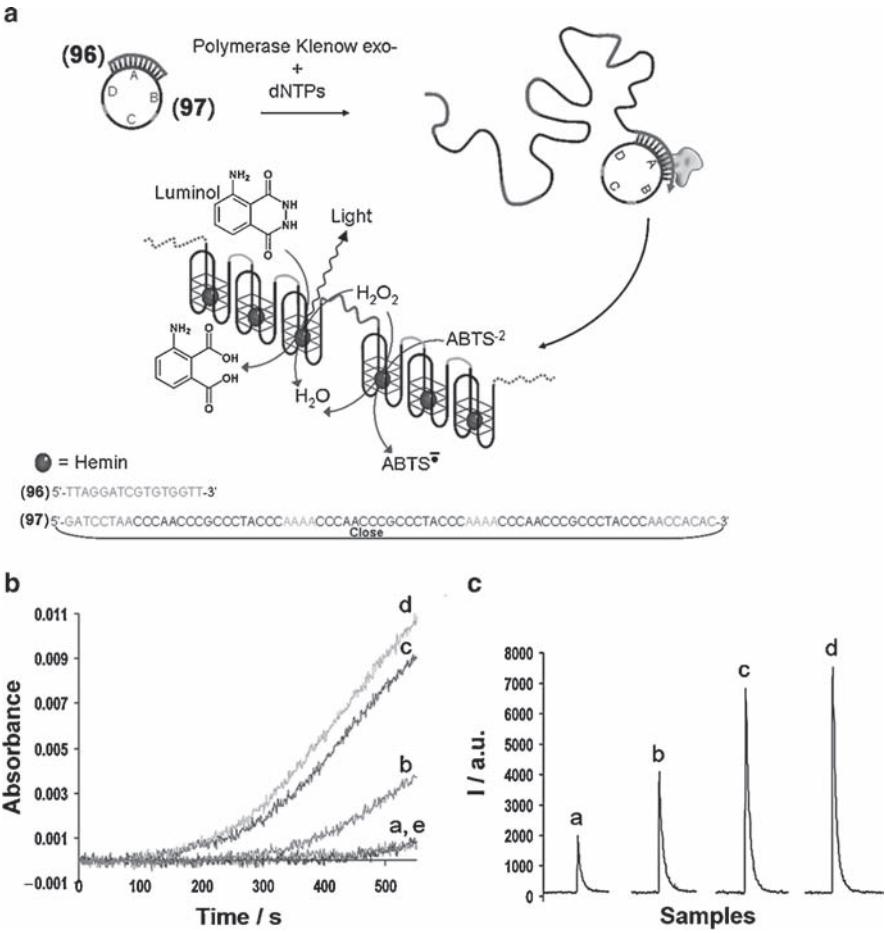

Fig. 8.31 (**a**) Detection of DNA hybridization by rolling-circle amplification (RCA) synthesizing DNAzyme chains. (**b**) Time-dependent absorbance changes upon analyzing the nucleic acid, (**96**), 2×10^{-8} M, for different time intervals by the RCA process that synthesizes the DNAzyme units: (*a*) 0 min, (*b*) 10 min, (*c*) 30 min, (*d*) 60 min, (*e*), analyzing (**96**) with the open circular DNA (**97**) (that was not treated with kinase and ligase to form the closed circular DNA). In experiments (*a*) to (*d*), the circular DNA, (**97**), 2×10^{-8} M, was present. (**c**) Chemiluminescence intensities observed upon the light emission by luminol/H_2O_2 by the RCA process at different time intervals and at the fixed concentrations of (**96**), 2×10^{-8} M, and (**97**), 2×10^{-8} M: (*a*) 0 min, (*b*) 10 min, (*c*) 30 min, (*d*) 60 min (Reproduced from ref. 101 by permission of The Royal Society of Chemistry)

by the replication and evolution of cutter units that enhance the consumption of the fuel and the generation of the fluorescence product. The analysis of the Tay–Sachs mutant by this Fok I–nucleic acid machine achieved a sensitivity that corresponded to 1×10^{-14} M.

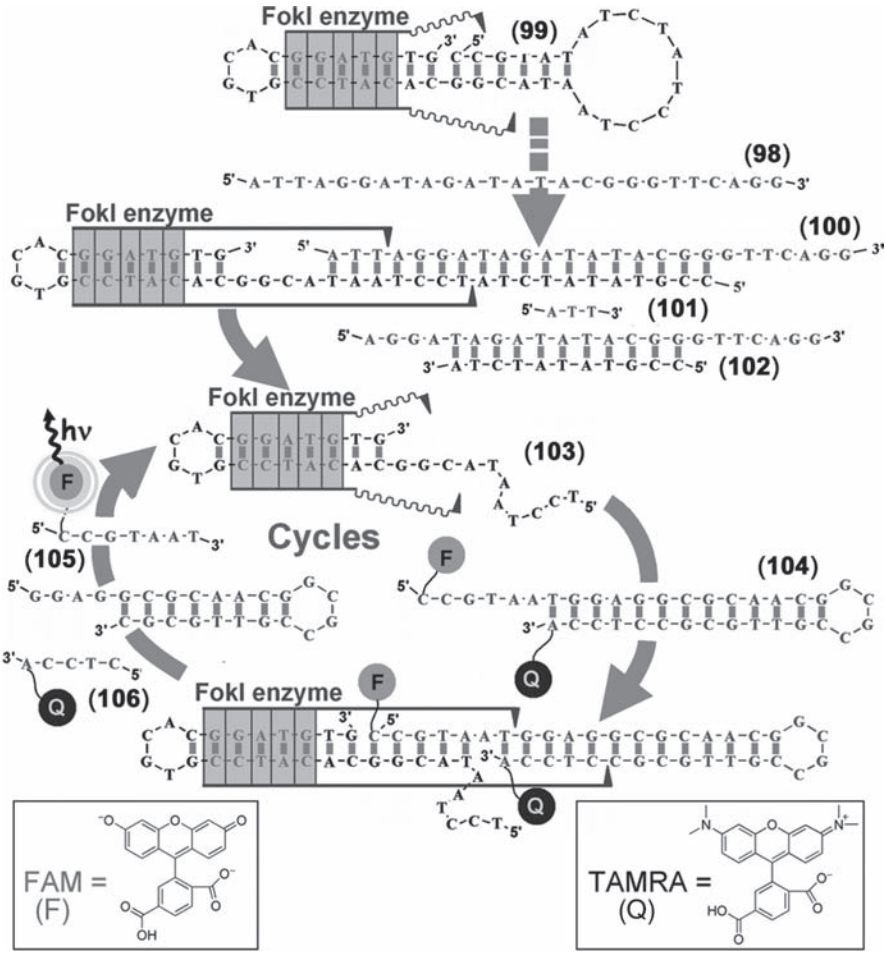

Fig. 8.32 Amplified detection of DNA using Fok I/DNA as a biocatalytic template for the scission of a fluorophore/quencher fuel substrate to the fluorescencent waste product (Reproduced with permission from ref. 103. Copyright Wiley-VCH Verlag GmbH & Co. KGaA)

8.7 Photoelectrochemical Detection of DNA

The photoexcitation of semiconductor NPs (quantum dots) results in the transfer of valence band electrons to the conduction band, thus yielding electron-hole pairs. The electron-hole recombination leads to size-controlled fluorescence of the semiconductor quantum dots. This property was extensively used by applying the quantum dots as optical labels for biorecognition events and, specifically, DNA detection.[105–107] The coupling of semiconductor NPs to electrodes allows, however,

an alternative path for the utilization of the electron-hole pairs in the generation of photocurrents (Fig. 8.33). The transfer of the photoexcited conduction band electrons to the electrode with the concomitant reduction of the valence band holes by an electron donor (Fig. 8.33a) yields an anodic photocurrent, while the ejection of the conduction band electrons to a solution-solubilized electron acceptor with the concomitant transfer of electrons from the electrode to the valence band holes yields a cathodic photocurrent (Fig. 8.33b). The photoelectrochemical functions of semiconductor NPs are extensively used in the development of light to electrical energy conversion systems.[108,109] The labeling of biorecognition complexes occurring on electrode surfaces with semiconductor NPs allows the use of the photoelectrochemical phenomenon, and the current resulting upon the photoexcitation of the NPs, as an electronic transduction means.

The amplified photoelectrochemical readout of DNA recognition events occurring on electrode surfaces was reported with the use of CdS NPs as photocurrent generation labels[110] (Fig. 8.34a). An Au electrode was modified with the probe thiolated nucleic acid, (**107**). The target DNA, (**108**), was hybridized at its 3′-end with the sensing interface, and the thiolated nucleic acid (**109**)-modified CdS NPs, and then hybridized to the 5′-end of the target DNA. The (**107**)-nucleic acid-functionalized CdS NPs were hybridized with (**108**), and the modified NPs were then hybridized with the first layer of CdS NPs. Subsequently, the (**109**)-functionalized CdS NPs were hybridized with the target DNA, (**108**), and the particles were linked as a third NP generation onto the electrode. By a stepwise and sequential procedure, a controlled number of CdS NP layers cross-linked by the analyte DNA were generated on the electrode. The transduced photocurrent was controlled by the number of CdS NP generations formed on the electrodes (Fig. 8.34b). The inefficient photocurrents generated by the CdS NPs bridged to the electrode by the respective duplex DNA hybrids was attributed to poor electrical contacting between the NPs and the electrode due to the inefficient charge transport through the duplex DNA bridges. To

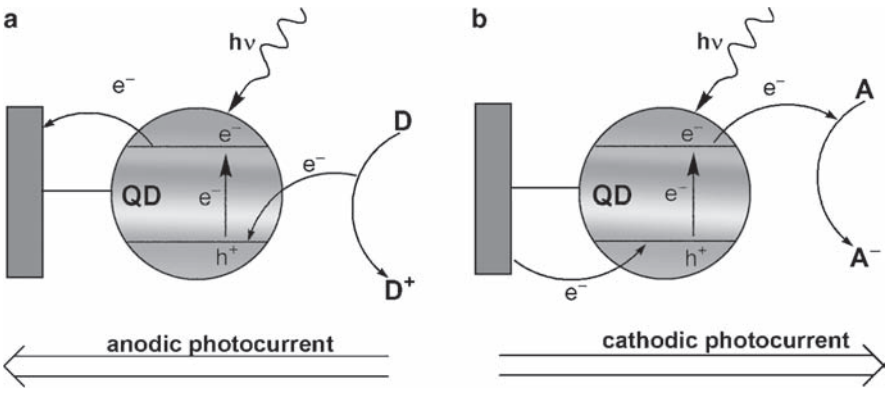

Fig. 8.33 Photocurrent generated by semiconductor NPs associated with electrodes: (**a**) anodic photocurrent; (**b**) cathodic photocurrent

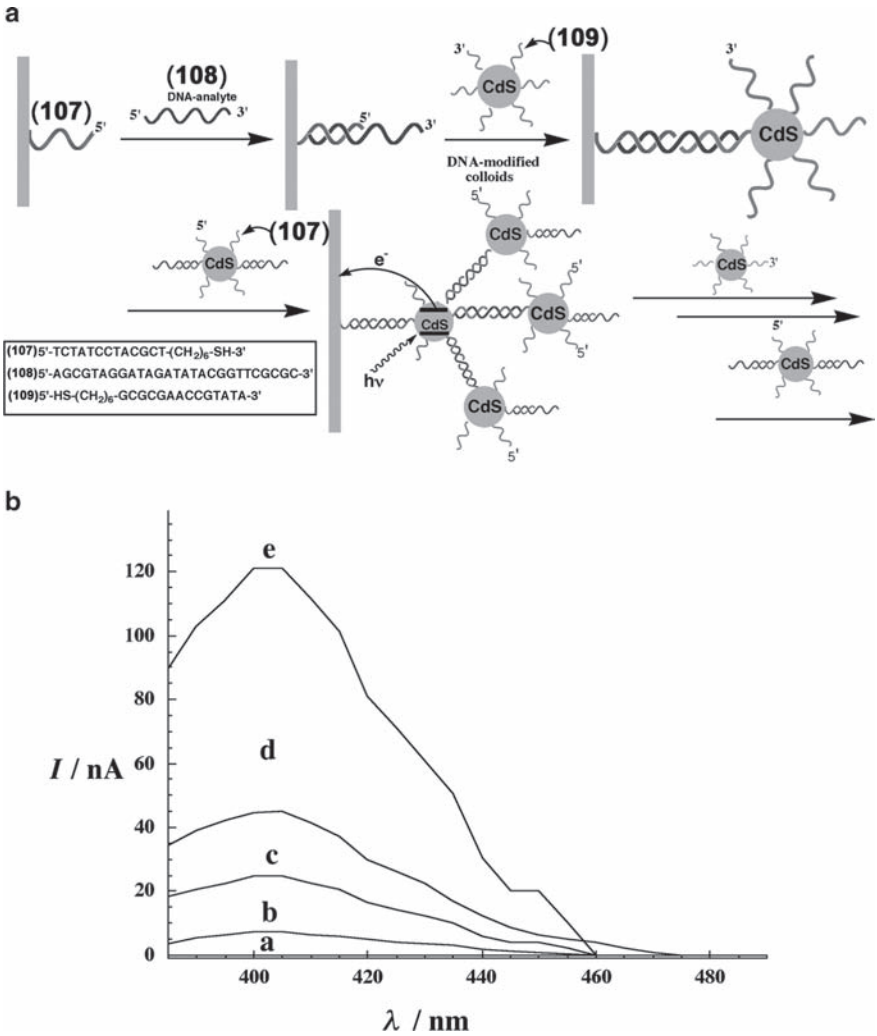

Fig. 8.34 (**a**) The assembly of an oligonucleotide/DNA-cross-linked array of CdS nanoparticles on a Au electrode, and the photoelectrochemical response of the nanoarchitecture. (**b**) Photocurrent action spectra of Au electrodes that include controlled numbers of oligonucleotide/DNA-cross-linked CdS nanoparticle layers: *a*, before the deposition of CdS nanoparticles; *b–e*, one to four oligonucleotide/DNA-cross-linked CdS nanoparticle layers (Reproduced with permission from ref. 110. Copyright Wiley-VCH Verlag GmbH & Co. KGaA)

overcome this limitation, and to specifically monitor double-stranded DNA structures associated with the electrode, redox-active intercalators specific to the duplex DNA structures were incorporated into the hybrids, and these acted as charge relays that shuttled the electrons between the CdS semiconductor NPs and the electrode.[111] The dithiol-tethered single-stranded DNA was assembled on an Au electrode, and

it was subsequently hybridized with a complementary dithiolated ssDNA to yield a double-stranded DNA. The resulted surface was treated with CdS NPs to yield a semiconductor nanoparticle-modified electrode surface. The irradiation of the dsDNA/CdS-NPs-functionalized electrode in the presence of triethanolamine (TEOA) as electron donor resulted in an anodic low-intensity photocurrent. The observed generated photocurrent was attributed to an imperfect structure of the CdS NPs/DNA assembly that resulted in direct contact between the NPs and the electrode, rather than from charge transport through the DNA. The DNA duplex structure linked to the CdS NPs and bridging them to the electrode was employed, however, as a medium to incorporate redox-active intercalators that mediate electron transport from the NPs to the electrode. It was found that methylene blue (MB), a typical intercalator for the DNA duplex, facilitated the generation of the enhanced photocurrent. An anodic photocurrent was generated in the system in the presence of TEOA as electron donor and methylene blue intercalated into the dsDNA, and while applying a potential of 0 V (vs. SCE) on the electrode. At this potential, MB exists in its oxidized state that acts as an electron acceptor of the photoexcited conduction band electrons. The resulting photocurrent was about fourfold higher than that recorded in the absence of the intercalator. The enhanced photocurrent was attributed to the trapping of conduction-band electrons by the intercalator units and their transfer to the electrode that was biased at 0 V, thus retaining the intercalator units in their oxidized form. The oxidation of TEOA by the valence band holes led, then, to the formation of the steady-state anodic photocurrent. Application of a potential of −0.4 V (vs. SCE) on the electrode, a potential that retained the intercalator units in their reduced state, led to a cathodic photocurrent in the presence of O_2 acting as an electron acceptor. The photocurrent observed in the system could be reversibly cycled between anodic or cathodic currents, depending on the applied potential on the electrode.

8.8 Conclusions and Perspectives

Different amplification procedures for the electronic or optical readout of DNA analyses were discussed. Despite the significant advances in the development of amplification routes, one has to realize that any amplification requires enhanced complexities of the analytical protocols that are reflected by additional components or analysis steps. From a practical point of view, additional ingredients and added analytical steps mean increased costs and longer analysis time intervals. The impressive progress in developing amplified biosensing schemes for DNA suggests, however, that several of the analytical protocols reached ripeness for practical applications. To reach this goal, a systematic comparison of the different methods would be desirable. A further, frequently raised question in the field of amplified DNA biosensing relates to the preferred mode of the sensor readout: electronic or optical. Answers to this issue may be driven by personal preferences of the different researchers, but a clear-cut conclusion is impossible at this stage. Several challeng-

ing topics, however, need further research, and amplified DNA biosensing technologies that address the parallel analysis of many targets, the reusability of the sensor devices, the evaluation of solution versus surface-confined assays, and particularly the cost-effectiveness of the systems need to be addressed. It seems that no single method could be defined, and the selection of the method would depend on different factors, such as the number of analytes to be detected in parallel, the nature and co-additives in the analyzed samples, the place of analysis, and the personal skills (analytical laboratory, point-of-care, field tests, etc.). Also, the progress in the field suggests that new exciting technologies for amplified DNA detection will emerge. In this context, the ultrasensitive detection of DNA by DNA-based machines is a promising approach to pursue, and isothermal analysis paths that substitute for the legendary PCR process seem to be achievable. We can certainly envisage numerous practical applications of the amplified detection schemes of DNA in clinical diagnostics (analysis of pathogens or genetic mutations), environmental and homeland security (analysis of pathogens), and forensic applications.

Acknowledgments Our research on amplified DNA analyses is supported by the Israel Ministry of Science and Technology, and by the Johnson & Johnson Corporation.

References

1. Amine, A., Mohammadi, H., Bourais, I. and Palleschi, G. (2006) Enzyme inhibition-based biosensors for food safety and environmental monitoring. Biosens. Bioelectron. 21:1405–1423.
2. Rodriguez-Mozaz, S., de Alda, M.J.L. and Barcelo, D. (2006) Biosensors as useful tools for environmental analysis and monitoring. Anal. Bioanal. Chem. 386:1025–1041.
3. Sadik, O.A., Land, W.H. and Wang, J. (2003) Targeting chemical and biological warfare agents at the molecular level. Electroanalysis 15:1149–1159.
4. Caminade, A.M., Padie, C., Laurent, R., Maraval, A. and Majoral, J.P. (2006) Uses of dendrimers for DNA microarrays. Sensors 6:901–914.
5. Epstein, J.R., Biran, I. and Walt, D.R. (2002) Fluorescence-based nucleic acid detection and microarrays. Anal. Chim. Acta 469:3–36.
6. Sapsford, K.E., Pons, T., Medintz, I.L. and Mattoussi, H. (2006) Biosensing with luminescent semiconductor quantum dots. Sensors 6:925–953.
7. Katz, E. and Willner, I. (2003) Probing biomolecular interactions at conductive and semiconductive surfaces by impedance spectroscopy: routes to impedimetric immunosensors, DNA-sensors, and enzyme biosensors. Electroanalysis 15:913–947.
8. Gooding, J.J. (2002) Electrochemical DNA hybridization biosensors. Electroanalysis 14: 1149–1156.
9. Drummond, T.G., Hill, M.G. and Barton, J.K. (2003) Electrochemical DNA sensors. Nat. Biotechnol. 21:1192–1199.
10. Duman, M., Saber, R. and Piskin, E. (2003) A new approach for immobilization of oligonucleotides onto piezoelectric quartz crystal for preparation of a nucleic acid sensor for following hybridization. Biosens. Bioelectron. 18:1355–1363.
11. Mulvaney, P. (1996) Surface plasmon spectroscopy of nanosized metal particles. Langmuir 12:788–800.
12. Alvarez, M.M., Khoury, J.T., Schaaff, T.G., Shafigullin, M.N., Vezmar, I. and Whetten, R.L. (1997) Optical absorption spectra of nanocrystal gold molecules J. Phys. Chem. B 101: 3706–3712.

13. Hutter, E. and Fendler, J.H. (2004) Exploitation of localized surface plasmon resonance. Adv. Mater. 16:1685–1706.
14. Mirkin, C.A., Letsinger, R.L., Mucic, R.C. and Storhoff, J.J. (1996) A DNA-based method for rationally assembling nanoparticles into macroscopic materials. Nature (Lond.) 382:607–609.
15. Elghanian, R., Storhoff, J.J., Mucic, R.C., Letsinger, R.L. and Mirkin, C.A. (1997) Selective colorimetric detection of polynucleotides based on the distance-dependent optical properties of gold nanoparticles. Science 277:1078–1081.
16. Storhoff, J.J., Elghanian, R., Mucic, R.C., Mirkin, C.A. and Letsinger, R.L. (1998) One-pot colorimetric differentiation of polynucleotides with single base imperfections using gold nanoparticle probes. J. Am. Chem. Soc. 120:1959–1964.
17. Reynolds, R.A., Mirkin, C.A. and Letsinger, R.L. (2000) Homogeneous, nanoparticle-based quantitative colorimetric detection of oligonucleotides. J. Am. Chem. Soc. 122:3795–3796.
18. Souza, G.R. and Miller, J.H. (2001) Oligonucleotide detection using angle-dependent light scattering and fractal dimension analysis of gold-DNA aggregates. J. Am. Chem. Soc. 123:6734–6735.
19. Jin, R.C., Wu, G., Li, Z., Mirkin, C.A. and Schatz, G.C. (2003) What controls the melting properties of DNA-linked gold nanoparticle assemblies? J. Am. Chem. Soc. 125:643–654.
20. Miao, W. and Bard, A.J. (2003) Electrogenerated chemiluminescence. 72. Determination of immobilized DNA and C-reactive protein on Au(111) electrodes using tris(2,2′-bipyridyl) ruthenium(II) labels. Anal. Chem. 75:5825–5834.
21. Palecek, E. (1960) Oscillographic polarography of highly polymerized deoxyribonucleic acid. Nature (Lond.) 188:656–657.
22. Hashimoto, K., Ito, K. and Ishimori, Y. (1994) Sequence-specific gene detection with a gold electrode modified with DNA probes and an electrochemically active dye. Anal. Chem. 66:3830–3833.
23. Jelen, F., Erdem A. and Palecek, E. (2002) Cyclic voltammetry of echinomycin and its interaction with double-stranded and single-stranded DNA adsorbed at the electrode. Bioelectrochemistry 55:165–167.
24. Takenaka, S., Yamashita, K., Takagi, M., Uto Y. and Kondo H. (2000) DNA sensing on a DNA probe-modified electrode using ferrocenylnaphthalene diimide as the electrochemically active ligand. Anal. Chem. 72:1334–1341.
25. Fan, C., Plaxco, K.W. and Heeger, A.J. (2003) Electrochemical interrogation of conformational changes as a reagentless method for the sequence-specific detection of DNA. Proc. Natl. Acad. Sci. USA 100:9134–9137.
26. Shin, J.K., Kim, D.S., Park, H.J. and Lim, G. (2004) Detection of DNA and protein molecules using an FET-type biosensor with gold as a gate metal. Electroanalysis 16:1912–1918.
27. Nicolini, C., Erokhin, V., Facci, P., Guerzoni, S., Ross, A. and Pashkevitch, P. (1997) Quartz balance DNA sensor. Biosens. Bioelectron. 12:613–618.
28. De Lumley-Woodyear, T., Campbell, C.N. and Heller, A. (1996) Direct enzyme-amplified electrical recognition of a 30-base model oligonucleotide. J. Am. Chem. Soc. 118:5504–5505.
29. Caruana, D.J. and Heller, A. (1999) Enzyme-amplified amperometric detection of hybridization and of a single base pair mutation in an 18-base oligonucleotide on a 7-μm-diameter microelectrode. J. Am. Chem. Soc. 121:769–774.
30. Ikebukuro, K., Kohiki, Y. and Sode, K. (2002) Amperometric DNA sensor using the pyrroquinoline quinone glucose dehydrogenase-avidin conjugate. Biosens. Bioelectron. 17: 1075–1080.
31. Patolsky, F., Weizmann Y. and Willner, I. (2002) Redox-active nucleic-acid replica for the amplified bioelectrocatalytic detection of viral DNA. J. Am. Chem. Soc. 124:770–772.
32. Carpini, G., Lucarelli, F., Marrazza, G. and Mascini, M. (2004) Oligonucleotide-modified screen-printed gold electrodes for enzyme-amplified sensing of nucleic acids. Biosens. Bioelectron. 20:167–175.
33. Patolsky, F., Lichtenstein, A. and Willner, I. (2003) Highly sensitive amplified electronic detection of DNA by biocatalyzed precipitation of an insoluble product onto electrodes. Chem. Eur. J. 9:1137–1145.

34. Patolsky, F., Lichtenstein, A., Kotler, M. and Willner, I. (2001) Electronic transduction of polymerase or reverse transcriptase induced replication processes on surfaces: highly sensitive and specific detection of viral genomes. Angew. Chem. Int. Ed. 40:2261–2265.
35. Patolsky, F., Zayats, M., Katz, E. and Willner, I. (1999) Precipitation of an insoluble product on enzyme-monolayer-electrodes for biosensor applications: characterization by Faradaic impedance spectroscopy, cyclic voltammetry and microgravimetric quartz-crystal-microbalance analyses. Anal. Chem. 71:3171–3180.
36. Patolsky, F., Lichtenstein A. and Willner I. (2001) Detection of single-base DNA mutations by enzyme-amplified electronic transduction. Nat. Biotechnol. 19:253–257.
37. Crowther, J.R. (1995) ELISA: theory and practice. Humana, Totowa, NJ.
38. Douillard, J.Y. and Hoffmann, T. (1983) Enzyme-linked immunosorbent-assay for screening monoclonal-antibody production using enzyme-labeled second antibody. Methods Enzymol. 92E:168–174.
39. Shlyahovsky, B., Pavlov, V., Kaganovsky, L. and Willner, I. (2006) Biocatalytic evolution of a biocatalyst marker: towards the ultrasensitive detection of immunocomplexes and DNA analysis. Angew. Chem. Int. Ed. 45:4815–4819.
40. Pavlov, V., Shlyahovsky, B. and Willner, I. (2005) Fluorescence detection of DNA by the catalytic activation of an aptamer/thrombin complex. J. Am. Chem. Soc. 127:6522–6523.
41. Patolsky, F., Katz, E. and Willner, I. (2002) Amplified DNA detection by electrogenerated biochemiluminescence and by the catalyzed precipitation of an insoluble product on electrodes in the presence of the doxorubicin intercalator. Angew. Chem. Int. Ed. 41:3398–3402.
42. Breaker, R.R. (2002) Engineered allosteric ribozymes as biosensor components. Curr. Opin. Biotechnol. 13:31–39.
43. Ellington, A.D. and Szostak, J.W. (1990) In vitro selection of RNA molecules that bind specific ligands. Nature (Lond.) 346:818–822.
44. Tuerk, C. and Gold, L. (1990) Systematic evolution of ligands by exponential enrichment-RNA ligands to bacteriophage-T4 DNA polymerase. Science 249:505–510.
45. Travascio, P., Li, Y.F. and Sen, D. (1998) DNA-enhanced peroxidase activity of a DNA aptamer–hemin complex. Chem. Biol. 5:505–517.
46. Travascio, P., Bennet, A.J., Wang, D.Y. and Sen, D. (1999) A ribozyme and a catalytic DNA with peroxidase activity: active sites versus cofactor-binding sites. Chem. Biol. 6:779–787.
47. Xiao, Y., Pavlov, V., Niazov, T., Dishon, A., Kotler, M. and Willner, I. (2004) Catalytic beacons for the detection of DNA and telomerase activity. J. Am. Chem. Soc. 126:7430–7431.
48. Pavlov, V., Xiao, Y., Gill, R., Dishon, A., Kotler, M. and Willner, I. (2004) Amplified chemiluminescence surface detection of DNA and telomerase activity using catalytic nucleic acid labels. Anal. Chem. 76:2152–2156.
49. Niazov, T., Pavlov, V., Xiao, Y., Gill, R. and Willner, I. (2004) DNAzyme-functionalized Au nanoparticles for the amplified detection of DNA or telomerase activity. Nano Lett. 4:1683–1687.
50. Fu A.H., Gu, W.W., Larabell, C. and Alivisatos, A.P. (2005) Semiconductor nanocrystals for biological imaging. Curr. Opin. Neurobiol. 15:568–575.
51. Medintz, I.L., Uyeda, H.T., Goldman, E.R. and Mattoussi, H. (2005) Quantum dot bioconjugates for imaging, labelling and sensing. Nat. Mater. 4:435–446.
52. Hoshino, A., Fujioka, K., Manabe, N. and Yamaya, S. (2005) Simultaneous multicolor detection system of the single-molecular microbial antigen with total internal reflection fluorescence microscopy. Microbiol. Immunol. 49:461–470.
53. Patolsky, F., Gill., R., Weizmann, Y., Mokari, T., Banin, U. and Willner, I. (2003) Lighting-up the dynamics of telomerization and DNA replication by CdSe–ZnS quantum dots. J. Am. Chem. Soc. 125:13918–13919.
54. Polsky, R., Gill, R., Kaganovsky, L. and Willner, I. (2006) Nucleic acid-functionalized Pt nanoparticles: catalytic labels for the amplified electrochemical detection of biomolecules. Anal. Chem. 78:2268–2271.
55. Gill, R., Polsky, R. and Willner, I. (2006) Pt nanoparticles functionalized with nucleic acid act as catalytic labels for the chemiluminescent detection of DNA and proteins. Small 2: 1037–1041.

56. Wang, J. (2005) Nanomaterial-based amplified transduction of biomolecular interactions. Small 1:1036–1043.
57. Park, S.J., Taton, T.A. and Mirkin, C.A., (2002) Array-based electrical detection of DNA with nanoparticle probes. Science 295:1503–1506.
58. Möller, R., Csáki, A., Köhler, J.M. and Fritzsche, W. (2001) Electrical classification of the concentration of bioconjugated metal colloids after surface adsorption and silver enhancement. Langmuir 17:5426–5430.
59. Urban, M., Möller R. and Fritzsche, W. (2003) A paralleled readout system for an electrical DNA-hybridization assay based on a microstructured electrode array. Rev. Sci. Instrum. 74:1077–1081.
60. Moreno-Hagelsieb, L., Lobert, P.E., Pampin, R., Bourgeois, D., Remacle J. and Flandre, D. (2004) Sensitive DNA electrical detection based on interdigitated Al/Al_2O_3 microelectrodes. Sens. Actuat. B 98:269–274.
61. Li, D., Yan, Y., Wieckowska, A. and Willner, I. (2008) Amplified electrochemical detection of DNA through the aggregation of Au nanoparticles on electrodes and the incorporation of methylene blue into the DNA-crosslinked structure. Chem. Commun. 3544–3546.
62. Taton, T.A., Mirkin, C.A. and Letsinger, R.L. (2000) Scanometric DNA array detection with nanoparticle probes. Science 289:1757–1760.
63. Taton, T.A., Lu, G.L. and Mirkin, C.A. (2001) Two-color labeling of oligonucleotide arrays via size-selective scattering of nanoparticle probes. J. Am. Chem. Soc. 123:5164–5165.
64. Storhoff, J.J., Marla, S.S., Bao, P., Hagenow, S., Mehta, H., Lucas, A., Garimella, V., Patno, T., Buckingham, W., Cork, W. and Muller, U.R. (2004) Gold nanoparticle-based detection of genomic DNA targets on microarrays using a novel optical detection system. Biosens. Bioelectron. 19:875–883.
65. Bao, P., Huber, M., Wei, T.-F., Marla, S.S., Storhoff, J.J. and Müller, U.R. (2005) SNP identification in unamplified human genomic DNA with gold nanoparticle probes. Nucleic Acids Res. 33:e15.
66. Nam, J.-M., Stoeva, S.I. and Mirkin, C.A. (2004) Bio-bar-code-based DNA detection with PCR-like sensitivity. Am. Chem. Soc. 126:5932–5933.
67. Stoeva, S.I., Lee, J.-S., Thaxton, C.S. and Mirkin, C.A. (2006) Multiplexed DNA detection with biobarcoded nanoparticle probes. Angew. Chem. Int. Ed. 45:3303–3306.
68. Cai, H., Xu, Y., Zhu, N., He, P. and Fang, Y. (2002) An electrochemical DNA hybridization detection assay based on a silver nanoparticle label. Analyst 127:803–809.
69. Wang, J., Xu, D., Kawde, A.-N. and Polsky, R. (2001) Metal nanoparticle-based electrochemical stripping potentiometric detection of DNA hybridization. Anal. Chem. 73:5576–5581.
70. Wang, J., Liu, G. and Zhu, Q. (2003) Indium microrod tags for electrochemical detection of DNA hybridization. Anal. Chem. 75:6218–6222.
71. Martin, C.R. (1995) Template synthesis of electronically conductive polymer nanostructures. Acc. Chem. Res. 28:61–68.
72. Zhu, N., Zhang, A., Wang, Q., He, P. and Fang, Y. (2004) Lead sulfide nanoparticle as oligonucleotides labels for electrochemical stripping detection of DNA hybridization. Electroanalysis 16:577–582.
73. Wang, J., Liu, G., Polsky, R. and Merkoçi, A. (2002) Electrochemical stripping detection of DNA hybridization based on cadmium sulfide nanoparticle tags. Electrochem. Commun. 4:722–726.
74. Wang, J., Liu, G. and Merkoçi, A. (2003) Electrochemical coding technology for simultaneous detection of multiple DNA targets. J. Am. Chem. Soc. 125:3214–3215.
75. Kerman, K., Saito, M., Morita, Y., Takamura, Y., Ozsoz, M. and Tamiya, E. (2004) Electrochemical coding of single-nucleotide polymorphisms by monobase-modified gold nanoparticles. Anal. Chem. 76:1877–1884.
76. Liu, G., Lee, T.M.H. and Wang, J. (2005) Nanocrystal-based bioelectronic coding of single nucleotide polymorphisms, J. Am. Chem. Soc. 127:38–39.
77. Wang, J., Xu, D.K., Kawde, A.N. and Polsky, R. (2001) Metal nanoparticle-based electrochemical stripping potentiometric detection of DNA hybridization. Anal. Chem. 73:5576–5581.

78. Wang, J., Polsky, R. and Xu, D.K. (2001) Silver-enhanced colloidal gold electrochemical stripping detection of DNA hybridization. Langmuir 17:5739–5741.
79. Buttry, D.A. and Ward, M.D. (1992) Measurement of interfacial processes at electrode surfaces with the electrochemical quartz crystal microbalance. Chem. Rev. 92:1355–1379.
80. Zhou, X.C., O'Shea, S.J. and Li, S.F.Y. (2000) Amplified microgravimetric gene sensor using Au nanoparticle modified oligonucleotides. Chem. Commun. 11:953–954.
81. Patolsky, F., Ranjit, K.T., Lichtenstein, A. and Willner, I. (2000) Dendritic amplification of DNA analysis by oligonucleotide-functionalized Au-nanoparticles. Chem. Commun. 1025–1026.
82. Liu, T., Tang, J. and Jiang, L. (2004) The enhancement effect of gold nanoparticles as a surface modifier on DNA sensor sensitivity. Biochem. Biophys. Res. Commun. 313:3–7.
83. Han, S., Lin, J., Satjapipat, M., Baca, A.J. and Zhou, F. (2001) A three-dimensional heterogeneous DNA sensing surface formed by attaching oligodeoxynucleotide-capped gold nanoparticles onto a gold-coated quartz crystal. Chem. Commun. 609–610.
84. Willner, I., Patolsky, F., Weizmann, Y. and Willner, B. (2002) Amplified detection of single-base mismatches in DNA using microgravimetric quartz-crystal-microbalance transduction. Talanta 56:847–856.
85. Weizmann, Y., Patolsky, F. and Willner, I. (2001) Amplified detection of DNA and analysis of single-base mismatches by the catalyzed deposition of gold on Au-nanoparticles. Analyst 126:1502–1504.
86. Wang, J., Polsky, R., Merkoçi, A. and Turner, K.L. (2003) "Electroactive beads" for ultrasensitive DNA detection. Langmuir 19:989–991.
87. Kawde, A.-N. and Wang, J. (2004) Amplified electrical transduction of DNA hybridization based on polymeric beads loaded with multiple gold nanoparticle tags. Electroanalysis 16:101–107.
88. Wang, J., Liu, G., Jan, M.R. and Zhu, Q. (2003) Electrochemical detection of DNA hybridization based on carbon-nanotubes loaded with CdS tags. Electrochem. Commun. 5: 1000–1004.
89. Patolsky, F., Lichtenstein, A. and Willner, I. (2001) Electronic transduction of DNA sensing processes on surfaces: amplification of DNA detection and analysis of single-base mismatches by tagged liposomes. J. Am. Chem. Soc. 123:5194–5205.
90. Xu, Y., Cai, H., He, P.-G. and Fang, Y.-Z. (2004) Probing DNA hybridization by impedance measurement based on CdS-oligonucleotides. Electroanalysis 16:150–155.
91. Yurke, B., Turberfield, A.J., Mills, A.P., Simmel, F.C. and Neumann, J.L. (2000) A DNA-fuelled molecular machine made of DNA. Nature (Lond.) 406:605–608.
92. Bath, J., Green, S.J. and Turberfield, A.J. (2005) A free-running DNA motor powered by a nicking enzyme. Angew. Chem. Int. Ed. 44:4358–4361.
93. Tian, Y. and Mao, C. (2004) Molecular gears: a pair of DNA circles continuously rolls against each other. J. Am. Chem. Soc. 126:11410–11411.
94. Tyagi, S. and Kramer, F.R. (1996) Molecular beacons: probes that fluoresce upon hybridization. Nat. Biotechnol. 14:303–308.
95. Beyer, S. and Simmel, F.C. (2006) A modular DNA signal translator for the controlled release of a protein by an aptamer. Nucleic Acids Res. 34:1581–1587.
96. Beissenhirtz, M. and Willner, I. (2006) DNA-based machines. Org. Biomol. Chem. 4: 3392–3401.
97. Bath, J., Andrew, J. and Turberfield, J. (2007) DNA nanomachines. Nature (Lond.) 2: 275–284.
98. Liedl, T., Sobey, T.L. and Simmel, F.C. (2007) DNA-based nanodevices. Nanotoday 2: 36–41.
99. Weizmann, Y., Beissenhirtz, M., Cheglakov, Z., Nowarski, R., Kotler, M. and Willner, I. (2006) A virus spotlighted by an autonomous DNA machine. Angew. Chem. Int. Ed. 45:7384–7388.
100. Beissenhirtz, M., Elnathan, R., Weizmann, Y. and Willner, I. (2007) The aggregation of Au nanoparticles by an autonomous DNA machine detects viruses. Small 3:375–379.
101. Cheglakov, Z., Weizmann, Y., Basnar, B., Willner, I. (2007) Diagnosing viruses by the rolling-circle amplified synthesis of DNAzymes. Org. Biomol. Chem. 5:223–225.

102. Tian, Y., He, Y. and Mao, C.D. (2006) Cascade signal amplification for DNA detection. ChemBioChem 7:1862–1864.
103. Weizmann, Y., Cheglakov, Z., Pavlov, V. and Willner, I. (2006) Autonomous fueled mechanical replication of nucleic acid templates for the amplified optical detection of DNA. Angew. Chem. Int. Ed. 45:2238–2242.
104. Weizmann, Y., Cheglakov, Z., Pavlov, V. and Willner, I. (2006) An autonomous fueled machine that replicates catalytic nucleic acid templates for the amplified optical analysis of DNA. Nat. Protocols 1:554–558.
105. Gerion, D., Chen, F., Kannan, B., Fu, A., Parak, W.J., Chen, D.J., Majumdar, A. and Alivisatos, A.P. (2003) Room-temperature single-nucleotide polymorphism and multiallele DNA detection using fluorescent nanocrystals and microarrays. Anal. Chem. 75: 4766–4772.
106. Pathak, S., Choi, S.K., Arnheim, N. and Thompson, M.E. (2001) Hydroxylated quantum dots as luminescent probes for in situ hybridization. J. Am. Chem. Soc. 123:4103–4104.
107. Xiao, Y. and Barker, P.E. (2004) Semiconductor nanocrystal probes for human metaphase chromosomes. Nucleic Acids Res. 32:e28.
108. Kamat, P.V. (2007) Meeting the clean energy demand: nanostructure architectures for solar energy conversion. J. Phys. Chem. C 111:2834–2860.
109. Adams, D.M., Brus, L., Chidsey, C.E.D., Creager, S., Creutz, C., Kagan, C.R., Kamat, P.V., Lieberman, M., Lindsay, S., Marcus, R.A., Metzger, R.M., Michel-Beyerle, M.E., Miller, J.R., Newton, M.D., Rolison, D.R., Sankey, O., Schanze, K.S., Yardley, J. and Zhu, X.Y. (2003) Charge transfer on the nanoscale: current status. J. Phys. Chem. B 107:6668–6697.
110. Willner, I., Patolsky, F. and Wasserman, J. (2001) Photoelectrochemistry with controlled DNA-cross-linked CdS nanoparticle arrays. Angew. Chem. Int. Ed. 40:1861–1864.
111. Gill, R., Patolsky, F., Katz, E. and Willner, I. (2005) Electrochemical control of the photocurrent direction in intercalated DNA/CdS nanoparticle systems. Angew. Chem. Int. Ed. 44:4554–4557.

Part III
Other Emerging Analytical Applications

Chapter 9
Aptamers in Affinity Separations: Capillary Electrophoresis

Jeffrey W. Guthrie, Yuanhua Shao, and X. Chris Le

Abstract Assays employing aptamers in capillary electrophoresis (CE), including competitive and noncompetitive assays, fluorescence polarization (FP) assays, nonequilibrium capillary electrophoresis of equilibrium mixtures, and affinity-polymerase chain reaction-CE assays, are summarized. These assays can be used to estimate dissociation rate and equilibrium binding constants, determine binding stoichiometries, study molecular interactions, and quantitatively determine specific analytes (e.g., proteins) in complex media. They can potentially be completed in under 60 s, detect zeptomol (10^{-24}) amounts of analyte, be utilized in complex media with little or no cross reaction, and target a number of different analytes of biological, environmental, and clinical importance. This chapter briefly overviews the process of aptamer selection using CE and discusses the various CE-based bioanalytical methods that have been used to study biomolecular interactions.

9.1 Introduction

Capillary electrophoresis (CE) employs narrow capillary tubes and high electric field strengths for high-efficiency separation of a wide range of analytes. Separation occurs in free-zone CE because the electric field applied to the capillary differentially attracts analytes in accordance to their mass-to-charge ratios, resulting in differing mobilities for each analyte toward the detector. The strength of CE lies in its speed of separation, high resolution, and high mass sensitivity. As a result, many of the newly emerging CE applications have played specifically to these strengths. One such application was in the human genome project. Capillary array electrophoresis

J.W. Guthrie, and X.C. Le
Department of Laboratory Medicine and Pathology, University of Alberta
jeff.guthrie@ualberta.ca
xc.le@ualberta.ca

Y. Shao
College of Chemistry and Molecular Engineering, Peking University
yhshao@pku.edu.cn

Y. Li and Y. Lu (eds.), *Functional Nucleic Acids for Analytical Applications*,

substantially increased the throughput of genome sequencing, accomplishing as much in 2 weeks as had been done in an entire year.[1]

Many recent studies have reported assays employing affinity capillary electrophoresis (ACE),[2–11] a collection of techniques in which high-affinity binding is used in conjunction with CE separation to determine analytes. The premise of affinity separations is that the electrophoretic mobilities are influenced by reversible molecular interactions taking place before and/or during the separation process, which is usually accomplished by employing an affinity reagent such as an antibody or aptamer that reversibly binds to the target of interest. This process effectively alters the mobility of the target by changing its mass-to-charge ratio, thus facilitating the separation of the target from the rest of the matrix. The most sensitive detection is by laser-induced fluorescence (LIF) of labeled affinity probes.

In most cases, the affinity reagent is an antibody. Antibodies have high affinity and selectivity for their targets, and they have been developed for a large variety of analytes; however, aptamers have recently been used as an alternative to antibodies in affinity separations.

9.2 Aptamers

Aptamers are short, synthetic nucleic acid sequences that are specifically selected to have high affinities for their targets. They are usually 20–60 bases in length, and assume characteristic secondary structures that are mainly responsible for their binding affinity and selectivity to a given target (see Chapter 2 for a thorough discussion on aptamers). Figure 9.1 shows the characteristic secondary structure of the thrombin-binding DNA aptamer that has been extensively used to study and determine the blood clotting protein thrombin.

Aptamers are commonly compared to antibodies as affinity reagents because of their selectivity and affinity for their targets. However, aptamers have several

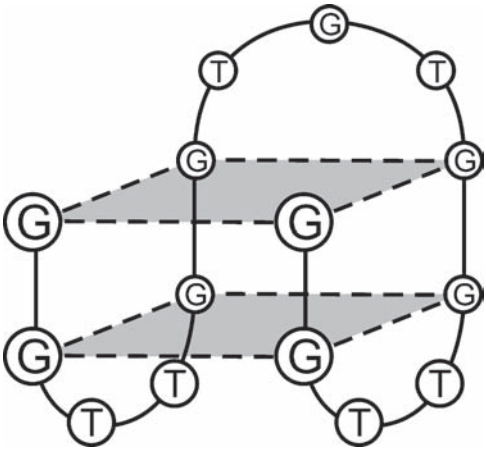

Fig. 9.1 Secondary structure of the thrombin-binding aptamer. The characteristic G-quartet motif (shown by *dashed lines*) is necessary for the specific recognition of thrombin

advantages over antibodies, such as ease of production, higher stability, batch-to-batch reproducibility, long shelf life, easy modification, and sometimes greater target affinity. As a result, aptamers have been increasingly used in assays traditionally dominated by antibodies. Aptamers are generated synthetically via a combinatorial chemistry method called systematic evolution of ligands by exponential enrichment (SELEX).[12,13] Once selected, cloned, and sequenced, aptamers can be readily synthesized and amplified by the polymerase chain reaction (PCR), ensuring reproducible batch-to-batch properties. SELEX and its variations have been thoroughly discussed in previous chapters. Here, only a brief description of aptamer selection using CE is given.

9.2.1 Aptamer Selection Using Capillary Electrophoresis

Aptamer selection using CE allows aptamer selection to occur in free solution (Fig. 9.2), which ensures that all possible binding sites on the target are available for binding to potential aptamers. The recent application of CE to SELEX has resulted in a great improvement in selection efficiency and comparable aptamer affinity for protein targets.[14] The obvious limitation of CE-SELEX, however, is that it requires the nucleic acids to exhibit a significant mobility shift when binding to the target if they are to be separated from the nonbinding sequences. Smaller targets would be expected to have only a minimal effect on the mobility of the nucleic acid sequences upon complexation, making collection of these binding sequences difficult.

CE-SELEX was first introduced by Mendonsa and coworkers (see Fig. 9.2).[14–17] It has been used to select aptamers for human IgE,[14,15] the reverse transcriptase of the type 1 human immunodeficiency virus (HIV-1 RT),[17] farnesyltransferase,[18] ricin toxin,[19] MutS protein,[20,21] and protein kinase C-δ.[22] Typical K_d values of aptam-

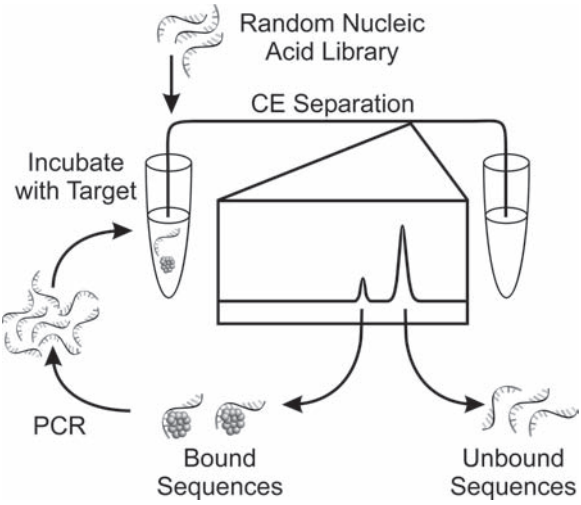

Fig. 9.2 Schematic of CE-SELEX. A random nucleic acid library of ~10^{13}–10^{15} sequences is incubated with the target to initiate aptamer–target binding. The mixture is injected into the capillary where the bound sequences are separated from the unbound sequences. Bound sequences are collected, PCR amplified, and introduced into the next round of selection

ers obtained via CE-SELEX for proteins are in the low nM range, but have been recorded as low as 180 pM.[17] CE-SELEX has also been successfully applied to small targets such as neuropeptide Y, which is smaller than the DNA in the library used for selection.[16]

Krylov and coworkers developed an aptamer selection process to generate "smart aptamers."[18,20,21] Smart aptamers are defined as aptamers with predefined kinetic and/or thermodynamic parameters.[20,21] The K_d values of the highest affinity aptamers for MutS protein and farnesyltranserase were 3.6 and 0.5 nM, respectively.

The same authors also developed a method for selecting aptamers by non-SELEX methods.[23] The DNA library was first incubated with the target as usual, and CE separation was used to partition the bound from unbound sequences. Instead of PCR amplification, the bound sequences were directly collected in a new vial containing the target, and the mixture was subject to separation again. This procedure was repeated three times, and was not tested further for increased aptamer affinity. The aptamers had K_d values of the order of 0.3 μM, which was comparable to CE-SELEX, which uses multiple rounds of partitioning and PCR amplification. This approach requires a relatively high concentration of the library molecules to have sufficient numbers of bound aptamer molecules after the three consecutive CE separations.

9.3 Assays Employing Aptamers in Capillary Electrophoresis

9.3.1 Competitive and Noncompetitive Assays

Competitive and noncompetitive assays are commonly used to study structure–function relationships between proteins, to aid in drug discovery, and to determine protein concentrations in complex media. In the competitive assay format, a labeled analyte competes with an unlabeled analyte for the binding site on a limited number of corresponding ligands. CE separation results in two peaks, one of the free labeled analyte and another of the complex between the labeled analyte and the ligand. By measuring the relative intensities of the labeled analyte and the analyte–ligand peaks, the original concentration of the unlabeled analyte can be determined. In noncompetitive assays, the analyte is added to a solution containing a labeled ligand. The analyte can be directly quantified by measuring the analyte–ligand complex after electrophoretic separation.

Noncompetitive assays offer a number of advantages over competitive assays. They have larger linear dynamic ranges, better detection limits, and the ability to distinguish between cross-reactive species. However, because antibodies are most commonly used as the ligand, the development of noncompetitive assays has been limited. Some of the main problems are that homogenous labeling of antibodies is difficult, resulting in broad bands, the nature of antibodies makes their electro-

phoresis difficult to predict, and separation of the antibody from the analyte may be difficult when binding results in small changes in electrophoretic mobility. These problems have since been addressed by using improved labeling procedures, antibody fragments, and "shift ligands" that act as "charge modulators."[4]

Aptamers have offered another alternative for the development of noncompetitive assays as they do not have the same limitations as antibodies. In particular, the use of aptamers as the affinity ligand can facilitate the separation of the aptamer from the aptamer–analyte complex because of the large negative charge on the aptamer, which greatly affects the mass-to-charge ratio of the complex. An additional advantage to the high density of negative charges is that analyte focusing can be accomplished to improve assay performance; this can be done by field amplification stacking,[24] transient anion isotachophoresis,[25–27] and pH-mediated stacking.[28] Wang et al. developed a DNA-driven focusing method for the human immunodeficiency virus type 1 reverse transcriptase (HIV-1 RT) and its aptamer.[10] By changing the pH and composition of the incubation buffer relative to the running buffer, they were able to effectively focus the aptamer–HIV-1 RT complex peak, resulting in a 70- to 120-fold increase in sensitivity and a threefold increase in separation efficiency. Increased efficiency allowed the use of shorter capillaries (16 cm) and resulted in migration times of less than 30 s.

To date, noncompetitive assays using aptamers as the labeled analyte have been mainly used for the study of protein–DNA interactions and to detect low concentrations of proteins in biological media. The first example of a noncompetitive assay using aptamers was done by Kennedy and coworkers, who employed an affinity probe capillary electrophoresis (APCE) assay for the rapid detection of human IgE and thrombin.[6] Aptamers for both targets had been previously isolated and had K_d values of 10 and 200 nM, respectively.[29,30] Aptamers were fluorescently labeled using fluorescein isothiocyanate for LIF detection using an argon ion laser at 488 nm. The capillary was coated with polyacrylamide to reduce adsorption of the proteins to the inner walls of the capillary during electrophoresis. Sample preparation consisted of heating the aptamer to 70°C and letting it cool slowly to ensure it was in its most favorable thermodynamic conformation. Samples of aptamer and protein were incubated for 3 min before introduction into the capillary by hydrodynamic injection and electrokinetic separation. The assays for IgE and thrombin were each complete in under 60 s and had detection limits of 46 pM for IgE and 40 nM for thrombin. The linear dynamic range for IgE was 10^5.

To test the selectivity of the assay, a set of control experiments was conducted; these consisted of incubating the IgE aptamer with IgG to determine if the aptamer would form complexes with a structurally similar protein, incubating IgE with a thrombin aptamer to show that IgE did not bind to other DNA sequences, and removing Mg^{2+} from the medium to disrupt the conformation of the aptamer. In all cases, the results showed that the assay was specific to IgE. The assay was also conducted in human serum, which may contain high concentrations of potential interferences. The results showed that human serum had little effect on the separation and quantification of the assay (Fig. 9.3). A competitive assay was also performed in which a labeled aptamer competed with an unlabeled aptamer for the binding

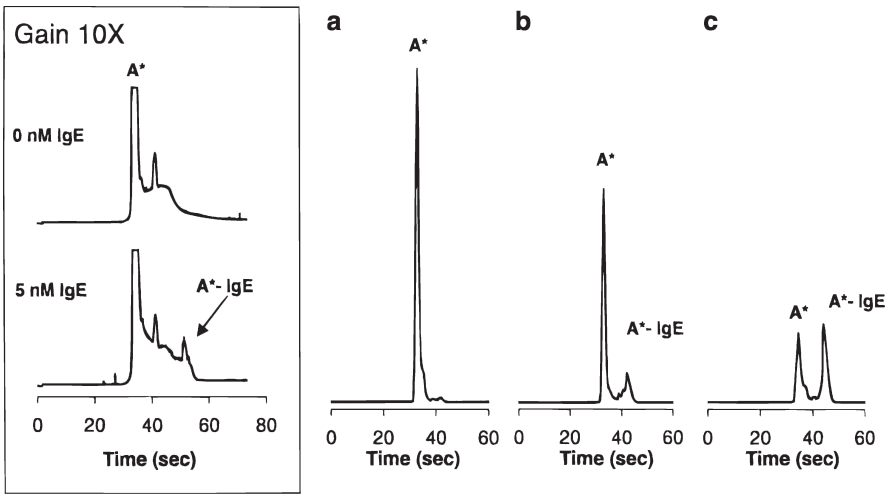

Fig. 9.3 Determination of IgE in reconstituted human serum. *A** is the labeled aptamer. Each sample contained a final concentration of 300 nM A* and 0, 100, and 400 nM IgE in **a–c**, respectively. The *inset* demonstrates the high sensitivity analysis of a sample containing 0 and 5 nM IgE with 300 nM A* (Reproduced with permission from ref. 6)

site on the IgE. As the concentration of the unlabeled aptamer increased from 0 to 400 nM, the free labeled aptamer peak increased, which showed that both labeled and unlabeled aptamers compete for the same site on IgE, although the labeled aptamer had a lower affinity for IgE (64 nM) than the unlabeled aptamer (8 nM). This difference was probably caused by slight conformational differences of the aptamer resulting from a bulky dye hanging off the 5′-end.

Kennedy et al. followed up their initial study[6] by examining more closely the electrophoretic conditions required for good separation and complex migration.[4] The same aptamer–IgE and aptamer–thrombin system was used to test the effect of buffer and electric field on separation and complex stability. It was found that buffer composition had a large effect on complex stability, with MOPS [3-(N-morpholino) propanesulfonic acid]-phosphate buffer resulting in longer migration times and the lowest survivability of the complex during separation versus TGK buffer [25 mM tris(hydroxyl-amino)methane, 192 mM glycine, 5 mM K_2HPO_4], which had migration times nearly twice as fast as MOPS-phosphate. Electric field was expected to affect complex survivability, as higher fields would result in less time on the capillary and less time for dilution of the complex during electrophoresis. However, higher fields proved deleterious to complex stability due to capillary heating and possible dissociation of the complex. Although higher electric fields (1,500 V/cm) did result in greater complex peak heights and a two-fold better limit of detection (LOD) compared to lower field strengths (150 V/cm), it also showed that the ratio of the relative peak heights to internal standard were lower, meaning that the complex was degrading. Reasons for this were not explored, but it was suggested that molecular collisions resulting from high complex velocities within the capillary may promote dissociation, or the high field strength may separate complexes that

do dissociate on the column, preventing them from recombination with their ligand, which could occur at lower field strengths. Lower field strengths were better for complex stability but worse for sensitivity because of dilution effects.

Pavski and Le developed an assay for the determination of HIV-1 RT using two aptamers, RT26 and RT12.[9] These aptamers had been previously isolated, and had binding constants of 1 and 2 nM, respectively.[31] They were fluorescently labeled with carboxyfluorescein for LIF detection. A calibration curve was constructed, showing that the protein could be detected with a linear range of 0–50 nM. This value is a very narrow dynamic range, probably a result of the high binding constant or kinetics of the assay favoring early binding saturation. It was noted that sample stability was problematic when using very low concentrations of the protein, which was likely the result of working at concentrations near the binding constant of the aptamer. To examine the specificity of the aptamer for HIV-1 RT, the authors tested other reverse transcriptases as well as the effect of sample matrix. The results using reverse transcriptases from the enhanced avian myeloblastosis virus and the Moloney murine leukemia virus incubated with HIV-1 RT separately and together, at concentrations up to two orders of magnitude higher than HIV-1 RT, showed no significant difference in the peak heights compared to samples containing only aptamer and HIV-1 RT. Heat-denatured HIV-1 RT was also tested, and no binding to the aptamer was observed. Using an undiluted sample matrix of RPMI cell culture medium containing 10% fetal bovine serum, known to inhibit HIV-1 RT activity, showed significant depression of the complex peak; however, medium diluted 100-fold showed no significant interference.

Haes et al. developed an ACE assay using an RNA aptamer specific for ricin, a toxic, ribosome-inactivating protein.[7] Both premixed and on-column mixed samples were tested. It was found that the peak areas for the on-column mixed samples were larger than the premixed samples, indicating that there was less time for complex dissociation with the on-column mixing. To test the ability of the method to detect ricin in complex samples, bovine serum albumin and casein were added separately at varying concentrations to the ricin sample matrix. On-column mixing showed that the presence of both proteins decreased the signal from the ricin–aptamer complex; however, they were still able to detect as little as 500 pM ricin in the samples with up to 100 μg/ml nonspecific proteins present. In addition, the authors tested the effect of RNase A, an RNA nuclease, which has the potential to be present in any ricin sample analysis. It was found that RNase does in fact degrade the aptamer during on-column mixing; however, the ricin–aptamer complex still formed and could be detected. The detection limit, however, increased from 500 pM to 1 nM at RNase concentrations of 100 ng/ml due to the loss of viable aptamer concentration.

Huang et al. studied protein–protein interactions using thrombin, antithrombin III (ATIII), and antihuman thrombin (AHT) using the thrombin aptamer in a competitive assay.[8] They first studied the binding structure of the aptamer, and its stability in the G-quartet structure in the presence of K^+, Rb^+, NH^+, Sr^{2+}, Ba^{2+}, Li^+, Na^+, Ca^{2+}, Cs^+, and Mg^{2+}, because the aptamer can only bind to thrombin in this form, not in the linear form. They found that both K^+ and Ba^{2+}, which have ionic radii that fit within the G-quartet structure,[32] were able to stabilize the aptamer and allowed

separation of the aptamer in the G-quartet structure from the aptamer in the linear form. However, Ba^{2+} was deemed unsuitable to study protein–protein and protein–DNA interactions because of peak broadening from a reduced electro-osmotic flow, increased separation time, and decreased resolution. Thrombin quantification was accomplished by using a fluorescently labeled aptamer and measuring the decrease in the peak associated with the G-quartet form of the aptamer. Because long capillaries were used (25 cm), peaks from the aptamer–thrombin complex were not observed; the only evidence of complexation was a tailing peak from the G-quartet aptamer peak. The limit of detection (LOD) was calculated to be 9.8 nM, and the K_d was 20 nM, which were both lower than previous reports (LOD = 40 nM; K_d = 450 and 240 nM). A competitive assay was able to quantify thrombin–ATIII complexes with a limit of detection of 2.1 nM, showing that binding of ATIII to exocyte II of thrombin destabilized the formation of the thrombin–aptamer complex, which was likely caused by conformational change in thrombin rendering the binding of the aptamer to exocyte I unstable. The same experiment done using AHT and a sulfonated hirudin fragment showed no effect on aptamer binding.

9.3.2 Fluorescence Polarization Assays

Fluorescence polarization (FP) is an intrinsic property of molecules in response to excitation by plane-polarized light. It is based on the observation that when fluorescent molecules are excited with plane-polarized light, the emitted light remains fixed in the same plane as the excitation plane (i.e., the light remains polarized) so long as the molecules remain stationary during excitation. However, molecules in solution are subject to rotation. As a result, if the molecule tumbles quickly with respect to the fluorescence lifetime (typically a few nanoseconds), fluorescence is emitted in both vertical and horizontal planes with respect to the excitation light, and the fluorescence is depolarized. However, if the molecule tumbles slowly with respect to the fluorescence lifetime, the observed fluorescence remains significantly polarized (Fig. 9.4).

Larger molecules are characterized by higher polarization values, as their rotational relaxation time is longer (slower rates of rotation), whereas smaller molecules have lower or negligible polarization values due to their shorter rotational relaxation times (faster rates of rotation) (Fig. 9.4). Thus, the extent of fluorescence polarization (FP) can be measured and used to determine molecular interactions and to develop assays that make use of molecular interaction events. ACE has been combined with FP to elucidate additional information about the binding of the aptamer to the target, such as binding stoichiometries.

Fu et al. recently followed up the ACE study done by Pavski and Le by using a polarization assay to determine the binding stoichiometries of four aptamers to HIV-1 RT.[5] The aptamers RT26, RT12, and ODN93 were chosen as polymerase inhibitors of HIV-1 RT; RT26 and RT12 target the polymerase activity of HIV-1 RT whereas ODN93 targets the RNase H region. RTlt49 is a shorter aptamer

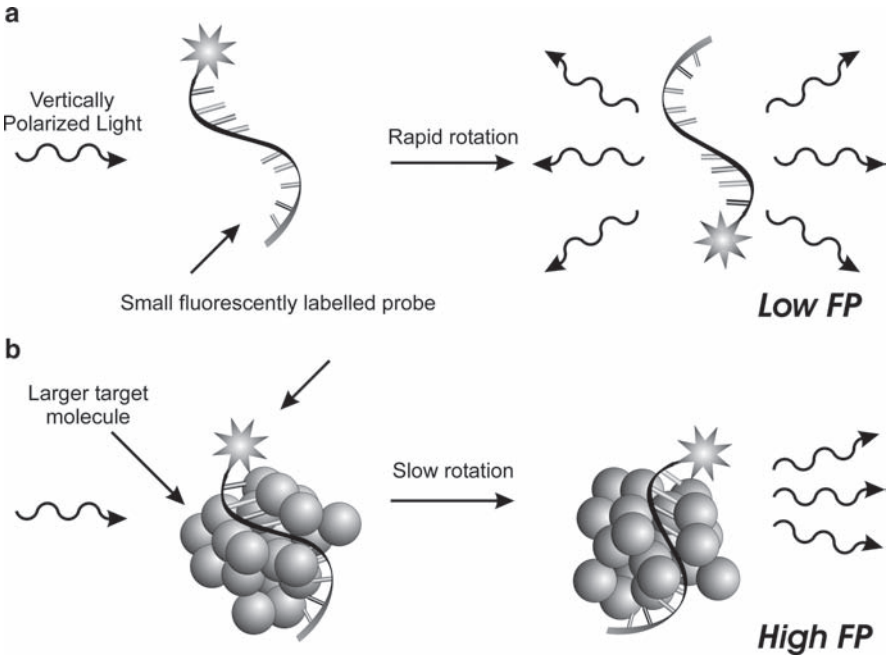

Fig. 9.4 Schematic diagram of the fluorescence polarization (*FP*) difference between a small molecule (**a**) and a large, affinity-bound molecule (**b**). When plane-polarized light is used to excite the fluorescently labeled probe alone, the rapid rotation of the small molecule results in depolarization of the emitted fluorescence, resulting in low FP. When the same light is used to excite a larger molecule, such as when the probe is bound to a much larger protein target, the slow rotation of the large molecule maintains the polarization, resulting in high FP

(49-mer vs. 84-mer, 81-mer, and 81-mer configurations of RT12, RT26, and ODN93, respectively), and lacks the 3′-GGGG and CCCC structures common to the other three aptamers. To study the binding stoichiometry, titration experiments were conducted with CE/LIF. The results suggested the presence of two binding stoichiometries using RT12 and RT26, represented by two peaks. To further confirm the presence of two different complexes, CE-laser-induced fluorescence polarization was employed using all four aptamers. It was shown that ODN93 also formed two binding stoichiometries whereas RTlt49 only formed one. This finding suggested that RT12, RT26, and ODN93 were able to bind to both the p51 and p66 subunits of HIV-1 RT whereas RTlt49 was not. This difference was attributed to the lack of the G-quartet structure, which only allowed RTlt49 to bind to the p66 subunit of HIV-1 RT, and not the p51 unit that contains the RNase H activity. The measured FP values of the three 1:2 complexes were lower than those of the 1:1 complexes (Fig. 9.5). This result seems counterintuitive, because a 1:2 complex is larger in size than a 1:1 complex and would result in slower rotation and higher FP values. The reason for significantly lower FP values was attributed to fluorescence resonance energy transfer (FRET) between the two identical fluorophores within

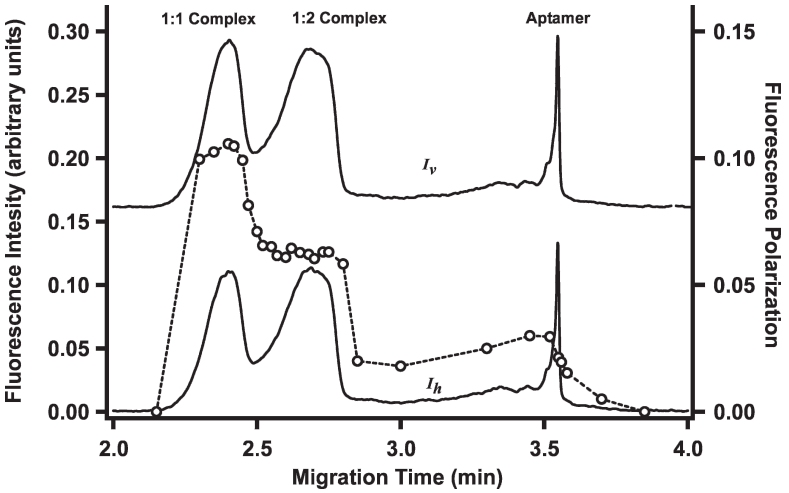

Fig. 9.5 Electropherograms showing vertically (I_v) and horizontally (I_h) polarized fluorescence and polarization of the aptamer RT26 and its complex with HIV-1 RT. Polarization values are appended on I_h and are represented by *open circles* (--o--). Two stoichiometries were observed, as shown by the two peaks at 2.3 and 2.7 min. The polarization value of the 1:2 complex was lower than the 1:1 complex, probably a result of FRET (Reprinted with permission from ref. 5)

the same 1:2 complex. FRET depends on the distance between the fluorophores (FRET may occur when the distance is <100 Å), the degree of spectral overlap of the absorption of the acceptor and the emission of the donor, and the relative orientation of the two fluorophores. In this work, the close proximity of the fluorophores attached to the aptamers once bound to the protein probably resulted in FRET. The authors also reported a linear calibration plot between 0 and 35 nM for the quantification of HIV-1 RT. They also noted that the linearity in this range was only possible if peak areas of both the 1:1 and 1:2 complexes were considered as a whole, and not as separate measures.

9.3.3 Nonequilibrium Capillary Electrophoresis of Equilibrium Mixtures

Berezovski and Krylov introduced nonequilibrium capillary electrophoresis of equilibrium mixtures (NECEEM) as a method to determine both the equilibrium binding constant, K_d, and the kinetic decay constant, k_1, for protein–DNA interactions in a single experiment.[3,18] NECEEM employs low-affinity aptamers as affinity probes for the quantitative analysis of analytes as opposed to high-affinity aptamers used in ACE. Briefly, an equilibrium mixture containing both protein and DNA was prepared. After equilibration, a plug of the equilibrium mixture was injected into the capillary using a running buffer devoid of the protein or aptamer. Since the

complex was no longer in equilibrium with free DNA and free protein, the complex underwent exponential decay from dissociation. Using fluorescently labeled aptamers, the resulting electropherogram typically has two peaks and an exponential decay curve adjacent to one of the peaks. Binding constants (K_d) were extracted by calculating the ratio of the areas under the DNA peak and the combination of the second peak and exponential decay curve. The kinetic decay constant was calculated by fitting the exponential curve to a single-exponential function. From this, the bimolecular rate constant, k_1, was determined from the equation $k_1 = k_{-1}/K_d$.

NECEEM was used to study the interactions between thrombin and a single-stranded DNA that binds to thrombin.[3] For NECEEM to be useful, there must be sufficient separation between the free aptamer peak and the protein–aptamer complex peak. To accomplish this, affinity-mediated NECEEM was employed, where a single-stranded DNA-binding protein (SSB) from *Escherichia coli* was added to the running buffer. SSB nonspecifically binds to the single-stranded DNA aptamer but not to the protein. Thus, the presence of SSB in the binding buffer was expected to both change the mobility of the DNA and preclude binding of the protein to the aptamer during NECEEM. In this study, the electropherograms consisted of two components: an initial peak corresponding to the free aptamer, and an exponential curve corresponding to the decay of the aptamer–thrombin complex. The aptamer–thrombin peak was not observed and was shown to have completely dissociated during its migration through the capillary (Fig. 9.6). The K_d was found to

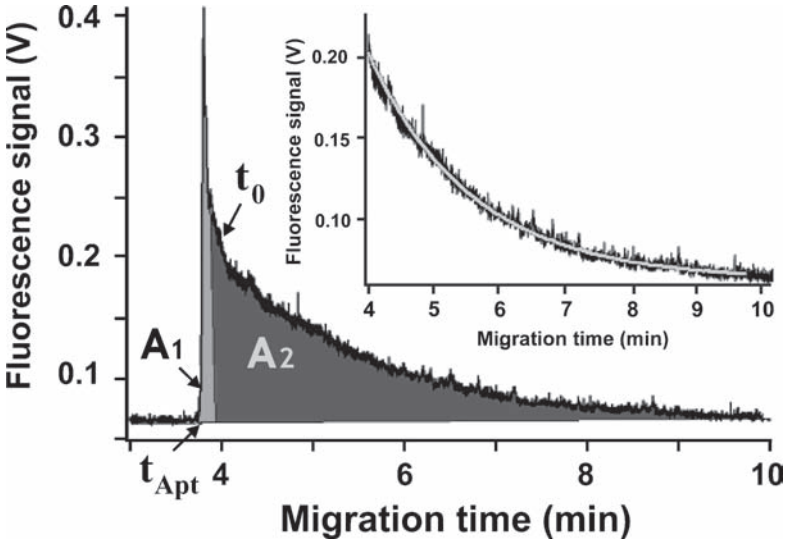

Fig. 9.6 NECEEM electropherogram generated using thrombin and its aptamer. The peak corresponds to the free aptamer and the exponential decay curve is from the dissociation of the aptamer–thrombin complex. To determine the K_d and k_{off}, areas A1 and A2 as well as the migration time of the aptamer (t_{Apt}) were required. The *inset* illustrates the fitting of the experimental decay curve with a single exponential function for the determination of k_{-1} (Reprinted with permission from ref. 3)

be 240 ± 16 nM, which is consistent with previous reports of 200 nM.[30] The kinetic rate constant, k_{-1}, was found to be (8.8 ± 1.0) × 10^{-3} s^{-1}. This result was noted to be a value characteristic of the separation buffer, and not the incubation buffer, and it showed that 99.3% of the aptamer–thrombin complex had dissociated during separation. By using the K_d value, the authors reported a detection limit of 60 nM protein and a linear dynamic range of two orders of magnitude.

Berezovski et al. later studied the interaction of *Taq* DNA polymerase with an aptamer using temperature-controlled NECEEM.[2] This method allowed the determination of temperature-dependent equilibrium and kinetic constants, as well as thermodynamic values of the protein–DNA interaction. Their results showed that the equilibrium stability did not change significantly between 15°C and 36°C; however, it decreased sharply at $T > 36$°C, which was in perfect agreement with previous data. The temperature dependence was attributed to a conformational change of the aptamer, where the initial conformation was more temperature stable than the second conformation. The value of k_1 was shown to mimic the temperature dependence of K_d, whereas the k_{-1} values did not show such a dramatic change above 36°C; this suggested that temperature played a greater role in complex formation than complex dissociation. They also studied a SSB with ssDNA in the same manner. This system was also found to undergo a temperature-dependent conformational change in K_d, which was attributed to the multimerization of the protein. The thermodynamic data for ΔH and ΔS showed that the *Taq* DNA polymerase–aptamer system was entropy driven at low temperatures and enthalpy driven at high temperatures, whereas the driving forces for the SSB/ssDNA system were the opposite.

9.3.4 Affinity-Polymerase Chain Reaction CE Methods

One of the main drawbacks of the previously described methods is that they cannot be used to determine ultratrace concentrations of proteins in a biological sample. Detection limits are commonly in the nanomolar (nM) range, which are still orders of magnitude higher than the concentrations of low abundance proteins in real samples. PCR can be used to exponentially amplify nucleic acid sequences, which drastically reduces the detection limits; however, there is no comparable technique for amplification of proteins.

To detect ultratrace protein concentrations, Zhang et al. have recently developed an ultrasensitive aptamer-based affinity-PCR technique and demonstrated its application for the determination of trace amounts of HIV-1 RT.[11] This method was used to indirectly measure the protein concentrations by PCR amplification of an HIV-1 RT-bound aptamer. Figure 9.7 shows the principle and operation of the assay. A previously isolated aptamer (RT 26, 1 nM) was incubated with HIV-1 RT, and an aliquot of the mixture was separated by CE. After the fraction containing only the aptamer–protein complex was collected, the aptamer was dissociated from the protein, amplified by PCR, and detected. The typical CE injection of 10 nl 30 fM HIV-1 RT corresponded to a detection limit of approximately 180 molecules of

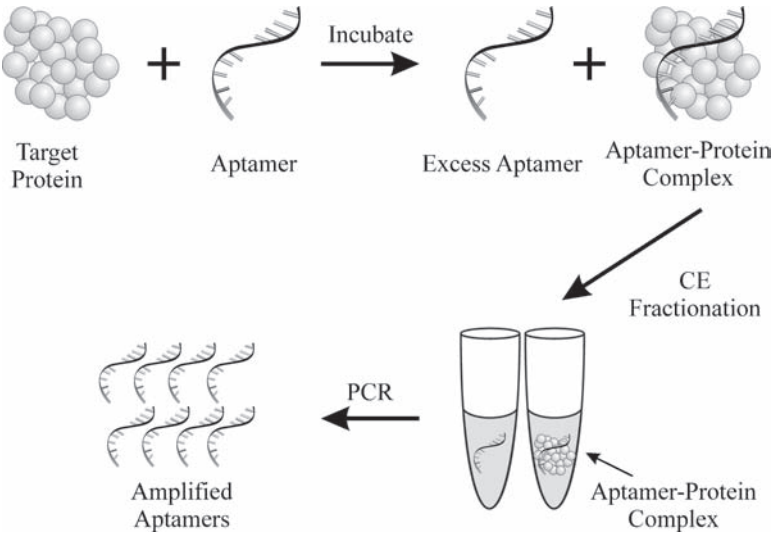

Fig. 9.7 Affinity aptamer amplification assay for proteins. The protein was first incubated with the aptamer to form an aptamer–protein complex. Separation and fractionation of the protein–aptamer complex from excess aptamers was conducted by CE. After the fraction containing only the aptamer–protein complex was collected, the aptamer was dissociated from the protein and amplified by PCR. The amplified aptamers were indirect measures of the protein concentration

HIV-1 RT, which represents detection limits orders of magnitude better than those of the traditional methods. This method was shown to be specific to HIV-1 RT in the presence of human IgG and RNase H. Both the specific recognition by aptamers and the CE separation aided in increasing the specificity of the assay. This assay is advantageous since the PCR method is able to amplify low concentrations of the aptamer, allowing indirect measurements of protein concentrations. However, careful attention should be paid to the collection of CE fractions and PCR amplification of the aptamer to avoid any contamination that could be amplified by PCR.

9.4 Conclusions

Aptamers have been used in many different applications; however, their use in affinity separations with CE has so far been understudied. One of the main reasons that only a handful of applications have been reported since the first paper[6] in 1998 is that the availability of high-quality aptamers for a given target is limited. The Aptamer Database currently lists just over 300 publications for aptamers selected by in vitro methods.[33] The actual number of available aptamers is less than the number of publications, because some report the selection of different aptamers for the same target and still others are reviews. In addition, many of the reported aptamers are RNA sequences, which are generally unsuitable for assays in biological media

as they are readily degraded by RNases.[34,35] So far, CE assays have been limited to using DNA aptamers for IgE, HIV-1 RT, thrombin, antithrombin (III), antihuman thrombin, ricin toxin, *Taq* polymerase, and platelet-derived growth factor (PDGF) isomers.[36,37] This dearth can be addressed by developing improved SELEX methods that make the process of selecting high-affinity DNA aptamers less time consuming and more reliable.

The first report of CE-SELEX emerged in 2004, and it has shown its utility for selecting both high-affinity aptamers in fewer rounds than conventional SELEX and lower-affinity aptamers that may be useful in electrochromatographic methods, as described in the next chapter (Chapter 10). Future trends are toward improving the existing methods and developing new SELEX methods for the selection of aptamers for small molecules of biological and environmental importance. So far, only one report has shown this to be feasible[16]; however, targets that are even smaller will require the development of new methodologies, as separation of target-bound from unbound nucleic acids requires a significant mobility shift not observed while using such small targets. If successful, this will be a vast improvement over the conventional affinity column- (or bead-) based SELEX method,[13] which is the only method currently used for the selection of aptamers for small targets.

CE affinity separations have undergone some improvements and modifications: examples include DNA-driven focusing by Wang et al. to improve separation and peak shape,[10] amplification of affinity aptamers by Zhang et al. for ultratrace detection,[11] NECEEM by Berezovski et al. to use low-affinity aptamers to quantitatively analyze proteins,[3,18] and tunable aptamer capillary electrophoresis developed by Zhang et al. for detection of multiple proteins and protein isomers.[37] Further development of CE affinity assays and its future success likely lies in the further development of miniature, fast, and multidimensional separation methods.[36] In addition, although CE has already been proven for high-throughput analysis,[1] aptamers have so far not played a role in this development. High-throughput analysis along with increased separation speed and improved detection limits toward clinically relevant concentrations may drive affinity CE to more clinical and diagnostic applications, such as the development of pharmaceutical drugs and the early detection of diseases.

References

1. Dovichi, N.J. and Zhang, J. (2000) How capillary electrophoresis sequenced the human genome. Angew. Chem. Int. Ed. 39:4463–4468.
2. Berezovski, M. and Krylov, S.N. (2005) Thermochemistry of protein–DNA interaction studied with temperature-controlled nonequilibrium capillary electrophoresis of equilibrium mixtures. Anal. Chem. 77:1526–1529.
3. Berezovski, M., Nutiu, R., Li, Y. and Krylov, S.N. (2003) Affinity analysis of a protein–aptamer complex using nonequilibrium capillary electrophoresis of equilibrium mixtures. Anal. Chem. 75:1382–1386.
4. Buchanan, D.D., Jameson, E.E., Perlette, J., Malik, A. and Kennedy, R.T. (2003) Effect of buffer, electric field, and separation time on detection of aptamer–ligand complexes for affinity probe capillary electrophoresis. Electrophoresis 24:1375–1382.

5. Fu, H., Guthrie, J.W. and Le, X.C. (2006) Study of binding stoichiometries of the human immunodeficiency virus type 1 reverse transcriptase by capillary electrophoresis and laser-induced fluorescence polarization using aptamers as probes. Electrophoresis 27:433–441.
6. German, I., Buchanan, D.D. and Kennedy, R.T. (1998) Aptamers as ligands in affinity probe capillary electrophoresis. Anal. Chem. 70:4540–4545.
7. Haes, A.J., Giordano, B.C. and Collins, G.E. (2006) Aptamer-based detection and quantitative analysis of ricin using affinity probe capillary electrophoresis. Anal. Chem. 78:3758–3764.
8. Huang, C., Cao, Z., Chang, H. and Tan, W. (2004) Protein–protein interaction studies based on molecular aptamers by affinity capillary electrophoresis. Anal. Chem. 76:6973–6981.
9. Pavski, V. and Le, X.C. (2001) Detection of human immunodeficiency virus type 1 reverse transcriptase using aptamers as probes in affinity capillary electrophoresis. Anal. Chem. 73:6070–6076.
10. Wang, H., Lu, M. and Le, X.C. (2005) DNA-driven focusing for protein–DNA binding assays using capillary electrophoresis. Anal. Chem. 77:4985–4990.
11. Zhang, H., Wang, Z., Li, X. and Le, X.C. (2006) Ultrasensitive detection of proteins by amplification of affinity aptamers. Angew. Chem. Int. Ed. 45:1576–1580.
12. Tuerk, C. and Gold, L. (1990) Systematic evolution of ligands by exponential enrichment: RNA ligands to bacteriophage T4 DNA polymerase. Science 249:505–510.
13. Ellington, A.D. and Szostak, J.W. (1990) In vitro selection of RNA molecules that bind specific ligands. Nature (Lond.) 346:818–822.
14. Mendonsa, S.D. and Bowser, M.T. (2004) In vitro evolution of functional DNA using capillary electrophoresis. J. Am. Chem. Soc. 126:20–21.
15. Mendonsa, S.D. and Bowser, M.T. (2004) In vitro selection of high-affinity DNA ligands for human IgE using capillary electrophoresis. Anal. Chem. 76:5387–5392.
16. Mendonsa, S.D. and Bowser, M.T. (2005) In vitro selection of aptamers with affinity for neuropeptide Y using capillary electrophoresis. J. Am. Chem. Soc. 127:9382–9383.
17. Mosing, R.K., Mendonsa, S.D. and Bowser, M.T. (2005) Capillary electrophoresis: SELEX selection of aptamers with affinity for HIV-1 reverse transcriptase. Anal. Chem. 77:6107–6112.
18. Berezovski, M., Drabovich, A., Krylova, S.M., Musheev, M., Okhonin, V., Petrov, A. and Krylov, S.N. (2005) Nonequilibrium capillary electrophoresis of equilibrium mixtures: a universal tool for development of aptamers. J. Am. Chem. Soc. 127:3165–3171.
19. Tang, J., Xie, J., Shao, N. and Yan, Y. (2006) The DNA aptamers that specifically recognize ricin toxin are selected by two in vitro selection methods. Electrophoresis 27:1303–1311.
20. Drabovich, A., Berezovski, M. and Krylov, S.N. (2005) Selection of smart aptamers by equilibrium capillary electrophoresis of equilibrium mixtures (ECEEM). J. Am. Chem. Soc. 127:11224–11225.
21. Drabovich, A.P., Berezovski, M., Okhonin, V. and Krylov, S.N. (2006) Selection of smart aptamers by methods of kinetic capillary electrophoresis. Anal. Chem. 78:3171–3178.
22. Mallikaratchy, P., Stahelin, R.V., Cao, Z., Cho, W. and Tan, W. (2006) Selection of DNA ligands for protein kinase C-δ. Chem. Commun. (Cambridge, United Kingdom) 30:3229–3231.
23. Berezovski, M., Musheev, M., Drabovich, A. and Krylov, S.N. (2006) Non-SELEX selection of aptamers. J. Am. Chem. Soc. 128:1410–1411.
24. Burgi, D.S. (1993) Large volume stacking of anions in capillary electrophoresis using an electroosmotic flow modifier as a pump. Anal. Chem. 65:3726–3729.
25. Auriola, S., Jaaskelainen, I., Regina, M. and Urtti, A. (1996) Analysis of oligonucleotides by on-column transient capillary isotachophoresis and capillary electrophoresis in polyethylene glycol-filled columns. Anal. Chem. 68:3907–3911.
26. Shihabi, Z.K. (2000) Stacking in capillary zone electrophoresis. J. Chromatogr. A 902:107–117.
27. Wanders, B.J. and Everaerts, F.M. (1994) Isotachophoresis in capillary electrophoresis. In: Landers, J.P. (ed.) Handbook of capillary electrophoresis. CRC Press, Ann Arbor, MI, pp. 111–127.
28. Xiong, Y., Park, S.R. and Swerdlow, H. (1998) Base stacking: pH-mediated on-column sample concentration for capillary DNA sequencing. Anal. Chem. 70:3605–3611.

29. Davis, K., Abrams, B., Lin, Y. and Jayasena, S. (1996) Use of a high affinity DNA ligand in flow cytometry. Nucleic Acids Res. 24:702–706.
30. Bock, L.C., Griffin, L.C., Latham, J.A., Vermaas, E.H. and Toole, J.J. (1992) Selection of single-stranded DNA molecules that bind and inhibit human thrombin. Nature (Lond.) 355:564–566.
31. Schneider, D.J., Feigon, J., Hostomsky, Z. and Gold, L. (1995) High-affinity ssDNA inhibitors of the reverse transcriptase of type 1 human immunodeficiency virus. Biochemistry 34:9599–9610.
32. Kankia, B.I. and Marky, L.A. (2001) Folding of the thrombin aptamer into a G-quadruplex with Sr^{2+}: stability, heat, and hydration. J. Am. Chem. Soc. 123:10799–10804.
33. Lee, J.F., Hesselberth, J.R., Meyers, L.A. and Ellington, A.D. (2004) Aptamer database. Nucleic Acids Res. 32:D95–D100.
34. Brumbt, A., Ravelet, C., Grosset, C., Ravel, A., Villet, A. and Peyrin, E. (2005) Chiral stationary phase based on a biostable L-RNA aptamer. Anal. Chem. 77:1993–1998.
35. Nutiu, R. and Li, Y. (2005) In vitro selection of structure-switching signaling aptamers. Angew. Chem. Int. Ed. 44:1061–1065.
36. Kennedy, R.T. (1999) Bioanalytical applications of fast capillary electrophoresis. Anal. Chim. Acta 400:163–180.
37. Zhang, H., Li, X.-F. and Le, X.C. (2008) Tunable aptamer capillary electrophoresis and its application to protein analysis. J. Am. Chem. Soc. 130:34–35.

Chapter 10
Aptamers in Affinity Separations: Stationary Separation

Corinne Ravelet and Eric Peyrin

Abstract The use of DNA or RNA aptamers as tools in analytical chemistry is a very promising field of research because of their capabilities to bind specifically the target molecules with an affinity similar to that of antibodies. Notably, they appear to be of great interest as target-specific ligands for the separation and capture of various analytes in affinity chromatography and related affinity-based methods such as magnetic bead technology. In this chapter, the recent developments of these aptamer-based separation/capture approaches are addressed.

10.1 Introduction

The development of the systematic evolution of ligands by exponential enrichment (SELEX) procedure[1–3] has allowed the discovery of aptamers against various targets such as ions, small organics, positively and negatively charged peptides, and proteins, viruses, and tissues.[4] The use of aptamers as tools in analytical chemistry is a very promising and exciting field of research for reasons of their capabilities to bind specifically the target molecules, with an affinity similar to that of antibodies. For example, aptamers typically bind target proteins with dissociation constants in the picomolar to nanomolar range with specificity constants of 10^3 or greater when comparing aptamer binding to the target versus related nontarget proteins. Aptamers can even distinguish between proteins that differ by only a few amino acids.[5] Furthermore, aptamers present numerous advantages over antibodies.[6] Aptamers can be regenerated within minutes via a denaturation-renaturation step and are, at least for DNA aptamers, relatively stable over time. The in vitro selection conditions (buffer composition, temperature, etc.) can be manipulated to obtain binding properties desirable for specific assays. As the specific binding pocket of the aptamers can be commonly elucidated by chemical and enzymatic footprinting, it is also possible to change their sequence

C. Ravelet and E. Peyrin
Département de Pharmacochimie Moléculaire UMR 5063 CNRS,
Institut de Chimie Moléculaire de Grenoble FR 2607, Université Joseph Fourier, France
eric.peyrin@ujf-grenoble.fr

Y. Li and Y. Lu (eds.), *Functional Nucleic Acids for Analytical Applications*,

at critical, precise locations to modulate the selectivity and the kinetic parameters of binding. The aptamers can be produced by chemical synthesis at a relatively high degree of purity, resulting in little or no batch-to-batch variation, and reporter molecules can be attached to aptamers at precise locations. Finally, they are produced through an in vitro process that does not require animals. Taking into account all these attractive background features, various analytical aptamer-based formats have been exploited, including enzyme-linked oligonucleotide assays, biosensors (called aptasensors), flow cytometry, or capillary electrophoresis/capillary electrochromatography (see other chapters of this book). The use of aptamers as target-specific ligands in liquid chromatography (and magnetic bead technology) for separation and capture of various analytes such as biopolymers or small molecules have also received much attention during the past few years. This chapter focuses on the potentials of such DNA and RNA oligonucleotides in such an affinity separation field.

10.2 Use of Aptamers as Specific Ligands for the Capture of Biopolymers

Affinity chromatography and related affinity-based techniques such as magnetic bead technology are rapidly becoming the methods of choice in various fields such as biochemistry, biotechnology or pharmaceutical sciences. All these techniques make use of a biological interaction for the separation, analysis, and purification of specific analytes within a sample. The specific ligand of interest is classically immobilized on a surface covalently or via a streptavidin–biotin interaction. The simplest operating scheme for the analyte capture involves the contact of the sample with the affinity matrix under conditions in which the target analyte will bind to the immobilized ligand with high affinity. Because of the specificity of the analyte–ligand interaction, undesirable solutes in the sample tend to have little or no affinity for the immobilized ligand. The elution buffer is then applied to dissociate the retained analyte. Although various immobilized specific ligands have been used for the purification of analytes in liquid chromatography and magnetic bead technology, the most popular format takes advantage of the high affinity and specificity offered by antibodies to create efficient immunoaffinity separation systems. However, there are some constraints that reduce the effectiveness of antibodies. The linkage of antibodies to chromatographic support or magnetic beads often results in couplings that are not uniform, leading to reduced binding capacity, and can allow leaching of the antibody from the surface. Furthermore, antibodies present a relatively larger size, which limits the ligand density at the bead surface. Finally, the elution/release conditions can be harsh, requiring extremes of pH, detergents, organic solvents, or chaotropic salts, leading to denaturation of the antibody and possibly the target (a protein, for example).

Expected advantages of aptamers relative to antibodies for the separation and capture by affinity-based methods include smaller size, enabling higher density on the surface, novel approaches for elution, and the possibility to immobilize the ligand to the support at a precise location. Moreover, a number of recent reports have shown

Table 10.1 Use of aptamers as specific ligands for biopolymer capture in affinity chromatography and magnetic bead technology

Targets	Oligos[a]	Methodologies	Applications immobilized aptamers	Refs
L-selectin	DNA	LC[b]/elution by EDTA	Purification of recombinant human L-selectin-Ig fusion protein from Chinese hamster ovary cell-conditioned medium Target capture	7
Thrombin	DNA	Capillary LC/elution by 8 M urea at 50°C	Target capture	8
HCV RNA polymerase and replicase	RNA	Chip/elution by photolytic method	Target capture	9, 10
Thyroid transcription factor 1	DNA	Magnetic beads/elution by DNase treatment	Purification of TTF1 in the soluble fraction of bacterial lysates	11
Aptamer tags				
Streptomycin	RNA	Sreptomycin matrix/elution by 10 µM streptomycin	Purification of yeast and phage RNA-binding proteins, group II intron, viral and bacterial noncoding RNA-binding proteins noncoding RNA-binding mRNAs Purification of RNAse P	12–14
Sephadex	RNA	Sephadex matrix/elution by denaturants or soluble dextran	Purification of RNAse P	18
Streptavidin	RNA	Sreptavidin matrix/elution by 5 mM *d*-biotin	Purification of RNAse P	17, 18
Tobramycin	RNA	Tobramycin matrix/elution by 5 mM tobramycin	Purification and identification of prespliceosomes	15

[a]Oligos: oligonucleotides
[b]LC: liquid chromatography

great interest in the use of DNA or RNA aptamers as immobilized affinity ligands in liquid chromatography and magnetic bead technology to purify proteins (Table 10.1).

Drolet and coworkers have presented the first work concerning the use of an immobilized DNA aptamer as an affinity stationary phase in liquid chromatography.[7] An aptamer of 36 nucleotides in length, displaying a high specificity and affinity (K_d of 2 nM) for human L-selectin, was applied to the chromatographic capture of recombinant L-selectin-Ig fusion protein from Chinese hamster ovary cell-conditioned medium. The 5′-biotinylated anti-L-selectin DNA aptamer was immobilized on a streptavidin Sepharose support, which was packed in a short column. After loading onto the aptamer affinity column, the L-selectin-Ig fusion protein was eluted under conditions that do not denature proteins: based on the known divalent cation dependence of the active tertiary structure of the aptamer, a linear ethylenediaminetetraacetic acid (EDTA) gradient appeared to be very efficient to release the captured protein. Application of the aptamer column as the initial purification step has resulted in a 1,500-fold purification with an 83% single-step recovery, demonstrating that aptamers can be effective as affinity capture reagents. However, it was also noted by the authors that the DNA aptamer was degraded by the nucleases present in the cell culture media, underlining the general limitation of the aptamer-based purification approach in biological media.

More recently, the use of a thrombin-binding DNA aptamer as a protein capture system in affinity capillary chromatography has been reported.[8] A 5′-thiol-modified aptamer (15 nucleotides) has been covalently attached to the inner surface of a bare fused silica capillary via an organic linker to serve as the stationary phase. After protein capture at 25°C by incubation overnight, the bound thrombin was released using an elution scheme involving 8 M urea and a capillary temperature of 50°C. Eluate was collected after each step (load, wash, and elute), and relative amounts of protein each were compared using fluorescence spectroscopy. The protein identity was confirmed using matrix-assisted laser desorption ionization-time of flight (MALDI-TOF) mass spectrometry analysis. The results showed that the aptamer stationary phase was able to bind approximately three times as much thrombin as the control columns (scrambled sequence oligonucleotide or bare column), in the presence or absence of human serum albumin. This finding suggested that nonspecific thrombin retention occurred, dependent on the protein adsorption to the exposed regions of the fused silica surface. Due to the low surface coverage of the aptamer phase or an inefficient capture by the stationary phase, only around 0.08 thrombin molecules/nm^2 were captured in this system, for an estimated stationary-phase density of two aptamers attached/nm^2.[8]

Via an elegant elution strategy based on a photolytic method, the detection of hepatitis C virus (HCV) RNA polymerase and replicase from a protein mixture using a microbead affinity chromatography on a chip has been achieved.[9,10] The RNA aptamer directed against the protein was coupled to the beads using a Fmoc photo-cleavable linker, and the aptamer-immobilized beads were loaded and packed in a microfluidic chip composed of a transparent microchannel. A protein sample was injected onto the microchamber and incubated for 5–30 min. After washing, the microchannel was irradiated by UV light at 360 nm and the captured

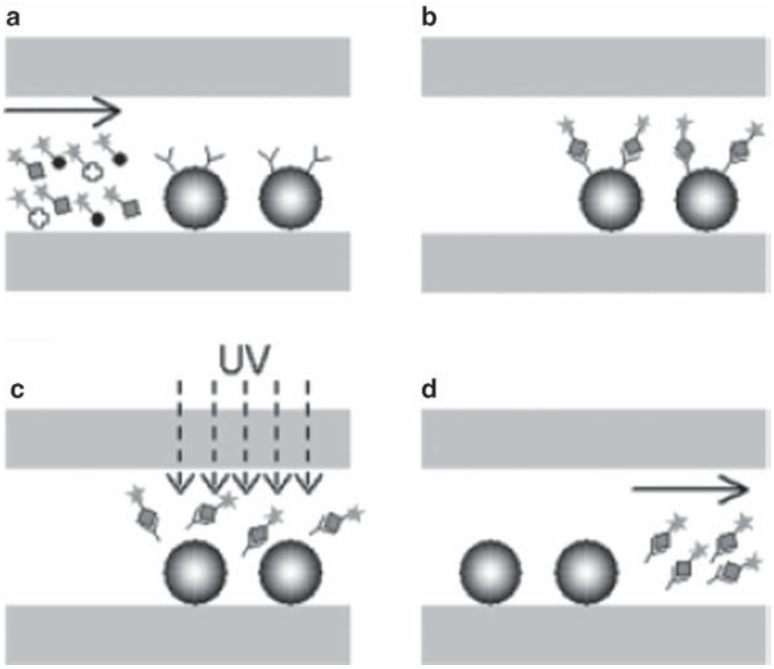

Fig. 10.1 Schematic view of microaffinity purification process using photolytic elution method: (**a**) injection of the protein mixture into the microchip packed with RNA aptamer-modified microbeads; (**b**) purification of the target protein; (**c**) UV irradiation; (**d**) analysis of the photolytically eluted protein (Reproduced with permission from ref. 10. Copyright [2005], Wiley)

protein was eluted with the pumped flow of mobile phase (Fig. 10.1). In the first approach for the detection of HCV RNA polymerase,[9] subsequent trypsin treatment was performed and the peptide mixture was concentrated and applied to MALDI-TOF mass spectrometry analysis. The detection limit of this system was estimated to be around 10 fmol HCV RNA polymerase. In the second approach for the analysis of HCV RNA replicase,[10] the protein was labeled with fluorescein, and the eluted target was quantitatively detected via the fluorescence intensity measurement using a confocal microscope. It has been shown that such a system was able to detect the HCV RNA replicase from a mixture containing 170 fmol target protein.

Doyle and coworkers have reported the affinity purification of thyroid transcription factor 1 (TTF1) using an antiprotein DNA aptamer immobilized on magnetic beads.[11] The aptamer-based affinity method was performed in a single purification step from a complex mixture of proteins in the soluble fraction of bacterial lysates. A solution of biotinylated anti-TTF1 aptamer (K_d ~50 nM) was mixed with streptavidin magnetic beads for 30 min. After a washing procedure, an aliquot of cleared lysate spiked with the target protein was added to the modified magnetic beads. Elution of the TTF1 protein from the affinity matrix was carried out using a recombinant DNase treatment. The recovery of purified TTF1 protein was around

25–50% of the total protein bound to the affinity support. In contrast with the observation reported by Romig et al. for the purification of L-selectin, detrimental effects from DNase activity in the TTF1 purification from bacterial lysates were not observed by these authors.

10.2.1 Aptamers as Affinity Tags

As an alternative to their use as immobilized specific ligands for affinity-based purification techniques, aptamers have been also successfully employed as affinity tags for the capture of biopolymers in affinity chromatography. An aptamer tag is selected against an immobilized target and embedded in or fused to either end of any RNA of interest. The resulting hybrid RNA can then be immobilized on an affinity column via the interaction between the aptamer tag and the matrix-immobilized target. Subsequently, a complex protein mixture or total cellular lysate is applied to the matrix, and elution with a free target solution allows efficient recovery of specific species such as ribonucleoproteins or RNA–RNA complexes (see Table 10.1). The general principle is illustrated in Fig. 10.2 by the antitobramycin RNA aptamer tag.

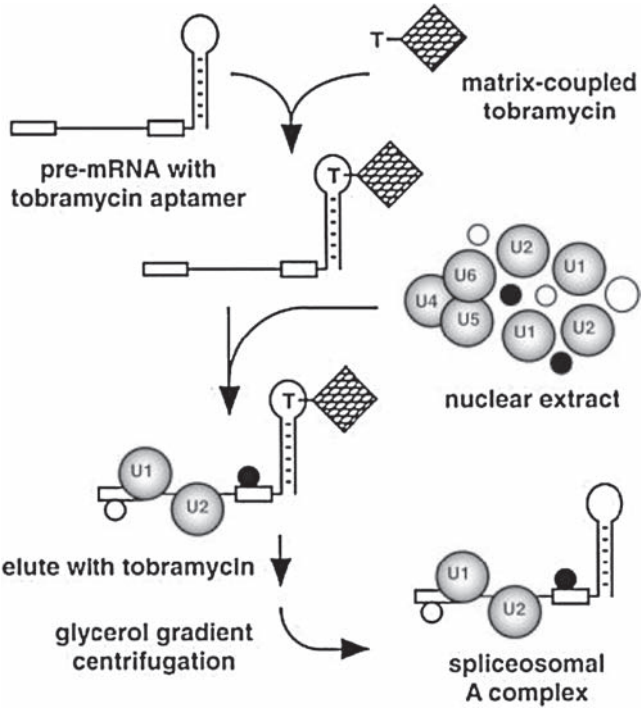

Fig. 10.2 Principle of the aptamer-based affinity tag method using an antitobramycin RNA aptamer (Reproduced with permission from ref. 15. Copyright [2002], National Academy of Sciences, USA)

Bachler et al. first described an affinity-purification method for the isolation of specific RNA-binding proteins using an in vitro-transcribed hybrid RNA.[12] The hybrid RNA consisted of an aptamer sequence with high binding specificity to the antibiotic streptomycin and a putative protein-binding RNA sequence. The streptomycin-binding RNA aptamer (referred as StreptoTag) was selected using a dihydrostreptomycin-coupled Sepharose and was shown to bind to the antibiotic with K_d of 1 μM, only in the presence of magnesium ions. StreptoTag fusion RNAs were created directly by polymerase chain reaction (PCR) and subsequent in vitro transcription. The templates of hybrid RNAs contained the protein-binding sites for the MS2 coat proteins (hairpin from MS2 replicase mRNA; wild-type, K_d < 1 nM; mutant, K_d in the low millimolar range) or for the U1A spliceosomal protein (stem-loop II of U1 snRNA: K_d in the low nanomolar range). Hybrid RNAs and proteins from crude extracts were incubated and the samples were applied to the streptomycin affinity column. After washes for the removal of nonspecific RNA-binding proteins, the bound proteins were recovered from the matrix by elution with a 10 μM streptomycin solution. This procedure appeared of interest as it allowed protein isolation from extracts in high yield and purity in only one round. The aptamer tag and the biotin tag strategies were compared. The purification efficiency of the StreptoTag methodology was found to be higher than that using the biotin–streptavidin system, which led to copurification of nonspecifically binding proteins. In addition, the MS2 coat protein could be isolated with a mutant RNA motif, indicating that such StreptoTag approach was able to detect weak RNA–protein interactions. This strategy has been subsequently applied to purify novel yeast group II intron-binding proteins, small ncRNA-binding proteins, and ncRNA-binding mRNAs.[13]

The method and StreptoTag sequence have been further optimized by Schroeder and coworkers for the isolation of low-abundance proteins with complex RNA-binding targets.[14] First, three modifications of the original StreptoTag aptamer were designed by modifications of the stem or the hairpin bulge involved in the streptomycin binding. It was found that the modification of the hairpin apex (formation of a GCAA tetraloop) was responsible for a 80% increase in stability for binding to the streptomycin-coupled column. Second, the method was adapted to use larger, less well defined test RNA molecules (up to at least 550 nt) to identify new RNA-binding targets. It was demonstrated that this optimized StreptoTag procedure allowed the isolation of low-abundance mouse mammary tumor virus long terminal repeat binding proteins from human cell extract.

Alternative intrinsic RNA aptamer tags have been described by other authors. Hartmuth et al. have described the use of an antitobramycin aptamer to tag the pre-mRNA.[15] The aptamer displayed a high affinity for tobramycin under physiological conditions (K_d, 5 nM). The hybrid RNA (aptamer–pre-mRNA) was created by PCR and transcription. The tagged pre-mRNA was first immobilized on tobramycin matrix (60–70% was bound) and subsequently incubated with nuclear extract under splicing conditions. The matrix was washed, and bound material was eluted with 5 mM tobramycin. To isolate the formed prespliceosomes, the tobramycin eluates were submitted to glycerol fraction centrifugation, then to

sodium dodecyl sulfate-polyacrylamide gel electrophoresis (SDS/PAGE), and the protein composition was analyzed by MALDI-MS or LC-MSMS. More than 70 proteins were identified by this approach, including proteins that are known to be involved in the pre-mRNA splicing but also several new prespliceosomal proteins.[15]

Engelke and coworkers have designed two intrinsic RNA aptamer tags directed against Sephadex and streptavidin.[16–18] D8 (33-nt) and S1 (44-nt) aptamers were isolated as minimal binding motifs for Sephadex and streptavidin, respectively. The D8 Sephadex-binding aptamer was found to bind specifically to the Sephadex G-100 without binding to other similar matrices such as Sepharose and Sephacryl. Using a Sephadex G-100 affinity matrix and elution schemes with denaturants or by competition with soluble dextran, the D8 aptamer can be selectively isolated from a complex mixture of RNA from human tissue culture cells (HeLa) with an enrichment of at least 60,000 fold over a control RNA.[16] The S1 streptavidin-binding RNA aptamer was originally selected to bind streptavidin in either streptavidin-agarose beads or polyacrylamide gel electrophoretic mobility shift assays. The S1 tag bound to streptavidin with high affinity (K_d, 70 nM). This binding can be disrupted in the presence of *d*-biotin, probably because the binding site might be at or near the biotin-binding pockets of streptavidin. Alternatively, the binding of biotin could cause a conformational change on streptavidin. The S1 tag was first evaluated as an affinity motif to recover ribonucleoprotein complexes from crude cellular lysates. The RNA subunit of *Saccharomyces cerevisiae* nuclear RNase P was chosen as a model RNA to be tagged with the streptavidin aptamer. Nuclear RNase P has one 369-nt RNA subunit (*RPR1* RNA) and at least nine integral protein subunits. The S1 tag was inserted into a nonessential loop at the end of a stem of the *RPR1* RNA. Lysates containing the tagged complexes were incubated with streptavidin-agarose and eluted under native conditions with a binding buffer containing 5 mM *d*-biotin. In addition, elution with biotin under mild conditions resulted in recovering RNase P with its activity preserved.[17] Srisawat and Engelke have also compared the one-step isolation of RNase P after tagging the *RPR1* RNA subunit with either the D8 Sephadex aptamer or the S1 streptavidin motif.[18] Both Sephadex or streptavidin tags enabled the specific and rapid isolation of tagged RNase P at a 20–30% level. The authors suggested that higher levels of purity could be attained by using a double-tagged RNA with the two aptamers and by performing two sequential purification steps.

Overall, there are some major advantages of using aptamer tags over conventional tags such as biotin for the identification and purification of RNA binding partners. A RNA aptamer motif can be incorporated during synthesis of the RNA of interest in vivo and can be adapted to isolate native in vivo-assembled ribonucleoproteins by expression of the hybrid RNA. It could allow the isolation of complexes that might not assemble when RNA is incubated with cellular extracts in vitro.[13] Furthermore, as reported by Schroeder and coworkers, the aptamer tags allow eluting RNA-binding species under native conditions, without coeluting nonspecifically bound contaminants.[12]

10.3 Use of Aptamers as Specific Ligands for the Separation/Capture of Small Molecules and Enantiomers

10.3.1 Immobilized Aptamers for the Separation/Capture of Small Molecules

Kennedy and coworkers have been the first researchers to report an immobilized aptamer that can selectively retain and separate related target compounds by affinity chromatography.[19] Using the target specificity of the antiadenosine DNA aptamer, these authors have described the preparation and characterization of an aptamer affinity nanocolumn for the analysis and separation of adenosine and various derivatives such as NAD, AMP, ATP, and ADP (Table 10.2). The 3′-biotinylated DNA aptamer was immobilized to the streptavidin chromatographic surfaces via a streptavidin–biotin bridge. The DNA-modified beads were packed in fused silica capillaries of low internal diameter (150 or 50 μm). Using frontal analysis, it has been found that: (i) the aptamer immobilization did not alter the adenosine-binding properties of the oligonucleotide and (ii) a greater surface coverage (about three-fold) was obtained relatively to that classically obtained for antibodies. The various species were separated in isocratic conditions in relationship to their different dissociation constant values (Fig. 10.3). The influence of the operating parameters such as particle diameter, capillary internal diameter, buffer composition, ionic strength, and mobile-phase pH were evaluated to obtain optimal separation. It appeared notably

Table 10.2 Use of aptamers as specific ligands for separation or capture of small molecules and enantiomers in liquid chromatography (LC)

Oligos[a]	Targets	Separation systems small molecules	Selectivity	Refs
DNA	Adenosine and analogues	Nano-LC[b]	From ~2 to ~20 (pH 7.6, 20 mM NaCl)	19, 20
Enantiomers				
DNA	Vasopressin	Narrowbore LC	nd[c]	21
DNA	Adenosine	Micro-LC	3.6 (20°C)	22
DNA	Tyrosinamide	Micro-LC	~80 (20°C)	22
RNA/L-RNA	Arginine	Micro-LC	nd	25
L-RNA	Aromatic amino acids: tyrosine, tryptophan, DOPA…	Micro-LC	From 1.3 to ~30 (10°C)	28
L-RNA	Histidine	Micro-LC	~20 (10°C, pH 5.5)	27

[a]Oligos: oligonucleotides
[b]LC: liquid chromatography
[c]Not determined due to the too low retention factor of the nontarget enantiomer

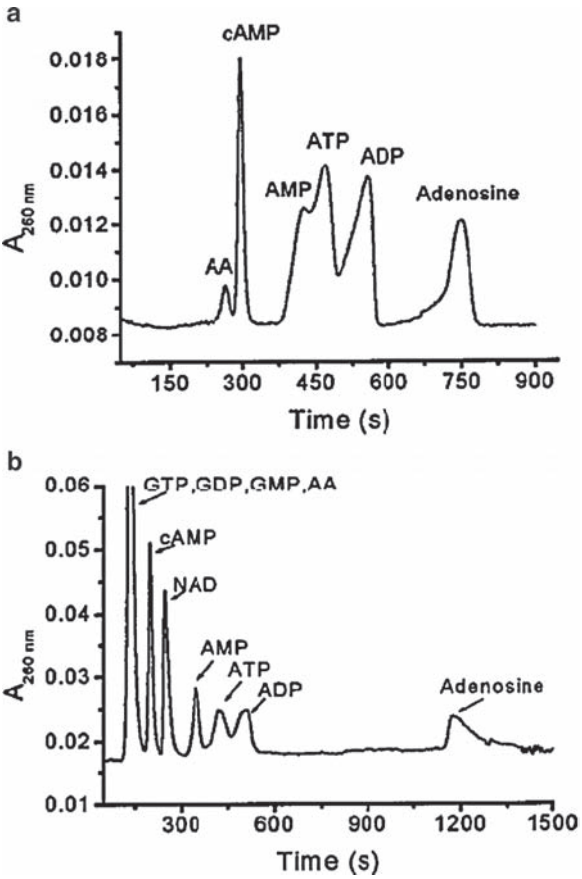

Fig. 10.3 Chromatograms illustrating selective retention and separation of a mixture of adenosine and anlogues with 20 mM KH_2PO_4, 20 mM NaCl, 10 mM $MgCl_2$ at pH 6.6, as mobile phase. (**a**) Column was 20 cm long by 150-µm-i.d. capillary, packed with POROS streptavidin-aptamer. Flow rate, 0.072 cm/s; injection volume, 80 nl. (**b**) Column was 7 cm long by 50 µm i.d., packed with CPG streptavidin-aptamer porous glass beads. Flow rate, 0.050 cm/s; injection volume, 10 nl (Reproduced with permission from ref. 19. Copyright [2001], American Chemical Society)

that when Mg^{2+} was removed from the column, the affinity of all the analytes was no longer observed (except of some residual retention of adenosine), probably because of the loss of the active Mg^{2+}-dependent tertiary structure.

Such an aptamer affinity nanocolumn was further used to develop an efficient adenosine assay in microdialysis samples.[20] Using an aqueous mobile phase containing 20 mM Mg^{2+}, adenosine was strongly retained on the column. Various elution schemes have been tested to optimize the target UV detection. Although the elution by chelation of Mg^{2+} with EDTA would be a suitable approach, a large background disturbance was observed in the chromatograms due to the large change in EDTA concentration. So, a competitive elution with divalent cation such as Ni^{2+}, which is presumed to complex nitrogen atoms in adenosine involved in binding to the

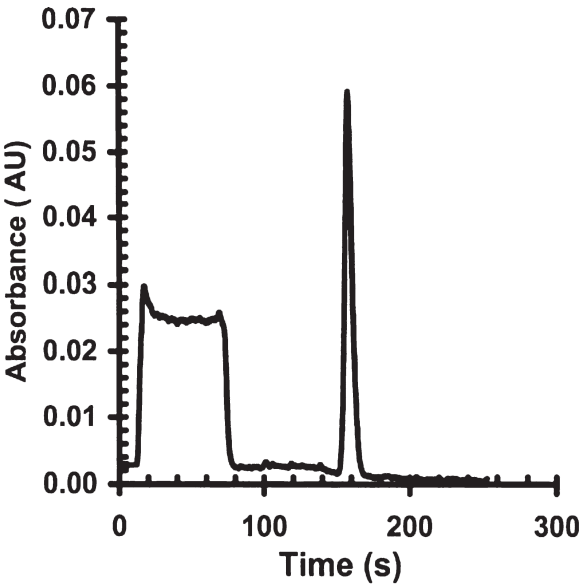

Fig. 10.4 Chromatogram illustrating gradient elution of 1.2 µM adenosine (2 µl injected) from an antiadenosine DNA aptamer nanocolumn 70 × 0.15 (i.d) mm. Mobile phase A consists of 20 mM Tris, 20 mM NaCl, 20 mM $MgCl_2$ at pH 6.6; mobile phase B consists of 20 mM Tris, 20 mM NaCl, and 20 mM $NiCl_2$ at pH 3.45. The gradient is 2% B from 0 to 72 s, with a linear increase to 90% B from 72 to 180 s (Reproduced with permission from ref. 20. Copyright [2003], Elsevier)

aptamer, was preferred (Fig. 10.4). Up to 6 µl of 1.2 µl adenosine could be injected onto the nanocolumn without loss of adenosine. The detection limit was found to be around 120 fmol. Such a chromatographic assay has been successfully applied to the determination of the adenosine concentration in microdialysis samples (without required preparation) collected from the somatosensory cortex of chloral-anesthetized rats.

10.3.2 Immobilized Aptamers for the Separation of Enantiomers

Although the aptamers were not selected, in most cases, for an enantioselective binding, the efficient monitoring of the selection procedure has often allowed a very high specificity exemplified by the capability of the aptamer to bind the target stereospecifically. Extreme enantioselectivities, ranging from about 100 to more than 10,000, have been reported for various compounds including oligopeptides, amino acids, and derivatives or nucleosides. Due to these stereoselective binding features, aptamers appear to be excellent potential elements for the development of chiral assays. A new class of target-specific chiral stationary phases for enantiomeric separation in liquid chromatography has been reported by our group (see Table 10.2).

First, the enantiomers of arginine-vasopressin have been separated using an immobilized 55-nt DNA aptamer known to bind stereospecifically the D-enantiomer of the oligopeptide.[21] The immobilization was achieved using the biotin–streptavidin interaction, as previously described by Kennedy and coworkers.[19] The influence of various parameters (such as column temperature, eluent pH, and salt concentration) on the L- and D-peptide retention has been investigated to provide information about the binding mechanism and then to define the utilization conditions of the aptamer column. A very significant enantioselectivity was obtained in the optimal binding conditions, the D-peptide being strongly retained by the column while the L-peptide eluted in the void volume. It has been shown by a complete thermodynamic analysis that dehydration at the binding interface, charge–charge interactions, and adaptive conformational transitions all contributed to the specific D-peptide–aptamer complex formation. Furthermore, it was established that the aptamer column was stable during an extended period of time.

In a further work, such approach has been extended to the chiral resolution of small molecules of biological interest.[22] The DNA aptamers used have been selected against the D-adenosine and L-tyrosinamide enantiomers. An apparent enantioseparation factor of around 3.5 (at 20°C) was observed for the anti-D-adenosine aptamer chiral stationary phase while a very high enantioselectivity was obtained with the immobilized anti-L-tyrosinamide aptamer; this allowed obtaining baseline resolution even at a relative high column temperature (Fig. 10.5). The results were particularly interesting because they showed that, although the DNA aptamers were not selected for enantioselective binding via a counterselection with the nontarget enantiomer, they were however able to discriminate the enantiomers. As expected by Famulok and coworkers,[23] it seems likely that an efficient SELEX procedure for high-affinity binding would result in the isolation of enantiospecific oligonucleotides. Of course, a necessary condition is that the target immobilization to the matrix must allow an adequate exposure of the enantiomer's key functional groups to the oligonucleotide pool during the in vitro selection. The anti-D-adenosine aptameric stationary phase can be used for 2 months without loss of selectivity, while some performance degradation was observed for the anti-L-tyrosinamide column over this period.

Most of the aptamers reported in the literature are related to RNA sequences (70% of aptamers are RNAs). Furthermore, the ability of RNA aptamers to bind their target with very high stereoselectivities has been also observed.[23,24] Thus, the enantioselective properties and the stability of an anti-L-arginine D-RNA aptamer target-specific chiral stationary phase have been tested.[25] It was found that such immobilized ligand was very quickly degraded by RNases under usual chromatographic utilization and storage. To overcome this severe limitation for practical use, it appeared fundamental to develop an RNA molecule intrinsically resistant to the classical cleaving RNases. A very interesting strategy involving the mirror-image approach has been successfully developed to design biostable L-RNA ligands (Spiegelmers) for potential therapeutic or diagnostic applications.[26] As the structure of nucleases is inherently chiral, the RNases accept only a substrate in the correct chiral configuration, i.e., the "natural" D-oligonucleotide. Therefore, L-oligonucleotides are expected to be unsusceptible to the naturally occurring

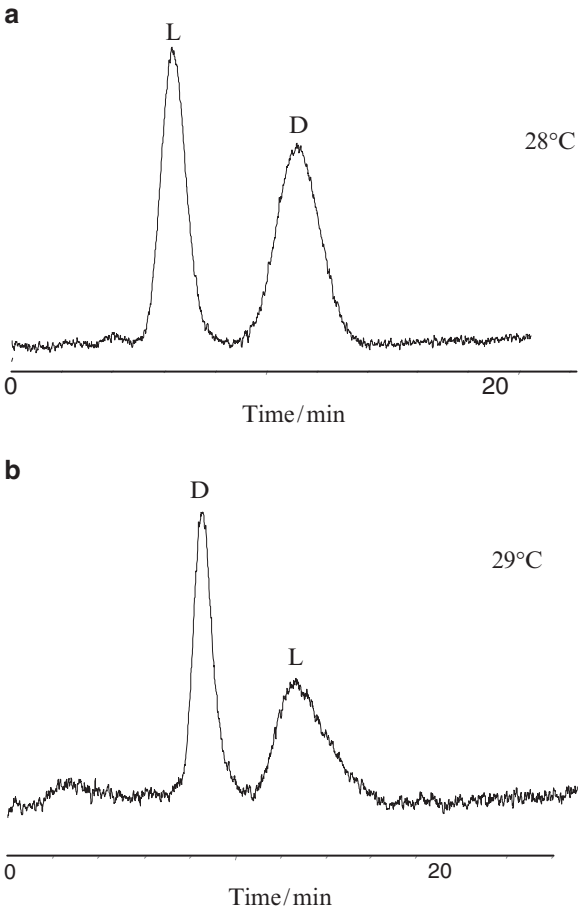

Fig. 10.5 (**a**) Chromatographic resolution of adenosine enantiomers using a D-adenosine target-specific DNA aptamer as CSP: column, 370 × 0.76 (i.d.) mm; mobile phase, phosphate buffer 20 mM, KCl 25 mM, $MgCl_2$ 1.5 mM, pH 6.0; amount of D-, L-adenosine injected, 70 pmol; injection volume, 100 nl; flow rate, 50 µl/min; detection at 260 nm. (**b**) Chromatographic resolution of tyrosinamide enantiomers using a L-tyrosinamide target-specific DNA aptamer as CSP: column, 250 × 0.76 (i.d.) mm; mobile phase, phosphate buffer 20 mM, KCl 25 mM, $MgCl_2$ 1.5 mM, pH 6.0; amount of D-, L-tyrosinamide injected, 70 pmol; injection volume, 100 nl; flow rate, 20 µl/min; detection at 224 nm

enzymes. This concept has been successfully applied to create a biostable RNA chiral stationary phase. It was demonstrated that a chiral stationary phase based on L-RNA, that is the mirror image of the "natural" D-RNA aptamer, was stable for an extended period of time (about 1,600 column volumes of mobile phase) under usual chromatographic conditions of storage and experiments.[25] In addition, as expected from the principle of chiral inversion, i.e., the mirror image of the "natural" aptamer recognizes with the same affinity and specificity the mirror image of the target,

D-arginine interacted with the L-RNA stationary phase while L-arginine was not significantly retained by the column. This result explains the reversed elution order of enantiomers relative to that obtained using the various D-RNA columns.[25]

Subsequently, an immobilized anti-D-histidine L-RNA aptamer microcolumn has been described and the retention and enantioselective properties of the CSP have been evaluated.[27] The minimal sequence of the 40-mer RNA aptamer used was obtained via a SELEX procedure directed against L-histidine. This oligonucleotide was known to strongly discriminate between L- and D-histidine (K_d ~10 µM for L-histidine and ~10,000 µM for D-histidine). As previously designed, the mirror-image approach was applied to create a biostable L-RNA CSP to use such aptamers in a routine chromatographic context. The effects of the variation of different operating parameters, including the mobile-phase pH and the $MgCl_2$ concentration, as well as the column temperature, on solute retention were assessed. The results suggested that: (i) the protonated form of histidine was involved in the stereospecific RNA binding and (ii) Mg^{2+} was essential for the target enantiomer binding to the specific aptamer sites. From a practical point of view, it appeared that the baseline resolution in a minimum analysis time can be achieved at a column temperature of 35°C for an eluent containing 10 mM $MgCl_2$, pH 5.5.[27]

Another major drawback of the aptamers is related to the too-high target specificity obtained from the SELEX procedure. For a broad application in the chiral separation field, such a high specificity is assumed to be of poor practical interest as each aptamer CSP is expected to resolve only one racemate. However, we have recently reported an aptamer-based chiral stationary phase that was able to resolve racemates of not only the target but also various related compounds.[28] The enantiomers of tyrosine and analogues (11 enantiomeric pairs) were separated using an immobilized anti-tyrosine-specific L-RNA aptamer (see Table 10.2). It was found also that the immobilized RNA aptamer can be used under hydro-organic mobile-phase conditions without alteration of the stationary phase stability (about 3 months of experiments).

10.4 Conclusions

As discussed in this chapter, DNA or RNA aptamers appear to be a new kind of target-specific ligands of very great interest for the separation, purification, and quantification of analytes in liquid chromatography and related methods. They can be used as immobilized specific ligands or as affinity tags. It can be anticipated that new, future developments will further enhance the usefulness of such molecular tools in the separation science field.

However, it is also important to point out that some major drawbacks could limit the broad practical applications of aptamers in routine analysis. As discussed in this chapter, aptamer degradation by nucleases can be problematic, notably when the aptamers are used for the analysis of species in biological fluids; this has been resolved, for chiral targets, by applying the mirror-image strategy.[25,26] Alternatively,

the use of other kinds of nuclease-resistant aptamers is possible.[29] Furthermore, because of the relatively high cost of the aptamers, the applications have been limited in most cases to miniaturized systems including chips and micro/nano liquid chromatography. These constraints probably preclude, at least at the present time, the large-scale preparative applications.

Another major problem is related to the SELEX methodology. Although highly efficient, this method requires sophisticated equipment, relatively expensive reagents, and can be time consuming. Furthermore, the number of aptamers directed against small molecules of importance such as drugs is relatively restricted at this time. However, the new improved methods of selection recently developed[11,30] could allow rapid generation of new aptamers of great interest for the development of efficient analytical tools in the pharmaceutical or biochemical fields.

References

1. Ellington, A.D. and Szostak, J.W. (1990) In vitro selection of RNA molecules that bind specific ligands. Nature (Lond.) 346:818–822.
2. Robertson, D.L. and Joyce, G.F. (1990) Selection in vitro of an RNA enzyme that specifically cleaves single-stranded DNA. Nature (Lond.) 344:467–468.
3. Tuerk, C. and Gold, L. (1990) Systematic evolution of ligands by exponential enrichment: RNA ligands to bacteriophage T4 DNA polymerase. Science 249:505–510.
4. Jayasena, S.D. (1999) Aptamers: an emerging class of molecules that rival antibodies in diagnostics. Clin. Chem. 45:1628–1650.
5. Collett, J.R., Cho, E.J. and Ellington, A.D. (2005) Production and processing of aptamer microarrays. Methods 37:4–15.
6. O'Sullivan, C.K. (2002) Aptasensors – the future of biosensing? Anal. Bioanal. Chem. 372:44–48.
7. Romig, T.S., Bell, C. and Drolet, D.W. (1999) Aptamer affinity chromatography: combinatorial chemistry applied to protein purification. J. Chromatogr. B 731:275–284.
8. Connor, A.C. and McGown, L.B. (2006) Aptamer stationary phase for protein capture in affinity capillary chromatography. J. Chromatogr. A 1111:115–119.
9. Cho, S., Lee, S., Chung, W., Kim, Y., Lee, Y. and Kim, B. (2004) Microbead-based affinity chromatography chip using RNA aptamer modified with photocleavable linker. Electrophoresis 25:3730–3739.
10. Chung, W., Kim, M., Cho, S., Park, S., Kim, J., Kim, Y., Kim, B. and Lee, Y. (2005) Microaffinity purification of proteins based on photolytic elution: toward an efficient microbead affinity chromatography on a chip. Electrophoresis 26:694–702.
11. Murphy, M.B., Fuller, S.T., Richardson, P.M. and Doyle, S.A. (2003) An improved method for in vitro evolution of aptamers and applications in protein detection and purification. Nucleic Acids Res. 31:e110.
12. Bachler, M., Schroeder, R. and von Ahsen, U. (1999) StreptoTag: a novel method for the isolation of RNA-binding proteins. RNA 5:1509–1516.
13. Windbichler, N. and Schroeder, R. (2006) Isolation of specific RNA-binding proteins using the streptomycin-binding RNA aptamer. Nat. Protocols 1:637–640.
14. Dangerfield, J.A., Windbichler, N., Salmons, B., Gunzburg, W.H. and Schroeder, R. (2006) Enhancement of the StreptoTag method for isolation of endogenously expressed proteins with complex RNA binding targets. Electrophoresis 27:1874–1877.

15. Harmuth, K., Urlaub, H., Vornlocher, H.P., Will, C.L., Gentzel, M., Wilm, M. and Luhrmann, R. (2002) Protein composition of human prespliceosomes isolated by a tobramycin affinity-selection method. Proc. Natl. Acad. Sci. USA 99:16719–16724.
16. Srisawat, C., Goldstein, I.J. and Engelke, D.R. (2001) Sephadex-binding RNA ligands: rapid affinity purification of RNA from complex RNA mixtures. Nucleic Acids Res. 29:e4.
17. Srisawat, C. and Engelke, D.R. (2001) Streptavidin aptamers: affinity tags for the study of RNAs and ribonucleoproteins. RNA 7:632–641.
18. Srisawat, C. and Engelke, D.R. (2002) RNA affinity tags for purification of RNAs and ribonucleoprotein complexes. Methods 26:156–161.
19. Deng, Q., German, I., Buchanan, D. and Kennedy, R.T. (2001) Retention and separation of adenosine and analogues by affinity chromatography with an aptamer stationary phase. Anal. Chem. 73:5415–5421.
20. Deng, Q., Watson, C.J. and Kennedy, R.T. (2003) Aptamer affinity chromatography for rapid assay of adenosine in microdialysis samples collected in vivo. J. Chromatogr. A 1005:123–130.
21. Michaud, M., Jourdan, E., Villet, A., Ravel, A., Grosset, C. and Peyrin, E. (2003) A DNA aptamer as a new target-specific chiral selector for HPLC. J. Am. Chem. Soc. 125:8672–8679.
22. Michaud, M., Jourdan, E., Ravelet, C., Villet, A., Ravel, A., Grosset, C. and Peyrin, E. (2004) Immobilized DNA aptamers as target-specific chiral stationary phases for resolution of nucleoside and amino acid derivative enantiomers. Anal. Chem. 76:1015–1020.
23. Geiger, A., Burgstaller, P., von der Eltz, H., Roeder, A. and Famulok, M. (1996) RNA aptamers that bind L-arginine with sub-micromolar dissociation constants and high enantioselectivity. Nucleic Acids Res. 24:1029–1036.
24. Majerfeld, I., Puthenvedu, D. and Yarus, M. (2005) RNA affinity for molecular L-histidine; genetic code origins. J. Mol. Evol. 61:226–235.
25. Brumbt, A., Ravelet, C., Grosset, C., Ravel, A., Villet, A. and Peyrin, E. (2005) Chiral stationary phase based on a biostable L-RNA aptamer. Anal. Chem. 77:1993–1998.
26. Klussmann, S., Nolte, A., Bald, R., Erdmann, A. and Furste, J.P. (1996) Mirror-image RNA that binds D-adenosine. Nat. Biotechnol. 14:1112–1115.
27. Ruta, J., Grosset, C., Ravelet, C., Fize, J., Villet, A., Ravel, A. and Peyrin, E. (2007) Chiral resolution of histidine using an anti-D-histidine L-RNA aptamer microbore column. J. Chromatogr. B 845:186–190.
28. Ravelet, C., Boulkedid, R., Ravel, A., Grosset, C., Villet, A., Fize, J. and Peyrin, E. (2005) A L-RNA aptamer chiral stationary phase for resolution of target and related compounds. J. Chromatogr. A 1076:62–70.
29. Green, L.S., Jellinek, D., Bell, C., Beebe, L.A., Feistner, B.D., Gill, S.C., Jucker, F. and Janjic, N. (1995) Nuclease-resistant nucleic acid ligands to vascular permeability factor/vascular endothelial growth factor. Chem. Biol. 2:683–695.
30. Mendonsa, S.D. and Bowser, M.T. (2005) In vitro selection of aptamers with affinity for neuropeptide Y using capillary electrophoresis. J. Am. Chem. Soc. 127:9382–9383.

Chapter 11
Aptamer Microarrays

Heather Angel Syrett, James R. Collett, and Andrew D. Ellington

Abstract In vitro selection can yield specific, high-affinity aptamers. We and others have devised methods for the automated selection of aptamers and have begun to use these reagents for the construction of arrays. Arrayed aptamers have proven to be almost as sensitive as their solution-phase counterparts and when ganged together can provide both specific and general diagnostic signals for proteins and other analytes. We describe here technical details regarding the production and processing of aptamer microarrays, including blocking, washing, drying, and scanning. We also discuss the challenges involved in developing standardized and reproducible methods for binding and quantitating protein targets. Although signals from fluorescent analytes or sandwiches are typically captured, it has proven possible for immobilized aptamers to be uniquely coupled to amplification methods not available to protein reagents, thus allowing for protein-binding signals to be greatly amplified. Into the future, many of the biosensor methods described in this book can potentially be adapted to array formats, thus further expanding the their utility and applications for aptamer arrays.

11.1 Introduction

The rise of in vitro selection methods has led to the development of aptamer array technologies similar to those that have previously been popularized for nucleic acid probes and antibodies. To take full advantage of aptamer arrays, three different prob-

H.A. Syrett and J.R. Collett
University of Texas – Austin, Institute for Cellular and Molecular Biology
angelita@mail.utexas.edu

J.R. Collett
Pacific Northwest National Laboratory, Richland, WA
james.collett@pnl.gov

A.D. Ellington
University of Texas – Austin, Department of Chemistry and Biochemistry
andy.ellington@mail.utexas.edu

Y. Li and Y. Lu (eds.), *Functional Nucleic Acids for Analytical Applications*,

lems must be solved: first, how large numbers of aptamers can be created; second, how these aptamers can be immobilized so as to retain function; and third, how the data from aptamer arrays can best be interpreted. In this chapter, we provide updates on solutions to all three of these problems.

11.2 Development of High-Throughput Selection Methods

11.2.1 The In Vitro Selection Scheme

Almost 2 decades ago, methods were devised for isolating high-affinity nucleic acid species, termed "aptamers," from large random-sequence pools.[1–3] This process has sometimes been termed SELEX, for "systematic evolution of ligands by exponential enrichment."

In vitro selection of nucleic acid aptamers typically begins with the chemical synthesis of a pool of DNA templates that includes a central randomized sequence region of 30–100 nucleotides. The random region is flanked by constant regions that can be used for amplification of the pool. One constant region often contains an RNA polymerase recognition sequence for transcription by T7 RNA polymerase. Even though long random-sequence pools could potentially contain upward of $4^{100} = 1.6 * 10^{60}$ sequences, a typical pool will have a diversity of only 10^{13}–10^{15} unique species due to the limitations of chemical DNA synthesis. After synthesis, the single-stranded DNA pool is amplified via the polymerase chain reaction (PCR) method to generate a double-stranded DNA (dsDNA) library that contains multiple copies of each initial sequence; the double-stranded library can be further transcribed in vitro to yield an RNA pool. In a typical selection, the nucleic acid pool will be incubated with a target protein, and this binding reaction will be passed through a nitrocellulose filter to capture protein-bound species. The filter is washed to remove nonspecifically and weakly bound nucleic acids, and any aptamers that remain are eluted from the filter under denaturing conditions (i.e., 7 M urea and 100°C). These aptamers can be amplified for subsequent rounds of selection by some combination of reverse transcription, PCR, and in vitro transcription.

The progress of selections for antiprotein aptamers are typically monitored using a variant of the same filter-binding assay. The aptamer pool is radiolabeled by incorporation of an α-^{32}P nucleoside triphosphate during enzymatic synthesis or by addition of a 5′-^{32}P phosphate via gamma-labeled ATP and polynucleotide kinase. The radiolabeled pool is incubated with its target protein and then filtered through a sandwich of nitrocellulose and nylon. Protein-bound species are captured on the upper nitrocellulose layer, and any remaining, nonbinding species are captured on the lower layer of nylon (Fig. 11.1). The percent of nitrocellulose-bound species provides an indication of what fraction of the population contains aptamers. If this assay is carried out as a function of protein concentration, then the average dissociation constant (K_d) of the population for its protein target can be determined. In a typical selection, no apparent increases in affinity may be observed for several

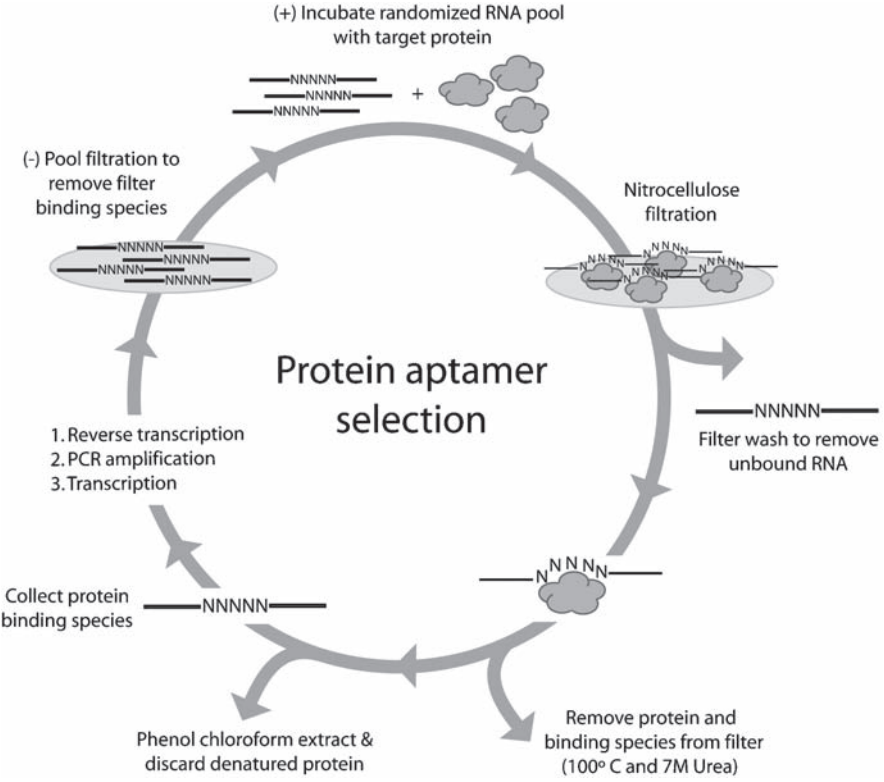

Fig. 11.1 In vitro selection for protein-binding RNA species via nitrocellulose filtration capture

rounds, and then affinity will quickly increase and level off. Although the ultimate affinities of aptamers are largely functions of the target protein, buffer, and stringency of selection, in our experience and that of others, aptamers with picomolar to low nanomolar dissociation constants can often be identified after 8–12 rounds of selection.[4] To date, more than 450 successful in vitro selections of aptamers have been published (aptamer.icmb.utexas.edu).[5]

11.2.2 High-Throughput Selection

In vitro selection methods have proven to be powerful, but they are also somewhat slow and laborious. Typically, each round of selection with an RNA pool takes at least a day, even for a skilled practitioner, and an entire selection against even a single target can take months to complete. Bottlenecks include both the methods used for sieving the pool, which are difficult to parallelize, and the amplification and purification of the selected species. Although many molecular biology methods such as PCR and in vitro transcription can be readily parallelized, but only if quality

control assays, such as sizing and quantitating the resultant products, are omitted. Unfortunately, because in vitro selection experiments can result in the survival of the survivor, rather than the survival of the fittest, it is essential that some form of quality control be included to prevent the accumulation of foreshortened amplicons or filter-binding species. Therefore, moving past the bottlenecks inherent in manual selection experiments as they are currently carried out requires one of several innovations: either the development of more robust separation methods that may not require extensive quality control, or the development of automated methods which can be parallelized by sheer brute force.

Even if these problems can be solved, a major problem confronting the large-scale development of binding reagents of any type (including antibodies) is what can be called the "target problem." It is difficult to find or purify protein targets representing an entire proteome, and especially individual modification states of the proteome. There are a number of methods by which the target problem can be solved, and these are examined as well.

11.2.2.1 Alternative Selection Modalities

The manual selection procedure just described has great advantages for the selection of aptamers against single targets because the stringency and progress of selections can be readily monitored by researchers. However, in the absence of automation this procedure is inherently difficult to parallelize: only a limited number of filtration selections or assays can be carried out by even a highly trained individual in a day (on the order of ten, but typically fewer). To improve the throughput of aptamer selections, one alternative is to adapt selections to analytical methods and machines that have been designed for high-throughput sample handling. For example, a number of devices are now available for monitoring protein interactions via surface plasmon resonance spectroscopy (i.e., Biacore), and aptamers have been selected by fractionating the flow during the dissociation phase of the binding reaction.[6,7] In addition to potentially increasing the throughput of binding reactions, one advantage of this method is that only the tightest binding species with the slowest dissociation rates can be captured.

Capillary electrophoresis has also been employed as a fast and efficient means of selectively partitioning single-stranded (ss) DNA-binding species. This process, similar in effect to gel electrophoresis, separates molecules based on size and charge through a voltage-induced ionic gradient in a fused silica capillary. Equilibration following loading can lead to molecules eluting in the following order: (1) target proteins that do not bind pool; (2) target molecules which bind weakly to pool; (3) pool and bound target complexes; (4) pool molecules that bind weakly to target; and (5) pool molecules which do not bind target.[8] Krylov's group pioneered this technique, producing ssDNA aptamers against protein farnesyl transferase and h-Ras with nanomolar range K_d values in one to three cycles of capillary electrophoresis (CE), respectively, and so-called smart aptamers against the thermostable DNA mismatch protein MutS.[8,9] Both the Krylov and Bowser groups have also combined this novel separation technique with a PCR amplification enrichment

step (so-called CE-SELEX). After three rounds of CE-SELEX, the Krylov group found no improvement in overall pool binding.[9] Bowser's group, however, reported the selection of highly specific, high-affinity ssDNA aptamers against human IgG after four rounds of CE-SELEX[10] and ssDNA aptamers against human immunodeficiency virus (HIV)-1 reverse transcriptase (RT) after four rounds with K_d values of 180 pM – a value better than that exhibited by similar aptamers selected in a more traditional manner.[11]

11.2.2.2 Automated Selection

Although the use of more complex analytical devices can increase the throughput of an individual researcher, the time-consuming steps of amplification and nucleic acid purification remain. Therefore, the Ellington laboratory has focused on automating the entire selection procedure. In 1998, the in vitro selection of functional nucleic acids was adapted to a Biomek 2000 liquid-handling robot that could perform five rounds of selection unattended (Fig. 11.2).[12] Since then, the robotic protocols and equipment have advanced to the point that automated selections against multiple protein targets can now be completed on a single Biomek 2000 robot within 2–3 days.[13–16] However, it is likely that automated selections into the future will be carried out on miniaturized devices.[17]

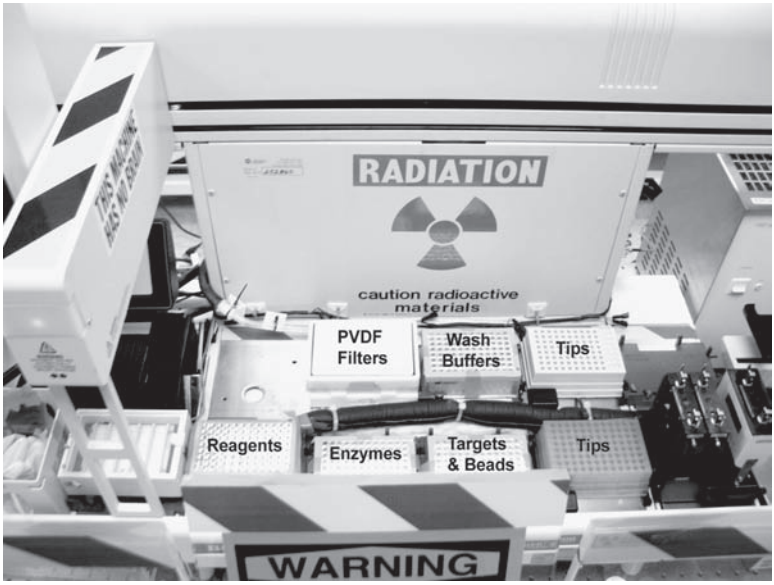

Fig. 11.2 Biomek 2000 liquid handling workstation selection robot. The entire automated in vitro selection system consists of a Beckman Coulter Biomek 2000 robot, integrated with a thermal cycler, magnetic particle separator, vacuum filtration manifold, pipette tip carousel, and enzyme cooler. All components are computer controlled

The shortened DNA molecules (deoxyribozyme candidates) are isolated by polyacrylamide gel electrophoresis (PAGE) (V) and amplified by polymerase chain reaction (PCR) with the use of two DNA primers, P1 and P2 (VI). Another PCR step is then conducted (VII) in which a ribo-terminated primer (P3, replacing P2 in VI) is used to introduce a ribonucleotide into the double-stranded PCR product. To recover the deoxyribozyme strands, the PCR products are treated with NaOH, thereby cleaving the ribonucleotide linkages, resulting in DNA fragments of unequal lengths (VIII). The middle-sized DNA fragment, which represents the deoxyribozyme strand, is purified by PAGE (IX), phosphorylated at the 5′-end by PNK (X) and subjected to the next selection cycle. When the cleavage activity of the population reaches a desirable level, standard cloning and sequencing protocols are applied to obtain the sequences of the final DNA pool. Eventually, several cloned species are arbitrarily chosen to assess their catalytic activities and fluorescence-signaling capabilities.

Although there have been a number of reviews of manual selection methods,[18] we briefly describe here some of the variables that also affect automated selection (see also Ellington et al.[16]).

To begin an automated selection, an appropriate pool must be designed and synthesized. As amplification takes place completely on the robotic workstation without the benefit of gel purification between selection cycles, it is even more important than usual to utilize pool and primer combinations that can be amplified without the generation of artifacts (i.e., primer dimers[19]). We have successfully used a N30 pool that had already been used for the manual selection of several antiprotein aptamers.[20,21] This pool utilized primers that base paired weakly (A:T rich) at their 3′-ends, thus reducing the probability of mispriming events. In contrast, a K30 pool that had strongly pairing (G:C rich) 3′-ends generated high molecular weight amplicons during automated selection. To date, most of our automated selections have been with RNA pools,[12–15,22] but automated selections have also been carried out with single- and double-stranded DNA pools.[23] It is likely selections with modified nucleotides (i.e., 2′-fluoropyrimidines or 2′-*O*-methylpyrimidines) can also be automated.

Once a protein target has been chosen, it is typically immobilized on beads to promote facile manipulation by the somewhat clumsy robotic pipettors. Biotin capture on streptavidin beads provides a versatile, modular platform for target conjugation. Alternatively, selection targets could also potentially be conjugated to bead surfaces through a variety of other methods including immobilized metal affinity chromatography (IMAC),[24] protein A or G interaction,[25–27] epoxy or tosyl group chemistry,[28,29] or antibody-coated beads.[30] However, we have not explored most of these methods, in part because of the fear of increasing the probability of selecting nucleic acids that bind to the beads themselves. For example, although histidine-tagged proteins can be immobilized via IMAC, the positive charge on both the tag and the nickel chelate may prove to be an irresistible target for the nonspecific binding and selection of negatively charged nucleic acids.

To initiate selection, the nucleic acid pool (10^{13}–10^{15} molecules) is incubated with the immobilized, biotinylated target. The slurry of beads and target-bound nucleic acid species is transferred to a filter manifold adapted to the robotic work surface, and unbound or weakly bound nucleic acids are washed away. Higher affinity

binding species that persist are subsequently liberated from beads and target by simply boiling the beads in water, and the selected nucleic acids are amplified by some combination of reverse transcription, PCR, and in vitro transcription. Both elution and amplification steps are carried out in the same tube on a thermal cycler on the robot. Again, the lack of purification between steps is discomfiting, but workable. Unpurified PCR product is used as template in the following RNA transcription reaction, and unpurified RNA transcript is transferred to the binding reaction for the next round. Because some residual salts, metabolites, and proteins are carried through, care must be taken to avoid the inadvertent buildup of reaction components. In addition, while the automation of nucleic acid capture and amplification may seem relatively simple, the multiple decisions that are normally made during the course of an experiment by a human researcher cannot be made by the robot, which of course just performs rote tasks. However, the advantage of robotic workstations is that while entire selections must be carried out from start to finish before the results can be evaluated, many different selection parameters (binding buffers, target concentrations, wash volumes, elution temperatures) can be quickly evaluated and a thorough optimization of selection conditions can be undertaken.[31]

Ultimately, it is hoped that brute force automation will allow us to undertake very large aptamer development projects. The multichannel pipetting capabilities of the robots should permit the selection of eight targets in parallel. Assuming 18 rounds of selection per target, this will be a throughput of roughly 16 targets per week per robot. Because of the modularity of the hardware and chemistry components, automated in vitro selection technology should also be portable to other, potentially even higher throughput workstations that might execute up to 384 selections in parallel. With this capacity, the construction of proteomic biosensor arrays can be envisioned.[32]

11.2.2.3 The Target Problem

In Vitro Transcription and Translation

The expression of gene libraries in organisms still requires the cumbersome purification of every protein. Although this can be accomplished, the idiosyncrasies of protein expression and purification are not well suited to routine application to selection procedures. Therefore, we have attempted to adapt the in vitro transcription and translation (TnT) of genes to the generation of targets for in vitro selection. To that end, and in collaboration with Andrew Hayhurst and the Georgiou laboratory at the University of Texas at Austin, we have developed a system wherein proteins may be expressed via TnT with an amino terminal peptide tag for in situ biotinylation. After examination of a large number of prokaryotic- and eukaryotic-based commercially available kits, we ultimately found that the Roche RTS 100 *Escherichia coli* HY kit worked best with the automated selection procedures we had established, and also gave some of the highest levels of expression for our templates. After translation, biotin protein ligase (BPL), the product of the *birA* gene[33–35] may be used to covalently link the ε-amino group of a single lysine residue in the appended peptide to biotin.[36] The biotin ligase may be either cotranslated or added exogenously.

Yeast Expression Libraries

The Snyder group at Yale has made significant advances in developing and streamlining the process of high-throughput protein preparation and attachment of target proteins to microarray slides. In doing so, they have successfully overexpressed 119 of the 122 known yeast protein kinases in small-scale 96-well format preparations. In the first demonstration of their system, they overexpressed N-terminal glutathione-*S*-transferase kinase fusion proteins, then purified them via GST:glutathione bead affinity capture and printed onto silanized slides via a covalent sulfhydryl cross-linking attachment.[37] Arrays were assayed for phosphorylation activity in the context of 17 known substrates, and several previously unknown correlations were discovered. As a result of their work and the work of others, a number of yeast open reading frame (ORF) libraries are now commercially available that are designed to overexpress fusion proteins tagged for purification or in vivo labeling. Both Open Biosystems (Huntsville, AL, USA) and Invitrogen (Carlsbad, CA, USA) offer a variety of collections of these yeast ORF libraries.

Combining high-throughput protein production and printing in one fell swoop, the LaBaer group have developed a system wherein a combination of target protein-encoding plasmid along with capture antibody are both printed onto microarray slides at once. After an on-slide TnT reaction, target proteins with a C-terminal glutathione-*S*-transferase (GST) tag are captured with proximally located anti-GST antibodies. C-terminal tag-based capture therefore serves the dual purpose of attaching protein to the slide while at the same time indicating successful protein translation.[38]

11.3 Development of Aptamer Microarrays

Assuming that aptamers against a wide array of targets can be made, the question becomes how these aptamers can be adapted to microarray technologies. In theory, this should be simple, given that aptamers are like other nucleic acid probes, and methods for the production of gene expression arrays are now quite robust. In practice, though, aptamers function very differently from simple hybridization probes. Aptamers must retain their tertiary structures following immobilization and must be immobilized in such a way that the array surface does not sterically hinder binding by the protein target. Neither consideration applies to nucleic acid hybridization, where even nonspecific immobilization of long nucleic acids by electrostatic interactions with polylysine is apparently good enough to yield specific hybridization. We have gone to some lengths to solve the immobilization and printing problem, likely just in time to be overtaken by the technology arc associated with light-directed array synthesis.

Assuming that aptamers can be immobilized without loss of function, a second (but easier) question is how binding to aptamers immobilized (or synthesized) on a surface can be sensitively detected.

11.3.1 Aptamer Immobilization on Arrays

As with other types of microarrays, the way in which aptamers are immobilized on slides will govern whether the solution-phase character of aptamers is retained and whether arrays can be used reproducibly. Several approaches to the problem of aptamer immobilization have been employed by our group and others.[39–41] Initially, we attempted to attach our aptamers to polylysine slides, commonly used to immobilize oligonucleotide probes for cDNA hybridization on gene expression microarrays. However, we found that polylysine capture routinely inhibited aptamer function, presumably because the aptamers were unfolded by electrostatic interactions between their negatively charged phosphodiester backbones and the positively charged lysine. In contrast, aptamers retained their functionality if they were immobilized in a more directed manner via biotin/streptavidin or covalent linkers to a substrate surface.[42–44]

One simple method for immobilization has involved transcribing aptamers with a 5′-terminal biotin and immobilizing them on custom-made NeutrAvidin- or streptavidin-coated slides (Pierce Biotechnology, Rockford, IL, USA). By incorporating biotinyl-GpG into in vitro transcription reactions at a 3:2 molar ratio of biotinyl-GpG to GTP, many transcripts will initiate with the biotinylated analogue. Unfortunately, although a maximum of 40% biotinylation can frequently be achieved, there is enough variability that the yield of each batch must be quantified using a gel-shift assay. A difficult obstacle when considering printing hundreds or even thousands of aptamers, this is a problem we address further in Section 11.3.3.3 (RT detection via antibody sandwich assay). We have also previously found that a high loading of streptavidin was necessary to ensure the robust capture and detection of protein analytes (hence the need for custom slides[42]) and that NeutrAvidin in general yielded lower background/autofluorescence.

While we have successfully printed aptamers that are conjugated to the surface via a generic 18-nucleotide linker appended to the aptamer 3′-terminus, it is likely that the length and composition of this biotin–aptamer linker can have an effect on binding function. This effect may be difficult to predict. For example, Yang et al.[45] found that a slightly longer 3′-linker to biotin (C3-biotin versus dT-biotin) yielded slightly better protein-dependent signals with a surface amplification scheme involving rolling-circle amplification (RCA), while Cho et al.[46] found that no linker was better for a similar scheme in which ATP was being detected.

One way to avoid steric problems might be to extend one of the constant regions of the aptamer, providing an additional sequence buffer ahead of the folded, functional structure. To better control the reproducibility of immobilization, we therefore sought to append aptamers to surface via the simple expedient of hybridization to a complementary, immobilized oligonucleotide. We initially examined anchoring via locked nucleic acids (LNAs; Fig. 11.3). LNAs are a novel class of conformationally restricted ribonucleotide analogue first described by Wengel and coworkers in 1998.[47] The rigidity of the locked ribose ring results in greatly increased melting temperatures by enhancing base stacking and backbone stability.[48] Most

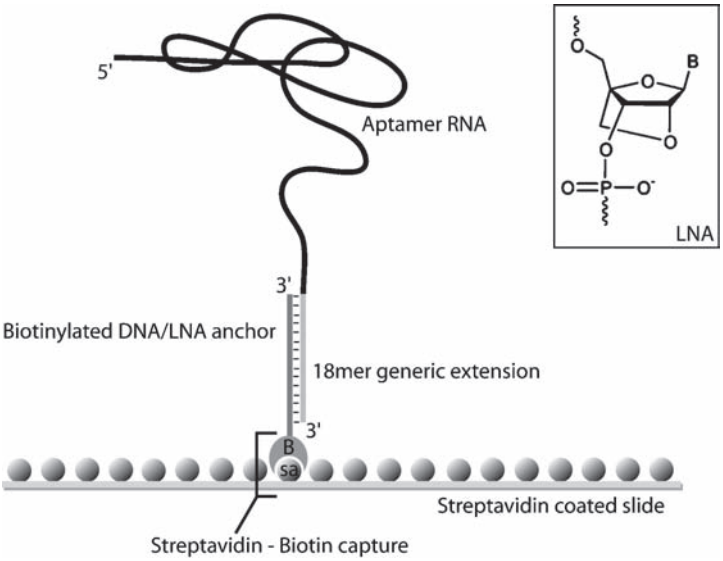

Fig. 11.3 Locked nucleic acid (LNA) anchoring of aptamers to streptavidin- or NeutrAvidin-coated slides (Pierce Biotechnology, Rockford, IL, USA). Anchor and aptamer are hybridized via an 18-mer generic 3′-aptamer extension before slide attachment. The melting temperature of this hybrid is roughly 80°C. *Inset* shows the ribose derivative structure of an LNA, with a methylene unit linking the 2′-oxygen and 4′-carbon

importantly, biotinylated LNAs can be obtained from commercial suppliers such as IDT (Coralville, IA, USA). The oligonucleotide anchors were designed to be complementary to aptamers whose 3′-constant (reverse priming) regions had been extended. It was thought that this would both avoid interference with aptamer structure and extend the aptamer away from the surface, avoiding steric effects that might occur during protein binding. It should be noted that the extension sequences should be chosen so as not to cause the aptamers to misfold. The design of the extension sequence can readily take into account the constant regions of a given set of aptamers, but choosing the extension in the context of many different aptamer sequences in parallel will likely prove to be much more difficult.

Aptamers can be immobilized either by hybridizing the LNA to the aptamers and printing, or by hybridizing the aptamers to a preprinted LNA. From a strictly practical perspective, hybridization in a tube before printing is a more controlled situation. It minimizes the potential for nonspecific aptamer–slide binding and also reduces the number of on-slide hybridization steps, which are typically messier and require more reagents.

Aptamers readily retain target-binding function following LNA-mediated immobilization, as can be seen in the results shown in Fig. 11.6 of Section 11.3.3.3. Although the strength and specificity conferred by the rigidity of the LNA backbone led us to choose the LNA anchors over DNA, it is reasonable to assume that anchoring could be carried out through hybridization to other types of nucleic acids, as well. Again, it is recommended that the original selections be carried out in the context of whatever linker is going to be used for immobilization.

Irrespective of whether attachment to streptavidin- or Neutravidin-coated slides is direct or via a LNA, we have found that aptamer arrays must be printed under conditions of high humidity to maintain the integrity of the protein and the biotin–avidin attachment. Furthermore, assays must be performed almost as soon as the slides have been printed, which means that arrayer calibration, printing, and the many steps of assaying must take place serially and continuously. Even printing and assaying just a few slides can require working throughout a 12- to 15-h day. For this reason, we are currently optimizing methods for the covalent attachment of amine-modified LNAs to epoxy-coated slides. Covalently attached LNA slides can either be prepared in advance, or LNAs can be used to capture aptamers from solution and then conjugated to a slide. In either case, the use of more sturdy covalent attachments in place of the biotin–streptavidin linkage should improve slide longevity and assay practicability.

Other groups have used different approaches for the preparation of functional nucleic acid arrays. Corn's group used T4 ligase to attach RNA aptamers endwise to ssDNA microarrays with a ligation efficiency of 85% ± 10%, as measured by surface plasmon resonance imaging (SPRI).[49] While this method is not readily adaptable to a multiplex format, it is potentially an excellent tool for the sensitive detection of targets and for the examination of binding kinetics. SPRI chips have been used to accurately detect human thrombin at concentrations as low as 500 fM and vascular endothelial growth factor (VEGF) at 1 pM.[50]

11.3.2 Printing Aptamer Arrays

Beyond choosing an immobilization substrate and chemistry, there are practical issues involved in how to actually print aptamer arrays. We have tried where possible to follow many of the procedures associated with printing gene expression arrays, in large measure because this latter technology is mature and many of the difficulties we might otherwise face have already been worked out.

Following aptamer biotinylation or hybridization to biotinylated LNA anchors, aptamers are printed onto NeutrAvidin- or streptavidin-coated custom glass slides (Pierce Biotechnology). However, before large-scale automated aptamer array printing, we deemed it necessary to show experimental proof-of-principle on a small scale. To test printing geometry and on-slide assays in small-scale experiments, we printed one or two aptamer arrays using a convenient and easy-to-wield manual arraying device made by V & P Scientific (San Diego, CA, USA). After small-scale optimization of conditions, we felt confident to proceed to the automated setting.

Large-scale automated printing was achieved using a custom-built automated arrayer whose specifications were developed by the Brown laboratory at Stanford University.[51] We use an 8-pin setup with the DeRisi print head, and arrays are printed as two columns of eight blocks running the length of the slide, with a block center-to-center spacing of 9 mm conveniently in register with a Rainin 8-channel p200 manual pipettor. With this geometry in mind, aptamer samples are loaded

into 384-well plates and transferred to slides via an 8-pin arrayer (although the reservoir plate pattern is also compatible with a 32-pin array configuration).

It was thought that prevention of drying during printing, biotin capture, and subsequent assay steps should result in improved signal image and data acquisition. Therefore, a humidity chamber was constructed to enclose the DeRisi arrayer, and printing buffer was supplemented with 5% (v/v) glycerol. Humidity in the chamber was maintained at 75–85% via a manually controlled Vicks personal steam inhaler (Proctor and Gamble, Cincinnati, OH, USA) and monitored using a small digital hygrometer (VWR, West Chester, PA, USA).

Before assaying, remaining unprinted surface is blocked (passivated) before target binding and antibody sandwich detection. Passivation of the unprinted slide surface can be accomplished by incubating the printed slide with a mixture of binding buffer containing 1× Roche Western Blocker and 0.5% Tween 20.

11.3.3 Assaying Aptamer Arrays

11.3.3.1 Incubating Arrays with Protein Targets

After printing, blocks of printed aptamers may be partitioned for assaying. There is a wide variety of partitioning devices available ranging from hydrophobic pens to disposable adhesive wells, depending on the arrangement of printed spots and desired assay conditions. We have had successful results with our printing format using Flexwell adhesive pads or reusable Fast Frame slide partitioning devices (Grace Bio-Labs, Bend, OR, USA). SureSeal Perfusion chamber adhesive pads (Schleischer & Schuell, Keene, NH, USA) have also been used successfully and have the advantage of providing an enclosed flow-through chamber.

Once printed, arrays can be used to assay proteins in one of several ways, the two most common of which are to either directly label the target protein and hybridize it to the array, or to use the array to capture unlabeled proteins for a sandwich assay. In the following sections, we discuss these two different assay methods and show their use in real-world examples. In particular, we show how direct labeling was used for the detection of hen egg white lysozyme (Section 11.3.3.2), and how antibody sandwiches were used for the detection of HIV-1 reverse transcriptase (Section 11.3.3.3).

11.3.3.2 Aptamer Microarray Detection of Hen Egg White Lysozyme

Some earlier important demonstrations of protein detection microarrays used direct labeling of protein for ratiometric quantification against reference sample.[52,53] By initially adopting a well-known labeling procedure, we were able to better optimize print and assay experimental conditions for multiplex aptamer arrays.[42] Drawing from current microarray literature, we tested a range of buffers and assay conditions and optimized conditions for the specific capture of fluorescently labeled target

proteins, either alone in binding buffer or in competition with labeled intracellular proteins from cell lysates.[42,54] Figure 11.4 briefly compares the salient attributes of cDNA and biotinylated aptamer arrays.

Aptamer microarrays were used to screen the affinity and specificity of a pool of robotically selected antilysozyme RNA aptamers. Aptamers were transcribed in vitro in reactions supplemented with biotinyl-guanosine 5′-monophosphate, which leads to the specific addition of a 5′-biotin moiety (as described above), and then spotted on streptavidin-coated microarray slides. The 5′-biotinylated aptamers were transcribed in vitro and purified via denaturing PAGE. Purified aptamers were then diluted into antilysozyme selection buffer and thermally equilibrated into their active conformations by heating to 70°C for 3 min and then gradually cooling to 4°C. Aptamers were spotted onto custom streptavidin-coated slides as described above and incubated at room temperature and 75–85% humidity to allow the biotinylated oligonucleotides to be captured by the streptavidin. After capture, the unprinted surface was blocked with binding buffer supplemented with bovine serum albumin and Tween-20 for 1 h, followed by multiple washes to remove non-biotinylated aptamers. The printed surface was then incubated with Cy3-labeled protein, thoroughly washed in blocking buffer, and rinsed in SB (10 mM sodium hydroxide adjusted to pH 8.5 using boric acid) before drying and imaging.

After the completion of an assay, slide image data were collected using an Axon Instruments 4000B microarray scanner. Emission intensity data for the Cy3 (570 nm) label are collected after excitation at 532 nm, and Cy5 (670 nm) emission intensity data were collected upon excitation at 635 nm. GenePix software (Molecular Devices, Sunnyvale, CA, USA) is used to assign Cy3 as green in

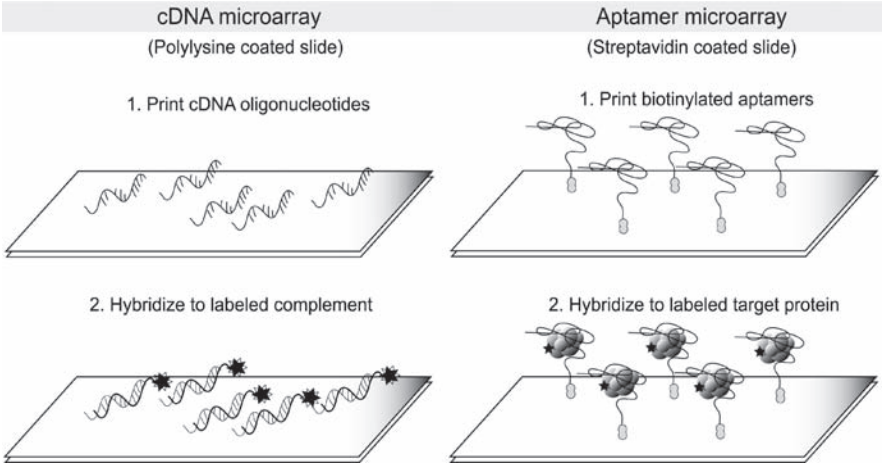

Fig. 11.4 A schematic comparison of DNA and aptamer microarrays. A typical cDNA microarray where DNA is printed on polylysine slides for hybridization capture of cDNA (*left*) is compared to an aptamer microarray printed with 5′-biotinylated RNA aptamers onto a streptavidin coated slide for capture of fluorescently labeled target proteins (*right*)

color and Cy5 as red, and each spot was manually flagged based on the quality of the image. After flagging, background subtracted intensity was calculated and slides were normalized against a SYBR555 nucleic acid dye-stained control slide. In experiments where data were collected from both channels, the background signals for Cy3 and Cy5 were normalized on reference slides (treated with equimolar amounts of Cy3 and Cy5) by adjusting the photomultiplier tube voltage and laser power during scanning and by normalizing data in the GenePix program.

Biotinylated antilysozyme RNA aptamers spotted on microarray slides retained their ability to bind and capture lysozyme (Fig. 11.5; microarray slide after treatment with 1 µg/ml Cy3-labeled lysozyme). To test signal response and lower limits of detection of the aptamers, ten identically spotted microarray slides were each treated with Cy3-lysozyme in selection buffer, at concentrations ranging from 100 fg/ml to 100 µg/ml. All the aptamers produced a signal with a mean spot signal-to-noise (SNR) ratio greater than 2 and a mean spot pixel intensity saturation of less than 5% at two or more consecutive orders of magnitude of lysozyme concentration; the dynamic ranges of binding is shown in Fig. 11.5. The best SNR among all aptamers across all concentrations was shown by clone 7 at 10 ng/ml Cy3-lysozyme, with a mean SNR of 78 (standard deviation = 5.7) and a lower limit of detection of 1 pg/ml (70 fM). Aptamers on the microarray retained their specificity for target protein in the presence of a 10,000-fold (w/w) excess of T-4 cell lysate protein. The RNA aptamer microarrays performed comparably to current antibody microarrays and within the clinically relevant ranges of many disease biomarkers.

While we have successfully used the direct labeling of proteins to test our aptamer microarrays, there are some attendant problems. Efficiency of protein labe-

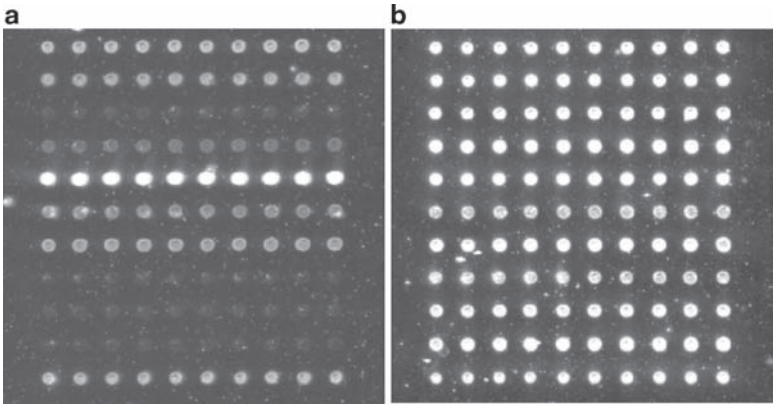

Fig. 11.5 Antilysozyme aptamer array. (**a**) Biotinylated RNA antilysozyme aptamers on a streptavidin-coated slide after treatment with Cy3-labeled lysozyme at 1 g/ml in selection buffer. Each row contains ten replicate spots of a single aptamer clone isolated from an in vitro selection against hen egg white lysozyme. (**b**) Identically arrayed spots of the same aptamer clones as in **a** after treatment with SYBR 555 nucleic acid stain

ling varies from batch to batch, requiring time-consuming optimization of assay conditions leading to inconsistency in assayed binding. Further, direct labeling methods introduce signal variations between aptamers, likely because multiple different epitopes on a protein can be labeled and different aptamers can have different affinities for these different conjugates. Similarly, heterogeneity in labeling may make attempts to quantitate protein concentrations using aptamer arrays more problematic. There is also evidence from a number of laboratories[55,56] and in our own work (unpublished datak) that interactions between oligonucleotides and fluorophores conjugated to target analytes confound interpretation of fluorescent signals in microarray assays.

Because of problems with direct labeling, an increasing trend is reported toward using enzyme-linked immunosorbent assay (ELISA)-style sandwich assay schemes for the quantitative detection of proteins using arrays.[57–61] The influence of established practices and reagent markets for quantitative ELISAs – originally introduced in 1971 – have the advantage of 35 years of evolution not yet established in the field of microarray techniques.[62]

11.3.3.3 Aptamer Microarray Detection of HIV-1 Reverse Transcriptase

Given our success with adapting RNA aptamers selected to function in the context of aptamer microarrays,[42,54,63] it seemed likely that we should be able to prepare aptamer arrays for detecting and typing HIV-1 reverse transcriptase (RT). Forty-two anti-RT aptamers selected in our lab were once again hybridized to the 5′-biotinylated bt-1890a-LNA anchor oligonucleotide and spotted on slides. As a negative control, the naïve pool (70.15-N30) was also immobilized.

In the arrays for detecting reverse transcriptase, we modified the labeling protocol to accommodate an antibody sandwich assay. Surface-bound aptamers are allowed to bind to the protein target of interest and washed to dislodge any unbound species; primary antibody is then allowed to bind to the protein surface, then after another round of washing, fluorescently labeled secondary antibody that specifically binds the primary is added and allowed to bind; excess is washed away.

To test sandwich detection methods on RNA aptamer microarrays, we obtained unlabeled primary polyclonal rabbit antibodies against our target proteins and Cy3-labeled goat antirabbit polyclonal secondary antibodies. Labeled secondary antibodies used in fluorescent detection of binding were available commercially through a variety of companies (e.g., Amersham, Santa Cruz, and AbCam). Sandwich assay reagent concentrations had to be optimized for each batch of primary and secondary antibody by performing a checkerboard series of dilutions for the various components across multiple microarray slides that had been partitioned into 16 wells with Flexwell adhesive pads.[64] To optimize conditions for binding assays, serially diluted unlabeled protein from 8.5 nM to 8.5 pM was added to the

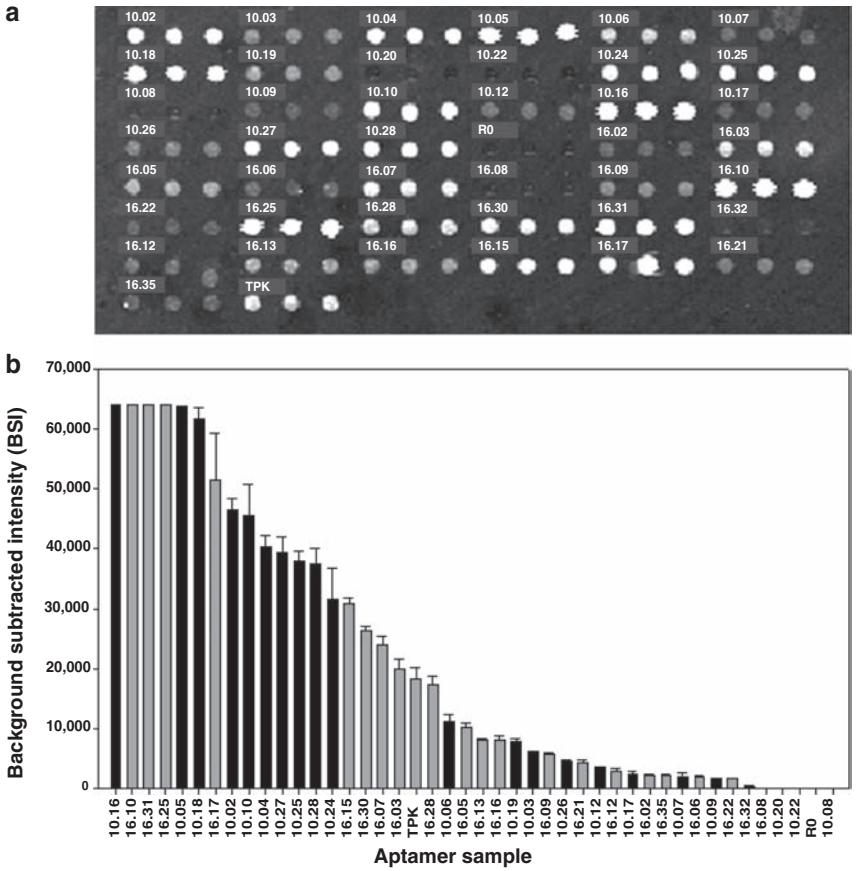

Fig. 11.6 Microarray capture of WT RT with antibody sandwich detection. (**a**) Microarray printed with 42 triplicate anti-WT RT aptamers treated with unlabeled 850 pM WT RT, followed by sandwich detection using a primary rabbit polyclonal antibody (1:4,000), and a Cy3-labeled goat antirabbit secondary antibody (1:1,000). Naïve R0 pool RNA and Tuerk pseudoknot RNA were used as negative and positive controls, respectively. (**b**) Rank-ordered graph of averaged BSI values of microarray spots for aptamer samples shown in **a**

wells and allowed to bind for 30 min, followed by a 2-h incubation with unlabeled primary antibody at dilutions of 500:1, 1,000:1, 2,000:1, and 4,000:1, and a 1-h incubation with Cy3-labeled secondary antibody at 250:1, 500:1, 1,000:1, and 2,000:1 (Fig. 11.6).

Wells were extensively washed with binding buffer after each incubation. After the final wash, wells were more thoroughly rinsed and centrifuged dry and then imaged. Optimal signal intensities for a broad range of aptamers (see Fig. 11.6) were obtained with 850 pM unlabeled HIV-1 RT, with a primary antibody dilution of 1:4,000 and the Cy3-labeled secondary antibody dilution of 1:1,000.

11.4 Data Analysis

Our analysis methods for aptamer microarrays have been influenced by antibody ELISA microarrays that employ standard curves drawn from serially diluted recombinant antigens to predict absolute protein concentrations in unknown samples.[60,61] Other analytical approaches have been demonstrated for affinity capture microarrays, including two-color ratiometric assays that (in a manner similar to spotted DNA microarrays) compare signals from reference samples mixed with experimental samples to estimate relative abundances of multiple proteins in solution.[65,66] Because aptamers may be in many cases directly interchangeable with antibodies for affinity capture applications, it is well worth perusing recent reviews on antibody microarrays to get a broader idea of the variety of ways aptamers might be deployed in the microarray format.[61,67–69]

Our own efforts for defining and improving the analytical performance of our nascent aptamer microarrays have thus far mainly relied on testing serial dilutions of recombinant protein analytes in buffer solutions or in mixtures with complex biological fluids such as cell lysates. As described above, our aptamer microarray slides are divided into 16 separate blocks, with each block having an identically printed set of 25–50 aptamers printed in triplicate. In this way, limited sets of aptamers may be tested in 16 parallel assays on a single slide. Most often, an eightfold-dilution series is performed in each of the two columns of eight blocks on each slide. This experimental format differs significantly from typical DNA gene expression microarrays, where a single sample is applied to a single slide that may be printed with 100,000 or more spots. Accordingly, we have found that most database and analysis software designed for gene expression microarrays such Gene Pix Acuity (Axon) proved to be inappropriate for our task of constructing binding affinity curves for each of the 25–50 aptamers in our multiplexed assays. In time, we determined that the open source BioArray Software Environment (BASE)[70] was flexible enough to suit our needs.

BASE is a web-enabled microarray database system that was designed to be compatible with the Microarray Gene Expression object model (MAGE-OM).[71,72] Accordingly, instead of referring to the oligoprobes on the slides and cDNA in the samples in literal, rigid terms, BASE uses more abstract data classes such as “reporters” and “biomaterials” that are more easily extensible to the context of protein capture microarrays. The current version (BASE 2.x; download and documentation at http://base.thep.lu.se) was entirely written in the object-oriented Java language using a plug-in architecture that provides local microarray facility administrators with a high degree of freedom to adapt BASE to match their particular needs.

A very attractive feature of BASE for us has been the batch data importer plug-in (written by Micha Bayer of the Scottish Crop Research Institute) that allows us to upload multiple Gene Pix Results (.gpr) files at one time. Data contained in each GPR file for all the spots (reporters) on a slide (such as name, fluorescent intensity data, block, row, column, etc.) are collectively and automatically saved to the

back-end MySQL database as elements of a "raw bioassay" item. The raw bioassay may then be associated within BASE with specific annotations about the assay from which it came, such as the date, the name of the experimenter(s), experimental protocols, scanner laser and PMT settings, and the biomaterials (analytes, blockers, detection antibodies, etc.) that were applied to the microarray slide.

To analyze data within BASE, raw bioassays are assigned to an "experiment," where together, they comprise a "bioassay set." The bioassay set may then be filtered to remove spots that were flagged as bad during scanning or to limit analysis to a specific subset of the data. In addition, the data may be transformed by statistical plug-ins to perform, for instance, a normalization. At each point in the data filtering/transformation process, simple plotting tools may be accessed to get a snapshot view of the current data set. As of yet, there is no consensus as to best approach for normalization of affinity capture microarray data. Several recent publications, however, specifically address the standardization of antibody microarray procedures and data.[59,61,73,74] Readers are directed to these references for more detailed treatment of the topic.

For presenting data, we currently find it most convenient to group the data within a bioassay set according to serial dilution series and then to export the data in a tab-text format. Once exported, the data may then be taken into a graphing program such as SigmaPlot, where they may be assembled as affinity binding curves.

11.5 Other Approaches

While we have primarily focused on printed aptamer arrays that mimic conventional gene expression microarrays, a variety of other aptamer array technologies can be contemplated. In particular, into the future we envision that even automated printing will be quickly and economically displaced by light-directed synthesis of aptamer arrays. Advances in the production of DNA oligonucleotide chips via light-directed chemical synthesis using maskless array synthesis (MAS) technology have resulted in the commercial availability of custom-fabricated chips with up to 768,000 probes for gene expression profiling (NimbleGen, Madison, WI, USA). Given the interchangeability of the now-commonplace phosphoramidite chemistry for producing either DNA or RNA oligonucleotides, it is reasonable to expect that chips thus printed with hundreds of thousands of DNA or RNA oligonucleotides produced via MAS technology may become widely available.

Beyond alternative methods for creating arrays, there are many different alternatives for probing arrays. Photo-cross-linking aptamers have been generated that can covalently capture proteins. Thus, photoaptamers contain reactive 5-bromo-2′-deoxyuridine (BrDU) in place of thymidine bases, which can cross-link with aromatic or sulfur-containing groups on the protein surface following irradiation with near-UV light (310 nm).[77,78] Golden and coworkers used mass spectrometry to characterize the photo-cross-linking of a BrDU single-stranded DNA photoaptamer to basic fibroblast growth factor (bFGF).[79] Further studies showed that the bFGF

photoaptamer specifically cross-links with its target protein (bFGF) in the presence of similar proteins (VEGF, PDGF, and aFGF) in human serum.[80,81] As proof-of-principle of this novel proteomic and diagnostic tool, a multiplex of 17 photoaptamers against a variety of proteins was printed on microarrays and successfully assayed for specific photo-cross-linking in human serum.[82]

Because aptamers are nucleic acids, it may also be possible to couple nucleic acid amplification technologies with arrays to improve signal-to-noise ratios. Aptamers can be coupled to nucleic acid enzymes to form allosteric catalysts, aptazymes. We have generated aptayzme ligases that are responsive to both small molecules and proteins.[83,84] An adenosine-sensing DNA aptazyme was immobilized on a glass slide and in the presence of ATP catalyzed the ligation of a circular, padlock probe.[46] This probe could subsequently be amplified using RCA and the concatamers detected by hybridization to fluorescent probes. In essence, ATP signal was converted into an immobilized, amplified nucleic acid. The ATP-dependent aptazyme-based sensor in concert with RCA exhibited high selectivity against structurally similar GTP, CTP, and UTP and proved to be useful for the sensitive quantitation of its target in a multiplex array format.[85] Building on these results, we have also generated a structure-switching aptamer that can ligate to form a circle in the presence of a protein analyte, platelet-derived growth factor (PDGF).[45] Real-time RCA could be used to specifically quantitate PDGF down to the low nanomolar range (limit of detection = 0.4 nM), even against a background of cellular lysate. The aptamer was also adapted to RCA on surfaces, although quantitation proved to be more difficult. One of the great advantages of these methods described here is that they can be immediately adapted to almost any aptamer and do not require two or more affinity reagents as do sandwich assays.

References

1. Ellington, A.D. and Szostak, J.W. (1990) In vitro selection of RNA molecules that bind specific ligands. Nature (Lond.) 346(6287):818–822.
2. Tuerk, C. and Gold, L. (1990) Systematic evolution of ligands by exponential enrichment: RNA ligands to bacteriophage T4 DNA polymerase. Science 249(4968):505–510.
3. Bock, L.C., et al. (1992) Selection of single-stranded DNA molecules that bind and inhibit human thrombin. Nature (Lond.) 355(6360):564–566.
4. Nimjee, S.M., Rusconi, C.P. and Sullenger, B.A. (2005) Aptamers: an emerging class of therapeutics. Annu. Rev. Med. 56:555–583.
5. Lee, J.F., et al. (2004) Aptamer database. Nucleic Acids Res. 32(database issue):D95–D100.
6. Khati, M., et al. (2003) Neutralization of infectivity of diverse R5 clinical isolates of human immunodeficiency virus type 1 by gp120-binding 2′F-RNA aptamers. J. Virol. 77(23):12692–12698.
7. Misono, T.S. and Kumar, P.K. (2005) Selection of RNA aptamers against human influenza virus hemagglutinin using surface plasmon resonance. Anal. Biochem. 342(2):312–317.
8. Berezovski, M., et al. (2005) Nonequilibrium capillary electrophoresis of equilibrium mixtures: a universal tool for development of aptamers. J. Am. Chem. Soc. 127(9):3165–3171.
9. Berezovski, M., et al. (2006) Non-SELEX selection of aptamers. J. Am. Chem. Soc. 128(5):1410–1411.

10. Mendonsa, S.D. and Bowser, M.T. (2004) In vitro selection of high-affinity DNA ligands for human IgE using capillary electrophoresis. Anal. Chem. 76(18):5387–5392.
11. Mosing, R.K., Mendonsa, S.D. and Bowser, M.T. (2005) Capillary electrophoresis-SELEX selection of aptamers with affinity for HIV-1 reverse transcriptase. Anal. Chem. 77(19):6107–6112.
12. Cox, J.C., Rudolph, P. and Ellington, A.D. (1998) Automated RNA selection. Biotechnol. Prog. 14(6):845–850.
13. Cox, J.C. and Ellington, A.D. (2001) Automated selection of anti-protein aptamers. Bioorg. Med. Chem. Lett. 9(10):2525–2531.
14. Cox, J.C., et al. (2002) Automated selection of aptamers against protein targets translated in vitro: from gene to aptamer. Nucleic Acids Res. 30(20):e108.
15. Cox, J.C., et al. (2002) Automated acquisition of aptamer sequences. Comb. Chem. High-Throughput Screen. 5(4):289–299.
16. Ellington, A.D., et al. (2005) Automated in vitro selections and microarray applications for functional RNA sequences. In: The RNA world. Cold Spring Harbor Laboratory Press, Cold Spring Harbor, NY, pp. 683–719.
17. Hybarger, G., et al. (2006) A microfluidic SELEX prototype. Anal. Bioanal. Chem. 384(1): 191–198.
18. Jhaveri, S.D. and Ellington, A.D. (2000) In vitro selection of RNA aptamers to a protein target by filter immobilization. In: Beaucage, S.L., et al. (eds.) Current protocols in nucleic acid chemistry. Wiley, New York, pp. 9.3.1–9.3.25.
19. Crameri, A. and Stemmer, W.P. (1993) 10(20)-fold aptamer library amplification without gel purification. Nucleic Acids Res. 21(18):4410.
20. Bell, S.D., et al. (1998) RNA molecules that bind to and inhibit the active site of a tyrosine phosphatase. J. Biol. Chem. 273(23):14309–14314.
21. Pollard, J., Bell, S.D. and Ellington, A.D. (2000) Design, synthesis, and amplification of DNA pools for in vitro selection. In: Beaucage, S.L., et al. (eds.) Current protocols in nucleic acid chemistry. Wiley, New York, pp. 9.2.1–9.2.23.
22. Goertz, P., Cox, J.C. and Ellington, A.D. (2004) Automated selection of aminoglycoside aptamers. J. Assoc. Lab. Autom. 9:150–154.
23. Sooter, L.J. and Ellington, A.D. (2004) Automated selection of transcription factor binding sites. J. Assoc. Lab. Autom. 9:277–284.
24. Liu, J.J., Hartman, D.S. and Bostwick, J.R. (2003) An immobilized metal ion affinity adsorption and scintillation proximity assay for receptor-stimulated phosphoinositide hydrolysis. Anal. Biochem. 318(1):91–99.
25. Worlock, A.J., et al. (1991) The use of paramagnetic beads for the detection of major histocompatibility complex class I and class II antigens. Biotechniques 10(3):310–315.
26. McKay, S.J. and Cooke, H. (1992) hnRNP A2/B1 binds specifically to single stranded vertebrate telomeric repeat TTAGGGn. Nucleic Acids Res. 20(24):6461–6464.
27. McKay, S.J. and Cooke, H. (1992) A protein which specifically binds to single stranded TTAGGGn repeats. Nucleic Acids Res. 20(6):1387–1391.
28. Froystad, M.K., et al. (1998) A role for scavenger receptors in phagocytosis of protein-coated particles in rainbow trout head kidney macrophages. Dev. Comp. Immunol. 22(5–6):533–549.
29. Laine, S., et al. (2003) In vitro and in vivo interactions between the hepatitis B virus protein P22 and the cellular protein gClqR. J. Virol. 77:12875–12880.
30. Pyle, B.H., Broadaway, S.C. and McFeters, G.A. (1999) Sensitive detection of *Escherichia coli* 0157:H7 in food and water by immunomagnetic separation and solid-phase laser cytometry. Appl. Environ. Microbiol. 65:1966–1972.
31. Stovall, G.M., Cox, J.C. and Ellington, A.D. (2004) Automated optimization of aptamer selection buffer conditions. J. Assoc. Lab. Autom. 9(3):117.
32. Rajendran, M. and Ellington, A.D. (2002) Selecting nucleic acids for biosensor applications. Comb. Chem. High-Throughput. Screen. 5(4):263–270.
33. Chapman-Smith, A. and Cronan, J.E. Jr. (1999) The enzymatic biotinylation of proteins: a post-translational modification of exceptional specificity. Trends Biochem. Sci. 24(9):359–363.

34. Saviranta, P., et al. (1998) In vitro enzymatic biotinylation of recombinant fab fragments through a peptide acceptor tail. Bioconjug. Chem. 9(6):725–735.
35. Cull, M.G. and Schatz, P.J. (2000) Biotinylation of proteins in vivo and in vitro using small peptide tags. Methods Enzymol. 326:430–440.
36. McAllister, H.C. and Coon, M.J. (1966) Further studies on the properties of liver propionyl coenzyme A holocarboxylase synthetase and the specificity of holocarboxylase formation. J. Biol. Chem. 241(12):2855–2861.
37. Zhu, H., et al. (2000) Analysis of yeast protein kinases using protein chips. Nat. Genet. 26(3):283–289.
38. Ramachandran, N., et al. (2004) Self-assembling protein microarrays. Science 305(5680): 86–90.
39. Stadtherr, K., Wolf, H. and Lindner, P. (2005) An aptamer-based protein biochip. Anal. Chem. 77(11):3437–3443.
40. Stoltenburg, R., Reinemann, C. and Strehlitz, B. (2005) FluMag-SELEX as an advantageous method for DNA aptamer selection. Anal. Bioanal. Chem. 383(1):83–91.
41. Bini, A., Minunni, M., Tombelli, S., Centi, S. and Mascini, M. (2007) Analytical performances of aptamer-based sensing for thrombin detection. Anal. Chem. 79(7):3016–3019.
42. Collett, J.R., Cho, E.J. and Ellington, A.D. (2005) Production and processing of aptamer microarrays. Methods 37(1):4–15.
43. Kirby, R., et al. (2004) Aptamer-based sensor arrays for the detection and quantitation of proteins. Anal. Chem. 76(14):4066–4075.
44. McCauley, T.G., Hamaguchi, N. and Stanton, M. (2003) Aptamer-based biosensor arrays for detection and quantification of biological macromolecules. Anal. Biochem. 319(2):244–250.
45. Yang, L., et al. (2007) Real-time rolling circle amplification for protein detection. Anal. Chem. 79(9):3320–3329.
46. Cho, E.J., et al. (2005) Using a deoxyribozyme ligase and rolling circle amplification to detect a non-nucleic acid analyte, ATP. J. Am. Chem. Soc. 127(7):2022–2023.
47. Wengel, J., et al. (2001) LNA (locked nucleic acid) and the diastereoisomeric alpha-L-LNA: conformational tuning and high-affinity recognition of DNA/RNA targets. Nucleosides Nucleotides Nucleic Acids 20(4–7):389–396.
48. You, Y., et al. (2006) Design of LNA probes that improve mismatch discrimination. Nucleic Acids Res. 34(8):e60.
49. Li, Y., Lee, H.J. and Corn, R.M. (2006) Fabrication and characterization of RNA aptamer-microarrays for the study of protein–aptamer interactions with SPR imaging. Nucleic Acids Res. 34:1–9.
50. Li, Y., Lee, H.J. and Corn, R.M. (2007) Detection of protein biomarkers using RNA aptamer microarrays and enzymatically amplified surface plasmon resonance imaging. Anal. Chem. 79(3):1082–1088.
51. DeRisi, J., Iyer, V. and Brown, P.O. (1999) The MGuide: a complete guide to building your own microarrayer. Biochemistry Department, Stanford University, Palo Alto, CA.
52. Haab, B.B., Dunham, M.J. and Brown, P.O. (2001) Protein microarrays for highly parallel detection and quantitation of specific proteins and antibodies in complex solutions. Genome Biol. 2(2):1–3.
53. Miller, J.C., et al. (2003) Antibody microarray profiling of human prostate cancer sera: antibody screening and identification of potential biomarkers. Proteomics 3(1):56–63.
54. Collett, J.R., et al. (2005) Functional RNA microarrays for high-throughput screening of antiprotein aptamers. Anal. Biochem. 338(1):113–123.
55. Martinez, M.J., et al. (2003) Identification and removal of contaminating fluorescence from commercial and in-house printed DNA microarrays. Nucleic Acids Res. 31(4):e18.
56. Timlin, J.A., et al. (2005) Hyperspectral microarray scanning: impact on the accuracy and reliability of gene expression data. BMC Genomics 6(1):72.
57. Schweitzer, B., et al. (2002) Multiplexed protein profiling on microarrays by rolling-circle amplification. Nat. Biotechnol. 20(4):359–365.
58. Nielsen, U.B. and Geierstanger, B.H. (2004) Multiplexed sandwich assays in microarray format. J. Immunol. Methods 290(1–2):107–120.

59. Perlee, L., et al. (2004) Development and standardization of multiplexed antibody microarrays for use in quantitative proteomics. Proteome Sci. 2(1):9.
60. Varnum, S.M., Woodbury, R.L. and Zangar, R.C. (2004) A protein microarray ELISA for screening biological fluids. Methods Mol. Biol. 264:161–172.
61. Zangar, R.C., Daly, D.S. and White, A.M. (2006) ELISA microarray technology as a high-throughput system for cancer biomarker validation. Expert Rev. Proteomics 3(1):37–44.
62. Engvall, E. and Perlman, P. (1971) Enzyme-linked immunosorbent assay (ELISA). Quantitative assay of immunoglobulin G. Immunochemistry 8(9):871–874.
63. Soderberg, O., et al. (2006) Direct observation of individual endogenous protein complexes in situ by proximity ligation. Nat. Methods 3(12):995–1000.
64. Crowther, J.R. (2000) The ELISA guidebook. Methods Mol. Biol. 149(III–IV):1–413.
65. Nielsen, U.B., et al. (2003) Profiling receptor tyrosine kinase activation by using Ab microarrays. Proc. Natl. Acad. Sci. USA 100(16):9330–9335.
66. Zhou, H., et al. (2004) Two-color, rolling-circle amplification on antibody microarrays for sensitive, multiplexed serum-protein measurements. Genome Biol. 5(4):R28.
67. MacBeath, G. (2002) Protein microarrays and proteomics. Nat. Genet. 32(suppl):526–532.
68. Pavlickova, P., Schneider, E.M. and Hug, H. (2004) Advances in recombinant antibody microarrays. Clin. Chim. Acta 343(1–2):17–35.
69. Wingren, C. and Borrebaeck, C.A. (2006) Antibody microarrays: current status and key technological advances. Proteomics 10(3):411–427.
70. Saal, L.H., et al. (2002) BioArray Software Environment (BASE): a platform for comprehensive management and analysis of microarray data. Genome Biol. 3(8):SOFTWARE0003.1–3.6.
71. Whetzel, P.L., et al. (2006) The MGED ontology: a resource for semantics-based description of microarray experiments. Bioinformatics 22(7):866–873.
72. Spellman, P.T., et al. (2002) Design and implementation of microarray gene expression markup language (MAGE-ML). Genome Biol. 3(9):RESEARCH0046.
73. Hamelinck, D., et al. (2005) Optimized normalization for antibody microarrays and application to serum-protein profiling. Mol. Cell Proteomics 4(6):773–784.
74. Master, S.R., Bierl, C. and Kricka, L.J. (2006) Diagnostic challenges for multiplexed protein microarrays. Drug Disc. Today 11(21–22):1007–1011.
75. White, A.M., et al. (2006) ProMAT: protein microarray analysis tool. Bioinformatics 22(10):1278–1279.
76. Daly, D.S., et al. (2005) Evaluating concentration estimation errors in ELISA microarray experiments. BMC Bioinform. 6:17.
77. Dietz, T.M. and Koch, T.H. (1987) Photochemical coupling of 5-bromouracil to tryptophan, tyrosine and histidine, peptide-like derivatives in aqueous fluid solution. Photochem. Photobiol. 46(6):971–978.
78. Dietz, T.M. and Koch, T.H. (1987) Photochemical reduction of 5-bromouracil by cysteine derivatives and coupling of 5-bromouracil to cystine derivatives. Photochem. Photobiol. 49(2):121–129.
79. Golden, M.C., et al. (1999) Mass spectral characterization of a protein-nucleic acid photocrosslink. Protein Sci. 8(12):2806–2812.
80. Golden, M.C., et al. (2000) Diagnostic potential of PhotoSELEX-evolved ssDNA aptamers. J. Biotechnol. 81(2–3):167–178.
81. Smith, D., et al. (2003) Sensitivity and specificity of photoaptamer probes. Mol. Cell Proteomics 2(1):11–18.
82. Petach, H., et al. (2004) Processing of photoaptamer microarrays. Methods Mol. Biol. 264:101–110.
83. Robertson, M.P. and Ellington, A.D. (2004) Design and optimization of effector-activated ribozyme ligases. Nucleic Acids Res. 28(8):1751–1759.
84. Robertson, M.P., Knudsen, S.M. and Ellington, A.D. (2004) In vitro selection of ribozymes de-pendent on peptides for activity. RNA 10(1):114–127.
85. Yang, L. and Ellington, A.D. (2007) Real-time PCR detection of protein analytes with conformation-switching aptamers. Nucleic Acids Res. (submitted).

Chapter 12
The Use of Functional Nucleic Acids in Solid-Phase Fluorimetric Assays

Nicholas Rupcich, Razvan Nutiu, Yutu Shen, Yingfu Li, and John D. Brennan

Abstract The past 15 years have seen a revolution in the area of functional nucleic acid (FNA) research since the demonstration that single-stranded RNA and DNA species can be used for both ligand binding and catalysis. An emerging area of application for such species is in the development of solid-phase fluorimetric assays for biosensing, proteomics, and drug screening purposes. In this chapter, the methods for immobilization of functional nucleic acids are briefly reviewed, with emphasis on emerging technologies such as sol-gel encapsulation. Methods for generating fluorescence signals from aptamers and nucleic acid enzymes are then described, and the use of such species in solid-phase fluorimetric assays is then discussed. Unique features of sol-gel based materials for the development of solid-phase assays are highlighted, and some emerging applications of immobilized FNA species are discussed.

12.1 Introduction

The past 40 years have seen an ever-growing use of selective biological recognition elements, such as proteins or single-stranded DNAs, for the development of solid-phase bioassays and biosensors. Immobilization of proteins (mainly enzymes and antibodies) has resulted in a wide range of sensors for analytes that span small molecules and metals to proteins and viruses. Immobilization of single-stranded DNA[1,2] and molecular beacons[3] has allowed the development of highly selective genosensors and gene arrays that can be used for detection of pathogenic organisms, genetic markers, or single nucleotide polymorphisms. However, there were drawbacks of protein and DNA-based sensors, including the poor stability of

N. Rupcich, R. Nutiu, Y. Shen, Y. Li, and J.D. Brennan
Department of Chemistry, McMaster University, Hamilton, Ontario, L8S 4M1, Canada
brennanj@mcmaster.ca

Y. Li
Department of Biochemistry and Biomedical Sciences, McMaster University, Hamilton Ontario, L8N 3Z5, Canada

Y. Li and Y. Lu (eds.), *Functional Nucleic Acids for Analytical Applications*,

many immobilized proteins and a lack of versatility for nucleic acid-based sensors beyond detection of complementary DNA, which restricted the development of sensors for many small-molecule- and protein-based analytes.

The development of functional nucleic acids (FNA), and in particular molecular beacons (MB), DNA/RNA aptamers, ribozymes, and deoxyribozymes (also known as DNA enzymes, DNAzymes, or catalytic DNA) during the past 15 years has led to a revolution in the area of biosensors and bioassays. Aptamers, which are single-stranded nucleic acids that are generated by in vitro selection,[4,5] have been reported for a variety of ligands (targets) including metabolites and proteins.[6,7] The high affinity of aptamers,[8,9] and their properties of precise molecular recognition,[10,11] along with the simplicity of in vitro selection and the inherent stability of DNA species, make aptamers attractive as molecular receptors and sensing elements. Deoxyribozymes, which are single-stranded DNA molecules with catalytic capabilities,[12–16] have also been created by in vitro selection, and can perform diverse chemical transformations such as RNA cleavage,[17,18] RNA ligation,[19,20] DNA cleavage,[21] DNA ligation,[22,23] and DNA phosphorylation.[24,25] These species possess many unique properties relative to proteins, including chemical stability, the ability to withstand denaturation and renaturation cycles, cost efficiency, ease of site-specific labeling, as well as the simplicity of the in vitro selection method for DNAzyme generation. These features have led to these species becoming desirable alternatives to traditional protein-based enzymes and ribozymes for applications such as fluorescence-based biosensing.[26]

In addition to the advantages outlined above, DNA aptamers and DNAzymes have two other key advantages over proteins as biorecognition elements. First, it is possible to tune the properties of such species to provide desired levels of affinity, selectivity, or catalytic rate for a wide range of analytes, or to allow operation under unusual conditions of temperature or pH,[27] which is generally not possible with proteins. A second major advantage of such species is the ability to prepare the optimized FNA by standard solid-phase synthetic methods. This ability allows for the incorporation of specially modified nucleic acids during synthesis, which makes it easy to place signaling molecules (i.e., fluorophores, quenchers, or redox species) into specific locations within the DNA sequence to make the FNA species compatible with fluorescence or electrochemical sensors, or to incorporate biotinylated nucleotides into specific locations for immobilization to avidin-coated surfaces.

To realize the full potential of biological recognition elements for applications such as multianalyte biosensing, metabolite profiling, reporting enzymatic activity, or affinity capture of specific analytes, it is necessary to immobilize such species on a suitable surface or within a suitable material. Both proteins[28,29] and single-stranded DNA species[1,2] have been immobilized onto a range of surfaces, typically through physical adsorption, covalent binding, or affinity-based interactions such as that between avidin and biotin,[2] to create analytical devices such as microarrays, affinity columns, and biosensors. However, proteins often suffer from issues related to control of orientation and denaturation during and after covalent immobilization,[28,30] while modification of the DNA is often required to conjugate functional groups to allow covalent binding to occur.[31] Physiosorption of either proteins or DNA, while simpler to perform, can

lead to dissociation of bound biomolecules under certain pH and ionic strength conditions, and may prevent proper folding of proteins or functional nucleic acids such as aptamers or DNAzymes.[30,31] Furthermore, proteins and DNA immobilized by such methods are prone to degradation by proteases and nucleases, respectively. Because of these issues, there is a need for new methods for immobilization of functional biomolecules and, in particular, functional nucleic acids.

An emerging method for bioimmobilization is entrapment of biomolecules into sol-gel-derived silica materials. Although widely reported as a method for immobilization of both soluble and membrane-bound proteins,[32–36] reports on the entrapment of DNA into sol-gel-derived materials are few and are generally restricted to studies on the nature of nucleotide–silica interactions[37] or the use of DNA as a silica templating agent.[38] While it has been suggested that DNA-based biorecognition elements could potentially be entrapped with sol-gel-derived materials,[35,39] until recently there was only one report on DNA immobilization involving sol-gel materials.[40]

In this chapter, we provide a brief overview of methods to immobilize FNA species onto solid surfaces, and describe in some detail the methods used to generate fluorescence signals from immobilized aptamer and DNAzyme species and the use of tethered FNA species for biosensing and proteomics applications. A brief overview of the sol-gel entrapment method is then provided, followed by a description of work that has been done using entrapped DNA aptamers and DNA enzymes. The use of sol-gel entrapment methods for coimmobilization of both FNA and protein species is also described as a means to develop a new enzyme activity assay, with emphasis on the use of layered immobilization constructs for assay optimization. Finally, a brief discussion of emerging applications of immobilized FNA species is provided, highlighting new directions for optical biosensing and high-throughput screening.

12.2 Traditional Methods for DNA Immobilization

Methods for the immobilization of functional nucleic acids have been reviewed recently,[31] and hence only a brief overview of traditional immobilization methods is presented here. It is worth noting that most immobilization methods have been developed with the goal of using the immobilized nucleic acid for detection of complementary DNA strands that bind through Watson–Crick base-pairing interactions. However, most methods have been shown to be amenable to FNAs, although in certain cases special precautions must be taken to achieve optimal performance for such species.

As noted by Di Giusto and King,[31] there are four general methods for DNA or RNA immobilization, which are adsorption onto activated surfaces, entrapment of nucleic acids into polymeric matrixes, affinity binding to suitably modified surfaces, and covalent attachment of nucleic acids to surfaces (Fig. 12.1). These methods can be employed with a wide range of surfaces, including polymers, gels, silica, graphite, metal oxides, or pure metals such as gold, and may also be utilized for

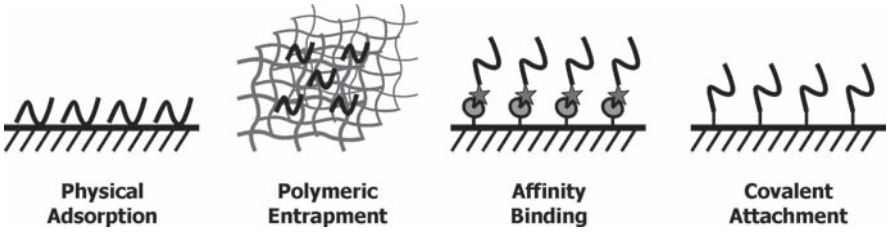

Fig. 12.1 Four general methods for DNA and RNA immobilization

immobilization onto specialized substrates such as silica or gold nanoparticles or carbon nanotubes to form fiberoptic sensors, microarrays, electrochemical sensors, or bead-based assays.

Adsorption is the simplest method to implement and generally makes use of hydrophobic, electrostatic, or hydrogen bonding interactions between the nucleic acid and the surface. However, it is not possible to control the orientation of the FNA, and binding through multiple points of contact can restrict conformational mobility; this can be particularly problematic for FNAs as such species often require significant conformational changes to generate an analytical signal (see Section 12.3.1). It is also possible that adsorption can alter the active conformation of FNAs, causing them to lose binding affinity. In addition, small changes in pH or ionic strength can lead to desorption of the FNA, which makes calibration of sensors difficult.

Matrix entrapment generally employs water-soluble organic polymers such as acrylamide, or electroactive polymers such as polypyrrole or polyanaline to produce a conductive polymer matrix. The FNA can either be entrapped or covalently bound to the matrix, with the latter method circumventing potential issues with leaching of the FNA. A potential advantage of such materials is the ability to form a three-dimensional layer of the nucleic acid, which can lead to much higher binding site density. However, a disadvantage is the difficulty in controlling pore size so as to retain conformational mobility and accessibility while avoiding leaching. These issues can be addressed using inorganic or organic/inorganic composite polymers for entrapment of FNA; this possibility is described in more detail in Section 12.4.

The availability of a wide range of modified nucleotides and the ability to insert such species into specific locations within a nucleic acid via standard solid-phase synthetic methods makes it straightforward to immobilize nucleic acids with a specific orientation using either affinity interactions or covalent attachment strategies. Affinity-based methods for immobilization of FNA almost exclusively involve the use of the high-affinity avidin–biotin interaction, which has a dissociation constant of 10^{-15} M. An advantage of this technique is the ability to label the FNA with biotin at either at the 3′- or 5′-end, or even in the center of the nucleic acid strand, to control the orientation of the FNA on the surface. In certain cases the need for an avidin underlayer can restrict electron transfer and thus compromise electrochemical sensors, but this is not an issue for fluorescence-based sensors.

The most prevalent method for immobilization of FNA is through covalent attachment to surfaces. Amine- and carboxylic acid-modified nucleic acids are readily available and can be immobilized to suitably modified surfaces (aldehyde, epoxy, amine) using appropriate coupling agents. Thiol-modified nucleic acids can also be utilized for direct binding to gold surfaces through coordination bonds. In many cases the surface can be initially derivatized with a spacer such as a short polyethylene glycol linker to minimize unwanted interactions between the FNA and the surface, improving performance. An important attribute of covalent immobilization is the ability to control the density of the nucleic acid to provide either high binding site density or a higher degree of conformational flexibility for the bound biomolecule.[31]

An issue with the immobilization of FNA species onto surfaces by any of the above methods is the potential for degradation by exonucleases when such species are to be used for in vivo analysis. Two methods exist to overcome this problem. First, the FNA can be placed in a polymer matrix or within a semipermeable membrane to exclude nucleases on the basis of size; this is an acceptable method for small-molecule sensing applications but is not appropriate for larger analytes. Another approach is to use a nucleic acid that has been modified to increase its resistance to degradation by nucleases. As noted by Di Giusto and King,[31] species such as locked nucleic acids (LNA), containing a 2′-*O*,4′-*C*-methylene bridge, or 2′-*O*,4′-*C*-*C*-ethylene-bridged nucleic acids (ENA) can significantly reduce the rate of degradation, as can oligo-2′-*O*-methylribonucleotides or other variants at the 2′-sugar position. The use of phosphorothioate backbone nucleic acids or peptide nucleic acids (PNA) also protect against nuclease attack, but in some cases can alter the energetics of hybridization, making it necessary to optimize temperature and ionic strength conditions for optimal selectivity and affinity.

12.3 Assays Utilizing Immobilized Functional Nucleic Acids

A wide range of assays that utilize immobilized FNAs have been reported in the past 10 years, and these have been reviewed extensively.[31,41] Applications that utilize tethered nucleic acids have ranged from the use of immobilized FNA species as affinity chromatography phases[42,43] to their use as selective capture agents for matrix-assisted laser desorption/ionization (MALDI) mass spectrometry.[44] A range of colorimetric sensors have been developed based on DNA-directed assembly or disassembly of gold nanoparticle aggregates,[45,46] whereas FNA species modified with redox probes have been widely employed for electrochemical sensors.[47] Immobilized FNA species have also been used for label-free sensing using impedance,[48] surface plasmon resonance,[49] quartz crystal microbalance,[50] or cantilever-based transduction methods.[51]

In this section a brief review of various fluorescence-signaling methods is provided, followed by an overview of fluorescence assays that have been developed

using tethered FNA species. Advantages and disadvantages of various fluorescence assay formats are described, along with interesting features of the different immobilization formats as supports for different assay platforms. In the interests of space, only assays utilizing planar surfaces are described. However, it is noted that there is a large body of work that utilizes FNA and other species bound to nanoparticles for a range of assays, as reviewed by Lu[52] and Mirkin.[53]

12.3.1 Methods of Fluorescence Signaling

The use of FNAs for fluorescence assay and sensor development has been recently reviewed,[54] and only key features of different systems are highlighted here. Fluorescence-based sensors have been developed utilizing a range of fluorescence signal readouts, including changes in intensity, wavelength, polarization, or fluorescence resonance energy transfer (FRET) signals.

Perhaps the most straightforward method for developing FNA-based solid-phase fluorescence assays is to use FNA species to detect fluorescent analytes, or as capture agents for fluorescence-based competitive binding assays.[77] Several examples exist that involve capture of small fluorescent molecules or fluorescently labeled proteins,[55] or the capture of proteins using photoaptamers followed by labeling.[56] These assays are described in more detail below.

More advanced fluorescence sensor formats utilize fluorescently labeled FNA species that undergo alterations in fluorescence anisotropy[57] or intensity[58] upon ligand binding. However, in most cases the total change in signal can be quite small (i.e., Jhaveri et al., reported an intensity increase of only 45% upon binding of ATP to the ATP-binding aptamer).[58]

More recently, specially designed nucleotide sequences have been prepared with both a fluorophore and a quencher moiety present. Such systems initially have a fluorescently labeled nucleotide (***F***) in close proximity to a quencher (dabcyl, blackhole quencher, nanogold) -modified nucleotide (***Q***), resulting in a low fluorescence signal. A range of probes have been utilized, with more recent examples including species such as quantum dots,[59] which have particular advantages for multiplexed assays.[60] Alteration of the nucleotide conformation, either by hybridization with a complementary target, binding of a nonnucleic acid target or catalytic cleavage or an engineered active site, results in spatial separation of the fluorophore and quencher, increasing the fluorophore–quencher distance and producing a large increase in fluorescence intensity.[54] In a related method, fluorescently tagged MB or aptamer species have been bound to metal surfaces to produce metal-dependent quenching of the signal.[61] Upon analyte binding, the fluorophore moves away from the surface, and fluorescence emission intensity is enhanced.

Early work on dequenching-based fluorescence-signaling DNA systems centered around the use of molecular beacons for detection of complementary DNA species.[3,62,63] These probes undergo self-complementary hybridization to form a hairpin structure that places the ***F*** and ***Q*** moieties in close proximity (Fig. 12.2a).

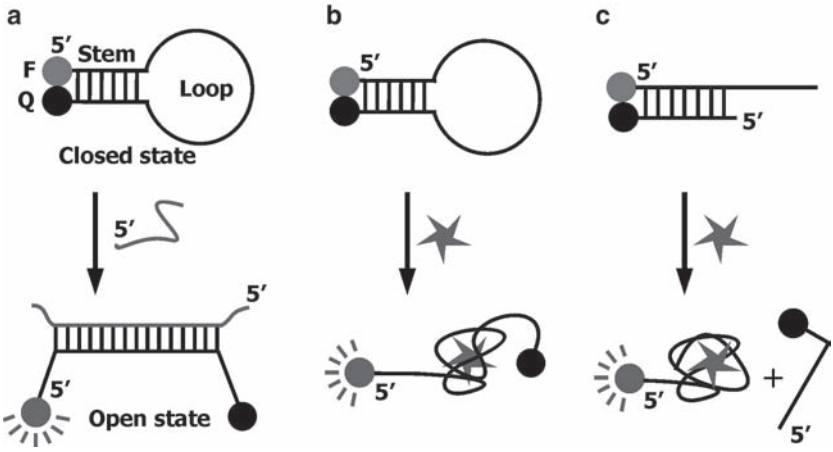

Fig. 12.2 Signaling DNA probes. (**a**) Molecular beacons for detection of nucleic acid targets. Aptamer beacons (**b**) and structure-switching signaling aptamers (**c**) for detection of nonnucleic acid targets. *F*, fluorophore; *Q*, quencher

The stem is normally five to seven nucleotides long while the loop of the hairpin is designed to be complementary to the desired target. Upon binding of target the MB moves from the "closed" to the "open" state, which leads to separation of the ***F*** and ***Q*** moieties, accompanied by a several-fold increase in emission intensity. MB systems can be designed to have high selectivity for perfectly complementary targets relative to those with single nucleotide polymorphisms (SNPs), making them highly useful for genosensing. Furthermore, the use of different labels allows for multiplexing of the emission signal to allow multianalyte sensing. MB systems can also be modified with a fluorophore–quencher pair by hybridization of ***F***-DNA and ***Q***-DNA to primer regions that extend beyond the normal stem region to form tripartite molecular beacons,[64] allowing for facile screening of different ***F-Q*** pairs to optimize signaling.

While MB species are excellent recognition elements for genosensing, they are not directly amenable to detection of nonnucleic acid targets. A method to extend the utility of MB species is to replace the loop region with an aptamer sequence to create an aptamer beacon, so that binding of the target to the aptamer results in a switch from the closed to the open state.[65] Several variants on this concept have been reported, but all rely on disruption or formation of a stem that controls the distance between ***F***- and ***Q***-labeled nucleotides (Fig. 12.2b).

A related concept for generating a change in fluorescence is to simply label the terminal nucleotides in an aptamer sequence with a fluorophore and quencher, and to then make use of conformational changes in the aptamer upon target binding to change the spatial separation of the terminal nucleotides.[66] However, this method often results in a loss in intensity upon target binding, which leads to poorer detection limits. Furthermore, this method requires that the aptamer undergo a fairly specific conformational change to ensure that the terminal nucleotides undergo large changes

in separation upon target binding; this is not always the case, and it is difficult to engineer into existing aptamers.

A more versatile method for converting aptamers to fluorescence-signaling aptamers is the creation of structure-switching signaling aptamers[67] (see Fig. 12.2c). This method exploits the fact that all aptamers can adopt two conformations: a weak duplex structure with a complementary DNA and a stronger complexed structure with the target. In this case a ***F***-DNA strand is hybridized to a primer region extending from the aptamer, while a ***Q***-DNA strand is hybridized over a region spanning the primer and aptamer regions, with the quencher adjacent to the fluorophore. Upon binding of a target, the aptamer undergoes a structural switch that destabilizes hybridization to the ***Q***-DNA, resulting in displacement of the quencher and an increase in fluorescence intensity. An advantage of this method is that a single aptamer can be labeled with a variety of different fluorophores or quenchers by simply altering the ***F***-DNA and ***Q***-DNA species. Thus, individual aptamers can be labeled with different ***F/Q*** pairs to allow for multiplexed detection of different analytes based on unique excitation and/or emission wavelengths for each aptamer.

A range of methods have also been developed to create fluorescence-signaling ribozymes and deoxyribozymes. The basis of most signaling enzyme systems is to have binding of a target molecule elicit catalytic activity, which then results in either cleavage of a RNA-bearing substrate or ligation of two nucleic acid strands, with the former method being by far the most widely employed.[54] By labeling the substrate nucleotide(s) with a fluorophore–quencher (or donor–acceptor) pair (Fig. 12.3), the spatial proximity of the ***F-Q*** (or ***D-A***) pair is altered by cleavage or ligation, generating a signal. This approach has been used for detection of metals, small molecules, nucleic acids, and proteins. As an example, a DNAzyme for Pb(II) was developed by Li and Lu and used for fluorimetric detection of lead.[68,69] A DNA-based substrate bearing a fluorophore, quencher, and ribonucleotide cleavage site was annealed to the lead-dependent DNAzyme. Addition of Pb(II) activated the catalytic DNA, resulting in cleavage of the ribo-linkage and an increase in fluorescence.

Catalytic molecular beacons have also been developed using an MB motif to control the activity of a DNAzyme.[70] In the absence of target, a ***F/Q***-labeled substrate containing a ribonucleotide is only partially annealed to the DNAzyme because of blockage of one of the substrate-binding arms as a result of formation of a closed stem, preventing cleavage. Upon target binding, the MB stem dissociates and the substrate-binding arm associates with the ***F/Q***-labeled substrate. Upon full hybridization with the DNAzyme, the ribo-linkage is cleaved, and fluorescence emission increases.

The concept of using an aptamer rather than a MB for allosteric control of ribozyme and DNAzyme catalysis has recently been reported. In this case, the aptamer is linked to the nucleic acid enzyme by a "communication module," which allows the aptamer to inhibit the catalytic action of the enzyme.[71,72] Upon target binding, the aptamer adopts a folded conformation that releases a substrate-binding sequence within the communication module, resulting in full substrate binding and catalysis (Fig. 12.3).

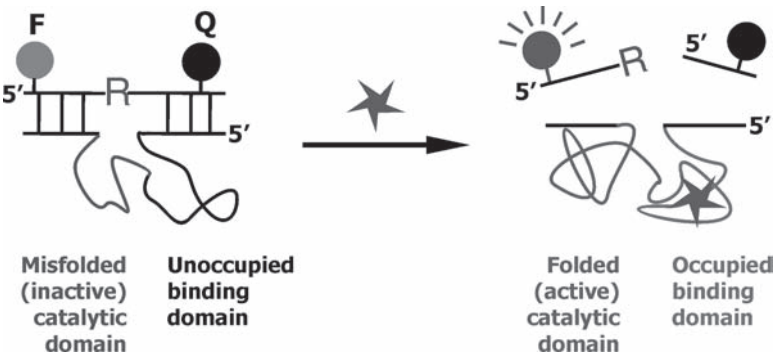

Fig. 12.3 An RNA-cleaving, fluorescence-signaling, ligand-dependent nucleic acid enzyme. *F*, fluorophore; *Q*, quencher; *R*, ribonucleotide as the cleavage site

A key issue with the systems outlined above is the use of end-labeled substrates, which is usually required to minimize perturbation of the region surrounding the ribo-linkage in existing DNAzyme substrates; this results in a relatively large distance between the fluorophore and quencher in the substrate, and thus a high initial fluorescence signal. A recent advance that led to improved signaling efficiency for DNAzyme systems was the design of a new substrate that utilized a fluorophore–quencher pair which immediately flanked the ribonucleotide cleavage site.[73] In this case, the ***F***-*R*-***Q*** motif was present in the substrate during the selection process so that only DNAzymes that could cleave the modified substrate were selected. The intact substrate had extremely low signal levels, and the cleavage of the substrate led to greater than tenfold increases in emission intensity. Furthermore, the substrate specificity depended on the presence of the ***F*** and ***Q*** moieties; alteration of the fluorophore or removal of the ***F*** or ***Q*** led to significantly reduced catalytic rates. Such species have been used as substrates for metal ion-sensitive, pH-sensitive, and allosteric ATP-sensitive DNAzymes, all with good signaling efficiency.[54,74]

12.3.2 Fluorescence Sensors Based on Immobilized Functional Nucleic Acid Species

Examples of immobilized aptamer sensors are numerous, and only selected papers are reviewed to highlight specific classes of sensors. Some of the earliest work with immobilized fluorescence-signaling aptamers was based on monitoring changes in the emission properties of aptamer-bound dyes as a result of target binding. For example, work by Heftjie and coworkers[57] utilized a covalent binding method to attach fluorescently labeled thrombin-binding aptamers to the surface of an evanescent wave sensor (Fig. 12.4). In this case, binding of thrombin increased the polarization of the fluorophore, resulting in a highly reproducible signal and

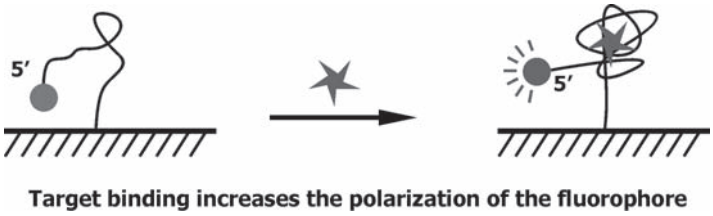

Fig. 12.4 A fluorescent sensor with an immobilized, fluorophore-labeled aptamer. The target is detected via changes in the evanescent-wave-induced fluorescence anisotropy of the immobilized aptamer

excellent detection limits (0.7 πmol thrombin) but a relatively limited dynamic range (three orders of magnitude).

A more common approach for detection of analytes is through the use of immobilized molecular beacons or aptamer beacons. The first reports in this area focused on the development of fiberoptic sensors that utilized MB systems bound by affinity or covalent interactions. For example, Tan's group developed a biotinylated MB that was bound to a planar silica surface derivatized with physisorbed avidin that was cross-linked with glutaraldehyde.[3] The MB-derivatized slide was incorporated into an internal reflection fluorescence instrument to allow evanescent excitation of the MB fluorescence. Upon introduction of complementary DNA, a 2.5-fold enhancement in fluorescence was observed over a period of ~30 min (versus a tenfold enhancement in 20 min in solution). The sensor could be used to detect sub-nanomolar levels of DNA. In a follow-up study, the MB was bound to streptavidin-coated optical fibers and used to detect γ-actin mRNA sequences via changes in evanescently excited fluorescence.[75] A detection limit of 1.1 nM was obtained, although the signaling magnitude and response kinetics were again much worse than that in solution, possibly due to a fraction of MB that was either initially unfolded or inaccessible to target.

This use of fiberoptic sensors has also been extended to aptamer beacons, which are formed by replacing the loop of the traditional MB with an aptamer. For example, Yu and coworkers developed a thrombin-binding MB and interfaced it to an optical fiber by affinity interactions.[76] The sensor showed a thrombin-dependent increase in emission intensity, and again the performance characteristics were worse than in solution.

12.3.3 Multianalyte Arrays Utilizing Immobilized Molecular Beacon Species

The examples noted above, while demonstrating the potential of MB and aptamer beacon systems for sensing, were relatively limited in performance owing to the ability to detect only a single species. Given the fact that conventional DNA

microarray technology was relatively mature by the year 2000, it was clear that this would be a major direction for the application of immobilized FNA species. Early work on the development of a multianalyte sensor platform used a hybrid of fiberoptic and array technologies. Walt and coworkers reported on the development of aptamer-linked silica microspheres that were distributed randomly within microwells etched into the distal tip of an imaging fiber bundle.[77] Thrombin-binding aptamers were bound to one set of beads and a second oligonucleotide was bound on separate beads to account for nonspecific binding. The beads were incubated with a mixture of fluorescently labeled thrombin and nonlabeled thrombin (analyte) in a competitive assay format, captured on the tip of the imaging fiber bundle and imaged. The fiber array could detect 10 nM thrombin with a dynamic range of three orders of magnitude, although there was some interference from albumin observed with the sensor.

More recent work on FNA-based microarrays has focused on the development of multianalyte arrays fabricated by contact or noncontact printing of multiple aptamers in a spatially defined pattern on a planar surface, or by synthesis of aptamers on chip. The methods used to immobilize DNA onto arrays are reviewed in detail by Heise and Bier,[78] and thus are not covered here.

There are many examples of FNA microarrays, and only a selection of studies is presented here. Chapter 11 of this volume covers the development and application of aptamer arrays in more detail. Early microarray studies focused on fabrication of arrays of molecular beacons and utilized a variety of substrates and immobilization chemistries. For example, MBs have been covalently immobilized onto three-dimensional photopolymerized acrylamide gel arrays,[79] and were able to discriminate complementary and noncomplementary DNA with a fivefold difference in intensity, with a 100-fold higher signal than similar two-dimensional arrays. More recently, Yao and Tan developed a MB array using biotinylated linkers to bind MBs to avidin-coated surfaces.[80] The length of the linker, pH, and ionic strength were optimized to extend the MB away from the surface of the substrate and maximize signaling capacity, and once optimized the array provided a 5.5-fold enhancement upon target binding, a significant improvement relative to approximately twofold enhancements observed in earlier work with immobilized MB systems (see above). Work by Malayer and coworkers[81] demonstrated the development of an MB array for detection of the 16S rRNA of the bacterium *Francisella tularensis*. In this case, the MB was covalently immobilized onto aldehyde- or hydrogel-modified slides and was used to discriminate complementary and mismatched sequences. It was demonstrated that the MB array showed poor discrimination between matched targets and those with up to three mismatches, particularly if mismatches were in terminal regions of the targets. Interestingly, the ability to discriminate between matched and mismatched targets improved as the temperature of the assay was increased to a value just below the melting temperature of the matched target. However, this study clearly demonstrated that use of single MB sequences for determination of SNPs could be fraught with poor selectivity, arguing for the need for multiplexed analysis. The most recent study to employ MB arrays involved the development of an array to detect *Escherichia coli* O157:H7.[82] This system uses

wavelength-shifting MB systems based on the use of a donor–acceptor pair rather than the conventional fluorophore–quencher system employed in the majority of MB arrays. The ability to detect hybridization via a color shift avoids false-negative signals that may arise from photobleaching or washing-off of donor probes. The array could detect as little as 1 ng/μl of *E. coli* marker genes, with changes in the ratio of red to green fluorescence (due to FRET) being as high as 30-fold in the presence of ~10 ng/μl cDNA.

An interesting variation on traditional MB systems that makes clever use of immobilized MBs is the modulation of fluorescence as a result of quenching by metal surfaces.[83] Such systems utilize MBs bound to nanoparticle or planar gold surfaces via thiol-modified terminal groups. In the "closed" state, the fluorophore on the other terminus is quenched by its close proximity to the gold surface via metal-induced quenching. Upon binding to a target (genes from methicillin-resistant *Staphylococcus aureus*, MRSA), the probe moves several nanometers away from the surface, and the fluorescence is enhanced by a factor of up to 20-fold, as shown in Fig. 12.5.[61] Further optimization of the density of the MB on the surface (via addition of mercaptopropanol spacers) and the nucleotides in the stem of the MB led to a significant increase in signal enhancement (100-fold) relative to the unoptimized system.[84] An important aspect of the optimization was the ability to provide sufficient space to allow hybridization to occur, while at the same time capping the gold surface to prevent unwanted interactions between the DNA and the metal. This platform could be used to produce microarrays that could discriminate SNPs with a tenfold difference in intensity relative to complementary DNA. However, the immobilized MB could be reused only a limited number of times because of loss of the MB from the gold surface during regeneration.

Most recently, this methodology has been extended to catalytic molecular beacons on gold surfaces.[85] A thiolated version of the Pb(II) dependent DNAzyme (17E) was immobilized onto a Au surface along with mercaptohexanol spacer molecules and hybridized with a complementary fluorophore-labeled substrate nucleotide to form a double-stranded structure. Introduction of lead results in cleavage of the substrate and release of the fluorophore into solution, where it is detected

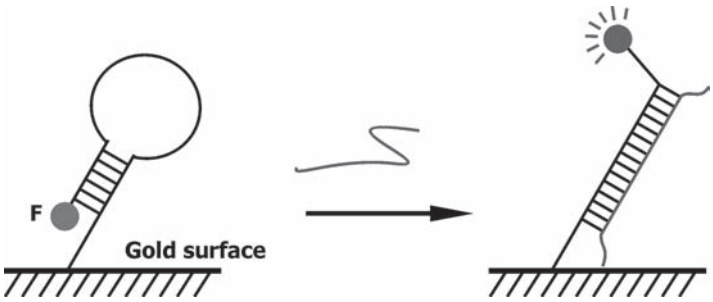

Fig. 12.5 A biosensor with molecular beacon immobilized on gold surface, which acts as the quencher

after removal of the DNAzyme modified substrate. In this format, an eightfold increase in intensity was observed upon addition of Pb(II), although selectivity relative to other divalent metal ions was poor (only threefold difference in intensity). While such a scheme does not make use of metal-induced quenching, it shows the potential of using self-assembled DNAzyme monolayers for generation of fluorescence signals.

12.3.4 Multianalyte Arrays Utilizing Immobilized Aptamers

Although significant work has been done on MB microarrays, these systems are inherently limited to detection of DNA or RNA targets. To overcome this issue, a large number of groups have developed a range of aptamer-based microarrays for detection of proteins and small molecules.

Several studies have utilized nonlabeled aptamer arrays for the detection of fluorescently labeled proteins, or for capture of proteins followed by on-array labeling or detection using fluorescently labeled secondary antibodies. For example, Lindner and coworkers reported on a comparison between DNA aptamers and monoclonal antibodies for detection of labeled proteins on microarrays.[86] This study demonstrated that aptamers could be used for protein detection with performance that was equivalent to or better than antibody-based arrays, although it must be noted that this study utilized a limited number of aptamers. It will be necessary to prepare arrays with a much larger number of aptamers to a wide range of analytes to make this technology competitive with antibody arrays.

A series of studies from Ellington's group have focused on the development of protein-sensing RNA aptamer microarrays. An early study utilized lysozyme- or ricin-binding aptamers on beads, which were dispensed into the wells of an array-based "electronic tongue".[87] Biotinylated agarose beads were derivatized with streptavidin and used to capture biotinylated aptamers. Bound proteins were detected based on the emission of a label on the protein and could be regenerated and reused over many assay cycles. A more conventional RNA microarray was fabricated by preparing biotinylated RNA aptamers for lysozyme by in vivo transcription and spotting these onto streptavidin-coated slides.[88] A total of 24 different lysozyme-binding aptamers, derived from an automated in vitro selection protocol, were spotted along with two clone pools and tested for binding to fluorescently labeled lysozyme. In this manner, it was possible to rapidly identify the highest affinity aptamer from the set of clones or to select clones with specific affinities or dynamic ranges. Overall, this study showed that automated selection combined with high-throughput screening of aptamer affinity on microarrays could be used to rapidly identify optimal aptamers for desired targets. Detailed methods for the fabrication, processing, and analysis of such microarrays have recently been reported,[89] as have methods for optimizing aptamer arrays for multiprotein analysis, including choice of surface chemistry, orientation of the aptamer, and type of assay and washing buffer.[55]

An interesting variant on aptamer microarrays is the use of photoaptamer arrays for protein detection. Early work by Gold and coworkers suggested that arrays of aptamers with photoreactive 5-bromodeoxyuridine groups could be used to capture target proteins onto specific locations on an array. Irradiation with UV light could then be used to photo-cross-link the protein permanently to the aptamer, allowing for harsh washing steps to remove nonspecifically bound proteins. Protein-specific stains could then be added to determine the presence and/or concentration of protein in the original sample.[90] To demonstrate the concept, photoaptamer microarrays were developed by pin-printing photoaptamers onto amine-derivatized slides to allow covalent binding and were used for protein detection.[56] Introduction of a sample of proteins was performed, followed by photo-cross-linking and washing. The array was then exposed to either a general protein-binding stain such as NHS-AlexaFluor555 or to a specific fluorescently tagged antibody to allow for general or specific detection of bound proteins, respectively. The arrays were demonstrated to be capable of detecting proteins in either buffer or diluted serum, and in optimal cases had detection limits in the low fM range. Use of antibody-based staining allowed for more selective determination of proteins, as the protein had to bind selectively to both the photoaptamer and secondary antibody, minimizing false positives. Furthermore, the use of a cross-linking reaction increased the stringency of the array based assay, as nonprotein species that might nonselectively adsorb to the aptamer were not covalently captured and thus were removed during the harsh washing step.

Two issues with the this aptamer array system are the need for multiple washing steps and for labeling of captured targets, either before or after capture or for development of competitive binding assays. This need results in added complexity for the assay and significantly limits that application of such arrays for small-molecule analysis, as neither staining nor secondary antibody binding is possible in this case. To overcome these issues, significant work has been done to utilize signaling aptamers in microarray-based assays for both protein and small-molecule analysis.

An early study employed signaling aptamers composed of either RNA or DNA to prepare a microarray on a planar waveguide surface.[91] The array was excited evanescently by total internal reflection, and the emission was detected through a polarizing beamsplitter to produce two images, one for parallel polarized light and one for perpendicularly polarized light, thus allowing for a fluorescence anisotropy based assay on the array. Initial studies showed that the binding of thrombin to array elements containing thrombin-binding aptamer resulted in a significant increase in anisotropy for these spots and resulted in a detection limit of ~1 nM. A microarray was constructed using four aptamers to different proteins and demonstrated excellent selectivity for detection of different proteins in cell lysates and serum, although some cross reactivity was noticed. The authors also reported that the RNA aptamers had poor stability relative to DNA aptamers owing to the presence of ribonucleases in the biological samples tested, and suggested that modified RNA species would be required to overcome this problem.

A second signaling aptamer array system was developed using a strategy wherein a RNA aptamer against human immunodeficiency virus (HIV)-1 Tat was split into two nonfunctional units, one of which (the anchor oligo) was immobilized on

aldehyde-coated slides in an array pattern by covalent interactions. In the presence of target, the other half of the aptamer (hybridizing oligo), which was labeled with a fluorescent probe, reassembled on the surface, resulting in an increase in fluorescence intensity.[92] The assay was shown to be amenable to detection of protein in buffer, but was unable to detect proteins in HeLa cell extracts even with added RNase inhibitors to minimize degradation of the RNA aptamer, again highlighting the need for modified RNA aptamers. A further disadvantage of this assay format relative to the methods described above was the need to add the hybridizing oligo in solution and to perform washing steps to remove nonselectively bound oligo species to minimize fluorescence background signals.

An interesting demonstration of an immobilized signaling aptamer system for protein detection involved the use of DNA tiles containing a fluorescently labeled thrombin aptamer sequence to allow self-assembly of DNA tiles onto a surface via assembly of "sticky ends" (Fig. 12.6).[93] This approach resulted in a periodic DNA structure on the surface that had a thrombin-binding aptamer every 27 nm within the array. The signaling aptamer underwent an increase in intensity greater than twofold upon thrombin binding, leading to a useable signal. An interesting aspect of this work was the ability to capture the analyte in solution in the first step, followed by assembly of the DNA tiles along with the captured protein to produce a fluorescent pattern on a surface. This method produced higher overall intensity values relative to adding protein to a preformed array, presumably due to the ability to avoid surface effects such as inaccessibility of bound aptamers.

A final example of a signaling aptamer array system utilized a polythiophene–DNA aptamer aggregate for detection of thrombin.[94] The basis of this system is the formation of a tight complex between polythiophene and ssDNA, which results in effective quenching of polythiophene fluorescence. Upon binding of either complementary DNA or a protein target, the DNA adopts a different structure, which leads to a significant enhancement in polythiophene emission. An array was fabricated with Cy-3-labeled antithrombin aptamers via covalent immobilization of the DNA, which was preassociated with the polymer, to an aldehyde surface. Addition of thrombin resulted in a conformational change in the DNA that allowed for dequenching of the polymer fluorescence and hence efficient energy transfer to the Cy-3 labels. The presence of several Cy-3-labeled DNA aptamers within the polymer–aptamer complex led to enhanced emission from the acceptor and resulted

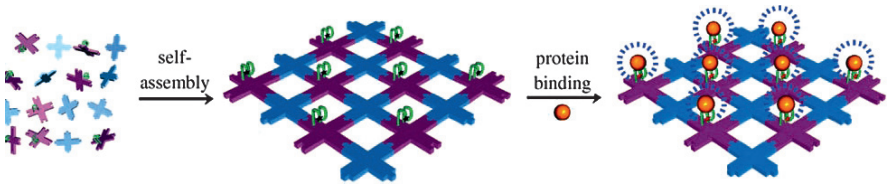

Fig. 12.6 A biosensor that uses DNA tiles containing a fluorescently labeled aptamer (Reproduced with permission from ref. 93. Copyright [2006] Wiley)

in a detection limit in the low pM range. The array also demonstrated excellent selectivity for thrombin over nontarget proteins, likely because of the inability of such proteins to induce the necessary conformational change in the aptamer to generate a signal. In this manner, issues with signals arising from nonspecific binding of proteins were avoided.

While there are several examples of signaling aptamer microarrays, as noted above, it is noteworthy that there are few reports of arrays fabricated with signaling deoxyribozymes, although Ellington did report on a DNAzyme array that utilized radioactivity for detection,[95] while Breaker and coworkers reported on riboswitch arrays for analysis of complex mixtures.[96] Such species might be expected to provide good resistance against changes in emission owing to nonspecific binding, because only specific binding should lead to catalysis and thus generation of a signal. As noted below, there are solid-phase assays involving signaling aptamers and DNAzymes that are moving in this direction.

12.4 Sol-gel Immobilization Methods

12.4.1 The Sol-gel Process for Biomolecule Entrapment

While there has been significant progress in the development of DNA immobilization protocols during the past 20 years, as noted here, many of the methods result in monolayer or submonolayer coverage and thus can suffer from poor sensitivity. In the case of FNAs, there is also the potential for surface-mediated changes in FNA conformation and mobility, which could potentially reduce activity and long-term stability and lead to the degradation of FNA by nucleases.[31]

As noted in Section 12.1, an emerging route for bioimmobilization involves the entrapment of biological components into inorganic silicate matrixes or organic-inorganic nanocomposite materials formed by a low temperature sol-gel processing method (Fig. 12.7). The key papers demonstrating the potential of this method for protein immobilization were published in the early 1990s by the groups of Avnir[97] and Dunn and Zink.[98] These groups and others demonstrated that a series of enzymes, antibodies, and ligand-binding proteins could be entrapped with high

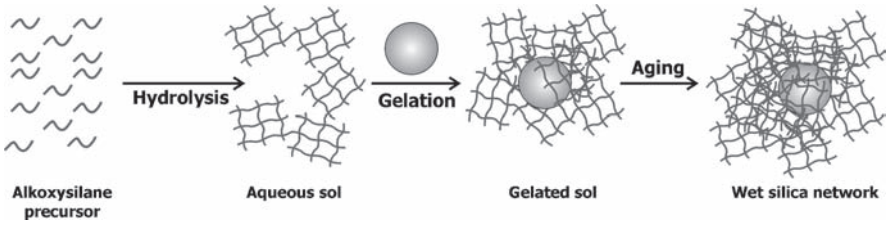

Fig. 12.7 Low-temperature sol-gel processing method for entrapment of biomacromolecules

activity into glasses derived from alkoxysilanes such as tetraethyl orthosilicate (TEOS) using a general protocol similar to that outlined in Fig. 12.7. The formation of the material begins with the partial or complete hydrolysis of a suitable precursor to form an aqueous sol, which is an aqueous suspension of silica nanostructures (oligomers, colloids, fibrils, etc.). The precursors can consist of tetraalkoxysilanes, mono-, di-, or tri-alkyl alkoxysilanes, or may comprise functional groups such as alkenyl, aryl, amino, carboxyl, or thiol as well as redox-active moieties, flavins, or quinones. Other metal centers such as Al, Ti, V, or Ce may also be used to alter the material properties. The hydrolysis reaction itself can be either acid- or base catalyzed, and more advanced precursors, such as diglycerylsilane,[99] can be hydrolyzed at neutral pH and liberate the biocompatible byproduct glycerol, which helps to stabilize biomolecules.

Following hydrolysis, the sol is mixed with a buffered aqueous solution containing the biomolecule along with any catalysts, drying control additives, polymers, templating agents, redox species, or fillers that may be required to modify the properties of the final material. The change in pH along with the presence of added salts and catalysts promotes a large-scale polymerization reaction over a period of minutes to hours, resulting in gelation of the sol and entrapment of the biomolecule. The initial gels are soft and have high water content (50–80%) and large pores (up to 200 nm diameter). Aging of the wet silica network over a period of days to weeks promotes further condensation and strengthens the network. During this stage, entrapped alcohol and/or water resulting from the initial hydrolysis and condensation reactions will be removed from the matrix, causing the matrix to shrink by 10–30%, the pore diameters to decrease by about 25%, and the relative proportion of siloxane to silanol groups to increase owing to coarsening of the material.[100] Finally, the aged material can be partially dried, resulting in the loss of most of the interstitial water, further cross-linking of the matrix, shrinkage of the pores to the range of 2–20 nm, and overall shrinkage of the material by 10–85% of its initial volume, depending on the types of precursors and processing conditions used.

In addition to enzymes and antibodies, sol-gel materials have been used to entrap a wide variety of biological species, including regulatory proteins, membrane-bound proteins, and even whole cells.[32–36] However, this immobilization platform did not gain significant popularity for the entrapment of DNA species, mainly because most DNA sensors were targeted to binding of large complementary DNA strands, and thus immobilization by simple size exclusion was not possible.

With the emergence of functional nucleic acids, and the use of these species for detection of small molecules, the sol-gel platform became amenable to entrapment of FNA species for small-molecule sensing. Potential advantages of sol-gel-derived silicate materials for immobilization of FNA species are as follows: (a) they can be made to be optically transparent, making them ideal for the development of optical sensors; (b) they are open to a wide variety of chemical modifications based on the inclusion of various polymer additives, redox modifiers, and organically modified silanes to create organic–inorganic composite materials; (c) they have a tunable pore size and pore distribution, which allows small molecules and ions to diffuse into the matrix while large biomolecules remain trapped in the pores,

allowing size-dependent bioanalysis; and (d) they can be made in a variety of forms (thin films, bulk glasses, powders, microarrays, etc.) to allow for development of novel bioanalytical devices. Specific examples of FNA entrapment within sol-gel materials, including both aptamers and DNAzymes, are provided in the following sections.

12.4.2 Immobilization of Molecular Beacons onto Sol-gel Materials

The earliest work involving the interfacing of FNA species and sol-gel supports involved the immobilization of biotinylated molecular beacons onto sol-gel materials that contained entrapped biotin-derivatized BSA which were coated, post gelation, with a layer of streptavidin. The SA layer acted as a bridge to link the MB species to the sol-gel material.[101] The advantages of utilizing sol-gel materials, relative to formation of MB monolayers on solid supports, included a faster response time, improved long-term stability for the immobilized MB, and a higher loading of MB owing to the high surface area of the sol-gel material, which led to improved detection limits. The sol-gel immobilized MB showed high sensitivity for detection of target DNA and good selectivity against single-base mismatches, indicating good potential for SNP analysis. Although the sol-gel method showed significant advantages for immobilization of biotinylated FNA species, there is no follow-up study reported in which this method is used for the immobilization of either aptamers or DNAzymes.

12.4.3 Entrapment of DNA Aptamers Within Sol-gel Materials

Our groups provided the first report on the entrapment of a functional nucleic acid within a sol-gel-derived material.[102] In this work, a structure-switching signaling aptamer was entrapped into a range of sol-gel materials derived from the biocompatible precursors sodium silicate or diglycerylsilane. A number of factors were found to affect the performance of the entrapped aptamer, including the type of precursor, the presence of additives, and the length of the Q-DNA. Our results showed that entrapment in any material resulted in a slight reduction in the signaling level relative to solution (tenfold vs 12-fold), with signaling levels decreasing dramatically if cationic silanes were included in the material. The rate of signal evolution was also decreased by a factor of approximately tenfold, and up to 50% of the aptamer was able to leach from the material. However, of the aptamer that was retained, more than 90% of the entrapped aptamer remained accessible to externally added small molecules. Overall, the results indicated that aptamers could be entrapped with retention of conformational freedom, although inclusion of

cationic silanes, such as aminopropyltriethoxysilane (APTES), resulted in the DNA backbone of the aptamer electrostatically binding to the matrix, with an inability to undergo a structural switch upon introduction of ATP.

As shown in Fig. 12.8a, the entrapped ATP-binding aptamer retained selectivity for ATP over other nucleotide triphosphates (such as GTP). The aptamer also retained sensitivity to ATP concentration that was similar to that observed in solution. Importantly, the dynamic range of the entrapped aptamer matched well with the physiological range of ATP, and thus the sensor could potentially be used for direct detection of ATP without the need for sample dilution. The aptamer retained full signaling capability for at least 30 days when aged in buffer solution, and required 3 months before signaling ability was completely lost, likely owing to continued evolution of the sol-gel matrix, which could lead to pore collapse and subsequent restriction of dynamic motion for the entrapped DNA.[103]

One of the key advantages of entrapping the aptamer within the silica matrix was that it provided a steric barrier to entry of digestive enzymes which could degrade the biomolecule. Addition of DNAse I to the aptamer in solution results in an increased fluorescence signal (5.5-fold in 1 h, eightfold maximum) from DNA degradation (see Fig. 12.8b), due to dehybridization of the QDNA and/or release of the fluorescein-labeled nucleotide, causing an overall increase in distance between the fluorescein- and dabcyl-labeled nucleotides. Digestion of the FNA immobilized by standard avidin–biotin affinity interactions was essentially identical to that obtained in solution, indicating no protection of the aptamer in this case. On the other hand, the entrapped aptamer underwent only a very minor change in fluorescence intensity (~18%), likely because of digestion of a small fraction (<2%) of the aptamer

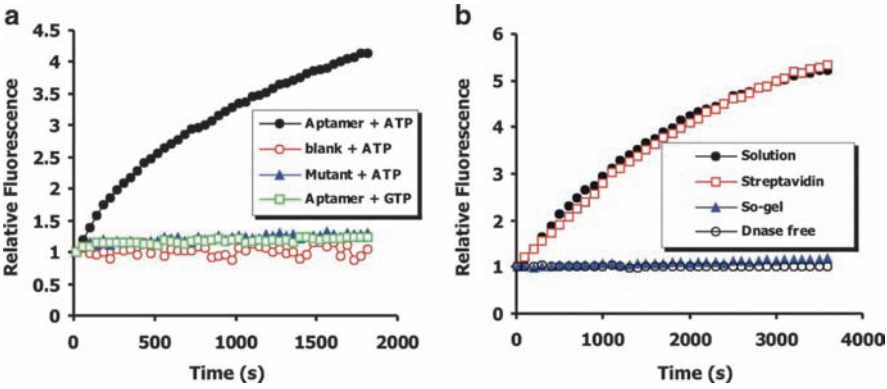

Fig. 12.8 Performance of ATP-binding DNA aptamer entrapped in silica sol-gel. (**a**) Comparison of selectivity of the aptamer and an inactive mutant. All analyses were done using 0.5 mM of the specified analyte: ●, aptamer + ATP; ○, blank; ▲, mutant + ATP; □, aptamer + GTP. (**b**) Changes in emission intensity of structure-switching aptamers upon exposure to DNase: ●, aptamer in solution; □, aptamer immobilized on a streptavidin-coated microwell; ▲, aptamer entrapped in sodium silicate; ○, DNase free control. (Reproduced with permission from ref. 102. Copyright [2005] American Chemical Society)

that resided close to the surface of the silica monolith. These results indicate that the DNA was not accessible to the DNAse I, and thus was well protected from digestion owing to the mesoporous silica matrix.

12.4.4 Entrapment of DNA Enzymes in Sol-gel Materials

To further assess the potential of sol-gel based materials for entrapment of FNA species, three fluorescence-signaling DNA enzymes, denoted as OA-II, OA-III, and OA-IV,[104] were examined (the secondary structures of these DNAzymes are shown in Fig. 12.9), each of which contains the ***F-R-Q*** element described above and exhibits distinct profiles of divalent metal ion specificities. PAGE studies previously showed that OA-II was active in the presence of Mg(II) and Ni(II), OA-III strictly used Mn(II), while OA-IV required both Mn(II) and Cd(II) to produce cleavage of the ribo-linkage. The signaling abilities of the deoxyribozymes were examined both in solution and in a range of polar and organic–inorganic composite sol-gel materials to determine if materials that were not optimal for protein entrapment (i.e., those that were partially hydrophobic and evolved alcohol byproducts) might be suitable for the entrapment of metal sensing DNAzymes.[105] Figure 12.10 shows the relative fluorescence enhancement obtained for OA-III upon addition of divalent metals to the enzymes in solution and when entrapped in the various sol-gel materials.

In solution, the signal enhancement was about 14-fold, with full signal development within 10 min. Upon entrapment, the signal enhancements and rates of signal development were highly dependent on the type of sol-gel material used. As shown in Fig. 12.10, some of the materials resulted in essentially no signal enhancements upon addition of metals, while other materials resulted in significant signal enhancements; all materials showed slower responses than in solution. Overall, the data showed that composite materials formed from 40% methyltrimethoxysilane (MTMS) and 60% tetramethylorthosilicate (TMOS) provided the best performance for the entrapped DNAzyme, resulting in the highest signal enhancements, highest signaling rates and lowest degree of leaching (similar observations were made with OA-II and OA-IV). It is likely that such materials have a balance of hydrophobic

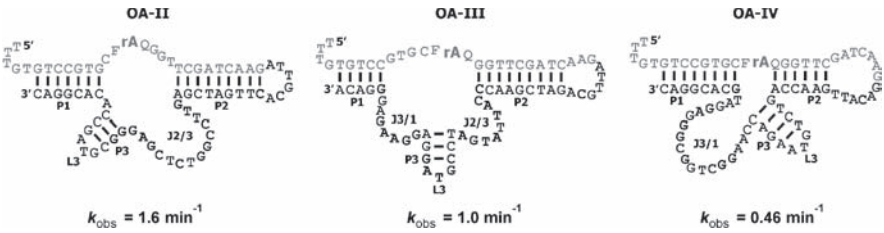

Fig. 12.9 Putative secondary structures of metal sensing deoxyribozymes: OA-II, OA-III, and OA-IV (Reproduced with permission from ref. 105. Copyright [2007] American Chemical Society)

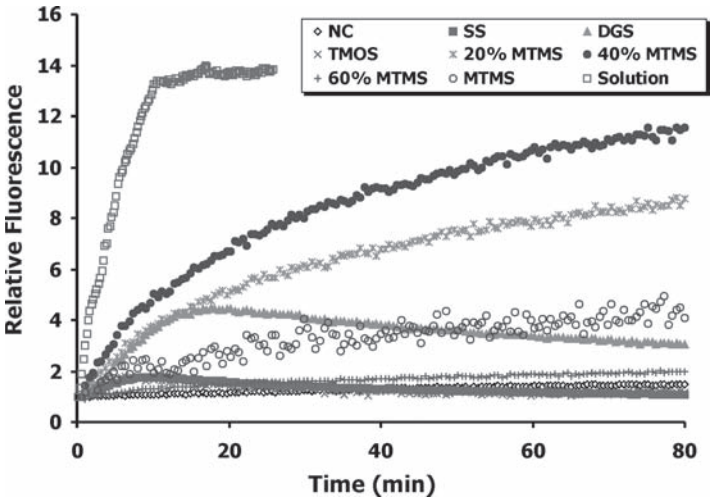

Fig. 12.10 Kinetic responses for OA-III in solution and in various sol-gel materials (Reproduced with permission from ref. 105. Copyright [2007] American Chemical Society)

and hydrophilic character that allows for retention of DNAzymes within the pores while also allowing facile entry of divalent metal ions with minimal metal–silica interactions.

To demonstrate multiplexed sensing, a DNAzyme array was prepared in a 384-well plate format that contained each of the three active DNAzymes as well as specific mutant sequences to act as a quenching control to avoid issues with metal-induced quenching of fluorescence from the signaling DNAzymes.[106] The active DNAzymes and mutant species were entrapped in both 40% MTMS/60% TMOS and sodium silicate gels, along with appropriate blanks, and imaged after addition of a series of metal ions (Fig. 12.11a).

The active DNAzyme samples exhibited the expected patterns of fluorescence enhancement based on the previous PAGE studies. OA-II was sensitive primarily to Ni(II), with a minor enhancement in the presence of Mn(II); OA-III was most sensitive to the presence of Mn(II), either when alone or combined with Cd(II); while OA-IV required both Mn(II) and Cd(II) for maximum signal enhancement, regardless of the type of sol-gel material used (Fig. 12.11a).

Figure 12.11b shows quantitative data derived from the array image obtained after addition of metal ions. These data were obtained by subtracting blanks and taking the ratio of intensity values for the DNAzyme relative to the mutant after metal addition. The data show that the enhancements range from 3.5-fold to four-fold for 40% MTMS samples and from two- to threefold for SS samples. In general, the MTMS samples showed higher enhancements than SS samples. However, in both cases the multiplexed data demonstrated the ability to detect multiple metals either alone or in mixtures, suggesting that there is potential for moving to a microarray format for multiplexed analysis using DNAzymes.

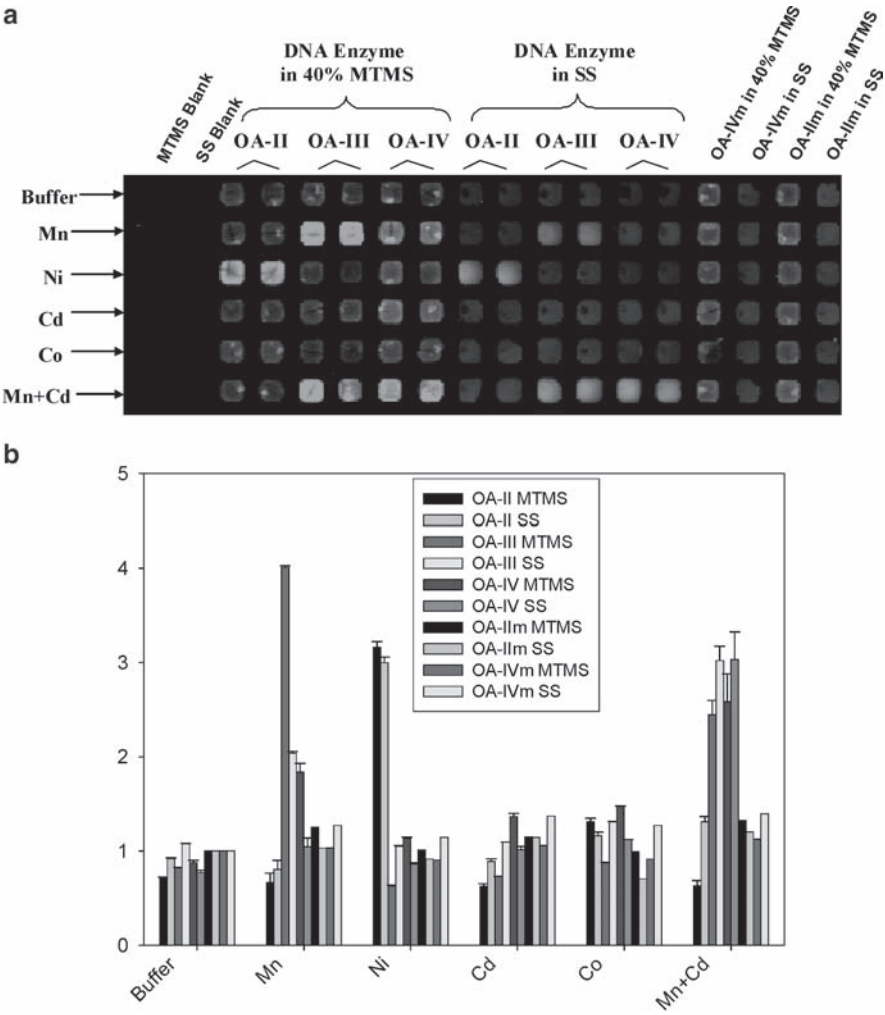

Fig. 12.11 (**a**) Fluorimages of a 384-microwell plate taken after the addition of divalent metal ions to entrapped DNAzymes. The final concentration of the DNAzyme in the gel was 250 nM. (**b**) Relative signal enhancements upon addition of various metals to DNAzymes and mutants, showing responses obtained from 40% MTMS and SS samples side by side for each DNAzyme in the presence of various metals (Reproduced with permission from ref. 105. Copyright [2007] American Chemical Society)

12.4.5 Layered Structures for Aptamer-Based HTS Assays

Particular advantages of sol-gel bioimmobilization include the ability to entrap both protein- and DNA-based species using a single immobilization method, and the ability to create three-dimensional structures using the polymeric silica system. A novel solid-phase assay was designed that utilized either a single sol-gel material

to co-entrap an enzyme and a fluorescence-signaling DNA aptamer, or separate layers of protein and aptamer, so that the DNA aptamer could be used to monitor the catalytic activity of an enzyme.[107] Adenosine deaminase (ADA), whose catalytic function is to convert adenosine to inosine, was used as the model enzyme, while the ATP-binding structure-switching signaling aptamer was used as the reporter.

The competition-based assay studied is illustrated in Fig. 12.12. In this system ADA converts adenosine to inosine and can be inhibited by erythro-9-(2-hydroxy-3-nonyl)adenine hydrochloride (EHNA). The ATP-dependent structure-switching signaling DNA aptamer has high affinity for adenosine and no affinity for inosine, and was used to monitor the action of ADA. When ADA is fully active, adenosine is depleted rapidly, and the aptamer signal should decrease with time. Upon inhibition of ADA by EHNA (I), the adenosine concentration should remain high and the aptamer reporter should be highly fluorescent.

The signaling ability of the entrapped ADA/EHNA/signaling aptamer system was studied within microwell plates using co-entrapment (mode A), the aptamer layered on top of the ADA (mode B), and ADA on top of the aptamer (mode C) to allow for segregation of different biomolecules into unique reaction zones. By using a layered reaction system, the biomolecule that is entrapped in the layer nearest to the solution interface receives the initial exposure to the substrate. Thus, the degree of binding or conversion of substrate in the upper layer determines the level of exposure of the subsequent layer to the substrate.

Figure 12.13 shows the signals obtained from each mode. Entrapment mode A exhibited a fluorescence response pattern (Fig. 12.13a) consisting of a rapid increase in fluorescence as aptamer binds adenosine, followed by a decrease as ADA converts

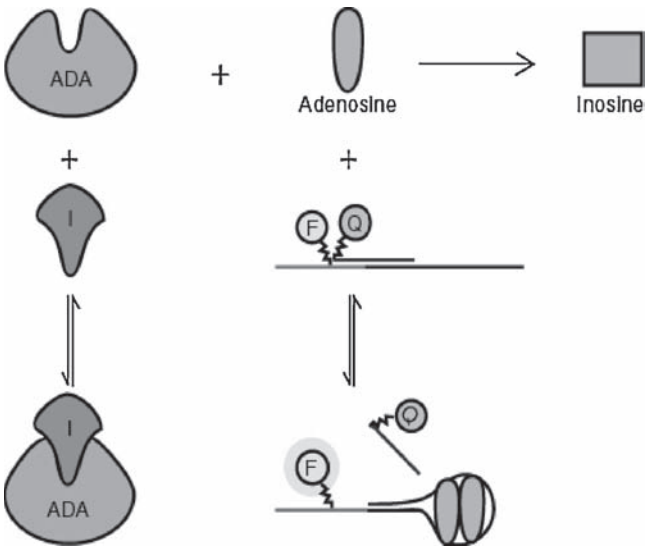

Fig. 12.12 The coupled assay involving ADA, an adenosine-binding DNA aptamer, and a small-molecule inhibitor (I). *F* and *Q* represent a fluorophore and a quencher, respectively (Reproduced with permission from ref. 107. Copyright [2006] Wiley)

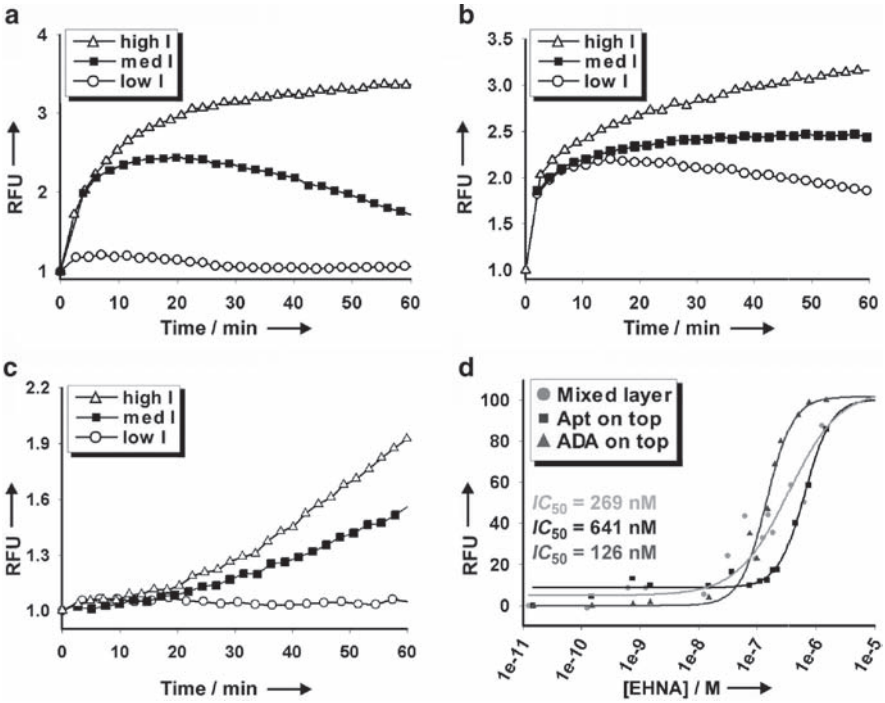

Fig. 12.13 (**a–c**) Signaling profiles of the ADA/EHNA/signaling aptamer systems entrapped in a single mixed layer, aptamer (*apt*) in the top layer and ADA at the bottom, and ADA on top and aptamer at the bottom, respectively. Samples contained EHNA (I) at 15 μM (Δ), 150 nM (■), and 15 pM (○) levels. (**d**) Normalized signal responses versus EHNA concentration in the single-layer system (*circles*), aptamer on top (*squares*), and ADA on top (*triangles*) (Reproduced with permission from ref. 107. Copyright [2006] Wiley)

adenosine to inosine. More active ADA resulted in a smaller increase and more rapid decrease owing to more rapid depletion of adenosine. The response was quite similar to that obtained from a solution assay,[108] except that the rate of the reaction was slowed substantially by the mass transfer limitations imposed by the silica matrix. For entrapment mode B, the signal increased relatively rapidly in the initial phase (<10 min) due to the binding of adenosine to the aptamer in the top layer (Fig. 12.13b). However, at a low level of EHNA (open circles), ADA remained highly active and led to a relatively rapid conversion of adenosine to inosine and a decrease in the fluorescence signal beyond 10 min. Conversely, at a high level of EHNA (open triangles), the activity of ADA was significantly inhibited, adenosine concentration remained high, and the signal continued to increase during the incubation period. Entrapment mode C led to no increase in the fluorescent signal over a period of at least 60 min when EHNA was used at a low level (Fig. 12.13c), consistent with adenosine being consumed before reaching the aptamer layer. Beyond 60 min there was a very slow increase in fluorescence, suggesting that ADA was

not able to fully consume all adenosine that was added. When ADA was strongly inhibited by EHNA (open triangles), the fluorescence response showed a relatively slow increase over the first 20 min, followed by a more rapid increase in intensity over a period of 40 min as adenosine penetrated into the aptamer layer. The slope of the response increased with increasing inhibitor concentration, reflecting the loss of ADA activity. It is noted that even after 2 h the system did not show the maximum expected signal, indicating that full equilibration of substrate into the bottom layer likely required a longer time. The data convincingly demonstrate that both ADA and the signaling aptamer remain active within silica and that the signaling aptamer can report the activity of ADA, regardless of which entrapment option is used.

The ability of each entrapment method to generate accurate inhibition constants was also assessed. For entrapment modes A and B, fitting the fluorescence responses to the concentration change of EHNA (see Fig. 12.13d, circles and squares) according to the Hill equation resulted in inaccurate IC_{50} values of 269 ± 15 and 641 ± 9 nM, respectively. Using a K_M value of 106 μM for ADA entrapped in silica,[109] K_I values of 26 and 61 nM were obtained, which are approximately fourfold to tenfold larger than the literature value of 6 nM.[110] The increase in the K_I value is most likely because the mixed system never attains equilibrium with respect to either the aptamer–adenosine or ADA–adenosine reactions, whereas the system with the aptamer in the top layer results in substrate depletion in the ADA layer. On the other hand, entrapment mode C (triangles in Fig. 12.13d) produced an IC_{50} of 126 ± 7 and a K_I of 12 nM, both of which were close to the reported values. The better accuracy of these values when ADA is in the top layer is most likely the result of the ability of the inhibitor to penetrate through the thinner upper layer (1.1 vs 2.3 mm for the mixed system) and thus establish equilibrium with the enzyme.

The use of layered entrapment systems for the separation of coupled assays can offer additional advantages. First, the spatial separation of biomolecules may allow biological species that are incompatible (such as a DNase and a DNA aptamer) to be coimmobilized, which would not be possible using a single monolith. Second, the thickness of each layer can either be increased to introduce a delay time (which provides time to perform multiple assay steps before reading), or decreased to accelerate the overall reaction. Finally, the concentration of biomolecule within each layer and the chemical composition of the individual silica layers can also be optimized to ensure that the molar ratio and activity of reagents is optimized. As aptamers can be generated by in vitro selection for virtually any target of interest[6] and structure-switching signaling aptamers can be either rationally designed for any known aptamer[67] or selected directly when there is no existing aptamer,[111] it is conceivable that many specific signaling aptamer–protein enzyme pairs can be developed in the future. Finally, while the foregoing example utilized aptamers that bind to the substrate of an enzyme, it is likely that even more straightforward assay formats could be developed with aptamers which bind products of enzymatic reactions,[112] since in this case there is no competition between the aptamer and enzyme for the product molecules. For example, a recently reported ADP-binding aptamer could be used to develop a universal solid-phase kinase assay to complement the previously described solution-based kinase assay.[113] Other aptamers that

could selectively bind NAD(P)H over $NAD(P)^+$ could also be used for a variety of redox enzyme assays, further extending the potential of this method for both sensing and high-throughput drug screening.

12.5 Emerging Applications

The examples outlined here demonstrate a wide range of potential applications for solid-phase assays using fluorescence-signaling FNAs, including biosensing, proteomics, and high-throughput screening using fiberoptic, waveguide, and microarray formats. In this section, a few emerging applications of DNA aptamers are considered, including recent advances in colorimetric detection using FNA species bearing gold nanoparticles for the development of "dipstick" tests, innovative signaling methods involving rolling-circle amplification, and emerging applications for FNA microarrays.

As already noted, an emerging area of interest in aptamer and DNAzyme-based detection is the development of rapid colorimetric assays, which in ideal cases removes the need for instrumentation to allow reading of a signal.[46] A recent article by Liu and coworkers[114] described the use of a lateral flow device containing ATP- or cocaine-binding aptamers bound to two types of DNA-modified gold nanoparticles, one (particle 1) containing a short sequence complementary to a primer extension of the aptamer, and the other (particle 2) containing a biotinylated DNA sequence that was complementary to the aptamer (Fig. 12.14a, b).

In the absence of target, the two types of particles form a large, multiparticle complex that is unable to migrate through the membrane of the lateral flow device. Upon addition of ATP or cocaine, the aptamer undergoes a structural switch to dissociate the DNA bound to particle 2 (similar to the structure switching signaling aptamers described above). The dissociated particle is small enough to move through the membrane of the flow device and is captured on a small strip of streptavidin placed at the top of the membrane (see Fig. 12.14c–e). The dipstick test allowed for rapid detection of target analytes present in both buffer and serum samples and showed good sensitivity for targets using detection with the naked eye.

Another recent report described the coupling of structure-switching signaling aptamers to cellulose as a first step in the development of bioactive paper materials for pathogen detection.[115] In this case, both physiosorption and covalent coupling methods were used to immobilize the ATP-dependent aptamer onto cellulose, and the fluorescence enhancement upon addition of ATP was determined. Aptamers that were adsorbed to the cellulose were easily washed off; however, covalently coupled aptamers bound to oxidized cellulose retained their structure-switching ability and were able to signal the presence of ATP.

Li and coworkers[116] also reported on a new method for amplifying the signals from aptamer-based sensors by using rolling-circle amplification (RCA). In this method, gold nanoparticles were used to immobilize DNA aptamers via thiol–gold interactions. A circular DNA template was added along with the special DNA

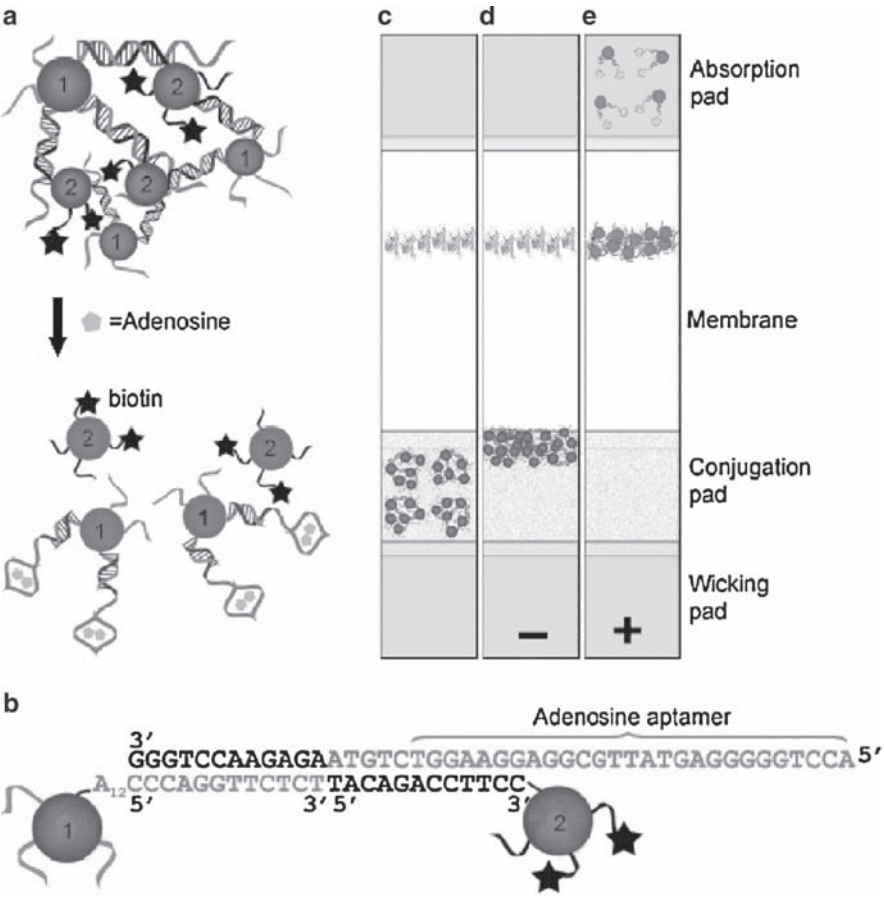

Fig. 12.14 A lateral flow device made of aptamer-gold nanoparticle assemblies. (**a**) Adenosine-induced disassembly of nanoparticle aggregates (*blue*) into dispersed nanoparticles (*red*). Biotin is shown as *black stars*. (**b**) The DNA aptamer arranged in the duplex form. (**c**) Device configuration. The aptamer–nanoparticle assembly is loaded on the conjugation pad; streptavidin is placed on the membrane (*cyan color*). (**d**), (**e**) Expected behavior of the aptamer–nanoparticle assembly in the absence and presence of adenosine, respectively (Reproduced with permission from ref. 114. Copyright [2006] Wiley)

polymerase ϕ29DNA polymerase, which resulted in the formation of a long DNA polymer with a specific repeating sequence unit. A fluorescently tagged DNA strand that was complementary to the repeat sequence was added and allowed for multiple labeling of each long DNA polymer, providing a large signal. Such a strategy has significant potential in many areas (i.e., developing periodic nano-assemblies), but in the case of sensors it is clear that this strategy could be coupled with a structure-switching aptamer so that the binding of an analyte determines the availability of a primer for RCA, which can then be used for polymer extension and labeling to amplify the signal.

Another area that is rapidly evolving is the further development of microarray technologies. As noted above, it is possible to form DNA with "sticky ends" to allow formation of DNA patterns on surfaces.[93] A very recent report has extended this idea to the formation of self-assembled DNA tile nano-arrays for multiplexed biosensing.[117] In this case, "A" tile-forming DNA strands bearing red or green fluorescent dyes are mixed in a specific ratio to produce a given color for encoding, and then mixed with a specific "B" detection tile-forming DNA that has a specific aptamer and a blue dye. The A and B tiles self-assemble to form a "blue-masked" region on a tiled array. Solutions containing various (A1 + A2):Bi combinations are then mixed so that each unique detection element resides within a specific color-coded tile. Addition of target releases the blue dye, revealing the specific coded color produced by the associated A tiles. In this way, multiplexed analysis can be performed. Such tile arrays can be self-assembled onto glass slides to produce solid-phase multiplexed fluorescence sensors.

A final example of an emerging application for microarrays is the use of "arrays of microarrays" to provide a means for ultrahigh-throughput screening. This approach relies on the formation of microarrays within the wells of microtiter plates.[118] Such an approach has been utilized with protein and small-molecule arrays to allow for multiplexed screening of protein–ligand interactions. In such a system, each well can carry up to 200 different species within an array, and each well can be interrogated with a different analyte to allow a "many versus many" screening platform to be developed. While this approach has not yet been applied to FNA species, it is clear that such an approach could be used in conjunction with the aptamer-based screening approaches outlined above to provide a highly multiplexed solid-phase assay for rapid compound screening.

12.6 Conclusions and Perspectives

In the past 15 years, a vast array of fluorescence sensors and assays have been developed with functional nucleic acids as the molecular recognition element. FNA species have several advantages over antibodies, including a wider versatility of targets (i.e., toxins, metals, whole cells, etc.), higher stability, ease of modification, and facile signal development, and, as shown here, ease of immobilization. Furthermore, it is possible to modify FNA species to make them less susceptible to degradation by nucleases, making them amenable to in vivo sensing. As a result, it is likely that such species will continue to expand in terms of their applications in the area of diagnostics and screening.

At this point, the majority of studies involving signaling FNA species have been done in solution and many investigations have utilized only "clean" samples. While such studies have been important in optimizing the signaling and binding properties of FNA species, there is a clear need to extend these studies to real samples to better evaluate performance in actual sensing settings. In the past decade there has been increasing emphasis on the development of solid-phase fluorescence assays

that utilize FNA, particularly for biosensor and microarray applications and more recently for high-throughput screening. However, once again most of the studies have been performed using well-behaved model systems, highlighting the need to expand such assays to more complex samples.

An emerging method for bioimmobilization is entrapment of biomolecules within sol-gel-derived materials. Although this approach has only been demonstrated in a few reports, there are significant opportunities for developing sensing devices, including multicomponent microarrays, via this method. The ability to entrap high amounts of FNA in a three-dimensional polymeric matrix has the potential to lead to increases in signal-to-noise ratios from small array elements, while the potential for layering of protein and FNA species could provide a method for novel microarray architectures for high-throughput screening. However, there is still much work to be done to better understand the properties of FNA within sol-gel materials so as to optimize entrapped aptamer performance. Advanced studies of aptamer dynamics, conformational mobility, and accessibility, along with studies on the long-term stability of entrapped FNA are needed to achieve this goal. Even so, the future of this method is bright.

References

1. Luderer, F. and Walschus, U. (2005) Immobilization of oligonucleotides for biochemical sensing by self-assembled monolayers: thiol-organic bonding on gold and silanization on silica surfaces. Top. Curr. Chem. 260:37–56.
2. Smith, C.L., Milea, J.S. and Nguyen, G.H. (2006) Immobilization of nucleic acids using biotin-strept(avidin) systems. Top. Curr. Chem. 261:63–90.
3. Fang, X., Liu, X., Schuster, S. and Tan, W. (1999) Designing a novel molecular beacon for surface-immobilized DNA hybridization studies. J. Am. Chem. Soc. 121:2921–2922.
4. Ellington, A.D. and Szostak, J.W. (1990) In vitro selection of RNA molecules that bind specific ligands. Nature (Lond.) 346:818–822.
5. Tuerk, C. and Gold, L. (1990) Systematic evolution of ligands by exponential enrichment: RNA ligands to bacteriophage T4 DNA polymerase. Science 249:505–510.
6. Wilson, D.S. and Szostak, J.W. (1999) In vitro selection of functional nucleic acids. Annu. Rev. Biochem. 68:611–647.
7. Famulok, M. (1999) Oligonucleotide aptamers that recognize small molecules. Curr. Opin. Struct. Biol. 9:324–329.
8. Green, L.S., Jellinek, D., Bell, C., Beebe, L.A., Fesitner, B.D., Gill, S.C., Jucker, F.M. and Janjic, N. (1995) Nuclease-resistant nucleic acid ligands to vascular permeability factor/vascular endothelial growth factor. Chem. Biol. 2:683–695.
9. Pagratis, N.C., Bell, C., Chang, Y.-F., Jennings, S., Fitzwater, T., Jellinek, D. and Dang, C. (1997) Potent 2′-amino-, and 2′-fluoro-2′-deoxyribonucleotide RNA inhibitors of keratinocyte growth factor. Nat. Biotechnol. 15:68–73.
10. Jenison, R.D., Gill, S.C., Pardi, A. and Polisky, B. (1994) High-resolution molecular discrimination by RNA. Science 263:1425–1429.
11. Geiger, A., Burgstaller, P., von der Eltz, H., Roeder, A. and Famulok, M. (1996) RNA aptamers that bind L-arginine with sub-micromolar dissociation constants and high enantioselectivity. Nucleic Acids Res. 24:1029–1036.
12. Achenbach, J.C., Chiuman, W., Cruz, R.P. and Li, Y. (2004) DNAzymes: from creation in vitro to application in vivo. Curr. Pharm. Biotechnol. 5:321–336.

13. Silverman, S.K. (2004) Deoxyribozymes: DNA catalysts for bioorganic chemistry. Org. Biomol. Chem. 2:2701–2706.
14. Joyce, G.F. (2004) Directed evolution of nucleic acid enzymes. Annu. Rev. Biochem. 73: 791–836.
15. Breaker, R.R. (2004) Natural and engineered nucleic acids as tools to explore biology. Nature (Lond.) 432:838–845.
16. Peracchi, A. (2005) DNA catalysis: potential, limitations, open questions. ChemBioChem 6: 1316–1322.
17. Breaker, R.R. and Joyce, G.F. (1994) A DNA enzyme that cleaves RNA. Chem. Biol. 1: 223–229.
18. Santoro, S.W. and Joyce, G.F. (1997) A general purpose RNA-cleaving DNA enzyme. Proc. Natl. Acad. Sci. USA 94:4262–4266.
19. Flynn-Charlebois, A., Wang, Y., Prior, T.K., Rashid, I., Hoadley, K.A., Coppins, R.L., Wolf, A.C. and Silverman, S.K. (2003) Deoxyribozymes with 2′-5′ RNA ligase activity. J. Am. Chem. Soc. 125:2444–2454.
20. Wang, Y. and Silverman, S.K. (2003) Deoxyribozymes that synthesize branched and lariat RNA. J. Am. Chem. Soc. 125:6880–6881.
21. Carmi, N., Balkhi, S.R. and Breaker, R.R. (1998) Cleaving DNA with DNA. Proc. Natl. Acad. Sci. USA 95:2233–2237.
22. Cuenoud, B. and Szostak, J.W. (1995) A DNA metalloenzyme with DNA ligase activity. Nature (Lond.) 375:611–614.
23. Sreedhara, A., Li, Y. and Breaker, R.R. (2004) Ligating DNA with DNA. J. Am. Chem. Soc. 126: 3454–3460.
24. Li, Y. and Breaker, R.R. (1999) Phosphorylating DNA with DNA. Proc. Natl. Acad. Sci. USA 96:2746–2751.
25. Achenbach, J.C., Jeffries, G.A., McManus, S.A., Billen, L.P. and Li, Y. (2005) Secondary-structure characterization of two proficient kinase deoxyribozymes. Biochemistry 44:3765–3774.
26. Nutiu, R., Mei, S.H.J., Liu, Z. and Li, Y. (2004) Engineering DNA aptamers and DNA enzymes with fluorescence-signaling properties. Pure Appl. Chem. 76:1547–1561.
27. Liu, Z., Mei, S.H.J., Brennan J.D. and Li, Y. (2003) An assemblage of signaling DNA enzymes with intriguing metal-ion specificities and pH dependences. J. Am. Chem. Soc. 125: 7539–7545.
28. Camarero, J.A. (2006) New developments for the site-specific attachment of protein to surfaces. Biophys. Rev. Lett. 1:1–28.
29. Weetall, H.H. (1993) Preparation of immobilized proteins covalently coupled through silane coupling agents to inorganic supports. Appl. Biochem. Biotechnol. 41:157–188.
30. Vandenberg, E.T., Brown, R.S. and Krull, U.J. (1994) Immobilization of proteins for biosensor development. In: Veliky, I.A. and Mclean, R.J.C. (eds.) Immobilized biosystems in theory and practical applications. Blackie, Glasgow, pp. 129–231.
31. Di Giusto, D.A. and King, G.C. (2006) Special-purpose modifications and immobilized functional nucleic acids for biomolecular interactions. Top. Curr. Chem. 261:131–168.
32. Gill, I. (2001) Bio-doped nanocomposite polymers: sol-gel bioencapsulates. Chem. Mater. 13:3404–3421.
33. Jin, W. and Brennan, J.D. (2002) Properties and applications of proteins encapsulated within sol-gel derived materials. Anal. Chim. Acta 461:1–36.
34. Pierre, A.C. (2004) The sol-gel encapsulation of enzymes. Biocat. Biotrans. 22:145–170.
35. Avnir, D., Coradin, T., Lev. O. and Livage, J. (2006) Recent bio-applications of sol-gel materials. J. Mater. Chem. 16:1013–1030.
36. Besanger, T.R. and Brennan, J.D. (2006) Entrapment of membrane proteins in sol-gel derived silica. J. Sol-gel Sci. Technol. 40:209–225.
37. Pierre, A., Bonnet, J., Vekris, A. and Portier, J. (2001) Encapsulation of deoxyribonucleic acid molecules in silica and hybrid organic-silica gels. J. Mater. Sci. Mater. Med. 12:51–55.
38. Numata, M., Sugiyasu, K., Hasegawa, T. and Shinkai, S. (2004) Sol-gel reaction using DNA as a template: an attempt toward transcription of DNA into inorganic materials. Angew. Chem. Int. Ed. Engl. 43:3279–3283.

39. Gill, I. and Ballesteros, A. (2000) Bioencapsulation within synthetic polymers (part 1): sol-gel encapsulated biologicals. Trends Biotechnol. 18:282–296.
40. Li, J., Tan, W., Wang, K., Yang, X., Tang, Z. and He, X. (2001) Optical DNA biosensor based on molecular beacon immobilized on sol-gel membrane. Proc. SPIE 4414 (International Conference on Sensor Technology: ISTC 2001) 2001:27–30.
41. Navani, N.K. and Li, Y. (2006) Nucleic acid aptamers and enzymes as sensors. Curr. Opin. Chem. Biol. 10:272–281.
42. Deng, Q., German, I., Buchanan, D. and Kennedy, R.T. (2001) Retention and separation of adenosine and analogues by affinity chromatography with an aptamer stationary phase. Anal. Chem. 73:5415–5421.
43. Rehder, M.A. and McGown, L.B. (2001) Open-tubular capillary electrochromatography of bovine b-lactoglobulin variants A and B using an aptamer stationary phase. Electrophoresis 22:3759–3764.
44. Dick, L.W. and McGown, L.B. (2004) Aptamer-enhanced laser desorption/ionization for affinity mass spectrometry. Anal. Chem. 76:3037–3041.
45. Elghanian, R., Storhoff, J.J., Mucic, R.C., Letsinger, R.L. and Mirkin, C.A. (1997) Selective colorimetric detection of polynucleotides based on the distance-dependent optical properties of gold nanoparticles. Science 277:1078–1080.
46. Liu, J. and Lu, Y. (2003) A colorimetric lead biosensor using DNAzyme-directed assembly of gold nanoparticles. J. Am. Chem. Soc. 125:6642–6643.
47. Di Giusto, D.A., Wlassoff, W.A., Giesebrecht, S., Gooding, J.J. and King, G.C. (2004) Multipotential electrochemical detection of primer extension reactions on DNA self-assembled monolayers. J. Am. Chem. Soc. 126:4120–4121.
48. Rodriguez, M.C., Kawde, A.N. and Wang, J. (2005) Aptamer biosensor for label-free impedance spectroscopy detection of proteins based on recognition-induced switching of the surface charge. Chem. Commun. 34:4267–4269.
49. Li, Y., Lee, H.J. and Corn, R.M. (2006) Fabrication and characterization of RNA aptamer microarrays for the study of protein–aptamer interactions with SPR imaging. Nucleic Acids Res. 34:6416–6424.
50. Liss, M., Petersen, B., Wolf, H. and Prohaska, E. (2002) An aptamer-based quartz crystal protein biosensor. Anal. Chem. 74:4488–4495.
51. Savran, C.A., Knudsen, S.M., Ellington, A.D. and Manalis, S.R. (2004) Micromechanical detection of proteins using aptamer-based receptor molecules. Anal. Chem. 76:3194–3198.
52. Lu, Y. and Liu, J. (2006) Functional DNA nanotechnology: emerging applications of DNAzymes and aptamers. Curr. Opin. Biotechnol. 17:580–588.
53. Rosi, N.L. and Mirkin, C.A. (2005) Nanostructures in biodiagnostics. Chem. Rev. 105: 1547–1562.
54. Nutiu, R., Billen, L.P. and Li, Y. (2006). Fluorescence-signaling nucleic acid-based sensors. In: Silverman, S.K. (ed.) Nucleic acid switches and sensors. Landes Bioscience/Springer, New York, pp. 49–74.
55. Cho, E.J., Collett, J.R., Szafranska, A.E. and Ellington, A.D. (2006) Optimization of aptamer microarray technology for multiple protein targets. Anal. Chim. Acta 564:82–90.
56. Bock, C., Coleman, M., Collins, B., Davis, J., Foulds, G., Gold, L., Greef, C., Heil, J., Heilig, J.S., Hicke, B., Nelson Hurst, M., Husar, G., Miller, D., Ostroff, R., Petach, H., Schneider, D., Vant-Hull, B., Waugh, S., Weiss, A. and Wilcox, S.K. (2004) Photoaptamer arrays applied to multiplexed proteomic analysis. Proteomics 4:609–618.
57. Potyrailo, R.A., Conrad, R.C., Ellington, A.D. and Hieftje, G.M. (1998) Adapting selected nucleic acid ligands (aptamers) to biosensors. Anal. Chem. 70:3419–3425.
58. Jhaveri, S., Kirby, R., Conrad, R., Maglott, E., Bowser, M., Kennedy, R.T., Glick, G. and Ellington, A.D. (2000) Designed signaling aptamers that transducer molecular recognition to changes in fluorescence intensity. J. Am. Chem. Soc. 122:2469–2473.
59. Levy, M., Cater, S.F. and Ellington, A.D. (2005) Quantum-dot aptamer beacons for the detection of proteins. ChemBioChem 6:2163–2166.
60. Liu, J. and Lu, Y. (2007) Quantum dot encoding of aptamer-linked nanostructures for one-pot simultaneous detection of multiple analytes. Anal. Chem. 79:4120–4125.

61. Du, H., Disney, M.D., Miller, B.L. and Krauss, T.D. (2003) Hybridization-based unquenching of DNA hairpins on Au surfaces: prototypical "molecular beacon" biosensors. J. Am. Chem. Soc. 125:4012–4013.
62. Tyagi, S. and Kramer, F.R. (1996) Molecular beacons: probes that fluoresce upon hybridization. Nat. Biotechnol. 14:303–308.
63. Tan, W., Fang, X., Li, J. and Liu, X. (2000) Molecular beacons: a novel DNA probe for nucleic acid and protein studies. Chem. Eur. J. 6:1107–1111.
64. Nutiu, R. and Li, Y. (2002) Tripartite molecular beacons. Nucleic Acids Res. 30:e94.
65. Hamaguchi, N., Ellington, A. and Stanton, M. (2001) Aptamer beacons for the direct detection of proteins. Anal. Biochem. 294:126–131.
66. Li, J.J., Fang, X. and Tan, W. (2002) Molecular aptamer beacons for real-time protein recognition. Biochem. Biophys. Res. Commun. 292:31–40.
67. Nutiu, R. and Li, Y. (2003) Structure-switching signaling aptamers. J. Am. Chem. Soc. 125: 4771–4778.
68. Li, J. and Lu, Y. (2000) A highly sensitive and selective catalytic DNA biosensor for lead ions. J. Am. Chem. Soc. 122:10466–10467.
69. Liu, J., Brown, A.K., Meng, X., Cropek, D.M., Istok, J.D., Watson, D.B. and Lu, Y. (2007) A catalytic beacon sensor for uranium with parts-per trillion sensitivity and millionfold selectivity. Proc. Natl. Acad. Sci. USA 104:2056–2061.
70. Stojanovic, M.N., de Prada, P. and Landry, D.W. (2001) Catalytic molecular beacons. ChemBioChem 2:411–415.
71. Hartig, J.S., Najafi-Shoushtari, S.H., Gruene, I., Yan, A., Ellington, A.D. and Famulok, M. (2002) Protein-dependent ribozymes report molecular interactions in real time. Nat. Biotechnol. 20: 717–722.
72. Achenbach, J.C., Nutiu, R. and Li, Y. (2005) Structure-switching allosteric deoxyribozymes. Anal. Chim. Acta 534:41–51.
73. Mei, S.H., Liu, Z., Brennan, J.D. and Li, Y. (2003) An efficient RNA-cleaving DNA enzyme the synchronized catalysis with fluorescence signaling. J. Am. Chem. Soc. 125:412–420.
74. Chiuman, W. and Li, Y. (2007) Efficient signaling platforms built from a small catalytic DNA and doubly labeled fluorogenic substrates. Nucleic Acids Res. 35:401–405.
75. Liu, X. and Tan, W. (1999) A fiber-optic evanescent wave DNA biosensor based on novel molecular beacons. Anal. Chem. 71:5054–5059.
76. Yu, S., Cai, X., Tan, X., Zhu, Y. and Lu, B. (2001) Fiber optic biosensor using aptamer as receptors. Proc. SPIE 4414 (International Conference on Sensor Technology: ISTC 2001) 2001:35–37.
77. Lee, M. and Walt, D.R. (2000) A fiber-optic microarray biosensor using aptamers as receptors. Anal. Biochem. 282:142–146.
78. Heise, C. and Bier, F.F. (2006) Immobilization of DNA on microarrays. Top. Curr. Chem. 261: 1–25.
79. Wang, H., Li, J., Liu, Q., Liu, H. and Lu, Z. (2001) Label-free DNA hybridization detection with molecular beacon immobilized in photopolymerized acrylamide gel microarray. Proc. SPIE 4601 (Micromachining and Microfabrication Process Technology and Devices), 256–259.
80. Yao, G. and Tan, W. (2004) Molecular-beacon-based array for sensitive DNA analysis. Anal. Biochem. 331:216–223.
81. Ramachandran, A., Flinchbaugh, J., Ayoubi, P., Olah, G.A. and Malayer, J.R. (2004) Target discrimination by surface-immobilized molecular beacons designed to detect *Francisella tularensis*. Biosens. Bioelectron. 19:727–736.
82. Kim, H., Kane, M.D., Kim, S., Dominguez, W., Applegate, B.M. and Savikhin, S. (2007) A molecular beacon DNA microarray system for rapid detection of *E. coli* O157:H7 that eliminates the risk of a false negative signal. Biosens. Bioelectron. 22:1041–1047.
83. Maxwell, D.J., Taylor, J.R. and Nie, S. (2002) Self-assembled nanoparticle probes for recognition and detection of biomolecules. J. Am. Chem. Soc. 124:9606–9612.
84. Du, H., Strohsahl, C.M., Camera, J., Miller, B.L. and Krauss, T.D. (2005) Sensitivity and specificity of metal surface-immobilized "molecular beacon" biosensors. J. Am. Chem. Soc. 127: 7932–7940.

85. Swearingen, C.B., Wernette, D.P., Cropek, D.M., Lu, Y., Sweedler, J.V. and Bohn, P.W. (2005) Immobilization of a catalytic DNA molecular beacon on Au for Pb(II) detection. Anal. Chem. 77:442–448.
86. Stadtherr, K., Wolf, H. and Lindner, P. (2005) An aptamer-based protein biochip. Anal. Chem. 77:4548–4554.
87. Kirby, R., Cho, E.J., Gehrke, B., Bayer, T., Park, Y.S., Neikirk, D.P., McDevitt, J.T. and Ellington, A.D. (2004) Aptamer-based sensor arrays for the detection and quantitation of proteins. Anal. Chem. 76:4066–4078.
88. Collett, J.R., Cho, E.J., Lee, J.F., Levy, M., Hood, A.J., Wan, C. and Ellington, A.D. (2004) Functional RNA microarrays for high-throughput screening of antiprotein aptamers. Anal. Biochem. 338:113–123.
89. Collett, J.R., Cho, E.J. and Ellington, A.D. (2005) Production and processing of aptamer microarrays. Methods 37:4–15.
90. Brody, E.N., Willis, M.C., Smith, J.D., Jayasena, S., Zichi, D. and Gold, L. (1999) The use of aptamers in large arrays for molecular diagnostics. Mol. Diagn. 4:381–388.
91. McCauley, T.G., Hamaguchi, N. and Stanton, M. (2003) Aptamer-based biosensor arrays for detection and quantification of biological macromolecules. Anal. Biochem. 319:244–250.
92. Yamamoto-Fujita, R. and Kumar, P.K.R. (2005) Aptamer-derived nucleic acid oligos: application to develop nucleic acid chips to analyze proteins and small ligands. Anal. Chem. 77:5460–5466.
93. Lin, C., Katilius, E., Liu, Y., Zhang, J. and Yan, H. (2006) Self-assembled signalling aptamer DNA arrays for protein detection. Angew. Chem. Int. Ed. 45:5295–5301.
94. Abérem, M.B., Najari, A., Ho, H.-A., Gravel, J.-F., Nobert, P., Boudreau, D. and Leclerc, M. (2006) Protein detecting arrays based on cationic polythiophene–DNA–aptamer complexes. Adv. Mater. 18:2703–2707.
95. Hesselbert, J.R., Robertson, M.P., Knudsen, S.M. and Ellington, A.D. (2003) Simultaneous detection of diverse analytes with an aptazyme ligase array. Anal. Biochem. 312:106–112.
96. Seetharaman, S., Zivarts, M., Sudarsan, N. and Breaker, R.R. (2001) Immobilized RNA switches for the analysis of complex chemical and biological mixtures. Nat. Biotechnol. 19:336–341.
97. Braun, S., Rappoport, S., Zusman, R., Avnir, D. and Ottolenghi, M. (1990) Biochemically active sol-gel-glasses: the trapping of enzymes. Mater. Lett. 10:1–5.
98. Ellerby, L.M., Nishida, C.R., Nishida, F., Yamanaka, S., Dunn, B., Valentine, J.S. and Zink, J.I. (1992) Encapsulation of proteins in transparent porous silicate glasses prepared by the sol-gel method. Science 255:1113–1115.
99. Brook, M.A., Chen, Y., Guo, K., Zhang, Z. and Brennan, J.D. (2004) Sugar-modified silanes: precursors for silica monoliths. J. Mater. Chem. 14:1469–1479.
100. Brinker, C.J. and Scherer, G.W. (1990) Sol-gel science: the physics and chemistry of sol-gel processing. Academic Press, San Diego, CA.
101. Wang, H., Li, J., Liu, Q., Liu, H. and Lu, Z. (2001) Label-free DNA hybridization detection with molecular beacon immobilized in photopolymerized acrylamide gel microarray. Proc. SPIE 4601 (Micromachining and Microfabrication Process Technology and Devices), 256–259.
102. Rupcich, N., Nutiu, R., Li, Y. and Brennan, J.D. (2005) Entrapment of fluorescent signaling DNA aptamers in sol-gel derived silica. Anal. Chem. 77:4300–4307.
103. Sui, X., Cruz-Aguado, J.A., Chen, Y., Zhang, Z., Brook, M.A. and Brennan, J.D. (2005) Properties of human serum albumin entrapped in sol-gel-derived silica bearing covalently tethered sugars. Chem. Mater. 17:1174–1182.
104. Chiuman, W. and Li, Y. (2006) Revitalization of six abandoned catalytic DNA species reveals a common three-way junction framework and diverse catalytic cores. J. Mol. Biol. 357:748–754.
105. Shen, Y., Mackey, G., Rupcich, N., Gloster, N.D., Chiuman, W., Li, Y. and Brennan, J.D. (2007) Entrapment of fluorescence-signaling DNA enzymes in sol-gel derived materials for metal ion sensing. Anal. Chem. 79:3494–3503.

106. Rupcich, N., Chiuman, W., Nutiu, R., Mei, S., Flora, K.K., Li, Y. and Brennan, J.D. (2006) Quenching of fluorophore-labeled DNA oligonucleotides by divalent metal ions: implications for selection, design and applications of signaling aptamers and signaling deoxyribozymes. J. Am. Chem. Soc. 128:780–790.
107. Rupcich, N., Nutiu, R., Li, Y. and Brennan, J.D. (2006) Solid-phase enzyme activity assay utilizing an entrapped fluorescence-signaling DNA aptamer. Angew. Chem. Int. Ed. Engl. 45:3295–3299.
108. Elowe, N.H., Nutiu, R., Allali-Hassani, A., Cechetto, J.D., Hughes, D.W., Li, Y. and Brown, E.D. (2006) Screening made simple for a difficult target with a signaling aptamer for deaminase activity. Angew. Chem. Int. Ed. Engl. 45:5648–5652.
109. Hodgson, R., Besanger, T.R., Brook M.A. and Brennan, J.D. (2005) Inhibitor screening using immobilized enzyme-reactor chromatography/mass spectrometry. Anal. Chem. 77: 7512–7519.
110. Agarwal, R.P. (1982) Inhibitors of adenosine deaminase. Pharmacol. Ther. 17:399–429.
111. Nutiu, R. and Li, Y. (2005). In vitro selection of structure-switching signaling aptamers. Angew. Chem. Int. Ed. Engl. 44:1061–1065.
112. Nutiu, R., Yu, J.M.Y. and Li, Y. (2004a) Signaling aptamers for monitoring enzymatic activity and for inhibitor screening. ChemBioChem 5:1139–1144.
113. Srinivasan, J., Cload, S.T., Hamaguchi, N., Kurz, J., Keene, S., Kurz, M., Boomer, R., Blanchard, J., Epstein, D., Wilson, C. and Diener, J.L. (2004) ADP-specific sensors enable universal assay of protein kinase activity. Chem. Biol. 11:499–508.
114. Liu, J., Mazumdar, D. and Lu, Y. (2006) A simple and sensitive dipstick test in serum based on lateral flow separation of aptamer-linked nanostructures. Angew. Chem. Int. Ed. 45: 7955–7959.
115. Su, S., Nutiu, R., Filipe, C.D.M., Li, Y. and Pelton, R. (2007) Adsorption and covalent coupling of ATP-binding DNA aptamers onto cellulose. Langmuir 23:1300–1302.
116. Zhao, W., Gao, Y., Kandadai, S.A., Brook, M.A. and Li, Y. (2006) DNA polymerization on gold nanoparticles through rolling circle amplification: towards novel scaffolds for three-dimensional periodic nanoassemblies. Angew. Chem. Int. Ed. 45:2409–2413.
117. Lin, C., Liu, Y. and Yan, H. (2007) Self-assembled combinatorial encoding nanoarrays for multiplexed biosensing. Nano Lett. 7:507–512.
118. Jones, R.B., Gordus, A., Krall, J.A. and MacBeath, G. (2006) A quantitative protein interaction network for the ErbB receptors using protein microarrays. Nature (Lond.) 439: 168–174.

Chapter 13
Functional Nucleic Acid Sensors as Screening Tools

Andrea Rentmeister and Michael Famulok

Abstract Functional nucleic acids such as aptamers and allosteric ribozymes can sense their ligands specifically, thereby undergoing structural alterations that can be converted into a detectable signal. The direct coupling of molecular recognition to signal generation in real time allows the generation of versatile reporters that can be applied in high-throughput screening (HTS). In the following chapter we describe different types of nucleic acids that have been applied successfully in screening approaches. We first refer to DNA and RNA aptamers, then consider allosteric ribozymes, and finally present examples of natural nucleic acids that were applied in screening assays.

13.1 Introduction

High-throughput screening (HTS) of compound libraries to identify small molecules that interact with target proteins or alter their catalytic activity is a major focus of pharmaceutical efforts. Therefore, universal assays that are amenable to a HTS format are highly desirable. Functional nucleic acid sensors have proven to be a valuable means to obtain and store information about a target and translate it into an easy read-out signal, such as fluorescence. Various artificial (e.g., aptamers, allosteric ribozymes) and natural functional nucleic acids (e.g., riboswitches) have been successfully adapted in a way that makes them useful for screening approaches. These adaptations mostly involve the introduction of one or two fluorescent dyes to generate a fluorescent signal in either the presence or the absence of the respective ligand and can be performed very easily with nucleic acids. The most common method applied in HTS uses Förster resonance energy transfer (FRET) from a fluorescent donor (F) to an acceptor molecule or quencher (Q) in

A. Rentmeister and M. Famulok
University of Bonn, Germany, LIMES Program Unit Chemical Biology & Medicinal Chemistry
andrea.rentmeister@uni-bonn.de
m.famulok@uni-bonn.de

Y. Li and Y. Lu (eds.), *Functional Nucleic Acids for Analytical Applications*,

close proximity to monitor ligand-induced structural changes within the nucleic acid sensors. If donor and acceptor are distant from each other, donor emission can be detected upon excitation of the donor. If donor and acceptor come in close proximity (1–10 nm), the acceptor emission is predominantly observed because of the FRET from the donor to the acceptor.

Fluorescence polarization (FP) is a less common but highly useful method to monitor the formation of complexes in a high-throughput format. Herein, dynamic binding events can be quantified by measuring the amount of depolarization after excitation of fluorescent molecules with polarized light. The extent of depolarization relates to the molecular weight of the excited molecule: if its molecular weight is high, it rotates and tumbles more slowly in space, and FP is preserved. If it is small, rotation and tumbling occur faster, and FP is reduced.[1]

Another feature of nucleic acids is their predictable base-pairing with complementary antisense oligodeoxynucleotides, which can be exploited to design deactivated allosteric aptazymes or signaling aptamers.

Artificial nucleic acid sensors comprise aptamers and allosteric ribozymes. Aptamers are single-stranded nucleic acids that bind their target molecules with high affinity and specificity and can be obtained by evolutionary selection methods. These functional nucleic acids are routinely selected from large combinatorial nucleic acid libraries (~10^{15}) against a variety of targets ranging from small molecules to proteins using a process called SELEX (systematic enrichment of ligands by exponential enrichment).[2–4] Moreover, they can be readily adapted in vitro to meet certain criteria, such as increasing stability, affinity, and specificity, or traceability. In addition, aptamers can be chemically synthesized in fairly large quantities. These properties make aptamers suitable for a variety of applications that require the reliable, specific, and sensitive detection of target compounds.

The combination of aptamers and ribozymes allows creating effector-mediated ribozymes, also known as aptazymes, reporter ribozymes, allosteric ribozymes, or ribo-reporters. Allosteric ribozymes are chimeric molecules that consist of an aptamer domain and a ribozyme module. Just like allosteric enzymes, their catalytic activity is regulated by binding of a ligand with their aptamer domain, distant from the active site.[5–8]

Recently, allosteric ribozymes and riboswitches have also been discovered in nature.[9,10] Just like their artificial counterparts, these RNAs specifically bind a ligand with their aptamer domain distant from the active site which leads to genetic regulation by altered base-pairing or self-cleavage.

Their mode of target recognition and binding makes both artificial and natural aptamers valuable for screening purposes: First, aptamers use their secondary and tertiary structures to recognize the three-dimensional shape of their target. Second, they undergo conformational changes upon ligand binding (which is also referred to as induced fit or adaptive binding).[11,12] Thus, aptamers allow ligand-dependent signal generation and provide a way to preserve structural information about their target.

13.2 Aptamers as Screening Tools

13.2.1 DNA Aptamers

Aptamers are known to bind their targets with high affinity and specificity. A DNA-aptamer against adenosine (A) can discriminate between closely related homologues such as adenosine mono-, di-, and triphosphate (AMP, ADP, and ATP) or the deaminated inosine. Nutiu et al. embedded the adenosine aptamer in a FRET-labeled nucleic acid construct.[13] They used an antisense sequence complementary to a part of the adenosine aptamer to bring the quencher in close proximity to the fluorescent dye (Fig. 13.1a). When the target is absent, the aptamer binds to the short quencher-labeled antisense strand, bringing the fluorophore and the quencher into close proximity for maximum fluorescence quenching. Upon introduction

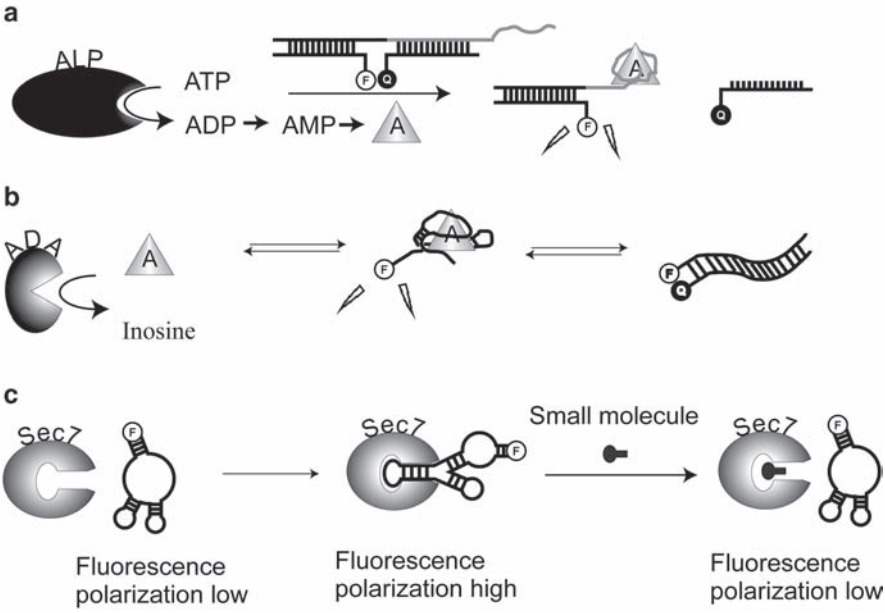

Fig. 13.1 Aptamers for inhibitor screening. (**a**) The activity of alkaline phosphatase (ALP) is reported by a DNA aptamer that binds to adenosine (*triangle*) produced in the reaction.[14] Binding of the aptamer to adenosine releases the quencher-labeled (*Q*) oligonucleotide, and fluorescence can be detected. (**b**) The activity of adenosine deaminase (ADA) is reported by a DNA aptamer that binds to adenosine (*triangle*) and has little affinity to inosine. As adenosine is transformed to inosine by ADA, the aptamer becomes available to complex with the quenching group (*Q*), resulting in decreasing fluorescence.[15] (**c**) Aptamer displacement screening assay by fluorescence polarization. The fluorescence-labeled aptamer exhibits low polarization in the unbound state (*left*). When bound to the *Sec7* domain of cytohesin 1, fluorescence polarization becomes high (*middle*). If a small molecule displaces the aptamer from the protein, fluorescence polarization becomes low (*right*)[16]

of the target however, the aptamer binds to adenosine and the quencher-labeled antisense oligodeoxynucleotide is released (Fig. 13.1a). FRET no longer can occur, and a fluorescence signal is detected.[13]

As adenosine is an important metabolite, this assay can be applied to monitor the activity of several enzymes. Li and coworkers demonstrated the use of their signaling aptamers for inhibitor screening of alkaline phosphatase (ALP)[14] and adenosine deaminase (ADA).[15]

ALP removes the 5′-phosphate groups from ATP, ADP, and AMP to convert each of these species to adenosine (Fig. 13.1a). The generation of adenosine from its phosphorylated precursors can be monitored because the signaling aptamer has a higher affinity for adenosine than for AMP, ADP, or ATP, respectively. As the signaling aptamer has a higher level of fluorescence in the presence of the product (adenosine) the transformation can be monitored conveniently by following the increase in the fluorescence intensity of the signaling aptamer (Fig. 13.1a). The fluorescent aptamer reporter allows both monitoring the activity of the enzyme in real time and screening for small-molecule inhibitors. Using a test screen in a 96-well plate, Nutiu et al. demonstrated that their structure-switching signaling aptamers are indeed suitable for high-throughput screening.[14]

As convenient fluorescence-based methods for the detection of ALP activity already exist, the signaling DNA aptamer technology was extended to screen small molecules for an otherwise problematic target,[15] adenosine deaminase (ADA). ADA is a key enzyme in purine metabolism, catalyzing the irreversible deamination of adenosine/deoxyadenosine to inosine/deoxyinosine. Despite the importance of the target, there is currently no simple, homogeneous, and sensitive assay available for ADA that is amenable to HTS. Elowe et al. used the DNA-signaling aptamer with high affinity for adenosine and almost no affinity for inosine to develop a screening assay for ADA (see Fig. 13.1b). The fluorescence signal is generated from a fluorescein group (F) at the 5′-end of the DNA aptamer and determined by the ratio of two different structural states, the adenosine-bound and -free forms of the aptamer. Only the adenosine-free form is capable of binding to the antisense DNA containing a quenching group (Q). As adenosine (A) is converted to inosine, the DNA duplex form of the aptamer predominates, leading to a decrease in fluorescence. Real-time monitoring of the adenosine-dependent fluorescent signal provides a convenient and homogeneous assay of ADA activity. Using this assay, Elowe et al. screened a collection of 44,400 commercial compounds with a Z′-factor of 0.51.[15] The Z′-factor is a statistical measure of the quality of the screening data in which a value of 0.5 or greater indicates a sensible signal window and limited variation associated with the high and low control data. Within 44,400 compounds, they found 47 hits in a primary screen. Retesting confirmed the activity of 12 of these compounds, which were further tested in the presence of nonspecific inhibitors such as reducing agents, detergent, or bovine serum albumin. Seven compounds remained that showed specific effects. These remaining compounds were analyzed by an HPLC assay. One of these compounds, MAC-0038732, was indeed an inhibitor of ADA. The other six compounds were falsely positive as a result of interference with a fluorescent signal.[15]

In conclusion, Elowe et al. used a fluorescence-signaling aptamer system in a simple, automated, and homogeneous assay of an otherwise problematic target, adenosine deaminase (ADA). The ability to routinely select aptamers as assay reagents coupled with the performance of fluorescence-signaling aptamers suggests that nucleic acid aptamers have exciting potential for this purpose.

13.2.2 RNA Aptamers

In principle, it should be possible to build up signaling aptamer systems from every aptamer. However, it would be desirable to apply aptamers for HTS without the need to build up new constructs. In the case of large ligands (e.g., proteins), aptamers can be applied directly for screening. Fluorescence polarization (FP) can be used to quantify dynamic binding events by measuring the amount of depolarization after excitation of fluorescent molecules with polarized light. Depolarization occurs due to rotation of a fluorescently labeled complex that is excited with linear polarized light within its fluorescence lifetime.[1] The bigger a complex, the more slowly it tumbles, leading to less depolarization and hence a higher value for fluorescence polarization. Thus, the fluorescently labeled aptamer alone will show less polarization than the aptamer–protein complex. If compounds from the screening library displace the aptamer from the aptamer–protein complex because they bind to the protein, the measured fluorescence polarization is again reduced.

This principle was successfully used by Hafner et al. to identify cytohesin-specific small molecules in a high-throughput screen.[16] As shown schematically in Fig. 13.1c, an RNA aptamer that specifically binds and inhibits the Sec-7 domain of small guanine nucleotide exchange factors (GEFs) and the cytohesin-1 Sec7 domain was used to establish an assay based on FP to identify cytohesin-specific small molecules which displace the aptamer from its target and adopt inhibitory activity. From a diverse library of synthetic chemicals, Hafner et al. identified a series of 1,2,4,-triazole derivatives as initial hits and selected the most promising compound, SecinH3, for synthesis and further studies. The inhibitory potential of the compound was assessed by guanine nucleotide exchange assays. The inhibition of cytohesins by the identified compound SecinH3 was demonstrated to lead to hepatic insulin resistance in mice. Furthermore, SecinH3 caused a phenocopy of the effect observed when steppke, the single cytohesin homologue in *Drosophila melanogaster*, was mutated. Thus, the results also demonstrate the potential of chemical biology and aptamer technology for HTS and for dissecting molecular mechanisms involved in the development of diseases.[16]

13.3 Allosteric Ribozymes as Screening Tools

Ribozymes can be tuned to specifically sense the presence of all kinds of molecules, even in complex mixtures, and transduce the information into an easy read-out signal, such as fluorescence. These allosteric ribozymes are also referred

to as aptazymes because they contain an aptamer moiety in addition to the catalytic domain. The information of the conformational change upon ligand binding in the aptamer moiety is "communicated" to the ribozyme's catalytic site. Most allosteric ribozymes are derived from the natural existing hammerhead and hairpin ribozymes; however, allosteric ribozymes with nonnatural catalytic domains have also been reported.

13.3.1 Generation of Allosteric Ribozymes

In principle, three different ways have proven successful for the generation of allosteric ribozymes. In a rational approach, allosteric ribozymes can be assembled in a modular fashion: an aptamer with desired affinity is appended to a ribozyme moiety. This approach was used to generate ATP- and theophylline-dependent hammerhead ribozymes[17] as well as oligonucleotide-dependent hairpin ribozymes.[18] Alternatively, allosteric selection can be used to generate allosteric ribozymes with new effector specificities from a random-sequence population. A random sequence is thereby introduced into a ribozyme, and species whose cleavage activity is activated or inactivated upon addition of the effector are isolated after several selection cycles.[19–21] Allosteric selection was used to render an RNA ligase ribozyme protein dependent.[22,23]

Third, in a mixed approach, the allosteric ribozyme is assembled from an aptamer and a ribozyme moiety and linked via a randomized bridge. In vitro selection is carried out to evolve a functional communication module. Ribozymes composed of a flavin mononucleotide (FMN)-binding aptamer and a hammerhead ribozyme could be turned into either allosterically activated or inhibited species by selection of different communication modules.[24]

13.3.2 Indirect Screening

Allosteric ribozymes can selectively monitor substrate or product formation during an enzymatic reaction. For example, a minimized ADP aptamer was used to construct a RiboReporter sensor that detects ADP in a background of ATP and generates a fluorescent signal[25] (Fig. 13.2a). The aptamer was appended to a hammerhead ribozyme core via a connecting stem consisting of randomized nucleotides and subjected to successive rounds of selection. Upon binding to ADP, the sensor undergoes self-cleavage and generates a fluorescent signal. The ADP RiboReporter sensor was used to monitor pERK2 protein kinase activity in a pilot screen of 77 test druglike compounds. The ADP RiboReporter sensor unambiguously identified microplate wells containing a known inhibitor (staurosporine), but no new functional molecules could be discovered in this test screen.[25]

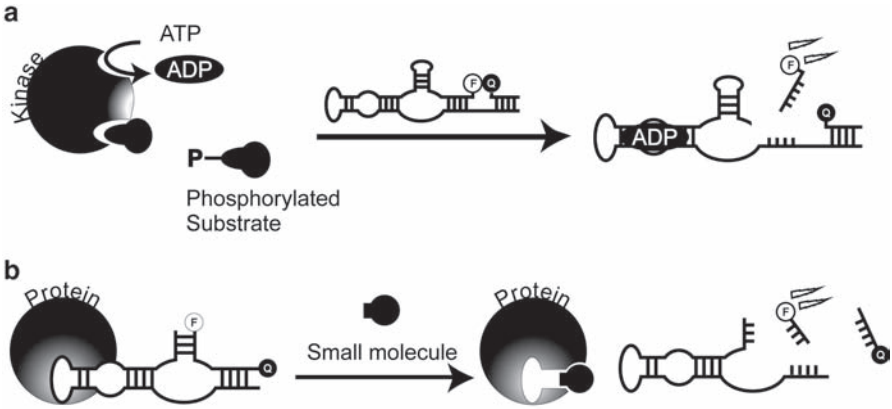

Fig. 13.2 Ribozymes for inhibitor screening. (**a**) A RiboReporter consisting of an ADP aptamer appended to the hammerhead ribozyme indirectly reports kinase activity by responding to ADP generated in the reaction.[25] ADP binding activates ribozyme cleavage and leads to release of the fluorescently labeled (*F*) oligonucleotide, which generates a fluorescence signal. (**b**) A protein-dependent hammerhead ribozyme directly reports molecular interactions of the bound protein with inhibitory small molecules.[26,27] Binding of a small molecule to the protein releases the protein from the ribozyme and thus triggers cleavage of the doubly labeled FRET probe, which causes fluorescence. These reporter ribozymes were used to identify a novel small-molecule inhibitor of the human immunodeficiency virus (HIV)-1 Rev protein

13.3.3 Direct Screening

Ribozymes have been engineered whose cleavage activities directly depend on proteins and peptides. Small molecules or other proteins that disrupt the binding between an aptazyme and its target can adversely affect the cleavage activity of the allosteric ribozyme. If the cleavage activity is transduced into an easy read-out signal, such as fluorescence, screening of novel interaction partners of a target protein can be performed. This approach was realized by Hartig et al. who fused the Rev-binding element (RBE) of HIV-1 to the hammerhead ribozyme to create a Rev-responsive ribozyme[26] (see Fig. 13.2b). Addition of the Rev protein triggered a conformational switch in the RBE rendering the ribozyme inactive (Fig. 13.2b, left). The cleavage activity that correlates with a fluorescent signal could be restored in the presence of a small molecule that competed with the RBE for Rev binding (Fig. 13.2b, right). By appending an HIV-1 reverse transcriptase (HIV-1-RT)-specific aptamer to the hammerhead ribozyme, Hartig et al. also engineered an HIV-1-RT-dependent hammerhead ribozyme that functions in a similar way.[27]

In a second approach, an anti-Rev aptamer was fused to the hammerhead ribozyme to generate an aptamer-inhibited ribozyme. In the absence of Rev, the aptamer domain hybridized to the hammerhead ribozyme to form a stem that prevented substrate annealing and hence cleavage. In the presence of the cognate-annealing protein or peptide, however, the aptamer formed a defined structure that rendered the hammerhead ribozyme substrate-binding site accessible for annealing

so that cleavage of the external FRET substrate occurred. Disruption of the aptamer–protein interaction by a small molecule allowed the original stem structure to form, again suppressing the generation of a fluorescence signal.

Both approaches of Hartig et al., the Rev-responsive ribozyme and the aptamer-inhibited ribozyme, were successfully applied for screening of small molecules binding to Rev. In a model screen of 96 antibiotics with both reporter systems, coumermycin A_1 was identified as a novel Rev-binding organic molecule that inhibited HIV-1 replication.[26]

Both the hairpin and hammerhead ribozymes also were extended by oligonucleotide sequences that rendered them susceptible to the antithrombin aptamer. They were regulated by the thrombin concentration. This assay was used to detect the α-thrombin–hirudin protein–protein interaction in a concentration-dependent manner. The thrombin-responsive reporter ribozymes might potentially be applicable in high-throughput screens for small molecules or peptides that function as superior thrombin inhibitors.

Other reporter ribozymes that sense the presence or activity status of a protein such as the protein-dependent ribozyme ligases[22] or the modified hairpin ribozyme[18,28] should also be readily convertible into screening formats.

13.4 Natural RNAs as Screening Tools

Functional nucleic acids such as aptamers and allosteric ribozymes can be obtained entirely in vitro by evolutionary selection methods for almost any kind of target. In some cases, however, Nature itself has already created functional nucleic acids that can be readily converted into probes and used for screening assays.

13.4.1 Riboswitches as Screening Tools

With the recent discovery that many bacteria utilize certain RNA domains, namely riboswitches and metabolite-dependent ribozymes, to regulate gene expression, a completely unexplored potential target class for new antibiotics has emerged.[29,30] Mayer et al. developed a high-throughput-compatible fluorescence-based assay that allowed direct monitoring of the *cis*-cleaving reaction catalyzed by the glmS ribozyme (Fig. 13.3a).[31] If small molecules can be found that activate the ribozyme in an analogous fashion to glucosamine-6-phosphate (GlcN6P), they are likely to exhibit antibiotic activity because they trigger destruction of the mRNA that encodes for a protein required for the synthesis of a bacterial cell wall precursor molecule.

Mayer et al. used an 81-nucleotide minimal ribozyme variant and FP to detect distinct, metabolite-dependent activation states of a catalytic riboswitch. The GlcN6P-triggered *cis*-cleaving reaction generated a fluorescent molecule from a

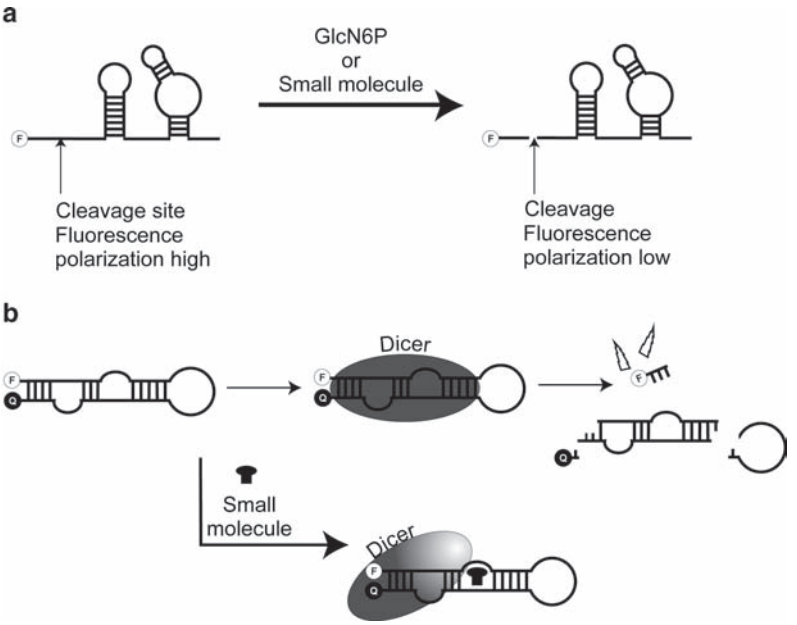

Fig. 13.3 Natural RNAs for inhibitor screening. (**a**) Schematic representation of the fluorescent-labeled glmS ribozyme and in *cis* cleavage induced by glucosamine-6-phosphate (GlcN6P) or a potential hit compound.[31] The inactive full-length ribozyme exhibits high fluorescence polarization (*left*). Activation of the ribozyme by GlcN6P or a potential hit compound triggers cleavage, releasing a short fluorescent-labeled fragment that shows low polarization (*right*). (**b**) A homogeneous assay for micro-RNA (miRNA) maturation. The doubly labeled pre-miRNA is hydrolyzed by *Dicer*, leading to increased fluorescence (*upper panel*). In the presence of an inhibitory small molecule that binds to the pre-miRNA, Dicer can no longer cleave, and no increase in fluorescence is detected[35]

high molecular weight 81-mer to a low molecular weight 4-mer showing different FP. This HTS-compatible assay could be used to screen compound libraries for small molecules that modulate bacterial riboswitches, which has implications for the practical development of new antimicrobial drugs. The obtained Z′-factor of 0.61 matched very well with industrial standards and showed that the assay is suitable for identifying active compounds.

Blount et al. developed a different high-throughput assay for the glmS ribozyme that relies on FRET.[32] This assay was used to identify active compounds from a library of GlcN6P analogues whose affinities for the ribozyme were verified by commonly used electrophoretic methods with radiolabeled RNA. The primary screen of a library of 960 compounds identified five active compounds, one of which was a GlcN6P analogue known to stimulate ribozyme activity. These results demonstrate that modern high-throughput screening techniques can be applied to the discovery of riboswitch-targeted drug compounds. Precedents for riboswitches as targets for antibiotic intervention exist: *S*-(2-aminoethyl)-L-cysteine (AEC) binds to the lysine riboswitch with only 30-fold-reduced affinity compared to

lysine,[33] and pyrithiamine, a thiamine analogue, exhibits antimicrobial action by binding to the TPP-responsive riboswitches in bacteria and fungi.[34]

13.4.2 Pre-miRNAs as Screening Tools

Micro-RNAs (miRNAs) are short, double-stranded, regulatory RNA molecules approximately 21 base pairs in length and of endogenous origin. They are cleaved from their inactive hairpin precursor molecules, the pre-miRNAs, by the enzyme Dicer. Many aspects of miRNA-mediated gene regulation are still unclear, but modified cellular miRNA expression patterns are often associated with diseases, especially many types of cancer. miRNAs may thus provide valid target molecules for new therapeutic approaches.

Davies and Arenz constructed a FRET-labeled pre-miRNA – the pre-let-7 RNA from *D. melanogaster* – to generate a fluorescence signal upon processing of the pre-miRNA to the miRNA by Dicer[35] (see Fig. 13.3b). In the presence of molecules that bind to the pre-miRNA and cause inhibition of Dicer-mediated processing, no fluorescence signal is observed. As a proof of concept, a dodecapeptide derived from the amino acid sequence of Dicer that inherently binds to pre-miRNAs was successfully tested. This assay should be suitable for identifying potential inhibitors of miRNA maturation. The selectivity of selected pre-miRNA ligands, however, remains to be elucidated.

13.5 Conclusions

Both artificial and natural functional nucleic acids have proven amenable and useful for high-throughput screening of inhibitors. Artificial functional nucleic acids such as aptamers and aptazymes can be generated quickly, easily, and entirely in vitro by evolutionary methods. Aptamers are available for a variety of targets ranging from small molecules to proteins. They exhibit superb binding affinities and can discriminate between closely related ligands. Most importantly, nucleic acid sensors can often be turned into reporter molecules by introducing fluorescent dyes using commercially available reagents and routine protocols, which allows transducing changes in their secondary structures into easy read-out signals. Moreover, the predictable base-pairing of nucleic acids allows the construction of reporter constructs from almost any functional sequence. In addition, some natural RNAs such as riboswitches and pre-miRNAs can be turned into molecular reporters and used directly for inhibitor screening.

Taken together, the examples presented in this chapter demonstrate that functional nucleic acids represent versatile tools for inhibitor screening that can also be applied in a high-throughput format. The majority of the assays described here meet criteria required for application in industry (e.g., the Z′-factor).

Acknowledgments We thank the DFG, the SFBs 645 and 704 for grants to M.F., and the Austrian Academy of Sciences for a grant to A.R. and the members of the Famulok lab. This work was supported by Aventis Gencell and by a grant from the Volkswagen Foundation (Priority program "conformational control") to M.F. We thank M. Blind, G. Mayer, D. Proske, and G. Sengle (Universitat Bonn) for helpful discussions as well as J. Crouzet, J.F. Mayaux, and M. Finer (Aventis Gencell) for support.

References

1. Owicki, J.C. (2000) Fluorescence polarization and anisotropy in high throughput screening: perspectives and primer. J. Biomol. Screen. 5:297–306.
2. Ellington, A.D. and Szostak, J.W. (1990) In vitro selection of RNA molecules that bind specific ligands. Nature (Lond.) 346:818–822.
3. Robertson, D.L. and Joyce, G.F. (1990) Selection in vitro of an RNA enzyme that specifically cleaves single-stranded DNA. Nature (Lond.) 344:467–468.
4. Tuerk, C. and Gold, L. (1990) Systematic evolution of ligands by exponential enrichment: RNA ligands to bacteriophage T4 DNA polymerase. Science 249:505–510.
5. Famulok, M. (2005) Allosteric aptamers and aptazymes as probes for screening approaches. Curr. Opin. Mol. Ther. 7:137–143.
6. Silverman, S.K. (2003) Rube Goldberg goes (ribo)nuclear? Molecular switches and sensors made from RNA. RNA 9:377–383.
7. Roth, A. and Breaker, R.R. (2004) Selection in vitro of allosteric ribozymes. Methods Mol. Biol. 252:145–164.
8. Breaker, R.R. (2002) Engineered allosteric ribozymes as biosensor components. Curr. Opin. Biotechnol. 13:31–39.
9. Winkler, W.C. and Breaker, R.R. (2003) Genetic control by metabolite-binding riboswitches. ChemBioChem 4:1024–1032.
10. Barrick, J.E., Corbino, K.A., Winkler, W.C., Nahvi, A., Mandal, M., Collins, J., Lee, M., Roth, A., Sudarsan, N., Jona, I., Wickiser, J.K. and Breaker, R.R. (2004) New RNA motifs suggest an expanded scope for riboswitches in bacterial genetic control. Proc. Natl. Acad. Sci. USA 101:6421–6426.
11. Yang, Y., Kochoyan, M., Burgstaller, P., Westhof, E. and Famulok, M. (1996) Structural basis of ligand discrimination by two related RNA aptamers resolved by NMR spectroscopy. Science 272:1343–1347.
12. Williamson, J.R. (2000) Induced fit in RNA–protein recognition. Nat. Struct. Biol. 7:834–837.
13. Nutiu, R. and Li, Y. (2003) Structure-switching signaling aptamers. J. Am. Chem. Soc. 125:4771–4778.
14. Nutiu, R., Yu, J.M.Y. and Li, Y. (2004) Signaling aptamers for monitoring enzymatic activity and for inhibitor screening. ChemBioChem 5:1139–1144.
15. Elowe, N.H., Nutiu, R., Allali-Hassani, A., Cechetto, J.D., Hughes, D.W., Li, Y. and Brown, E.D. (2006) Small-molecule screening made simple for a difficult target with a signaling nucleic acid aptamer that reports on deaminase activity. Angew. Chem. Int. Ed. Engl. 45:5648–5652.
16. Hafner, M., Schmitz, A., Grune, I., Srivatsan, S.G., Paul, B., Kolanus, W., Quast, T., Kremmer, E., Bauer, I. and Famulok, M. (2006) Inhibition of cytohesins by SecinH3 leads to hepatic insulin resistance. Nature (Lond.) 444:941–944.
17. Tang, J. and Breaker, R.R. (1997) Rational design of allosteric ribozymes. Chem. Biol. 4:453–459.
18. Najafi-Shoushtari, S.H., Mayer, G. and Famulok, M. (2004) Sensing complex regulatory networks by conformationally controlled hairpin ribozymes. Nucleic Acids Res. 32:3212–3219.

19. Piganeau, N., Thuillier, V. and Famulok, M. (2001) In vitro selection of allosteric ribozymes: theory and experimental validation. J. Mol. Biol. 312:1177–1190.
20. Piganeau, N., Jenne, A., Thuillier, V. and Famulok, M. (2001) An allosteric ribozyme regulated by doxycyline. Angew. Chem. Int. Ed. Engl. 40:3503.
21. Koizumi, M., Soukup, G.A., Kerr, J.N. and Breaker, R.R. (1999) Allosteric selection of ribozymes that respond to the second messengers cGMP and cAMP. Nat. Struct. Biol. 6:1062–1071.
22. Robertson, M.P. and Ellington, A.D. (2001) In vitro selection of nucleoprotein enzymes. Nat. Biotechnol. 19:650–655.
23. Robertson, M.P., Knudsen, S.M. and Ellington, A.D. (2004) In vitro selection of ribozymes dependent on peptides for activity. RNA 10:114–127.
24. Soukup, G.A. and Breaker, R.R. (1999) Engineering precision RNA molecular switches. Proc. Natl. Acad. Sci. USA 96:3584–3589.
25. Srinivasan, J., Cload, S.T., Hamaguchi, N., Kurz, J., Keene, S., Kurz, M., Boomer, R.M., Blanchard, J., Epstein, D., Wilson, C. and Diener, J.L. (2004) ADP-specific sensors enable universal assay of protein kinase activity. Chem. Biol. 11:499–508.
26. Hartig, J.S., Najafi-Shoushtari, S.H., Grune, I., Yan, A., Ellington, A.D. and Famulok, M. (2002) Protein-dependent ribozymes report molecular interactions in real time. Nat. Biotechnol. 20:717–722.
27. Hartig, J.S. and Famulok, M. (2002) Reporter ribozymes for real-time analysis of domain-specific interactions in biomolecules: HIV-1 reverse transcriptase and the primer-template complex. Angew. Chem. Int. Ed. Engl. 41:4263–4266.
28. Najafi-Shoushtari, S.H. and Famulok, M. (2007) DNA aptamer-mediated regulation of the hairpin ribozyme by human alpha-thrombin. Blood Cells Mol. Dis. 38:19–24.
29. Winkler, W.C. (2005) Riboswitches and the role of noncoding RNAs in bacterial metabolic control. Curr. Opin. Chem. Biol. 9:594–602.
30. Blount, K. and Breaker, R. (2006) Riboswitches as antibacterial drug targets. Nat. Biotechnol. 12:1558–1564.
31. Mayer, G. and Famulok, M. (2006) High-throughput-compatible assay for glmS riboswitch metabolite dependence. ChemBioChem 7:602–604.
32. Blount, K., Puskarz, I., Penchovsky, R. and Breaker, R. (2006) Development and application of a high-throughput assay for glmS riboswitch activators. RNA Biol. 3:77–81.
33. Sudarsan, N., Wickiser, J.K., Nakamura, S., Ebert, M.S. and Breaker, R.R. (2003) An mRNA structure in bacteria that controls gene expression by binding lysine. Genes Dev. 17:2688–2697.
34. Sudarsan, N., Cohen-Chalamish, S., Nakamura, S., Emilsson, G.M. and Breaker, R.R. (2005) Thiamine pyrophosphate riboswitches are targets for the antimicrobial compound pyrithiamine. Chem. Biol. 12:1325–1335.
35. Davies, B.P. and Arenz, C. (2006) A homogenous assay for micro RNA maturation. Angew. Chem. Int. Ed. Engl. 45:5550–5552.

Chapter 14
Nucleic Acids for Computation

Joanne Macdonald and Milan N. Stojanovic

Abstract Nucleic acids have many features that are ideal for molecular computation. Using nucleic acids, we have constructed a full set of molecular logic gates, with modular stem-loop-controlled deoxyribozymes as switches and single-stranded oligonucleotides as inputs and outputs. These gates have been combined to form basic computational circuits, including a half- and a full-adder, and can also be assembled into automata to perform complex computational tasks such as game playing. Our most advanced automaton to-date integrates more than 100 nucleic acid logic gates to play a complete game of tic-tac-toe encompassing 76 possible game plays. Inputs and outputs can also be coupled with upstream and downstream components, such as aptamers, sensors, secondary gate activation, and small-molecule release, indicating the potential for nucleic acid computation in the engineering of autonomous therapeutic and diagnostic molecular devices.

14.1 Introduction

Our group joined the field of DNA-based molecular computation relatively late; our first experiments were done almost 5 years after Adleman's seminal demonstration,[1] that is, solving a directed Hamiltonian path problem. At the time of our first publication in this field,[2] there was already growing concern[3] that DNA-based procedures might be unlikely to solve any computational problem that modern computers would not solve more quickly. Our decision to pursue molecular computation had little to do with a desire to compete with silicon. Rather, in the conducive environment of the Department of Medicine, we joined this field based on our realization that there are therapeutic problems that would benefit greatly from even the simplest application of solution-phase molecular logic, that is, Boolean

J. Macdonald and M.N. Stojanovic
The National Science Foundation Center for Molecular Cybernetics;
Division of Experimental Therapeutics, Department of Medicine,
Columbia University, New York, USA
mns18@columbia.edu

Y. Li and Y. Lu (eds.), *Functional Nucleic Acids for Analytical Applications*,

calculations. For example, the therapy for cancer using toxin immunoconjugates has been limited by concurrent development of toxic effects in normal cells. Thus, the most basic Boolean logic, such as an AND gate detecting two disease markers before killing a cell, could significantly improve therapy outcomes by enhancing specific delivery to target cells. The rapid success of our early approach[4,5] encouraged us to propose and to develop, step-by-step, more and more complex computational systems[6,7] based on nucleic acids, and to realize that there are other health care-related areas in which molecular computation could be potentially useful.[8] This chapter is an updated story of our work.

14.2 Logic Gates

14.2.1 Silicomimetic Approach

Our approach is called silicomimetic because we apply some simple concepts from modern digital (silicon) computing to the construction of molecular networks. While digital computers use currents and voltages to convey information, our system uses molecules for information processing, taking oligonucleotides as inputs and generating oligonucleotide outputs. Similar to digital computing, more complex circuits are built from basic computational elements called logic gates. Our molecular logic gates perform simple logical (Boolean) calculations on inputs to produce a single output based on a set of rules. Calculations are the intuitively named "AND," "OR," and "NOT," and their rules of operation are described in so-called truth tables (Figs. 14.1–14.3).[2,9] For example, an AND gate has two molecules as inputs, providing an output if both inputs are present; alternatively, a NOT gate, or inverter, has one input molecule and provides the output only if the input

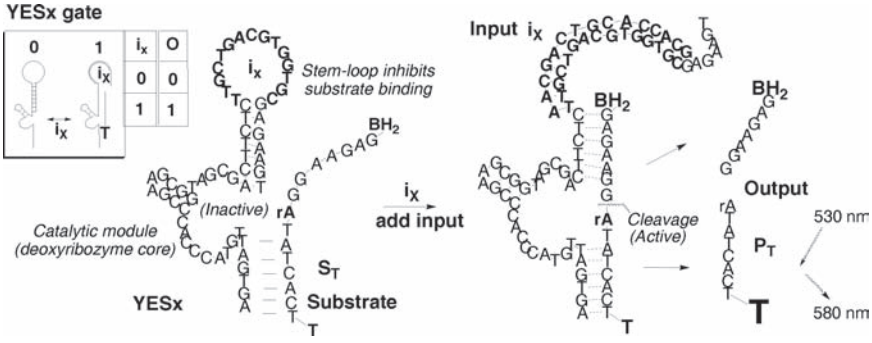

Fig. 14.1 Simplest deoxyribozyme-based logic gate. Addition of an inhibitory stem-loop region to a deoxyribozyme catalytic module creates a YES*x* gate (*left*), which is activated by the addition of a complementary input oligonucleotide (*ix*), cleaving a FRET-labeled substrate to produce a shortened oligonucleotide output. *Inset* shows a cartoon of all possible gate/input combinations and a truth table indicating output activation

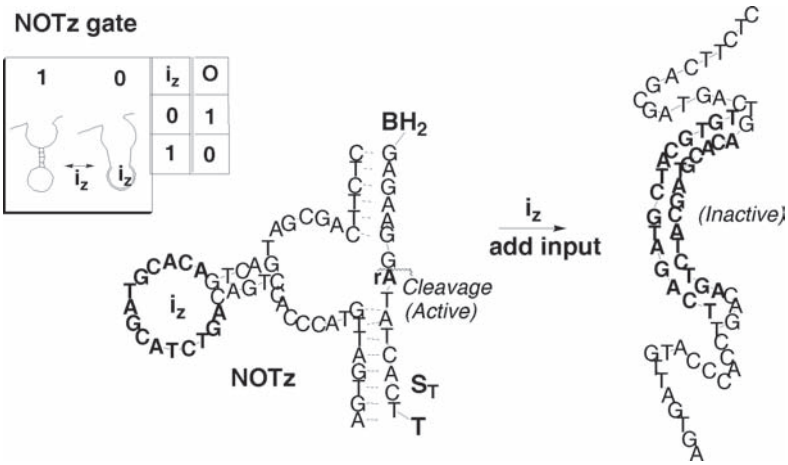

Fig. 14.2 Deoxyribozyme-based NOT logic gate. NOT *z* gates or inverters are created by the addition of a stem-loop within the catalytic region of the deoxyribozyme, such that the gate is active until a complementary input oligonucleotide (*iz*) is added, which breaks the structure of the deoxyribozyme and inactivates the gate. *Inset* shows a cartoon of all possible gate/input combinations and a truth table indicating output activation

is absent. More complex electronic circuits can be implemented by combining individual logic gates, and we have constructed several such circuits including a half-adder[4] and a full-adder,[6] which are described in Section 14.3.

In principle, any recognition event that influences structural or spectral changes, or influences downstream catalytic activity, can be reinterpreted as "logic gate" behavior. In many cases, even quite complex logical operations are possible with this approach,[10] and important advances can be made in the field of sensors or molecular electronics. These approaches are limited in a plug-and-play modularity, which restricts their power and implementation in solution. Our design is intended to be a generic "bottom-up" approach to enable full modularity for future implementation in complex solution-phase autonomous molecular devices.

14.2.2 Principles Behind Deoxyribozyme-Based Logic Gates

Our logic gates consist of two modules[11]: a catalytic module, usually a deoxyribozyme (nucleic acid catalyst); and a recognition module, usually a stem-loop oligonucleotide inspired by molecular beacons (see Figs. 14.1–14.3).[2,9] These two modules are combined such that any conformational change in the stem-loop region influences the catalytic activity of the enzyme. That is, the stem-loop provides allosteric control over the activity of the deoxyribozyme. Our simplest design uses positive regulation (Fig. 14.1): a stem-loop region blocks access of the deoxyribozyme substrate; upon binding of the complementary oligonucleotide to the loop,

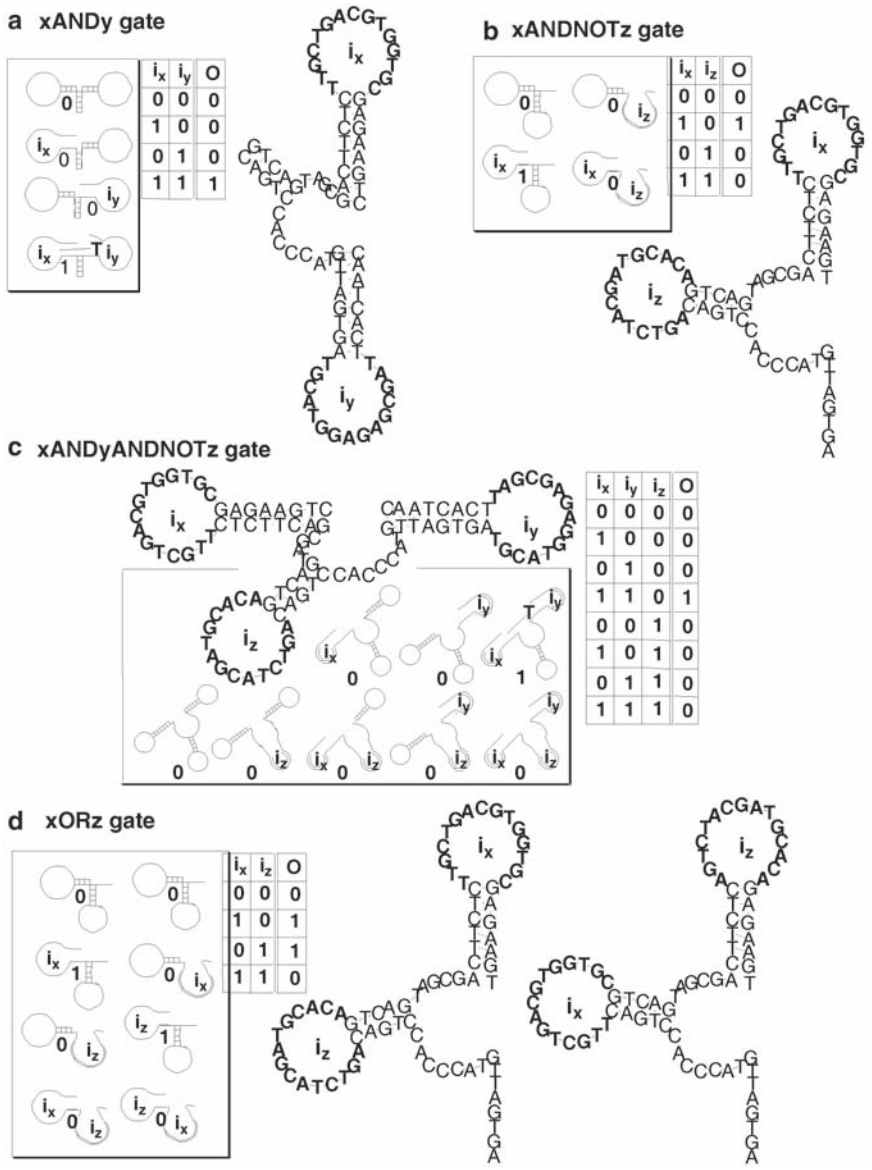

Fig. 14.3 Using YES and NOT modules, the complete set of logic gates can be made, including (**a**) *x AND y* gates, active only in the presence of *ix* AND *iy*; (**b**) *x ANDNOT z* gates, active in the presence of input *ix* but not input *iz*; (**c**) *x AND y ANDNOT z* gates, active in the presence of input *ix* and *iy* so long as a third inhibitory input *iz* is not present; and (**d**) *x OR z* gates, which are created by combining two ANDNOT gates, and are active in the presence of either *ix* or *iy*, but not in the presence of both inputs *ix* and *iy. Insets* show cartoons of all possible gate/input combinations and truth tables indicating output activation

the stem-loop region opens, allowing substrate binding and the catalytic reaction to proceed. Chemists call this molecule a YES gate, although a more proper name would be a detector or sensor gate. In an example of negative allosteric regulation (NOT gates; Fig. 14.2), a stem-loop region is embedded within the catalytic core of the deoxyribozyme, and the binding of a complementary oligonucleotide distorts this core, shutting down enzyme activity. The enzymatic module is crucial for building more complex circuits, because through multiple turnovers we provide a solution for increased fan-out (the maximum number inputs that the output of a single logic gate can feed).

Multiple-input gates can be constructed by the addition of two or more controlling modules attached to the same deoxyribozyme (Fig. 14.3). For instance, placement of two stem-loop controlling regions on the 5′- and 3′-ends of the deoxyribozyme creates an AND gate (Fig. 14.3a), which requires two inputs before the enzyme is activated; whereas placement of a positive regulating loop with a negative regulating loop gives an ANDNOT gate (Fig. 14.3b), which is active in the presence of one input so long as a second inactivating input is not present. Currently, up to three inputs can be generally implemented on a single gate (for example, the ANDANDNOT gate[5] in Fig. 14.3c), and other Boolean functions can be achieved through the combination of multiple gates (for instance the OR gate shown in Fig. 14.3d).

An important property of our gates is the modularity of the inputs. Virtually any deoxyribozyme can be combined with any stem-loop; this allows the use of arbitrary oligonucleotides as inputs, within some limitations. For example, oligonucleotide inputs with strong secondary structure cannot open the stem-loop region. Furthermore, at room temperature, an excess of inputs with single nucleotide mismatches are not clearly differentiated by gates, although there are differences in the initial enzyme reaction rates. While in many special cases two mismatched positions are clearly distinguished, the safe Hamming distance (the diversity required for two sequences to be recognized as separate inputs) appears to be three or more mismatches, with some exceptions such as if G*T mismatches prevail. Another feature of our gates is that the action of input oligonucleotides can be reversed by adding their complements,[12] and we utilized this property during the construction of our full-adder[6] (described in Section 14.3). The switching of gates from inactive to active state or vice versa is almost instantaneous upon addition of inputs.

14.2.3 Output Detection

The deoxyribozymes we used can either produce shorter oligonucleotides through phosphodiesterase activity,[11,13] or longer oligonucleotides through ligase activity.[14] In either case we can claim that our inputs and outputs are concordant, which means that they are the same type of molecules (oligonucleotides). This similarity is important for the construction of larger networks involving cascades, which is discussed in Section 14.5.

For both phosphodiesterase and ligase reactions, the formation of output can be distinguished based on the size of the product using gel electrophoresis. While we still use gels to screen new enzymes, in more complex circuits we implemented a rapid FRET (fluorescence resonance energy transfer) system[15–17] by labeling our substrate oligonucleotides with a 5′-fluorophore and a 3′-quencher (see Figs. 14.1, 14.4b). After cleavage by the deoxyribozyme, the fluorophore is

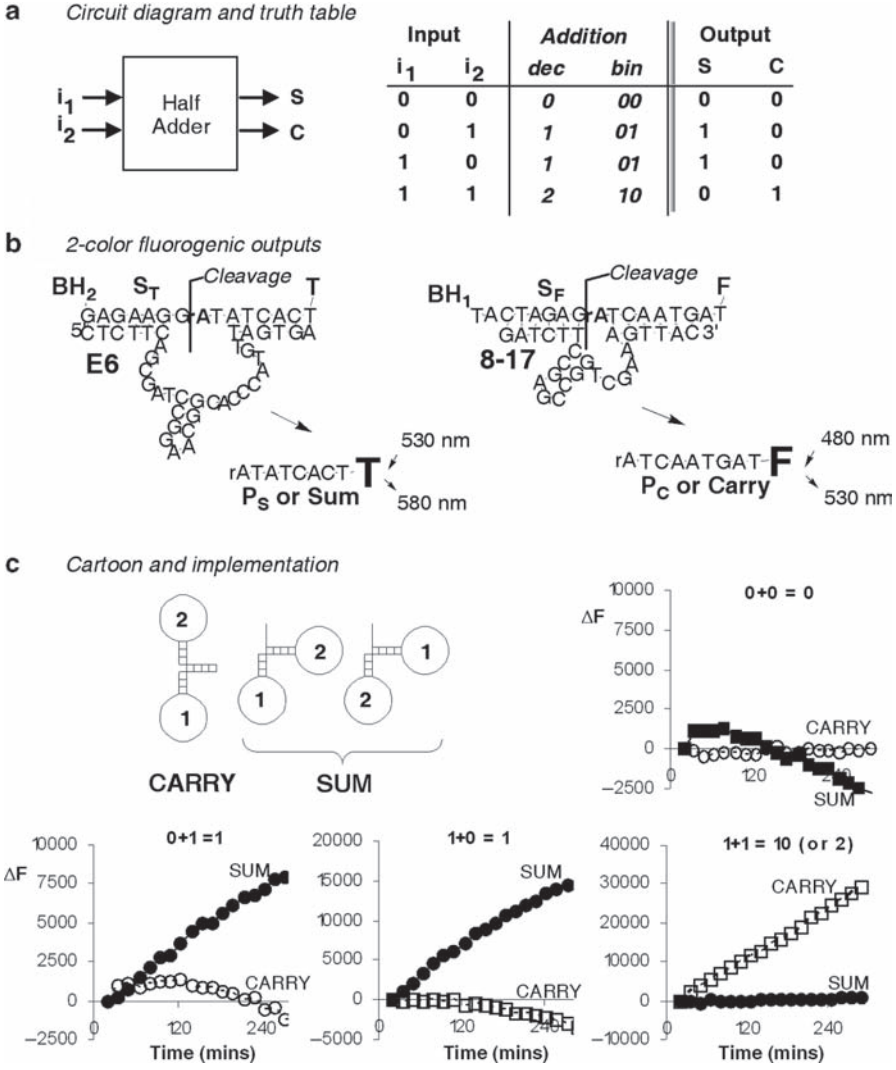

Fig. 14.4 Construction of a molecular half-adder. A half-adder adds two bits of information to produce a sum and carry digit, as shown in the circuit diagram and truth table (**a**). A molecular half-adder was constructed using a two-color fluorogenic output system (**b**) and three molecular logic gates (**c**), producing perfect digital behavior

separated from the quencher and increase of fluorescence is produced. This system is more difficult to design for ligases, so with ligase logic gates we cascaded them into downstream logic gates to accomplish visualization (see Section 14.5).

14.3 Adders: Circuits for Basic Arithmetical Operations

After initial demonstration of logic gates, the next key challenge for traditional digital computing is the ability to combine logic gates into circuits that perform basic arithmetic operations.[18] Such logic circuits are called adders, and in modern computers adders are used as fundamental units that are then cascaded to perform more complex arithmetic operations. A half-adder adds two binary digits (bits) to produce two binary outputs – denoted as a sum and a carry (Fig. 14.4a). A full-adder adds three binary digits, usually two bits and a carry from a previous addition step, and again produces two binary outputs notated as a sum and a carry (see Fig. 14.6a).

14.3.1 A Molecular Half-Adder

A half-adder can add in binary 00 + 00 = 00, 00 + 01 = 01 (and reverse), and 01 + 01 = 10 (notated in decimal as 0 + 0 = 0, 0 + 1 = 1, 1 + 0 =1, and 1 + 1 = 2). To construct a molecular half-adder we designed a system that could analyze the presence of two input molecules and generate two different output molecules in accordance with the following set of rules (see truth table; Fig. 14.4a): (1) the absence of both input molecules leaves the system as is, and neither of the outputs is produced, (2) the presence of any one (and only one) of the input molecules activates only the first output (the sum output), while (3) the presence of both inputs activates only the second output (the carry output). The sum output could be produced by the action of an exclusive OR (XOR) gate (see Fig. 14.3b), whereas the carry output required an AND gate (see Fig. 14.3a). Because an XOR gate in our system is actually built from two deoxyribozyme ANDNOT gates, our molecular half-adder needed a total of three deoxyribozyme logic gates.

Practically, to engineer a half-adder with deoxyribozymes, we had to expand our existing logic gate capability to systems with multiple outputs. We used combinations of the catalytic cores of deoxyribozymes E6[4,6,11] and 8–17[4,6,13] to cleave two different oligonucleotide substrate sequences, and labeled each substrate oligonucleotide with two different fluorophore/quencher combinations: namely, fluorescein (F) and black-hole quencher 1 (BHQ1), and tetramethylrhodamine (TAMRA) and black-hole quencher 2 (BHQ2). After some optimization of deoxyribozyme structures to show satisfactory digital behavior in mixtures, we successfully constructed a molecular half-adder[4] (Fig. 14.4c). The construction of this half-adder also demonstrated that two separate systems of our deoxyribozyme logic gates (an AND function and an XOR function) could operate in parallel within a single tube, without any interfering cross-talk.

14.3.2 A Molecular Full-Adder

A full-adder is similar to a half-adder except that it processes an additional input, usually a carry digit from a previous half-adder or adder. This ability to process a carry digit from a previous addition is paramount for the construction of more complex systems, and thus the construction of a full-adder is considered a fundamental challenge for any novel computational paradigm. Mechanistically, the full-adder produces two outputs according to the following rules (see Fig. 14.6a): (1) the presence of any one (and only one) of the input molecules activates only sum output; (2) the presence of any two inputs activates only the carry (C) output; (3) the presence of all three inputs activates both outputs; and (4) the absence of all three input molecules leaves the system as is, and neither output is produced. For instance, the mathematical phrase $1+1+1=3$, when converted into binary, would be written as $01+01+01=11$, and would result in the production of both a carry and a sum digit.

An exceptional high-school student, Harvey Lederman, proposed that by using a method similar to Bernie Yurke's fuel/antifuel addition,[12] we could construct a full-adder using a mixture of parallel components without the requirement for serial connections. He demonstrated that a generic three-input deoxyribozyme could be developed with stem-loops initially set to an open state by preincubation with complementary oligonucleotides[6]; the addition of inputs would then strip loops of these complementary oligonucleotides, returning them to closed states (Fig. 14.5).

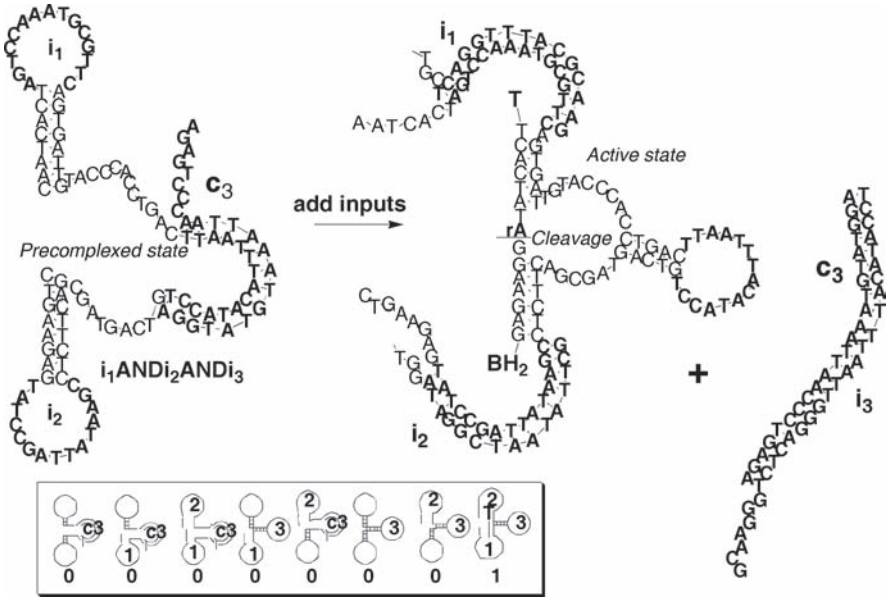

Fig. 14.5 A generic three-input gate constructed using precomplexed oligonucleotides

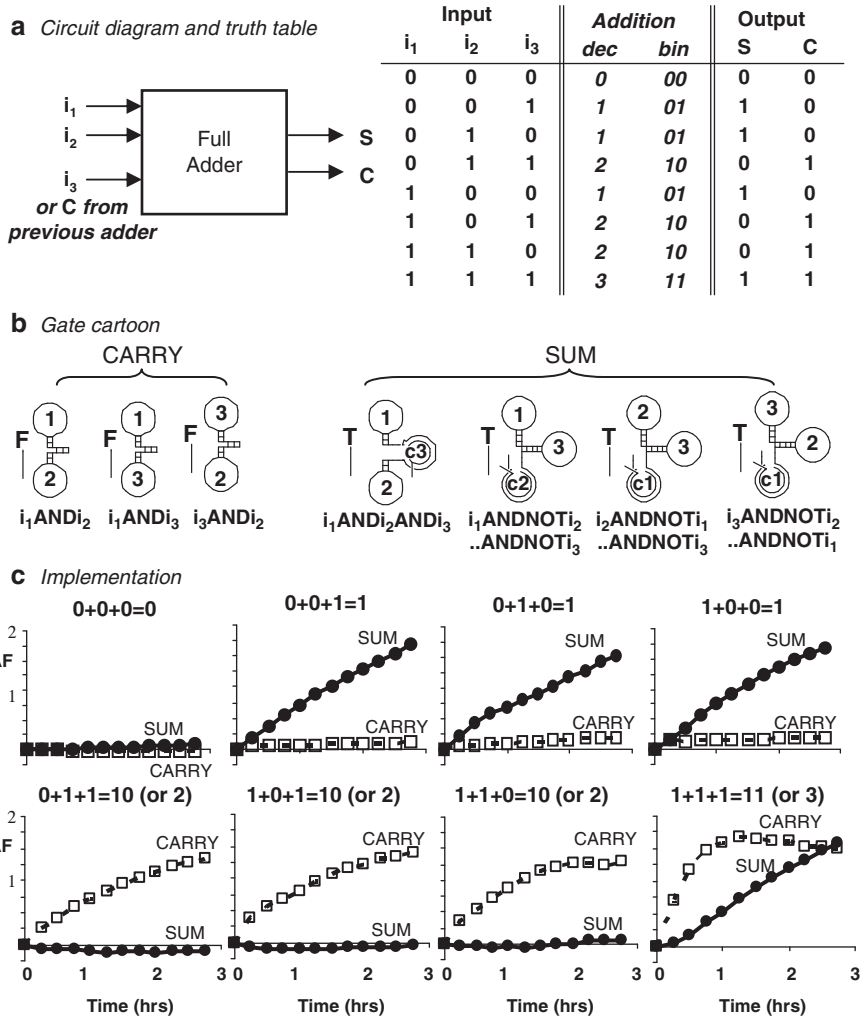

Fig. 14.6 Construction of a molecular full-adder. A full-adder adds three bits of information to produce a sum and carry digit, as shown in the circuit diagram and truth table (**a**). A molecular full-adder was constructed: three AND logic gates to produce the SUM digit, and four 3-input gates to produce the CARRY digit (**b**), producing perfect digital behavior (**c**)

His initial experimental demonstration enabled us to develop our molecular full-adder, which consisted of seven logic gates (Fig. 14.6b, c): three AND gates activating the TAMRA-labeled carry output, and four generic three-input gates appropriately activating the fluorescein-labeled sum output.[6]

Two design issues were identified during construction. First, at higher gate concentrations (total concentrations >1 μM), the gates influenced each other, and therefore much lower concentrations were required to attain perfect full-adder

behavior. It is likely that a judicious choice of oligonucleotides would allow the use of higher gate concentrations, although possibly at the expense of generality. As a second issue, we noticed that, despite the remarkable successes of modular design, we were not able to routinely rotate stem-loops to design all possible combinations of ANDNOTANDNOT gates. We expect that this apparent breakdown in modular design will likely be eliminated with the availability of improved oligonucleotide libraries that are specifically matched to the substrates and core enzymes sequences. Such libraries under development and are discussed further in Section 14.4.

14.4 Automata: Complex Decision Making and Scaled Integration

Automata are machines that change states according to a series of inputs and a set of rules that determine the changes between each state. We have focused on the construction of molecular automata that play tic-tac-toe (noughts and crosses) against a human player, since game playing is an unbiased test of the complexity that can be achieved by a new computation medium. We chose tic-tac-toe as one of the simplest games of perfect information. Our first automaton, MAYA,[5] plays a symmetry-pruned restricted game of tic-tac-toe, which allowed us to explore gate integration and decision making on a simplified scale. Our second automaton, MAYA-II,[7] plays an unrestricted game and was constructed to begin testing the engineering limits of our deoxyribozyme logic gate model. At this stage, games are played in 3×3 wells of 384-well plates (mimicking the nine fields of a tic-tac-toe game board). Human inputs are encoded with oligonucleotides, which are added to all the wells, and the automaton's response is observed by monitoring a fluorescence increase in a particular well. In MAYA, 8 inputs are used, encoding the position of the human move; whereas 32 inputs are used in MAYA-II, encoding both the position and the timing of the human move (Figs. 14.7–14.10).

14.4.1 MAYA

MAYA (an acronym derived from *m*olecular *a*rray of *Y*ES and *A*ND gates), plays a symmetry-pruned restricted game of tic-tac-toe: the automaton always goes first in the middle well, and the human player can respond by moving in one of the corner wells or one of the side wells (see Figs. 14.7, 14.10).[5] This simplification reduces our engineering effort to programming the automata to play a total of 19 legal game plays, 18 of which end in human defeat and one ending in draw. After the automaton's initial move (created by a constitutively active deoxyribozyme and the addition of magnesium, a required cofactor), the human player

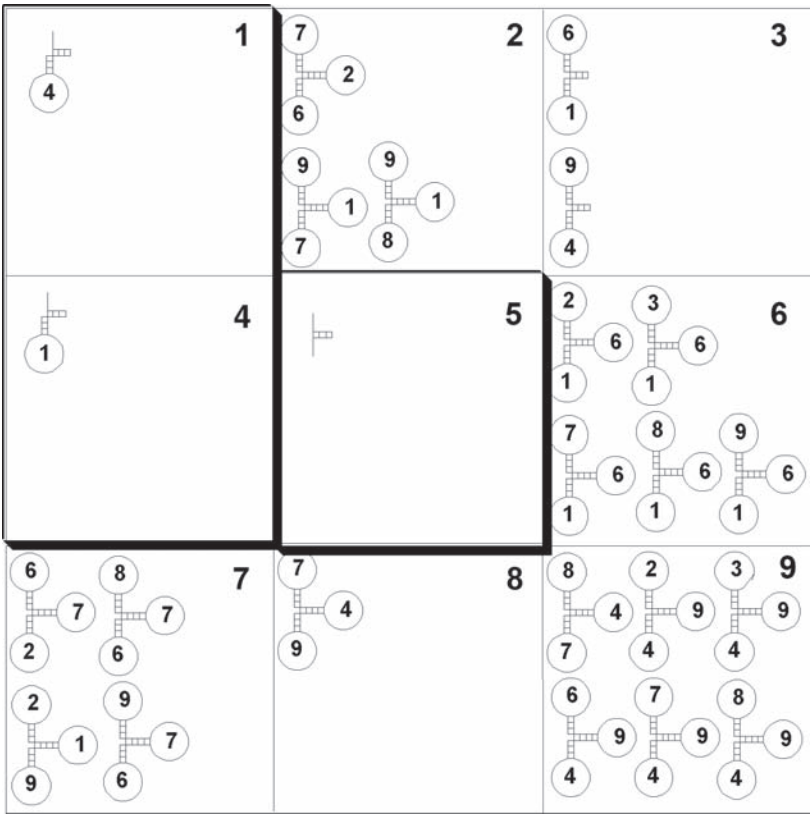

Fig. 14.7 Deoxyribozyme-based logic gates required for MAYA. The automaton moves first into square 5 (via a constitutively active deoxyribozyme). The human player's first move is restricted to square 1 and 4

makes a move by adding one of eight input DNA sequences to all the wells. The sequences are coded, and tell the automaton which well the human has chosen. For instance, to move into well 1 the human player will add input i1, and to move into well 4 the human player will add input i4. To calculate its next move, MAYA uses a network of 23 logic gates distributed in the remaining eight wells (Fig. 14.7). These gates react to the human player's input DNA, causing a single well to fluoresce, indicating the automaton's chosen well. The cycle of human player input followed by automaton response continues until there is a draw or a victory for the automaton. The automaton cannot be defeated as it plays according to a perfect strategy.

The increase from two to eight inputs, and the combination of 23 logic gates in eight wells, constituted at that time our largest test of the deoxyribozyme logic gate model: and MAYA excelled! Our eight-input DNA sequences were modular, and could be present in any of the three stem-loop positions within

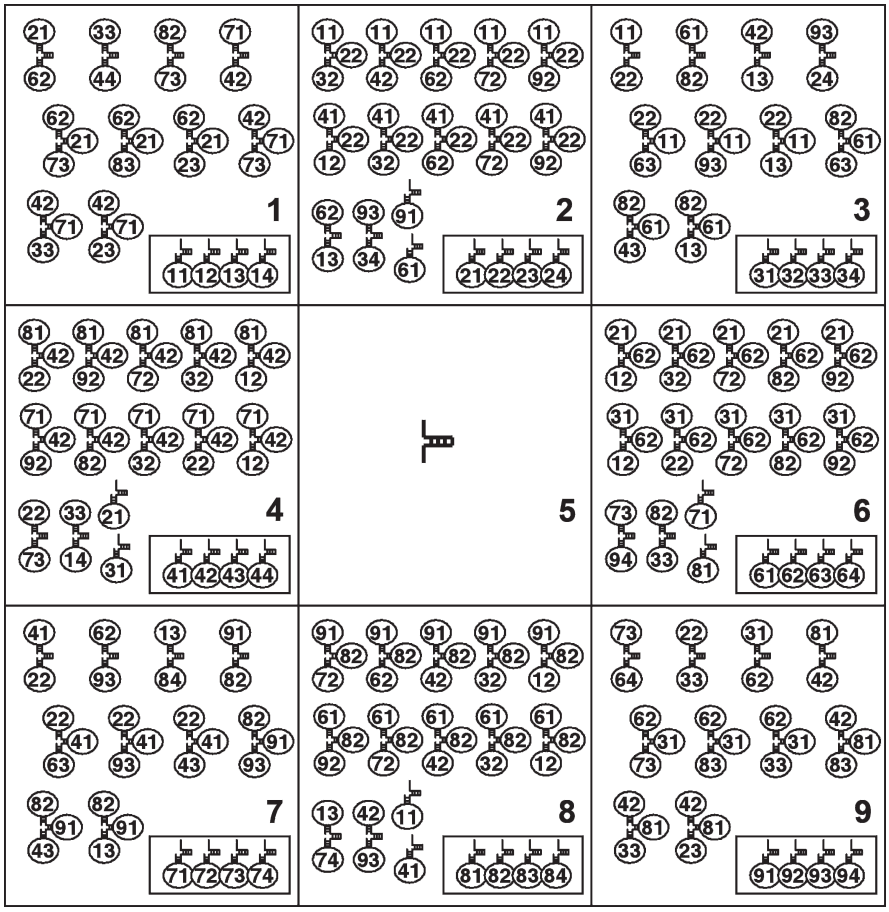

Fig. 14.8 Deoxyribozyme-based logic gates required for MAYA-II. The automaton moves first into square 5 (via a constitutively active deoxyribozyme). The human players first move is unrestricted. *Boxed gates* monitor human player moves

the E6 deoxyribozyme; extensive testing indicated the lack of erroneous moves. The only concern was some background fluorescence increase in wells not intended to respond. For instance, upon addition of i1 we noticed a strong and expected increase in well 4, but also a detectable increase in well 9 from the five partially activated ANDANDNOT gates. This observation suggested that error propagation in more complex networks could potentially lead to non-digital behavior. The digital behavior of individual gates can be perfected one gate at a time by increasing the lengths of inhibitory stems in the presence of specific inputs. This, however, suppresses the reaction rate in the presence of

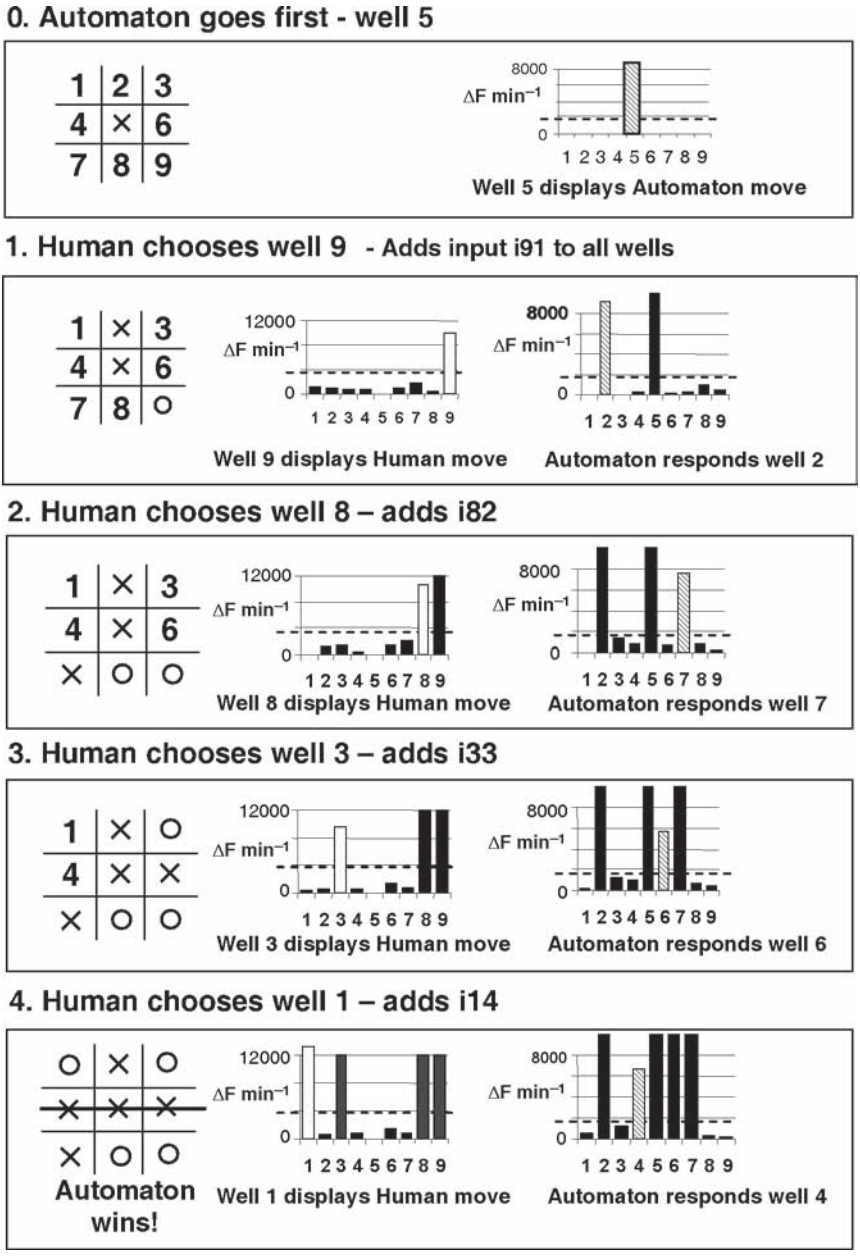

Fig. 14.9 An example game played with MAYA-II

activating oligonucleotides, leading to an increase in MAYA's "thinking time." Background stabilization was investigated further during the construction of our next automaton, MAYA-II, and is discussed below.

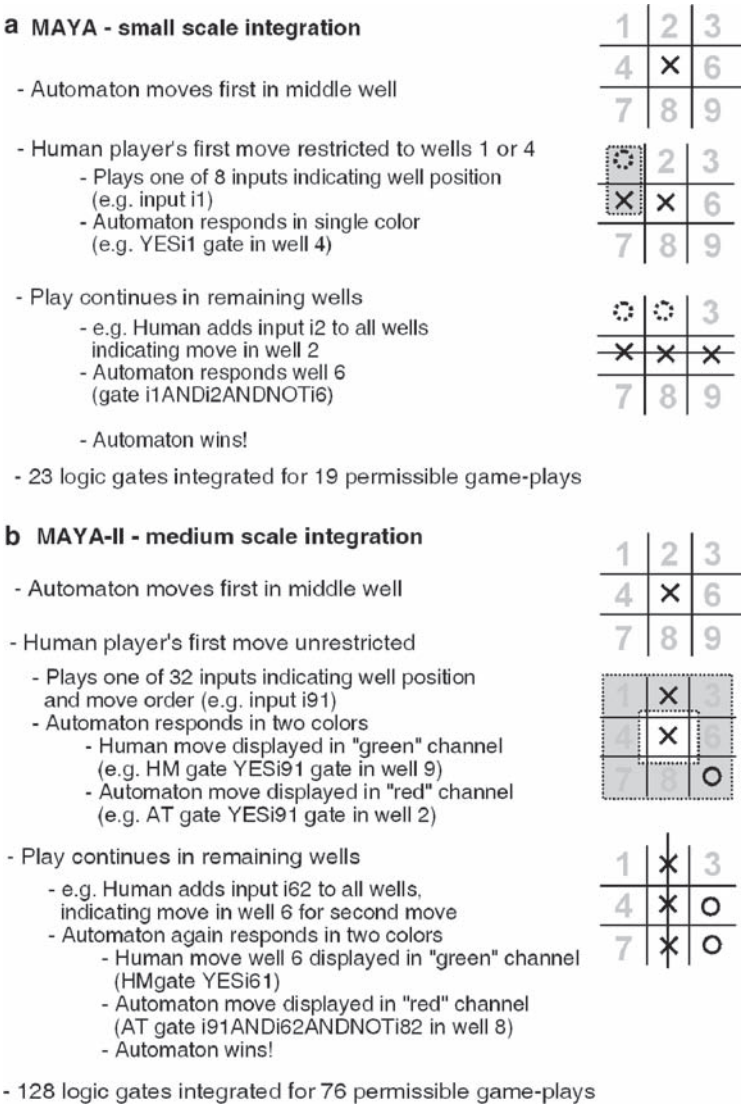

Fig. 14.10 Key features comparison of MAYA and MAYA-II

14.4.2 MAYA-II

After the successful implementation of MAYA, we decided to build a larger unrestricted tic-tac-toe playing automaton to probe the complexity to which our deoxyribozyme-based logic gates could be integrated; that is, the number of systems that can operate autonomously in a coordinated and meaningful fashion. The resultant version, MAYA-II,[7] plays an unrestricted non-symmetry-pruned complete game

of tic-tac-toe: the automaton still always goes first in the middle well, but the human players are unrestricted in their first move and may choose to play in any of the eight remaining wells (Figs. 14.8, 14.10). Using this format MAYA-II encompasses 76 permissible game plays. We also improved the user friendliness of the automaton (see Fig. 14.10), giving it a two-color fluorogenic output system to display both human and automaton moves (MAYA only displayed automaton moves with a single color). Similar to our adders (see Fig. 14.4b), human moves are displayed in a "green" channel (fluorescein fluorescence) and automaton moves are displayed in a "red" channel (TAMRA) fluorescence (Fig. 14.9).

Indicating a move in MAYA-II became slightly more complicated as the lack of human move restrictions required an increase from eight to 32 coded input sequences. These new inputs code both the well position and the order of the human move (their first, second, third, or fourth move). The inputs are labeled I[NM], where N is the board position and M is the order of the human move. For instance, to play into well 9 for the first move, the human would add input I91, but to play into well 9 on a second move the human would add input I92 (Fig. 14.9). To calculate its next move and to display human moves, MAYA-II uses a network of logic gates distributed in the remaining eight wells (see Fig. 14.8): a set of 32 YES gates based on the 8–17 deoxyribozyme distributed evenly in each well react to display the human player's move position in the "green" fluorescein channel; and a mixture of 96 E6 deoxyribozyme-based logic gates distributed in a symmetrical array to calculate the automaton's chosen well. The automaton remains undefeated as it plays according to a perfect strategy.

The biggest difficulty in the construction of MAYA-II was not the selection of inputs that did not cross react with each other, but rather the calibrating of individual gates to fall within a certain range of high and low fluorescence values. On the first try, nearly all the human move gates failed to show a response with the 32 input sequences selected; however, successful reengineering of the underlying deoxyribozyme provided an improved structure that accepted all the input sequences without need for further calibration. The automaton move gates were initially more promising, accepting nearly all the 32 input sequences to some degree of activity. However, it soon became apparent that some of the gates required careful engineering to titrate reasonable signal-to-noise ratios (i.e., some gates gave very high reaction rates with corresponding high background levels, whereas other gates gave low reaction rates with corresponding low background levels). We thus developed a set of design principles to allow gate titration,[19] and after careful testing and retesting we established a set of titrated gates. However upon mixing the gates, some showed concentration-dependent activity, as previously noted in our full-adder.[6] These gates were then either reengineered or their concentration adjusted, and consistent digital behavior of MAYA-II was finally achieved. The degree of engineering required for MAYA-II is not unlike traditional circuit construction in silicon electronics, where circuit and switch calibration to high and low voltage signals is also required. It would be preferable to create a system that minimizes the laborious trial and error of gate calibration, and we are currently analyzing our reengineering data for the construction of an oligonucleotide input reference library, for speedier construction of future gates.

Despite the engineering challenge, the success of MAYA-II indicates the maturity of our deoxyribozyme-based logic gates as a reasonably plug and play integrated system. In total, MAYA-II integrates 128 molecular logic gates, 32 input DNA sequences, and eight two-channel fluorescent outputs in solution, which more than quadruples the number of logic gates used in any previous solution-phase system. By integrating more than 100 logic gates, MAYA-II represents the first medium-scale integration of molecular logic gates in solution. The significance of this is similar to the significance of early silicon chips and semiconductors. MAYA-II shows that large-scale, higher-level computing using molecular logic gates is now a reality and that even larger molecular computers are feasible. For example, with the gates used in this chapter, we can regularly detect down to about 10 nM gate concentrations; the maximum total concentration of oligonucleotides in an individual well was approximately 1 μM, indicating that we could potentially operate up to 100 gates in parallel in a single tube. In MAYA-II, the maximum number of gates used per well was 18, significantly less than the theoretical maximum, but double the number used in MAYA.

14.5 Engineering Interelement Interfaces

All circuits described up to now use gates that operate in a parallel fashion. To achieve a higher complexity of computation and to control downstream actuators, serial operation is required, where outputs of upstream elements are connected to inputs of downstream elements. The deoxyribozymes can either produce shorter oligonucleotides through phosphodiesterase activity[11,13] or longer oligonucleotides through ligase activity.[14] In either case, we can claim that our inputs and outputs are concordant, which means that they are the same type of molecules (oligonucleotides), but each case presents us with a different challenge for integration, and we now discuss such issues.

We say that two gate elements are tied into a cascade when either the molecular or functional output of one upstream element is sensed by a second downstream element. This, in principle at least, allows arbitrary logical operations through cascading gates, although the delay in the activation of the next element in the cascade is of a great concern, as is the case in many other systems.[20,21]

14.5.1 Ligase–Phosphodiesterase Cascades

Our most straightforward cascade uses a ligase enzymatic module as an upstream element and a phosphodiesterase with attached YES gate stem-loop module as a downstream gate.[9] In this case, the product of a ligase gate reaction can bind to the stem-loop of a downstream phosphodiesterase gate (Fig. 14.11). In theory, ligases could also feed new substrates to phosphodiesterases, allowing us to reset circuits.

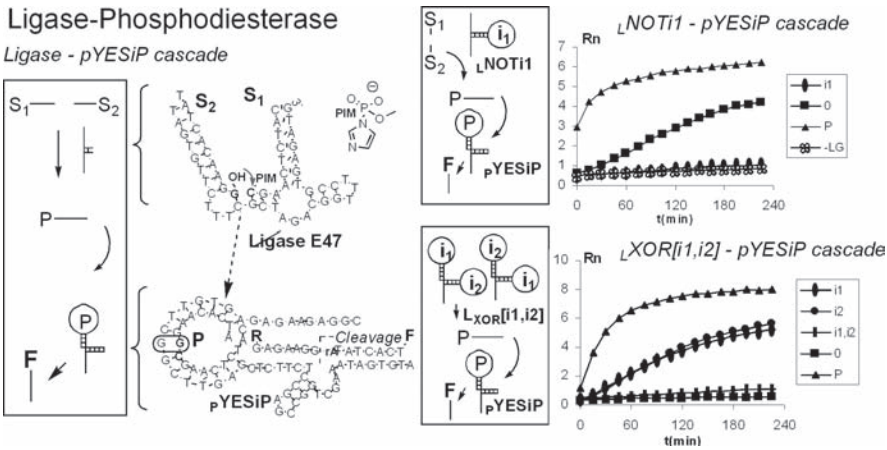

Fig. 14.11 Interelement interfaces. Logic gates can be cascaded into upstream and downstream elements. Ligase logic gates combine two short substrates into a longer product that feeds downstream phosphodiesterase gates. NOT (*top right*) and XOR (*bottom right*) ligase logic gates are demonstrated here

However our chosen ligase requires chemically activated phosphoimidazole groups (PIM) at the 3′-end of one substrate (Fig. 14.11), which makes reversibility more difficult to achieve. Similar to our phosphodiesterase logic gate design, we extended this simple cascade with modularly designed stem-loop regions into ligase E47 and developed a full set of logic gates.[9] To avoid activation by the cooperative action of two ligase substrates self-assembling on downstream phosphodiesterase gates, we introduced a mismatch in one of the substrates and the downstream stem loop. This step allows product alone to selectively activate downstream gates in the presence of a large excess of the two initial substrates.

The successful coupling of two gates into a cascade provided us with more than just a convenient read-out. To the best of our knowledge, this was the first artificial example of nonphotonic gate-to-gate communication of molecular scale in solution, with an upstream gate signaling its state to a reporting downstream gate. This result also offers a possible solution to a long-standing problem in solution-phase molecular computation, that is, construction of multicomponent circuits.

14.5.2 Phosphodiesterase–Phosphodiesterase Cascades

Coupling two phosphodiesterases is somewhat more challenging to design in solution. Noncatalytic single-turnover cascades were reported by Breaker's group in their alternative design of phosphodiesterase logic gates.[22] The challenge for multiple-turnover cascades arises from the inability to design trivial and general substrate–product pairs, in which a downstream gate would only interact with great

selectivity with the product. By definition, substrates for phosphodiesterases contain within their structures a complete product, and this substrate is present at the initial stages of the reaction in great excess. We attempted various designs to "hide" the inputs of downstream gates into conformationally shielded structures, but none of them provided us with satisfactory low background. In other words, while we are able to slow down the initial reaction rates of downstream gates in the presence of substrate, when compared to products this difference did not hold over the several hours needed for computation. This problem can be solved in solid state, but seems to require completely new thinking in solution.

An alternative design was more easily implemented. We used a substrate of an upstream logic gate as an inhibitor of a downstream NOT gate. In this way, only the active upstream gate can remove the inhibition imposed on the downstream gate. In principle, this design is general, and we have encoded both AND and OR logic into it. Also, multiple cascade levels are possible, although the increase in time of computation becomes an issue. We demonstrated (Stojanovic, 2003, unpublished) this approach by coupling of an upstream streptavidin sensor gate to a downstream NOT gate (Fig. 14.12).

14.5.2.1 Computational Control of Aptameric Actuators

Larger and more complex networks aside, we are also interested in the practical application of nucleic acid computation, which requires the engineering of an interface between nucleic acids and biological systems. For this, we need "actuators." Current aptamer technology provides a natural interface between nucleic acids and other molecules, both at the level of sensors (i.e., aptazymes or switches) and actuators. Dmitry Kolpashchikov in our group has developed an example system

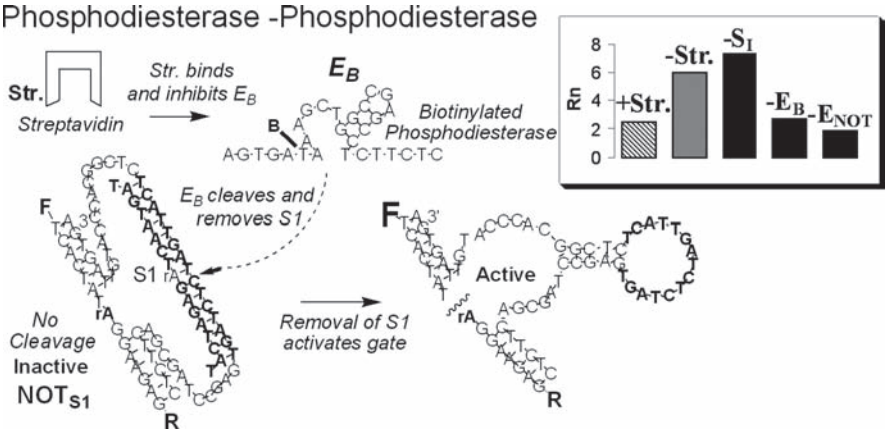

Fig. 14.12 Interelement interfaces. Phosphodiesterases can cleave downstream logic gate inputs and can in turn be inhibited by upstream binding elements such as biotin–streptavidin complexation

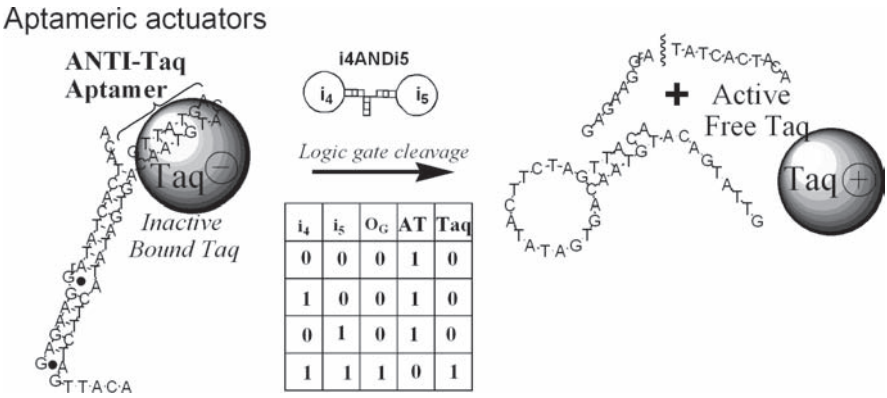

i_4	i_5	O_G	AT	Taq
0	0	0	1	0
1	0	0	1	0
0	1	0	1	0
1	1	1	0	1

Fig. 14.13 Interelement interfaces. Logic gates can control aptameric binding events, such as the binding and release of active Taq DNA polymerase

that provides control over both small molecules and proteins,[23] the next step in the development of autonomous therapeutic and diagnostic devices.

The logical control of aptamers is similar to our phosphodiesterase-phosphodiesterase cascades: the substrate of an upstream logic gate is used to keep a structure-switching aptamer[24–26] in an open state. The removal of substrate from solution switches the aptamer off and releases any bound ligand. In our initial studies of this design, we adapted two aptamers for logical control: one triggered the release of a small molecule (malachite green) and the second was able to control the enzymatic activity of Taq DNA polymerase (Fig. 14.13).[23]

Our initial studies indicate that this approach to aptamer control is likely general and that other aptamers are candidates for integration into molecular circuits. Through the process of in vitro selection and amplification (SELEX) using either natural or unnatural nucleotides, aptamers that are responsive to almost any molecular or ionic species can be isolated, suggesting that molecular computation can be connected to almost any other event on a molecular scale. The current work, although still not suitable for practical in vivo applications, marks a shift in the autonomous computational systems with therapeutic potential from catalytic[2,4–7,9] and stoichiometric antisense outputs[27] to the release of small molecules and control of enzymatic activity.

14.6 Conclusions and Future Visions

At this moment, we have established arbitrary Boolean calculations in solution, limited only by some cross-reactivity of various elements and our patience to wait for our computations to be observable (particularly for the cascades). So, the natural question is, What comes next? We are intrigued by opportunities to build increasingly complex networks of molecules, networks that will perhaps

be trainable, could be subjected to evolutionary processes, and that could show emergent properties. However, our biggest long-term challenge is to adapt this system to in vivo applications. This accomplishment will require a significant and coordinated effort to build fully reliable components that can operate in vivo and be integrated with sensory and drug delivery components.

Acknowledgments This material is based upon work supported by the National Science Foundation under Grants IIS-0324845, CCF-0523317, and CHE-0533065, Searle Fellowship to M.N.S. Milan Stojanovic is a Lymphoma and Leukemia Society Fellow.

References

1. Adleman, L.M. (1994) Molecular computation of solutions to combinatorial problems. Science 266:1021–1024.
2. Stojanovic, M.N., Mitchell, T.E. and Stefanovic, D. (2002) Deoxyribozyme-based logic gates. J. Am. Chem. Soc. 124:3555–3561.
3. James, K.D., Boles, A.R., Henckel, D. and Ellington, A.D. (1998) The fidelity of template-directed oligonucleotide ligation and its relevance to DNA computation. Nucleic Acids Res. 26:5203–5211.
4. Stojanovic, M.N. and Stefanovic, D. (2003) Deoxyribozyme-based half-adder. J. Am. Chem. Soc. 125:6673–6676.
5. Stojanovic, M.N. and Stefanovic, D. (2003) A deoxyribozyme-based molecular automaton. Nat. Biotechnol. 21:1069–1074.
6. Lederman, H., Macdonald, J., Stefanovic, D. and Stojanovic, M.N. (2006) Deoxyribozyme-based three-input logic gates and construction of a molecular full adder. Biochemistry 45:1194–1199.
7. Macdonald, J., Li, Y., Sutovic, M., Lederman, H., Pendri, K., Lu, W., Andrews, B.L., Stefanovic, D. and Stojanovic, M.N. (2006) Medium scale integration of molecular logic gates in an automaton. Nano Lett. 6:2598–2603.
8. Macdonald, J., Li, Y., Sutovic, M., Stefanovic, D. and Stojanovic, M. (2006) Genomes to systems conference 2006. Manchester, UK, p. BN-2.
9. Stojanovic, M.N., Semova, S., Kolpashchikov, D., Macdonald, J., Morgan, C. and Stefanovic, D. (2005) Deoxyribozyme-based ligase logic gates and their initial circuits. J. Am. Chem. Soc. 127:6914–6915.
10. de Silva, A.P., Leydet, Y., Lincheneau, C. and McClenaghan, N.D. (2006) Chemical approaches to nanometre-scale logic gates. J. Phys. Condensed Matter 18:S1847–S1872.
11. Breaker, R.R. and Joyce, G.F. (1995) A DNA enzyme with Mg(2+)-dependent RNA phosphoesterase activity. Chem. Biol. 2:655–660.
12. Yurke, B., Turberfield, A.J., Mills, A.P., Jr., Simmel, F.C. and Neumann, J.L. (2000) A DNA-fuelled molecular machine made of DNA. Nature (Lond.) 406:605–608.
13. Santoro, S.W. and Joyce, G.F. (1997) A general purpose RNA-cleaving DNA enzyme. Proc. Natl. Acad. Sci. USA 94:4262–4266.
14. Cuenoud, B. and Szostak, J.W. (1995) A DNA metalloenzyme with DNA ligase activity. Nature (Lond.) 375:611–614.
15. Hartig, J.S. and Famulok, M. (2002) Reporter ribozymes for real-time analysis of domain-specific interactions in biomolecules: HIV-1 reverse transcriptase and the primer-template complex. Angew. Chem. Int. Ed. 41:4263–4266.
16. Singh, K.K., Parwaresch, R. and Krupp, G. (1999) Rapid kinetic characterization of hammerhead ribozymes by real-time monitoring of fluorescence resonance energy transfer (FRET). RNA (New York) 5:1348–1356.

17. Stojanovic, M.N., de Prada, P. and Landry, D.W. (2000) Homogeneous assays based on deoxyribozyme catalysis. Nucleic Acids Res. 28:2915–2918.
18. McCluskey, E.J. (1986) Logic design principles: with emphasis on testable semicustom circuits. Prentice Hall, Englewood Cliffs, NJ.
19. Macdonald, J., Stefanovic, D. and Stojanovic, M.N. (2006) Solution-phase molecular-scale computation with deoxyribozyme-based logic gates and fluorescent readouts. In: Didenko, V.V. (ed.) Fluorescent energy transfer nucleic acid probes: designs and protocols, vol. 335. Humana Press, Totowa, NJ, pp. 343–363.
20. Noireaux, V., Bar-Ziv, R. and Libchaber, A. (2003) Principles of cell-free genetic circuit assembly. Proc. Natl. Acad. Sci. USA 100:12672–12677.
21. Seelig, G., Soloveichik, D., Zhang, D.Y. and Winfree, E. (2006) Enzyme-free nucleic acid logic circuits. Science 314:1585–1588.
22. Penchovsky, R. and Breaker, R.R. (2005) Computational design and experimental validation of oligonucleotide-sensing allosteric ribozymes. Nat. Biotechnol. 23:1424–1433.23.
23. Kolpashchikov, D.M. and Stojanovic, M.N. (2005) Boolean control of aptamer binding states. J. Am. Chem. Soc. 127:11348–11351.
24. Dirks, R.M. and Pierce, N.A. (2004) Triggered amplification by hybridization chain reaction. Proc. Natl. Acad. Sci. USA 101:15275–15278.
25. Dittmer, W.U., Reuter, A. and Simmel, F.C. (2004) A DNA-based machine that can cyclically bind and release thrombin. Angew. Chem. Int. Ed. 43:3550–3553.
26. Nutiu, R. and Li, Y. (2003) Structure-switching signaling aptamers. J. Am. Chem. Soc. 125: 4771–4778.
27. Benenson, Y., Gil, B., Ben-Dor, U., Adar, R. and Shapiro, E. (2004) An autonomous molecular computer for logical control of gene expression. Nature (Lond.) 429:423–429.

Chapter 15
DNAzymes in DNA Nanomachines and DNA Analysis

Yu He, Ye Tian, Yi Chen and Chengde Mao

Abstract This chapter discusses our efforts in using DNAzymes in DNA nanomachines and DNA analysis systems. 10–23 DNAzymes can cleave specific phosphodiester bonds in RNA. We use them to construct an autonomous DNA-RNA chimera nanomotor, which constantly extracts chemical energy from RNA substrates and transduces the energy into a mechanical motion: cycles of contraction and extension. The motor's motion can be reversibly turned on and off by a DNA analogue (brake) of the RNA substrate. Addition and removal of the brake stops and restarts, respectively, the motor's motion. Furthermore, when the RNA substrates are preorganized into a one-dimensional track, a DNAzyme can continuously move along the track so long as there are substrates available ahead. Based on a similar mechanism, a novel DNA detection system has been developed. A target DNA activates a DNAzyme to cleave RNA-containing molecular beacons (MB), which generates an enhanced fluorescence signal. A following work integrates two steps of signal amplifications: a rolling-circle amplification (RCA) to synthesize multiple copies of DNAzymes, and the DNAzymes catalyze a chemical reaction to generate a colorimetric signal. This method allows detection of DNA analytes whose concentration is as low as 1 pM.

15.1 Introduction

DNA nanotechnology is a rapidly evolving research field.[1] It takes advantage of the remarkable molecular recognition capability and highly predictable double helix structures of DNA molecules to build DNA nanostructures, either static[2] or dynamic.[3–5] Such structures have been used as scaffolds in nanofabrication, bioanalysis, or DNA computation. In this regard, DNA is a special building block for material engineering rather than its natural role – the genetic molecule of life. A more exciting future is expected if the biological properties and functions of DNA

Yu He, Ye Tian, Yi Chen, and C. Mao
Purdue University, Department of Chemistry
mao@purdue.edu

Y. Li and Y. Lu (eds.), *Functional Nucleic Acids for Analytical Applications*,

can be incorporated into the developing DNA nanotechnology. Several splendid works have been shown in this direction. For example, one of the most attractive features of DNA is its exponential multiplication by polymerase chain reaction (PCR) or molecular cloning. This property has been successfully employed to produce well-defined DNA nanostructures in large quantity.[6] Another attractive feature of DNA is that some DNA single strands with specific sequences have enzymatic activities, just as the normal protein enzymes or catalytic RNA (ribozyme) do. When incorporated into rationally designed DNA nanostructures or nanomachines, the DNA enzymes (DNAzymes) could catalyze chemical reactions to further tailor DNA nanostructures,[7] power mechanical motions,[8] or give out detectable signals.[9] In particular, this strategy is effective in building novel DNA nanomachines and benefiting applications in bioanalytics. In this chapter, we discuss this theme in detail along with several related examples.

Compared with protein enzymes and ribozymes, DNAzymes have several advantages for functioning in nanomachine systems: (1) They are stable and robust. Proteins and RNAs have serious problems of denaturation, oxidation, or degradation, but DNA is quite resistant to those problems. (2) DNAzymes do not require many additives or stabilizers, such as glycerol, bovine serum albumin (BSA), or dithiothreitol (DTT), which are normally essential for proper functions of many protein enzymes. (3) More importantly, DNAzymes are normal DNA molecules and possess all inherent attractive features of DNA molecules. The sequences of DNA enzymes, except the catalytic cores, can be designed arbitrarily as needed. Therefore, the DNAzyme molecules can be facilely incorporated into DNA nanomechanical systems with highly predicted association and geometry, acting as both functional and structural components of the system, thus leading to a precise control over both structures and functions.

15.2 Autonomous DNA Nanomachines Powered by DNAzyme

15.2.1 Autonomous DNA Nanotweezers

To achieve nanometer-scale mechanical motions in a controllable fashion is one of the key goals in nanotechnology. DNA appears as a superb candidate for construction of diverse nanomachines at the molecular level because of its nanometer-scale dimensions. The DNA duplex is 2-nm wide and 3.4-nm long per helical turn. Indeed, a number of DNA nanomechanical devices, or nanomachines/nanomotors, have been reported.[10–12] DNA nanomachines developed in the early stage perform mechanical motions by external interventions, such as sequentially adding DNA fuel strands[11,12] or changing environmental conditions.[10] To develop novel DNA nanomachines that can run autonomously is, then, an important challenge. Herein, we discuss a delicate autonomous DNA nanomachine that can continuously conduct open-and-close motions until the fuel is exhausted.[13] More interestingly, this nanomachine can be easily stopped and restarted by adding and removing a "brake."[14]

This synthetic DNA nanomachine superficially resembles some natural protein motors, such as myosins and kinesins.[15–18] Both systems contain enzymes (a DNAzyme or protein enzymes) as their "engines" and use chemicals (RNA or ATP) as fuels. During enzyme-catalyzed chemical reactions, the enzymes constantly extract chemical energies and convert them into mechanical energies. The mechanical motions in both systems are at the low-nanometer scale.

The DNA device contains an RNA-cleaving enzyme, named 10–23 DNAzyme,[19] which has resulted from an in vitro evolution. It is the 23rd clone after the tenth round of selection. The DNAzyme can cleave its RNA substrate with sequence specificity. During cleavage, the substrate releases chemical energy stored in the covalent bonds to power the mechanical motion of the nanomachine. The design of the DNA nanomachine is illustrated in Fig. 15.1. The DNA complex has a tweezers-like shape, with two rigid arms made of double-stranded DNA. The two

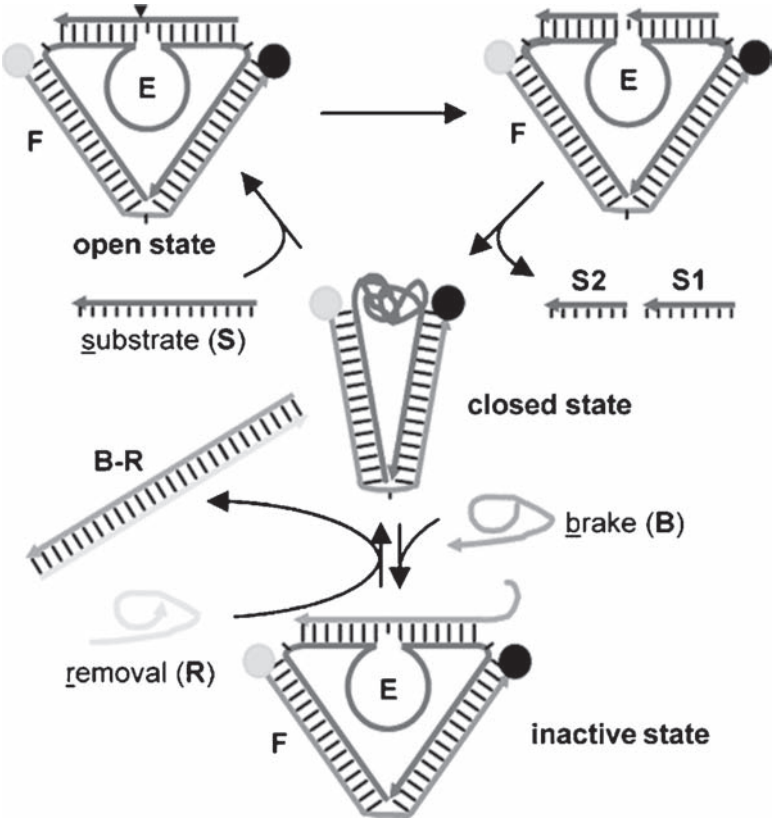

Fig. 15.1 Schematic representation of an autonomous DNA nanomachine. The DNA machine consists of two single strands: *E* and *F*. The E strand contains a 10–23 DNA enzyme domain. The motion of the device has been demonstrated by a fluorescence resonance energy transfer (FRET) technique. The F strand is labeled with a fuorophore, rhodamine green, at its 5′-end and a black hole quencher-1 (BHQ-1) at its 3′-end (Reproduced with permission from ref. 14)

arms connect at one end by a single nucleotide hinge and at the other end by a 29-nucleotide single-stranded DNAzyme. The DNAzyme contains a 15-nucleotide catalytic core that is flanked by two 7-nucleotide substrate-recognition segments at both sides. In the presence of divalent cations, for example, Mg^{2+}, the single-stranded DNAzyme forms a compact random coil driven by entropy maximization[20] and brings the two double helical arms closer. This is defined as a closed state. However, when the RNA substrate is added into the system, it will hybridize with the DNAzyme to form a bulged double-helical structure, thus pushing the two arms of the tweezers outward to reach an open state. Once bounded, the DNAzyme will cleave the substrate into two short fragments. The fragments have low affinity for the DNAzyme and will dissociate from the DNA device. Consequently, the DNAzyme becomes single stranded and collapses into a compact coil. The DNA device returns to its close conformation and is ready for the next motion cycle. So long as there are uncleaved substrates available, the nanodevice will continuously conduct the open–close motion cycle by cycle. It is worth pointing out that RNA is much less stable than its DNA counterpart. To improve the substrate stability, a DNA-RNA chimera is used as fuel in this system. In the substrate, only the two nucleotides flanking the phosphodiester to be cleaved are RNA; all others are DNA. Such DNA-RNA chimera can be efficiently cleaved by the DNAzyme, but are much more stable than RNA molecules.

This process is analogous to a car, which can keep running until all the gasoline is depleted. However, tight control is needed for the operation of a real car. For instance, a car should be able to stop and start at its driver's will, no matter how full the gasoline tank is. A similar function has been realized for the DNA machine by introducing a DNA "brake" into the system.[14] Similar to the DNA–RNA chimera substrate, the brake DNA can also bind to the recognition segments of the DNAzyme. In addition, it has two more nucleotides in the middle that are complementary to the DNAzyme catalytic core, which ensure that the brake DNA has a higher binding affinity to the DNAzyme than the substrate has. In the brake molecule, RNA residues are replaced with DNA counterparts; thus, the DNAzyme cannot cleave the brake DNA. Consequently, when the brake DNA strand exists, it will preferentially occupy the DNAzyme binding site and freeze the DNA device at the "open" state. To restart the motion, a nonpairing tail (a toehold) is designed for removing the brake that initiates a strand-displacement process when a fully complementary DNA single strand, called the "removal" strand, is added. Overall, with the combination of DNAzyme activity and strand-displacement strategy, the DNA device described here can work autonomously and be stopped and restarted readily.

15.2.2 An Autonomous and Processive DNA Walker

The development of nanotechnology is always inspired by the advancement and complexity of nature, and so is the fabrication of synthetic nanomechanical devices. Biological systems contain a rich family of nanomachines. Each nanomachine

can perform a specific function. Some motions are simple and some are quite complicated. For instance, kinesins[21,22] and myosins[23] are extensively studied molecular motors that autonomously and processively move along their corresponding protein tracks to transport cellular cargos. The motions performed by these biological motors are much more complicated than the simple open-and-close motions of the DNA tweezers described above. Those protein motors inspired us to develop a synthetic molecular device (walker) that is analogous to kinesins or myosins. To this end, a DNAzyme-powered DNA walker has been designed and constructed.[24]

This walking system contains a DNA walker (a DNAzyme) and a DNA-RNA chimera track (Fig. 15.2). The track is assembled from a long single-stranded DNA

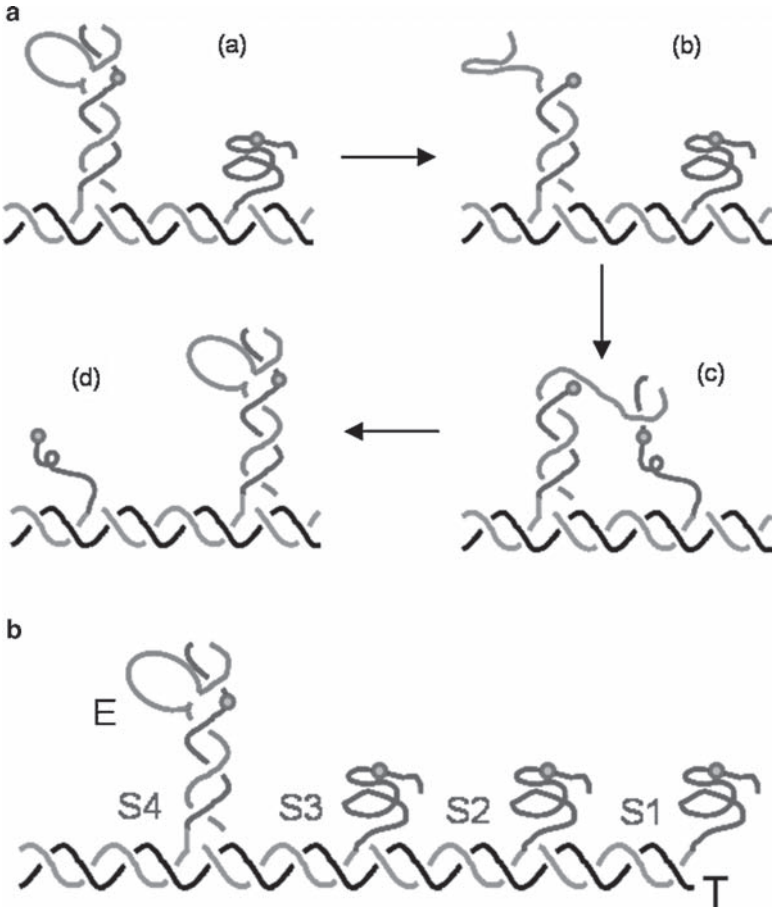

Fig. 15.2 Scheme of a DNA walking system. (**a**) The walking principle. (**b**) A construction with a walking DNAzyme at one end of its track. *T*, template DNA, single strand; *S1–S4*, substrates; *E*, a 10–23 DNAzyme; *black dots*, phosphodiester bonds to be cleaved by the DNAzyme (Reproduced with permission from ref. 24)

template (T) and four DNA-RNA chimera substrates (S1–S4). Each substrate has a positional DNA tag and an unpaired DNA-RNA chimera tail. The tags direct the substrates to designated locations along the track by hybridizing to the template strand (T); the tails can be recognized by the DNAzyme and are stations for the walker. The four substrates have different tags, but their tails are the same. The distance between any two adjacent stations is around 7 nm, defined by two helical turns. The walker is a 10–23 DNAzyme. Besides the 15-nucleotide catalytic core, the DNAzyme walker contains two flanking asymmetric recognition arms with lengths of 7 and 16 nucleotides, respectively. Once bound to a substrate, the walker cleaves the substrate and releases a short fragment of the substrate into the solution, leaving the 7-nucleotide recognition arm of the DNAzyme unpaired. Thus, the recognition arm will have a chance to pair with the adjacent uncleaved substrate, followed by a strand-displacement process. Finally, the entire DNAzyme dissociates from the cleaved substrate and moves to the new one. The whole process can be repeated so long as there are intact substrates available ahead on the track. Gel electrophoretic analysis shows that the DNAzyme walker moves stepwise from one side of the track to the other processively. During the whole moving process, the DNAzyme always remains on the track and no dissociation or intercomplex exchange exists. Although there are only four stations designed in the present system, there is no fundamental reason that prevents increasing the number of stations involved. This DNA walking system represents a biomimetic nanomotor that works autonomously and processively in modeling biological protein nanomotors. Moreover, this system might provide transportation behaviors that natural protein nanomotors cannot do. The rapidly evolving DNA nanotechnology allows one to design and construct aperiodically two-dimensional (2D) arrays.[25] Thus, we can construct arbitrarily designed 2D paths to guide the DNA walkers for controlled motion with 2D trajectories. Once the walker is linked with other nano-objects of interest, such as proteins, enzymes, or nanoparticles, the transportation of such nano-objects could be realized with precise control.

15.3 DNA Detection Systems Based on DNAzyme

15.3.1 DNAzyme-Mediated Amplification of Molecular Beacon Signal for DNA Detection

With the increasing demands in clinical diagnosis, gene therapies, and other biomedical studies, fast and sensitive methods for sequence-specific DNA/RNA detection become more and more important. Traditional methods, such as polymerase chain reaction (PCR), usually amplify the amount of the target molecules but require long processing time and specific experimental facilities and chemicals. To overcome these problems, a number of detection methods are developed by hybridizing the DNA/RNA molecule of interest with complementary oligonucleotide

probes labeled with radioactive isotopes, fluorescent dyes, quantum dots, and metallic or magnetic nanoparticles.[26–31] However, delicate procedures are often required in the preparation of these probes, and well-controlled and stringent wash after the hybridization has to be carried out to minimize the background caused by the free probes.

A DNAzyme-mediated signal amplification for DNA/RNA detection was developed to solve these problems. It is based on a catalytic molecular beacon (MB).[9,32] The MB is an enzyme substrate and only gives rise to a fluorescent signal upon the stimuli of the target DNA/RNA molecules, directly or indirectly. A MB is a single-stranded DNA molecule with a stem-loop structure; its two ends are labeled with a fluorescence dye (F) and a fluorescence quencher (Q), respectively.[33,34] At its native conformation, the fluorescence dye is in close proximity with the quencher and the fluorescence is strongly quenched. Thus, the background is low. Upon binding to the target DNA, the stem-loop structure of MB opens to form a DNA duplex. In this conformation, the fluorescence dye becomes well separated from the quencher and starts to fluoresce. One limitation of the traditional MB technique is that one target DNA molecule can activate only one MB molecule, which lacks a mechanism for signal amplification. To further improve detection sensitivity, catalytic molecular beacon systems have been developed,[9,32] by introducing a DNAzyme for signal amplification. Here, we have further improved this method.

In our approach, target DNA/RNA molecules do not interact with MBs directly to activate them to fluoresce. Instead, the target will activate an inhibited DNAzyme, which, in turn, will activate MBs to fluoresce. One target molecule activates one DNAzyme, but each DNAzyme activates multiple copies of MBs. Hence, the DNAzyme provides a means for signal amplification. Here, the DNAzyme used is a specific RNA-cleaving 10–23 DNAzyme, which has been used in our DNA nanodevices. All RNA residues of the substrate are replaced by DNA residues, except the residue 5′ to the cleavage site. Thus, the substrate (MB) is a DNA-RNA chimera molecule. The reserved RNA residue is located in the loop and subject to cleavage under the catalytic activity of the DNAzyme. In the MB stem, the two ends associate with each other by four base pairs (bp). The 4-bp-long duplex is stable enough to hold the two ends together. As they fall apart upon DNAzyme cleavage, the fluorescence dye is physically separated from the quencher and the fluorescent signal is generated.

To detect the target DNA molecule, the DNAzyme is adjusted accordingly.[35] The scheme is illustrated in Fig. 15.3. First, the DNAzyme has been extended at its 5′-end. This additional domain is a complementary sequence to the target DNA/RNA and contains an inhibitory segment and a toehold. The inhibitory segment is a DNA analogue of the DNA-RNA chimera loop of the MB substrate, so it can bind to the recognition arms of the DNAzyme, but is not cleavable by the DNAzyme. Consequently, the MB substrates are prevented from binding to the DNAzyme; thus, the DNAzyme is inactive. When the target DNA is introduced into the system, it will first bind to the unpaired toehold and gradually form a longer duplex along the 5′- to 3′-direction of the inhibitory segment through strand displacement. Finally, the inhibitory segment is completely removed from the enzyme domain,

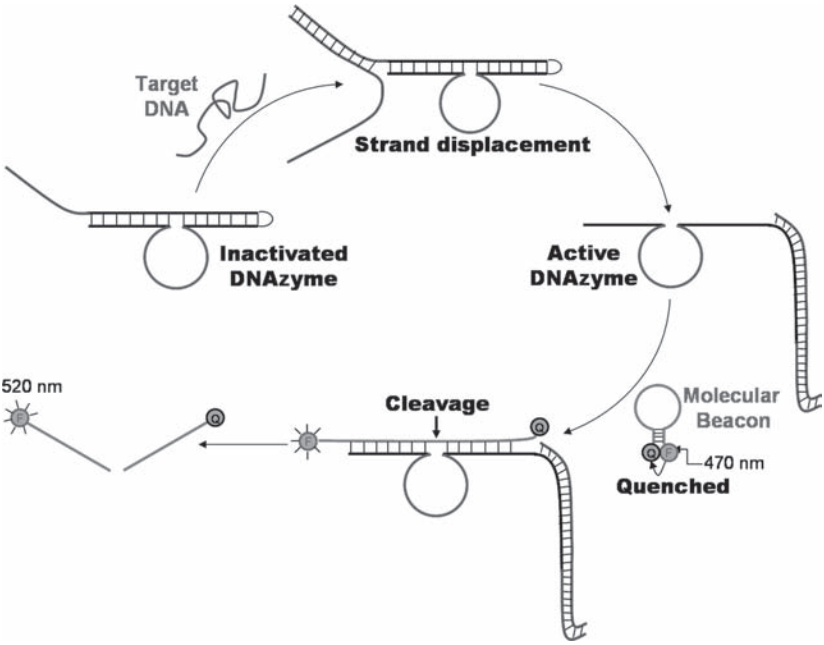

Fig. 15.3 Scheme of DNAzyme amplification of molecular beacon signal. The DNAzyme is composed of three portions: a catalytic core, two target recognition arms, and an inhibitory domain. Without target DNA, the active site of the DNAzyme is inactivated by the inhibitory domain. In the presence of target DNA, the inhibitory domain is removed by forming a longer duplex with the target DNA through strand displacement. The DNAzyme becomes active and starts to cleave the molecular beacon molecules. Thus, a strong fluorescent signal is generated (Reproduced with permission from ref. 35)

which activates the DNAzyme. Subsequently, the MBs are cleaved by the DNAzyme, which results in a strong fluorescent signal.

This method separates the target molecule recognition and signal read-out into two steps. The target DNA only activates the DNAzymes, then the activated DNAzymes constantly amplify the output signal through multiple turnover of MB cleavage, which improves the detection sensitivity. Furthermore, the high efficiency of 10–23 DNAzymes and the flexibility in designing the recognition arms make it adaptable to detect a variety of DNA/RNA molecules reliably and easily.

15.3.2 Cascade DNAzyme Signal Amplification for DNA Detection

To further increase detection sensitivity, another level of signal amplification beside DNAzyme has been introduced. The complete system contains two successive

levels of signal amplifications: one by a DNA polymerase (a protein enzyme) and the other by a DNA peroxidase (a DNAzyme). Here the DNAzyme used is a preidentified DNA peroxidase[36–38] that catalyzes chemical oxidizations by peroxides, which could generate detectable signals such as chemiluminescence, fluorescence, or color. This DNAzyme originally resulted from an in vitro selection experiment (SELEX), and can adopt a G-quadruplex conformation in solutions.

Willner and coworkers have explored a series of DNA detection methods based on this DNA peroxidase.[39,40] The target DNA molecule first triggers the opening of a hairpin DNA and activates the DNAzyme. Then the substrate [2,2′-azino-bis(3-ethylbenzthiazoline)-6-sulfonic acid, ABTS] is oxidized by H_2O_2 under the activity of the DNAzyme and generates detectable signals: colored products or chemiluminescence. However, if a target DNA molecule can only activate one DNAzyme, the detection will not be very sensitive. One solution is to introduce Au nanoparticles as biobarcodes to carry multiple copies of DNAzymes,[41] so that a stronger output signal will be generated.

An even more efficient way to improve the sensitivity is to use two successive steps of enzymatic amplifications[42] (Fig. 15.4). In the first amplification step, the target DNA does not interact with the DNAzyme directly, but initiates a rolling-circle amplification (RCA) reaction by serving as a primer. RCA is an isothermal method that uses a circular single-stranded template to synthesize long, repetitive single-stranded DNA.[43,44] The circular template for RCA in this system is deliberately coded with complementary sequences of both the target DNA and the DNA peroxidase. The target DNA will hybridize with the template. In the presence of a mixture of dATP, dGTP, dTTP, and dCTP, a DNA polymerase will extend the target DNA along the circular template over and over again, resulting in a long

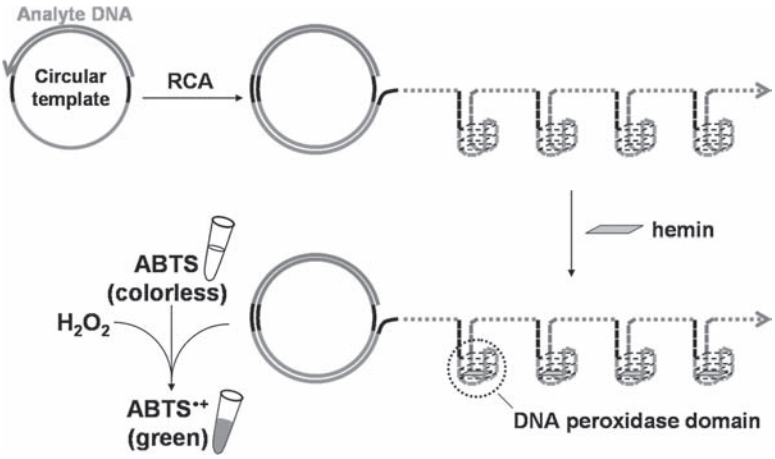

Fig. 15.4 Scheme of the cascade amplification of signal for DNA detection. *RCA*, rolling-circle amplification; *ABTS*, 2,2′-azino-bis(3-ethylbenzthiazoline)-6-sulfonic acid (Reproduced with permission from ref. 43)

DNA single strand that contains a series of DNA peroxidase domains. After being complexed with hemin, the DNA peroxidase becomes active and catalyzes the oxidation of ABTS by H_2O_2. The reaction product $ABTS^{\bullet+}$ has a blue-green color with a maximum absorption wavelength of 415 nm. It serves as a colorimetric output signal that can be conveniently monitored by a normal UV-vis spectrophotometer. Overall, each target DNA produces many copies of DNAzymes, and each DNAzyme produces many copies of colored, detectable chemicals. The complete system is composed of a two-step cascade amplification and has a high detection sensitivity. Experimentally, 1 pM target DNA has been detected. One particular attractive feature of this system is that it is an isothermal process and does not require temperature cycling.

RCA is a powerful isothermal amplification technique. It is not surprising that it has also been exploited in other related strategies to amplify signals. For example, Andrew Ellington has used RCA in conjunction with DNA ligases to detect proteins[45] and small molecules.[46]

15.4 Summary and Outlook

This chapter has discussed applications of DNAzymes for DNA nanomachines and DNA analysis. The currently reported work has shown great success with this strategy, which makes synthetic DNA nanomachines more intelligent and DNA analysis systems more sensitive. However, greater potential of the DNAzymes could be explored as there is plenty of scope in this newly emerged research field. Several conceivable research directions include the following: (1) With the well-established two-dimensional (2D) DNA crystals (periodic or aperiodic), we could design DNA paths on the DNA 2D crystals for DNA walkers. On such paths, the DNA walkers can intelligently choose the most reasonable route on their own. This would be an interesting branch in DNA computation and active manipulation of matters at the nanoscale. (2) If we incorporate the biological functions of DNA further into DNA nanotechnology, elegant DNA nanostructures and nanomachines could be introduced into cells or other organisms to interface with biological processes and perform gene detection, gene regulation, and gene therapy. DNAzymes are very likely to play important roles in turning these ambitious imaginings into reality.

Acknowledgments This work is supported by the NSF (EIA-0323452) and Purdue University (a start-up fund).

References

1. Seeman, N.C. (2003) DNA in a material world. Nature (Lond.) 421:427–431.
2. Feldkamp, U. and Niemeyer, C.M. (2006) Rational design of DNA nanoarchitectures. Angew. Chem. Int. Ed. 45:1856–1876.

3. Seeman, N.C. (2005) From genes to machines: DNA nanomechanical devices. Trends Biochem. Sci. 30:119–125.
4. Simmel, F.C. and Dittmer, W.U. (2005) DNA nanodevices. Small 1:284–299.
5. Kelly, T.R. (2005) Molecular motors: synthetic DNA-based walkers inspired by kinesin. Angew. Chem. Int. Ed. 44:4124–4127.
6. Shih, W.M., Quispe, J.D. and Joyce, G.F. (2004) A 1.7-kilobase single-stranded DNA that folds into a nanoscale octahedron. Nature (Lond.) 427:618–621.
7. Garibotti, A.V., Knudsen, S.M., Ellington, A.D. and Seeman, N.C. (2006) Functional DNAzymes organized into two-dimensional arrays. Nano Lett. 6:1505–1507.
8. Turberfield, A.J., Mitchell, J.C., Yurke, B., Mills, A.P., Blakey, M.I. and Simmel, F.C. (2003) DNA fuel for free-running nanomachines. Phys. Rev. Lett. 90:118–120.
9. Stojanovic, M.N., Prada, P. and Landry, D.W. (2001) Catalytic molecular beacons. ChemBioChem 2:411–415.
10. Mao, C., Sun, W., Shen, Z. and Seeman, N.C. (1999) A nanomechanical device based on the B–Z transition of DNA. Nature (Lond.) 397:144–146.
11. Yurke, B., Turberfield, A.J., Mills, A.P., Simmel, F.C. and Neumann, J.L. (2000) A DNA-fuelled molecular machine made of DNA. Nature (Lond.) 406:605–608.
12. Yan, H., Zhang, X., Shen, Z. and Seeman, N.C. (2002) A robust DNA mechanical device controlled by hybridization topology. Nature (Lond.) 415:62–65.
13. Chen, Y., Wang, M. and Mao, C. (2003) An autonomous DNA nanomotor powered by a DNA enzyme. Angew. Chem. Int. Ed. 43:3554–3557.
14. Chen, Y. and Mao, C. (2004) Putting a brake on an autonomous DNA nanomotor. J. Am. Chem. Soc. 126:8626–8627.
15. Vale, R.D. and Milligan, R.A. (2000) The way things move: looking under the hood of molecular motor proteins. Science 288:88–95.
16. Schliwa, M. and Woehlke, G. (2003) Molecular motors. Nature (Lond.) 422:759–765.
17. Alberts, B. (1998) The cell as a collection of protein machines: preparing the next generation of molecular biologists. Cell 92:291–294.
18. Sambongi, Y., Iko, Y., Tanabe, M., Omote, H., Iwamoto-Kihara, A., Ueda, I., Yanagida, T., Wada, Y. and Futai, M. (1999) Mechanical rotation of the c subunit oligomer in ATP synthase (F_0F_1): direct observation. Science 286:1722–1724.
19. Santoro, S.W. and Joyce, G.F. (1997) A general purpose RNA-cleaving DNA enzyme. Proc. Natl. Acad. Sci. USA 94:4262–4266.
20. Van Oijen, A.M., Blainey, P.C., Crampton, D.J., Richardson, C.C., Ellenberger, T. and Xie X.S. (2003) Single-molecule kinetics of λ exonuclease reveal base dependence and dynamic disorder. Science 301:1235–1238.
21. Asbury, C.L., Fehr, A.N. and Block, S.M. (2003) Kinesin moves by an asymmetric hand-over-hand mechanism. Science 302:2130–2134.
22. Yildiz, A., Tomishige, M., Vale, R.D. and Selvin, P.R. (2004) Kinesin walks hand-over-hand. Science 303:676–678.
23. Hammer, J.A. (1991) Novel myosins. Trends Cell Biol. 1:50–56.
24. Tian, Y., He, Y., Chen, Y., Yin, P. and Mao, C. (2005) A DNAzyme that walks processively and autonomously along a one-dimensional track. Angew. Chem. Int. Ed. 44:4355–4358.
25. Rothemund, P.W.K. (2006) Folding DNA to create nanoscale shapes and patterns. Nature (Lond.) 440:297–302.
26. Taton, T.A., Mirkin, C.A. and Letsinger, R.L. (2000) Scanometric DNA array detection with nanoparticle probes. Science 289:1757–1760.
27. Park, S.J., Taton, T.A. and Mirkin, C.A. (2002) Array-based electrical detection of DNA with nanoparticle probes. Science 295:1503–1506.
28. Chan, W.C.W. and Nie, S.M. (1998) Quantum dot bioconjugates for ultrasensitive nonisotopic detection. Science 281:2016–2018.
29. Maxwell, D.J., Taylor, J.R. and Nie, S.M. (2002) Self-assembled nanoparticle probes for recognition and detection of biomolecules. J. Am. Chem. Soc. 124:9606–9612.
30. Cao, Y.W.C., Jin, R.C. and Mirkin, C.A. (2002) Nanoparticles with Raman spectroscopic fingerprints for DNA and RNA detection. Science 297:1536–1540.

31. Zhao, X., Tapec-Dytioco, R., Wang, K. and Tan, W. (2003) Collection of trace amounts of DNA/mRNA molecules using genomagnetic nanocapturers. Anal. Chem. 75:3476–3483.
32. Li, J. and Lu, Y. (2000) A highly sensitive and selective catalytic DNA biosensor for lead ions. J. Am. Chem. Soc. 122:10466–10467.
33. Tyagi, S., Bratu, D.P. and Kramer, F.R. (1998) Multicolor molecular beacons for allele discrimination. Nat. Biotechnol. 16:49–53.
34. Bonnet, G., Tyagi, S., Libchaber, A. and Kramer, F.R. (1999) Thermodynamic basis of the enhanced specificity of structured DNA probes. Proc. Natl. Acad. Sci. USA 96:6171–6176.
35. Tian, Y. and Mao, C. (2005) DNAzyme amplification of molecular beacon signal. Talanta 67:532–537.
36. Travascio, P., Li, Y. and Sen, D. (1998) DNA-enhanced peroxidase activity of a DNA aptamer-hemin complex. Chem. Biol. 5:505–517.
37. Travascio, P., Witting, P.K., Mauk, A.G. and Sen, D. (2001) The peroxidase activity of a hemin-DNA oligonucleotide complex: free radical damage to specific guanine bases of the DNA. J. Am. Chem. Soc. 123:1337–1348.
38. Cano, A., Hernández-Ruiz, J., García-Cánovas, F., Acosta, M. and Arnao, M.B. (1998) An end-point method for estimation of the total antioxidant activity in plant material. Phytochem. Anal. 9:196–202.
39. Xiao, Y., Pavlov, V., Niazov, T., Dishon, A., Kotler, M. and Willner, I. (2004) Catalytic beacons for the detection of DNA and telomerase activity. J. Am. Chem. Soc. 126:7430–7431.
40. Pavlov, V., Xiao, Y., Gill, R., Dishon, A., Kotler, M. and Willner, I. (2004) Amplified chemiluminescence surface detection of DNA and telomerase activity using catalytic nucleic acid labels. Anal. Chem. 76:2152–2156.
41. Niazov, T., Pavlov, V., Xiao, Y., Gill, R. and Willner, I. (2004) DNAzyme-functionalized Au nanoparticles for the amplified detection of DNA or telomerase activity. Nano Lett. 4:1683–1687.
42. Tian, Y., He, Y. and Mao, C. (2006) Cascade signal amplification for DNA detection. ChemBioChem 7:1862–1864.
43. Fire, A. and Xu, S. (1995) Rolling replication of short DNA circles. Proc. Natl. Acad. Sci. USA 92:4641–4645.
44. Liu, D., Daubendiek, S.L., Zillman, M.A. and Kool, E.T. (1996) Rolling circle DNA synthesis: small circular oligonucleotides as efficient templates for DNA polymerases. J. Am. Chem. Soc. 118:1587–1594.
45. Yang, L., Fung, C.W., Cho, E.J. and Ellington, A.D. (2007) Real-time rolling circle amplification for protein detection. Anal. Chem. 79:3320–3329.
46. Cho, E.J., Yang, L., Levy, M. and Ellington, A.D. (2005) Using a deoxyribozyme ligase and rolling circle amplification to detect a non-nucleic acid analyte, ATP. J. Am. Chem. Soc. 127:2022–2023.

Index